UC Berkeley
SEMM Reports Series

Title
Computer Programs for Prestressed Concrete Box Girder Bridges

Permalink
https://escholarship.org/uc/item/8155w1hw

Authors
Scordelis, Alex
Chan, Esmond
Ketchum, Mark
et al.

Publication Date
1985-03-01

eScholarship.org Powered by the California Digital Library
University of California

REPORT NO.
UCB/SESM-85/02

STRUCTURAL ENGINEERING AND
STRUCTURAL MECHANICS

COMPUTER PROGRAMS FOR PRESTRESSED CONCRETE BOX GIRDER BRIDGES

by

A. C. SCORDELIS

E. C. CHAN

M. A. KETCHUM

P. P. VAN DER WALT

In cooperation with State of California,
Business and Transportation Agency,
Department of Transportation and the
U.S. Department of Transportation,
Federal Highway Administration

MARCH 1985

DEPARTMENT OF CIVIL ENGINEERING
UNIVERSITY OF CALIFORNIA
BERKELEY, CALIFORNIA

TECHNICAL REPORT STANDARD TITLE PAGE

1. Report No.	2. Government Accession No.	3. Recipient's Catalog No.

4. Title and Subtitle	5. Report Date
COMPUTER PROGRAMS FOR PRESTRESSED CONCRETE BOX GIRDER BRIDGES	March 1985
	6. Performing Organization Code
7. Author(s)	8. Performing Organization Report No.
A. C. Scordelis, E. C. Chan, M. A. Ketchum, P. P. van der Walt	UCB/SESM 85/02
9. Performing Organization Name and Address	10. Work Unit No.
Department of Civil Engineering University of California Berkeley, CA 94720	11. Contract or Grant No. F66SD02
	13. Type of Report and Period Covered
12. Sponsoring Agency Name and Address	Final Report
California Department of Transportation Sacramento, CA 95807	14. Sponsoring Agency Code RTA 13945 - F13844 UCB

15. Supplementary Notes

Prepared in cooperation with State of California, Business and Transportation Agency, Department of Transportation and the U.S. Department of Transportation, Federal Highway Administration.

16. Abstract

Three new computer programs are described which incorporate automatic prestressing and several other new features into three existing computer programs for the analysis of box girder bridges. The three new programs are MUPDI4 for the analysis of straight prismatic bridges using the folded plate elasticity method; CURDI4 for the analyses of circularly curved prismatic bridges using the finite strip method; and CELL4 for the analysis of bridges of arbitrary plan geometry, but constant depth, using the finite element method. These computer programs make it possible to perform detailed linear elastic analyses of a wide range of prestressed concrete box girder bridges in an expeditious and accurate manner with a minimum of simplifying assumptions. Both longitudinal and transverse prestressing may be specified by direct input or by automatic generation of the tendon profiles.

A detailed description of the input and output for MUPDI4, CURDI4 and CELL4 is presented together with the input data and selected output results for six numerical examples, which demonstrate the new capabilities of the programs and which also can be used for verification of the numerical results.

17. Key Words	18. Distribution Statement
Computer programs, box girders bridges, multi-cell bridges, straight, curved, arbitrary geometry, prestressed concrete, structural analysis, elastic analysis, folded plate method, finite strip method, finite element method.	Unlimited

19. Security Classif. (of this report)	20. Security Classif. (of this page)	21. No. of Pages	22. Price
Unclassified	Unclassified	349	

Form DOT F 1700.7 (8-69)

Department of Civil Engineering
Division of Structural Engineering
and
Structural Mechanics

UCB/SESM Report No. 85-02

COMPUTER PROGRAMS FOR PRESTRESSED CONCRETE BOX GIRDER BRIDGES

by

A. C. Scordelis
Professor of Civil Engineering

E. C. Chan
Assistant Research Engineer

M. A. Ketchum
Graduate Research Assistant

P. P. van der Walt
Graduate Research Assistant

In cooperation with

State of California
Department of Transportation
Under Research Technical Agreement
No. 13945-F13844

and

U. S. Department of Transportation
Federal Highway Administration

College of Engineering
Office of Research Services
University of California
Berkeley, California

March 1985

DISCLAIMER

The contents of this report reflect the views of the authors who are responsible for the facts and the accuracy of the data presented herein. The contents do not necessarily reflect the official views or policies of the State of California or the Federal Highway Administration. This report does not constitute a standard, specification or regulation.

TABLE OF CONTENTS

		Page
DISCLAIMER		i
TABLE OF CONTENTS		ii
LIST OF TABLES		v
LIST OF FIGURES		vi
1.	**INTRODUCTION**	1
2.	**PREVIOUS SOLUTIONS AND NEW FEATURES OF THE COMPUTER PROGRAMS**	5
	2.1 General Remarks	5
	2.2 Folded Plate Elasticity Method (MUPDI4)	6
	2.2.1 Straight Single Span Bridges	9
	2.2.2 Straight Continuous Span Bridges	9
	2.2.3 New Features of Program MUPDI4	12
	2.3 Finite Strip Method (CURDI4)	13
	2.3.1 Circularly Curved Bridges	14
	2.3.2 New Features of Program CURDI4	14
	2.4 Finite Element Method (CELL4)	16
	2.4.1 Bridges with Arbitrary Plan Geometry and Constant Depth	17
	2.4.2 New Features of Program CELL4	20
3.	**PRESTRESSING**	23
	3.1 General Remarks	23
	3.2 Tendon Discretization	25
	3.2.1 Panel Tendons	27
	3.2.2 Slab Tendons	27
	3.3 Definition of Tendon Profiles	28
	3.3.1 Direct Tendon Point Input	30
	3.3.2 Parametric Profile Generation	30
	3.4 Short Term Force Losses	32
	3.4.1 Friction Losses	32
	3.4.2 Anchor Slip Losses	35
	3.4.3 Influence of Stressing Procedure	37
	3.5 Final Tendon Forces	37
	3.6 Equivalent Loads	38
4.	**MUPDI4 - STRAIGHT BOX GIRDER BRIDGES**	42
	4.1 General Remarks	42
	4.2 Structural Modelling	42
	4.2.1 Folded Plate System	44
	4.2.2 Supporting Frames and Bents	47
	4.2.3 Unsupported Diaphragms	51
	4.3 Equivalent Loads from Prestressing	53
	4.3.1 Panel Tendons	53
	4.3.2 Slab Tendons	55
	4.4 Features of MUPDI4	56
	4.5 Computer Program Organization	56
	4.6 Computer Program Input and Output	58
	4.7 Special Considerations for the use of MUPDI4	59

Page

5. **CURDI4 - CIRCULARLY CURVED BOX GIRDER BRIDGES** 63
5.1 General Remarks 63
5.2 Structural Modelling 63
5.2.1 Finite Strip System 64
5.2.2 Supporting Frames and Bents 71
5.2.3 Unsupported Diaphragms 72
5.3 Equivalent Loads from Prestressing 73
5.3.1 Panel Tendons 73
5.3.2 Slab Tendons 75
5.4 Features of CURDI4 76
5.5 Computer Program Organization 77
5.6 Computer Program Input and Output 79
5.7 Special Considerations for the use of CURDI4 80

6. **CELL4 - BOX GIRDER BRIDGES OF ARBITRARY PLAN GEOMETRY** 84
6.1 General Remarks 84
6.2 Structural Modelling 86
6.2.1 General 86
6.2.2 Coordinate Systems and Sign Conventions 86
6.2.3 Material Laws 88
6.2.4 Deck Elements 90
6.2.5 Vertical Web Elements 90
6.2.6 Special Web Elements 90
6.2.7 Elastic Spring Supports 93
6.3 Equivalent Loads from Prestressing 93
6.4 Features of CELL4 96
6.5 Computer Program Organization 99
6.6 Computer Program Input and Output 100
6.7 Special Considerations for the use of CELL4 102

7. **NUMERICAL EXAMPLES** 104
7.1 Example 1 - Simply Supported Straight Single-Cell Box Girder Bridge with Curved Exterior Webs 105
7.1.1 Structure Geometry and Load Cases 105
7.1.2 Analytical Models 105
7.1.3 Discussion of Results 109
7.1.4 Conclusions 118
7.2 Example 2 - Simply Supported Straight Prestressed Single-Cell Box Girder Bridge with Vertical or Sloping Webs 119
7.2.1 Structure Geometry, Prestressing, and Load Cases . . . 119
7.2.2 Analytical Models 122
7.2.3 Discussion of Results 125
7.2.4 Conclusions 136
7.3 Example 3 - Two Span Straight Four-Cell Prestressed Box Girder Bridge with Vertical Exterior Webs 137
7.3.1 Structure Geometry, Prestressing, and Load Cases . . . 137
7.3.2 Analytical Models 139
7.3.3 Discussion of Results 142
7.3.4 Conclusions 161
7.4 Example 4 - Two Span Circularly Curved Single-Cell Prestressed Box Girder Bridge Model 162
7.4.1 Structure Geometry, Prestressing, and Load Cases . . . 162
7.4.2 Analytical Models 162
7.4.3 Discussion of Results 165
7.4.4 Conclusions 170

Page

7.5 Example 5 - Two Span Four-Cell Circularly Curved Prestressed Box Girder Bridge with Vertical Exterior Webs . . 171
7.5.1 Structure Geometry, Prestressing, and Load Cases . . . 171
7.5.2 Analytical Models 171
7.5.3 Discussion of Results 173
7.5.4 Conclusions 183
7.6 Example 6 - Three Span Multi-Cell Prestressed Box Girder Bridge of Arbitrary Plan Geometry 184
7.6.1 Structure Geometry, Prestressing, and Load Cases . . . 184
7.6.2 Analytical Models 187
7.6.3 Discussion of Results 191
7.6.4 Conclusions 212

8. **SUMMARY AND CONCLUSIONS** 213

9. **ACKNOWLEDGEMENTS** 214

10. **REFERENCES** 215

APPENDIX A -- Research Reports and Technical Papers Published on Box Girder Bridge Research at the University of California, Berkeley A1

APPENDIX B -- MUPDI4 USER'S GUIDE B1

APPENDIX C -- CURDI4 USER'S GUIDE C1

APPENDIX D -- CELL4 USER'S GUIDE D1

APPENDIX E -- LISTINGS OF INPUT DATA FOR EXAMPLES E1

LIST OF TABLES

Page

7.1.1 Total Section Bending Moments (ft-kips) and Vertical Shear Forces (kips) for Dead Load 113
7.1.2 Total Section Bending Moments (ft-kips), Vertical Shear Forces (kips) and Torsional Moments (ft-kips) for AASHTO Single Lane Live Load 117
7.2.1 Total Section Bending Moments (ft-kips) and Vertical Shear Forces (kips) for Dead Load 128
7.2.2 Total Section Bending Moments (ft-kips) and Vertical Shear Forces (kips) for Longitudinal Prestressing Without Friction . . 133
7.3.1 Transverse Distribution of Section Moments and Shears to Individual Girders under Dead Load 145
7.3.2 Transverse Distribution of Section Moments and Shears to Individual Girders under Prestressing 151
7.3.3 Transverse Distribution of Section Moments and Shears to Individual Girders under P13 Truck Load 157
7.5.1 Summary of Individual Girder and Total Section Moments (ft-kips) (Coarse Mesh 1) 175
7.5.2 Summary of Individual Girder and Total Section Shears (kips) (Coarse Mesh 1) 176
7.6.1 Summary of Vertical Reactions for Various Load Cases 193
7.6.2 Comparisons of Total Vertical Reactions (kips) by SAPIV and CELL4 (Case 2: Dead Load) 194
7.6.3 Comparisons of External and Internal Section Shears, Moments and Torques (Case 1: 1 ksf Uniform Load) 194
7.6.4 Comparison of Extrapolated Internal Shear Forces (kips) with External Support Reactions (kips) (Case 2: Dead Load) 195
7.6.5 Summary of Internal Shear at Various Sections for Different Load Cases 197
7.6.6 Summary of Internal Moment at Various Sections for Different Load Cases 198

LIST OF FIGURES

		Page
1.1	Elevations of Simple Span and Continuous Bridges	2
1.2	Straight, Curved, Skew and Arbitrary Plan Geometries	2
1.3	Typical Single- and Multi-Cell Cross-Sections	2
2.1	Displacements and Internal Forces on a Differential Element	7
2.2	Multi-Cell Prismatic Box Girder Bridges	7
2.3	Joint and Plate Edge Forces and Displacements in Global and Local Coordinate Systems	7
2.4	Analysis of a Box Girder Bridge on a Flexible Bent	10
2.5	Circularly Curved Box Girder Bridge Elements	15
2.6	Box Girder Bridge of General Geometry	18
2.7	Finite Elements used in CELL4 Program	18
2.8	Bridge with Arbitrary Plan Geometry and Constant Depth	19
3.1	Panel and Slab Tendons	24
3.2	Panel Tendon Discretization	26
3.3	Slab Tendon Discretization	26
3.4	Definition of Tendon Profiles	29
3.5	Definition of Tendon Geometry Parameters	31
3.6	Definition of Some Typical Tendon Geometries	31
3.7	Tendon Force Profile Under Jacking	33
3.8	Calculation of Friction Losses	33
3.9	Anchorage Slip Losses	36
3.10	Jacking From Both Ends	36
3.11	Segment Forces in a Smoothly Curved Tendon	39
3.12	Segment Forces in a Harped Tendon	40
3.13	Equivalent Loads at Tendon Points	40
4.1	Straight Bridge with Intermediate Diaphragms and Bents	43
4.2	Box Girder Bridge Cross Sections	43
4.3	Global Coordinate System for MUPDI4	46
4.4	Positive Element Local Axes and Element Results for MUPDI4	48
4.5	Fourier Representation of Concentrated Loads	49
4.6	Fourier Representation of Patch Loads.	50
4.7	Supporting Bent Coordinate System	52
4.8	Statically Equivalent Joint Loads	54
4.9	Longitudinal Symmetry and Antisymmetry	61
4.10	Transverse Symmetry and Antisymmetry	61
5.1	Global Coordinate System for CURDI4	65
5.2	Positive Element Local Axes and Element Results for CURDI4	67
5.3	Consistent Joint Loads for Prestress	74
6.1	Geometry, Cross-sections and Coordinate Systems for CELL4	85
6.2	Sign Convention for Internal Element Forces and Moments	87
6.3	Configuration, D.O.F. and Coordinate Systems for Special Web Element	91
6.4	Elastic Support Spring Element	94
6.5	Typical Prestressing Tendon Layouts	97
6.6	Geometry of a Prestressing Tendon Segment Passing Through a Finite Element	98
6.7	Reference Point Location and Sign Convention for Sectional Force Resultants	101

Page

7.1.1 Geometry and Loadings for Single Cell Box Girder Bridge with Curved Exterior Webs 106
7.1.2 Analytical Model 1 for Single Cell Box with Curved Exterior Webs 107
7.1.3 Analytical Model 2 for Single Cell Box with Curved Exterior Webs 108
7.1.4 Midspan Longitudinal Membrane Stresses σ_x (psi) for Dead Load 110
7.1.5 Midspan Transverse Moments M_y (in-lb/in) for Dead Load 111
7.1.6 Membrane Shear Stresses τ_{xy} (psi) at a Section Near the Support X =8.1 ft for Dead Load 112
7.1.7 Midspan Vertical Displacements (in.) and Transverse Moments M_y (in-lb/in) for Unsymmetrical Lane Live Load Using Fine Mesh Model 2 115
7.1.8 Longitudinal Variation of Vertical Displacements at Tops of Webs 1 and 2 for Unsymmetrical Lane Live Loading, Using Fine Mesh Model 2 116

7.2.1 Geometry for Single Cell Box Girder Bridge with Vertical or Sloping Exterior Webs 120
7.2.2 Loadings and Prestressing Tendon Profiles 121
7.2.3 Analytical Models for Single Cell Box with Vertical Exterior Webs 123
7.2.4 Analytical Models for Single Cell Box with Sloping Exterior Webs 124
7.2.5 Displacements and Longitudinal Stresses for Dead Load 126
7.2.6 Transverse Moments for Dead Load 127
7.2.7 Displacements and Longitudinal Stresses for Antisymmetric Live Load 130
7.2.8 Shear Stresses and Transverse Moments for Antisymmetric Live Load 131
7.2.9 Displacements and Longitudinal Stresses for Longitudinal Prestressing without Friction 132
7.2.10 Displacements and Longitudinal Stresses for Longitudinal Prestressing with Friction 134
7.2.11 Displacements and Transverse Moments for Transverse Slab Prestressing without Friction 135

7.3.1 Span Arrangement, Cross-Sectional Dimensions, and Tendon Profile for Two Span, Continuous, Prestressed, Four Cell Box Girder Bridge 138
7.3.2 Analytical Models for MUPDI4, CURDI4, and CELL4 Computer Solutions 140
7.3.3 P13 Truck Load Configuration and Position of P13 Truck on Bridge for Live Load Analysis 141
7.3.4 Longitudinal Variation of Vertical Displacements, Section Moments and Shears for Dead Load 144
7.3.5 Transverse Distribution of Transverse Moments, Longitudinal Membrane Stresses and Membrane Shear Stresses for Dead Load 147

Page

7.3.6 Longitudinal Variation of Vertical Displacements, Section Moments and Shears for Prestressing 150
7.3.7 Transverse Distribution of Transverse Moments, Longitudinal Membrane Stresses and Membrane Shear Stresses for Prestressing 153
7.3.8 Longitudinal Variation of Vertical Displacements, Section Moments and Shears for P13 Truck Load 156
7.3.9 Transverse Distribution of Transverse Moments, Longitudinal Membrane Stresses and Membrane Shear Stresses for P13 Truck Load 159

7.4.1 Geometry and Concentrated Point Load Position for Hood Plexiglass Model 163
7.4.2 Analytical Model of Cross-Section for CURDI4 Analysis 164
7.4.3 Prestressing Tendon Geometry 164
7.4.4 Stresses (MPa) at Middle of Loaded Span for Single 313N Point Load 166
7.4.5 Stresses (MPa) at Midspan Due to Prestressing 168
7.4.6 Longitudinal Variations of Vertical Displacement (mm) at the Tops of the Inner and Outer Webs 169

7.5.1 Plan Geometry and Section Locations for Circularly Curved Four Cell Bridge 172
7.5.2 Analytical Model 1 - (Coarse Mesh) of Cross-Section for CURDI4 Analysis 172
7.5.3 Analytical Model 2 - (Fine Mesh) of Cross-Section for CURDI4 Analysis 172
7.5.4 Longitudinal Membrane Stresses σ_x (psi) at Midspan Section B-B (Coarse Mesh 1) 178
7.5.5 Transverse Moments M_y (in-lb/in) at Midspan Section B-B (Coarse Mesh 1) 179
7.5.6 Transverse Moments M_y (in-lb/in) at Midspan Section B-B (Fine Mesh 2) 180
7.5.7 Vertical Displacements (in.) at Midspan Section B-B (Coarse Mesh 1) 181
7.5.8 Longitudinal Variations of Vertical Displacements (in.) at Tops of Inner Girder 1 and Outer Girder 5 (Coarse Mesh 1) 182

7.6.1 Geometry of the Bridge in Plan 185
7.6.2 Plan of Mesh, Section Locations, Tendon Profile and Cross-Sectional Dimensions 186
7.6.3 Summary of Various Load Cases 188
7.6.4 Longitudinal Variation of Section Shears and Moments for Dead Load 199
7.6.5 Longitudinal Variation of Section Shears and Moments for Prestress 200
7.6.6 Longitudinal Variation of Section Shears and Moments for AASHTO HS20 Truck Live Loads 201
7.6.7 Longitudinal Variation of Section Shears and Moments for AASHTO Lane Live Load 202

Page

7.6.8 Longitudinal Variation of Centerline Vertical Displacements for Dead Load and Prestress 203
7.6.9 Transverse Distribution of Vertical Displacements and Longitudinal Membrane Stresses at Midspan Section 3A (Span 3) for Dead Load 204
7.6.10 Transverse Distribution of Membrane Shear Stresses (ksf) at Sections 2B and 3B (Left and Right of Bent 2B) for Dead Load 205
7.6.11 Transverse Distributions of Vertical Displacements and Longitudinal Membrane Stresses at Midspan Section 3A (Span 3) for Prestress 206
7.6.12 Transverse Distribution of Membrane Shear Stresses (ksf) at Sections 2B and 3B (Left and Right of Bent 2B) for Prestress 207
7.6.13 Transverse Distribution of Vertical Displacements and Longitudinal Membrane Stresses at Midspan Section 3A (Span 3) for AASHTO HS 20 Truck Live Loads 208
7.6.14 Transverse Distribution of Membrane Shear Stresses (ksf) at Sections 2B and 3B (Left and Right of Bent 2B) for AASHTO HS 20 Truck Live Loads 209
7.6.15 Transverse Distribution of Vertical Displacements and Longitudinal Membrane Stresses at Midspan Section 3A (Span 3) for AASHTO Lane Live Load 210
7.6.16 Transverse Distribution of Membrane Shear Stresses (ksf) at Sections 2B and 3B (Left and Right of Bent 2B) for AASHTO Lane Live Loads 211

1. INTRODUCTION

Reinforced and prestressed concrete box girder bridges (Figs. 1.1, 1.2, 1.3) have been widely used as economic and aesthetic solutions for the overcrossings, undercrossings, separation structures and viaducts found in today's modern highway system. Both simple span and continuous bridges supported by single or multiple column bents are used (Fig. 1.1). These structures may be straight, curved, skewed, or of arbitrary plan geometry (Fig. 1.2). The typical cross section of such a box girder bridge (Fig. 1.3) consists of a top slab and a bottom slab connected monolithically by webs to form a cellular or box-like structure. Either single cell or multi cell cross sections may be used, depending on the span, width, and construction method used. The webs are generally vertical, but in some cases sloping or curved exterior webs are also used. Transverse diaphragms are placed at the end and interior support sections, and sometimes additional intermediate diaphragms are placed between supports. In recent years, because of the demand for longer spans, prestressed concrete box girder bridges have become the predominant bridge type for new construction in the California highway system.

Prestressing is used in these structures in order to increase maximum spans, control behavior, and limit weight. Post-tensioned tendons are generally used, both in the longitudinal direction where their use can result in more slender girders and longer maximum spans, and in some cases in the transverse direction where their use can reduce the number of webs required and increase the width of cantilever top slabs, resulting in a more efficient cross section.

Present and past designs of prestressed concrete box girder bridges usually have been based on linear elastic analyses of simplified models of uncracked homogeneous systems. Empirical formulas are often used to determine the transverse distribution of longitudinal girder moments and vertical shear forces in the webs due to design truck vehicle wheel loads.

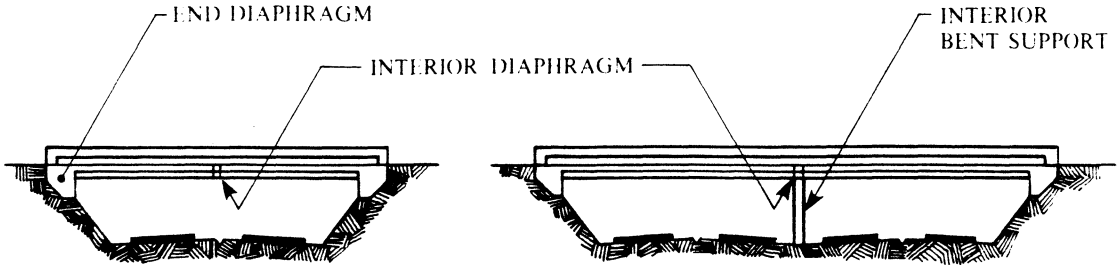

FIG. 1.1 ELEVATIONS OF SIMPLE SPAN AND CONTINUOUS BRIDGES

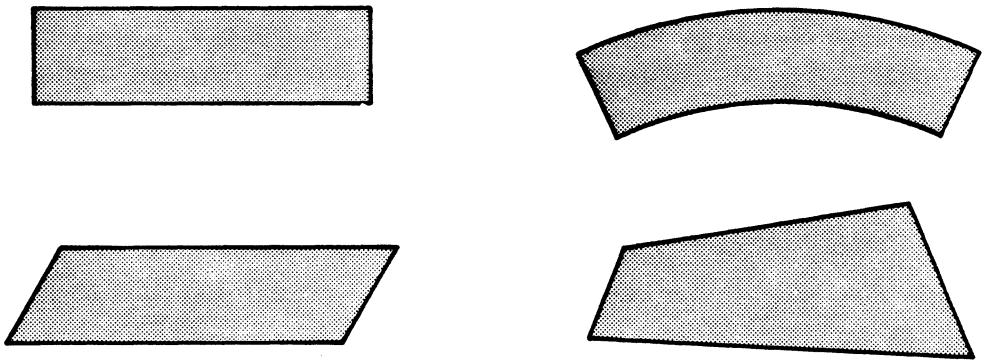

FIG. 1.2 STRAIGHT, CURVED, SKEW, AND ARBITRARY PLAN GEOMETRIES

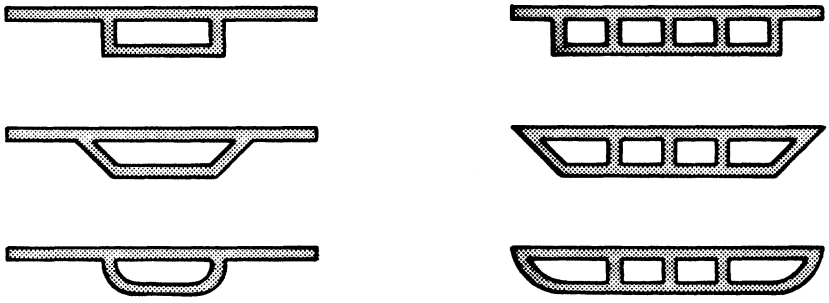

FIG. 1.3 TYPICAL SINGLE - AND MULTI-CELL CROSS-SECTIONS

Empirical formulas are also used to determine local transverse and longitudinal slab design moments. In many recent bridge specifications, an alternate load factor method of design based on ultimate strength calculations is permitted, but little guidance is given on how this can be applied to complex box girder bridge geometries. Basic knowledge of the nonlinear behavior and ultimate strength of concrete box girder bridges is lacking at the present time.

Prestressed concrete box girder bridges are complex spatial structures, and their behavior can be only roughly approximated using analysis techniques which do not reflect this fact. A common simplified analysis procedure used by some designers is to ignore any curvature or skewness and analyze an equivalent straight bridge taking the centerline length as the effective span and treating the entire bridge cross-section as a beam section. Judgment and experience are then used to extrapolate the results to the actual bridge geometry. A curved bridge system may also be approximated by a series of short straight one-dimensional beam segments and analyzed as a three dimensional frame using a standard three dimensional frame program. This type of analysis can give an indication of the longitudinal distribution of total reactions, internal total stress resultants, and centerline deflections, but can provide no information on the transverse distribution of these quantities or the internal forces in the individual plate type elements making up the cellular cross section. Furthermore, the elementary beam theory assumptions may be seriously in error for some box girder bridge types. As maximum spans and loads increase, the importance of more accurate analysis also increases, particularly for those structures whose configuration does not match those on which the empirical design rules are based.

An analytical solution of the true response of a concrete box girder under load is complicated by the usual factors common to other reinforced or prestressed concrete structural systems. It is a highly indeterminate structure; it is made of two materials, concrete and steel; under increasing load it can experience cracking and material nonlinearities and thus some redistribution of internal forces; and also the internal forces are time

dependent because of creep and shrinkage in the concrete. Nevertheless, as for other reinforced or prestressed concrete systems, such as frames, slabs, and shells, it has generally been accepted that for design purposes, the distribution of internal forces, moments and displacements in a box girder bridge due to applied loads can be based on linear elastic analyses of an uncracked homogeneous concrete system.

In a complete analysis of a multi-cell box girder bridge, all of the internal forces and displacements shown on a typical element in Fig. 2.1 taken from a deck or web plate of the bridge should be determined. The internal forces N_x, N_y and N_{xy} are termed membrane forces while M_x, M_y, M_{xy}, Q_x and Q_y are internal forces due to plate bending. In many approximate analyses certain internal forces are assumed to be negligible and are thus taken as zero.

Of prime interest from a design standpoint are those internal forces which determine the reinforcing or prestressing steel requirements for the bridge. These are N_x for the main longitudinal tension steel; N_{xy} for the diagonal tension steel; and M_y and N_y for the transverse steel.

The primary purpose of this research study was to write three new computer programs incorporating automatic prestressing and several other new features into three existing computer programs for box girder bridges. The three new programs are: MUPDI4 for the analysis of straight prismatic bridges; CURDI4 for the analysis of circularly curved prismatic bridges; and CELL4 for the analysis of bridges of arbitrary plan geometry. These computer programs make it possible to perform detailed linear elastic analyses of a wide range of prestressed concrete box girder bridges in an expeditious and accurate manner with a minimum of simplifying assumptions.

A detailed description of the input and output for MUPDI4, CURDI4 and CELL4 will be presented in this report together with six numerical examples which demonstrate the new capabilities of the programs and which also can be used for verification of the numerical results.

2. PREVIOUS SOLUTIONS AND NEW FEATURES OF THE COMPUTER PROGRAMS

2.1 General Remarks

A continuous research program on box girder bridges, directed towards improved design methods, has been conducted at the University of California, Berkeley, in which analytical and experimental studies have been carried out on the structural behavior of box girder bridges which are straight, skew, curved, or of arbitrary plan geometry. The results of this research program, which has been primarily sponsored by the State of California, Department of Transportation and the U. S. Department of Transportation, Federal Highway Administration, have been presented in detail in a number of research reports and technical papers. A list of these publications is given in Appendix A of this report.

As a part of this research program, a number of computer programs have been developed for the analysis of box girder bridges using folded plate, finite strip, finite element, and finite segment methods. A summary of many of these programs with examples may be found in reference [19].

Many analytical models and methods have been developed for the linear elastic analysis of box girder bridges. Among these are approximate methods based on simplified structural behavior such as the use of an elementary or extended beam method; an equivalent beam grillage or anisotropic slab to represent the system; exact and approximate methods based on folded plate theory; and numerical solutions based on finite strip, finite element, finite segment or finite difference methods. No attempt will be made to review all of these methods here. Instead, only previous solutions and computer programs on which the new programs, MUPDI4, CURDI4 and CELL4 are based will be described. These linear elastic analyses of an uncracked homogeneous structure give complete solutions for all of the internal forces, moments and displacements shown in Fig. 2.1 for any type or position of loading on the bridge. The linear elastic solutions and computer programs to be described

can be classified under the following methods of analysis: (1) folded plate elasticity method (MUPDI4); (2) finite strip method (CURDI4); (3) and finite element method (CELL4). Each of these methods has its advantages and disadvantages and the appropriate method should be carefully selected based on its advantages and applicability for the particular problem to be solved.

2.2 Folded Plate Elasticity Method (MUPDI4)

A multi-cell prismatic box girder bridge (Fig. 2.2) may be modelled analytically as a folded plate system consisting of an assembly of longitudinal plate elements interconnected at joints along their longitudinal edges and simply supported at the two ends. The known quantities input into the problem include the geometry, dimensions and material properties of the plate elements, the surface and joint loadings and the boundary conditions along the longitudinal joints. Each plate element selected is assumed to extend longitudinally over the entire span and transversely between designated joints on the cross-section (Fig. 2.3)

An analysis for applied loads with any arbitrary longitudinal distribution for straight or circularly curved bridges may be performed using a direct stiffness harmonic analysis. The applied loads are first resolved into Fourier series components. An analysis is made for the components of each particular harmonic and then the final results are obtained by summing the results for all harmonics used to represent the load. Once the solution technique, which involves extensive computations, has been developed for a single harmonic, it can be reused for any harmonic, and thus the method is ideally suited to the application of a digital computer.

The analysis for each harmonic load has the advantage that for straight or curved circular bridges such loads will produce displacements of the same variation and vice versa and thus a single characteristic value may be used to describe any force or displacement pattern. For example, the displacement pattern for the n-th harmonic:

$$r(x) = r_0 \sin \frac{n\pi x}{L} \quad \text{for straight bridges, or} \qquad (2.1)$$

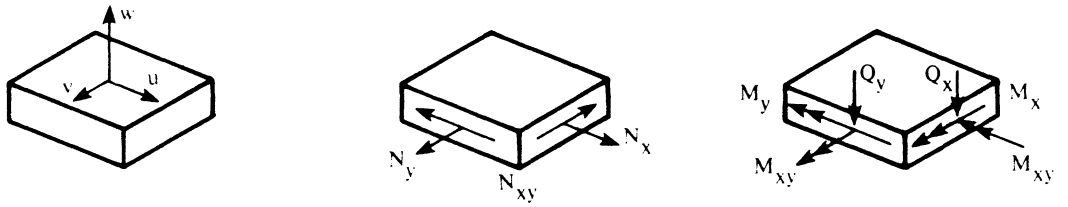

(a) DISPLACEMENTS (b) MEMBRANE FORCES (c) PLATE BENDING FORCES

FIG. 2.1 DISPLACEMENTS AND INTERNAL FORCES ON A DIFFERENTIAL ELEMENT

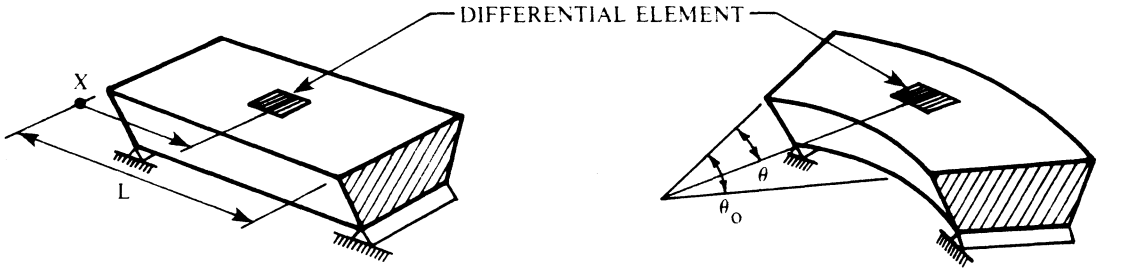

(a) STRAIGHT BRIDGE (b) CIRCULARLY CURVED BRIDGE

FIG. 2.2 MULTI-CELL PRISMATIC BOX GIRDER BRIDGES

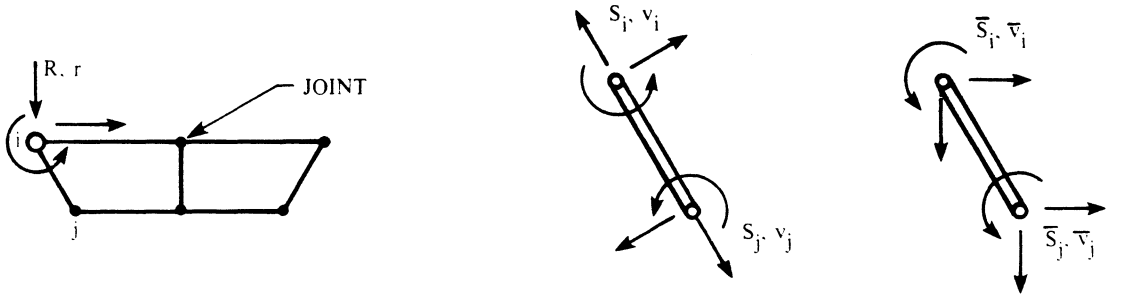

(a) JOINT - GLOBAL (b) PLATE - LOCAL (c) PLATE - GLOBAL

FIG. 2.3 JOINT AND PLATE EDGE FORCES AND DISPLACEMENTS IN GLOBAL AND LOCAL COORDINATE SYSTEMS

$$r(\Theta) = r_0 \sin \frac{n\pi\Theta}{\Theta_0} \qquad \text{for curved circular bridges} \qquad (2.2)$$

may be described by a single value r_0. L and Θ_0 define the span for the straight and circular bridges respectively (Fig. 2.2). This makes it possible to treat an entire joint as a single nodal point and to operate with single forces and displacements instead of functions. If the condition of static equilibrium and geometric compatibility are maintained at a nodal point they will automatically be satisfied along the entire longitudinal joint. Thus the three-dimensional prismatic bridge problem may be treated as a two-dimensional problem in the transverse direction. A direct stiffness method applied to such a system results in a structure stiffness matrix which is well conditioned for solution and with non-zero coefficients all grouped in a narrow band about the main diagonal.

Each longitudinal joint has four characteristic degrees of freedom; it can displace vertically and horizontally in the plane of the cross-section; it can move longitudinally tangent to the joint; and it can rotate about the axis tangent to the joint. These directions define a global coordinate system for displacements or forces at the joint (Fig. 2.3a).

The direct stiffness method is described in detail in many textbooks and other publications. Thus it need only be briefly outlined here by the following steps for loads applied at the joints.

1. Determine the 8 x 8 element stiffness matrix **k** in **S** = **kv** for each plate element, relating the edge forces **S** to the edge displacements **v** in the local coordinate system (Fig. 2.3b).
2. Transform the element stiffnesses from a local **k** (Fig. 2.3b) to a global **k'** (Fig. 2.3c) coordinate system. Assemble these 8 x 8 matrices into the structure stiffness matrix **K**, which for the structure in Fig. 2.3a would be a 24 x 24 matrix.
3. Solve the equilibrium equation, **R** = **Kr**, where **R** represents the applied loads, for the unknown joint displacements **r**.
4. Determine the plate element internal forces and displacements (Fig.

2.1) by expressions relating these quantities to the joint displacements.

The basic logic of a general computer program for the direct stiffness harmonic analysis is independent of the method chosen for determining the element stiffness matrices.

2.2.1 Straight Single Span Bridges

For straight bridges, formulas based on elasticity theory for the stiffness matrix coefficients defining membrane and plate bending action for isotropic, linearly elastic plates were first utilized to develop the computer program MULTPL (1965) [1,3,4,6] for straight single span bridges, simply supported at the two ends. The elasticity equations defining the plane stress problem for membrane loads in the plane of the plate and classical thin plate theory for loads normal to the plate are used to determine the necessary expressions for the fixed-edge forces and moments due to applied loads between the joints and also for the element stiffness matrix **k** in the local coordinate system needed in the direct stiffness harmonic solution. Results obtained by this elasticity method represent the most exact available solution for a linear elastic analysis of box girder bridges and they are often used to measure the accuracy of results by other methods.

2.2.2 Straight Continuous Span Bridges

The above solution for a single span bridge without interior supports was extended to continuous span bridges with interior rigid diaphragms in the computer program MUPDI (1966) [1,5,6] and to bridges with interior flexible diaphragms and supporting planar frame bents in the computer program MUPDI3 (1971) [2,6,7]. A force method of analysis is used in combination with the direct stiffness harmonic analysis described above.

For structures supported by flexible planar frame bents the redundants are taken as the interaction forces between the folded plate system and the bents (Fig. 2.4). The interaction forces are represented by a set of three joint forces at each longitudinal joint (Fig. 2.4d) consisting of vertical, horizontal and rotational components in the plane of the transverse cross-section. The analysis is carried out in the following sequence of steps:

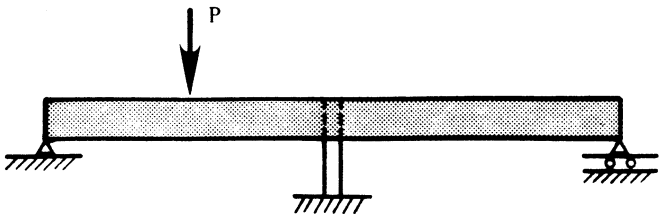

(a) ELEVATION OF STRUCTURE

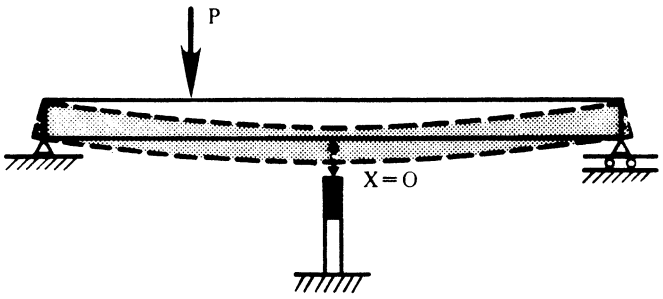

(b) PRIMARY STRUCTURE

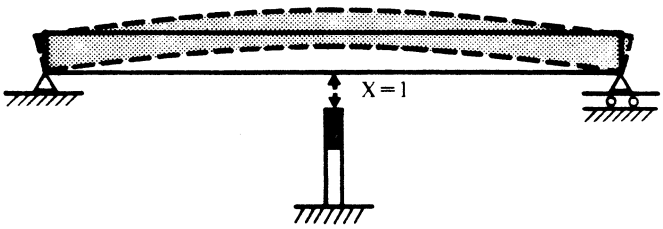

(c) UNIT REDUNDANT FORCES

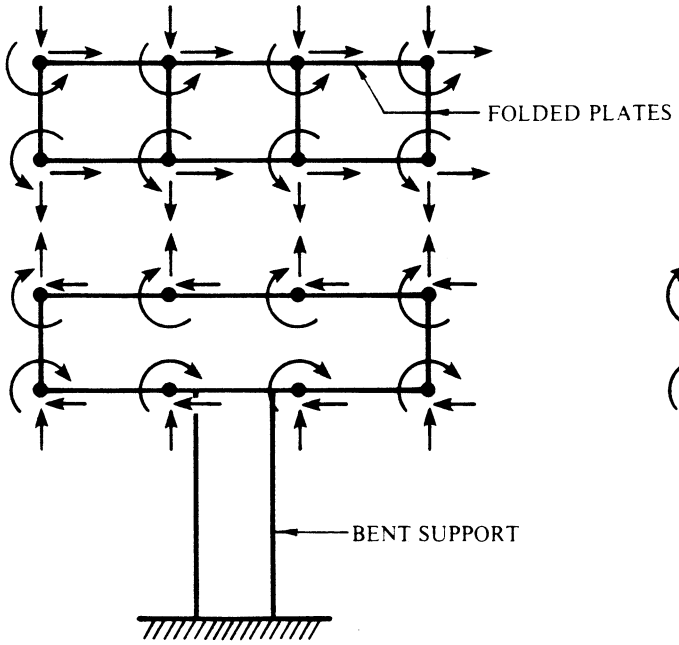

(d) JOINT REDUNDANT FORCES

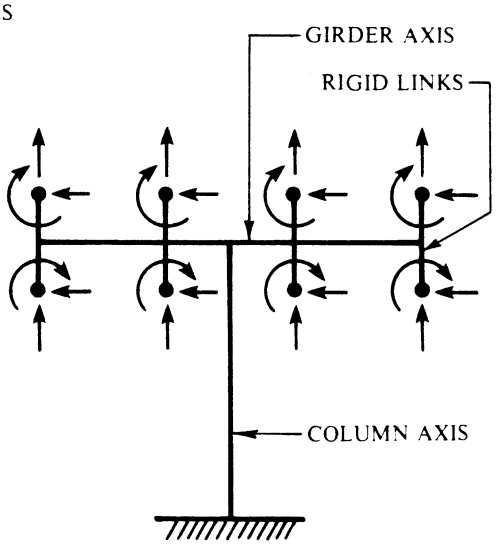

(e) IDEALIZED FRAME BENT

FIG. 2.4 ANALYSIS OF A BOX GIRDER BRIDGE ON A FLEXIBLE BENT

1. With the redundants **X** set equal to zero (Fig. 2.4b), the folded plate structure is analyzed for the given external applied load using a direct stiffness harmonic analysis as described above. A displacement vector δ_0 (24 x 1 in Fig. 2.4) is found for this case, which defines the displacements at the points where the redundants are to act.
2. The folded plate structure is next analyzed for unit values of each of the redundant forces **X** (Fig. 2.4c) and the corresponding flexibility matrix $\mathbf{F}_1$ (24 x 24 in Fig. 2.4) for the folded plate system is formed.
3. The idealized planar frame bent (Fig. 2.4e), composed of one dimensional elements, is then analyzed by the direct stiffness method. The total structure stiffness matrix for the frame bent is formed, and is solved for the flexibility matrix $\mathbf{F}_2$ (24 x 24 in Fig. 2.4) corresponding to the unit redundant forces.
4. Geometric compatibility requires that

$$\delta_0 + \delta_1 + \delta_2 = \mathbf{0} \qquad (2.3a)$$

$$\delta_0 + \mathbf{F}_1\mathbf{X} + \mathbf{F}_2\mathbf{X} = \mathbf{0} \qquad (2.3b)$$

or

$$\delta_0 + \mathbf{F}\mathbf{X} = \mathbf{0} \qquad (2.3c)$$

where

$$\mathbf{F} = \mathbf{F}_1 + \mathbf{F}_2 \qquad (2.4)$$

and thus the redundants may be found from Eq. 2.3c.

$$\mathbf{X} = -\mathbf{F}^{-1}\,\delta_0 \qquad (2.5)$$

5. The simply supported folded plate structure and the planar frame bent can now be analyzed, subjected to the known applied external loading and the known redundant forces, to determine the final stresses and displacements in the structure.

For interior diaphragms which are not externally supported, a similar force method is used to determine the redundants. However, in this case, because the diaphragms can undergo three degrees of rigid body motion in their own plane in addition to the deformation of the diaphragms themselves,

additional transformation and condensation of the flexibility matrices $\mathbf{F}_1$ and $\mathbf{F}_2$ are required. These are done automatically in the computer program MUPDI4 and are described in detail in Ref. [2].

2.2.3 New Features of Program MUPDI4

The new features of MUPDI4 may be summarized as follows:

1. The FORTRAN program, input specifications and output formats have been completely rewritten in order to utilize new numerical techniques and to simplify and clarify the features of the program.
2. Computer memory is dynamically allocated, in order to more efficiently utilize available computer resources.
3. Automatic prestressing options are available for the use of panel and slab tendons.
4. Automatic integration of plate element forces gives individual girder and total section moments, shears, and axial forces.
5. Multiple load cases can be analyzed in one computer run.

The new program MUPDI4 is capable of analyzing open or cellular straight prismatic folded plate structures simply supported at the two ends and with optional intermediate diaphragms or supports. Prestressing tendons may be located in any of the folded plate elements. The basic solution technique of MUPDI3 has been retained, but the program has been restructured and rewritten utilizing dynamic storage allocation techniques in order to eliminate any dimensional restraints on the size of problem that can be solved. Any arbitrary bridge cross section may be considered by suitable discretization as flat plate elements.

Automatic prestressing options have been added in MUPDI4 which permit the use of two types of unbonded post-tensioned tendons, designated as panel tendons and slab tendons. Panel tendons have a profile at the mid-thickness of the plate elements and extend over the length of the bridge, while slab tendons may have a profile across the thickness of the plate elements, but must be straight in plan and must be at right angles to the longitudinal axis of the bridge. Tendon profiles may be input either by direct input of coordinates of points on the tendon, or by specification of tendon geometry

parameters from which the actual tendon geometry is generated in the program as segments of parabolas and straight lines. Each tendon may be stressed from one or both ends, and short term losses in tendon force due to friction and anchor slip are automatically calculated.

Joint displacements, as well as internal forces and moments in the plate elements are output at selected locations as in MUPDI3. A new addition in MUPDI4 makes it possible to automatically integrate the plate element internal forces to give individual girder and total section moments, shears and axial forces. An option is provided to also output forces and displacements in the supporting flexible frame bents. Multiple load case capability has been added to MUPDI4, so that several load cases may be analyzed in one execution of the program.

2.3 Finite Strip Method (CURDI4)

When using the direct stiffness harmonic analysis, the direct application of elasticity theory to determine the stiffness matrix of plate elements which are not isotropic becomes exceedingly complex and resort must be made to simpler approaches. A theory known as the finite strip method is used in these cases. The finite strip method may be thought of as a special form of the finite element method. It approximates the behavior of each plate in a straight or circularly curved bridge (Fig. 2.2) by an assemblage of narrower longitudinal finite strips for which selected displacement patterns varying as harmonics longitudinally or circumferentially and as polynomials in the transverse direction are assumed to represent the behavior of the strip in the total structure. With these assumptions the displacement of any point in the strip can be expressed in terms of the eight nodal point displacements shown if Fig. 2.3b. Using successively strain-displacement relationships, a stress-strain law and thence either the principle of virtual displacements or the principle of minimum potential energy, the element stiffness matrix and also the generalized or consistent nodal forces for surface loads can be derived for the finite strip. The direct stiffness harmonic analysis can then proceed as described before in Section 2.2.

2.3.1 Circularly Curved Bridges

The finite strip method and direct stiffness harmonic analysis were used to develop the computer programs CURSTR (1970) [8,6,12,13,7], CURDI (1974) [10], and CURDIP (1980) [11] for box girder bridges which are circularly curved in plan (Fig. 2.5a) and made up of orthotropic plate elements. Each element, which may be a segment from a circular ring plate, a conical shell or a cylindrical shell (Figs. 2.5b, c, d), is idealized by a number of circumferential finite strips. Displacement patterns in each strip are assumed to vary as harmonics in the circumferential direction and in the transverse direction, a linear variation of the in-plane displacements and a cubic variation of the normal displacements, are assumed.

CURSTR can be used to analyze single span bridges and is similar in concept tp MULTPL for straight bridges. CURDI can be used to analyze curved continuous span bridges with interior radial diaphragms or supporting planar frame bents (Fig. 2.4) and is similar in concept to MUPDI3 for straight bridges. By setting the radius to a very large value in CURSTR or CURDI a close approximation to a straight bridge is obtained and thus, if desired, results from a finite strip method can be compared with those from the more exact folded plate elasticity method used in MULTPL and MUPDI3.

CURDIP was a first attempt to extend CURDI to take into account the effect of post-tensioned prestressing panel tendons. It had severe limitations in the number of panel tendons it could handle and also in the automatic generation capabilities of the panel tendon geometry. Slab tendons could not be treated in CURDIP.

2.3.2 New Features of Program CURDI4

The new program CURDI4 for circularly curved bridges was written after MUPDI4 for straight bridges had been completed. The method of analysis used in CURDI4 is computationally very similar to that used in MUPDI4 except that the basic structural element used in CURDI4 is a circumferential finite strip, while in MUPDI4 it is a straight folded plate element. Because of their similarity it was possible to incorporate into CURDI4 all of the new features of MUPDI4 already described in Section 2.2.3:

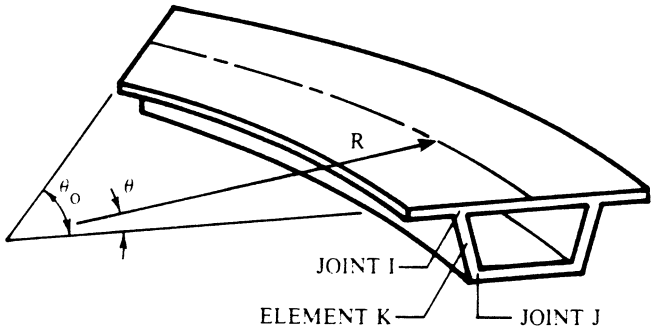

(a) CIRCULARLY CURVED BRIDGE

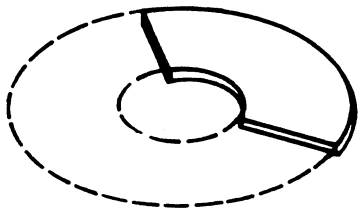

(b) RING PLATE ELEMENT

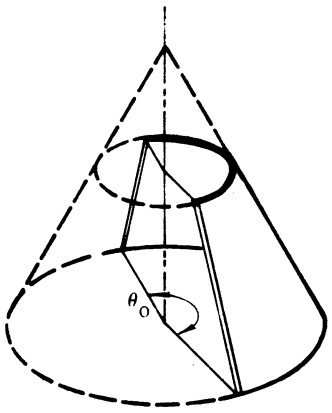

(c) CONICAL ELEMENT

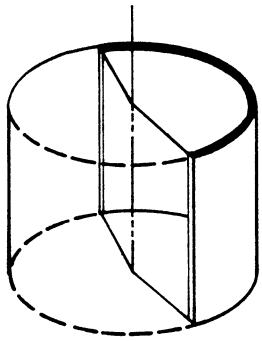

(d) CYLINDRICAL ELEMENT

FIG. 2.5 CIRCULARLY CURVED BOX GIRDER BRIDGE ELEMENTS

1. The FORTRAN program, input specifications and output formats have been completely rewritten in order to utilize new numerical techniques and to simplify and clarify the features of the program.
2. Computer memory is dynamically allocated, in order to more efficiently utilize available computer resources.
3. Automatic prestressing options are available for the use of panel and slab tendons.
4. Automatic integration of plate element forces gives individual girder and total section moments, shears, and axial forces.
5. Multiple load cases can be analyzed in one computer run.

CURDI4 provides important new analysis capabilities for circularly curved or straight bridges under dead load, prestressing and external live loads. The complex problem of generating three dimensional draped cable geometries and equivalent forces in curved bridges, which is not considered in MUPDI4, is solved automatically within the program. A tendon geometry and equivalent force generation scheme similar to that incorporated in MUPDI4 is adopted, but the scheme is extended to include tendon geometry generation on curves and the radial tendon force components caused by horizontal curvature of the box girder. Thus the output of CURDI4 can automatically include local stresses in the curved box girder strip elements (Fig. 2.5) due to horizontal curvature of the structure and its prestressing tendons. Options are included so that joint displacements, internal element displacements, and membrane and plate bending stresses or stress resultants, as well as the individual girder and total section moments, shears, and axial forces, can be output at any radial section in the structure. CURDI4 thus has the capability of providing a complete picture of both global and local stresses and displacements in curved prestressed box girder bridges.

2.4 Finite Element Method (CELL4)

The finite element method is described extensively in textbooks and in the technical literature. In the finite element method the actual continuum is replaced by an assembly of finite elements interconnected at nodal points

(Fig. 2.6). For a general box girder bridge system, the finite elements may consist of two dimensional shell or plate elements and transverse or longitudinal one dimensional frame type elements. Stiffness matrices which approximate the behavior in the continuum, are developed for the finite elements based on assumed displacement or stress patterns, after which an analysis based on the direct stiffness method may be performed to determine nodal point displacements and thence the internal stresses in the finite elements. The accuracy obtained is dependent on the assumptions used in deriving the stiffness matrices and on the fineness of mesh used in subdividing the structure. The results often satisfy compatibility, but not necessarily equilibrium in the continuum until a sufficiently fine mesh is used.

A number of investigators have developed general finite element shell programs which could be used for analyzing box girder bridges. However, if available, it is better to use special purpose programs which take advantage of the repetitive and special nature of these structures. These should provide the required accuracy in the results with a minimum of the following: (1) required amount of input preparation; (2) execution time in the computer; and (3) amount of output data reduction necessary for meaningful interpretation.

2.4.1 Bridges with Arbitrary Plan Geometry and Constant Depth

Many multicell box girder bridges used in separation and interchange structures fall into this category. The special purpose computer program CELL (1970) [14,6,15,16,7] was written especially for this type of bridge in which the bridge is made up of top and bottom horizontal deck slabs and vertical longitudinal webs and transverse diaphragms (Fig. 2.8).

The deck slabs are idealized by quadrilateral elements having a total of five degrees of freedom (DOF) per node, three translations and two rotations (Fig. 2.7a, b). The in-plane action of the quadrilateral elements is represented by the plane stress mixed model Q8D11 having two translational DOF at each corner node and three internal DOF (Fig. 2.7a). The mixed model is constructed using separate expansions for the displacement and strain

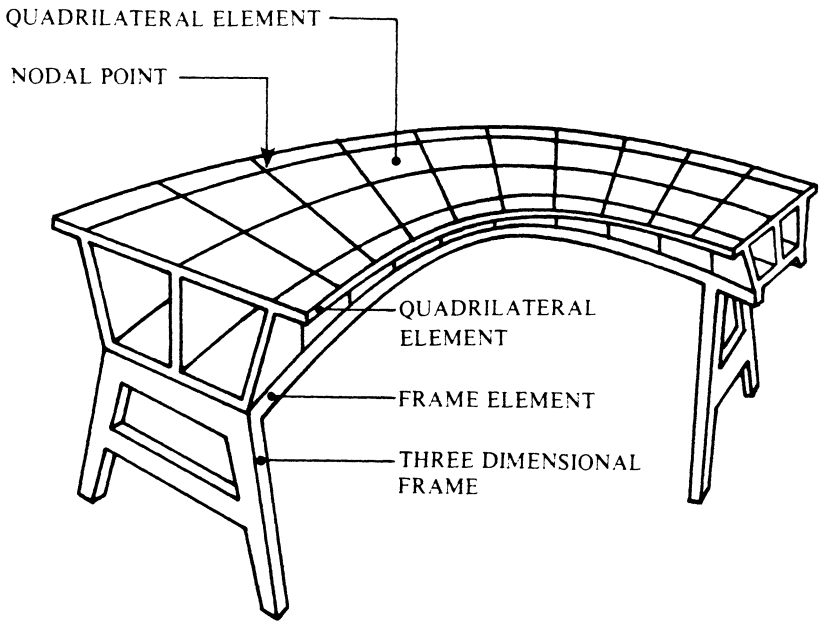

FIG. 2.6 BOX GIRDER BRIDGE OF GENERAL GEOMETRY

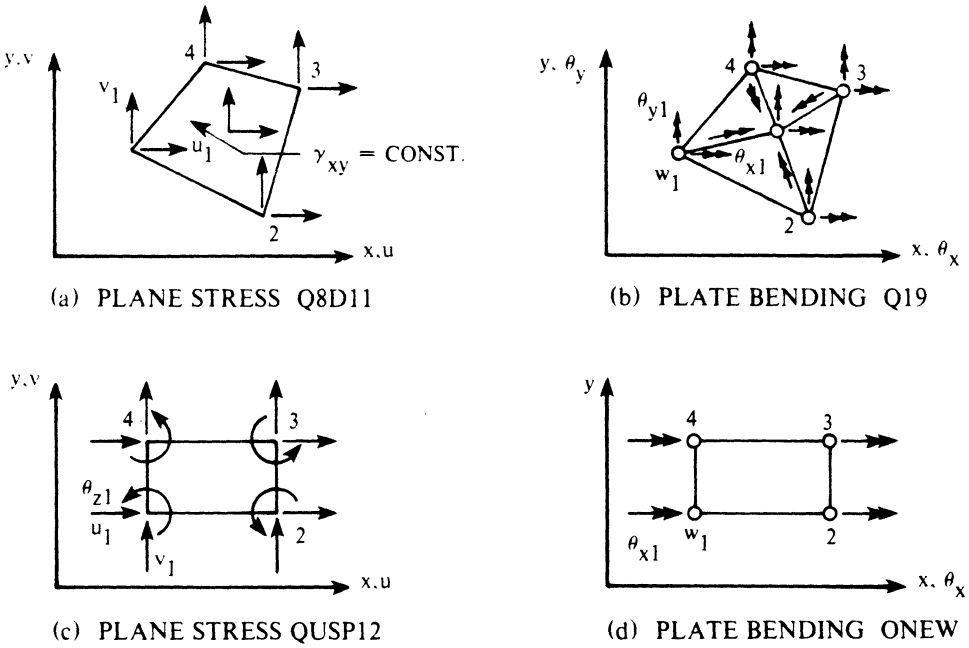

FIG. 2.7 FINITE ELEMENTS USED IN IN CELL4 PROGRAM

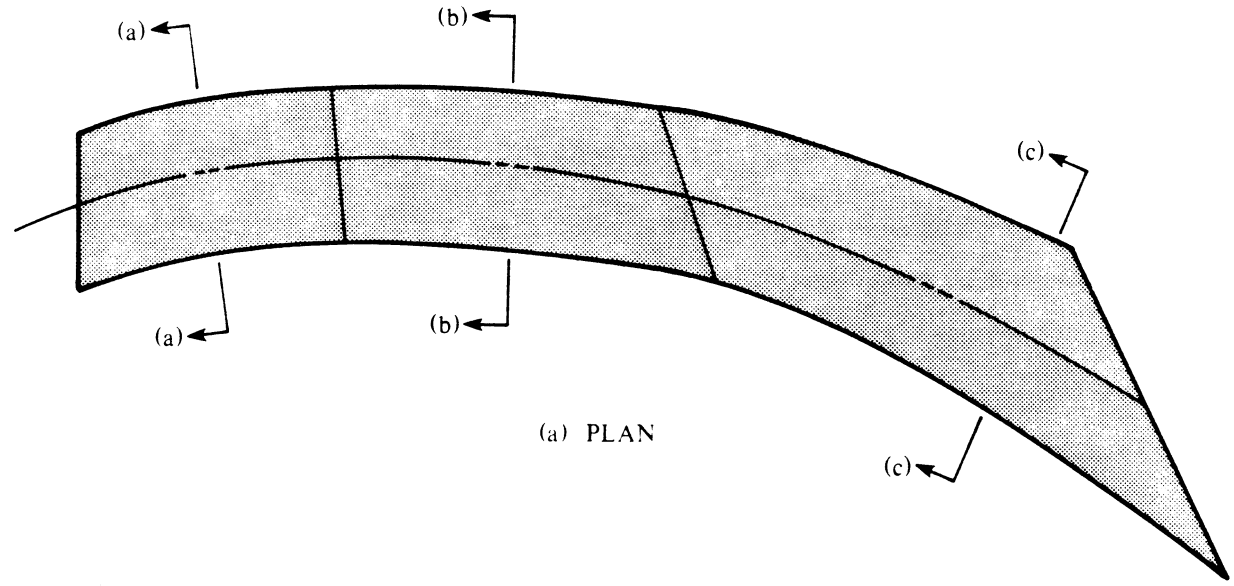

(a) PLAN

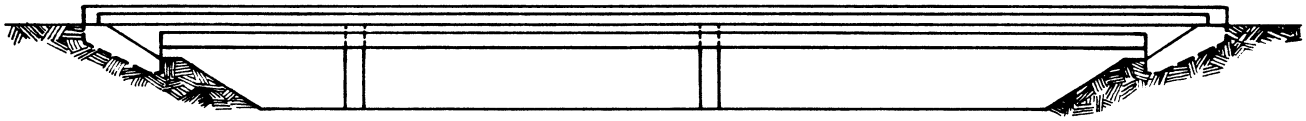

(b) ELEVATION

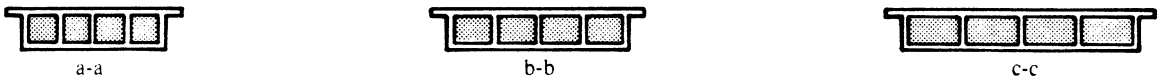

(c) CROSS-SECTIONS AT VARIOUS SECTIONS

FIG. 2.8 BRIDGE WITH ARBITRARY PLAN GEOMETRY AND CONSTANT DEPTH

fields. The variations of the u and v components of the displacement field are approximated by the standard bi-linear expansion for the eight corner node DOF and by bi-quadratic expansions for two of the internal DOF. The third internal DOF is used to enforce a constant shear-strain variation over the entire element, which produces a more flexible and better element. After the element stiffness is formed the three internal DOF are eliminated by an internal static condensation process. The quadrilateral plate bending element Q19 (Fig. 2.7b) used for the deck slabs is a compatible element made up of four subtriangles, each of which has eleven DOF associated with full cubic expansions of the w-displacement field and an enforced linear variation of the normal slope along one edge. In combining the four sub-elements, a quadrilateral with nineteen DOF is obtained. However, the seven internal DOF are eliminated by static condensation leaving the essential three DOF at each corner node, two rotations and one translation (Fig. 2.7b).

The vertical web elements of the bridge are idealized by special rectangular spar elements having a total of five DOF at each corner node, three translations and two rotations. A single element over the entire depth of the bridge can be used to capture the essential behavior of the web. The in-plane action of these elements is represented by the model QUSP12 (Fig. 2.7c). A bilinear expansion for u and v is associated with the two translational DOF at each node and a cubic variation in the x-direction of v is defined by the rotation $\Theta_{zi} = \partial v/\partial x$ at each node. The plate bending is represented by a simple one-way bending element ONEW having two DOF at each node, a rotation and a translation (Fig. 2.7d). Orthotropic plate properties and arbitrary loadings and boundary conditions can be treated in CELL. Automatic element and coordinate generation options which minimize the required input data, have made CELL a widely used program.

2.4.2 New Features of Program CELL4

The new features of CELL4 may be summarized as follows:

1. The FORTRAN program, input specifications and output formats have been completely rewritten in order to simplify and clarify the features of the program.

2. Special elements are included to simulate sloping or curved exterior webs.
3. External elastic spring elements in any direction may be placed at any node.
4. Automatic prestressing options are available for the use of panel and slab tendons.
4. Automatic integration of internal element forces gives the six stress resultants (three forces and three moments) for each individual girder and for the total section with respect to any prescribed set of orthogonal axes at a point in the section.
5. Multiple load cases can be analyzed in one computer run.

The new program CELL4 is capable of analyzing cellular bridge structures of constant depth with arbitrary plan geometry and boundary support conditions. The bridge may have vertical, sloping, or curved exterior webs. Prestressing tendons may be located in the top and bottom slabs and in the webs. The finite elements incorporated in the original CELL program have been retained for modelling the top and bottom slabs and vertical webs, while the sloping or curved exterior webs in CELL4 are modelled with new special web elements. External elastic spring elements have been incorporated to simulate the stiffness of supporting columns, bents, foundations, or reactions in arbitrary directions.

Automatic prestressing options have been added which permit the use of two types of unbonded post-tensioned tendons, designated as panel tendons and slab tendons. Panel tendons have a profile at the mid-thickness of the webs or of the horizontal top or bottom deck slabs. Slab tendons lie in the horizontal top or bottom slabs and must be straight in plan, but can have a profile in any plane perpendicular to the horizontal slabs. Tendon profiles may be input either by direct input of coordinates of points on the tendon at element boundaries, or by specification of tendon geometry parameters from which the actual tendon geometry is generated in the program as segments of parabolas and straight lines. Each tendon may be stressed from one or both ends, and short term losses in tendon force due to friction and anchor slip

are automatically calculated.

The addition of the panel and slab tendon prestressing option will permit the analysis of not only multicell box girders, but should also prove to be a useful tool in studying many problems encountered in single cell boxes with large cantilever overhangs such as found in prestressed segmental bridges. For example, questions regarding the shear lag and local stresses in the deck slabs induced by curved panel tendons in these horizontal slabs may be studied. In addition the tendency to go to larger and larger cantilevers and transverse spans between the webs has necessitated the use of transverse slab tendons producing local slab moments and stresses, which also may be studied with the prestressing option.

In analyzing bridge structures it is often useful to know the internal moments and forces that each individual girder contributes to the total internal stress resultants at a specified section. In a finite element displacement analysis, such as used in CELL4, while compatibility is generally satisfied, local equilibrium is not until the finite element mesh is sufficiently refined. Thus it is always advisable to make equilibrium checks of external and internal forces and moments. The incorporation of the automatic integration into CELL4 to give individual girder and total section stress resultants will greatly simplify this process. A study of the distribution of these quantities among the girders also gives a better understanding of load distribution in multi-cell box girder bridges.

The multiple load case capability of CELL4 permits several load cases to be analyzed in one execution of the program, for example: (1) dead load; (2) prestressing; (3) live load; and (4) any combination of (1), (2) and (3).

3. PRESTRESSING

3.1 General Remarks

Prestressing is used in concrete box girder bridges in order to increase maximum span, control behavior, and limit weight. Post-tensioned tendons are generally used, both in the longitudinal direction where their use can result in more slender girders and longer maximum spans, and in some cases in the transverse direction where their use can reduce the number of webs required and increase the width of cantilever top slabs, resulting in a more efficient cross section.

Many factors affect the behavior of concrete box girder bridges under the influence of prestressing. Prestressing can be considered as a set of equivalent loads on the structure, and an analysis of the structure under these loads is subject to all of the usual complicating factors common to all loadings on the system. These factors are briefly discussed in Chapter 1. In addition, the force in a tendon and the equivalent loads on the structure are influenced by short term and long term losses. Short term losses take place at the time of stressing and are due to friction between the tendon and duct as well as slippage at the anchorage when the stressing jack is removed. Long term losses take place during the life of the structure and are due to creep and shrinkage of the concrete and relaxation of the prestressing steel.

Automatic prestressing analysis options in MUPDI4, CURDI4 and CELL4 developed under this research program permit the use of two types of post-tensioned tendons, designated as panel tendons and slab tendons. Panel tendons (Fig. 3.1a,b) have a profile at the mid-thickness of the webs or of the top or bottom deck slabs, and extend over the length of the bridge. Slab tendons (Fig. 3.1c) lie in the top or bottom slabs or the webs, have a profile in a plane perpendicular to the slabs, and extend over the width of the bridge.

Tendon profiles may be specified either by direct input of coordinates of points along the length of the tendon, or by specification of tendon

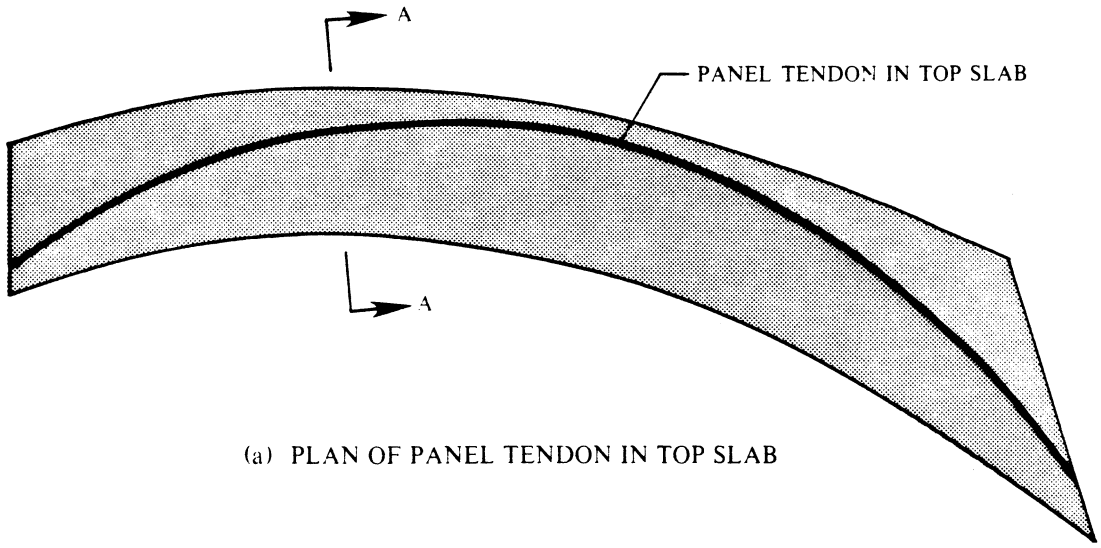

(a) PLAN OF PANEL TENDON IN TOP SLAB

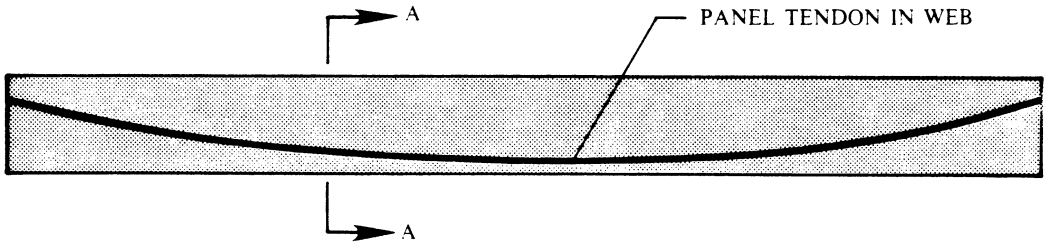

(b) ELEVATION OF PANEL TENDON IN WEB

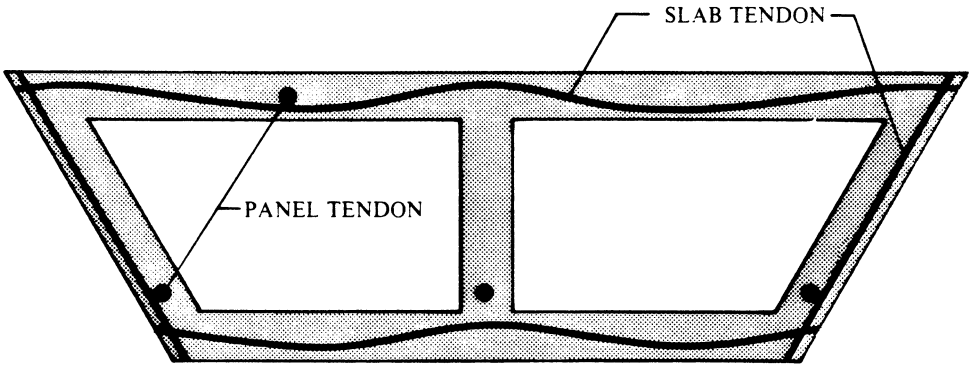

(c) SECTION A-A WITH SLAB AND PANEL TENDONS

FIG. 3.1 PANEL AND SLAB TENDONS

geometry parameters from which the actual tendon geometry is generated as segments of parabolas and straight lines. Within the programs, tendon profiles are made up of short straight segments approximating the actual tendon profile. Any number of slab and panel tendons may be specified, and the method of profile specification may vary from tendon to tendon.

Each tendon may be stressed from one or both ends, and short term losses in tendon force due to friction and anchor slip are automatically calculated. Long term losses are not calculated internally, and must be estimated and input to the programs by the engineer. Once the force distribution along the length of the tendon is known, the equivalent forces on the structure are calculated, and the analysis of the structure under prestressing is performed by treating these forces as another load case on the structure. Prestressing load cases may be combined with other load cases for checking of total stresses and displacements.

This chapter describes aspects of the prestressing analysis which are common to the three programs MUPDI4, CURDI4, and CELL4. These aspects include tendon profile definitions, computation of short term force losses due to friction and anchor slip, and computation of equivalent loads on the structure. Methods of application of the equivalent loads are described in Chapters 4 (MUPDI4), 5 (CURDI4), and 6 (CELL4).

3.2 Tendon Discretization

In order to describe a wide range of general tendon profiles, the actual curved tendon is approximated by subdivision into piece-wise linear segments intersecting at tendon points (Figs. 3.2, 3.3). The force in each segment is computed using methods presented in Sections 3.4 and 3.5. Then a system of equivalent point forces at the tendon points is computed using methods presented in Section 3.6. This set of equivalent forces is then treated as a prestressing load case in the analysis. Only the forces are applied to the structure, no stiffness contribution from the tendon is considered.

Panel tendons and slab tendons are discretized slightly differently by the programs; this is the basic reason for having two different tendon types.

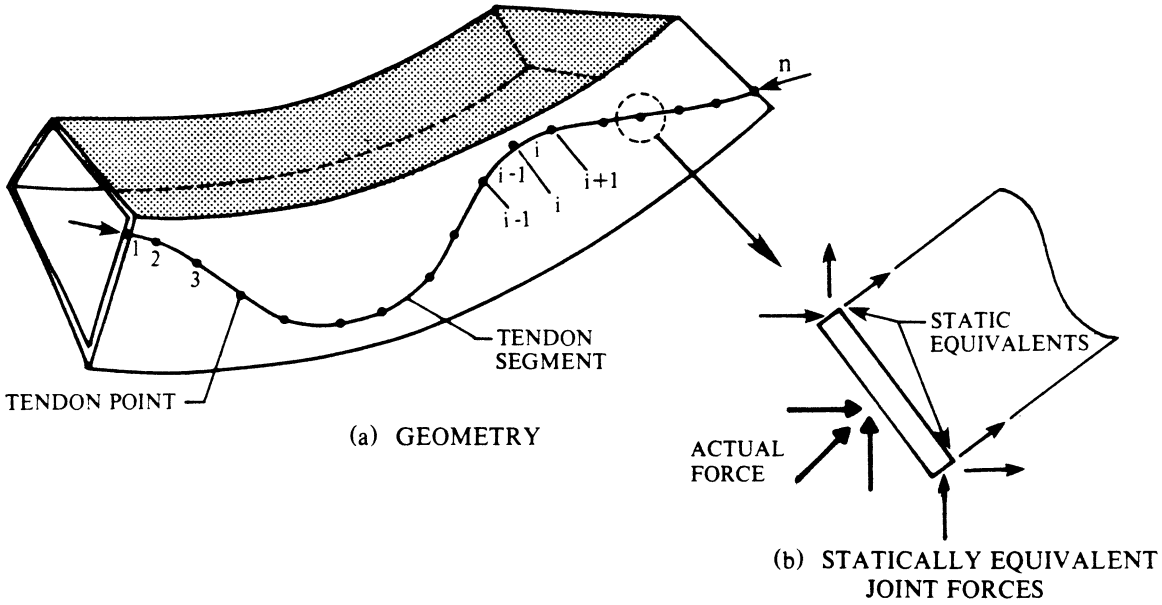

FIG. 3.2 PANEL TENDON DISCRETIZATION

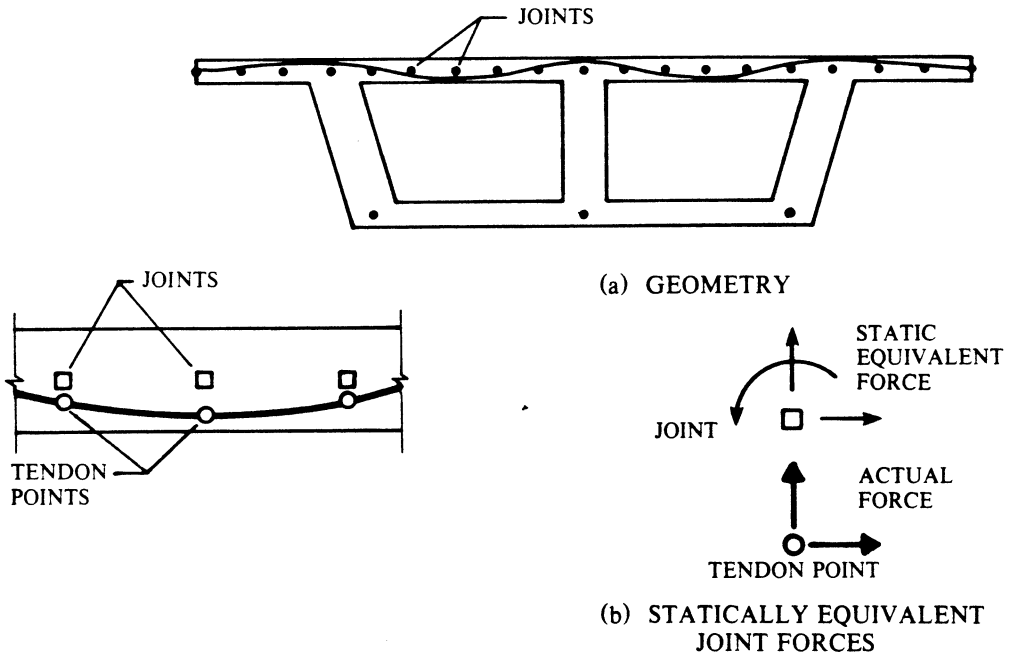

FIG. 3.3 SLAB TENDON DISCRETIZATION

Additionally, the three programs handle certain details of the discretization differently. However, most aspects other than application of the force to the structure are common to all three programs.

3.2.1 Panel Tendons

Panel tendons may be used to model longitudinal prestressing in top and bottom slab elements as well as in web elements. The discretization is defined for the general case of a curved inclined web (Fig. 3.2a). An arbitrarily curved prestressing tendon is approximated by subdivision into piece-wise linear segments intersecting at tendon points. The discretized geometry is completely defined by the set of coordinates of the tendon points, all of which must lie in plate elements.

Each tendon is discretized into n-1 straight segments defined by n tendon points (Fig. 3.2a). Once the equivalent forces acting on the structure at the tendon points are found, they are transformed to statically equivalent forces at the adjacent nodes or joints (Fig. 3.2b). Thus the final application of the equivalent force vector is as a set of nodal (or joint) forces, requiring mesh refinement in order to capture local behavior in regions of high tendon curvature. This method of load application also precludes the use of the programs for detailed analysis of anchorage block stresses.

In a typical multi cell concrete box girder bridge, each web may contain one or more tendons, and the tendon profiles in the different webs may be the same. In MUPDI4, CURDI4, and CELL4, it is possible to treat several physical tendons located in the same web as one analytical tendon. It is not possible, however, to treat tendons which are not located in the same web as one analytical tendon.

3.2.2 Slab Tendons

Slab tendons may be used to model transverse prestressing in top and bottom slab elements as well as vertical prestressing in web elements. The discretization is defined for the case of a draped tendon in a transversely prestressed top slab (Fig. 3.3a). The draped prestressing tendon is approximated by subdivision into piece-wise linear segments intersecting at

tendon points. The discretized geometry is completely defined by the set of coordinates of the tendon points, which should lie near nodal (or joint) lines.

Each tendon is discretized into n-1 straight segments defined by n tendon points (Fig. 3.3a). Once the equivalent forces acting on the structure at the tendon points are found, they are transformed to statically equivalent forces and moments at the adjacent nodes (Fig. 3.3b). Thus the final application of the equivalent force vector is as a set of nodal (or joint) forces and moments, requiring one or more nodes between webs in order to capture local slab bending moments due to tendon drape.

In a typical transversely prestressed concrete box girder bridge, slab tendons with similar geometry may be uniformly distributed over a significant length of the bridge. In MUPDI4, CURDI4, and CELL4, it may be possible to generate these uniformly distributed slab tendons as a slab tendon group, thus minimizing input and computation requirements.

3.3 Definition of Tendon Profiles

Tendon profile definitions are used to locate each prestressing tendon within the bridge structure. Tendon profiles for panel tendons (Fig. 3.4a) and slab tendons (Fig. 3.4b) are specified in similar fashions. First, the length of the bridge (for panel tendons) or the width of the bridge (for slab tendons) is divided into portions which usually correspond to the actual physical spans of the bridge between supports (for panel tendons) or between webs (for slab tendons).

Then the tendon point coordinates in each portion are defined, using either direct tendon point input or parametric tendon input. When direct tendon point input is used, the engineer must input the actual coordinates of the tendon points. When parametric tendon input is used, the programs generate the tendon profile as a series of parabolic and linear segments, based on a few simple input parameters. With either method of input, the program discretizes the actual tendon profile as a series of straight segments.

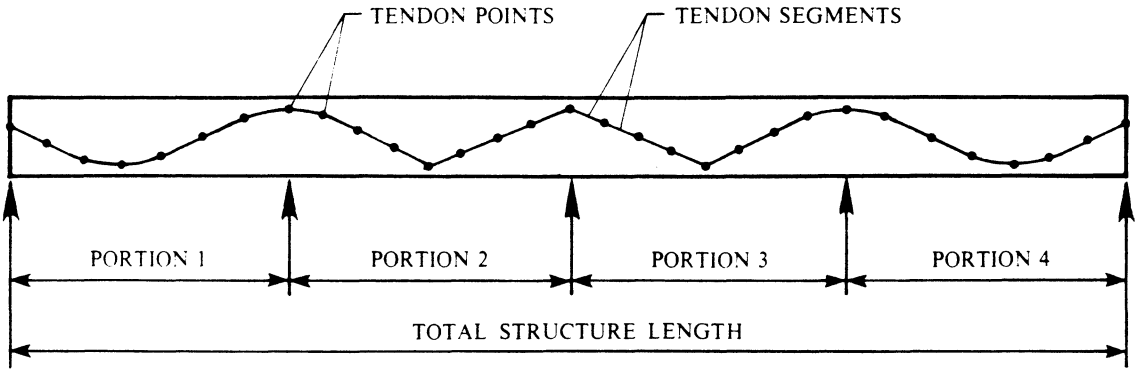

(a) PANEL TENDONS

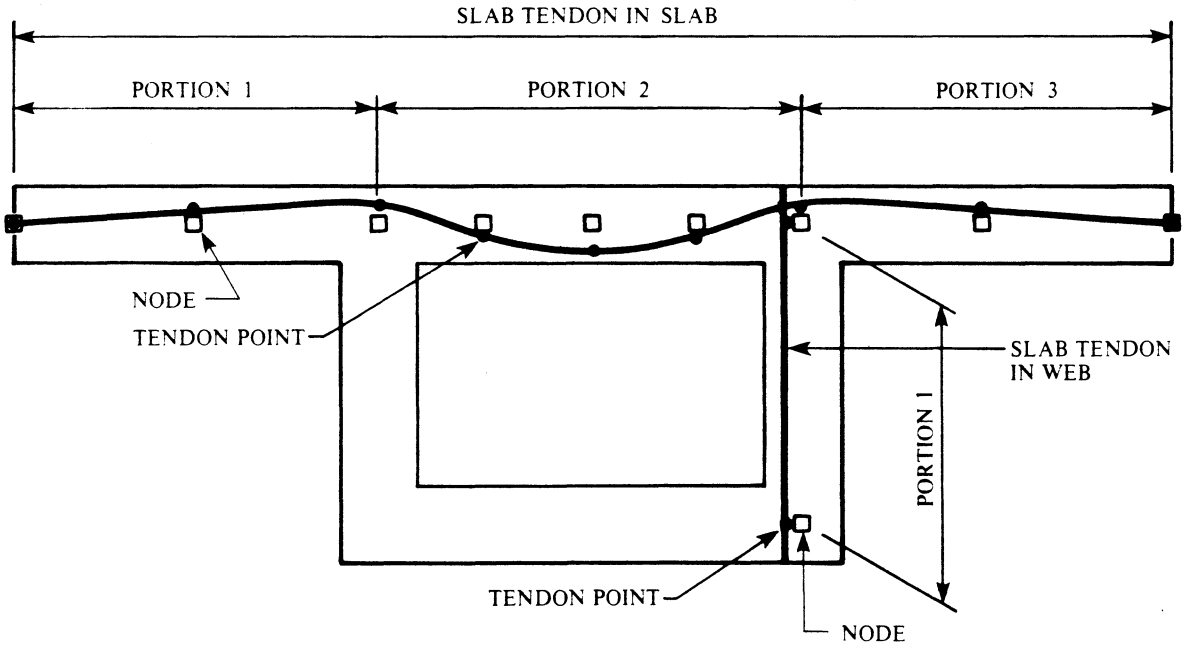

(b) SLAB TENDONS

FIG. 3.4 DEFINITION OF TENDON PROFILES

It is clear from Fig. 3.4a that portion 1 requires a considerably finer subdivision into segments than portion 2 to define the tendon geometry. Care should be taken in discretizing straight tendons in long segments, particularly in curved bridges where radial forces are distributed along the length of the tendon even when the tendon appears straight when viewed from some directions. In such cases short segments should be used.

3.3.1 Direct Tendon Point Input

The conceptually simplest approach for definition of tendon profiles is for the engineer to provide the program with the coordinates of the n tendon points used for the discretization. These coordinates must be carefully calculated, and depending on the program used and the type of tendon under consideration, there may be a number of constraints on the exact locations of the tendon points. These constraints are fully described in Chapters 4, 5, and 6 for each of the three programs.

For panel tendons in a three cell, three span bridge with twenty tendon segments per span, this approach requires the calculation of 244 sets of X,Y,Z tendon point coordinates. If the bridge is curved and has sloping exterior webs, this represents a tremendous computational task much better left to the computer. The parametric profile generation schemes implemented in the programs can perform this task for most typical tendon profiles.

In some cases where non typical tendon geometries are used, it may be necessary to resort to direct tendon point input. With careful selection of tendon portions, and with use of parametric generation in portions where it is possible, the use of direct tendon point input can be minimized.

3.3.2 Parametric Profile Generation

Prestressing tendon profiles in most concrete box girder bridges consist of combinations of parabolas "draped" between the supports of the slab or girder. In special cases, other geometries may be used, which can generally be specified as combinations of several paraboic and/or straight line segments. MUPDI4, CURDI4, and CELL4 have the capability of generating the tendon point coordinates for this type of tendon profile based on a minimum number of tendon geometry parameters.

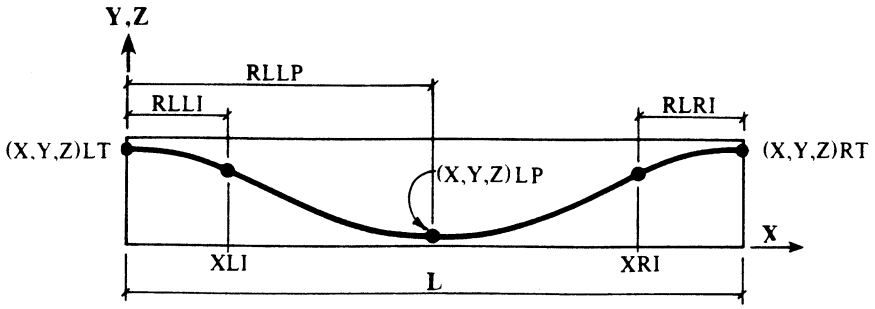

FIG. 3.5 DEFINITION OF TENDON GEOMETRY PARAMETERS.

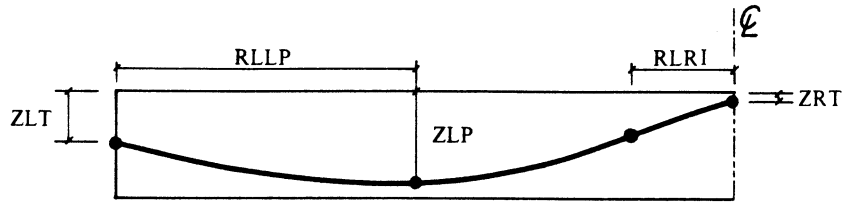

(a) CASE 1: LEFT SPAN OF TWO SPAN BRIDGE (RLLI =0)

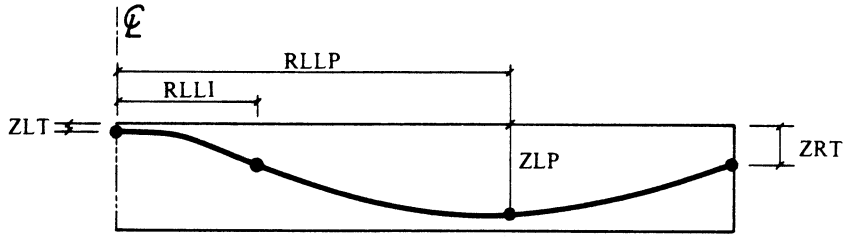

(b) CASE 2: RIGHT SPAN OF TWO SPAN BRIDGE (RLRI =0)

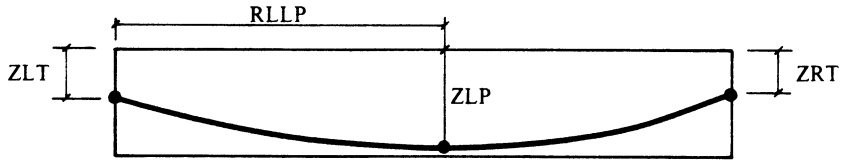

(c) CASE 3: TYPICAL SIMPLE SPAN (RLLI =RLRI =0)

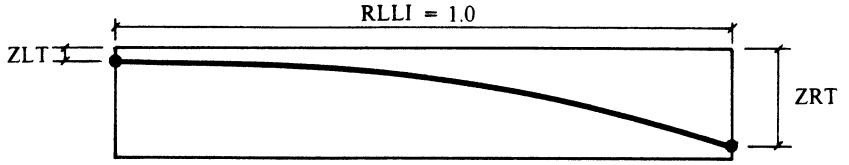

(d) CASE 4: TYPICAL CANTILEVER SPAN (RLLI =RLLP=1.0, RLRI =0)

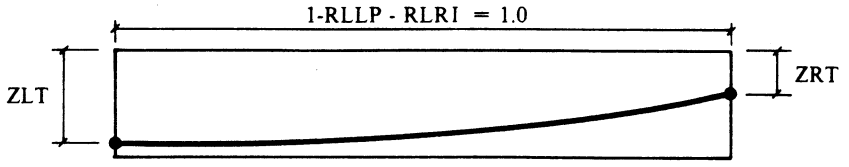

(e) CASE 5: TYPICAL CANTILEVER SPAN (RLLP=RLRI=RLLI=0)

FIG. 3.6 DEFINITION OF SOME TYPICAL TENDON GEOMETRIES

Given the length L of one span of a beam, the tendon profile may be uniquely specified by the following parameters (Fig. 3.5):

$(X,Y,Z)_{lt}$ - Coordinates of left tendon end
$(X,Y,Z)_{lp}$ - Coordinates of point of zero slope (low point)
$(X,Y,Z)_{rt}$ - Coordinates of right tendon end
L - $(X_{rt} - X_{lt})$ = Span Length
RLLI - $(X_{li} - X_{lt}) / L$
RLLP - $(X_{lp} - X_{lt}) / L$
RLRI - $(X_{rt} - X_{ri}) / L$

These parameters provide enough information to generate a profile made up of four parabolic segments with zero slope at locations lt, lp, and rt and tangent intersections at li, lp, and ri. The zero slope at ends lt and rt guarantees tangent intersections with neighboring spans. For curved spans, this profile can be developed onto the actual span geometry. This basic approach to parametric tendon point coordinate generation is implemented in MUPDI4, CURDI4, and CELL4.

Many other tendon profiles can be generated by the algorithms implemented in the three programs. By proper specification of parameters, most of the profile types found in prestressed concrete box girder bridges can be generated (Fig. 3.6). In special cases, it is possible to use more than one portion to represent one physical span of the bridge. This technique allows generation of very complex tendon geometries.

3.4 Short Term Force Losses

Short term losses in tendon force have two major causes: friction between the tendon and the duct during the jacking (stressing) operation, and slippage of the anchorage during transfer of the prestressing force from the jack to the anchorage assembly. Both of these causes result in a variation in force along the length of the tendon. Depending on the system, either one or both of these losses can significantly influence system behavior.

3.4.1 Friction Losses

Due to friction between the tendon and the duct during jacking, the tendon force at the jacking end is greater than the force at some distance away along the tendon (Fig. 3.7a). This friction loss can be considered in

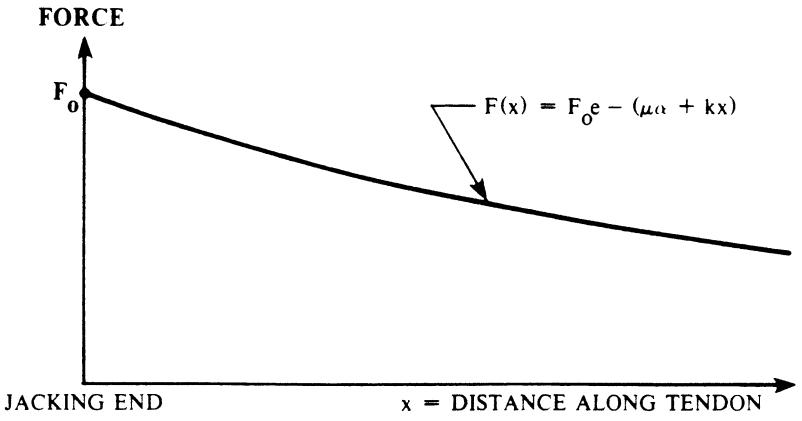

(a) ACTUAL TENDON FORCE PROFILE

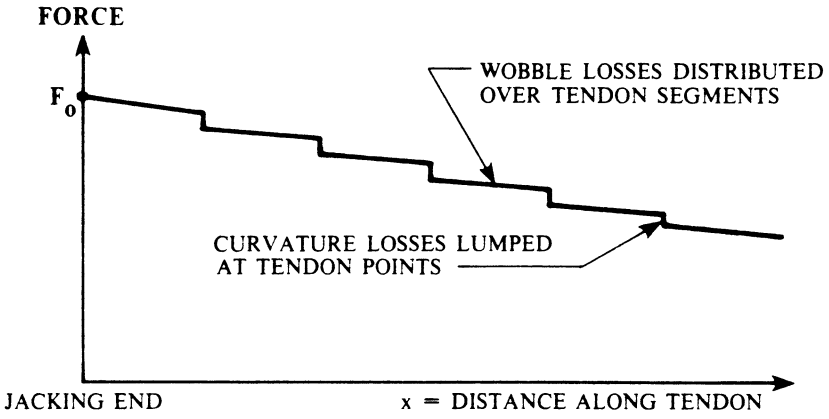

(b) DISCRETIZED TENDON FORCE PROFILE

FIG. 3.7 TENDON FORCE PROFILE UNDER JACKING

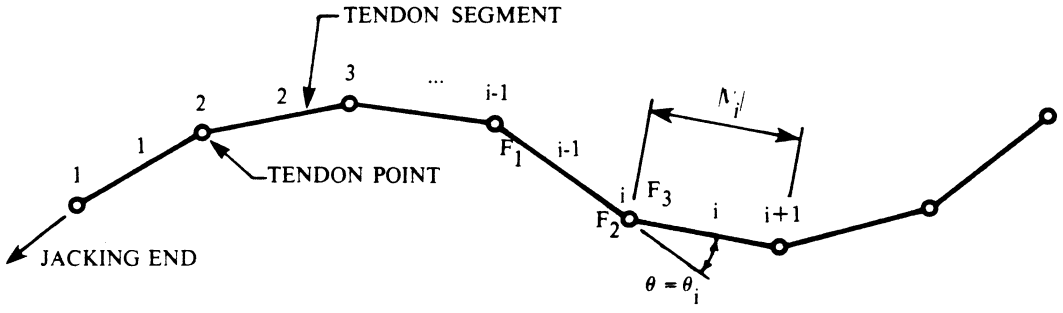

FIG. 3.8 CALCULATION OF FRICTION LOSSES

two parts: the length or wobble effect and the curvature effect. The length effect is the amount of friction loss that would occur in a straight tendon due to duct imperfections and construction practice, and is dependent on the coefficient of friction, the length of the tendon, and the workmanship and alignment of the duct. The curvature effect results from the intended curvature of the tendons, and is dependent on the coefficient of friction and the total angle change between the jacking end and the point under consideration.

The tendon force F_x at a distance x from the jacking end can be described by the following commonly used expression:

$$F_x = F_0 \, e^{-(\mu\alpha + kx)} \tag{3.1}$$

where F_0 = tendon force at jacking end

μ = curvature friction coefficient

α = cumulative angle (in radians) by which the tangent to the tendon profile has changed between the jack and location x

k = wobble friction coefficient

x = distance along tendon from jacking end to point considered

In the tendon discretization used in this study, the angle change is concentrated at the (n-2) interior tendon points, and the length is defined by the lengths of the (n-1) tendon segments. Thus the curvature losses are lumped at the tendon points and the wobble losses are distributed over each tendon segment (Fig. 3.7b). The friction loss expression (Eq. 3.1) must be reformulated in accordance with this approximation. The first step is to derive expressions for the length of each segment and the angle change in space at each tendon point.

Define vectors V_{i-1} and V_i from tendon point i to i-1 and from i to i+1 respectively:

$$\mathbf{V}_{i-1} = \begin{Bmatrix} X_{i-1} - X_i \\ Y_{i-1} - Y_i \\ Z_{i-1} - Z_i \end{Bmatrix} \; ; \; \mathbf{V}_i = \begin{Bmatrix} X_{i+1} - X_i \\ Y_{i+1} - Y_i \\ Z_{i+1} - Z_i \end{Bmatrix} \tag{3.2}$$

The angle Θ_i in space between tendon segments i and i-1 at tendon point i can be found from

$$\cos \theta_i = \frac{\mathbf{v}_{i-1} \quad \mathbf{v}_i}{|\mathbf{v}_{i-1}| \; |\mathbf{v}_i|} \tag{3.3}$$

where the dot denotes the scalar product of two vectors and | | denotes the length of a vector.

The force at each end of each tendon segment can be expressed in terms of these lengths and angle changes (Fig. 3.8). The force at one end of a segment in terms of the force at the other may be expressed as

$$F_2 = F_1 \, e^{-kL} \tag{3.4}$$

while the force at one side of a tendon point in terms of the force at the other may be expressed as

$$F_3 = F_2 \, e^{-\mu\theta} \tag{3.5}$$

where the locations of F_1, F_2, and F_3 relative to the jacking end are shown in Fig. 3.8.

These expressions are evaluated for each tendon segment and each interior tendon point to arrive at the discretized tendon force profile during jacking shown in Fig. 3.7b.

3.4.2 Anchor Slip Losses

Anchor slip losses take place when the jacking force is transferred from the jack to the permanent tendon anchorage assembly. The anchorage assembly typically displaces up to 3/8 inch during this operation, resulting in a change in stress in a length of the tendon near the anchorage (Fig. 3.9).

The change in stress and the length over which it is effective may be derived from fundametal principles: the friction force reverses direction when the slippage takes place, and the anchor slip displacement must equal the integral of the change in strain over the slip distance L_a:

$$d = \int_0^{La} \delta\varepsilon \, dx \tag{3.6}$$

This results in the "mirror image" type tendon force change over the anchor slip distance shown in Fig. 3.9.

A graphical interpretation of the fundamental principles may be taken in order to arrive at the computational approach used in MUPDI4, CURDI4, and CELL4. The area of region A B C (Fig. 3.9) of the tendon force diagram must

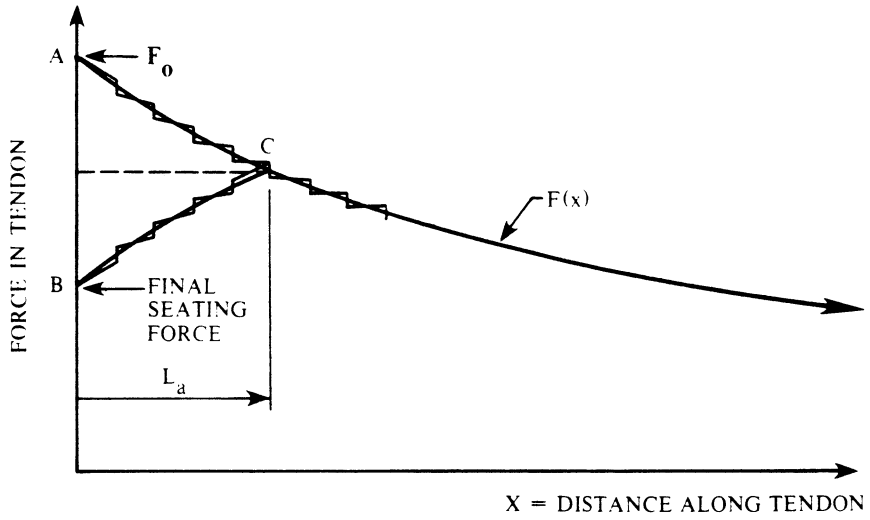

FIG. 3.9 ANCHORAGE SLIP LOSSES

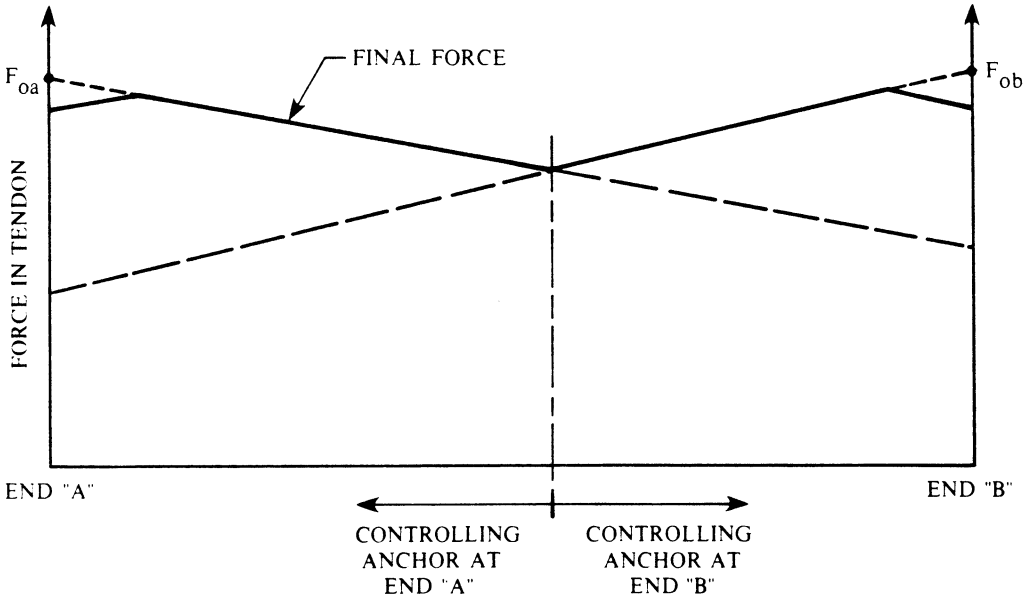

FIG. 3.10 JACKING FROM BOTH ENDS

equal the anchor slip displacement multiplied by (AE) of the tendon:

$$\text{Area (ABC)} = d\,AE \tag{3.7}$$

The tendon segments are scanned starting at the jacking end in order to locate point C which satisfies this equality (Eq. 3.7). After this point is located, all tendon forces between the jacking end and the point are modified to reflect the "mirrored" profile.

3.4.3 Influence of Stressing Procedure

In a real bridge structure different jacking procedures may be used for stressing the tendons: jacking from one of the two ends or jacking from both ends. Provisions have been made for these different procedures, and the friction and anchor slip loss algorithms function in all cases.

The procedure for one-end jacking is the same for jacking from either end of the tendon; the only difference is the order in which the tendon segments and tendon points are considered in the methods discussed in Section 3.4.1 and 3.4.2.

For two-end jacking the controlling anchorage must be determined for each tendon segment (Fig. 3.10). The procedure used is as follows: First, the segment forces are determined under jacking at tendon end 'A'. Next, the same procedure is initiated for jacking from tendon end 'B', but as each segment force is computed it is compared with the force already existing due to jacking from tendon end 'A'. When it is found that the force already existing in the segment (from end 'A' jacking) is higher than the force computed for end 'B' jacking, the end 'B' jacking procedure is terminated. This method closely approximates the physical situation in the actual tendon.

3.5 Final Tendon Forces

After the force is computed at each end of each tendon segment, an average force is computed in each tendon segment which is then used for computing equivalent loads. One of two methods must be specified for computing this average force. Method A is applicable to tendons with smooth profiles, while method B is applicable to harped tendons with concentrated angle changes. The differences in computed forces from the two methods are

generally small and have the greatest influence near the anchorages.

Consider a tendon with a smooth arbitrarily curved profile (Fig. 3.11). The actual tendon force profile is a smooth curve (Fig. 3.11b). The computed tendon force profile (Fig. 3.11c) has curvature friction losses lumped at the tendon points and wobble friction losses distributed over the segments. The best estimate of the actual tendon force profile from this computed force profile is found by connecting the plotted average forces at the tendon points with straight lines (Fig. 3.11c). The constant force in each tendon segment can then be found by averaging the segment end force values from this smoothed profile (Fig. 3.11d). This approach is used in averaging method A and is recommended for smooth curved tendon profiles.

Consider a harped tendon with concentrated angle changes in its profile (Fig. 3.12). The actual tendon force profile is the same as the computed force profile: piece-wise linear with steps at the harp points (Fig. 3.12b). The constant force in each tendon segment can be found by averaging the segment end force values from this unsmoothed force profile (Fig. 3.12c). This approach is used in averaging method B and is recommended for harped tendon profiles.

3.6 Equivalent Loads

Once the forces in all the tendon segments are known, the equivalent forces acting on the structure at each tendon point may be found. Consider tendon point i where tendon segments i-1 and i are connected (Fig. 3.13). The vectors from point i to i-1 and from i to i+1 are $\mathbf{V}_{i-1}$ and $\mathbf{V}_i$, respectively:

$$\mathbf{V}_{i-1} = \begin{Bmatrix} X_{i-1} - X_i \\ Y_{i-1} - Y_i \\ Z_{i-1} - Z_i \end{Bmatrix} ; \mathbf{V}_i = \begin{Bmatrix} X_{i+1} - X_i \\ Y_{i+1} - Y_i \\ Z_{i+1} - Z_i \end{Bmatrix} \qquad (3.7)$$

with direction cosines

$$C_{i-1} = \frac{\mathbf{V}_{i-1}}{|\mathbf{V}_{i-1}|} \quad ; \quad C_i = \frac{\mathbf{V}_i}{|\mathbf{V}_i|} \qquad (3.8)$$

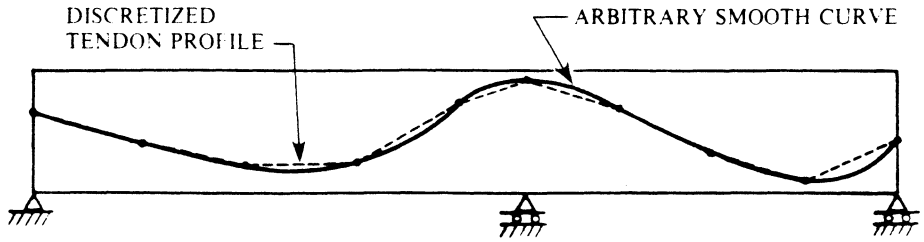

(a) STRUCTURE AND TENDON GEOMETRY

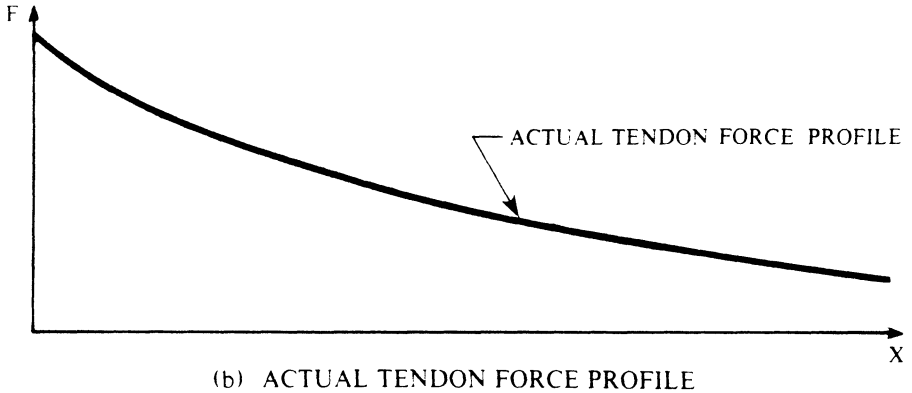

(b) ACTUAL TENDON FORCE PROFILE

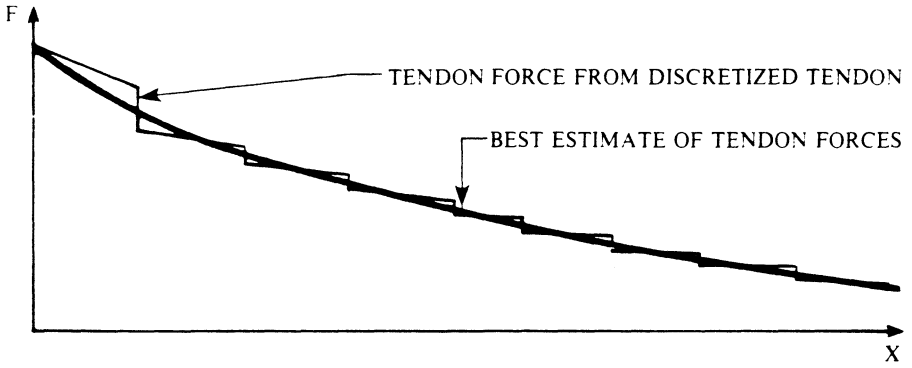

(c) BEST ESTIMATE OF TENDON FORCE PROFILE

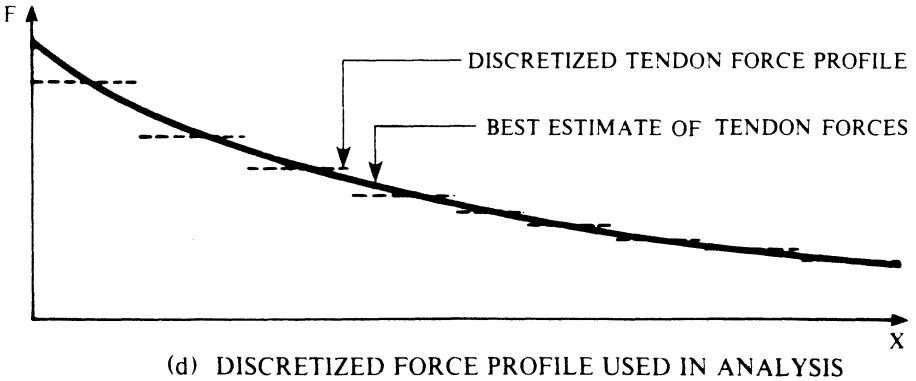

(d) DISCRETIZED FORCE PROFILE USED IN ANALYSIS

FIG. 3.11 SEGMENT FORCES IN A SMOOTHLY CURVED TENDON

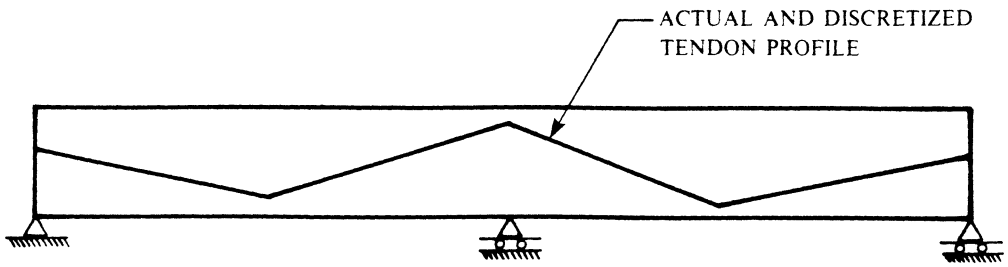

(a) STRUCTURE AND TENDON GEOMETRY

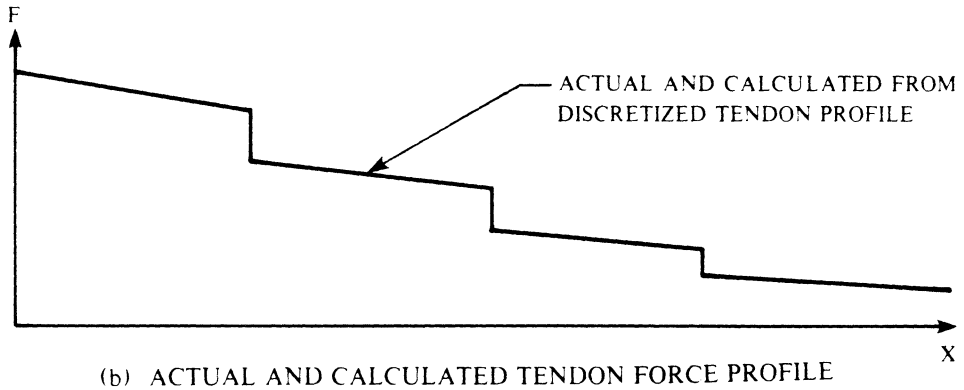

(b) ACTUAL AND CALCULATED TENDON FORCE PROFILE

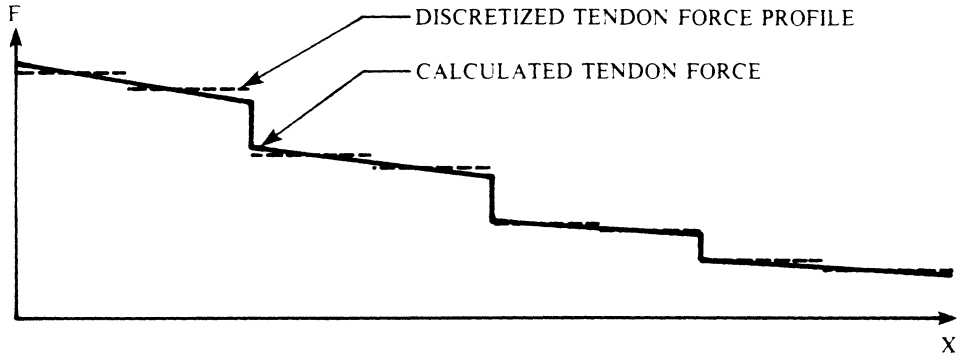

(c) DISCRETIZED FORCE PROFILE USED IN ANALYSIS

FIG. 3.12 SEGMENT FORCES IN A HARPED TENDON

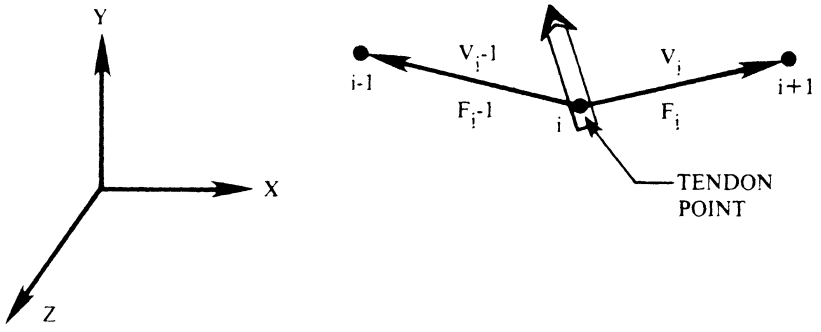

FIG. 3.13 EQUIVALENT LOADS AT TENDON POINTS

The tendon force vectors F'_{i-1} and F'_i can now be found:

$$F'_{i-1} = F_{t,i-1}\, C_{i-1} \tag{3.8a}$$

$$F'_i = F_{t,i}\, C_i \tag{3.9b}$$

The resulting equivalent load vector P_i at tendon point i, in terms of its three components, can now be found by simple vector addition:

$$P_i = F'_{i-1} + F'_i \tag{3.10}$$

Omitting the subscripts, the load vector P of Eq. 3.10 is referred to the fixed cartesian coordinate system XYZ, with components

$$P = \begin{Bmatrix} P_X \\ P_Y \\ P_Z \end{Bmatrix} \tag{3.11}$$

4. MUPDI4 - STRAIGHT BOX GIRDER BRIDGES

4.1 General Remarks

MUPDI4 is a computer program capable of analyzing straight prismatic folded plate bridge structures made up of isotropic plate elements. The continuous span structure must be simply supported at the two ends, but may have several interior diaphragms or supports between the two ends (Fig. 4.1). Any arbitrary bridge cross section may be considered by suitable discretization as flat plate elements (Fig. 4.2). Diaphragms may be defined by transverse flexible beams, and supports may be defined by transverse two dimensional planar rigid frame bents. A direct stiffness harmonic analysis is used for the folded plate system. Compatibility at the interior diaphragms and supporting bents is accomplished by a force method of analysis taking account of the flexibility of the folded plate, diaphragm, and supporting bent systems.

This chapter is intended as a description of MUPDI4 and guide to its use. There are additonal sections covering details of the application of prestressing loads, and the organization of the program. For a description of the theories and numerical approach used, refer to Chapter 2 of this report or References [1,2,5,6,7]. For the details of the prestressing analysis refer to Chapter 3 of this report.

4.2 Structural Modelling

The structural system is modelled as a combination of a folded plate structure and optional movable diaphragm or supported bent substructures. The first step in modelling the structure is to identify and number these three component types. The folded plate system must be straight, prismatic and simply supported at the two ends, but any arbitrary bridge cross section can be modelled (Fig. 4.2). The diaphragm or bent substructures may be located at any transverse vertical plane between the ends of the folded plate system. Supported rigid diaphragms are always assumed at the two ends.

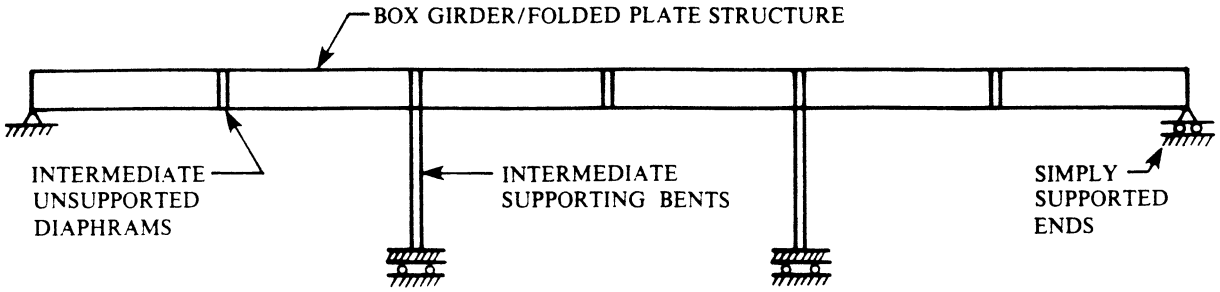

FIG. 4.1 STRAIGHT BRIDGE WITH INTERMEDIATE DIAPHRAGMS AND BENTS

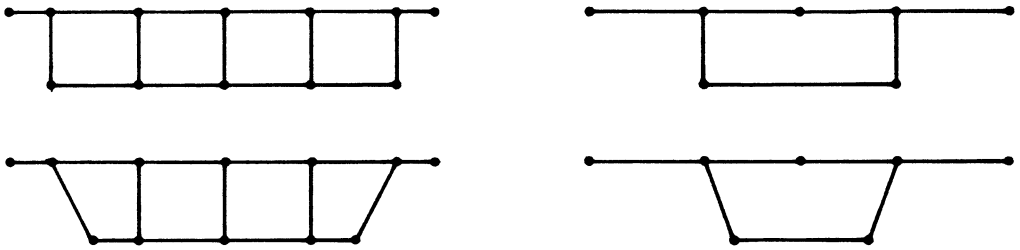

(a) MINIMUM NUMBER OF ELEMENTS

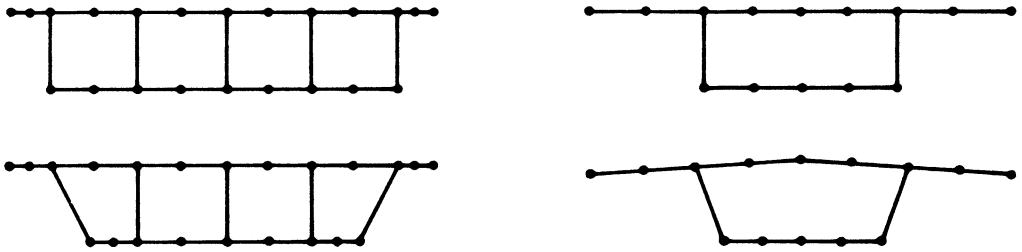

(b) ADDITIONAL ELEMENTS IN SLABS

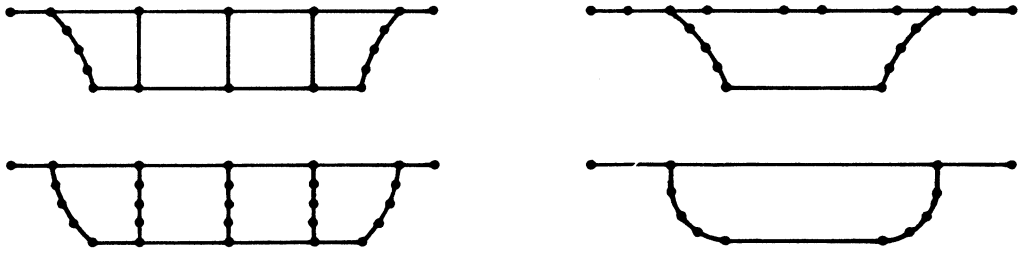

(c) ADDITIONAL ELEMENTS IN WEBS

FIG. 4.2 BOX GIRDER BRIDGE CROSS-SECTION

4.2.1 Folded Plate System

The folded plate system is modelled as an assembly of longitudinal plate elements possessing both membrane and plate bending stiffnesses. The elements extend over the full length of the structure and are interconnected at joints along their longitudinal edges. Elasticity theory is used for the isotropic plate elements. Uniform or partial surface loads, line loads, concentrated loads and prestressing may be applied anywhere on the structure.

Modelling a box girder as a folded plate system consists of identifying the cross section to be used and modelling it with constant thickness plate elements. Joint coordinates, isotropic elastic material properties, and element locations must be input to MUPDI4.

Structure geometry and loads are expressed in a right handed cartesian global coordinate system (Fig. 4.3). The longitudinal axis of the structure lies parallel to the X- axis. The total overall length of the structure is defined by its length along the X axis. The cross section has a constant description in the Y-Z plane along the length of the structure. The cross section can be oriented arbitrarily in the Y-Z plane, however for dead load application and stress integration the Z- axis is defined as vertical and the Y- axis as horizontal.

Joint coordinates and element locations define the subdivision of the cross section into folded plate elements. For a cross section with vertical or inclined webs (Fig. 4.2a), joints are required only at the intersections of the webs with the top and bottom slabs. When transverse prestressing is included, when the slabs are haunched, or when detailed analysis is required for concentrated loads between the webs, intermediate joints may be required between the webs (Fig. 4.2b). For a cross section with curved webs, or when detailed analysis is required for prestressing or concentrated loads in the webs, intermediate joints may be required in the webs (Fig. 4.2c). MUPDI4 will generate joints with uniform spacing along a straight line. Joint numbering should be selected so as to minimize the maximum absolute difference between joint numbers for any plate element. Plate elements may be numbered in any order, but numbering elements with identical geometry and

materials in groups will minimize numerical effort requirements.

Loads may be applied on the joints or the plate elements, and can be defined to act over either the full length or any partial length of the structure. Dead loads are automatically included as plate loads based on the specified weight densities (weight per unit volume of material) and thicknesses of the plates. Dead loads are generated positive downwards for input positive weight density and global Z- axis positive downward. Dead load can be added to any load case with the use of load case multipliers.

Joint loads include forces in the global X-, Y-, and Z- directions and moments about the global X- axis (Fig. 4.3). They are input as a total load centered at a specified X- coordinate along the joint, and uniformly distributed over a specified length of the joint. If the distribution length is specified as zero, the load is taken as concentrated. The total X- (longitudinal) force on the structure must add up to zero, due to the boundary conditions assumed in the plate formulation.

Surface loads on the plate elements include forces in the global Y- and Z- directions. They are input as load intensities over the projected area (or width) of the plate, centered at a specified X- coordinate along the plate, and extending over a specified length of the plate. If the length is specified as zero, the load is taken as a line load. Plate element forces are applied to the system as released fixed edge X- Y- and Z- direction forces and moments about the X- axis, computed using elasticity theory. Final results for displacements and stresses in the plate elements are the superposition of this fixed edge solution with the displacement solution. This formulation is capable of capturing the true nonlinear variations of internal stresses within the plate elements under load. However, concentrated loads, line loads, and surface loads over a partial width of a plate element are not allowed in MUPDI4. Therefore, whenever possible, joints should be put at the points of application of point loads and line loads. See also sections 4.3.1 and 4.7 for additional discussions.

All loads are expanded into Fourier series components for the harmonic series solution. The convergence rate of the series solution is influenced

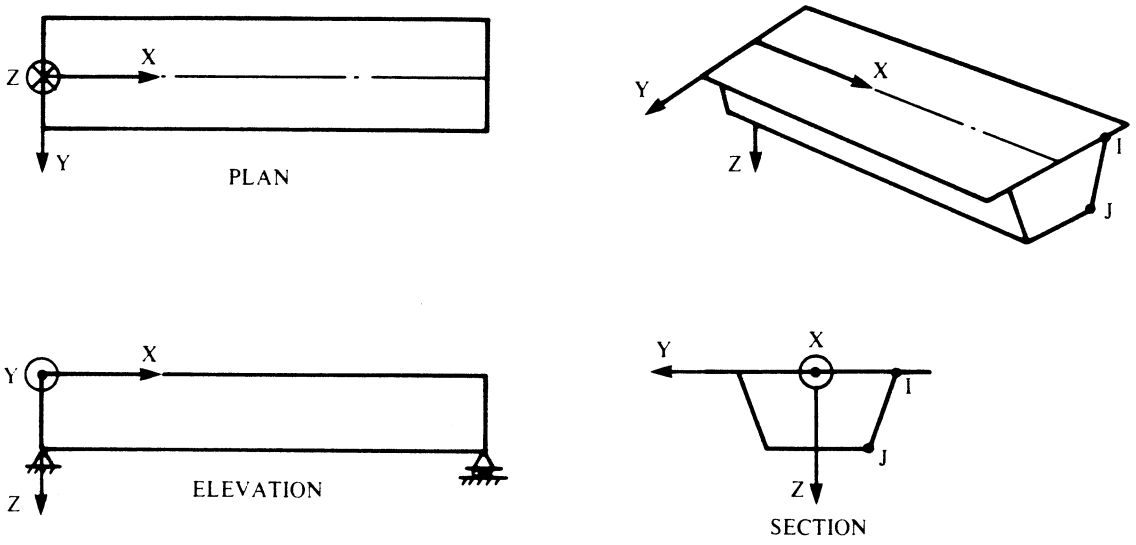

(a) ORIGIN AT LEFT SIMPLE SUPPORT

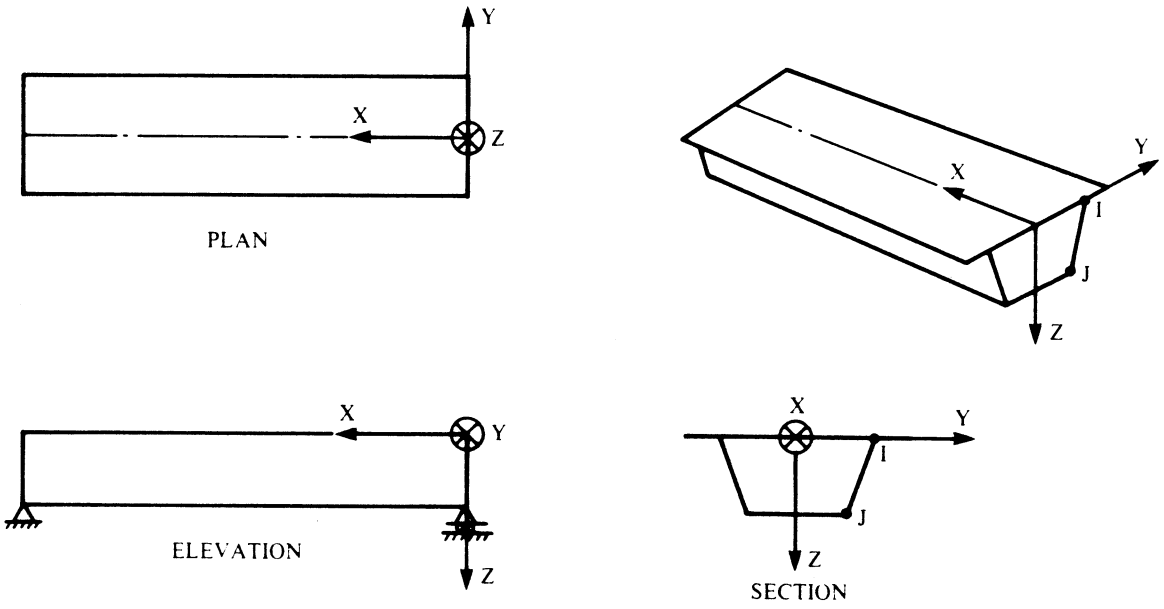

(b) ORIGIN AT RIGHT SIMPLE SUPPORT

FIG. 4.3 GLOBAL COORDINATE SYSTEM FOR PROGRAM MUPDI4

by the length of the load relative to the total structure length. Meyer [9] showed that for concentrated loads the stress resultants converge very slowly (Fig. 4.5), requiring a very large number of Fourier terms. By replacing the concentrated loads with patch loads distributed over a short length $_p$ with intensity p_0, so that $P = p_0 \delta_p$, the results converge faster (Fig. 4.6), requiring fewer Fourier terms. Thus most concentrated or line loads should be modelled as patch loads whenever possible.

Output consists of joint displacements, the plate element internal displacements, stresses or stress resultants, and the integrated section forces and moments. X- Y- and Z- direction joint displacements and joint rotations about the X- axis are output for all joints at specified locations along the X- axis (Fig. 4.3). Plate element internal results can be output selectively at specified locations along the X- axis and at equally spaced intervals across the width of each element (Fig. 4.4). Plate element internal displacements are output in the directions of the local u, v, and w element axes. Plate element internal stresses S_x, S_y and S_{xy}, and stress resultants N_x, N_y, N_{xy}, Q_x, Q_y, M_x, M_y and M_{xy} are output according to the sign convention shown in Fig. 4.4. Plate element internal stresses are numerically integrated at selected cross sections to arrive at individual girder and total section axial (X-) force, shear (Z-) force, and (Y-) moment. Integrated forces and moments are defined as positive when they are in the directions of the global axes on the positive cut face of the cross section. Total axial force is summed from N_x stresses; total shear force is summed from N_{xy} and Q_x stresses; total bending moment is summed from N_x stresses and M_x moments. The trapezoidal rule is employed for the integration, using the internal stresses obtained at the specified uniform interval across the plate. The accuracy of the integration is dependent on the interval chosen, particularly at locations with highly nonlinear stress distributions. Thus a large number of output locations across the width of the plate is required where precise integration is desired.

4.2.2 Supporting Frames and Bents

Intermediate supports of the folded plate system may be specified either

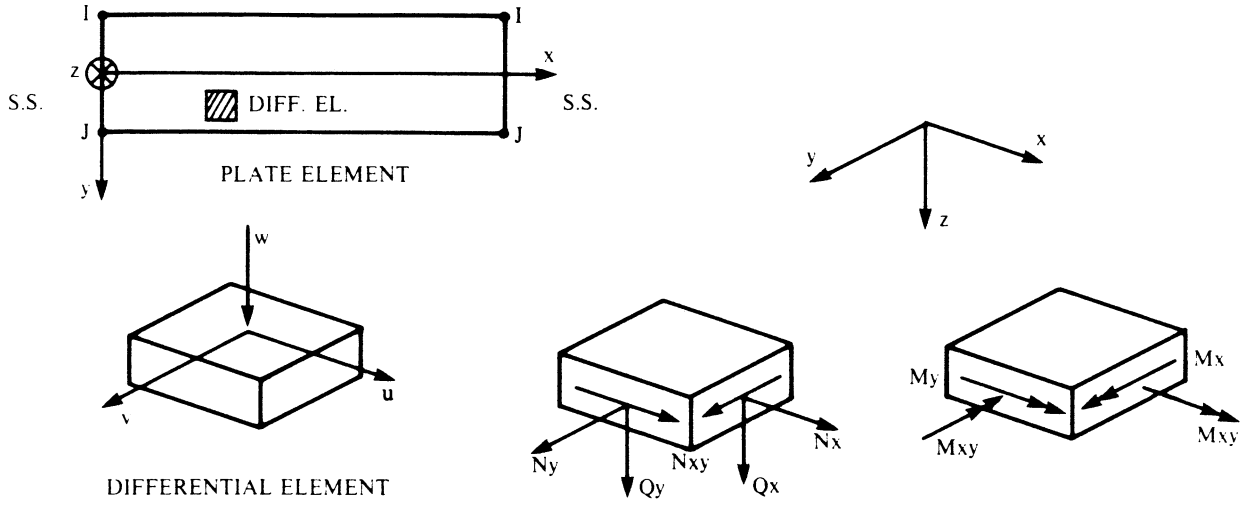

(a) ORIGIN AT LEFT SIMPLE SUPPORT

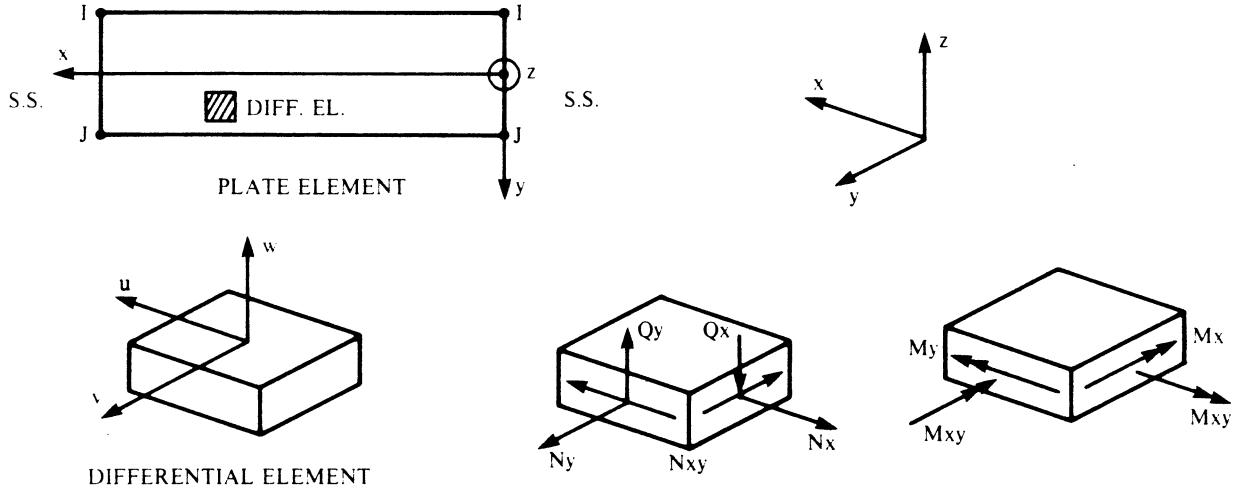

(b) ORIGIN AT RIGHT SIMPLE SUPPORT

FIG. 4.4 POSITIVE ELEMENT LOCAL AXES AND ELEMENT RESULTS FOR MUPDI4

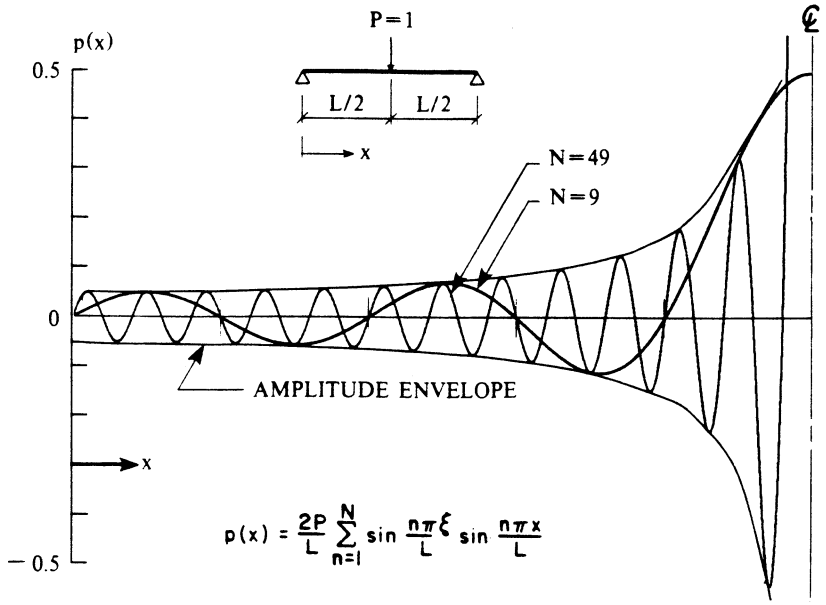

(a) VERTICAL LOAD AT MIDSPAN

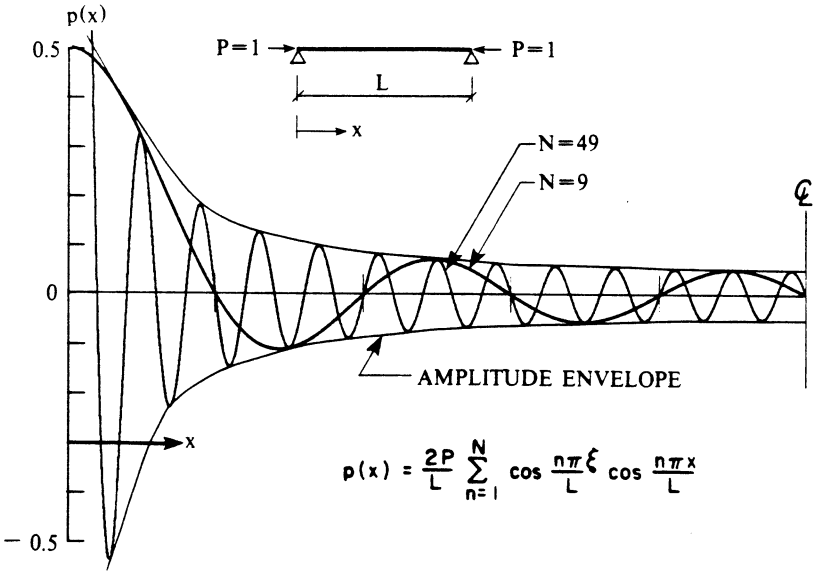

(b) LONGITUDINAL LOAD AT BOTH ENDS

FIG. 4.5 FOURIER REPRESENTATION OF CONCENTRATED LOADS

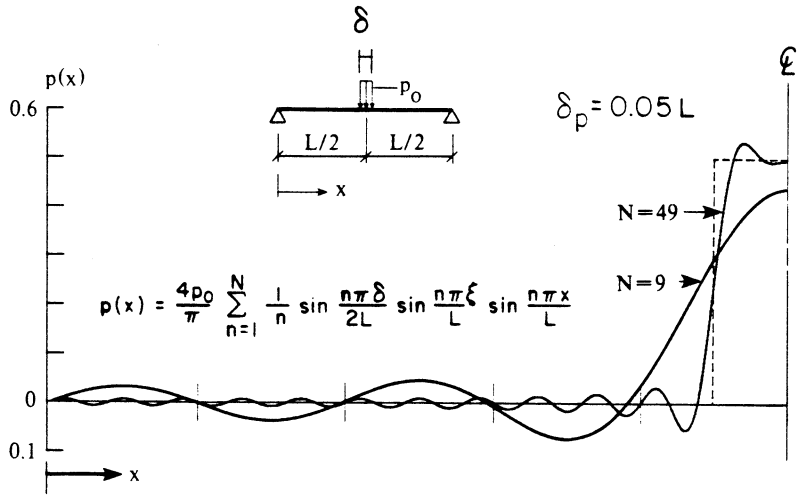

(a) VERTICAL LOAD AT MIDSPAN

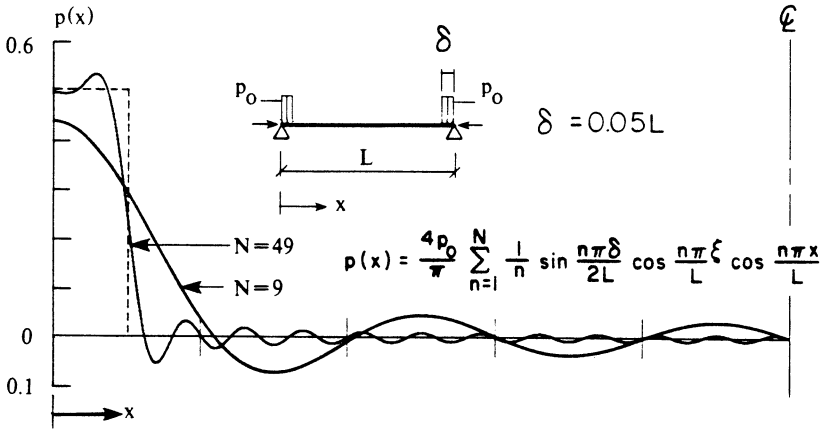

(b) LONGITUDINAL LOAD AT BOTH ENDS

FIG. 4.6 FOURIER REPRESENTATION OF PATCH LOADS

as rigid supports or as flexible bents. They must lie parallel to the global Y-Z plane. Displacement compatibility between the supports and the folded plate system is enforced for Y- and Z- displacements and X- rotations only, and is not enforced for X- displacements. Thus transverse interaction of the intermediate supports is considered, but longitudinal interaction is not considered.

No loads other than the internally computed interaction forces with the folded plate system are allowed on the supporting structures. Interaction forces are always printed in the output, but output of support internal displacements and stress resultants is possible only for flexible bents.

Rigid supports are entirely defined by their centerline X- coordinate and interaction thickness. Flexible bents are additionally defined as a plane frame system. Identical plane frames are assigned a type number, and frame description input is required only once for each frame type.

Each plane frame is located in its own X-Y coordinate system, which must lie parallel to the global Y-Z coordinate system (Fig. 4.7). Node coordinates and boundary conditions are input, as are elastic support stiffnesses, frame element material properties and element locations. The frame elements include bending, axial and shear deformations.

Output for the frames, when specified, includes interaction forces, node displacements, boundary spring forces and moments, and stress resultants at the ends of the elements.

4.2.3 Unsupported Diaphragms

Intermediate unsupported diaphragms may be specified either as rigid or as flexible. They must lie parallel to the global Y-Z plane. Displacement compatibility between the diaphragms and the folded plate system is enforced for Y- and Z- displacements and X- rotations only, and is not enforced for X- displacements. Thus transverse interaction of the intermediate diaphragms is considered, but longitudinal interaction is not considered.

No loads other than the internally computed interaction forces with the folded plate system are allowed on the diaphragms. Interaction forces are always printed in the output; no other output is available.

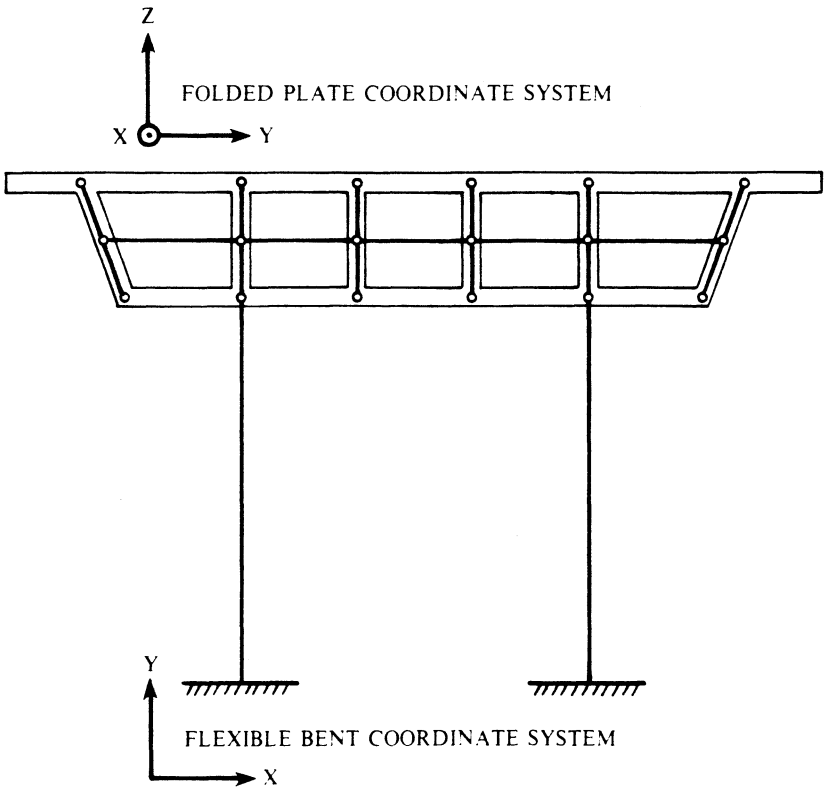

(a) NODE GEOMETRY AND DISPLACEMENTS

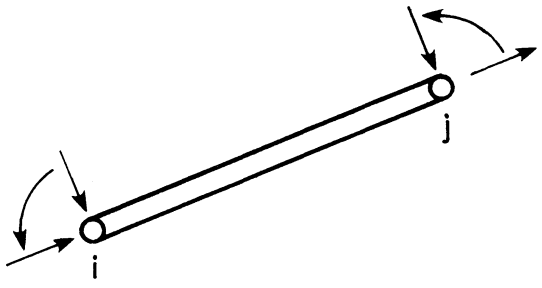

(b) BEAM ELEMENT END FORCES

FIG. 4.7 SUPPORTING BENT COORDINATE SYSTEM

Rigid diaphragms are entirely defined by their centerline X- coordinate and interaction thickness. Flexible diaphragms are additionally defined as a flexible straight beam parallel to the global Y- axis. Identical flexible diaphragms are assigned a type number, and diaphragm description input is required only once for each diaphragm type.

Each flexible diaphragm type is described by its Z- coordinate, material and section properties. Section properties can be computed interally based on input dimensions of the flexible diaphragm. The beam elements include bending, axial and shear deformations.

4.3 Equivalent Loads from Prestressing

Post tensioned prestressing tendons are classified as panel tendons or slab tendons. Panel tendons may lie in any element of the cross section and extend over the length of the folded plate system. Slab tendons may lie in any element of the cross section and must be parallel to the global Y-Z plane. For a description of the prestressing analysis and the modelling of the tendons, refer to Chapter 3 of this report. This section deals only with the final application of the equivalent prestressing loads to the folded plate structure.

4.3.1 Panel Tendons

For panel tendons, tendon points are uniformly spaced in each portion and tendon point loads consist of X- Y- and Z- direction concentrated forces acting on some plate element. These tendon point loads R are converted to statically equivalent joint forces R' acting on the two joints defining the plate element (Fig. 4.8a), according to the following relationship:

$$\text{Joint i:} \quad R'_i = R\, a/L \tag{4.1}$$

$$\text{Joint j:} \quad R'_j = R - R_i \tag{4.2}$$

where L is the width of the folded plate element and a is the distance from joint j to the tendon point. It is important to realize that this procedure ignores any local stresses between the joints due to the load. Thus, if it is desired to more accurately model local variations of internal stresses due to prestress loads applied between the joints, more plate elements should be used in the affected regions.

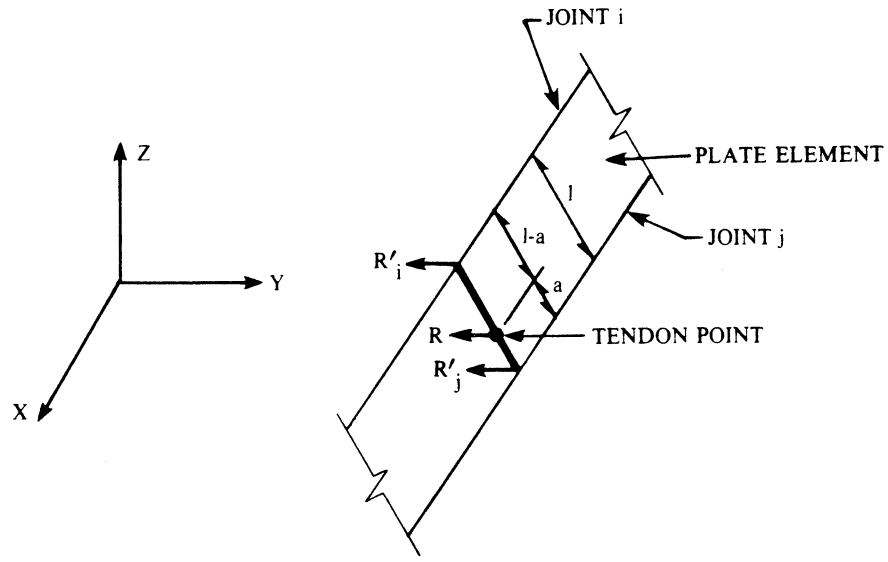

(a) PANEL TENDONS

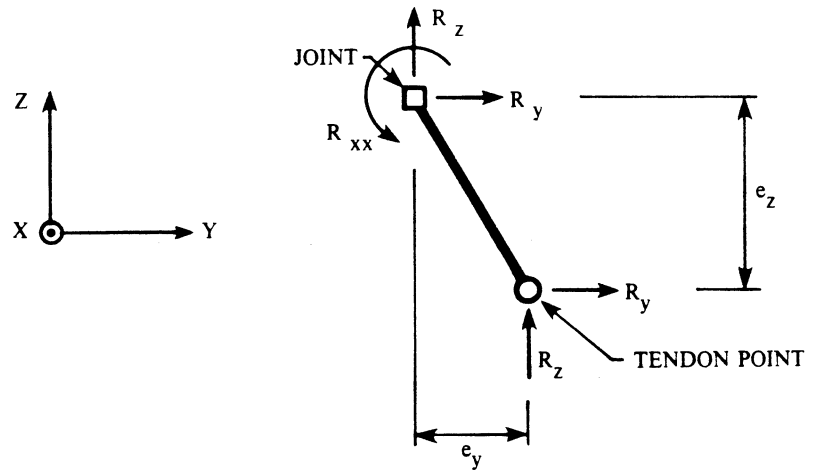

(b) SLAB TENDONS

FIG. 4.8 STATICALLY EQUIVALENT JOINT LOADS

Statically equivalent joint loads are applied to the joints as patch loads. The length of the patch load defaults to the tendon point spacing, but may be input as any value. Use of patch loads instead of concentrated loads speeds convergence of the solution and more closely approximates the actual load due to the prestressing tendon. A realistic solution of the local stresses behind the anchorages is not expected in any case, since in reality the structure is subjected to anchorage forces as the longitudinal normal stresses acting on the end anchorage plate, while in the harmonic analysis the anchorage forces can be introduced only as longitudinal shear forces acting on the longitudinal joints near the end anchorage.

4.3.2 Slab Tendons

For slab tendons, tendon points apply to a group of tendons with identical descriptions and spacing, and tendon point loads consist of Y- and Z- direction distributed forces acting near some joint. These tendon point loads R are converted to statically equivalent joint forces and moments R' acting on that joint (Fig. 4.8b), according to the following relationships:

$$R'_Y = R_Y \tag{4.3a}$$

$$R'_Z = R_Z \tag{4.3b}$$

$$R'_{XX} = R_Y\, e_z + R_Z\, e_y \tag{4.3c}$$

where e_y and e_z are the eccentricities of the tendon point from the joint in the Y- and Z- directions respectively. This approach may result in inaccurate modelling of transverse moments (M_y in Fig. 4.4) between joints for some tendon geometries. Thus, if it is desired to more accurately model local variations of internal stresses due to slab prestressing, more plate elements should be used in the affected regions.

These statically equivalent joint loads are applied to the joints as uniformly distributed loads over the extent of the length of the slab tendon group. If the length of the tendon group is specified as zero, the joint loads are applied as concentrated loads.

Since the convergence of the Fourier series is considerably slower for concentrated loads than for distributed loads, it may be necessary to use more harmonics if the length of the tendon group is specified as zero. Refer to

section 4.3.1 for more discussion of concentrated loads versus patch loads.

4.4 Features of MUPDI4

MUPDI4 has many unique features making it a desirable program for the analysis of straight prismatic prestressed box girder bridges. These features relate to the accuracy of the analysis, the simplicity of input preparation and the completeness of the output.

The analysis is in complete accordance with the theory of elasticity, so that important effects such as shear lag, warping, and transverse distortion are all automatically considered. Subdivision of simple cross sections into many elements is not required for convergence of the solution. Improving the precision of the final results requires increasing the number of harmonic terms only.

The prestressing analysis has all the features and capabilities described in Chapter 3. The solution technique accounts for the effects of prestressing and the distribution of its loads within the structure.

The computer program input is very simple: Discretize the girder cross section as folded plate elements, locate and describe the diaphragms and bents, generate the prestressing tendons, define locations for output of results, and describe all the loads.

Loads can be specified anywhere on the structure in any number of load cases. Load cases may be combined from factored dead load, prestressing, and external loads.

The output capabilities are very flexible. Joint displacements may be ouput at any location along the length of a joint. Plate element internal displacements, stress resultants, and stresses may be selectively printed at any location in the structure. Individual girder and total section axial forces, shears and moments may be printed for any cross sections. Displacements and stress resultants for the flexible supporting bents may also be printed.

4.5 Computer Program Organization

MUPDI4 is an updated and extended version of MUPDI3 [2,5,6]. The program has been restructured and in some cases rewritten to utilize new

numerical techniques and to implement all the new features. The program is written around a named in-core array data base [17] which dynamically allocates and manages all numerical array storage. The program was tested on the IBM 3081 Computer at the University of California, Berkeley using the IBM FORTRAN H compiler, and is written for easy transfer to other machines.

Program organization and flow may be described as follows:

1. Initialize database, input title and problem control data.
2. Input, generate and check folded plate system data, including joint coordinates, boundary conditions, plate element material properties and locations, output control specifications, joint and surface loads, and diaphragm/bent locations.
3. Generate and check slab tendon geometries, compute tendon forces, and find equivalent joint loads for slab tendons.
4. Generate and check panel tendon geometries, compute tendon forces, and find equivalent joint loads for panel tendons.
5. Input, generate and check flexible bent data, including node coordinates, boundary conditions, and beam element material properties and locations. Form flexible bent flexibility matrices and internal results recovery arrays.
6. Input, generate and check flexible diaphragm data. Form flexible diaphragm flexibility matrices.
7. Perform harmonic series solution of folded plate system for external load cases and unit generalized interaction forces. Save harmonic components of joint displacements on disk.
8. Sum folded plate system flexibility and initial displacement matrices from harmonic components. Transform these matrices for possible rigid body modes of movable diaphragms.
9. Sum total system flexibility matrix from folded plate system, flexible bent and flexible diaphragm components.
10. Solve flexibility system for generalized interaction forces. Transform these forces for movable diaphragms to actual interaction forces.

11. For each load case, sum final plate system joint displacements, internal element results and integrated section resultants from harmonic components due to external loads and interaction forces.
12. For each load case, find flexible bent joint displacements, boundary spring forces and frame element internal forces based on computed interaction forces.

4.6 Computer Program Input and Output

Data describing the bridge structure to be solved is provided in either a deck of cards or an an input file of card images, depending on the computer system used. The required detailed format for the input file is specified in the input manual (Appendix B). The basic organization of the input file is summarized below in terms of its major components.

1. Title: One line of problem description text to be printed with the output.
2. Structure Control Data: One line defining the number of joints, material types, plate elements, number of bents, etc.
3. Load and Prestressing Control Data: One line defining the number of load cases, joint loads, surface loads, panel and slab tendons.
4. Analysis Control Data: One line defining the number of harmonics, number of output cross sections, data check or execution mode, etc.
5. Joint Coordinates and Boundary Conditions: Describes the folded plate system cross section.
6. Plate Element Data: Defines material properties and locations of the plate elements in the cross section.
7. Diaphragm/Bent Interaction Data: Defines locations of diaphragms and bents along the length of the bridge.
8. Output Specifications: Defines options and locations for output of displacements, stresses, and girder moments.
9. Load Case Multipliers for Dead Load: Multipliers for the plate element dead load to be used for each load case.
10. Joint and Surface Loads: Defines external joint and plate element

surface loads.

11. Slab Prestressing Tendons: Defines transverse slab tendons in groups of tendons with uniform geometry and stressing.
12. Panel Prestressing Tendons: Defines longitudinal panel tendons one at a time.
13. Flexible Supporting Frame Bents: Defines the plane frame structures making up the flexible supporting bents.
14. Flexible Movable Diaphragms: Defines the beam structures making up the flexible movable diaphragms.

Computer program output consists first of a complete check printout of all the input and generated data describing the structure, the prestressing and loads. Then, depending on the features of the structure and the output specification requests, the following final results are printed for each load case:

1. The interaction (restraint) forces between each diaphragm or bent and the folded plate system.
2. Resulting four displacement components of each joint at each X-coordinate specified.
3. Optionally, internal element displacements, forces and stresses. Each component may be supressed or printed as required.
4. Optionally, individual girder and total section axial forces, shears and bending moments and percentages at each specified cross section.
5. Optionally, node displacements and member end forces for the flexible supporting bents.

4.7 Special Considerations for the use of MUPDI4

MUPDI4 provides a rapid solution for prismatic folded plate structures simply supported at the two ends and with optional interior diaphragms or supports. The diaphragms and supports may be either rigid or flexible but must be at right angles to the bridge axis. Diaphragms may be defined by flexible beams, while supports may be defined by two dimensional planar frame

bents. Surface loads, line loads, concentrated loads, and prestressing may be applied anywhere on the folded plate structure.

The maximum number of plates, joints, diaphragms, bents, and prestressing tendons is limited only by available high and low speed storage on the computer system used. In practical terms, there is no limit on the size or complexity of structure which can be analyzed with MUPDI4.

If the structure is symmetrical in the longitudinal direction about a transverse midspan plane, a great saving in computing effort may be achieved by taking advantage of the symmetry or anti-symmetry of the loading with respect to this transverse plane, if it exists. For the case of a symmetrical structure subjected to symmetrical loading (Fig. 4.9a), only the odd terms of the Fourier series have to be included. For anti-symmetrical loading (Fig. 4.9b), only the even terms have to be included. This can be accomplished by giving the appropriate instructions in the analysis control data.

Loadings to be considered when choosing whether or not to take advantage of symmetry include the external loads as well as the redundant forces from each diaphragm or bent applied individually. Thus, advantage of symmetrical loading can only be taken in simply supported structures and structures with only one center bent or diaphragm (Fig. 4.9a). No advantage of symmetrical loading may be taken for structures with more than one intermediate diaphragm or bent. In these cases all terms of the Fourier series must be used. Advantage of anti-symmetrical loading may be taken only in cases of simple spans with no intermediate diaphragms or bents (Fig. 4.9b).

If the cross section of the structure is symmetrical about a longitudinal plane, advantage of symmetry or anti-symmetry of the loading with respect to this plane may be taken by analyzing only half of the cross section and imposing appropriate boundary conditions at the longitudinal plane of symmetry (Fig. 4.10).

Since the actual force distribution on the structure is modelled as a truncated Fourier series, a suitable number of harmonics must be used to adequately approximate the applied loads and the interaction forces. The number of terms required depends on the number of intermediate diaphragms and

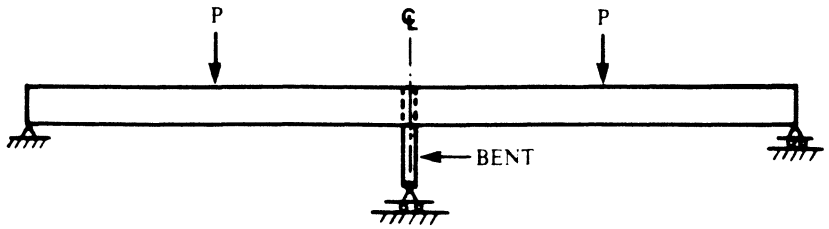

(a) SYMMETRICAL LOADING

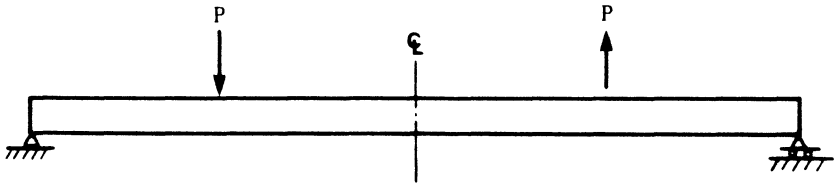

(b) ANTISYMMETRICAL LOADING

FIG. 4.9 LONGITUDINAL SYMMETRY AND ANTISYMMETRY

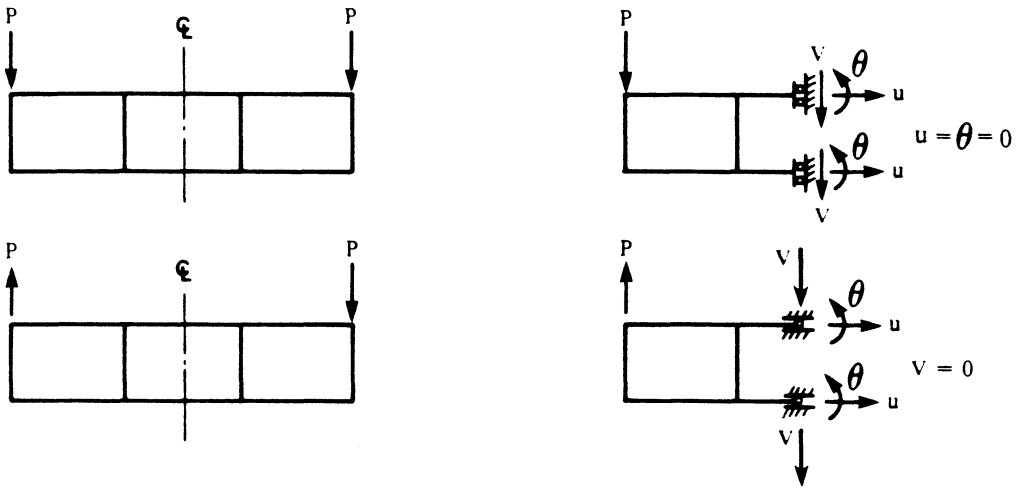

(a) LOADING (b) BOUNDARY CONDITIONS

FIG. 4.10 TRANSVERSE SYMMETRY AND ANTISYMMETRY

supports and the details of the external and influence coefficient loadings. (Very short loading lengths and concentrated loads require more terms than more uniform loads.) A convergence study, in which the problem is run completely two or more times using successively an increasing number of harmonics, is recommended for complex structures and whenever detailed information is desired on internal forces and moments in the vicinity of concentrated external loads or interaction redundant forces. The program should not be used for prediction of local bursting and spalling stresses behind prestressing anchorages, due to a basic difference in the method of application of load.

Plate element surface loads are applied in accordance with the theory of elasticity, so that local stresses within the elements under these loads are accurately predicted and no mesh refinement is required in order to reflect these effects. Prestressing tendon equivalent forces, however, are applied as statically equivalent joint loads. The effect of the actual tendon forces on local variations of internal forces and displacements is thus not included. To reflect these effects for prestressing tendons it is necessary to use more elements. Additional elements beyond the number required for stiffness modelling may also be required for certain load types, since concentrated loads and longitudinal line loads can be applied only at the joints, and plate element surface loads must be uniform over the entire width of the plate element.

The folded plate system and the intermediate diaphragms and supports are assumed to interact only at discrete points. If the intermediate diaphragms or supports are connected continuously to the folded plates, an averaging process must be used in order to properly interpret the internal forces and moments in the diaphragms or supports.

Although the program does not give the internal forces in the flexible movable diaphragms, it outputs the interaction forces. The internal forces may be calculated by analyzing these diaphragms as beams subjected to the interaction forces. This is a statically determinate problem.

5. CURDI4 - CIRCULARLY CURVED BOX GIRDER BRIDGES

5.1 General Remarks

CURDI4 is a computer program capable of analyzing circularly curved or straight prismatic folded plate bridge structures made up of orthotropic finite strip elements. The continuous span structure must be simply supported at the two ends, but may have several interior diaphragms or supports between the two ends (Fig. 4.1). Any arbitrary bridge cross section may be considered by a suitable discretization of finite strip elements (Fig. 4.2). Diaphragms may be defined by transverse flexible beams, and supports may be defined by transverse two dimensional planar rigid frame bents. A direct stiffness harmonic analysis is used for the finite strip system. Compatibility at the interior diaphragms and supporting bents is accomplished by a force method of analysis taking account of the flexibility of the finite strip, diaphragm, and supporting bent system.

This chapter is intended as a description of CURDI4 and as a guide to its use. There are additional sections covering details of the application of prestressing loads, and the organization of the program. For a description of the theories and numerical approach used, refer to Chapter 2 of this report or References [8, 9, 10]. For the details of the prestressing analysis refer to Chapter 3 of this report.

The method of analysis used in CURDI4 is computationally very similar to that used in MUPDI4, except that in CURDI4 a finite strip element is used instead of the folded plate element used in MUPDI4. The CURDI4 program, which was written after the MUPDI4 program, was closely patterned after MUPDI4, described in Chapter 4, to take full advantage of their similarity.

5.2 Structural Modelling

The structural system is modelled as a combination of a finite strip structure and optional moveable diaphragm or supported bent substructures.

The first step in modelling the structure is to identify and number these three component types. The finite strip system must be circularly curved or straight, prismatic and simply supported at the two ends, but any arbitrary bridge cross section can be modelled (Fig. 4.2). The diaphragm or bent substructures may be located at any radial vertical plane between the ends of the finite strip system. Supported rigid diaphragms are always assumed at the two ends.

5.2.1 Finite Strip System

The finite strip system is modelled as an assembly of circumferential or straight finite strip elements possessing both membrane and plate bending stiffnesses. The elements extend over the full length (circumference) of the structure and are interconnected at joints along their circumferential edges. Finite strip theory is used for the orthotropic finite strip elements. Uniform or partial surface loads, line loads, concentrated loads and prestressing may be applied anywhere on the structure.

Modelling a box girder as a finite strip system consists of identifying the cross section to be used and modelling it with constant thickness finite strip elements. Unlike the folded plate elasticity method (Chapter 4) more than one element between physical web/slab intersections may be required for an accurate solution. Joint coordinates, orthotropic elastic material properties, and element locations must be input to CURDI4.

5.2.1.1 Global Coordinate System, Joints and Elements

Structure geometry and loads are expressed in a right handed cylindrical global coordinate system (Fig. 5.1). A circumferential reference line is defined with a specified nonzero radius or as straight. The cross section is defined relative to this reference line. The length of the structure is defined by the horizontal radius to this reference line, and either the subtended angle or the circumferential length along this line. The Y-Z plane is locally orthogonal to the reference line (Fig. 5.1). The cross section thus has a constant description in the Y-Z plane

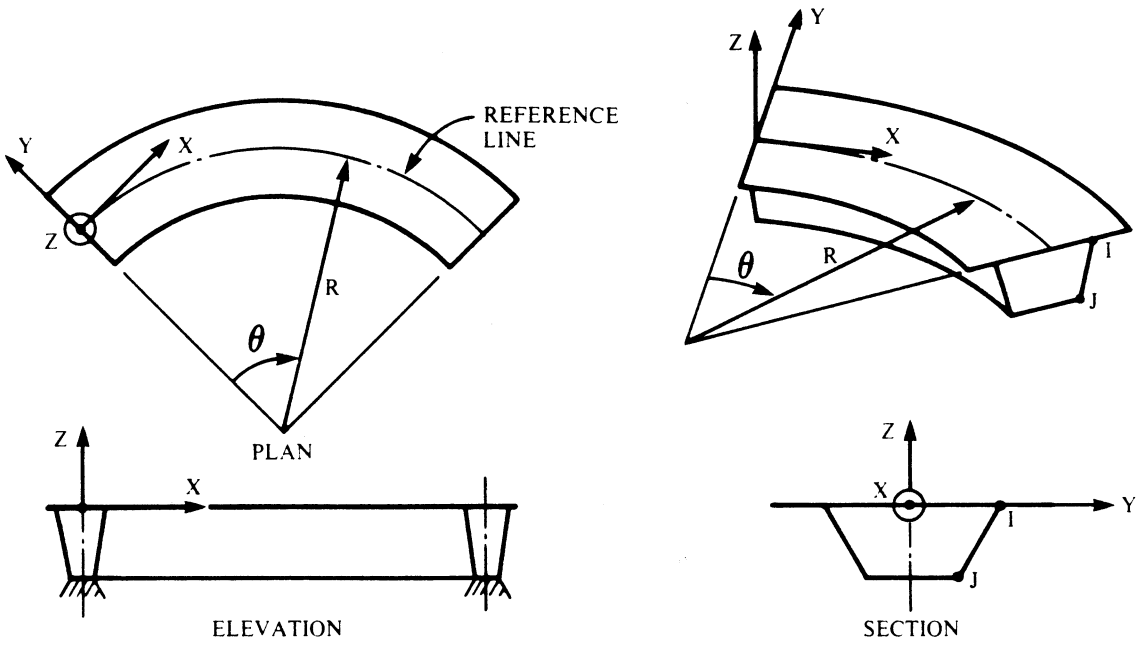

(a) ORIGIN AT LEFT SIMPLE SUPPORT

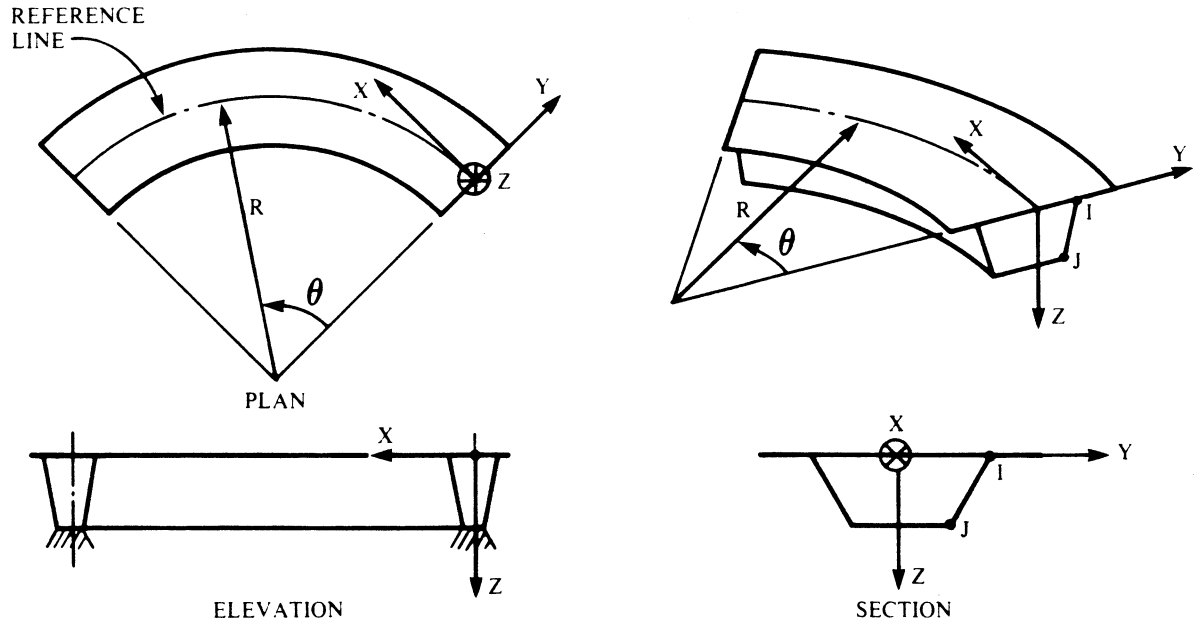

(b) ORIGIN AT RIGHT SIMPLE SUPPORT

FIG. 5.1 GLOBAL COORDINATE SYSTEM FOR CURDI4

over the length of the structure. The cross section can be oriented arbitrarily in the Y-Z plane. However, the Z axis must be vertical (usually downward) and the Y axis must be horizontal with the positive direction always outward radially away from the center of horizontal curvature, (Fig. 5.1).

Joint coordinates and element locations define the subdivision of the cross section into finite strip elements. The solution converges as the number of elements used increases, so that it may not be desirable to model entire webs or transverse slabs by only one element. For a cross section with vertical or inclined webs (Fig. 4.2a), relatively few joints may be required. When transverse prestressing is included, when the slabs are haunched, or when detailed analysis is required for concentrated loads between the webs, additional intermediate joints may be required between the webs (Fig. 4.2b). For a cross section with curved webs, or when analysis is required for prestressing or concentrated loads in the webs, additional intermediate joints may be required in the webs (Fig. 4.2c). CURDI4 will generate joints with uniform spacing along a straight line. Joint numbering should be selected so as to minimize the maximum absolute difference between joint numbers for any finite strip element. Finite strip elements may be numbered in any order.

5.2.1.2 Element Internal Stress Resultants and Material Laws

A typical element is defined by specifying the joint numbers I and J. In general, an element is a segment of a conical frustrum (Fig. 2.5). Positive element local axes displacements and internal stress resultants are shown in Fig. 5.2. The material law relating stress resultants and strains is assumed to be uniform, but may be isotropic or polar-orthotropic throughout the element.

The program has been written such that the material law can be input in one of three ways.

1. Isotropic material. Input only the following element properties: modulus of elasticity E and Poisson's ratio ν.

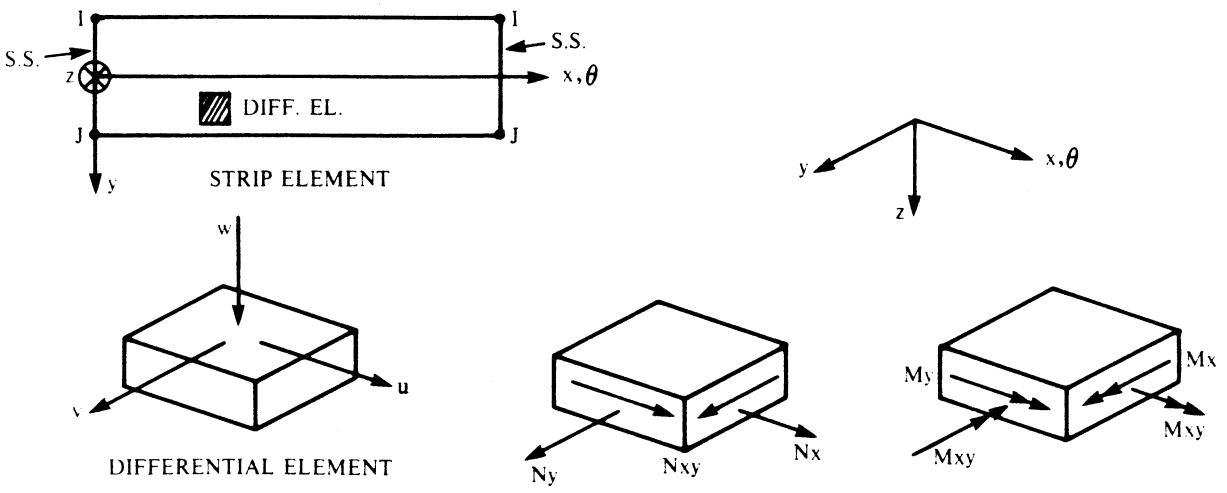

(a) ORIGIN AT LEFT SIMPLE SUPPORT

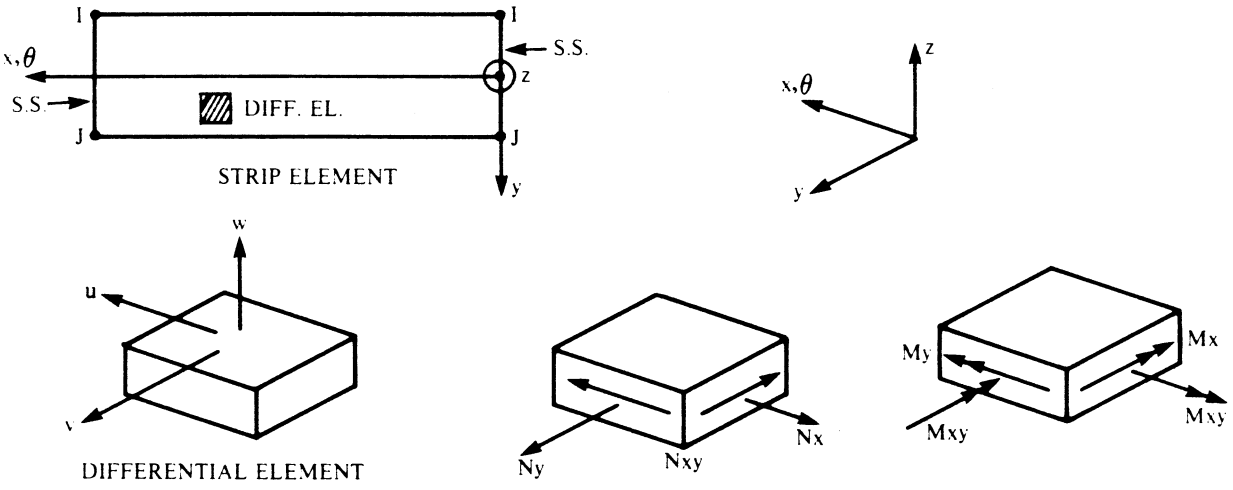

(b) ORIGIN AT RIGHT SIMPLE SUPPORT

FIG. 5.2 POSITIVE ELEMENT LOCAL AXES AND ELEMENT RESULTS FOR CURDI4

2. Polar-orthotropic material. Input all of the following element properties:

$$t^m,\ t^b,\ E_x^m,\ E_x^b,\ E_y^m,\ E_y^b,\ G^m,\ G^b,\ \nu_{xy}^m,\ \nu_{xy}^b$$

for each material which is defined by a unique set of the above quantities in the following material law, (Eq. 5.1):

$$\begin{Bmatrix} N_y \\ N_x \\ N_{yx} \\ M_y \\ M_x \\ M_{yx} \end{Bmatrix} = \begin{bmatrix} \frac{t^m E_y^m}{1-\nu_{yx}^m \nu_{xy}^m} & \nu_{xy}^m \frac{t^m E_x^m}{1-\nu_{yx}^m \nu_{xy}^m} & 0 & 0 & 0 & 0 \\ \nu_{yx}^m \frac{t^m E_y^m}{1-\nu_{yx}^m \nu_{xy}^m} & \frac{t^m E_x^m}{1-\nu_{yx}^m \nu_{xy}^m} & 0 & 0 & 0 & 0 \\ 0 & 0 & t^m G^m & 0 & 0 & 0 \\ 0 & 0 & 0 & \frac{(t^b)^3 E_y^b}{12(1-\nu_{yx}^b \nu_{xy}^b)} & \nu_{xy}^b \frac{(t^b)^3 E_x^b}{12(1-\nu_{yx}^b \nu_{xy}^b)} & 0 \\ 0 & 0 & 0 & \nu_{yx}^b \frac{(t^b)^3 E_y^b}{12(1-\nu_{yx}^b \nu_{xy}^b)} & \frac{(t^b)^3 E_x^b}{12(1-\nu_{yx}^b \nu_{xy}^b)} & 0 \\ 0 & 0 & 0 & 0 & 0 & \frac{(t^b)^3 G^b}{12} \end{bmatrix} \begin{Bmatrix} \varepsilon_y \\ \varepsilon_x \\ 2\varepsilon_{yx} \\ \kappa_y \\ \kappa_x \\ 2\kappa_{yx} \end{Bmatrix} \quad (5.1)$$

where the superscript "m" denotes "membrane" or in-plane characteristics, and superscript "b" denotes "bending" properties, t is the element thickness E and G the elastic and shear modulus, and ν Poisson's ratio. Subscripts y and x indicate the radial and circumferential directions, respectively. Note that symmetry of (Eq. 5.1) must be preserved so that:

$$\nu_{yx}^m = \frac{E_x^m}{E_y^m}\ \nu_{xy}^m$$

and

$$\nu_{yx}^b = \frac{E_x^b}{E_y^b}\ \nu_{xy}^b$$

3. Polar-orthotropic material. Input the constitutive relations directly in the form of:

$$d_{11},\ d_{12},\ d_{22},\ d_{33},\ d_{44},\ d_{45},\ d_{55},\ d_{66}$$

therefore, specify all independent elements of the constitutive matrix in the following Eq. (5.2):

$$\begin{Bmatrix} N_y \\ N_x \\ N_{yx} \\ M_y \\ M_x \\ M_{yx} \end{Bmatrix} = \begin{bmatrix} d_{11} & d_{12} & 0 & 0 & 0 & 0 \\ d_{21} & d_{22} & 0 & 0 & 0 & 0 \\ 0 & 0 & d_{33} & 0 & 0 & 0 \\ 0 & 0 & 0 & d_{44} & d_{45} & 0 \\ 0 & 0 & 0 & d_{54} & d_{55} & 0 \\ 0 & 0 & 0 & 0 & 0 & d_{66} \end{bmatrix} \begin{Bmatrix} \varepsilon_y \\ \varepsilon_x \\ 2\varepsilon_{yx} \\ \kappa_y \\ \kappa_x \\ 2\kappa_{yx} \end{Bmatrix} \quad (5.2)$$

This input option gives the user much freedom in defining his constitutive relations. Stiffeners in either direction and different amounts of reinforcement may be taken into account. In complex situations, the d-coefficient may be determined experimentally.

5.2.1.3 Types of Loading on Finite Strip System

Loads may be applied on the joints or the finite strip elements, and can be defined to act over either the full length or any partial length of the structure. Dead loads are automatically included as finite strip loads based on the specified weight densities (unit weight per volume of material) and thicknesses of the finite strips. Dead loads are generated positive downwards for input positive weight density and global Z axis positive downward.

Joint loads include forces in the global X, Y, and Z directions and moments about the global X axis (Fig. 5.1). They are input as a total load centered at a specified θ or X coordinate along the joint, and uniformly distributed over a subtended angle or length along the reference line. If the distribution length is specified as zero, the load is taken as concentrated. The total X (longitudinal) force on the structure must add up to zero, due to the boundary conditions assumed in the finite strip formulation.

Surface loads on the finite strip elements include forces in the

global Y and Z directions. They are input as load intensities over the projected area (or width) of the finite strip, centered at a specified θ or X coordinate along the finite strip, and uniformly distributed over a subtended angle or length along the reference line. If the length is specified as zero, the load is taken as a line load.

All loads that are applied between joints are converted to equivalent joint forces and moments acting on the two joints defining the relevant finite strip element. The actual loads are replaced by consistent joint loads such that the virtual work done by the consistent joint loads while undergoing the corresponding joint displacements equals the virtual work done by the actual loads undergoing associated displacements. The displacement fields are the same as that used in the finite strip stiffness computation. If the true variation in transverse bending moment and transverse axial force (M_y and N_y in Fig. 5.2) is anything else than linear for M_y and uniform for N_y over the width of a strip element for example, parabolic or bilinear, the consistent joint load approach will fail to give the correct variation of transverse moment and axial force between the relevant joints. When it is important to model these effects accurately, a finer finite strip mesh has to be used near the points of application of the loads that are applied between joints. Therefore, whenever possible, joints should be put at the points of application of point loads and longitudinal line loads. See also sections 5.3.1 and 5.7 for additional discussions.

All loads are expanded into Fourier series components for the harmonic series solution. The convergence rate of the series solution is influenced by the length of the load relative to the total structure length. Meyer [9] showed that for concentrated loads the stress resultants converge very slowly (Fig. 4.5), requiring a very large number of Fourier terms. By replacing the concentrated loads with patch loads distributed over a short length δ_p with intensity p_o, so that $P = p_o \delta_p$, the results converge faster (Fig. 4.6), requiring fewer Fourier terms. Thus most concentrated or line

loads should be modelled as patch loads whenever possible.

5.2.1.4 Output for Finite Strip System

Output consists of joint displacements, the finite strip element internal displacements, stresses or stress resultants (Fig. 5.2), and the integrated section forces and moments. The output can be printed selectively at specified locations along the structure length and at equally spaced intervals across the width of each element. Finite strip element internal stresses are numerically integrated at selected cross sections to arrive at individual girder and total section axial (X) force, shear (Z) force, and (Y) moment. Total axial force is summed from N_x stresses; total shear force is summed from N_{xy} stresses; total bending moment is summed from N_x stresses and M_x moments. The trapezoidal rule is employed, using the internal stresses obtained at the specified uniform interval across the finite strip. The accuracy of the integration is dependent on the interval chosen, particularly at locations with highly nonlinear stress distributions. Thus a larger number (about 4) of output locations across the width of the finite strip is required where more precise integration is desired.

5.2.2 Supporting Frames and Bents

Intermediate supports of the finite strip system may be specified either as rigid supports or as flexible bents. They must lie radially, parallel to the global Y-Z plane. Displacement compatibility between the supports and the finite strip system is enforced for Y and Z displacements and X rotations only, and is not enforced for X displacements. Thus transverse interaction of the supports is considered, but circumferential interaction is not considered.

No loads other than the internally computed interaction forces with the finite strip system are allowed on the supporting structures. Interaction forces are always printed in the output, but output of support internal displacements and stress resultants is possible only for flexible bents.

Rigid supports are entirely defined by their centerline X, θ coordinate and interaction thickness. Flexible bents are additionally defined as a plane frame system. Identical plane frames are assigned a type number, and frame description input is required only once for each frame type.

Each plane frame is located in its own X-Y coordinate system, which must lie parallel to the global Y-Z coordinate system (Fig. 4.7). Joint coordinates and boundary conditions are input, as are elastic support stiffnesses, frame element material properties and element locations. The frame elements include bending, axial and shear deformations.

Output for the frames, when specified, includes interaction forces, node displacements, boundary spring forces and moments, and stress resultants at the ends of the elements.

5.2.3 Unsupported Diaphragms

Intermediate unsupported diaphragms may be specified either as rigid or as flexible. They must lie parallel to the global Y-Z plane. Displacement compatibility between the diaphragms and the finite strip system is enforced for Y and Z displacements and X rotations only, and is not enforced for X displacements. Thus transverse interaction of the diaphragms is considered, but circumferential interaction is not considered.

No loads other than the internally computed interaction forces with the finite strip system are allowed on the diaphragms. Interaction forces are always printed in the output; no other output is available.

Rigid diaphragms are entirely defined by their centerline X, θ coordinate and interaction thickness. Flexible diaphragms are additionally defined as flexible straight beam. Identical flexible diaphragms are assigned a type number, and diaphragm description input is required only once for each diaphragm type.

Each flexible diaphragm type is described by its Z coordinate, material and section properties. Section properties can be computed

internally based on input dimensions of the flexible diaphragm. The beam elements include bending, axial and shear deformations.

5.3 Equivalent Loads from Prestressing

Post tensioned prestressing tendons are classified as panel tendons or slab tendons. Panel tendons may lie in the mid-thickness of any element of the cross-section and extend over the length of the finite strip system. Slab tendons may lie in any element of the cross-section and must be oriented radially, parallel to the global Y-Z plane. For a description of the prestressing analysis and the modelling of the tendons, refer to Chapter 3 of this report. This section deals only with the final application of the equivalent prestressing loads to the finite strip structure.

5.3.1 Panel Tendons

For panel tendons, tendon points are uniformly spaced in each portion and tendon point loads consist of X Y and Z direction concentrated forces acting on some finite strip element. These tendon point loads are converted to equivalent joint forces and moments acting on the two joints defining the finite strip element (Fig. 5.3a), using a consistent load approach in the finite strip formulation. The tendon point loads are replaced by joint loads such that the virtual work done by the joint loads while undergoing the corresponding joint displacements equals the virtual work done by the tendon point loads undergoing their associated displacements. The element displacement field assumed for this purpose is the same as used in the finite strip stiffness computation.

It is important to realize that this procedure whereby a load which is applied between joints is completely replaced by its virtual work equivalent at the joints totally ignores any local stresses between the joints due to the load. Thus in the finite strip element results, only the effect of the equivalent joint loads on the element stresses can be noticed, the transverse moment peak at the location of the point load due to prestress is absent. Also, if transverse moment (M_y in Fig. 5.2)

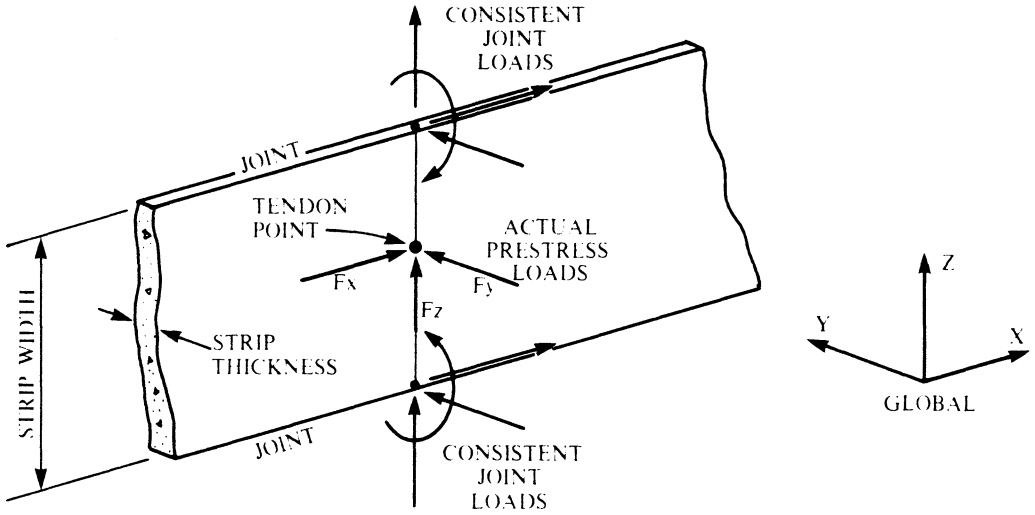

(a) PANEL TENDON LOADS

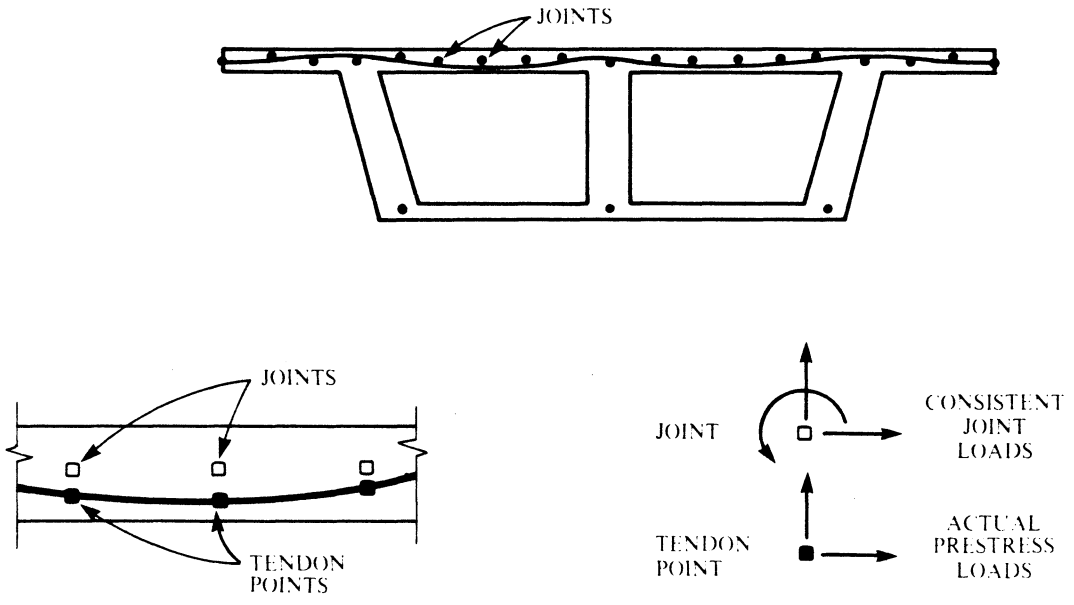

(b) SLAB TENDON LOADS

FIG. 5.3 CONSISTENT JOINT LOADS FOR PRESTRESS

equilibrium at joints is checked using the element transverse moment results, it will be found that moment equilibrium is not satisfied. In general, the transverse moment unbalance at joints decreases as the number of elements in the webs is increased (Fig. 4.2c). Thus, if it is desired to model local variations in moment, axial force, etc. due to prestress loads applied between joints more accurately, more finite strip elements should be used in the affected regions. The variation in transverse moment (M_y in Fig. 5.2) can be especially strong if the bridge is curved in plan, due to the radial component of the prestress point loads. The global structural behavior of the finite strip system, such as girder moments and shears, joint displacements, etc. is normally quite accurately computed using a rather coarse mesh even though the modelling of the local effects between joints might be relatively inaccurate.

Statically equivalent joint loads are applied to the joints as patch loads. This speeds convergence of the solution and more closely approximates the actual load due to the prestressing tendon. A realistic solution of the local stresses behind the anchorages is not expected since in reality the structure is subjected to anchorage forces as circumferential normal stresses acting on the end anchorage plate, while in the harmonic analysis the anchorage forces can be introduced only as circumferential shear forces acting on the circumferential joints near the end anchorage.

5.3.2 Slab Tendons

For slab tendons, tendon points apply to a group of tendons with identical descriptions and spacing, and tendon point loads consist of Y and Z direction distributed forces acting near some joint. These tendon point loads are converted to equivalent consistent joint loads and moments acting on that joint (Fig. 5.3b) by equating the virtual work done by the consistent joint loads while undergoing the corresponding joint displacements with the virtual work done by the tendon point loads undergoing their associated displacements. Thus the tendon point loads are

replaced by Y and Z direction forces and moments about the circumferential X axis. The joint loads are consistent within the finite strip formulation. This approach may result in an unsatisfactory modelling of transverse moments (M_y in Fig. 5.2) between joints. For a discussion see Section 5.3.1.

These statically equivalent joint loads are applied to the joints as uniformly distributed loads over the extent of the length of the slab tendon group. If the length of the tendon group is specified as zero, the joint loads are applied as concentrated loads.

Since the convergence of the Fourier series is considerably slower for concentrated loads than for patch loads, it might be necessary to use more harmonics if the length of the tendon group is specified as zero. Refer to Section 4.2.1 for a more complete discussion of concentrated loads versus patch loads.

5.4 Features of CURDI4

CURDI4 is capable of the analysis of three types of structures, namely straight prismatic folded plate structures, curved prismatic folded plate structures, and axisymmetric shells.

The program allows the specification of both orthotropic and the more usual isotropic material properties. Several options for the specification of these properties are implemented, including direct input of the constitutive relation matrix, allowing the analysis of voided slabs as well as folded plate structures.

The analysis is based on finite strip theory, which is a numerical technique which depends for its convergence on both the fineness of the mesh and the number of terms in the harmonic series. A relatively small number of elements will usually accurately model the longitudinal behavior of the structure. Since the finite strip element employed does not account for local transverse effects, a finer element subdivision may be required in order to capture local transverse bending moments, particularly in cases where loads are applied between joints.

Straight bridges may be modelled using two alternative approaches. One is to specify a large radius relative to the span length. The analysis then proceeds using curved finite strip theory. The alternative is to use the program's straight bridge option, in which case straight finite strip theory is used. Use of straight finite strip theory results in a decoupling of membrane and plate bending terms in the element stiffness matrix of an element. This yields fewer terms in the element stiffness matrix and simplification of element stress evaluations.

The prestressing analysis has all the features and capabilities described in Chapter 3. The solution technique accounts for the effects of prestressing and the distribution of its loads within the structure.

The computer program input is very simple: Discretize the girder cross sections as finite strips, locate and describe the diaphragms and bents, generate prestressing tendons, define locations for output of results, and finally describe all the loads.

Loads can be specified anywhere on the structure in any number of load cases. Load cases may be combined from factored dead load, prestressing, and external loads.

The output capabilities are very flexible. Finite strip element internal displacements, stress resultants, and stresses may be selectively printed at any location in the structure. Individual girder and total section axial forces, shears and moments may be printed for any cross sections. Displacements and stress resultants for the flexible supporting bents may also be printed.

5.5 Computer Program Organization

CURDI4 is an updated and extended version of CURDI. The program has been restructured and in some cases rewritten to utilize new numerical techniques. The program is written around a named in-core array data base which dynamically allocates and manages all numerical array storage. The program was tested on the IBM 3081 Computer at the University of California, Berkeley using the IBM FORTRAN H compiler, and is written for

easy transferability to other machines.

Program organization and flow may be described as follows:

1. Initialize database, input title and problem control data.
2. Input, generate and check finite strip system data, including joint coordinates, boundary conditions, finite strip element material properties and locations, output control specifications, joint and surface loads, and diaphragm or bent locations.
3. Generate and check slab tendon geometries, compute tendon forces, and find equivalent joint loads for slab tendons.
4. Generate and check panel tendon geometries, compute tendon forces, and find equivalent joint loads for slab tendons.
5. Input, generate and check flexible bent data, including node coordinates, boundary conditions, and beam element material properties and locations. Form flexible bent flexibility matrices and internal results recovery arrays.
6. Input generate and check flexible diaphragm data. Form flexible diaphragm flexibility matrices.
7. Perform harmonic series solution of finite strip system for external load cases and unit generalized interaction forces. Save harmonic components of joint displacements on disk.
8. Sum finite strip system flexibility and initial displacement matrices from harmonic components. Transform these matrices for possible rigid body modes of movable diaphragms.
9. Sum total system flexibility matrix from finite strip system, flexible bent and flexible diaphragm components.
10. Solve flexibility system for generalized interaction forces. Transform these forces for movable diaphragms to actual interaction forces.
11. For each load case, sum final finite strip system joint displacements, internal element results and integrated section resultants from harmonic components due to external loads and

interaction forces.

12. For each load case, find flexible bent joint displacements, boundary spring forces and frame element internal forces based on computed interaction forces.

5.6 Computer Program Input and Output

Data describing the bridge structure to be solved is provided in either a deck of cards or in an input file of card images, depending on the computer system used. The required format for the input file is specified in the input manual (Appendix C). The basic organization of the input file is summarized below in terms of its major components.

1. Title: One line of problem description text to be printed with the output.
2. Structure Control Data: One line describing the number of joints, number of finite strip elements, number of bents, etc.
3. Analysis Options: One line defining straight or curved finite strip theory, isotropic or orthotropic materials, axisymmetry, etc.
4. Load and Prestressing Data: One line defining the number of load cases, joint loads, surface loads, panel and slab tendons.
5. Analysis Control Data: One line defining the number of harmonics, data check or execution mode, number of output cross-sections, etc.
6 Geometry Control Data: One line specifying the angle subtended if the bridge is curved or the span if it is straight and the reference radius if it is curved.
7. Joint Coordinates and Boundary Conditions: Describes the finite strip system cross-section.
8. Finite Strip Element Data: Defines material properties and locations of the finite strip elements in the cross-section.
9. Diaphragm/Bent Interaction Data: Defines locations of diaphragms and bents along the length of the bridge.

10. Output Specifications: Defines options and locations for output of displacements, stresses, girder moments.
11. Load Case Multipliers for Dead Load: Multipliers for the finite strip element dead load to be used for each load case.
12. Joint and Surface Loads: Defines external joint and finite strip element surface loads.
13. Slab Prestressing Tendons: Defines transverse slab tendons in groups of tendons with uniform geometry and stressing.
14. Panel Prestressing Tendons: Defines longitudinal panel tendons one at a time.
15. Flexible Supporting Frame Bents: Defines the plane frame structures making up the flexible supporting bents.
16. Flexible Movable Diaphragms: Defines the beam structures making up the flexible moveable diaphragms.

Computer program output consists first of a complete check printout of all the input and generated data describing the structure, the prestressing and loads. Then, depending on the features of the structure and the output specification requests, the following final results are printed for each load case:

1. The interaction (restraint) forces between each diaphragm or bent and the finite strip system.
2. Resulting four displacement components of each joint at each θ or X coordinate specified.
3. Optionally, internal element displacements, forces and stresses. Each component may be supressed or printed as required.
4. Optionally, individual girder and total section axial forces, shears and bending moments and percentages at each specified cross-section.
5. Optionally, joint displacements and member end forces for the flexible supporting bents.

5.7 Special Considerations for the Use of CURDI4

CURDI4 provides a rapid solution for circularly curved prismatic folded plate structures simply supported at the two ends and with optional interior diaphragms or supports. The diaphragms and supports may be either rigid or flexible but must be oriented radially. Diaphragms may be defined by flexible beams, while supports may be defined by two dimensional planar frame bents. Surface loads, line loads, concentrated loads, and prestressing may be applied anywhere on the folded plate structure.

The maximum number of finite strip elements, joints, diaphragms, bents, and prestressing tendons is limited only by available high and low speed storage on the computer system used. In practical terms, there is no limit on the size or complexity of a structure which can be analyzed with CURDI4.

If the structure is symmetrical in the longitudinal direction about a transverse midspan plane, a great saving in computing effort may be achieved by taking advantage of the symmetry or anti-symmetry of the loading with respect to this transverse plane, if it exists. For the case of a symmetrical structure subjected to symmetrical loading (Fig. 4.9a), only the odd terms of the Fourier series have to be included. For anti-symmetrical loading (Fig. 4.9b), only the even terms have to be included. This can be accomplished by giving the appropriate instructions in the analysis control data.

Loadings to be considered when choosing whether or not to take advantage of symmetry include the external loads as well as the redundant forces from each diaphragm or bent applied individually. Thus, advantage of symmetrical loading can only be taken in simply supported structures and structures with only one center bent or diaphragm (Fig. 4.9a). No advantage of symmetrical loading may be taken for spans with more than one intermediate diaphragm or bent. In these cases all terms of the Fourier series must be used. Advantage of anti-symmetrical loading may be taken only in cases of simple spans with no intermediate diaphragms or bents (Fig. 4.9b).

When using the straight bridge option, if the cross section of the structureis symmetrical about a longitudinal plane, advantage of symmetry or anti-symmetry of the loading with respect to this plane may be taken by analyzing only half of the cross section and imposing appropriate boundary conditions at the longitudinal plane of symmetry (Fig. 4.10). In the case of a curved bridge, a symmetrical cross-section does not result in a symmetrical structure, so that transverse symmetry may not be used.

Since the actual force distribution on the structure is modelled as a truncated Fourier series, a suitable number of harmonics must be used to adequately approximate the applied loads and the interaction forces. The number of terms required depends on the number of intermediate diaphragms and supports and the details of the external and influence coefficient loadings. Very short loading lengths and concentrated loads require more terms than more uniform loads. A convergence study, in which the problem is run completely two or more times using successively an increasing number of harmonics, is recommended for complex structures and whenever detailed information is desired on internal forces and moments in the vicinity of concentrated external loads or interaction redundant forces. The program should not be used for prediction of local bursting and spalling stresses behind prestressing anchorages, due to a basic difference in the method of application of load.

Loads that are applied between joints, for example dead load, surface loads, concentrated loads and prestress are converted by the program to equivalent loads at the joints. The effect of the original loads on local variations of transverse bending moment (M_y in Fig. 5.2) is thus not included. To reflect these effects it is necessary to use more elements. A good check to see if the local effects have been captured accurately is to check transverse moment as well as transverse axial force (N_y in Fig. 5.2) equilibrium at the joints using the element results. A relatively small moment or axial force unbalance implies a relatively accurate modelling of local effects between joints. More finite strip elements in

the vicinity of loads applied between joints, in general, result in a more accurate approximation of local effects. It is to be noted, however, that although an element mesh might be too coarse to accurately model the local effects of loads applied between joints, it can still adequately model global structural behavior,such as joint displacements and integrated moments, axial forces and girder shears. Of particular importance is panel prestress in the webs of circularly curved bridges, since it has a radial component that bends the web transversely and thus might cause important local transverse bending in the web elements between joints. Slab tendons might also cause high local bending, the degree depending on the drape of the tendons. If point or patch loads due to trucks, etc. are to be applied directly to the finite strip system, it is good practice to put joints at the points of application of these loads wherever practical. In cases where it is unavoidable to have loads between joints, more elements in the vicinity of the loads will result in a more accurate local modelling of transverse moments, transverse axial forces, etc. Convergence studies in which the effects of progressively finer finite strip meshes are compared can be very useful whenever local effects between joints are important.

The folded plate system and the intermediate diaphragms and supports are assumed to interact only at discrete points. If the intermediate diaphragms or supports are connected continuously to the folded plates, an averaging process must be used in order to properly interpret the internal forces and moments in the diaphragms or supports.

Although the program does not give the internal forces in the flexible movable diaphragms, it outputs the interaction forces. The internal forces may be calculated by analyzing these diaphragms as beams subjected to the interaction forces. This is a statically determinate problem.

6. CELL4 - BOX GIRDER BRIDGE OF ARBITRARY PLAN GEOMETRY

6.1 General Remarks

CELL4 is a program based upon the finite element method and is particularly suited for the analysis of post-tensioned box girder bridges of constant depth which have arbitrary plan geometry and support conditions.

The bridge can be straight, curved or quadrilateral in plan (Fig. 6.1). The longitudinal interior webs must be vertical, but the longitudinal exterior webs can be vertical, sloping or curved. Transverse diaphragms can be modelled by vertical web elements or by special web elements in regions with sloping or curved exterior webs. The top and bottom deck slabs as well as the interior and the exterior webs may be prestressed.

Boundary conditions at any nodal point are arbitrary, allowing rigid supports as well as translational and rotational elastic supports, oriented in any arbitrary direction to simulate the stiffness of the supporting columns and bents.

For prestressing analysis an automatic input has been provided to define the geometry of the two types of post-tensioned unbonded tendons which can be used. These are panel and slab tendons as described in Chapter 3. Each tendon can be stressed either from one end A or both ends A and B, and losses due to friction and anchorage slip are accounted for by using the procedure described in Chapter 3.

In order to facilitate the interpretation of output, an automatic integration of internal forces to give individual girder and total sectional force resultants is incorporated. This will permit a better understanding of the load carrying mechanism in a complex bridge system, and also can be used to carry out equilibrium checks easily.

The theoretical bases and the implementation of the above features into CELL4 will be presented in this chapter. Numerical results from selected

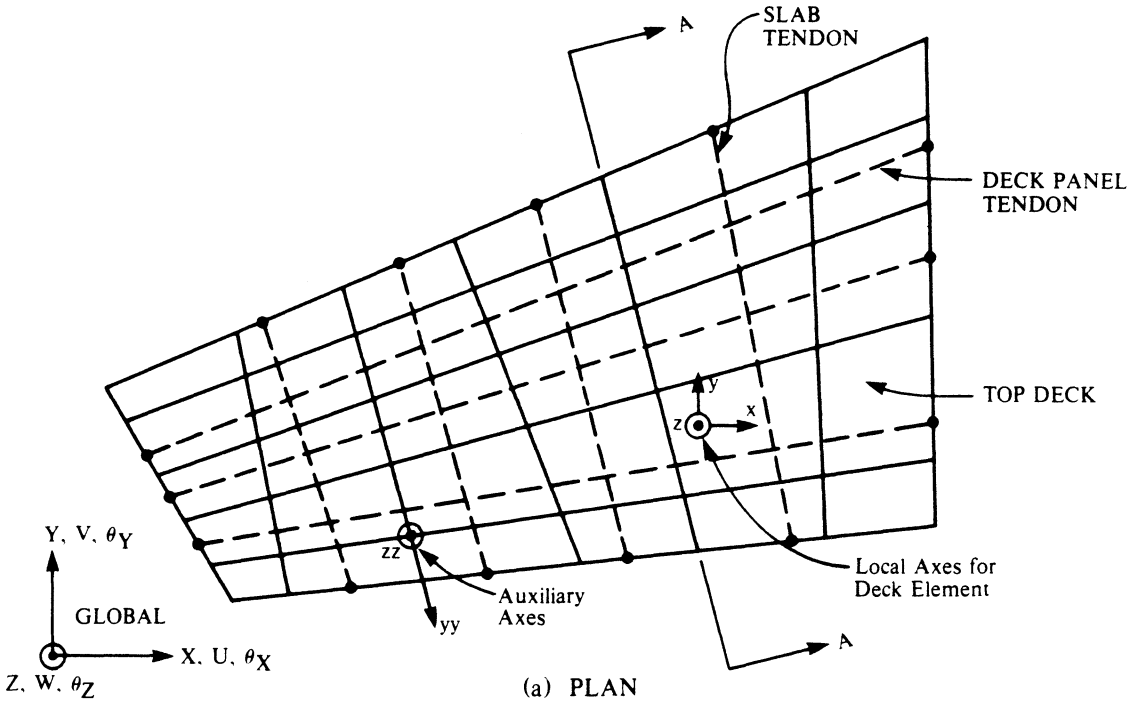

(a) PLAN

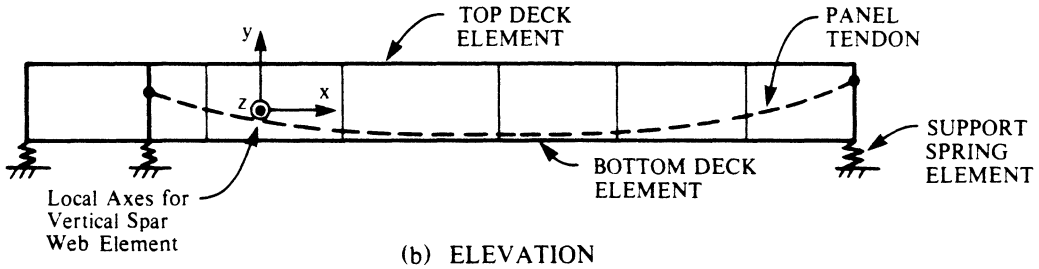

(b) ELEVATION

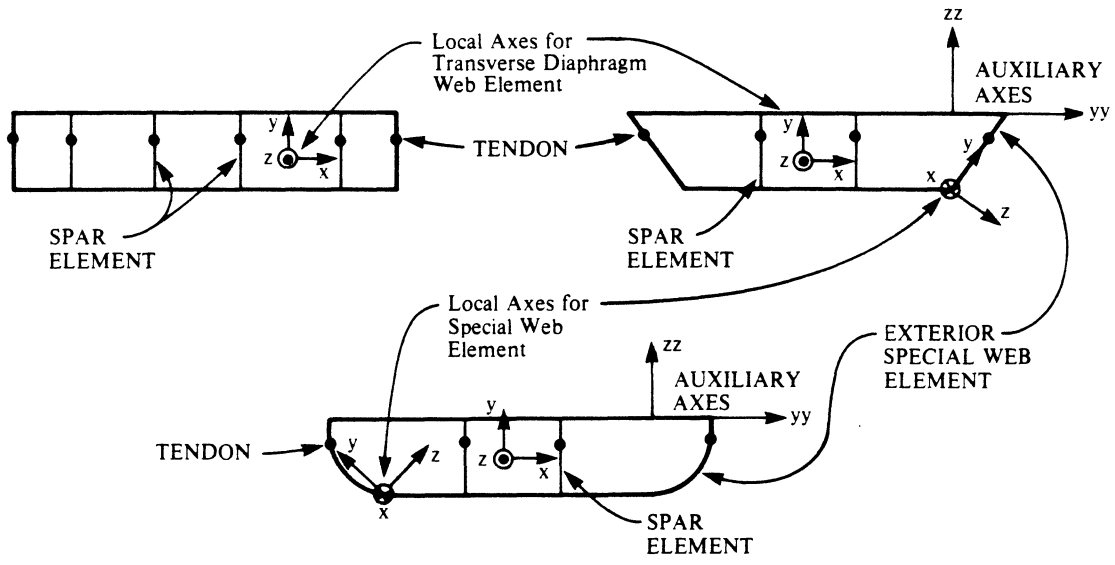

(c) TYPICAL CROSS-SECTIONS AT SECTION A-A

FIG. 6.1 GEOMETRY, CROSS-SECTIONS AND COORDINATE SYSTEMS FOR CELL4

examples used in verifying CELL4 will be described in Chapter 7.

6.2 Structural Modelling

6.2.1 General

The modelling of a cellular bridge system by the finite element method consists of a series of nodes interconnected by finite elements.

The structure (Fig. 6.1) has one set of right-handed Cartesian global axes, oriented in such a way that the global X- and Y-axes lie in a plane parallel to the top and bottom deck slabs of the structure. The global Z-axis is perpendicular to the X-Y plane, and is positive upwards from the top deck mid-surface. In addition, a number of sets of auxiliary axes yy and zz can be used, if desired, to describe the geometry of the exterior sloping or curved webs. The yy axis must be defined by two reference nodes on the top deck. The zz axis is parallel to the global Z axis.

The cellular system (Fig. 6.1) consists of deck elements representing the top and bottom deck slabs, rectangular spar elements for the vertical webs, and special web elements for the sloping or curved exterior webs. Furthermore, the system may be supported elastically at the nodes on elastic spring elements.

Prestressing in the panel tendons of the top deck, bottom deck, vertical webs, and exterior webs, as well as in the slab tendons of the top and bottom decks is possible by a suitable definition of tendon geometry and jacking forces.

6.2.2 Coordinate System and Sign Conventions

Each top and bottom deck node has nodal displacements U, V, W which are positive in the global directions X, Y, Z, and nodal rotations θ_X, θ_Y about the X, Y axes whose positive direction is given by the right-hand rule. For nodes lying between the top and bottom deck, the rotations θ_Z about the global Z axis are also included.

Each element is formed in a local right-handed Cartesian system x, y, z with x, y lying in the plane of the element as illustrated in Fig. 6.1. For

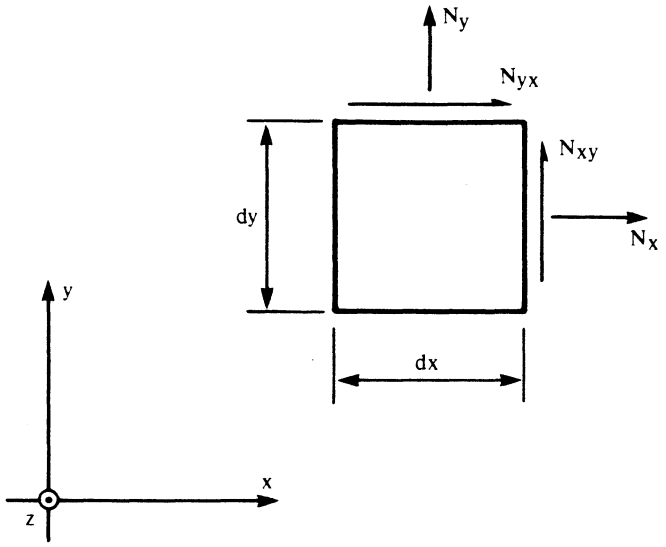

LOCAL ELEMENT AXES

(a) IN PLANE MEMBRANE STRESS RESULTANTS

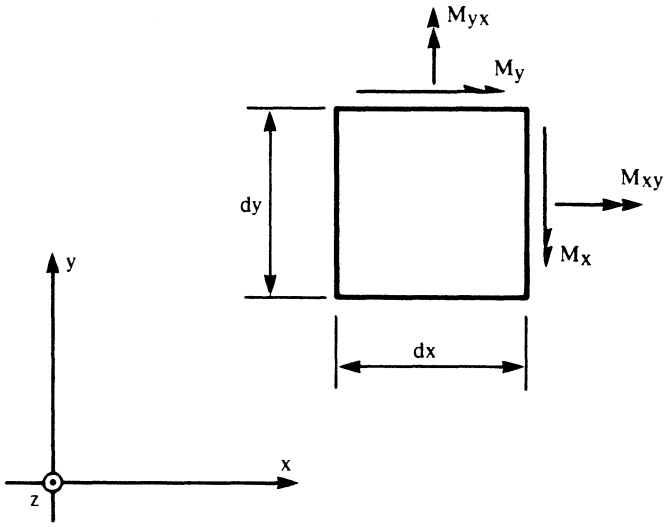

LOCAL ELEMENT AXES

(b) PLATE BENDING MOMENT RESULTANTS

FIG. 6.2 SIGN CONVENTION FOR INTERNAL ELEMENT FORCES AND MOMENTS

the deck elements only, the global and local systems are identical. The sign convention of the internal forces is referred to this local coordinate system and is indicated in Fig. 6.2.

6.2.3 Material Laws

The material properties can be specified at two levels, (a) a plane stress law relating stresses to strains, and (b) a law relating internal forces to strains and curvatures.

(a) Orthotropic and Isotropic Plane Stress Materials

The principal axes of orthotropy for each element are denoted by $\bar{x}_1$, $\bar{y}_1$, $\bar{z}_1$ where $\bar{x}_1$ forms an angle ϕ with the local element x-axis. The orthotropic stress-strain relation refers to these principal axes and is defined by:

$$\begin{Bmatrix} \bar{\sigma}_x \\ \bar{\sigma}_y \\ \bar{\tau}_{xy} \end{Bmatrix} = \begin{bmatrix} E_1/\chi & E_1\,\nu_{12}/\chi & 0 \\ E_2\,\nu_{21}/\chi & E_2/\chi & 0 \\ 0 & 0 & G_{12} \end{bmatrix} \begin{Bmatrix} \bar{\varepsilon}_x \\ \bar{\varepsilon}_y \\ \bar{\gamma}_{xy} \end{Bmatrix} \qquad (6.1)$$

E_1, E_2 = Elastic moduli in the $\bar{x}_1$ and $\bar{y}_1$ direction

ν_{12}, ν_{21} = Poisson's ratio with $E_1\,\nu_{12} = E_2\,\nu_{21}$ for symmetry. ν_{12} is defined as the ratio of the strain in the $\bar{x}_1$ direction to the strain in the $\bar{y}_1$ direction due to a uniaxial stress in the $\bar{y}_1$ direction.

$\chi = 1-\nu_{12}\,\nu_{21}$ = Denominator in material law

G_{12} = Shear modulus

The corresponding material law in the x, y coordinates requires a tensor transformation eliminating zero coefficients if $\phi \neq 0$.

For an isotropic material the constants degenerate to:

$$E_1 = E_2 = E, \quad \nu_{12} = \nu_{21} = \nu, \quad G_{12} = G$$

and the angle ϕ is not needed. The in-plane membrane stress resultant-strain relation is obtained by multiplying this matrix by h, where h is the plate thickness. The moment-curvature relation is obtained by multiplying this matrix by $h^3/12$.

(b) Anisotropic Stress Resultant-Strain and Moment-Curvature Relations

In order to increase the versatility of the program direct access is available to the material law relating stress resultants to strains and moments to curvatures. This capability makes it possible to take account, for instance, of stiffeners arranged along two skewed directions or of various levels of flexural action, such as two-way bending, one-way bending, or no bending action altogether. In-plane stress resultants are related to the strains by:

$$\{N\} = [DS]\{\varepsilon\}$$

$$\begin{Bmatrix} N_x \\ N_y \\ N_{xy} \end{Bmatrix} = \begin{bmatrix} DS(1) & DS(4) & DS(5) \\ & DS(2) & DS(6) \\ Sym. & & DS(3) \end{bmatrix} \begin{Bmatrix} \varepsilon_x \\ \varepsilon_y \\ \gamma_{xy} \end{Bmatrix} \tag{6.2}$$

Internal moments are related to the curvatures by:

$$\{M\} = [DM]\{\kappa\}$$

$$\begin{Bmatrix} M_x \\ M_y \\ M_{xy} \end{Bmatrix} = \begin{bmatrix} DM(1,1) & DM(1,2) & DM(1,3) \\ & DM(2,2) & DM(2,3) \\ Sym. & & DM(3,3) \end{bmatrix} \begin{Bmatrix} \kappa_x \\ \kappa_y \\ \kappa_{xy} \end{Bmatrix} \tag{6.3}$$

The coefficients of the material matrices [DS] and [DM] can be determined either by integration of the associated plane stress material law over the thickness, as it is done in (a), or by performing appropriate experiments to evaluate these coefficients.

6.2.4 Deck Elements

The deck element used in the analysis and developed for the original CELL program is represented by the mixed model Q8D11 plane stress element and the Q19 plate bending element (Fig. 2.7a,b). These are described briefly in Section 2.4.1, and in detail in [14, 15]. The element degenerates into a triangle by collapsing nodes 1 and 4.

The lack of invariance of the membrane stiffness with respect to coordinate rotation requires that the element be formed in local convected coordinate system (Fig. 2.7).

6.2.5 Rectangular Spar Elements

This element, also developed for the original CELL program, is especially suitable to represent the vertical web behavior by a single plane stress element over the depth of the bridge (Fig. 2.7c,d). The element is described briefly in Section 2.4.1 and in detail in [14, 15].

The enforcement of equal nodal rotations of $\omega = (dv/dx)$ between adjacent colinear spar elements results in equal shear strains $\gamma_{xy} = (\partial u/\partial y) + (\partial v/\partial x)$ at a node since $\partial u/\partial y$ is continuous. Because of this shear constraint, the shear stresses under concentrated loads cannot be calculated accurately with a coarse mesh at the point of application of a load. The element lengths must therefore be reduced in regions with discontinuities in shear, such as near supports or under load points. Interpolation and extrapolation of results for shear should be carried out in these cases to get a clear understanding of behavior.

6.2.6 Special Web Elements

This element (Fig. 6.3) is a special form of the deck element with appropriate transformations to take into account the arbitrary orientation of the element in space and the sloping and curved geometry of the exterior webs, resulting in any possible warped configuration. The resulting element has 5 D.O.F. per node in the local coordinate system, which when transformed to the global coordinate system becomes 6 D.O.F.

A typical element (Fig. 6.3) has nodes 1 and 4 lying above nodes 2 and 3.

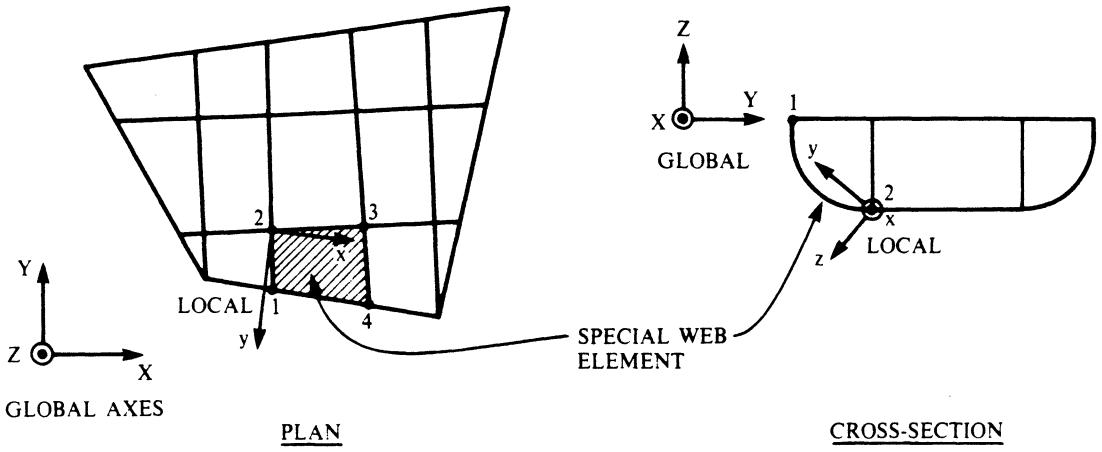

(a) BRIDGE WITH QUADRILATERAL GEOMETRY IN PLAN

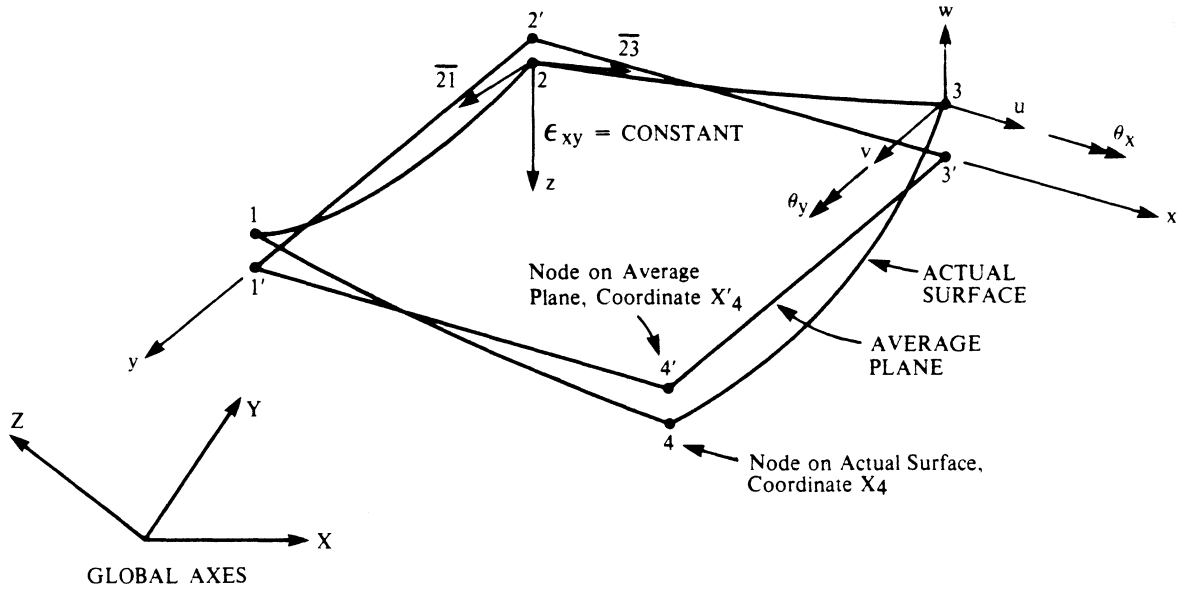

(b) TYPICAL SPECIAL WEB ELEMENT

FIG. 6.3 CONFIGURATION, D.O.F. AND COORDINATE SYSTEMS FOR SPECIAL WEB ELEMENT

The nodal coordinates are defined in the global XYZ system. Element local axes xyz are oriented in such a way that the local x axis lies either in a general longitudinal direction of the bridge for longitudinal web elements or in a general transverse direction for transverse web elements (Fig. 6.3a). The local y axis is normal to the plane formed by local x and local z axis, with the local z normal to the plane of the element. The shear stress calculated based on this local coordinate system will therefore always give the beam shear in the usual sense, and the stress along the local x axis will give the longitudinal membrane stress for a longitudinal web, independent of the orientation of the element.

The calculation of this local x, y and z coordinate system is as follows. A coplanar element is first identified by checking whether node 4 falls on the plane containing nodes 1, 2 and 3. For non-coplanar elements an average plane is calculated with new global coordinates X' and corner nodes 1', 2', 3' and 4' (see Fig. 6.3), which minimize the distance between the four corners from the averaged plane to the actual surface. The normal z-axis to the element can then be established as the vector product:

$$z = (\overline{23} \times \overline{21})/(\|\overline{23} \times \overline{21}\|) \qquad \text{for coplanar elements}$$

$$\text{or} \quad z = (\overline{2'3'} \times \overline{2'1'})/(\|\overline{2'3'} \times \overline{2'1'}\|) \qquad \text{for non-coplanar elements}$$

and the local x axis in a general longitudinal direction is then given by the vector product:

$$x = z \times Z, \quad Z = (0\ 0\ 1)$$

and the local y axis is normal to both x and z:

$$y = z \times x$$

When an element is non-coplanar, the stiffness k' in the averaged plane is first computed and then transformed to the actual surface geometry nodes

through the use of kinematic constraints. The final 24x24 stiffness matrix k with respect to the true surface is made up of 16 - 6x6 submatrices k_{IJ} determined as follows:

$$[k_{IJ}] = [A_I]^T[k'_{IJ}][A_J] \quad \text{for nodes I and J}$$

where

$$[A_I] = \left[\begin{array}{ccc|ccc} X_1 & X_2 & X_3 & (-X_2e_Z + X_3e_Y) & (X_1e_Z - X_3e_X) & (-X_1e_Y + X_2e_X) \\ Y_1 & Y_2 & Y_3 & (-Y_2e_Z + Y_3e_Y) & (Y_1e_Z - Y_3e_X) & (-Y_1e_Y + Y_2e_X) \\ Z_1 & Z_2 & Z_3 & (-Z_2e_Z + Z_3e_Y) & (Z_1e_Z - Z_3e_X) & (-Z_1e_Y + Z_2e_X) \\ \hline 0 & 0 & 0 & X_1 & X_2 & X_3 \\ 0 & 0 & 0 & Y_1 & Y_2 & Y_3 \\ 0 & 0 & 0 & Z_1 & Z_2 & Z_3 \end{array}\right] \quad (6.4)$$

and $e_I^T = (e_X\ e_Y\ e_Z)_I$ are eccentricities of the node I with respect to the averaged plane, computed as $e_I = X_I - X'_I$.

A sloping or curved exterior web can be modelled more accurately by increasing the number of the above special web elements to three or four over the depth of the web instead of just one.

6.2.7 Elastic Spring Supports

The elastic spring element (Fig. 6.4) can have specified translational and rotational stiffnesses. The direction of the constraint is either defined by the vector joining the two nodes, I and J, or by a cross product of two vectors a and b formed by nodes I, J, K and L which defines the plane normal to the constraint direction.

6.3 Equivalent Loads from Prestressing

It is assumed that the panel or slab tendon profile (Fig. 6.5) as well as the tendon forces are known along the tendon by using the procedure described in Chapter 3. The major difference in the approach used in CELL4 lies in the definition of tendon segment and the calculation of the equivalent nodal loads

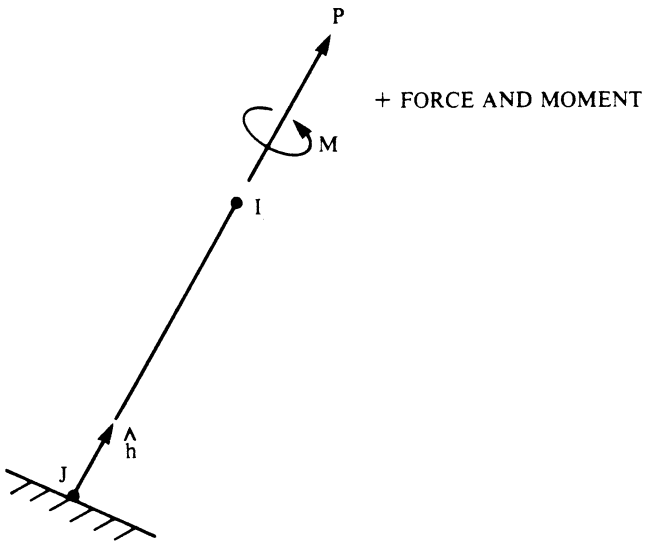

(a) CONSTRAINT DIRECTION DEFINED BY TWO NODES

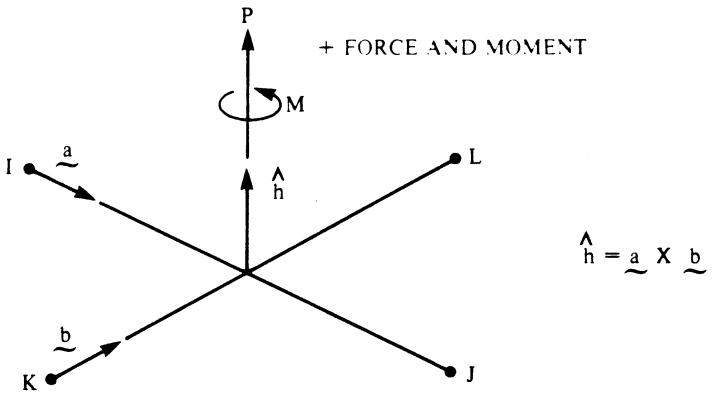

(b) CONSTRAINT DIRECTION NORMAL TO A DEFINED PLANE

FIG. 6.4 ELASTIC SUPPORT SPRING ELEMENT

due to prestressing.

A tendon segment is defined as the portion between two tendon points in which the tendon crosses an element boundary. Unlike MUPDI4 and CURDI4, the segments are of unequal lengths, and are largely dependent on the tendon and element geometries.

For the kind of tendon profiles permissible in the analysis, the deck panel tendons and the slab tendons can be made up of different parabolic segments, Fig. 6.5. In addition, the slab tendon profiles perpendicular to the deck slabs as well as the panel tendon profiles in the vertical webs can be described by the parametric input, described in Chapter 3, by substituting for the span length the projection of the tendon length on the global X-Y plane. However, to maintain generality, and to treat all exterior web geometries, the geometries of panel tendons in the special web elements used for sloping or curved exterior webs must be input by tendon points.

Once the tendon points are known (Fig. 6.6), the orientation V of this tendon segment can be found. For the general case of a slab tendon with end eccentricities e_{ZI} and e_{ZJ}, at tendon points I and J with respect to the mid-thickness of an element, the tendon force at tendon points I and J in the global coordinates are:

$$\begin{Bmatrix} P_X \\ P_Y \\ P_Z \\ M_X \\ M_Y \end{Bmatrix}_I = \bar{P} \begin{Bmatrix} V_X \\ V_Y \\ V_Z \\ -V_Y e_Z \\ +V_X e_Z \end{Bmatrix}_I \quad \text{and} \quad \begin{Bmatrix} P_X \\ P_Y \\ P_Z \\ M_X \\ M_Y \end{Bmatrix}_J = -\bar{P} \begin{Bmatrix} V_X \\ V_Y \\ V_Z \\ -V_Y e_Z \\ +V_X e_Z \end{Bmatrix}_J \tag{6.5}$$

$\bar{P}$ = $(P_I + P_J)(1/2)$ = average tendon force

V = direction cosine of the tendon segment

and the statical equivalent nodal loads due to prestressing are then obtained by distributing the tendon forces to adjacent nodes:

$$(P_{Xi} \quad P_{Xj} \quad P_{Xk} \quad P_{Xl}) = (a_I \quad a_J \quad b_J \quad b_I)P_X$$
$$(P_{Yi} \quad P_{Yj} \quad P_{Yk} \quad P_{Yl}) = (a_I \quad a_J \quad b_J \quad b_I)P_Y$$
$$(P_{Zi} \quad P_{Zj} \quad P_{Zk} \quad P_{Zl}) = (a_I \quad a_J \quad b_J \quad b_I)P_Z$$
$$(M_{Xi} \quad M_{Xj} \quad M_{Xk} \quad M_{Xl}) = (a_I M_{XI} \quad a_J M_{XJ} \quad b_J M_{XJ} \quad b_I M_{XI})$$
$$(M_{Yi} \quad M_{Yj} \quad M_{Yk} \quad M_{Yl}) = (a_I M_{YI} \quad a_J M_{YJ} \quad b_J M_{YJ} \quad b_I M_{YI})$$

where

$$M_{XI} = -P_{YI}e_{ZI}\ ,\ M_{XJ} = -P_{YJ}e_{ZJ}$$
$$M_{YI} = P_{XI}e_{ZI}\ ,\ M_{YJ} = P_{XJ}e_{ZJ}$$

l_I = length of side $\overline{il}$

l_J = length of side $\overline{jk}$

$a_I = \overline{lI'}/l_I$

$b_I = \overline{iI'}/l_I$

$a_J = \overline{kJ'}/l_J$

$b_J = \overline{jJ'}/l_J$

eccentricity e_Z = +ve for points above mid-depth of element

For the case of a panel tendon which always lies in a plane at the mid-thickness of the element, the moment eccentricities e_{ZI} and e_{ZJ} (Fig. 6.6) are zero and thus M_X and M_Y are also zero.

6.4 Features of CELL4

The new program CELL4 was developed on the IBM 4341 and IBM 3081, and was written in FORTRAN 66 in double precision. The program utilizes dynamic storage allocations which eliminate the restrictions on the problem size.

CELL4 has a data check option which only reads and echoes the input data with appropriate headings, with a minimum amount of calculations. This will facilitate data checking before the final analysis is made.

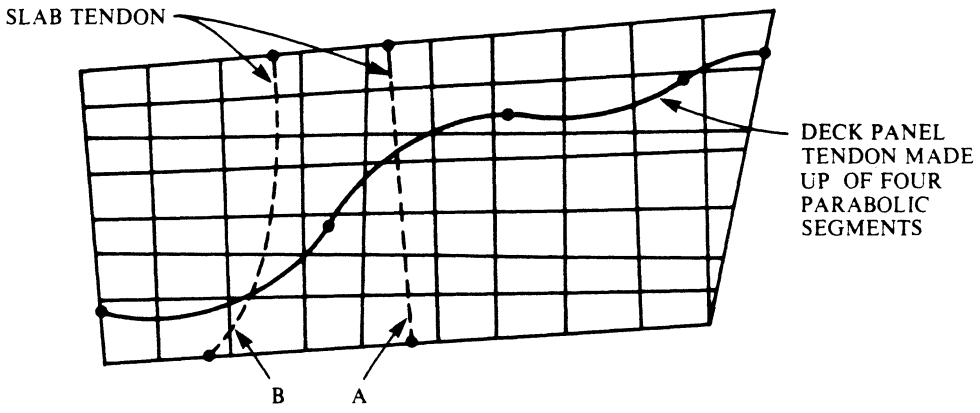

(a) PLAN OF TENDON PROFILES

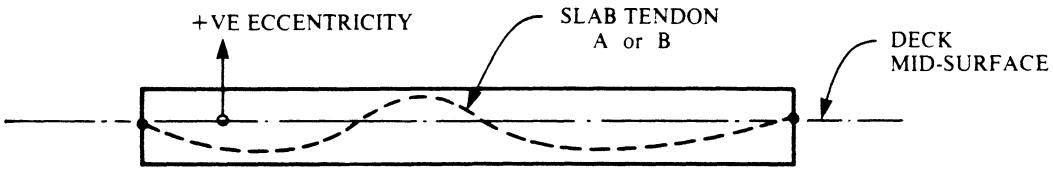

(b) TRANSVERSE SLAB TENDON PROFILE

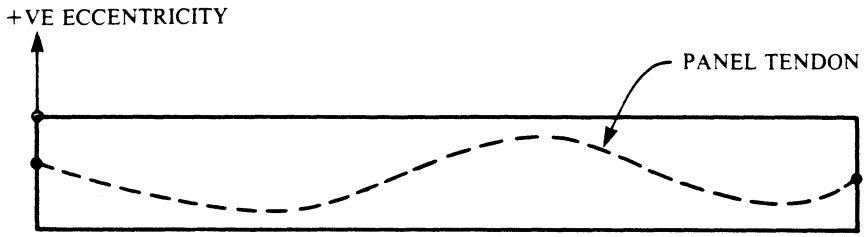

(c) LONGITUDINAL PANEL TENDON PROFILE IN VERTICAL WEB

FIG. 6.5 TYPICAL PRESTRESSING TENDON LAYOUTS

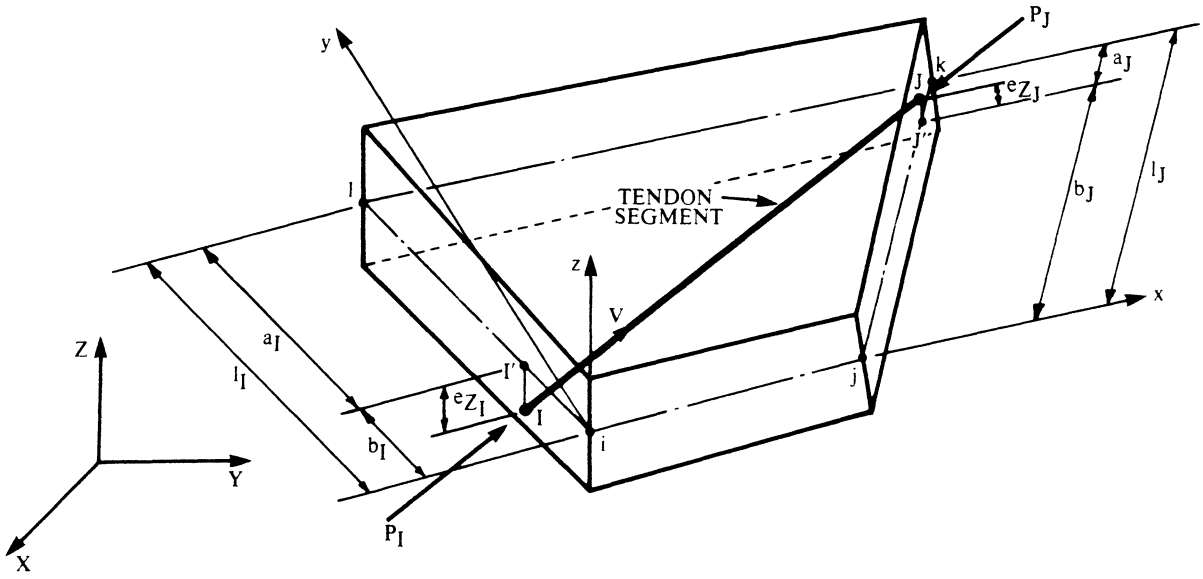

FIG. 6.6 GEOMETRY OF A PRESTRESSING TENDON SEGMENT PASSING THROUGH A FINITE ELEMENT

The capabilities of the CELL4 program have been described in some detail in Section 2.4.2. Among the most important new features are, first, its ability to analyze post-tensioned box girder bridges of arbitrary plan geometry with constant depth, and with sloping or curved exterior webs, by making use of an internal automatic prestressing generation option, and, second, its ability to perform an internal automatic integration of internal sectional force resultants from the calculated membrane stresses and output these results for each defined girder or the total section.

The program also permits the solution of multiple load cases and any combinations of dead load, various live loads, and a factored prestressing load. This factored prestressing load is useful in determining initial stresses and then final stresses under reduced prestress forces which account for long-term losses such as creep and shrinkage of the concrete, relaxation of the prestressing steel, etc.

6.5 Computer Program Organization

The computer program CELL4 consists of five different phases during the solution process.

(1) Input phase - The geometry of the structure and the tendons will be input and generated. Tendon forces will also be calculated.

(2) Stiffness formation - The element stiffnesses will be formed and assembled, and will be stored on tape.

(3) Load input - The loading and the prestressing load factor will be input, and the final load vector will be assembled.

(4) Solution phase - The structure stiffness matrix will be triangularized and stored, and back-substituted for nodal displacements for new load cases.

(5) Output phase - The nodal displacements, stresses and integrated sectional forces will be calculated and output if requested.

Step 3 is repeated as many times as the load cases require. The output can be very selective in order to minimize unnecessary calculations and the required input and output used by the computing system.

6.6 Computer Program Input and Output

The input to CELL4 is fix-formatted and consists of a series of lines input according to the format described in detail in Appendix D. Consistent units must be used unless otherwise specified.

The input includes a series of coordinates for the nodes. Generally, three types of nodes can be identified (Fig. 6.7).

Type 0: Node numbers which exist for both top and bottom deck elements.

Type 1: Nodes to which only top deck elements are attached. These are typically in the overhanging section of a bridge.

Type 2: Nodes lying in between the top and bottom deck plate elements. These are typically nodes belonging to a special web element.

The tendon geometries can be input directly using a point-by-point procedure or by making use of the automatic tendon geometry generation capabilities in CELL4.

The output consists of joint displacements in the global coordinates, and stresses either in the global directions or in the principal stress directions, or in some user-specified directions. Furthermore, the nodal stresses can be averaged from up to eight adjacent elements in any direction, either using one string of elements or using adjacent strings of elements. This averaging process is done separately for the deck, vertical web and special web elements.

Finally, the integrated internal sectional force resultants are output, which include the forces for individual girders as well as the total sectional force resultants summed from all the girders. The six components of forces

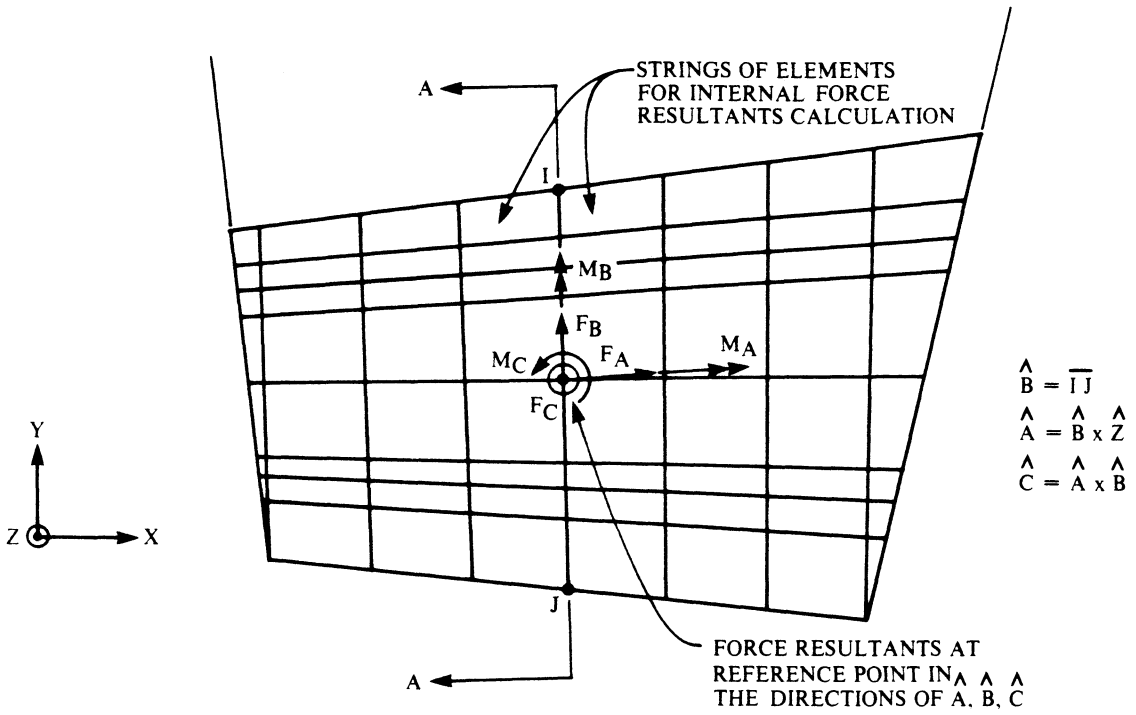

(a) PLAN

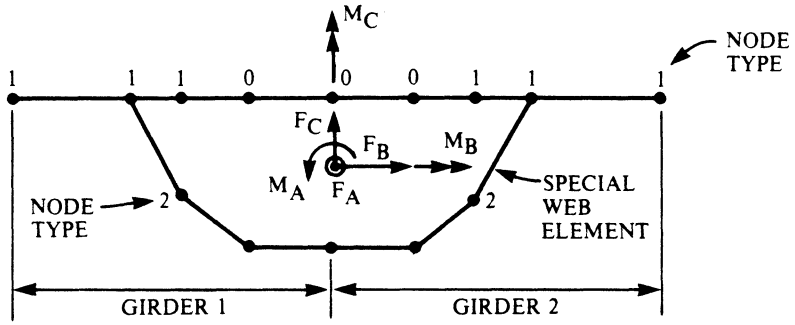

(b) CROSS-SECTION A-A

FIG. 6.7 REFERENCE POINT LOCATION AND SIGN CONVENTION FOR SECTIONAL FORCE RESULTANTS

(three forces and three moments) are output at the user's specified reference output point and output direction using stress results from either one string of elements or two adjacent strings of elements parallel to the section. The number of girders that make up the cross-section in which force resultants are computed is arbitrary. The only restriction is that the entire exterior web must be used as part of a girder. The user can specify up to ten individual girders in one section for the integrated forces output (Fig. 6.7).

6.7 Special Considerations for the Use of CELL4

In laying out the mesh for a structure, extreme care must be used to model the regions where shear stresses are discontinuous in the webs. In these regions a finer mesh must be used to achieve satisfactory results. The deck elements should be as rectangular as possible and large aspect ratios or excessive distortion of the element should be avoided. The nodal numbering sequence which gives a minimum nodal difference within an element should always be used.

In modelling the tendon, care must be used to avoid using too coarse a mesh for the structure, resulting in a tendon that crosses a given element more than twice. If this is the case, automatic tendon generation schemes should not be used, and those tendon points should be input directly.

Stress averaging should be used with care because there are many instances where the stresses are physically discontinuous. Averaging of membrane forces should not be done whenever the adjoining elements have unequal thicknesses.

When using two adjacent strips of elements to calculate the sectional force resultants, the elements so selected must lie side by side with a common boundary as shown in Fig. 6.7. The total number of elements must be an even number.

When integrating the internal sectional forces, it is best to use a section which almost lies perpendicular to the longitudinal direction. Highly

skewed sections or sections with adjacent elements having odd shapes or poor aspect ratios are poor choices for sectional force integration.

7. NUMERICAL EXAMPLES

In this chapter, six numerical examples, which demonstrate the capabilities of the new computer programs MUPDI4, CURDI4 and CELL4, are presented. Several of the examples are analyzed by more than one of the above programs so that the numerical results obtained can be compared and the different techniques required for interpretation discussed. Statical checks are also made to verify the results.

For each example, the following items are presented briefly: (1) purpose of the example; (2) structure geometry, prestressing and load cases; (3) analytical models used in the computer analyses; (4) summary and discussion of the numerical results; and (5) conclusions.

A complete list of all the input data used for all of the examples is given in Appendix E. A careful study of this input data together with the input instructions given in Appendices B, C and D for MUPDI4, CURDI4 and CELL4 should be very useful in implementing the programs. Details regarding the analytical models such as nodal point numbering, element numbering, etc. used in the examples can only be determined from a study of the input data given in Appendix E.

Finally, the examples demonstrate where care should be used in modeling the structure analytically and in interpreting certain results.

7.1 Example 1 - Simply Supported Straight Single-Cell Box Girder Bridge with Curved Exterior Webs

This example has been chosen to demonstrate the capability of CELL4 and MUPDI4 in modelling a box girder bridge with curved exterior webs, and the accuracy of CELL4 in predicting the behavior of such a bridge. For these purposes, the finite element analysis results from CELL4 are compared with those from MUPDI4, which is known to give accurate results for this example.

7.1.1 Structure Geometry and Load Cases

A straight single cell two lane box girder bridge (Fig. 7.1.1) with a total top deck width of 30 ft. and a single simple span of 162 ft., simply supported at the two ends by rigid end diaphragms and having curved exterior longitudinal webs, was chosen for the analysis.

The cross-section (Fig. 7.1.1a) had the following section properties: distances from the cgc of the section to the fibers at the mid-thickness of the top and bottom slabs of c_t = 1.996 ft and c_b = 3.654 ft; cross-sectional area A = 59.03 ft^2 and moment of inertia about cgc I = 314.56 ft^4.

The concrete material properties were: modulus of elasticity E = 3600 ksi; Poisson's ratio ν = 0.15; and unit weight density w = 155 pcf giving a dead load of the bridge of 9.15 kips per longitudinal ft.

The bridge was subjected to two different loading conditions (Fig. 7.1.1):

Case 1 - Dead load of the bridge.

Case 2 - AASHTO lane live load without impact and lane reduction factors acting on a single lane.

7.1.2 Analytical Models

The analytical models used for both the CELL4 and the MUPDI4 analyses are shown in Figs. 7.1.2 and 7.1.3. Note that the actual curved exterior web was discretized by a series of flat elements in all cases.

The effects of the discretized geometry for the curved webs on the

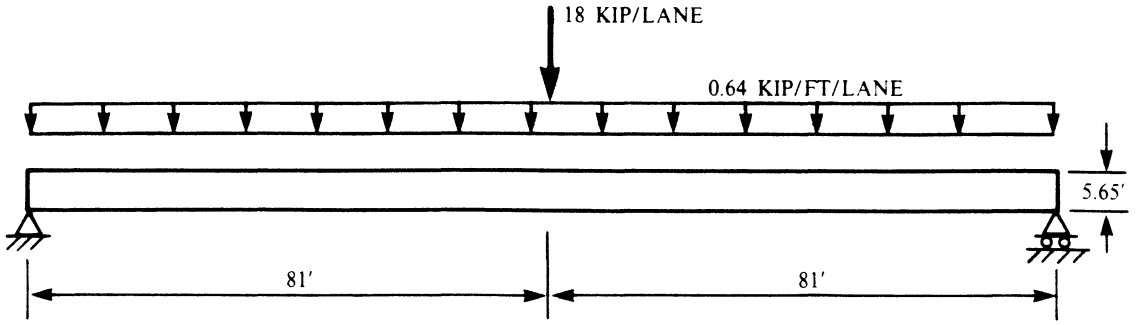

(a) ELEVATION AND AASHTO LANE LIVE LOAD

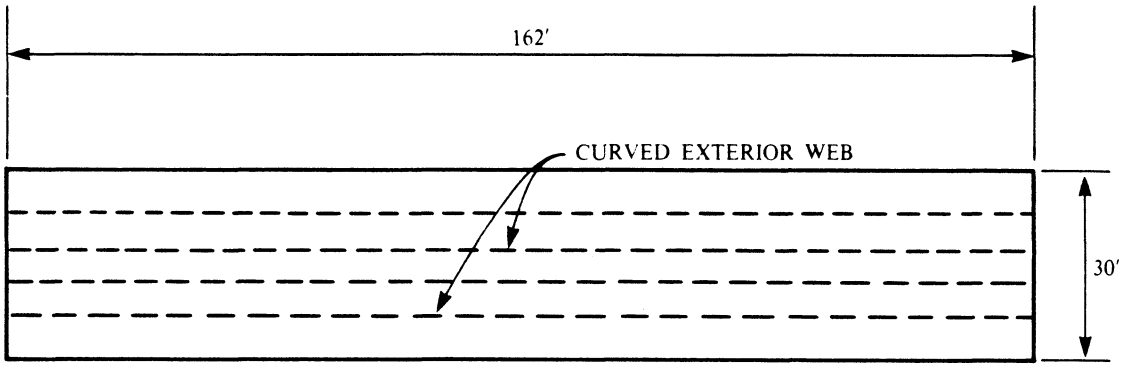

(b) PLAN

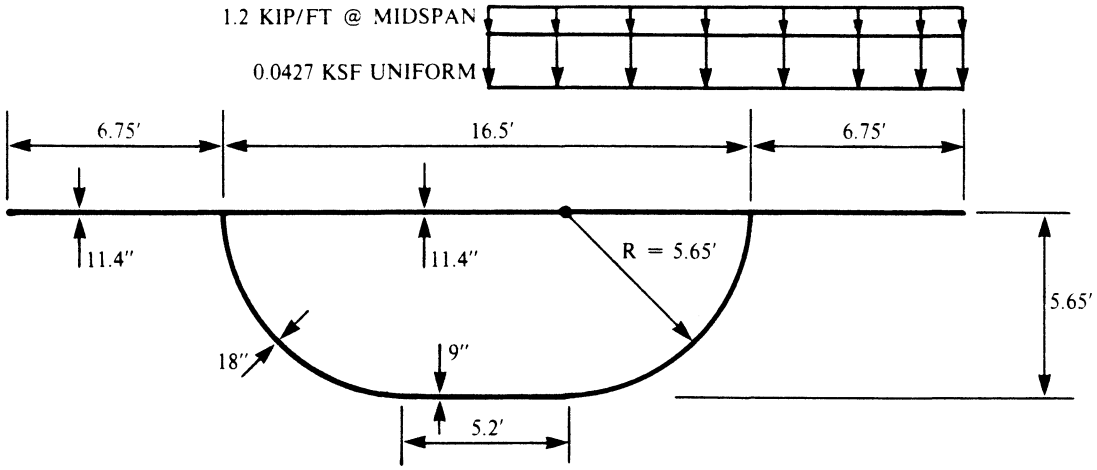

(c) CROSS-SECTION AND AASHTO LANE LIVE LOAD

FIG. 7.1.1 GEOMETRY AND LOADINGS FOR SINGLE CELL BOX GIRDER BRIDGE WITH CURVED EXTERIOR WEBS

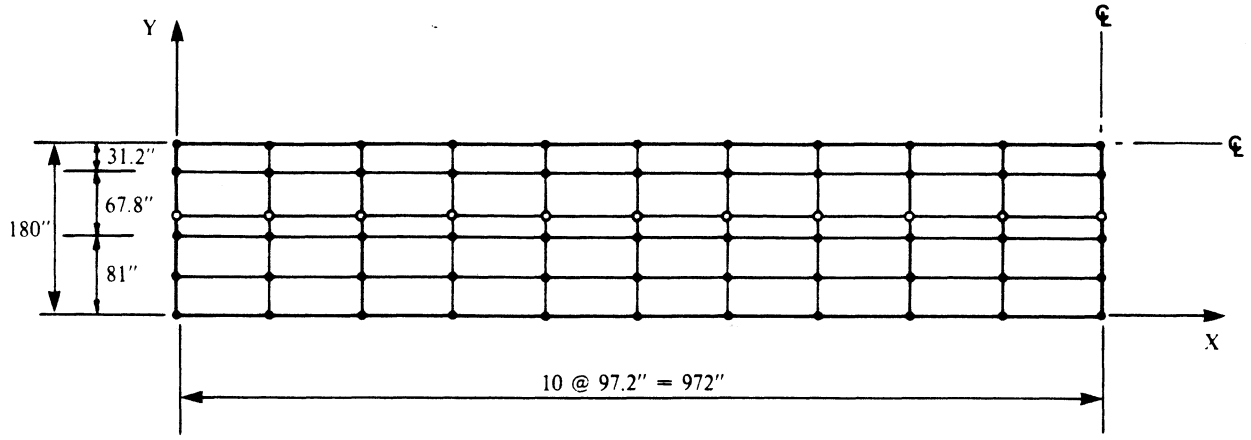

(a) PLAN OF COARSE MESH 1 FOR CELL4

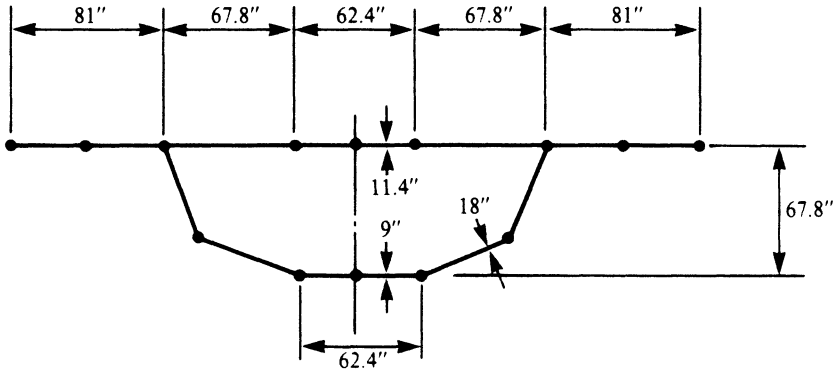

(b) CROSS-SECTION OF COARSE MESH 1 FOR CELL4

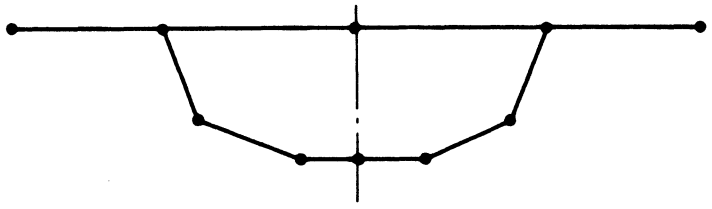

(c) CROSS-SECTION OF COARSE MESH 1 FOR MUPDI4

FIG. 7.1.2 ANALYTICAL MODEL 1 FOR SINGLE CELL BOX WITH CURVED EXTERIOR WEBS

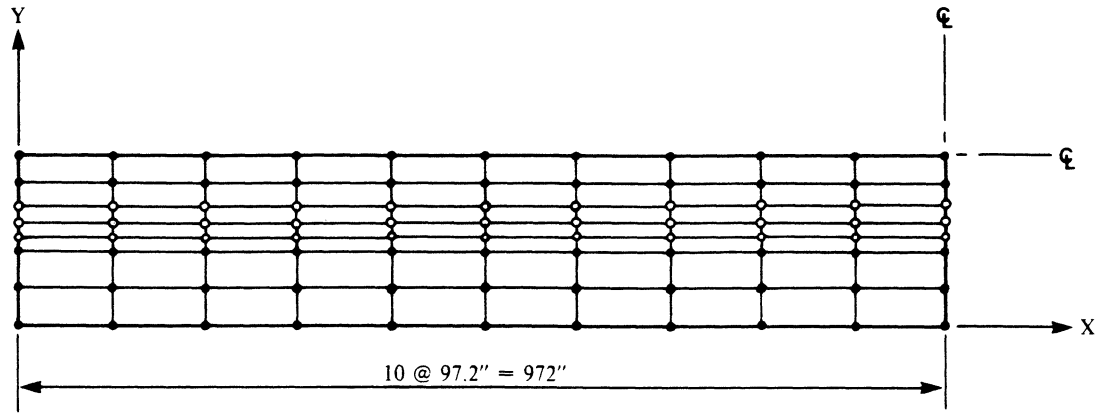

(a) PLAN OF FINE MESH 2 FOR CELL4

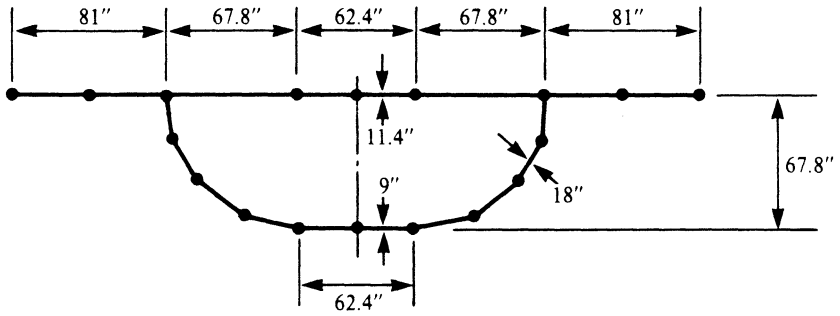

(b) CROSS-SECTION OF FINE MESH 2 FOR CELL4

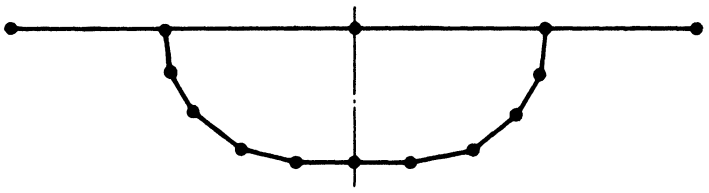

(c) CROSS-SECTION OF FINE MESH 2 FOR MUPDI4

FIG. 7.1.3 ANALYTICAL MODEL 2 FOR SINGLE CELL BOX WITH CURVED EXTERIOR WEBS

analytical results was also studied using two different mesh layouts for the curved webs, designated as coarse mesh model 1 (Fig. 7.1.2) and fine mesh model 2 (Fig. 7.1.3). Models 1 and 2 are identical except they use two and four web elements, respectively, in modelling each curved exterior web.

The end diaphragms in MUPDI4 are rigid, while in CELL4 they are modelled using a coarse mesh of triangular elements in order to investigate this diaphragm modelling effect on the CELL4 results. 100 Fourier Series terms are used in the MUPDI4 analysis.

7.1.3 Discussion of Results

7.1.3.1 Case 1 - Dead Load

Under dead load, the longitudinal stresses σ_x from CELL4 and MUPDI4 are in good agreement for the two curved web models 1 and 2 (Fig. 7.1.4) The stresses are almost uniform across the top and bottom decks of the bridge and are close to those predicted by beam theory, which gives midspan stresses of -1323 psi and +2421 ksi at the mid-thicknesses of the top and bottom deck slabs, respectively.

The transverse bending moments M_y (Fig. 7.1.5) from CELL4 and MUPDI4 are also in good agreement for the fine mesh model 2, but the comparison is not as good for coarse mesh model 1. The largest discrepancy occurs in the exterior curved webs (Fig. 7.1.5).

The membrane shear stresses, τ_{xy} (Fig. 7.1.6) in the curved webs give unsatisfactory agreement between CELL4 and MUPDI4 for coarse mesh model 1, but indicate improvement in fine mesh model 2. It should be noted that those shear stress values obtained by averaging of nodal quantities from adjacent elements in CELL4 give a good representation of the actual shear stress. It is therefore necessary to use more deck elements along with nodal stress averaging in CELL4 to capture a better representation of the membrane shear stress distribution in the top and bottom decks.

For statical control, and to perform equilibrium checks, the longitudinal variation of the total section bending moment and the vertical

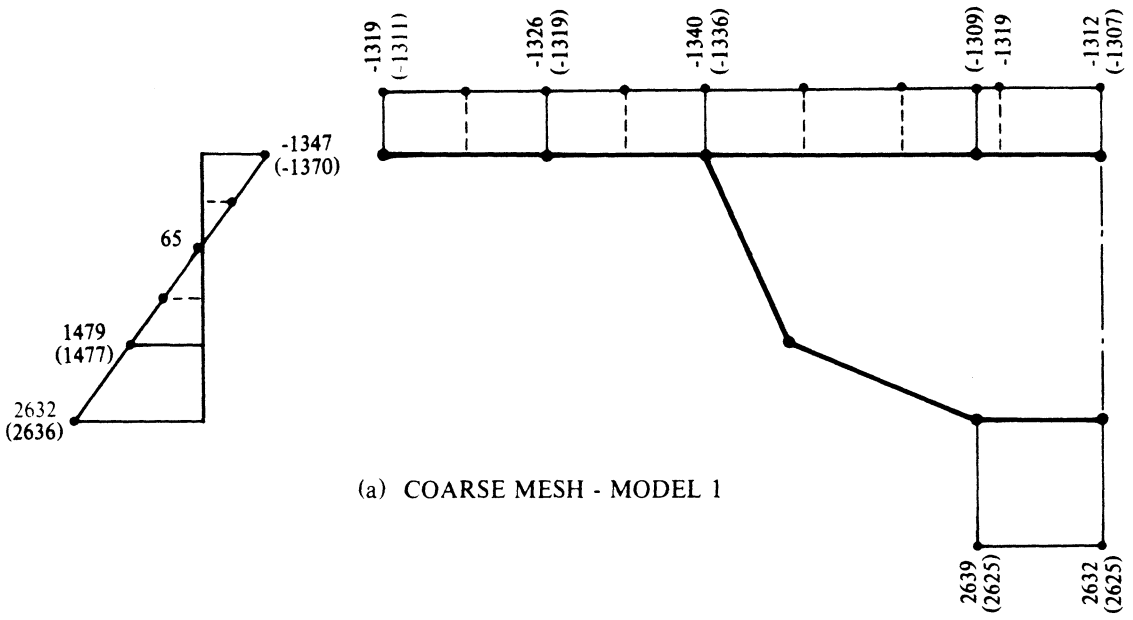

(a) COARSE MESH - MODEL 1

MUPDI4 xxx ------

CELL4 (xxx) ——————

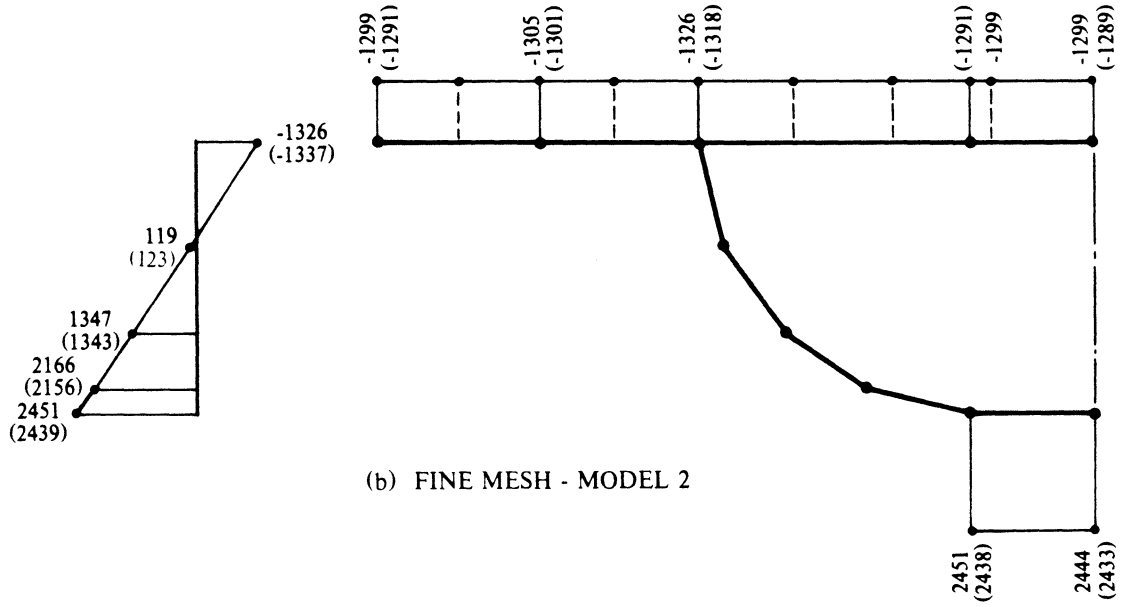

(b) FINE MESH - MODEL 2

FIG. 7.1.4 MIDSPAN LONGITUDINAL MEMBRANE STRESSES σ_x (psi) FOR DEAD LOAD

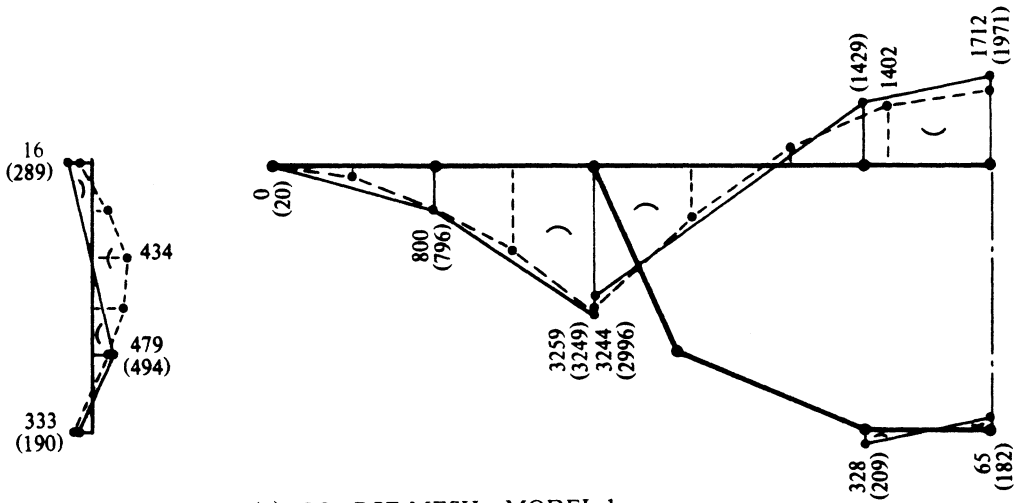

(a) COARSE MESH - MODEL 1

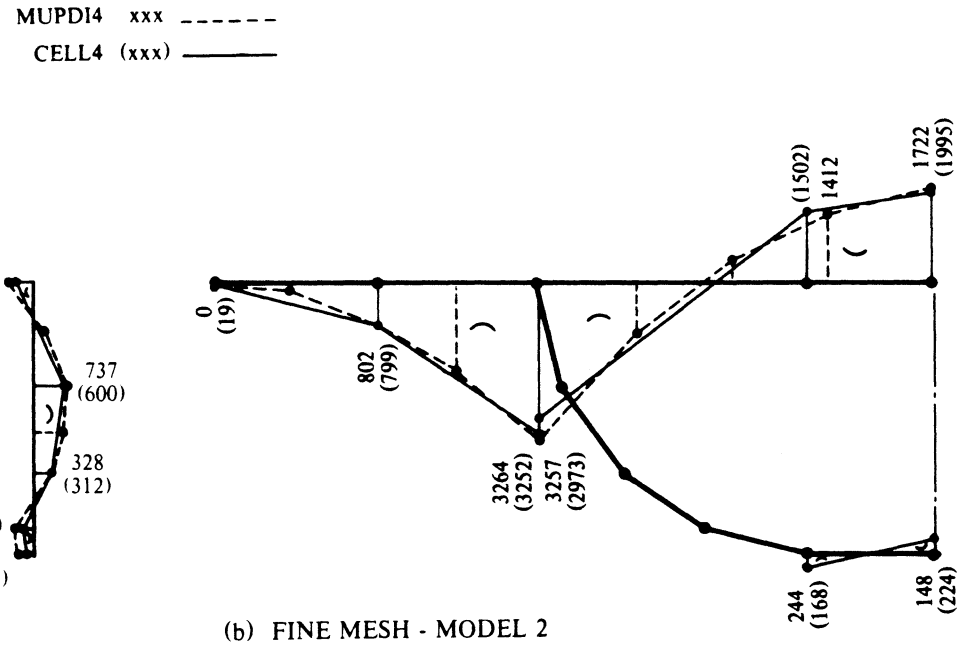

(b) FINE MESH - MODEL 2

FIG. 7.1.5 MIDSPAN TRANSVERSE MOMENTS M_y (in-lb/in) FOR DEAD LOAD

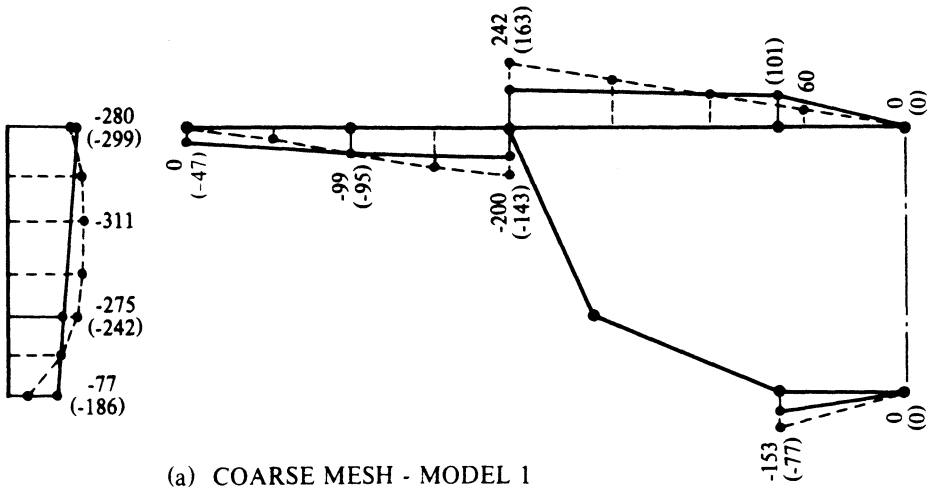

(a) COARSE MESH - MODEL 1

MUPDI4 xxx
CELL4 (xxx)

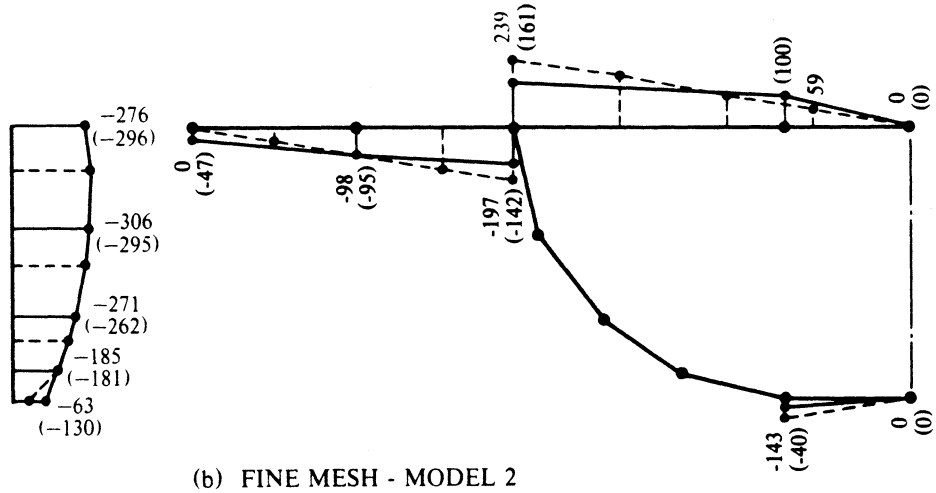

(b) FINE MESH - MODEL 2

FIG. 7.1.6 MEMBRANE SHEAR STRESSES τ_{xy} (psi) AT A SECTION NEAR THE SUPPORT X = 8.1 ft FOR DEAD LOAD

TABLE 7.1.1 TOTAL SECTION BENDING MOMENTS (FT-KIPS) AND VERTICAL SHEAR FORCES (KIPS) FOR DEAD LOAD

DISTANCE FROM SUPPORT	MOMENT (FT-KIPS)			SHEAR (KIPS)		
(FT)	BEAM THEORY	MUPDI4	CELL4	BEAM THEORY	MUPDI4	CELL4
(1)	(2)	(3)	(4)	(5)	(6)	(7)
0	0	0	2828	741	729	641
8.1	5702	5690	5540	667	660	636
16.2	10804	10777	10447	593	587	588
24.3	15306	15267	14878	518	514	508
32.4	19208	19158	18710	445	441	437
40.5	22510	22450	21951	370	367	364
48.5	25210	25144	24605	296	294	291
56.7	27311	27239	26668	222	220	218
64.8	28812	28735	28141	148	147	146
72.9	29712	29633	29026	74	73	73
81.0	30012	29932	29320	0	0	0

shear force resultant at various sections along the span were calculated automatically in CELL4 and in MUPDI4 by integrating the appropriate stress components from the plate elements, and the results are tabulated and compared with beam theory results in Table 7.1.1. Note for the dead load case, results are symmetrical about vertical planes through the midspan and midwidth of the bridge. Beam theory results provide values which satisfy statics.

The correlations of results from MUPDI4 and beam theory are generally good, except at the locations of the two end diaphragms. The CELL4 (model 2) results which were obtained by integrating the internal stresses from two adjacent strings of elements, are also in good agreement with those from beam theory, provided that the integrated sections are at a short distance away from the end supports. For sections near the supports it is necessary to refine the mesh and use extrapolation procedures to obtain good agreement.

7.1.3.2 Case 2 - AASHTO Lane Live Load

The AASHTO lane live load on one lane of the bridge (Fig. 7.1.1) should yield results which are symmetrical about a vertical plane through the midspan of the bridge, but will yield results which are unsymmetrical about a vertical plane through the midwidth of the bridge. Thus the bridge is under a combination of bending, torsion and transverse distortion. The ability to model these basic deformation modes will form the basis for testing the accuracy of the CELL4 and MUPDI4 analytical models. While elementary beam theory cannot be used to predict the transverse distribution of stresses and displacement, it can still be used to check total section moments and vertical shears from CELL4 and MUPDI4 to see if they satisfy total statics. The transverse distribution of the vertical displacements (Fig. 7.1.7a) and the transverse bending moments (Fig. 7.1.7b) indicate satisfactory aggreement exists between the CELL4 (fine mesh model 2) and the MUPDI4 results. The agreement between the displacements is somewhat better than for transverse bending moments.

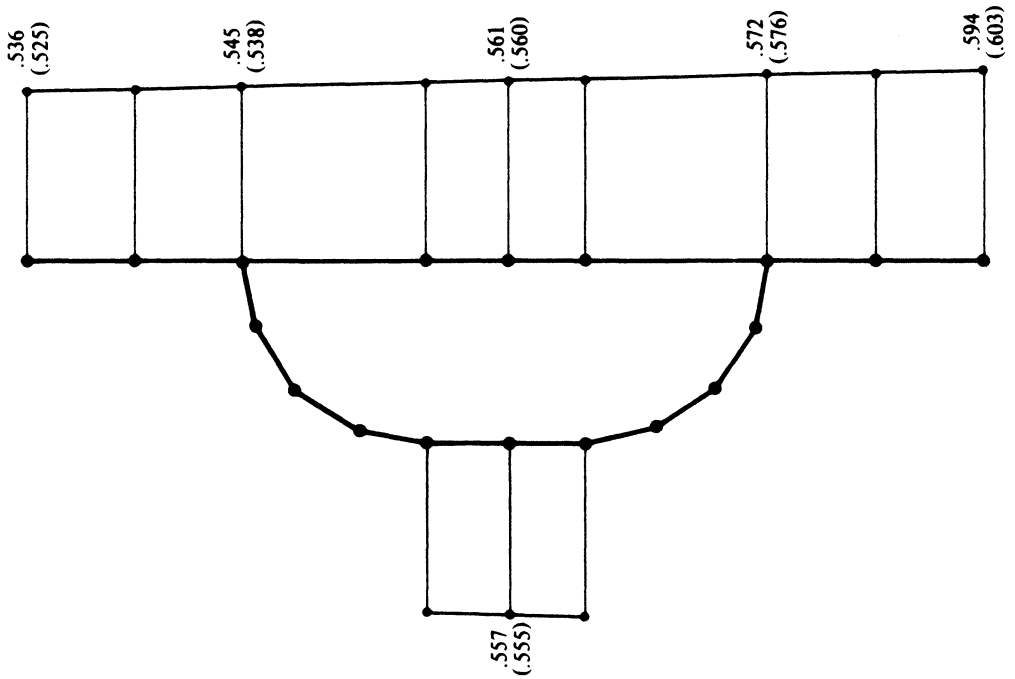

(a) VERTICAL DISPLACEMENT (in.)

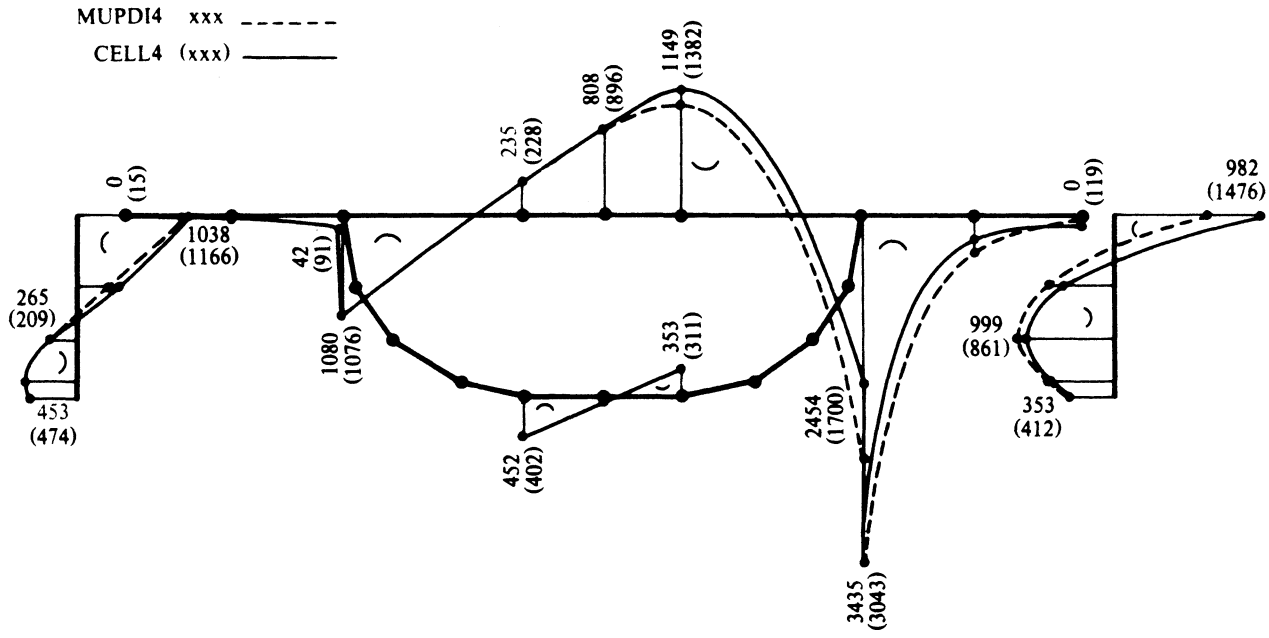

(b) TRANSVERSE BENDING MOMENT (in-lb/in)

FIG. 7.1.7 MIDSPAN VERTICAL DISPLACEMENTS (in.) AND TRANSVERSE MOMENTS M_y (in-lb/in) FOR UNSYMMETRICAL LANE LIVE LOAD USING FINE MESH MODEL 2

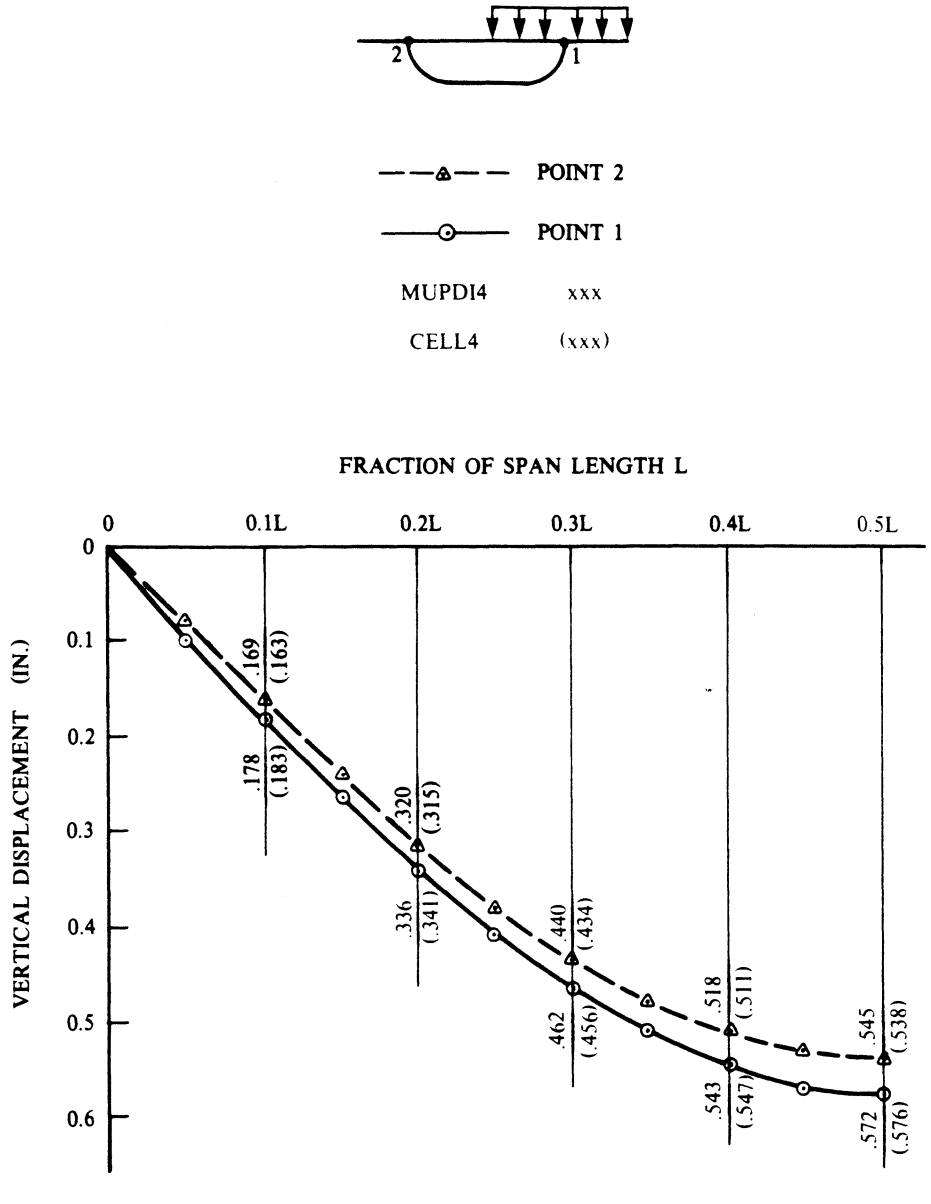

FIG. 7.1.8 LONGITUDINAL VARIATION OF VERTICAL DISPLACEMENTS AT TOPS OF WEBS 1 AND 2 FOR UNSYMMETRICAL LANE LIVE LOADING, USING FINE MESH MODEL 2.

TABLE 7.1.2 TOTAL SECTION BENDING MOMENTS (FT-KIPS), VERTICAL SHEAR FORCES (KIPS) AND TORSIONAL MOMENTS (FT-KIPS) FOR AASHTO SINGLE LANE LIVE LOAD

DISTANCE FROM SUPPORT	MOMENT (FT-KIPS)			SHEAR (KIPS)			TORQUE (FT-KIPS)	
(FT)	BEAM THEORY	MUPDI4	CELL4	BEAM THEORY	MUPDI4	CELL4	BEAM THEORY	CELL4
(1)	(2)	(3)	(4)	(5)	(6)	(7)	(8)	(9)
0	0	0	0	61	60	53	457	418
8.1	471	472	461	56	55	53	418	399
16.2	902	902	876	50	50	50	379	362
24.3	1289	1290	1258	45	45	44	340	324
32.4	1635	1636	1599	40	40	40	301	291
40.5	1939	1939	1897	35	35	34	262	250
48.6	2201	2201	2155	30	30	29	223	210
56.7	2420	2421	2372	25	24	24	184	176
64.8	2599	2599	2548	19	19	19	145	139
72.9	2735	2735	2679	14	14	13	106	96
81.0	2828	2823	2734	9	0	10	67	71

It can be observed in Figs. 7.1.7 and 7.1.8 that the box cross section is fairly stiff in resisting torsion, because only a small increase occurs in the vertical displacements on the loaded portion of the bridge as compared to the unloaded portion for this unsymmetrical loading.

Again the longitudinal variations of the total section bending moments, vertical shears, and torsional moments as given in Table 7.1.2 indicate good agreement between CURDI4 and CELL4 results and good statical checks with the results from beam theory, except near the end supports.

7.1.4 Conclusions

The analyses indicate that MUPDI4 and CELL4 can accurately predict the behavior of a box girder bridge with curved exterior webs. The modelling of the actual curved surface by a series of flat elements is justified by the fast rate of convergence in the results between coarse mesh model 1 and fine mesh model 2.

The actual number of flat elements required to model the entire depth of a given exterior web is a function of the curvature of the surface. Successive mesh refinement should be made in order to arrive at the final mesh layout for the exterior web. Generally, three to four elements are found to be sufficient to model a quarter circle.

The discretization of the diaphragm in CELL4 by a coarse mesh layout of triangular elements appears to have very little influence on the overall results. However, it is advisable to use a more regular mesh layout and avoid using triangular elements if possible.

7.2 Example 2 - Simply Supported Straight Single Cell Prestressed Box Girder Bridge with Vertical or Sloping Exterior Webs

This example demonstrates the capabilities of MUPDI4 and CELL4 in analyzing a straight, single cell, prestressed concrete bridge with either vertical or sloping exterior webs. Unlike Example 1, which had a curved exterior web, no discretization error is involved in modelling the web geometries in Example 2.

The capabilities of MUPDI4 and CELL4 to model longitudinal panel prestressing tendons in the webs and transverse slab tendons in the top slab are also illustrated. The results of the prestressing analyses can be used to compare the effects of the different modelling of the equivalent loads due to prestressing, by treating them as nodal loads in the finite element method used in CELL4 and as patch loads using the Fourier series of the harmonic analysis in MUPDI4.

7.2.1 Structure Geometry, Prestressing and Load Cases

The plan geometry of the bridge (Fig. 7.2.1) is similar to that of Example 1, with a total top deck width of 30 ft. and a single simple span of 162 ft., simply supported at the two ends by rigid end diaphragms.

The two cross-sections (Fig. 7.2.1) had identical section properties as follows: distances from the cgc of the section to the fibers at the mid- thickness of the top and bottom deck slabs of c_t = 1.941 ft and c_b = 3.709 ft; cross-sectional area A = 56.32 ft^2; and moment of inertia about the cgc I = 318.32 $ft.^4$

The concrete material properties were: modulus of elasticity E = 3600 ksi; Poisson's ratio ν = 0.15; and unit weight density w = 155 pcf giving a dead load of the bridge of 8.73 kips per longitudinal ft.

A total of five different loading cases were analyzed for each of the two cross-sections:

Case 1 - Dead load of the bridge.

Case 2 - A theoretical pair of AASHTO lane live loads (Fig. 7.2.2), antisymmetric about a vertical plane through the mid-width

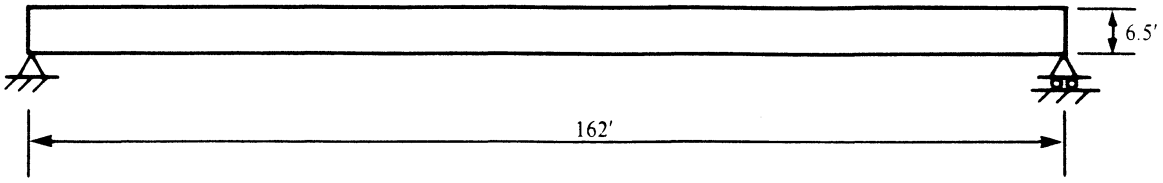

(a) ELEVATION

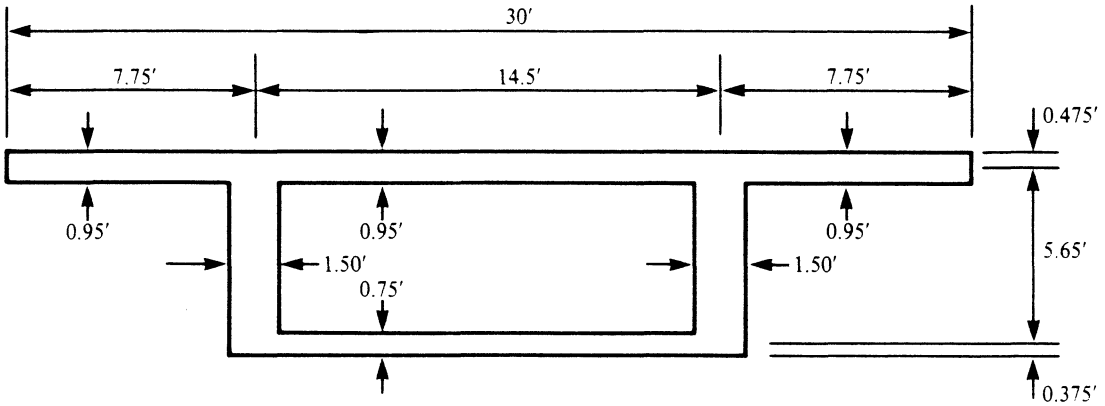

(b) VERTICAL WEB SECTION

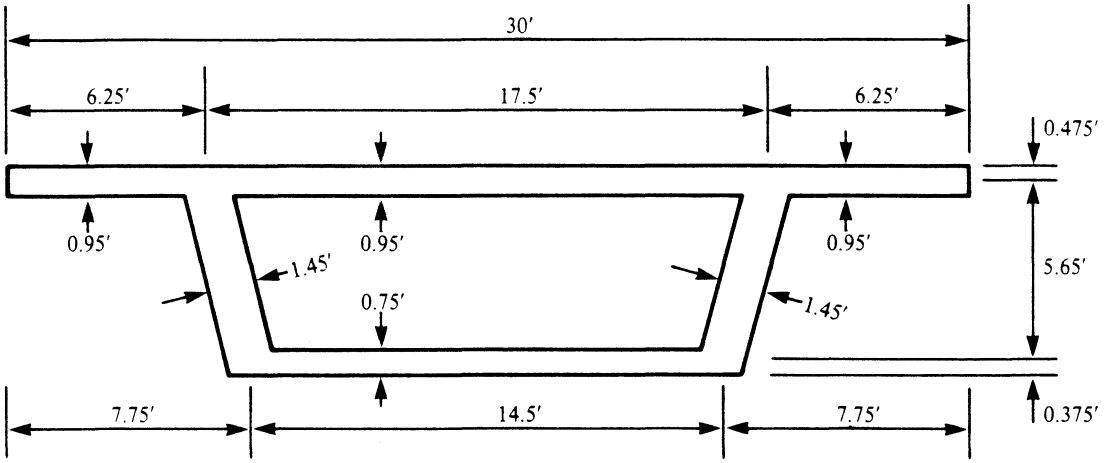

(c) SLOPING WEB SECTION

FIG. 7.2.1 GEOMETRY FOR SINGLE CELL BOX GIRDER BRIDGE WITH VERTICAL OR SLOPING EXTERIOR WEBS

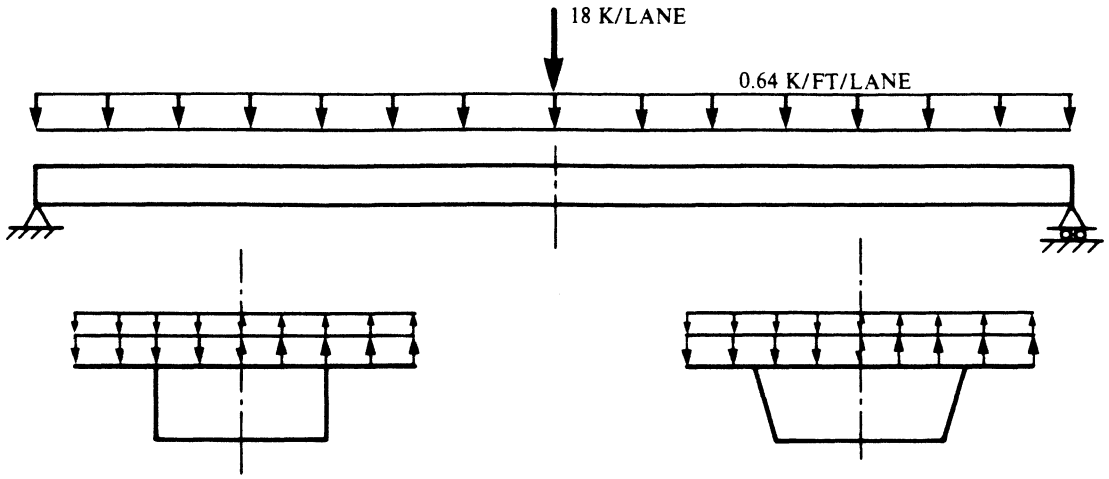

(a) ANTISYMMETRIC AASHTO LANE LIVE LOAD

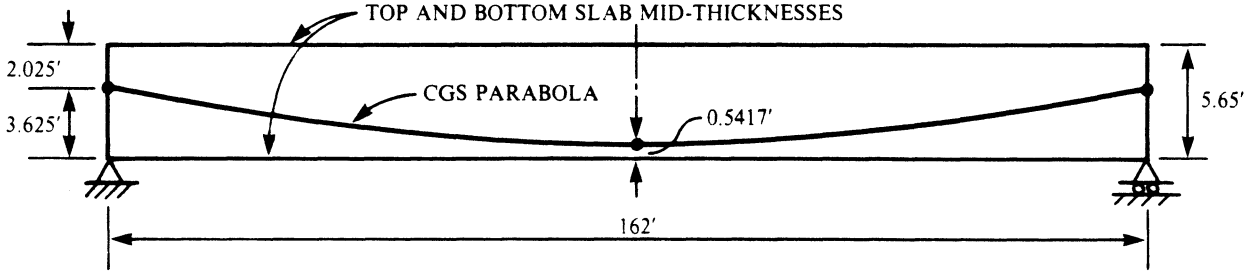

(b) LONGITUDINAL WEB PANEL TENDON PROFILE
(Not to Scale)

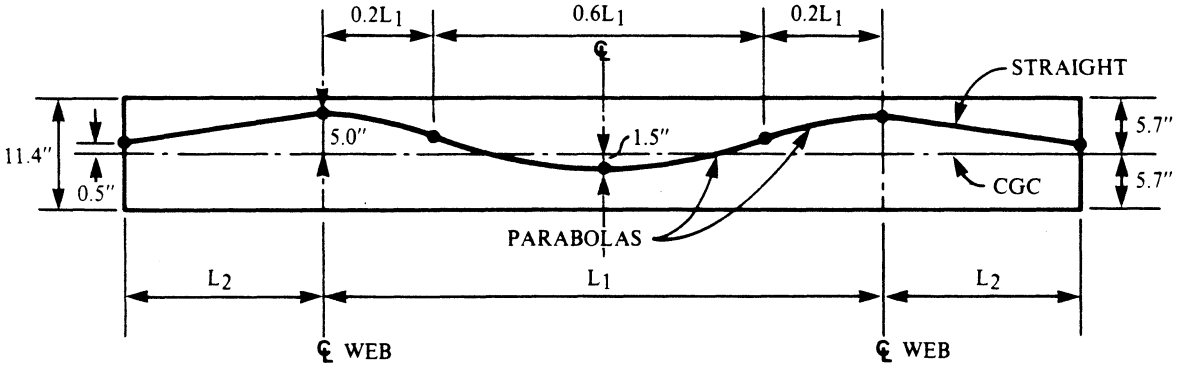

(c) TRANSVERSE TOP SLAB TENDON PROFILE
(Not to Scale)

FIG. 7.2.2 LOADINGS AND PRESTRESSING TENDON PROFILES

of the bridge.

Case 3 - Longitudinal prestressing by one panel tendon in each web, neglecting friction and anchor slip. Each tendon has a parabolic profile (Fig. 7.2.2) and a jacking force of 3640 kips per web.

Case 4 - Longitudinal prestressing by one panel tendon in each web, with the same tendon profile as in Case 3, but including friction and anchor slip. Symmetrical jacking forces from both ends of the bridge are 4266 kips per web. Wobble and curvature friction coefficients of $K = 0.0002/ft$ and $\mu = 0.25/radian$ and an anchorage set of 3/16 in. at each jacking end were assumed.

Case 5 - Transverse prestressing by slab tendons in the top slab (Fig. 7.2.2), neglecting friction, and spaced longitudinally to provide a transverse prestress force of 30 kips per longitudinal ft. of top slab.

7.2.2 Analytical Models

The analytical models for CELL4 and MUPDI4 analyses are shown in Fig. 7.2.3 and 7.2.4. Due to symmetry of the structure and the loadings, only one quarter of the structure was analysed by CELL4 utilizing symmetric boundary conditions for transversely symmetric loadings (Cases 1, 3, 4, 5) and antisymmetric boundary conditions for transversely antisymmetric loadings (Case 2. This resulted in a considerable saving of data input and computer effort by CELL4. For MUPDI4, the entire cross-section was used since the input was simpler and the computer effort was quite small.

Each web was modelled by one single element in both the CELL4 and MUPDI4 analytical models (Fig. 7.2.3 and 7.2.4), and the rigid end diaphragms were modelled as simply supported ends, where no vertical movement was permitted.

The actual dead (Case 1) and antisymmetric live (Case 2) loads and the prestressing loads (Case 3, 4, 5) were represented by statically

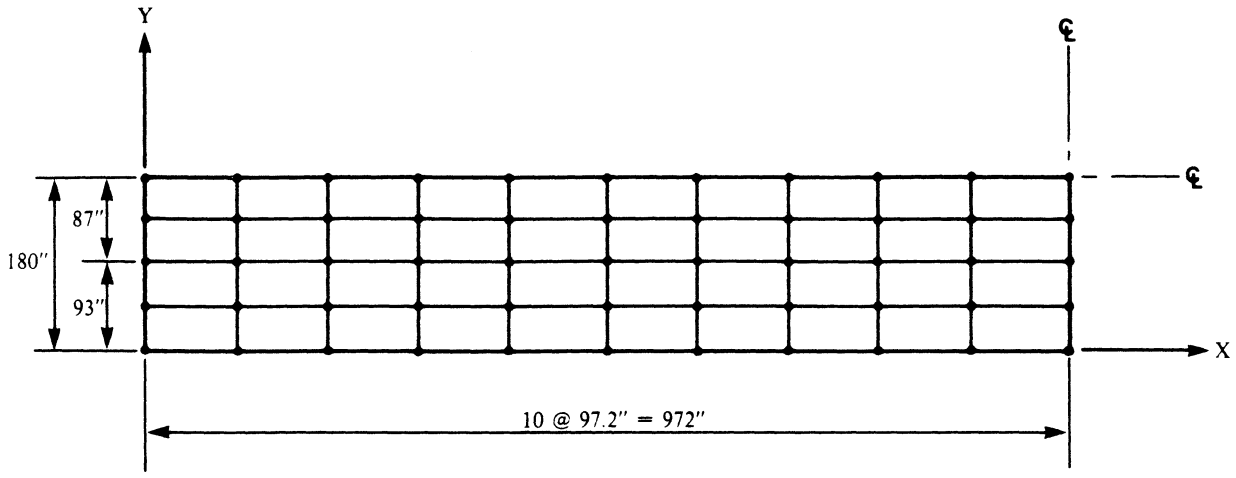

(a) PLAN OF MESH FOR CELL4

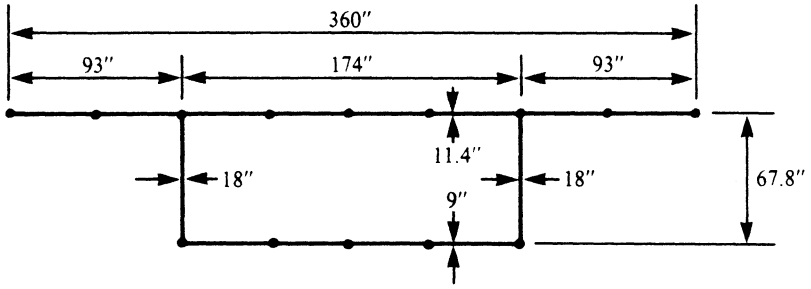

(b) CROSS-SECTION OF MESH FOR CELL4

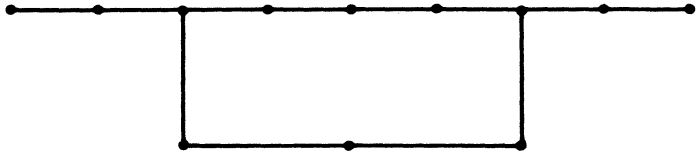

(c) CROSS-SECTION OF MESH FOR MUPDI4

FIG. 7.2.3 ANALYTICAL MODELS FOR SINGLE CELL BOX WITH VERTICAL EXTERIOR WEBS

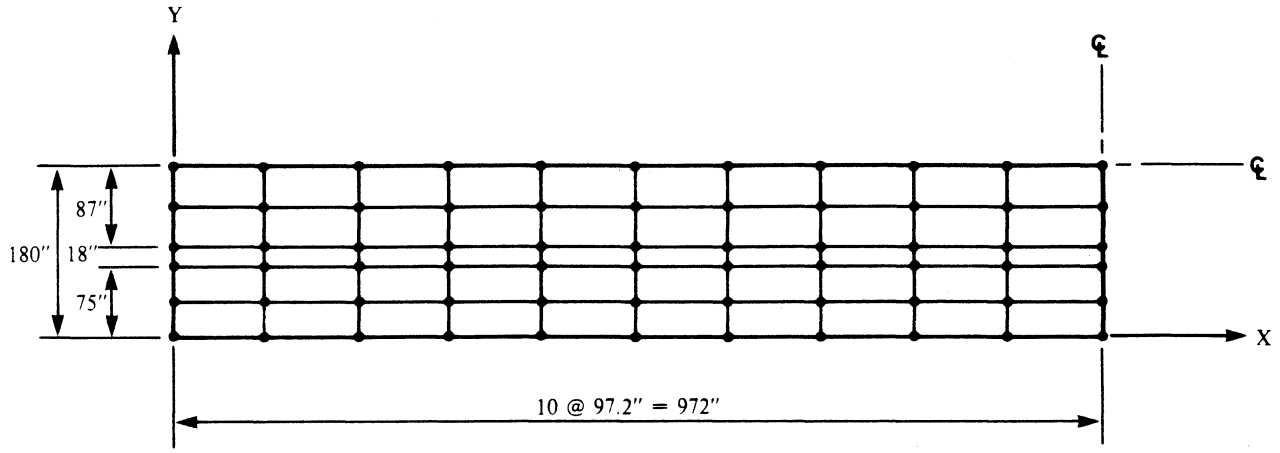

(a) PLAN OF MESH FOR CELL4

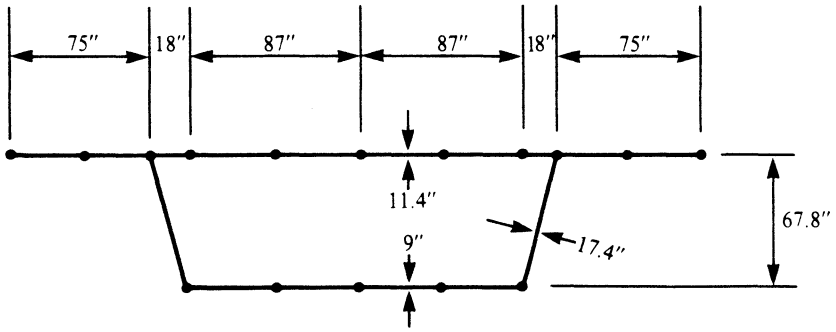

(b) CROSS-SECTION OF MESH FOR CELL4

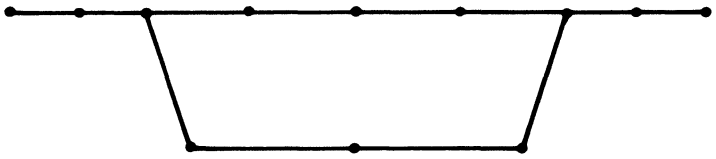

(c) CROSS-SECTION OF MESH FOR MUPDI4

FIG. 7.2.4 ANALYTICAL MODELS FOR SINGLE CELL BOX WITH SLOPING EXTERIOR WEBS

equivalent nodal loads in CELL4, whereas, patch loads were used for prestress loads and uniform surface loads were used to represent the dead and antisymmetric live load in MUPDI4. 100 Fourier Series terms were used in the MUPDI4 analyses.

For transverse prestressing in the top slab, a single slab tendon is used for every 8.1 ft of bridge length, with an equivalent jacking force of 243 kips (or 30 kips/ft). In order to simplify the input, the prestressing tendon profiles in the top slab and in the webs were input according to the parametric input described in Chapter 3 in both the MUPDI4 and CELL4 analyses.

7.2.3 Discussion of Results

7.2.3.1 Dead Load

Results for this load case 1 are symmetrical about vertical planes through the midspan and midwidth of the bridge. The transverse distributions of vertical displacements, the longitudinal membrane stresses and the transverse bending moments are shown in Figs. 7.2.5 and 7.2.6 for the two cross-sectional geometries. Good agreement between results from the CELL4 and MUPDI4 analyses can be noted. As expected, the vertical displacements and the longitudinal stresses are almost uniform across the width of the section indicating essentially elementary beam theory behavior, which gives longitudinal stresses of -1213 psi and +2317 psi at the top and bottom. In addition, the numerical results for the two cross-sectional geometries are very similar due to their identical moments of inertia. Some differences in the transverse bending moments occur because of different transverse spans of the top slabs between the webs for the two geometries.

For statical control, and to perform equilibrium checks, the longitudinal variation of the total section bending moment and the vertical shear force resultant at various sections were calculated in CELL4 and MUPDI4 by integrating the appropriate stress components from the plate elements, and the results are tabulated and compared with beam theory

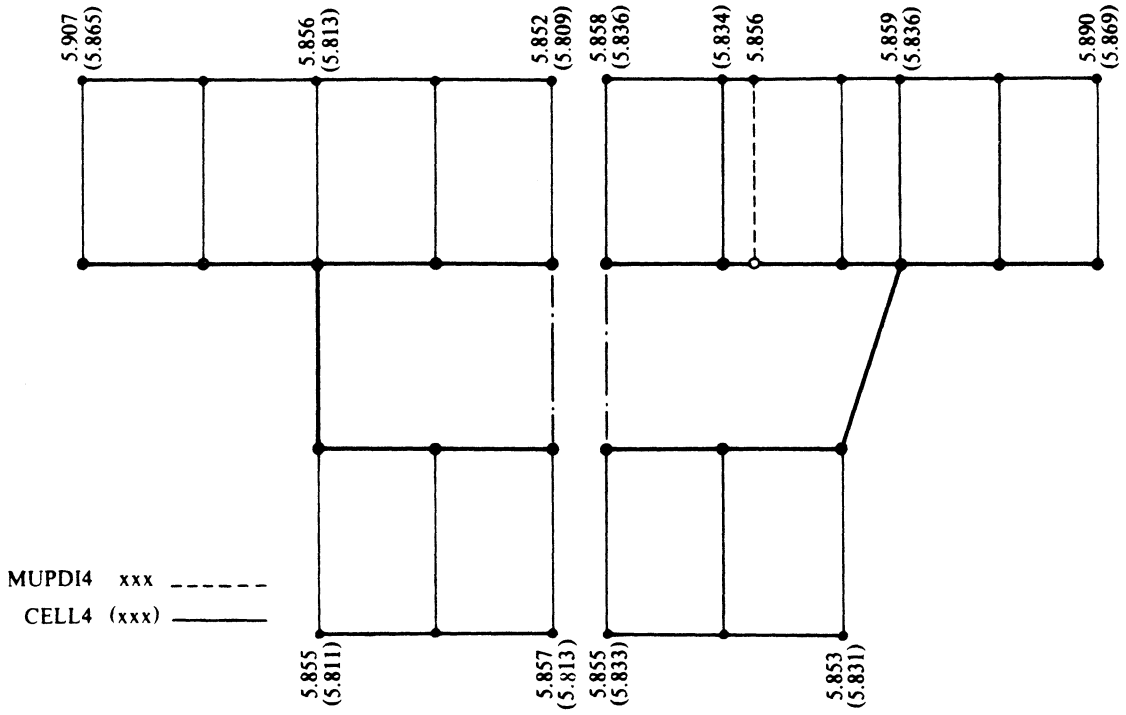

(a) MIDSPAN VERTICAL DISPLACEMENTS (in.)

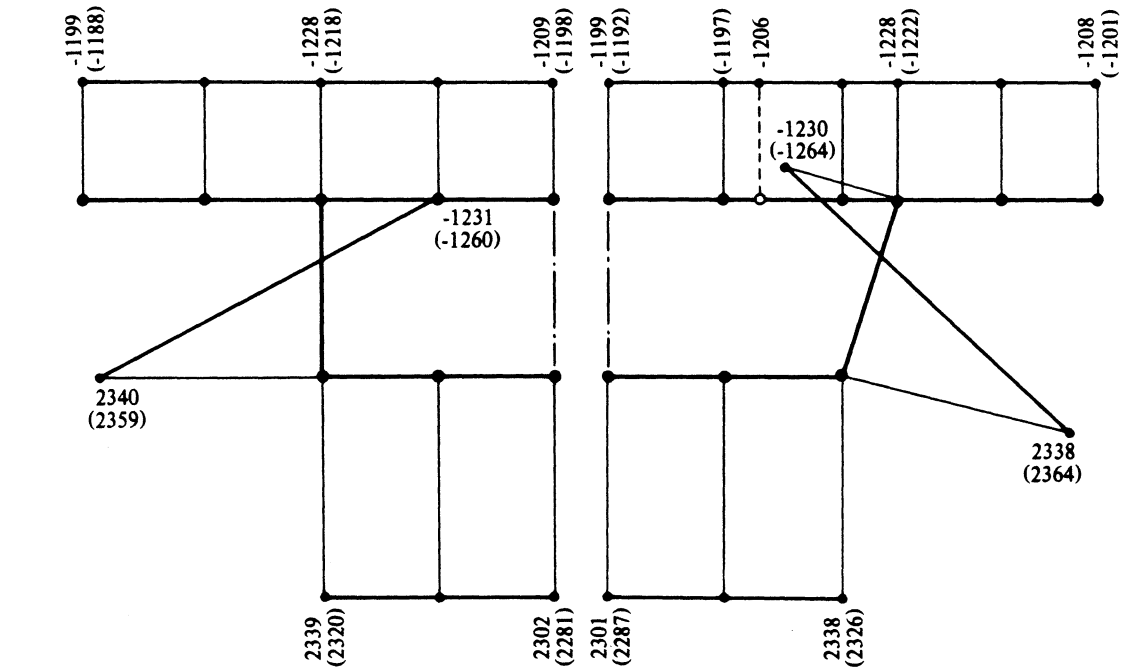

(b) MIDSPAN LONGITUDINAL MEMBRANE STRESSES σ_x (psi)

FIG. 7.2.5 DISPLACEMENTS AND LONGITUDINAL STRESSES FOR DEAD LOAD

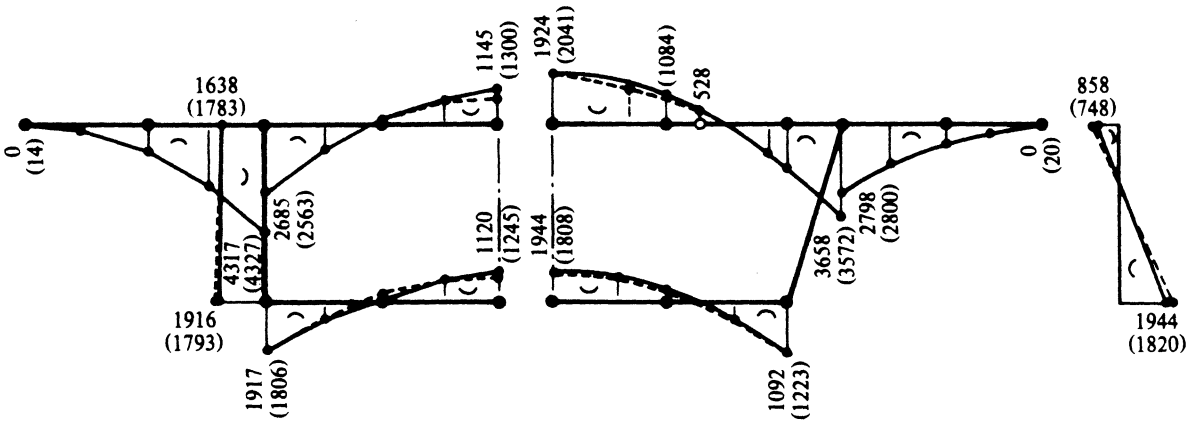

(a) MIDSPAN TRANSVERSE MOMENTS M_y (in-lb/in)

MUPDI4 xxx ------

CELL4 (xxx) ——————

FIG. 7.2.6 TRANSVERSE MOMENTS FOR DEAD LOAD

TABLE 7.2.1 TOTAL SECTION BENDING MOMENTS (FT-KIPS) AND VERTICAL SHEAR FORCES (KIPS) FOR DEAD LOAD

DISTANCE FROM SUPPORT	MOMENT (FT-KIPS)			SHEAR (KIPS)		
(FT)	BEAM THEORY	MUPDI4	CELL4	BEAM THEORY	MUPDI4	CELL4
(1)	(2)	(3)	(4)	(5)	(6)	(7)
0	0	0	0	707	698	642
8.1	5441	5446	5331	636	632	620
16.2	10309	10314	10096	566	563	562
24.3	14605	14610	14376	495	492	490
32.4	18329	18333	18078	424	422	420
40.5	21480	21484	21212	354	352	350
48.6	24056	24062	23775	283	281	280
56.7	26061	26066	25768	212	211	210
64.8	27494	27498	27192	141	141	140
72.9	28352	28357	28047	71	70	70
81.0	28639	28644	28330	0	0	0

results in Table 7.2.1. Beam theory results provide values which satisfy statics. Results shown in Table 7.2.1 are for the cross-section with sloping webs, but results for the cross-section with vertical webs were essentially the same. The correlation of results between MUPDI4, CELL4 and beam theory are generally good, except for CELL4 at locations near the end supports, where it is necessary to refine the mesh and use extrapolation procedures to get better agreements.

7.2.3.2 Antisymmetric Live Load

Results for this load case 2 are symmetrical and antisymmetrical, respectively, about vertical planes through the midspan and midwidth of the bridge.

The transverse distributions of vertical displacements, longitudinal membrane stresses and transverse moments at midspan are shown in Figs. 7.2.7 and 7.2.8 and for membrane shear stresses at a section 8.1 ft from the end support in Fig. 7.2.8. Agreement between CELL4 and MUPDI4 values are generally good. The MUPDI4 values, based on elasticity theory, can be considered to be very accurate. CELL4 values, based on the finite element method, are dependent on the mesh size used, especially for local effects such as the transverse slab moments. Also, a study of the membrane shear stresses for CELL4, Fig. 7.2.8 indicates the higher order special web element used for the sloping web gives better results than the spar web element used for vertical webs.

7.2.3.3 Longitudinal Prestressing Without Friction

Results for this load case 3 are symmetrical about vertical planes through the midspan and midwidth of the bridge.

The transverse distribution of the vertical displacements and longitudinal membrane stresses at midspan given in Fig. 7.2.9 indicate good agreement between CELL4 and MUPDI4, thus verifying the two different methods used to model the equivalent prestressing loads.

Again, the longitudinal variations of the total section bending moments and vertical shears as given in Table 7.2.2 indicate good agreement

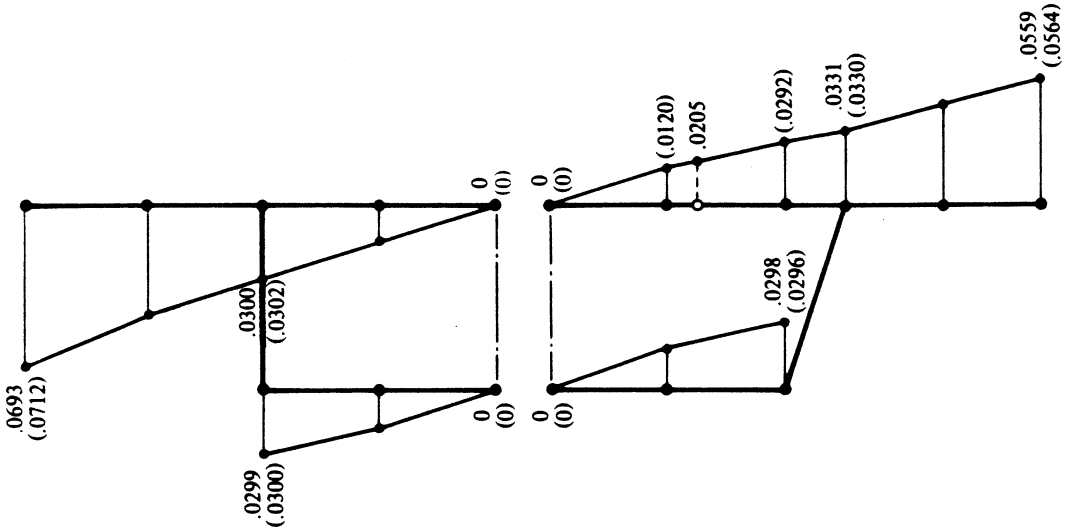

(a) MIDSPAN VERTICAL DISPLACEMENTS (in.)

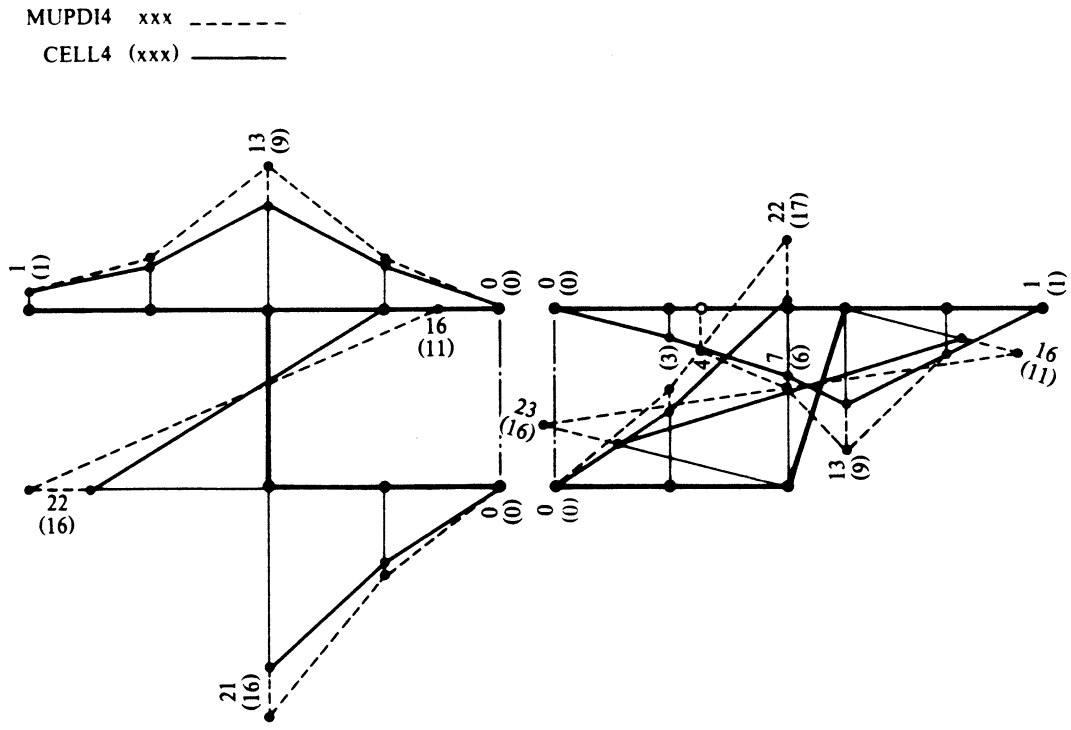

(b) MIDSPAN LONGITUDINAL MEMBRANE STRESSES σ_x (psi)

FIG. 7.2.7 DISPLACEMENTS AND LONGITUDINAL STRESSES FOR ANTISYMMETRIC LIVE LOAD

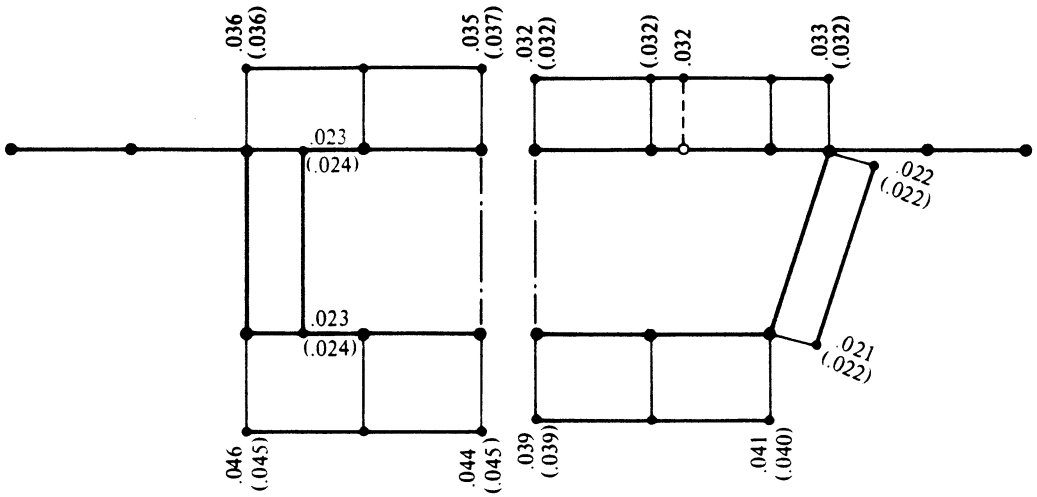

(a) MEMBRANE SHEAR STRESSES τ_{xy} (psi) AT x=8.1 ft.

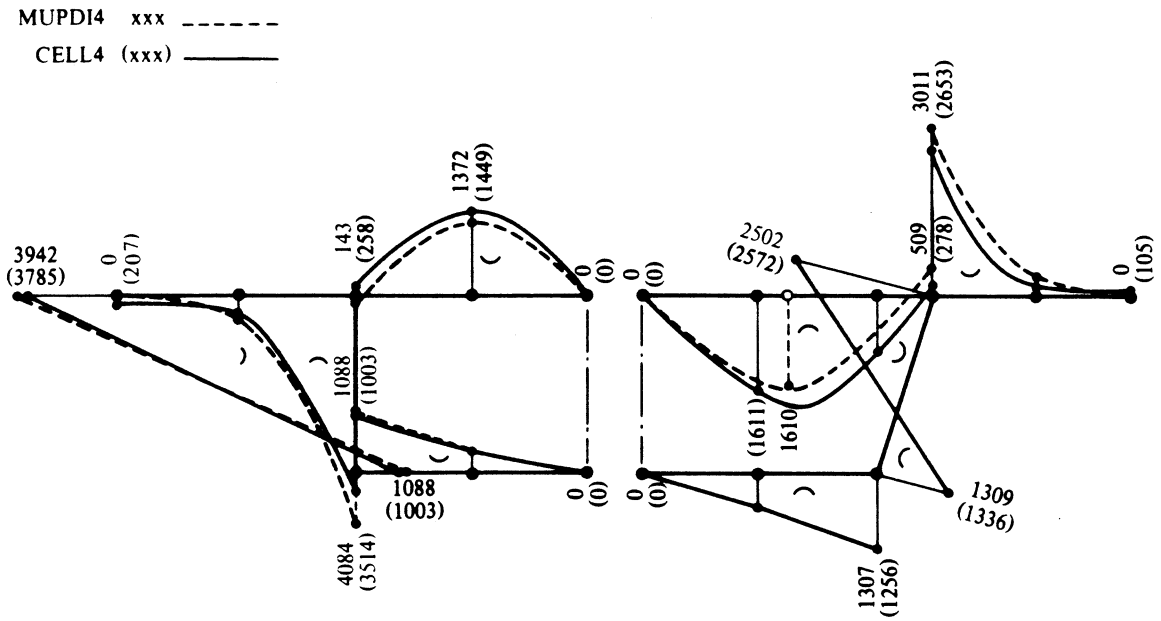

(b) MIDSPAN TRANSVERSE MOMENTS M_y (in-lb/in)

FIG. 7.2.8 SHEAR STRESSES AND TRANSVERSE MOMENTS FOR ANTISYMMETRIC LIVE LOAD

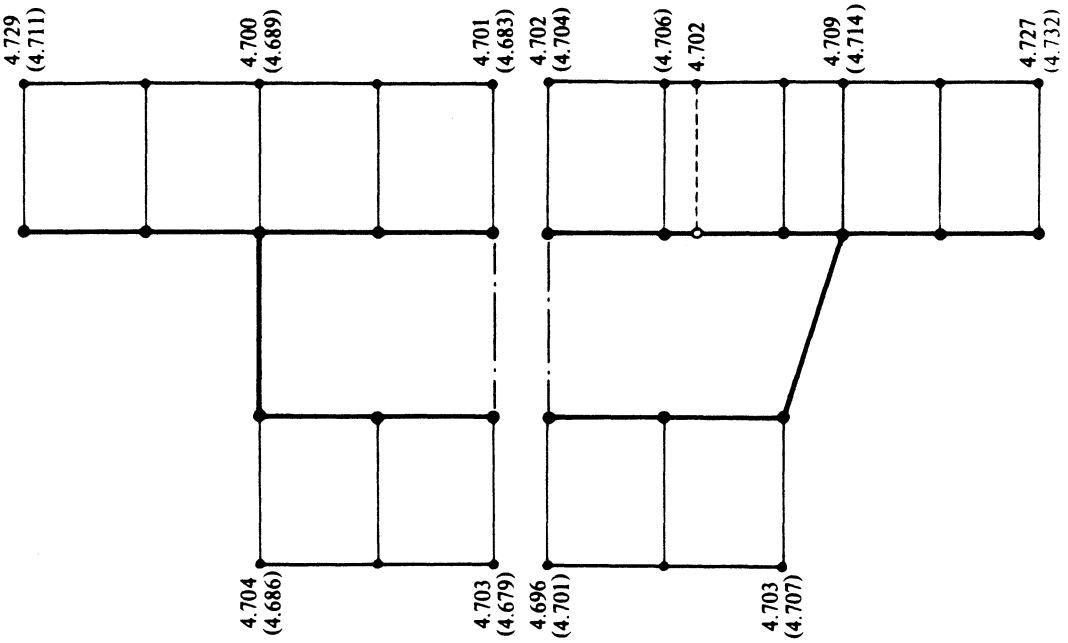

(a) MIDSPAN VERTICAL DISPLACEMENTS (in.)

MUPDI4 xxx ------
CELL4 (xxx) ——————

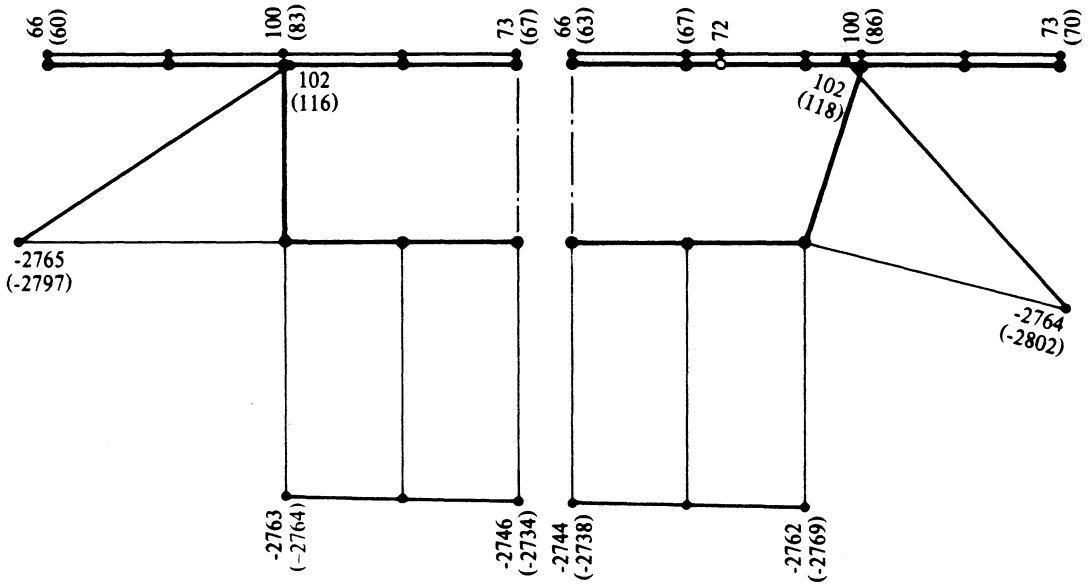

(b) MIDSPAN LONGITUDINAL MEMBRANE STRESSES σ_x (psi)

FIG. 7.2.9 DISPLACEMENTS AND LONGITUDINAL STRESSES FOR LONGITUDINAL PRESTRESSING WITHOUT FRICTION

TABLE 7.2.2 TOTAL SECTION BENDING MOMENTS (FT-KIPS) AND VERTICAL SHEAR FORCES (KIPS) FOR LONGITUDINAL PRESTRESSING WITHOUT FRICTION

DISTANCE FROM SUPPORT	MOMENT (FT-KIPS)			SHEAR (KIPS)		
(FT)	BEAM THEORY	MUPDI4	CELL4	BEAM THEORY	MUPDI4	CELL4
(1)	(2)	(3)	(4)	(5)	(6)	(7)
0	0	0	- 2537	-553	- 48	-502
8.1	- 3945	- 4817	- 4923	-498	-496	-486
16.2	- 7752	- 8619	- 8476	-442	-439	-440
24.3	-11110	-11989	-11833	-387	-385	-384
32.4	-14021	-14906	-14763	-332	-330	-328
40.5	-16484	-17380	-17215	-276	-275	-274
48.6	-18499	-19401	-19230	-221	-220	-220
56.7	-20066	-20978	-20795	-166	-165	-164
64.8	-21186	-22101	-21913	-111	-110	-110
72.9	-21857	-22778	-22585	- 55	- 55	- 54
81.0	-22082	-23002	-22810	0	0	- 28

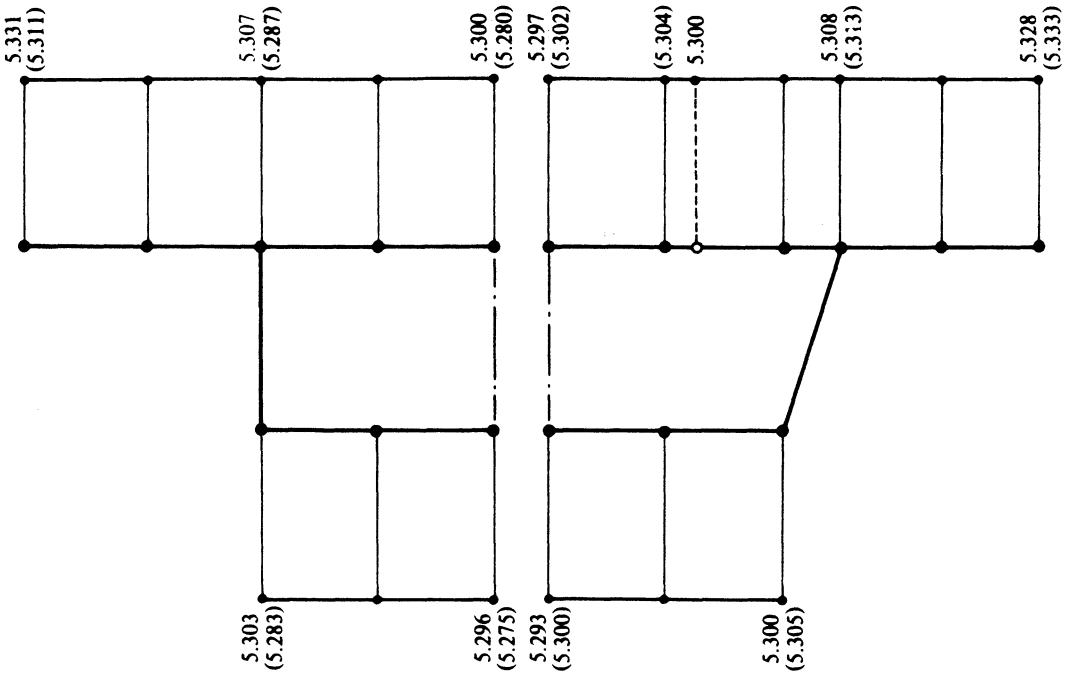

(a) MIDSPAN VERTICAL DISPLACEMENTS (in.)

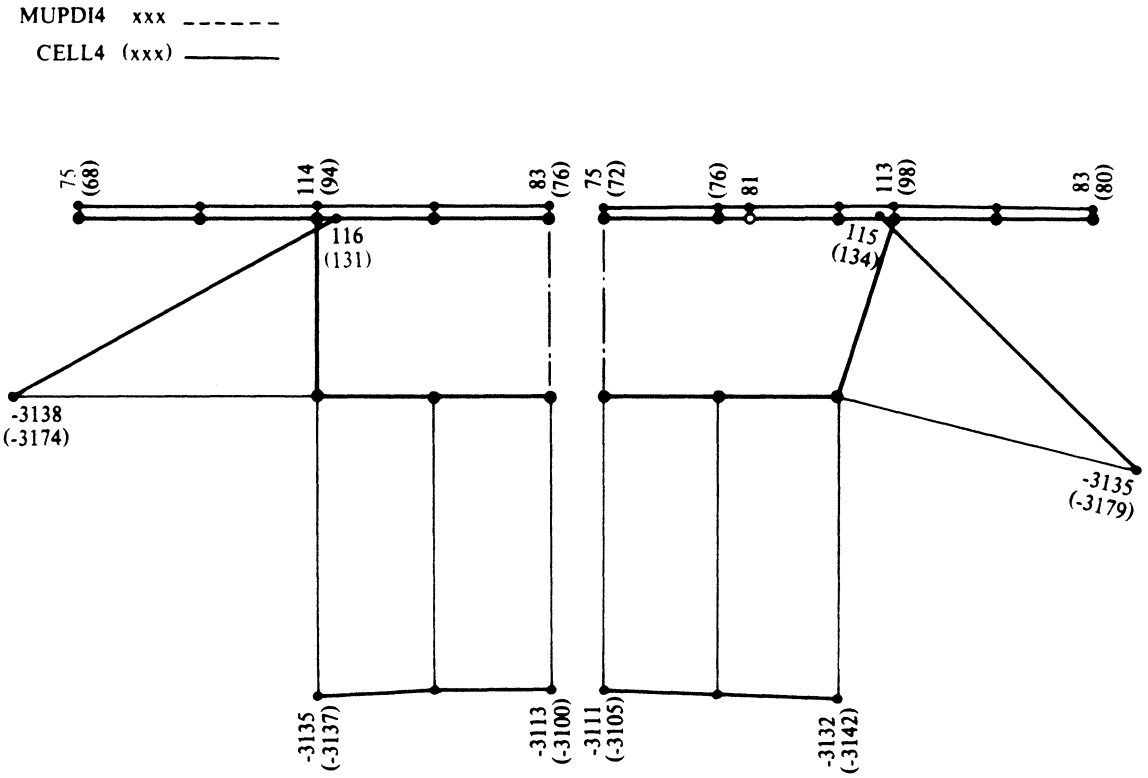

(b) MIDSPAN LONGITUDINAL MEMBRANE STRESSES σ_x (psi)

FIG. 7.2.10 DISPLACEMENTS AND LONGITUDINAL STRESSES FOR LONGITUDINAL PRESTRESSING WITH FRICTION

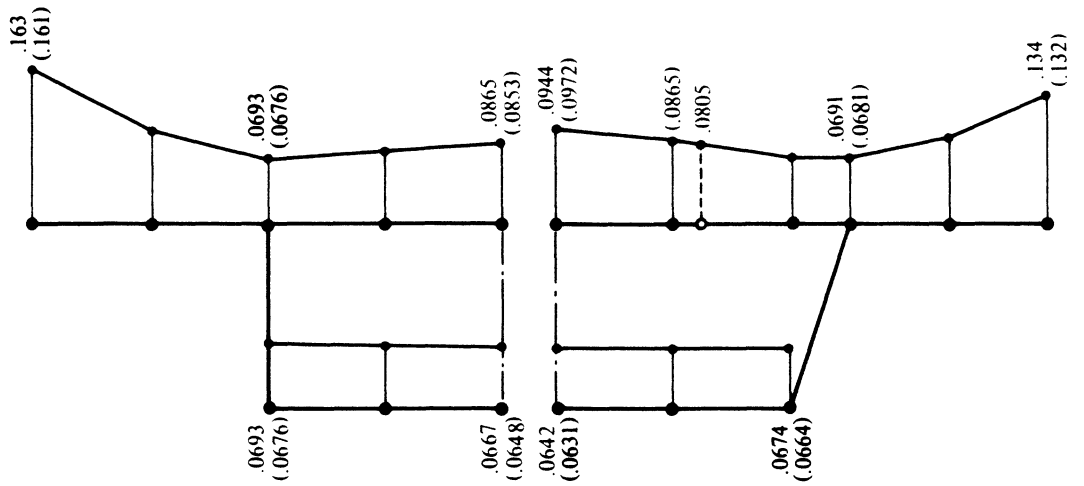

(a) MIDSPAN VERTICAL DISPLACEMENTS (in.)

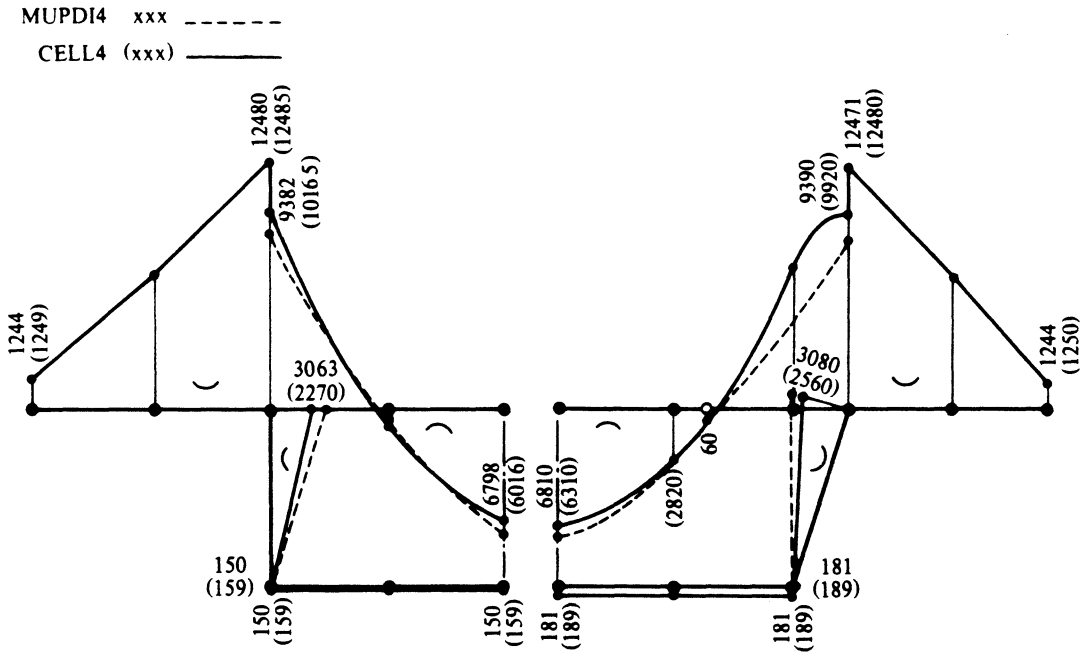

(b) MIDSPAN TRANSVERSE MOMENTS M_y (in-lb/in)

FIG. 7.2.11 DISPLACEMENTS AND TRANSVERSE MOMENTS FOR TRANSVERSE SLAB PRESTRESSING WITHOUT FRICTION

between CELL4 and MUPDI4 results and good statical checks with the results from beam theory except near the end supports. Results for section moments and shears for both cross-sections were essentially the same.

7.2.3.4 Longitudinal Prestressing with Friction

This load case 4 tests the ability of the two programs to account for friction and anchor set.

Good agreement between CELL4 and MUPDI4 values of vertical displacements and longitudinal stresses at midspan can be seen in Fig. 7.2.10.

7.2.3.5 Transverse Slab Prestressing Without Friction

This load case 5 tests the ability of the two programs to model local bending due to top slab transverse prestressing. The equivalent prestress loads for this case (Fig. 7.2.2) are self equilibrating for any transverse slab strip.

The transverse distribution of vertical displacements and transverse moments at midspan are shown in Fig. 7.2.11, and indicate satisfactory agreement between CELL4 and MUPDI4 values. Better agreement could be achieved by refining the mesh size used in CELL4.

7.2.4 Conclusions

The analyses indicate that MUPDI4 and CELL4 can satisfactorily predict the behavior of a box girder bridge with vertical or sloping exterior webs, subjected to dead load, live load, and longitudinal or transverse prestressing.

Agreement between the two programs is best for displacements, longitudinal stresses and section moments and shears. If local effects such as slab moments or stress concentrations are of interest they must be carefully interpreted and the mesh layout used in CELL4 for external loads and prestressing must be refined. Results from more than one mesh size may be necessary to achieve a desired accuracy.

7.3 Example 3 - Two Span Straight Four-Cell Prestressed Box Girder Bridge with Vertical Exterior Webs

This example demonstrates the capabilities of the MUPDI4, CURDI4, and CELL4 computer programs in analyzing a realistic prestressed concrete multi-cell box girder bridge under general loadings, and allows a comparison of the results of the three programs for such a structure. Differences in the results of the programs, as well as different techniques required for interpretation of the results in order to provide the displacements and internal stresses required for design, are all illustrated.

7.3.1 Structure Geometry, Prestressing and Loads

The bridge chosen for this example (Fig. 7.3.1) is a two span straight prestressed concrete box girder bridge used as a continuous bridge design example in the Post-Tensioning Institute's Post-Tensioned Box Girder Bridge Manual [18]. The box girder cross section, material properties, span arrangement, tendon profiles, and prestressing force requirements are all taken directly from that design example. The purpose of this analysis example is to analyse the bridge with MUPDI4, CURDI4, and CELL4, and to compare and discuss the results.

The bridge has a four-cell cross section (Fig. 7.3.1b) with vertical exterior webs and short cantilever slabs. This is a typical cross section type for a three lane California bridge. The span arrangement (Fig. 7.3.1a) is unsymmetrical with 150 ft and 162 ft spans. Diaphragms are located at each of the three supports. Longitudinal prestressing panel tendons are used in each web. Transverse slab tendons are not used.

Prestressing is idealized as one panel tendon in each web, with a constant effective force of 1580 kips per web. Friction and anchorage slip losses are neglected. This prestressing force would most likely be provided by several tendons in each web, but the analysis is simplified with no sacrifice in accuracy by lumping together the several actual tendons in one web as one tendon. The tendon profile (Fig. 7.3.1c) is the same in each web, and is taken directly from the P.T.I. design example including the reverse

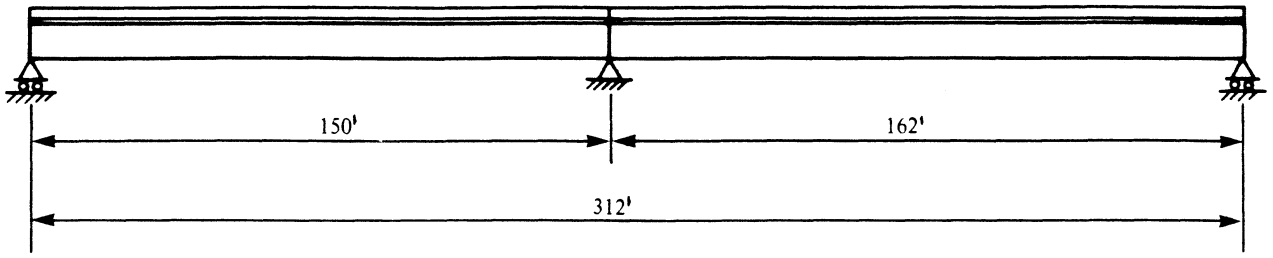

(a) SPAN ARRANGEMENT

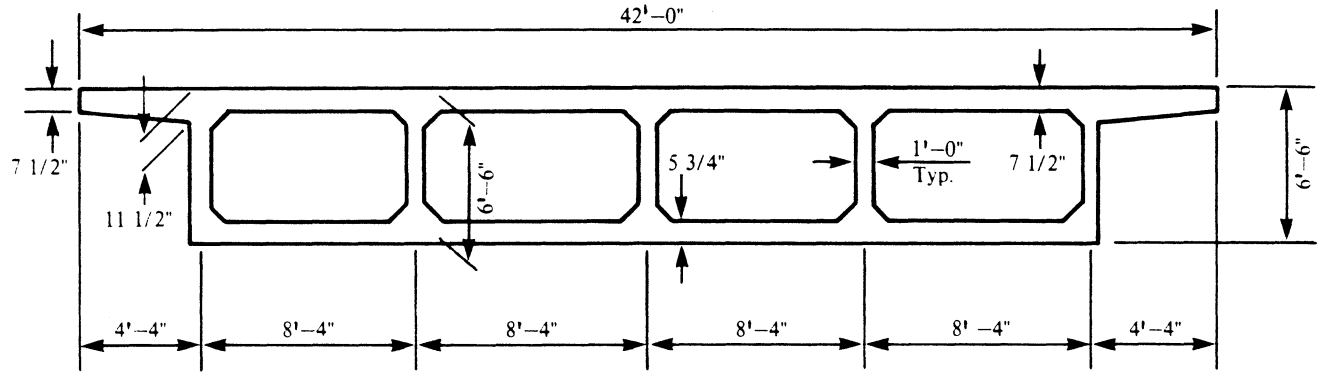

(b) CROSS-SECTIONAL DIMENSIONS

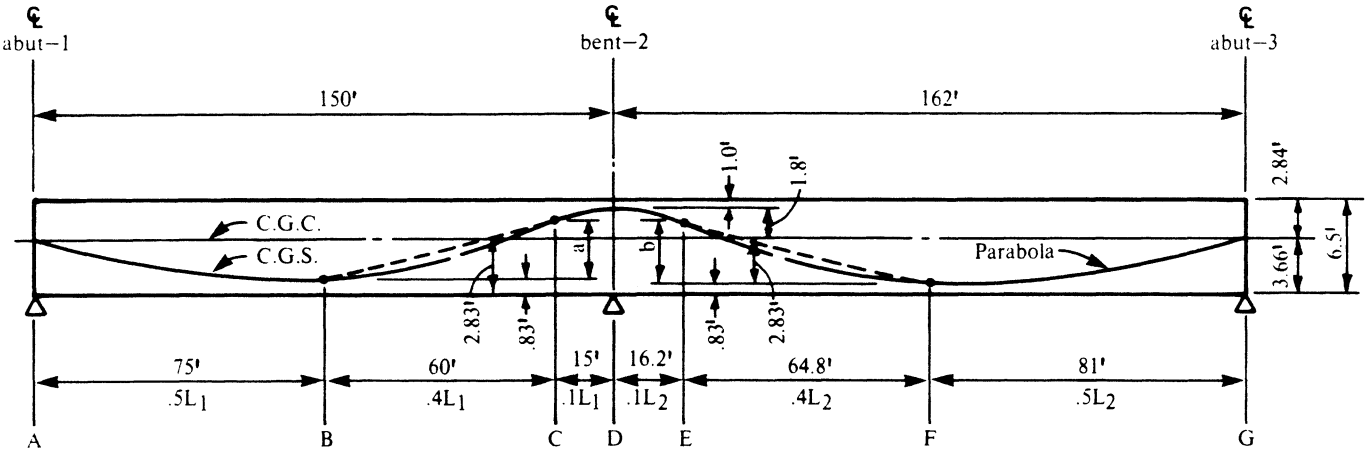

(c) PANEL TENDON PROFILE IN VERTICAL WEBS

FIG. 7.3.1 SPAN ARRANGEMENT, CROSS-SECTIONAL DIMENSIONS, AND TENDON PROFILE FOR TWO SPAN , CONTINUOUS, PRESTRESSED, FOUR CELL BOX GIRDER BRIDGE

curvature over the interior support.

A total of three different loading cases are considered in the analysis. They may be summarized as follows:

Case 1 - Dead Load of Bridge

Case 2 - Prestressing (losses not considered)

Case 3 - Overload Permit Design Vehicle (P-13) in one lane

Dead load of the bridge is considered using the automatic options in each program. Prestressing loads are generated automatically using the parametric form of input described in Chapter 3. The overload permit vehicle loading is a heavy truck-wheel pattern shown in Fig. 7.3.3. The permit vehicle is located at the center of the 162 foot span in an exterior lane. No impact is applied.

7.3.2 Analytical Models

Three different analytical models are used in this example (Fig. 7.3.2), one for each computer program used.

For all three models, the cross-section assumed is identical in which the fillets and haunched cantilevers shown in Fig. 7.3.1 are ignored. Thus the entire top slab has a constant thickness of 7.5 in.; the bottom slab of 5.75 in.; and all the webs of 12.0 in. This idealized cross-section has the following section properties: distances from the cgc of the section to the fibers at the mid-thickness of the top and bottom deck slabs of c_t = 2.55 ft and c_b = 3.40 ft; cross sectional area A = 71.96 ft^2; and moment of inertia about the cgc I = 448.13 ft^4.

The MUPDI4 model (Fig. 7.3.2a) consists of plate elements the length of the structure. One element between webs is sufficient for modelling the top and bottom slabs due to the elasticity element used, resulting in a total of 15 elements and 12 joints. 80 Fourier Series terms are used.

The CURDI4 model (Fig. 7.3.2b) consists of straight finite strip elements the length of the structure. Two elements between webs are used for the top and bottom slabs in order for the finite strip elements to accurately predict local bending moments, and each web is subdivided into two elements,

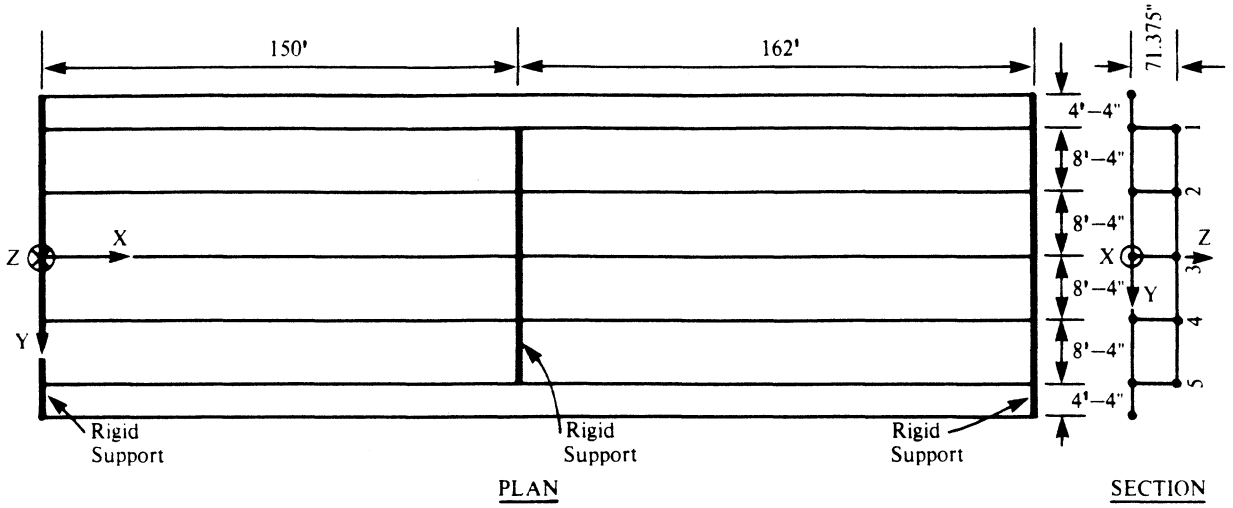

(a) MUPDI4

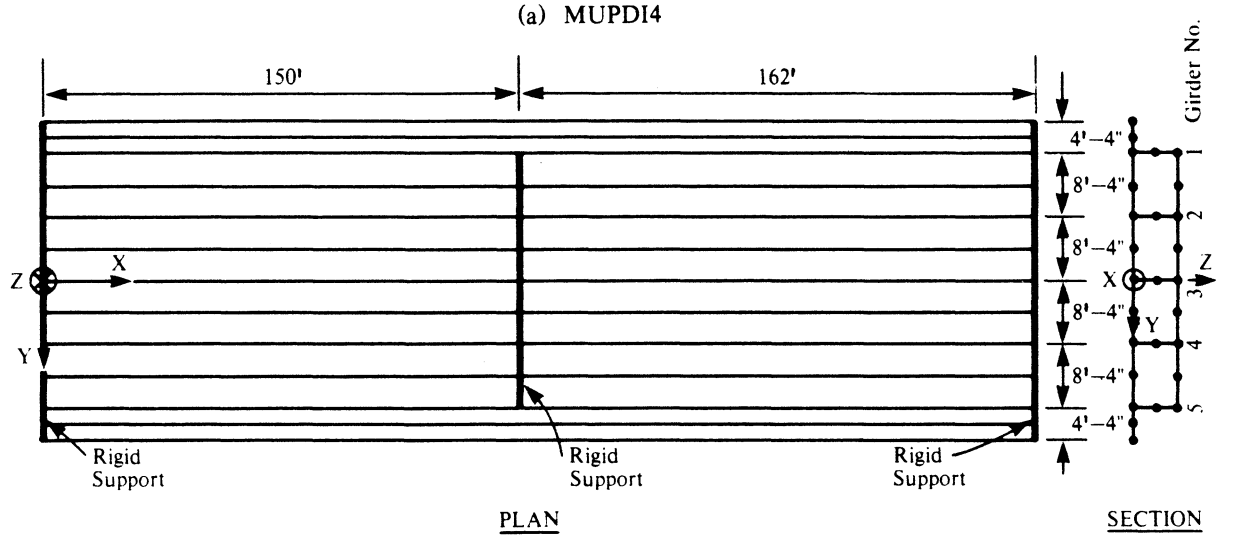

(b) CURDI4

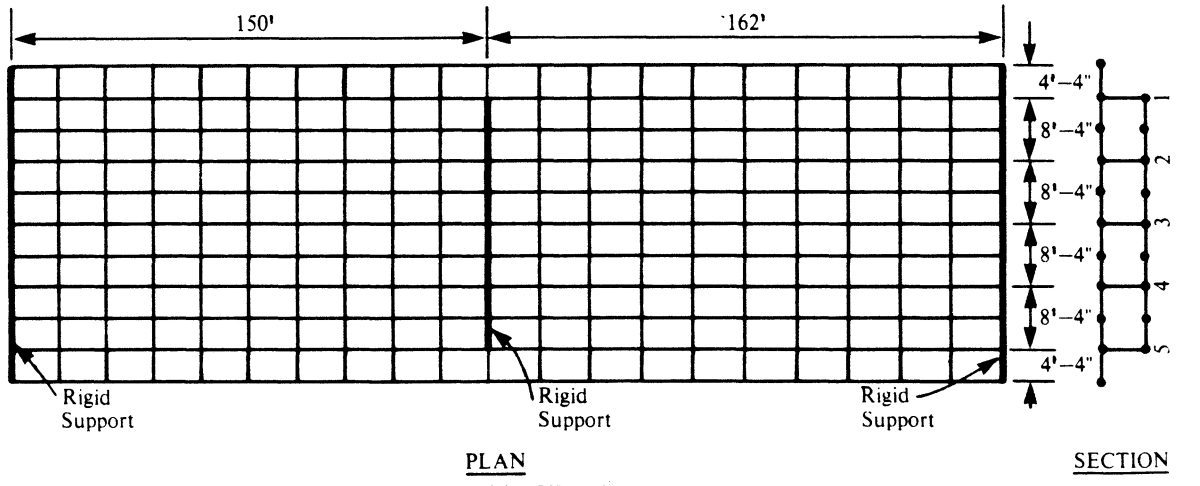

(c) CELL4

FIG. 7.3.2 ANALYTICAL MODELS FOR MUPDI4, CURDI4 AND CELL4 COMPUTER SOLUTIONS

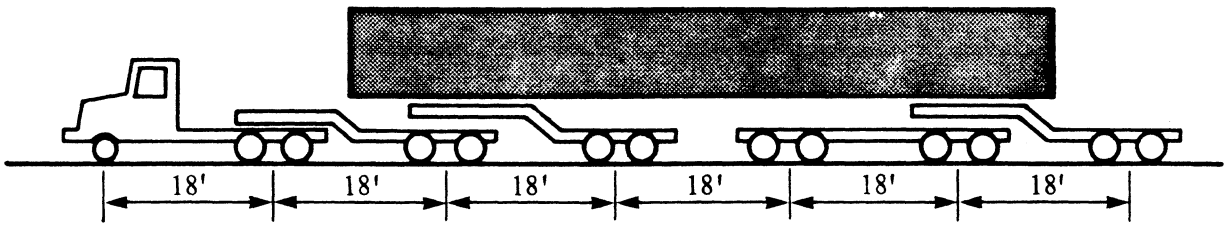

(a) TRUCK ELEVATION

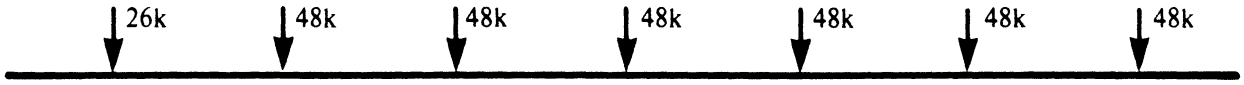

(b) TOTAL AXLE LOADS ON BRIDGE

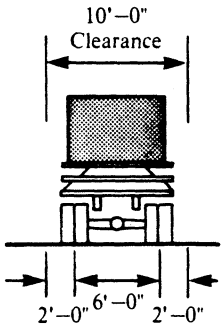

(c) TRUCK SECTION

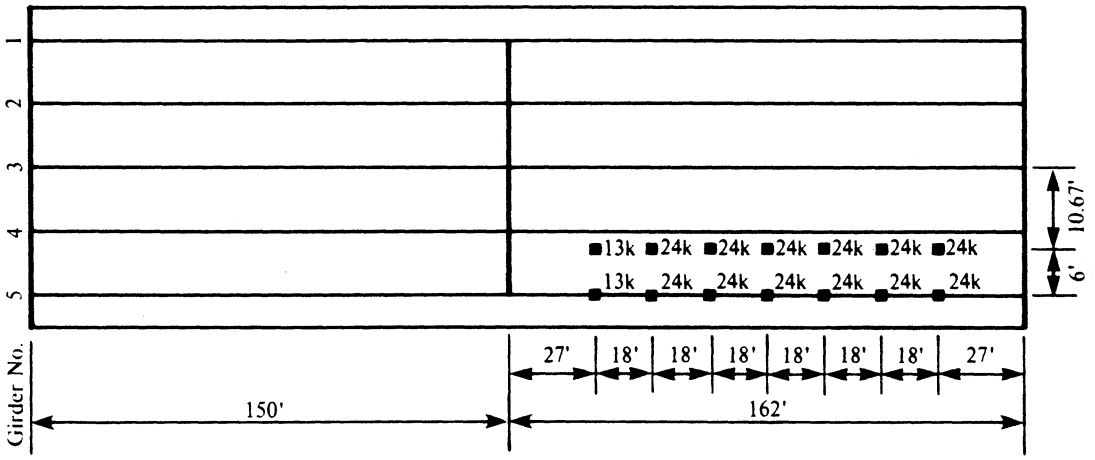

(d) POSITION OF WHEEL LOADS ON BRIDGE

FIG. 7.3.3 P13 TRUCK LOAD CONFIGURATION AND POSITION OF P13 TRUCK ON BRIDGE FOR LIVE LOAD ANALYSIS

resulting in a total of 30 elements and 27 joints. 100 Fourier Series terms are used.

The CELL4 model (Fig. 7.3.2c) is a finite element mesh with one element over the depth of each web, two elements between webs for top and bottom slabs and ten elements over the length of each span, resulting in a total of 460 elements and 231 nodes.

In each of these models, each span of each prestressing tendon is subdivided into ten straight segments.

The overload permit vehicle loading is modelled with statically equivalent joint or nodal loads (Fig. 7.3.3). The statically equivalent loads may be found by considering the top slab to be a simple grillage of simple span beams supported at the actual joints or nodes. Then the reactions are the equivalent loads.

Material properties assumed for the three models were taken directly from the PTI design example: Elastic modulus of 3600 ksi; Poisson's ratio of 0.17; and concrete unit weight of 0.155 kcf for modelling dead load.

7.3.3 Discussion of Results

A detailed summary of the various results of the analysis for the three loading cases is shown in Figures 7.3.4 through 7.3.9 and in Tables 7.3.1 through 7.3.3. Only those results most important to understanding the behavior of the bridge are presented and discussed. In general, good agreement is found between the results of the three different analyses. Significant differences will be explained in the text below.

7.3.3.1 Dead Load Results

Dead load results are illustrated in Figures 7.3.4 and 7.3.5 and in Table 7.3.1.

Displacements

Vertical displacement profile of Girder 1 under dead load is shown in Fig. 7.3.4a. The displacement is uniform across the width of the bridge, with nearly identical displacements at each girder line. MUPDI4 and CURDI4 give nearly identical results, while CELL4 gives slightly smaller (stiffer)

displacements, as expected from the finite element idealization.

Girder Bending Moments

Total cross section bending moment under dead load is shown in Fig. 7.3.4b. The distribution of this moment to each individual girder is shown in Table 7.3.1a.

The total bending moments from MUPDI4 and CURDI4 (Fig. 7.3.4b) are essentially identical at all locations. The CELL4 solution agrees well with the MUPDI4 and CURDI4 solutions in all locations except at the center support, where the finite element solution truncates the peak of the bending moment diagram. This truncation is evident in both Fig. 7.3.4b and Table 7.3.1a, and could be reduced by further mesh refinement in the CELL4 model and extrapolation of the results.

The distribution of the total moments to the individual girders (Table 7.3.1a) is nearly uniform, with the exterior girders resisting slightly less total moment because of their absence of a bottom cantilever. Percentage distributions from MUPDI4 and CURDI4 are identical, and differ with those of CELL4 by only one percent.

Girder Shears

Total cross section shear force under dead load is shown in Fig. 7.3.4c. The distribution of this shear to each individual girder is shown in Table 7.3.1b.

The total shear forces from MUPDI4 and CURDI4 (Fig. 7.3.4c) are essentially identical except at the interior support where CURDI4 gives slightly higher values. The CELL4 solution agrees well with the MUPDI4 and CURDI4 solutions except at the supports, where the finite element solution truncates the peak of the shear diagram. This truncation is evident in both Fig. 7.3.4c and Table 7.3.1b, and could be reduced by mesh refinement and extrapolation of results for CELL4.

The distribution of the total shears to the individual girders (Table 7.3.1b) is nearly uniform. CELL4 gives a slightly different distribution at the extreme ends, due to the different boundary condition idealization of the finite element method.

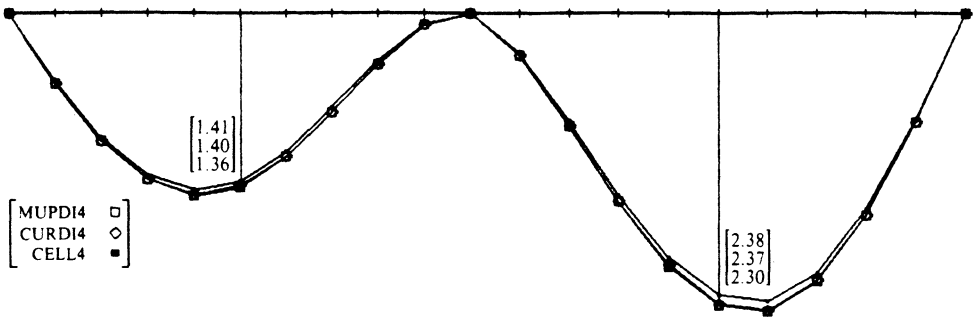

(a) VERTICAL DISPLACEMENTS (in.) FOR GIRDER 1

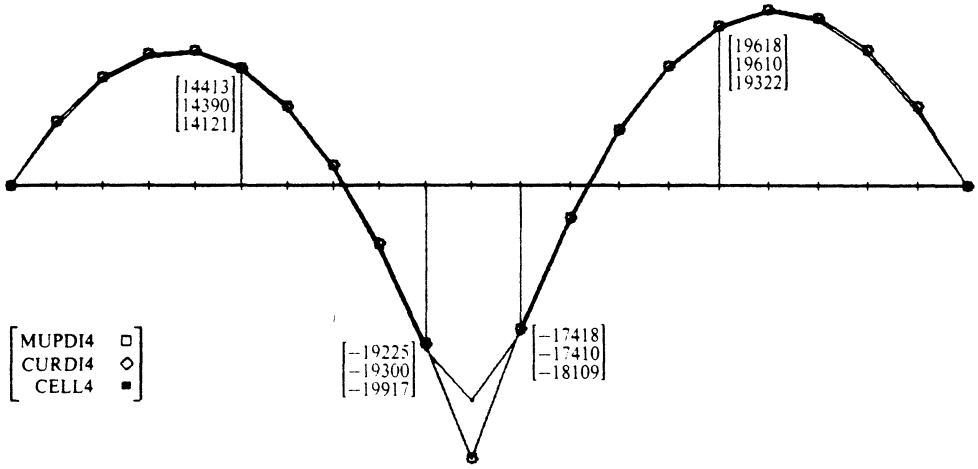

(b) SECTION MOMENTS (ft-kips)

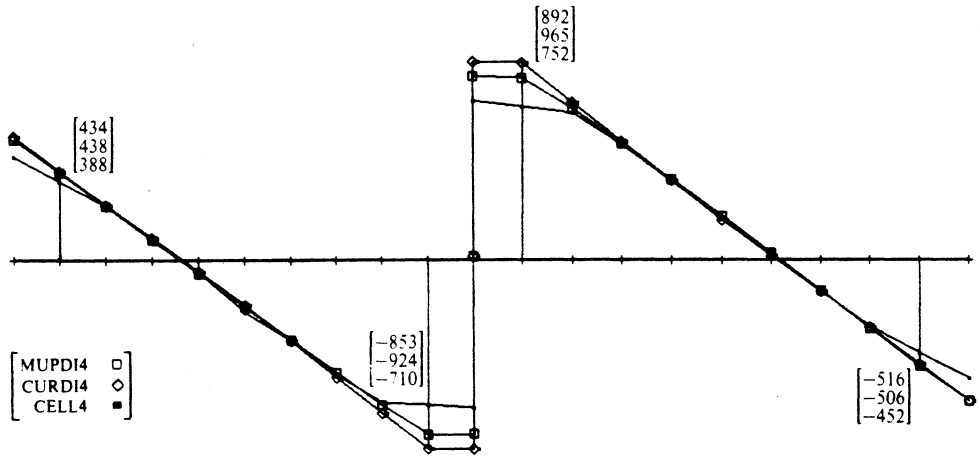

(c) SECTION SHEARS (kips)

FIG. 7.3.4 LONGITUDINAL VARIATION OF VERTICAL DISPLACEMENTS, SECTION MOMENTS AND SHEARS FOR DEAD LOAD

TABLE 7.3.1 TRANSVERSE DISTRIBUTION OF SECTION MOMENTS AND SHEARS TO INDIVIDUAL GIRDERS UNDER DEAD LOAD

GIRDER	SECTION	a) MOMENTS UNDER DEAD LOAD						SECTION	b) SHEARS UNDER DEAD LOAD					
		MUPDI4		CURDI4		CELL4			MUPDI4		CURDI4		CELL4	
		FT-KIPS	%	FT-KIPS	%	FT-KIPS	%		KIPS	%	KIPS	%	KIPS	%
(1)	(2)	(3)	(4)	(5)	(6)	(7)	(8)	(9)	(10)	(11)	(12)	(13)	(14)	(15)
1	x = 75 ft	2453	17.0	2448	17.0	2549	18.1	x = 15 ft	85.1	19.6	85.8	19.6	79.3	20.4
2		3171	22.0	3166	22.0	3007	21.3		87.9	20.2	88.6	20.2	76.5	19.7
3		3166	22.0	3162	22.0	3008	21.3		88.5	20.4	89.1	20.4	76.6	19.7
4		3171	22.0	3166	22.0	3007	21.3		87.9	20.2	88.6	20.2	76.5	19.7
5		2453	17.0	2448	17.0	2549	18.1		85.1	19.6	85.8	19.6	79.3	20.4
TOTAL		14413	100	14390	100	14121	100		434.5	100	437.9	100	388.2	100
1	x = 150 ft	- 5860	17.6	- 5889	17.7	- 4753	18.0	x = 135 ft	-155.8	18.3	-168.3	18.2	-132.4	18.6
2		- 7180	21.6	- 7171	21.6	- 5626	21.3		-180.0	21.1	-195.4	21.1	-148.1	20.8
3		- 7151	21.5	- 7156	21.5	- 5619	21.3		-181.8	21.3	-197.3	21.3	-149.3	21.0
4		- 7180	21.6	- 7171	21.6	- 5626	21.3		-180.0	21.1	-195.4	21.1	-148.1	20.8
5		- 5860	17.6	- 5889	17.7	- 4753	18.0		-155.8	18.3	-168.3	18.2	-132.4	18.6
TOTAL		-33233	100	-33280	100	-26377	100		-853.4	100	-924.6	100	-710.5	100
1	x = 231 ft	3339	19.0	3337	17.0	3494	18.1	x = 166.2 ft	164.3	18.4	177.0	18.4	141.6	18.8
2		4315	22.0	4313	22.0	4111	21.3		187.3	21.0	203.0	21.0	155.8	20.7
3		4310	22.0	4308	22.0	4111	21.3		189.1	21.2	204.9	21.2	156.9	20.9
4		4315	22.0	4313	22.0	4111	21.3		187.3	21.0	203.0	21.0	155.8	20.7
5		3339	17.0	3337	17.0	3494	18.1		164.3	18.4	177.0	18.4	141.6	18.8
TOTAL		19618	100	19610	100	19322	100		892.4	100	964.0	100	751.8	100
1								x = 295.8 ft	-101.5	19.7	-99.6	19.7	-92.4	20.5
2									-104.2	20.2	-101.9	20.2	-88.8	19.7
3									-104.8	20.3	-102.4	20.3	-88.8	19.7
4									-104.2	20.3	-102.4	20.3	-88.8	19.7
5									-101.5	19.7	-99.6	19.7	-92.7	20.5
TOTAL									-516.3	100	-505.5	100	-451.8	100

Transverse Bending Moments at X = 231 feet

The transverse distribution of transverse bending moments in the walls of the box girder cross section under dead load is shown in Fig. 7.3.5a.

In the top and bottom slab elements, MUPDI4 predicts the expected parabolic distribution while CURDI4 and CELL4 do not. MUPDI4's elasticity theory solution is capable of capturing this behavior mode, while CURDI4's and CELL4's numerical solutions are not. The CURDI4 and CELL4 results must be adjusted for local element bending effects to precisely predict transverse bending under distributed loads.

In the web elements, the three programs give essentially identical results. CELL4 gives erroneous results in the exterior webs, due to the approximation in the top slab imbalance. This could be reduced by finer discretization of the top slab cantilever.

Longitudinal Membrane Stresses at X = 231 feet

The transverse distribution of longitudinal membrane stresses in the walls of the box girder cross section under dead load is shown in Fig. 7.3.5b.

At all locations the three programs give essentially identical results, with nearly linear variations in stress in all webs and very little reduction of stress in the slabs between the webs. This suggests that beam theory should be adequate for prediction of longitudinal membrane stresses under dead load.

Membrane Shears at X = 166.2 feet

The transverse distribution of membrane shear stresses in the walls of the box girder cross section under dead load is shown in Fig. 7.3.5c.

In the webs, where most of the vertical section shear is resisted, MUPDI4 gives the parbolic shear stress variation predicted by elasticity theory, while CURDI4 overestimates the parabolic distribution with a bilinear approximation and CELL4 underestimates the parabolic distribution with a linear approximation. This is the source of the discrepancies between the three programs noted in Fig. 7.3.4c.

In the top and bottom slabs, MUPDI4 gives the expected linear shear stress variation, while CURDI4 and CELL4 do not. Note, however, that the

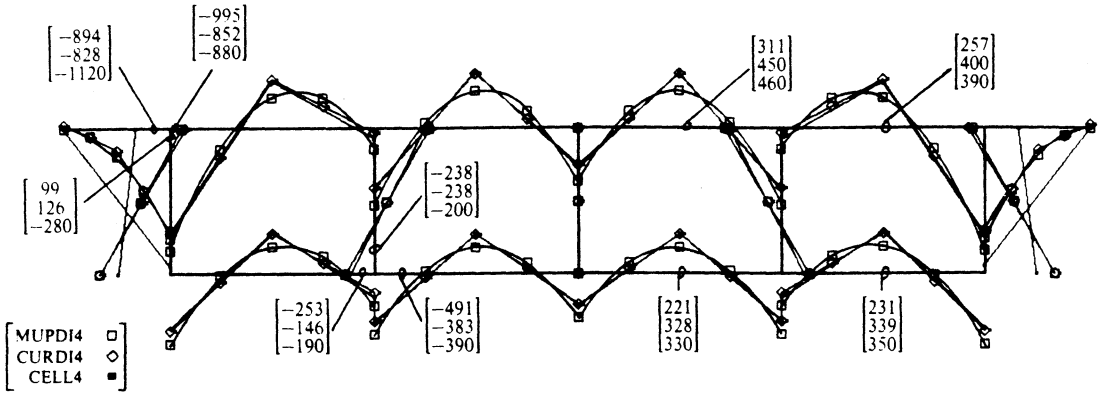

(a) TRANSVERSE MOMENTS M_y (in-lb/in) AT x=231 ft.

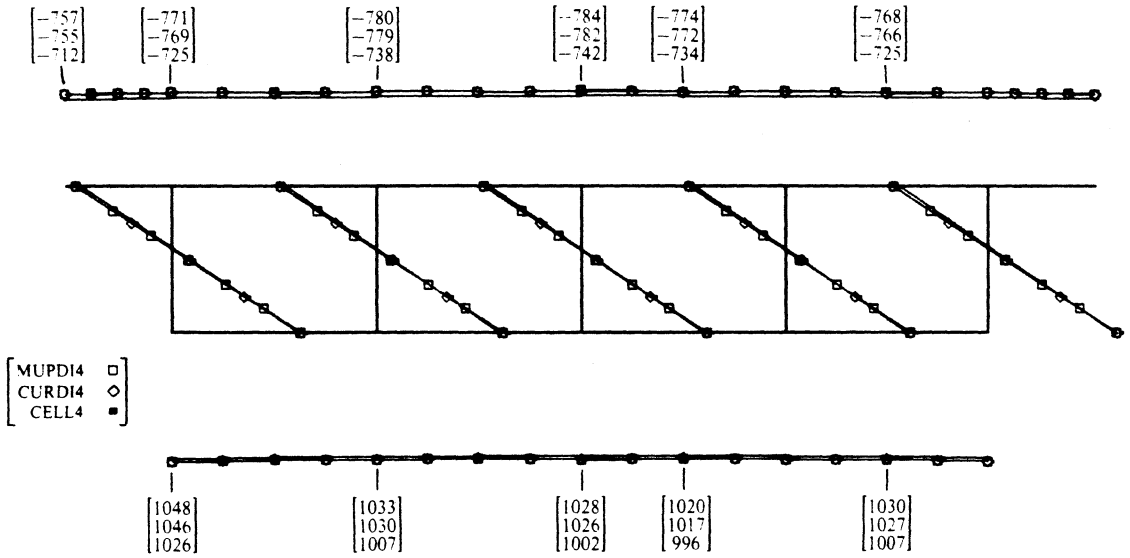

(b) LONGITUDINAL MEMBRANE STRESSES σ_x (psi) AT x=231 ft.

FIG. 7.3.5 TRANSVERSE DISTRIBUTION OF TRANSVERSE MOMENTS, LONGITUDINAL MEMBRANE STRESSES AND MEMBRANE SHEAR STRESSES FOR DEAD LOAD

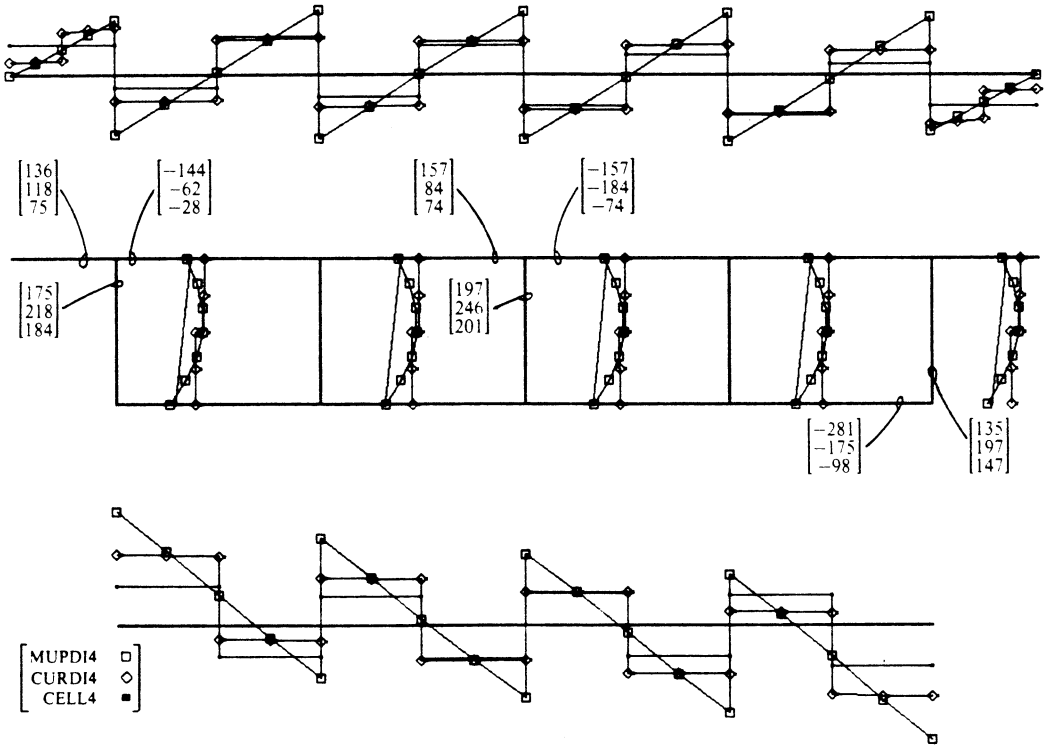

(c) MEMBRANE SHEAR STRESSES τ_{xy} (psi) AT x=166.2 ft.

FIG. 7.3.5 TRANSVERSE DISTRIBUTION OF TRANSVERSE MOMENTS, LONGITUDINAL MEMBRANE STRESSES AND MEMBRANE SHEAR STRESSES FOR DEAD LOAD

CURDI4 and CELL4 solutions give accurate results at element midpoints. With mesh refinement the CURDI4 and CELL4 solutions will converge to the MUPDI4 result.

7.3.3.2 Prestressing Results

Prestressing results are illustrated in Figures 7.3.6 and 7.3.7 and in Table 7.3.2.

Displacements

Vertical displacement profile of Girder 1 under prestressing is shown in Fig. 7.3.6a. The displacement is uniform across the width of the bridge, with nearly identical displacements at each girder line. MUPDI4 and CURDI4 give identical results, while CELL4 gives slightly smaller (stiffer) displacements, as expected from the finite element idealization.

Girder Bending Moments

Total cross section bending moment under prestressing is shown in Fig. 7.3.6b. The distribution of this moment to each individual girder is shown in Table 7.3.2a.

The total bending moments from MUPDI4 and CURDI4 (Fig. 7.3.6b) are essentially identical at all locations. The CELL4 solution predicts slightly shifted bending moments, and truncates the peak of the bending moment diagram at the center support. This truncation is evident in both Fig. 7.3.6b and Table 7.3.2a, and could be reduced by further mesh refinement in the CELL4 model and extrapolation of the results.

The distribution of the total moments to the individual girders (Table 7.3.2a) is nearly uniform, with the exterior girders resisting slightly less total moment in positive moment zones. Percentage distributions from MUPDI4 and CURDI4 are nearly identical, and differ with those of CELL4 by only one percent.

Girder Shears

Total cross section shear force under prestressing is shown in Fig. 7.3.6c. The distribution of this shear to each individual girder is shown in Table 7.3.2b.

The total shear forces from MUPDI4 and CURDI4 (Fig. 7.3.6c) are

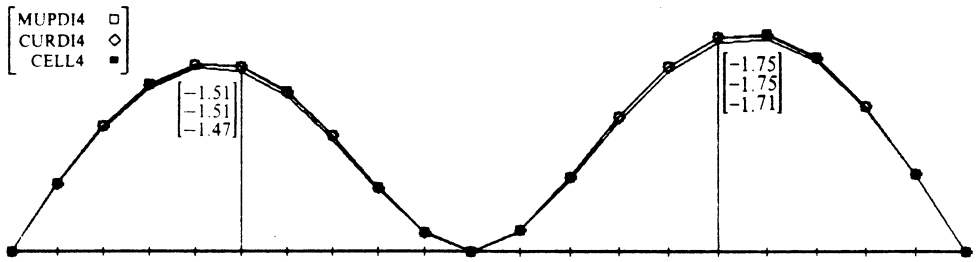

(a) VERTICAL DISPLACEMENTS (in.) FOR GIRDER 1

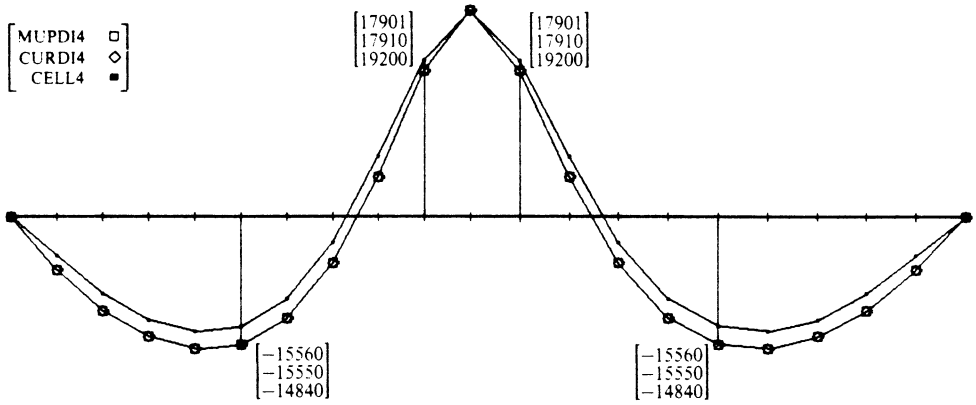

(b) SECTION MOMENTS (ft-kips)

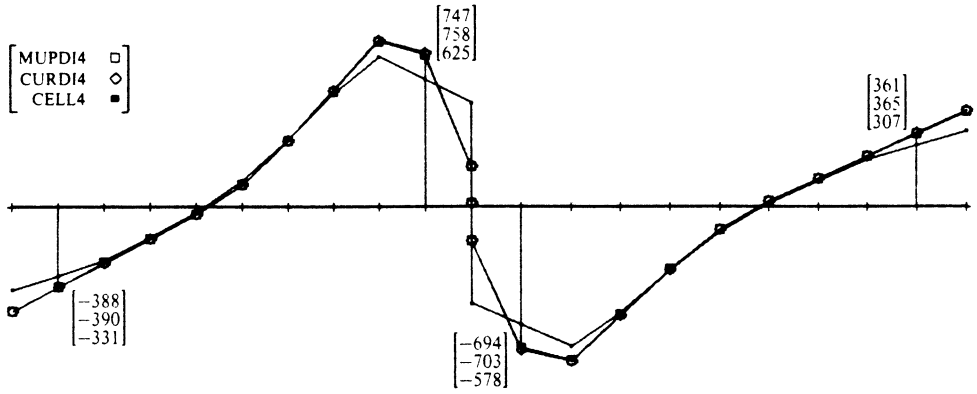

(c) SECTION SHEARS (kips)

FIG. 7.3.6 LONGITUDINAL VARIATION OF VERTICAL DISPLACEMENTS, SECTION MOMENTS AND SHEARS FOR PRESTRESSING

TABLE 7.3.2 TRANSVERSE DISTRIBUTION OF SECTION MOMENTS AND SHEARS TO INDIVIDUAL GIRDERS UNDER PRESTRESSING

GIRDER	SECTION	a) MOMENTS UNDER PRESTRESSING						SECTION	SHEARS UNDER PRESTRESSING					
		MUPDI4		CURDI4		CELL4			MUPDI4		CURDI4		CELL4	
		FT-KIPS	%	FT-KIPS	%	FT-KIPS	%		KIPS	%	KIPS	%	KIPS	%
(1)	(2)	(3)	(4)	(5)	(6)	(7)	(8)	(9)	(10)	(11)	(12)	(13)	(14)	(15)
1	x = 75 ft	- 2186	14.1	- 2183	14.0	- 2031	13.7	x = 15 ft	-70.8	18.3	-71.1	18.2	-60.9	18.4
2		- 3732	24.0	- 3729	24.0	- 3594	24.2		-81.8	21.1	-82.2	21.1	-69.1	20.9
3		- 3726	23.9	- 3723	24.0	- 3590	24.2		-83.6	21.3	-83.2	21.3	-71.1	21.5
4		- 3732	24.0	- 3729	24.0	- 3594	24.2		-81.8	21.1	-82.2	21.1	-69.1	20.9
5		- 2186	14.1	- 2183	14.0	- 2031	13.7		-70.8	18.3	-71.1	18.2	-60.9	18.4
TOTAL		-15560	100	-15550	100	-14840	100		-387.8	100	-398.8	100	-331.2	100
1	x = 150 ft	4908	19.4	4914	19.4	4726	20.1	x = 135 ft	139.9	18.7	141.0	18.6	118.9	19.0
2		5189	20.5	5169	20.4	4678	19.9		155.4	20.8	158.3	20.9	128.6	20.6
3		5167	20.4	5156	20.4	4655	19.8		156.1	20.9	159.1	21.0	129.4	20.7
4		5189	20.5	5169	20.4	4672	19.9		155.4	20.8	158.3	20.9	128.6	20.6
5		4908	19.4	4914	19.4	4726	20.1		139.9	18.7	141.0	18.6	118.9	19.0
TOTAL		25361	100	25320	100	23464	100		746.8	100	757.8	100	624.5	100
1	x = 231 ft	- 2185	14.1	- 2183	14.0	- 2032	13.7	x = 166.2 ft	-129.7	18.7	-130.2	18.5	-109.5	18.9
2		- 3732	24.0	- 3729	24.0	- 3594	24.2		-144.7	20.8	-147.0	20.9	-119.4	20.7
3		- 3726	24.0	- 3723	24.0	- 3589	24.2		-145.6	21.0	-147.9	21.1	-120.2	20.8
4		- 3732	24.0	- 3729	24.0	- 3594	24.2		-144.7	20.8	-147.0	20.9	-119.4	20.7
5		- 2185	14.1	- 2183	14.0	- 2032	13.7		-129.7	18.7	-130.2	18.5	-109.5	18.9
TOTAL		-15559	100	-15550	100	-14842	100		-694.6	100	-702.5	100	-577.9	100
1								x = 295.8 ft	65.6	18.2	66.5	18.2	56.7	18.4
2									76.2	21.1	76.9	21.1	63.9	20.8
3									77.2	21.4	78.0	21.4	66.3	21.6
4									76.2	21.1	76.9	21.1	63.9	20.8
5									65.6	18.2	66.5	18.2	56.7	18.4
TOTAL									360.7	100	364.7	100	307.4	100

essentially identical. The CELL4 solution agrees well with the MUPDI4 and CURDI4 solutions except at the supports, where the finite element solution truncates the peak of the shear diagram. This truncation is evident in both Fig. 7.3.6c and Table 7.3.2b, and could be reduced by mesh refinement and extrapolation of results for CELL4.

The distribution of the total shears to the individual girders (Table 7.3.2b) is nearly uniform. The three programs agree very well in their prediction of percentage distribution of total prestressing moment to the individual girders.

Transverse Bending Moments at X = 231 feet

The transverse distribution of transverse bending moments in the walls of the box girder cross section under prestressing is shown in Fig. 7.3.7a.

The three programs predict essentially identical transverse bending moments for this load case, due to the fact that no element loadings are applied. Note that these bending moments are mainly of the same sign as the transverse bending moments due to dead load.

Longitudinal Membrane Stresses at X = 231 feet

The transverse distribution of longitudinal membrane stresses in the walls of the box girder cross section under prestressing is shown in Fig. 7.3.7b.

At all locations the three programs give essentially identical results, with nearly linear variations in stress in all webs and very little reduction of stress in the slabs between the webs. This suggests that beam theory should be adequate for prediction of longitudinal membrane stresses under prestressing.

Membrane Shears at X = 166.2 feet

The transverse distribution of membrane shear stresses in the walls of the box girder cross section under prestressing is shown in Fig. 7.3.7c.

In the webs, where most of the vertical section shear is resisted, MUPDI4 gives a parbolic shear stress variation, while CURDI4 overestimates the parabolic distribution with a bilinear approximation and CELL4 underestimates the parabolic distribution with a linear approximation. This is the source

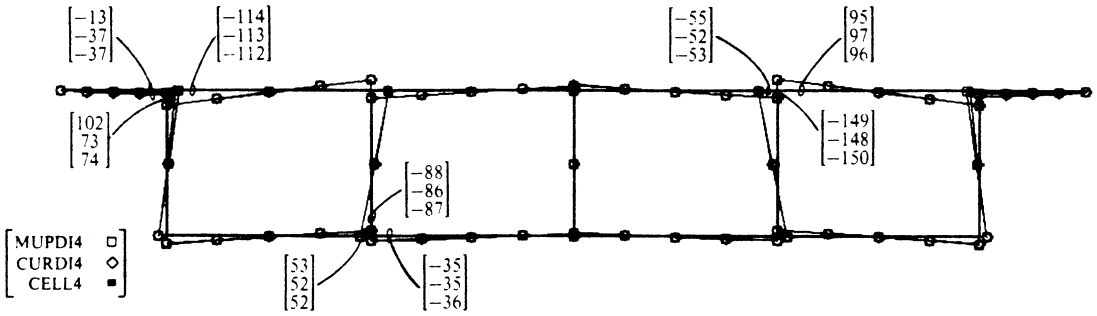

(a) TRANSVERSE MOMENTS M_y (in-lb/in) AT x=231 ft.

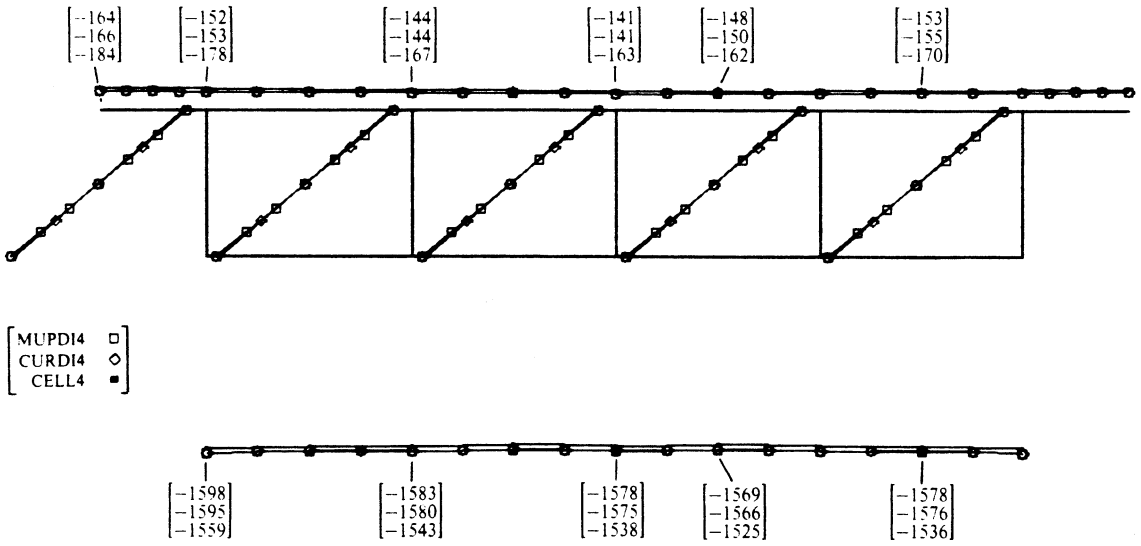

(b) LONGITUDINAL MEMBRANE STRESSES σ_x (psi) AT x=231 ft.

FIG. 7.3.7 TRANSVERSE DISTRIBUTION OF TRANSVERSE MOMENTS, LONGITUDINAL MEMBRANE STRESSES AND MEMBRANE SHEAR STRESSES FOR PRESTRESSING

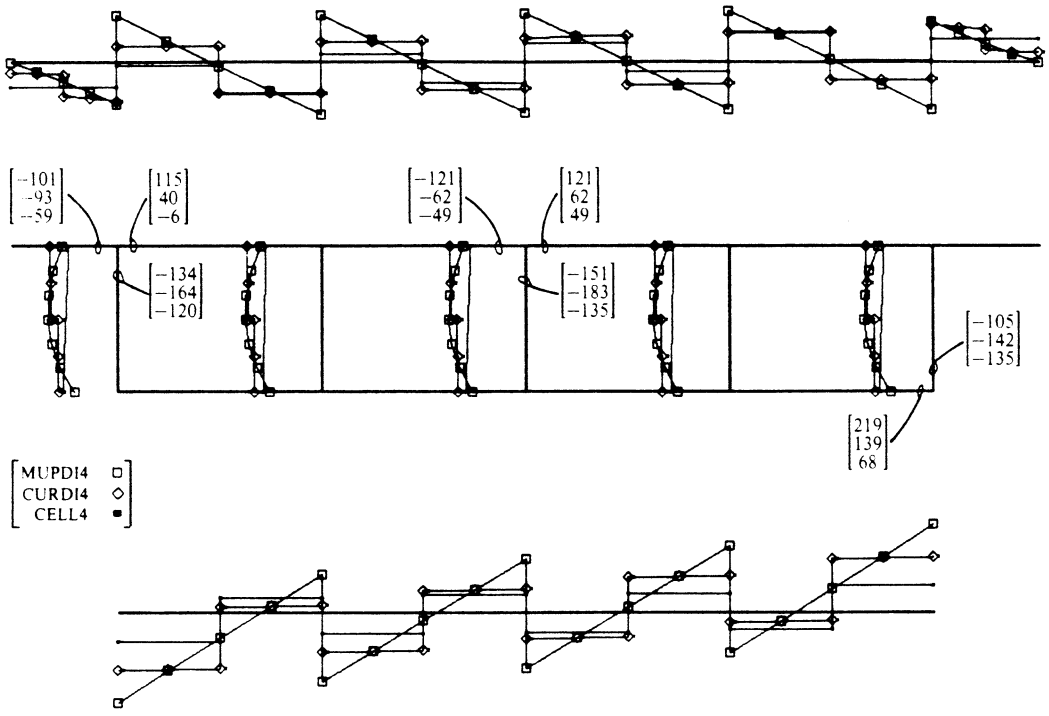

(c) MEMBRANE SHEAR STRESSES τ_{xy} (psi) AT x=166.2 ft.

FIG. 7.3.7 TRANSVERSE DISTRIBUTION OF TRANSVERSE MOMENTS, LONGITUDINAL MEMBRANE STRESSES AND MEMBRANE SHEAR STRESSES FOR PRESTRESSING

of the discrepancies between the three programs noted in Fig. 7.3.6c. Note, however, that none of the predicted web shear stresses are precise for this loading case, since the actual tendon load, applied in the web element, is lumped in the programs to the adjacent node or joint line. Additional web elements may be used in MUPDI4 and CURDI4 to refine the prediction.

In the top and bottom slabs, MUPDI4 gives the expected linear shear stress variation, while CURDI4 and CELL4 do not. Note, however, that CURDI4 and CELL4 give accurate results at element midpoints. With mesh refinement the CURDI4 and CELL4 solutions will converge to the MUPDI4 result.

7.3.3.3 P13 Truck Load Results

P13 Truck Load results are illustrated in Figures 7.3.8 and 7.3.9 and in Table 7.3.3.

Displacements

Vertical displacement profiles of Girders 1 and 5 under P13 truck load are shown in Fig. 7.3.8a. MUPDI4 and CURDI4 give nearly identical results, while CELL4 gives slightly smaller (stiffer) displacements, as expected from the finite element idealization.

Girder Bending Moments

Total cross section bending moment under P13 truck load is shown in Fig. 7.3.8b. The distribution of this moment to each individual girder is shown in Table 7.3.3a.

The total bending moments from MUPDI4 and CURDI4 (Fig. 7.3.8b) are essentially identical at all locations. The CELL4 solution predicts slightly smaller bending moments under the load, but agrees with MUPDI4 and CURDI4 at other cross sections.

The distribution of the total moments to the individual girders (Table 7.3.3a) shows that the girder under the load resists only about three percent more of the load under eccentric truck load than it does under dead load. This illustrates the ability of a multi cell box girder bridge to distribute concentrated loads to the entire section. Percentage distributions from MUPDI4 and CURDI4 are nearly identical, and differ with those of CELL4 by only one percent.

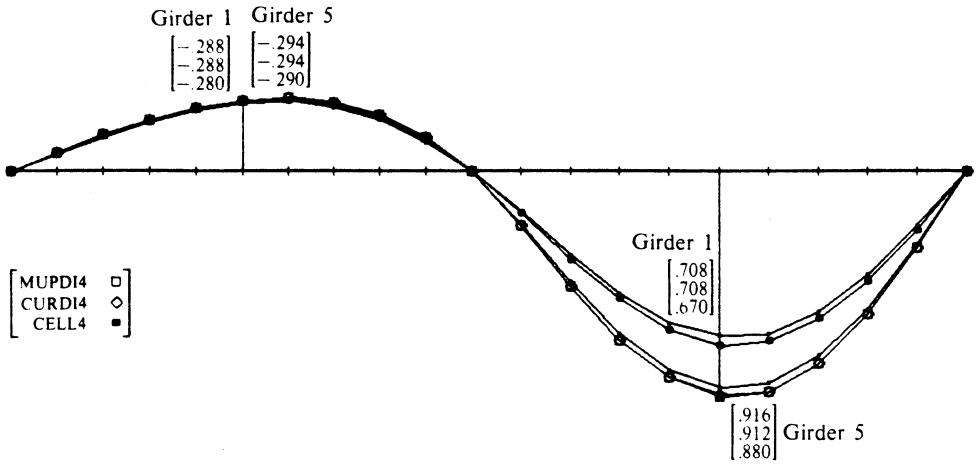

(a) VERTICAL DISPLACEMENTS (in.) FOR GIRDERS 1 AND 5

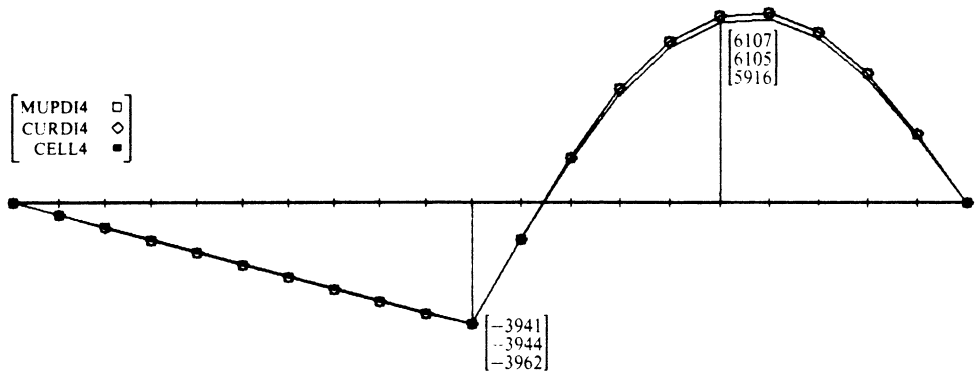

(b) SECTION MOMENTS (ft-kips)

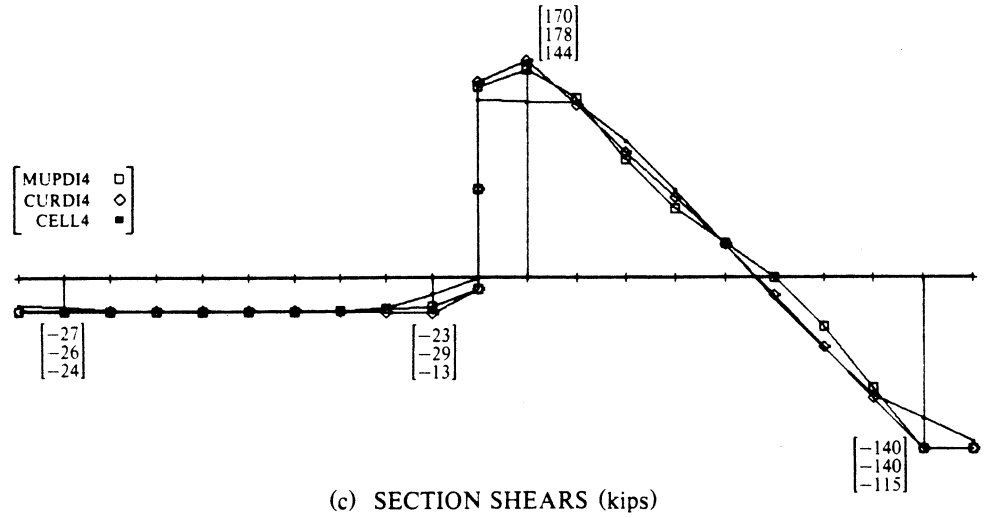

(c) SECTION SHEARS (kips)

FIG. 7.3.8 LONGITUDINAL VARIATION OF VERTICAL DISPLACEMENTS, SECTION MOMENTS AND SHEARS FOR P13 TRUCK LOAD

7.3.3 TRANSVERSE DISTRIBUTION OF SECTION MOMENTS AND SHEARS TO INDIVIDUAL GIRDERS UNDER P13 TRUCK LOAD

GIRDER	SECTION	a) MOMENTS UNDER P13 TRUCK LOAD						SECTION	b) SHEARS UNDER P13 TRUCK LOAD					
		MUPDI4		CURDI4		CELL4			MUPDI4		CURDI4		CELL4	
		FT-KIPS	%	FT-KIPS	%	FT-KIPS	%		KIPS	%	KIPS	%	KIPS	%
(1)	(2)	(3)	(4)	(5)	(6)	(7)	(8)	(9)	(10)	(11)	(12)	(13)	(14)	(15)
1	x = 75 ft	- 347	17.3	- 347	17.1	- 368	18.5	x = 15 ft	- 4.8	17.7	- 4.8	17.8	- 4.5	18.8
2		- 445	22.2	- 445	22.1	- 427	21.5		- 5.2	19.3	- 5.2	19.4	- 4.6	19.2
3		- 440	22.0	- 440	22.0	- 422	21.2		- 5.3	19.8	- 5.3	19.8	- 4.6	19.2
4		- 436	21.8	- 437	21.9	- 418	21.0		- 5.5	20.4	- 5.5	20.3	- 4.8	20.0
5		- 335	16.7	- 336	17.0	- 354	17.8		- 6.2	22.9	- 6.1	22.7	- 5.6	23.3
TOTAL		-2002	100	-2004	100	-1990	100		-27.1	100	-26.9	100	-24.0	100
1	x = 150 ft	- 546	13.9	- 550	13.9	- 452	14.2	x = 135 ft	- 0.9	4.0	- 1.1	3.6	- 0.6	4.6
2		- 704	17.9	- 706	17.9	- 570	17.9		- 3.5	15.2	- 4.4	14.9	- 2.1	16.2
3		- 814	20.7	- 814	20.7	- 656	20.6		- 5.4	23.4	- 6.5	22.3	- 3.8	29.2
4		- 987	25.1	- 983	24.9	- 778	24.5		- 7.6	33.0	- 9.4	32.0	- 5.0	38.5
5		- 890	22.6	- 892	22.6	- 725	22.8		- 5.6	24.4	- 7.9	27.1	- 1.5	11.5
TOTAL		-3941	100	-3944	100	-3181	100		-23.1	100	-29.3	100	-13.0	100
1	x = 231 ft	944	15.5	946	15.5	971	16.4	x = 166.2 ft	8.0	4.7	9.1	5.1	7.3	5.1
2		1250	20.5	1251	20.5	1171	19.8		21.9	12.8	23.1	13.0	18.8	13.0
3		1319	21.6	1318	21.6	1245	21.0		27.7	16.3	29.2	16.4	23.9	16.6
4		1428	23.4	1426	23.4	1340	22.7		45.5	26.7	47.3	26.6	37.6	26.1
5		1166	19.1	1164	19.1	1188	10.1		67.5	39.6	69.2	38.9	56.6	39.3
TOTAL		6107	100	6105	100	5916	100		170.6	100	177.8	100	144.2	100
1								x = 295.8 ft	- 3.7	2.6	- 4.5	3.2	- 3.3	2.9
2									- 14.6	10.4	- 14.8	10.6	- 12.7	11.0
3									- 18.9	13.5	- 19.1	13.7	- 16.4	14.3
4									- 38.4	27.4	- 38.0	27.2	- 30.4	26.4
5									- 64.7	46.1	- 63.2	45.3	- 52.2	45.4
TOTAL									-140.3	100	-139.6	100	-115.0	100

Girder Shears

Total cross section shear force under P13 truck load is shown in Fig. 7.3.8c. The distribution of this shear to each individual girder is shown in Table 7.3.3b.

The total shear forces from MUPDI4 and CURDI4 (Fig. 7.3.6c) are essentially identical. The CELL4 solution agrees well with the MUPDI4 and CURDI4 solutions except at the supports, where the finite element solution truncates the peak of the shear diagram. This truncation is evident in both Fig. 7.3.8c and Table 7.3.3b, and could be reduced by mesh refinement and extrapolation of results for CELL4.

The distribution of the total shears to the individual girders (Table 7.3.3b) shows that the girder under the load resists nearly half the total shear in the section. The multi cell box girder does not distribute shear to adjacent girders as efficiently as it distributes moments. The three programs agree very well in their prediction of percentage distribution of total P13 truck load moment to the individual girders.

Transverse Bending Moments at X = 231 feet

The transverse distribution of transverse bending moments in the walls of the box girder cross section under P13 truck load is shown in Fig. 7.3.9a.

The three programs predict essentially identical transverse bending moments for this load case, except for directly under the load. Here, CELL4 differs from MUPDI4 and CURDI4 because the truck load was lumped to the mid-slab node as well as to the nodes at the webs, resulting in the positive mid slab moments shown.

Longitudinal Membrane Stresses at X = 231 feet

The transverse distribution of longitudinal membrane stresses in the walls of the box girder cross section under P13 truck load is shown in Fig. 7.3.9b.

At most locations the three programs give similar results, with nearly linear variations in stress in all webs and very little reduction of stress in the slabs between the webs. Under the load in girders 4 and 5, MUPDI4 and CURDI4 predict higher peaks in stress and greater reduction in stress in the

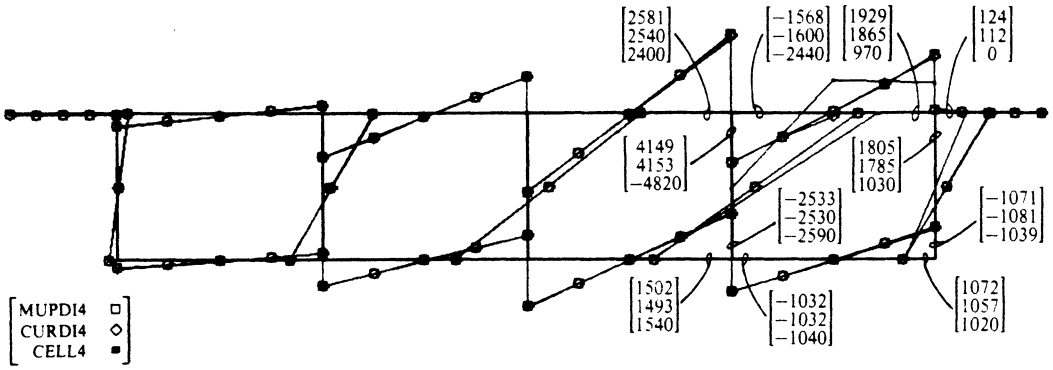

(a) TRANSVERSE MOMENTS M_y (in-lb/in) AT x=231 ft.

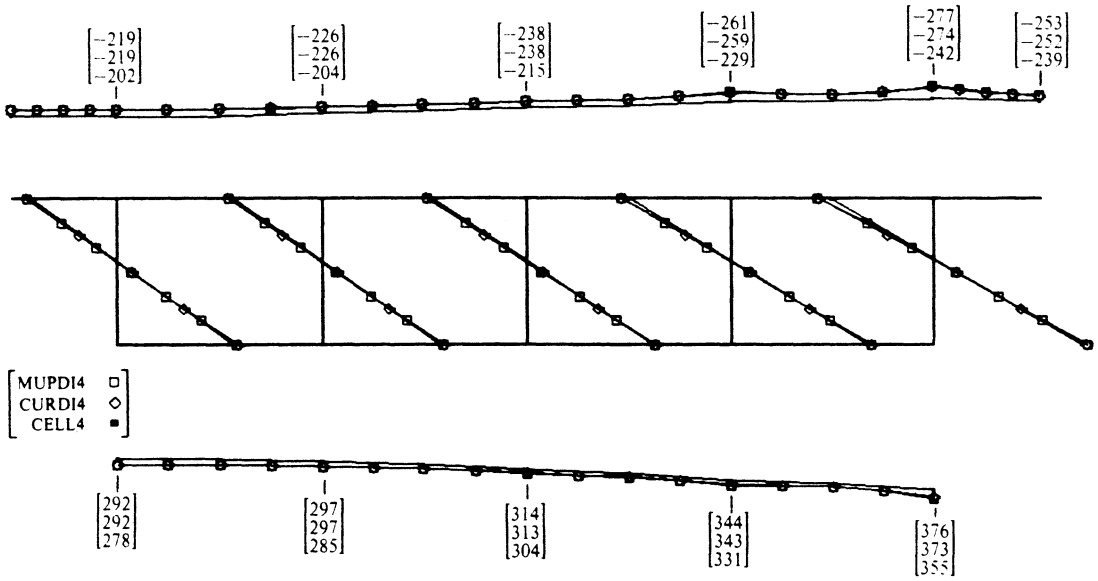

(b) LONGITUDINAL MEMBRANE STRESSES σ_x (psi) AT x=231 ft.

FIG. 7.3.9 TRANSVERSE DISTRIBUTION OF TRANSVERSE MOMENTS, LONGITUDINAL MEMBRANE STRESSES AND MEMBRANE SHEAR STRESSES FOR P13 TRUCK LOAD

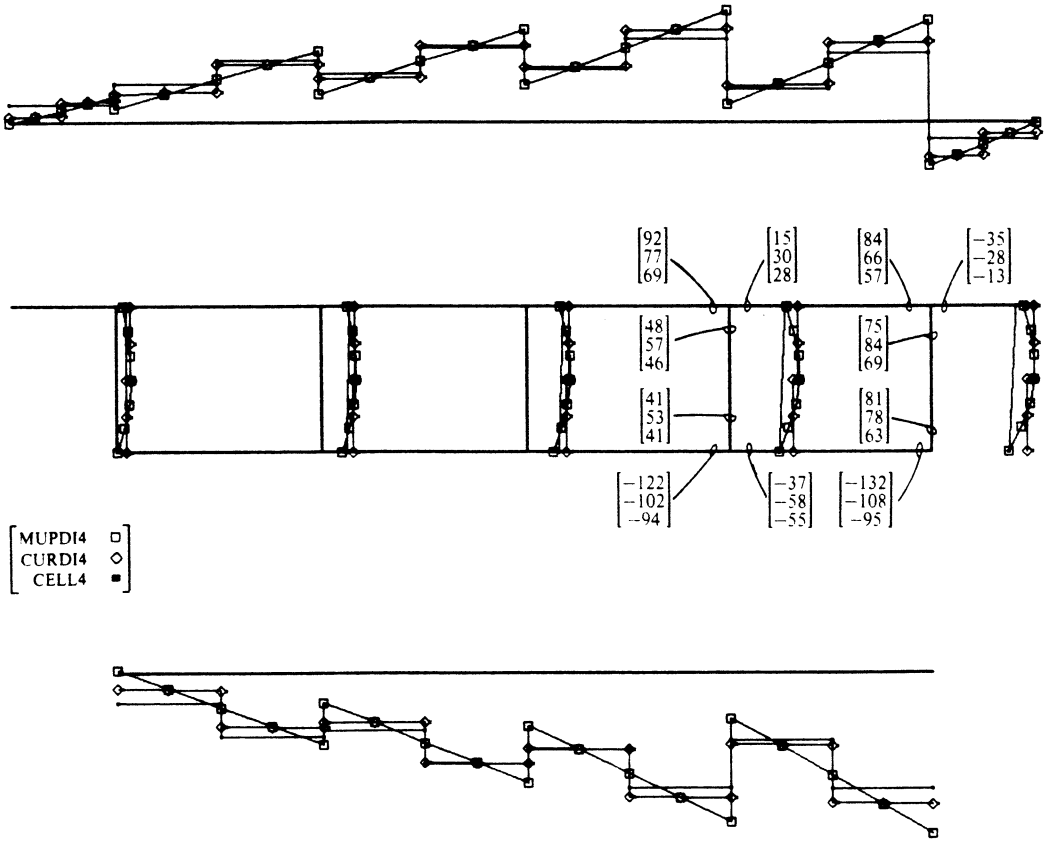

(c) MEMBRANE SHEAR STRESSES τ_{xy} (psi) AT x=166.2 ft.

FIG. 7.3.9 TRANSVERSE DISTRIBUTION OF TRANSVERSE MOMENTS, LONGITUDINAL MEMBRANE STRESSES AND MEMBRANE SHEAR STRESSES FOR P13 TRUCK LOAD

slabs between the webs, due to their more refined model. The CELL4 result could be improved by further mesh refinement.

Membrane Shears at X = 166.2 feet

The transverse distribution of membrane shear stresses in the walls of the box girder cross section under P13 truck load is shown in Fig. 7.3.9c.

In the webs, where most of the vertical section shear is resisted, MUPDI4 gives a parbolic shear stress variation, while CURDI4 overestimates the parabolic distribution with a bilinear approximation and CELL4 underestimates the parabolic distribution with a linear approximation. This is the source of the discrepancies between the three programs noted in Fig. 7.3.8c. Additional web elements may be used in CURDI4 to refine the prediction.

In the top and bottom slabs, MUPDI4 gives the expected linear shear stress variation, while CURDI4 and CELL4 do not. Note, however, that the CURDI4 and CELL4 solutions give accurate results at element midpoints. With mesh refinement the CURDI4 and CELL4 solutions will converge to the MUPDI4 result. Note that membrane shears in the top and bottom slabs form a large force couple which resists a large portion of the section torsion due to the eccentric load.

7.3.4 Conclusions

This example illustrates the capabilities of MUPDI4, CURDI4 and CELL4 in the analysis of a realsitic multi cell prestressed concrete highway bridge structure. In most cases the results of the three programs agree quite well, and show that they can provide a complete picture of the behavior of such a bridge structure under load.

7.4 Example 4 - Two Span Circularly Curved Single-Cell Prestressed Bridge Model with Sloping Webs

This example demonstrates the application of the CURDI4 computer program in analyzing a continuous, two span, prestressed curved box girder bridge with sloping webs, and compares the numerical results with the results obtained from the experimental study of a small scale model.

7.4.1 Structure Geometry, Prestressing and Load Cases

The structure is a plexiglass model studied extensively by Hood [20]. The model consists of straight plexiglass segments glued together and is circularly curved in plan with a centerline radius of 2000 mm (Fig. 7.4.1a). It has supported diaphragms at the two ends and at the center, dividing it into two equal spans. The cross section is a single cell box girder with sloping webs and haunched bottom slab, top slab, and top slab cantilevers (Fig. 7.4.1b).

Two different load cases have been analyzed and compared with the results of the model study:

Case 1 - A single vertical 313 N load on the top slab at its intersection with the interior web, at the center of one span only (Fig. 7.4.1a):

Case 2 - Two prestressing tendons, one in each web, following a piecewise parabolic profile, including the effects of curvature friction (Fig. 7.4.3).

Material properties are considered to be isotropic, based on measurements of the model by Hood [20]. Hood reports a modulus of elasticity of 6536 MPa and a Poisson's ratio of 0.321.

7.4.2 Analytical Model

The structure is modelled analytically with two elements in each web, ten elements in the top deck slab, and two elements in the bottom soffit slab (Fig. 7.4.2). The supports are modelled as rigid supported diaphragms. The idealized cross-section (Fig. 7.4.2) had the following section properties: distance from cgc of the section to the fibers at the

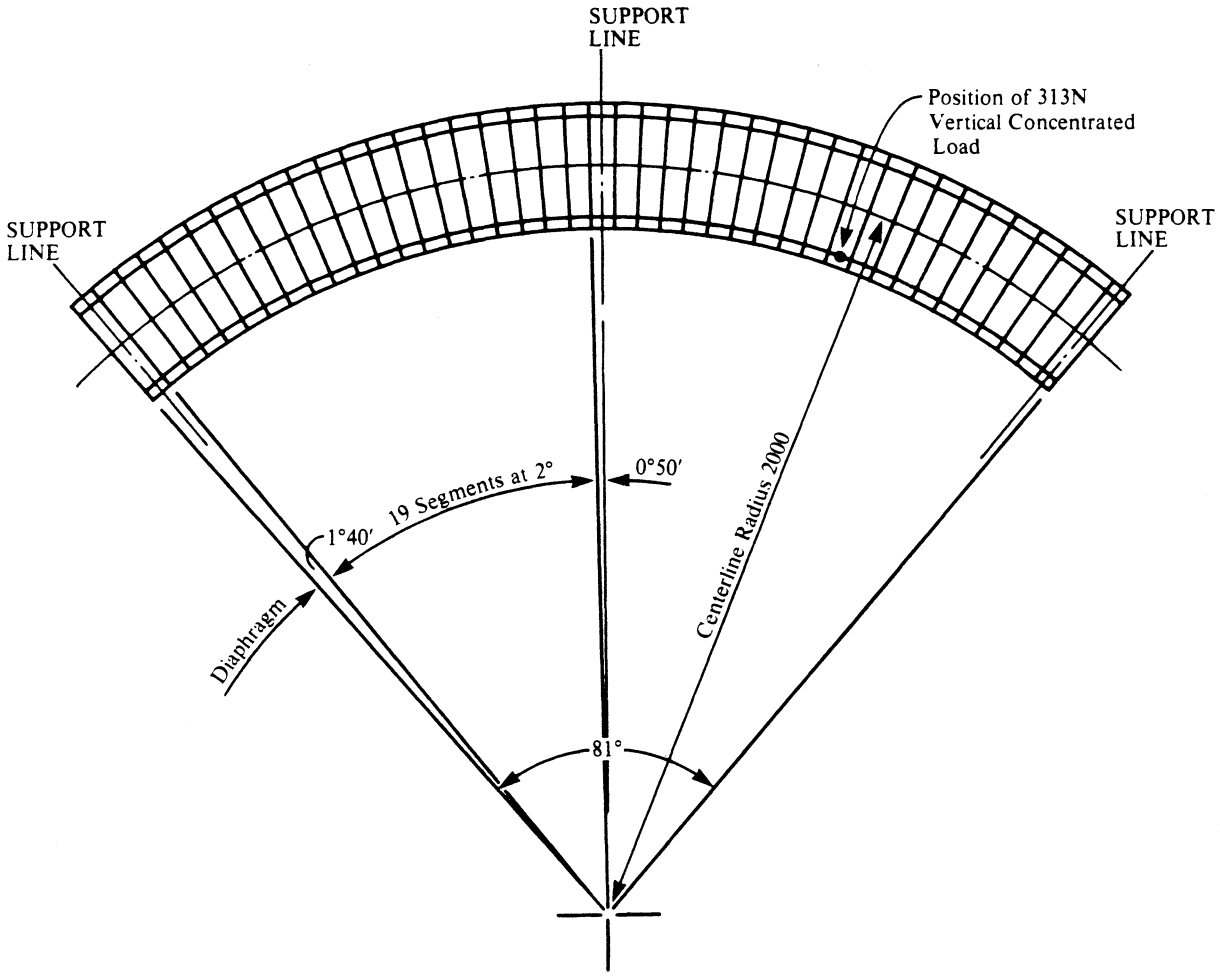

(a) PLAN GEOMETRY

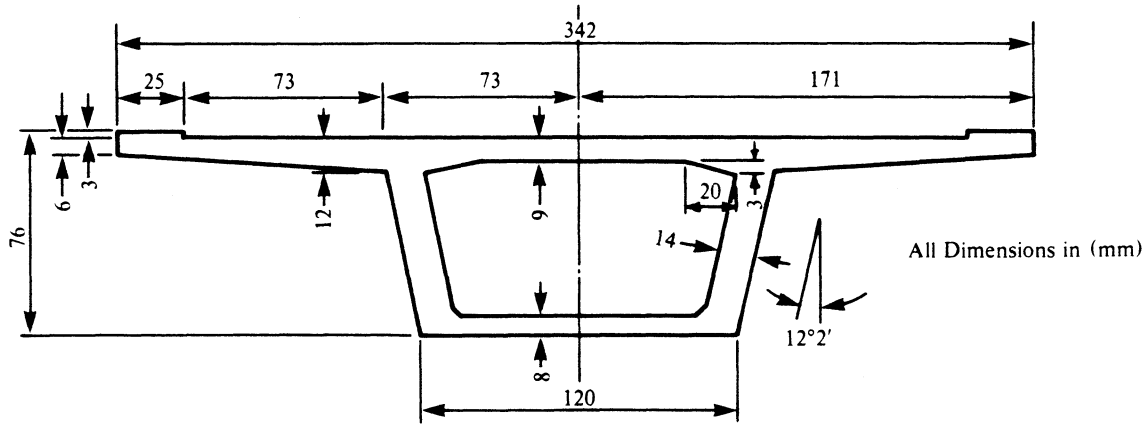

(b) TYPICAL SECTION DIMENSIONS

FIG. 7.4.1 GEOMETRY AND CONCENTRATED POINT LOAD POSITION FOR HOOD PLEXIGLASS MODEL

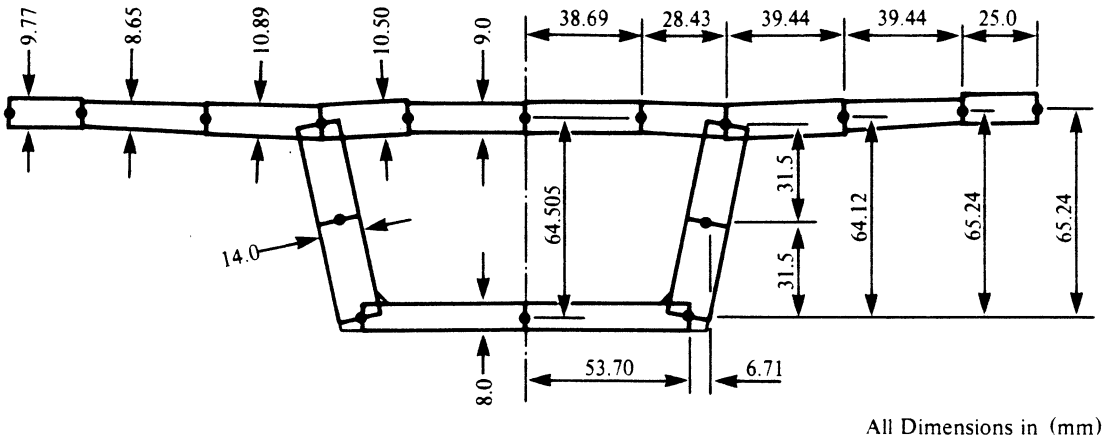

FIG. 7.4.2 ANALYTICAL MODEL OF CROSS-SECTION FOR CURDI4 ANALYSIS

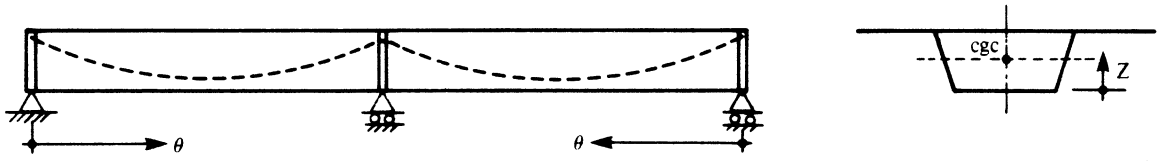

θ[°]	Z[mm]	θ[°]	Z[mm]
0°50′	40.04	20°50′	12.72
2°50′	33.69	22°50′	14.43
4°50′	28.12	24°50′	16.96
6°50′	23.37	26°50′	20.28
8°50′	19.43	28°50′	24.44
10°50′	16.29	30°50′	29.38
12°50′	13.95	32°50′	35.14
14°50′	12.44	34°50′	41.70
16°50′	11.73	36°50′	47.81
18°50′	11.82	38°50′	50.72

FIG. 7.4.3 PRESTRESSING TENDON GEOMETRY

mid-thickness of the bottom deck slab c_b = 45.18 mm; cross-sectional area A = 5986 mm^2; and moment of inertia about the cgc I = 3.9 x 10^6 mm^4.

The tendon profile (Fig. 7.4.3) is defined by coordinates as given by Hood [20]. The tendons in the model were jacked from both end supports with a prestressing force of 2224 N per web. Hood [20] measured a loss of prestressing force of 6% from the end supports to the center support, assuming a uniform friction loss. Since reliably measured friction coefficients are not available, a curvature friction coefficient of μ = 0.08 is chosen for the CURDI4 analysis. Wobble friction is assumed to be zero. The chosen friction coefficients give a loss of prestress force of about 6%.

The concentrated load is simulated as a patch load of length 8 mm along the span and zero width transverse to the span. Hood [20] used a pad size of 8 mm by 20 mm experimentally. 100 Fourier Series terms are used in the CURDI4 analysis.

7.4.3 Discussion of Results

7.4.3.1 Case 1 - Single 313N Vertical Point Load

The longitudinal tangential stresses found by CURDI4 at a section at the middle of the loaded span agree quite well with the experimental results of Hood (Fig. 7.4.4a). Stresses shown are at the mid-thickness of each plate element.

The transverse radial stresses at the same section at the inner and outer faces of each plate element also agree quite well with the experimental values (Fig. 7.4.4b) in the top and bottom slabs and at most points in the webs. The largest discrepancy occurs at the inner face at the top of the inner web directly under the concentrated load, emphasizing the need for a finer finite strip mesh in this vicinity and the need to carefully study results for stresses directly under concentrated loads.

The longitudinal variations of the vertical displacement at the tops of the inner and outer webs as found by CURDI4 (Fig. 7.4.6a) indicates a small difference at the midspan of the unloaded span, but essentially no

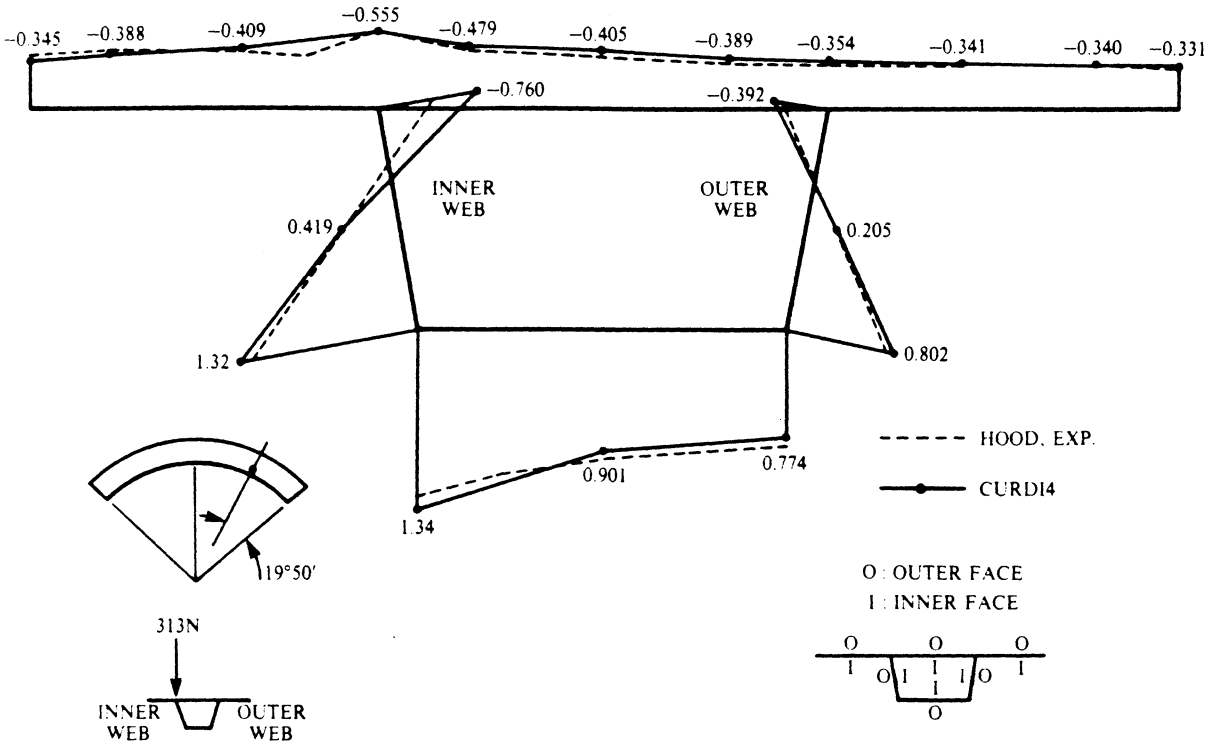

(a) LONGITUDINAL TANGENTIAL STRESSES (MPa)

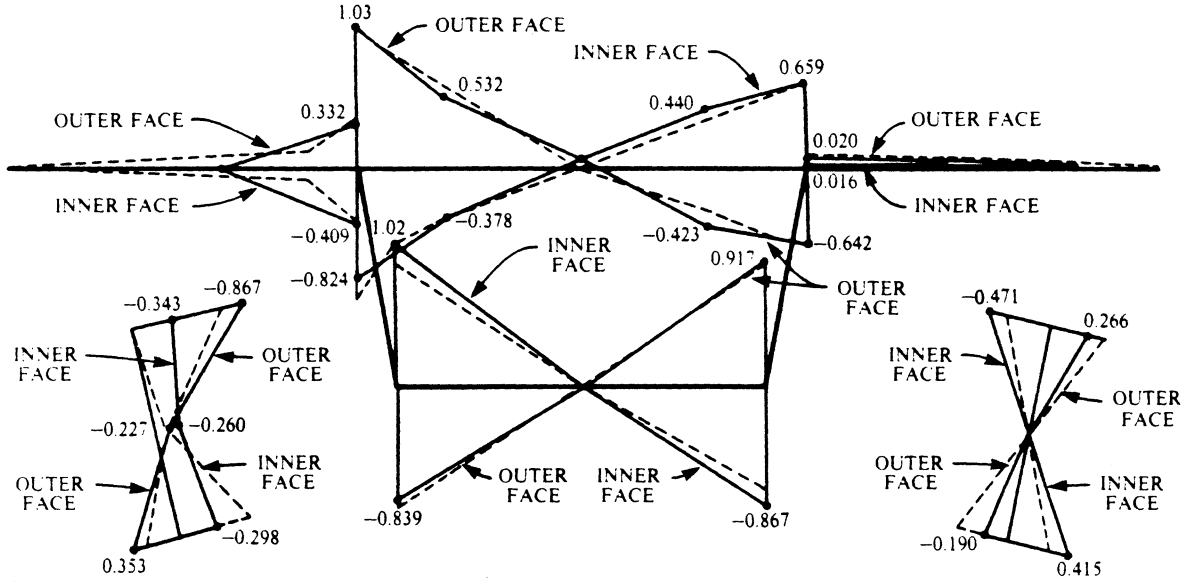

(b) TRANSVERSE RADIAL STRESSES (MPa)

FIG. 7.4.4 STRESSES (MPa) AT MIDDLE OF LOADED SPAN FOR SINGLE 313N POINT LOAD

difference at the midspan of the loaded span.

7.4.3.2 Case 2 - Prestressing

The longitudinal tangential stresses found by CURDI4 at the same midspan section as for Case 1, but due to prestressing alone, are compared with experimental values by Hood in Fig. 7.4.5a. It can be seen that the CURDI4 compressive stresses in the top slab are smaller and in the bottom slab larger than those found experimentally by Hood. An approximate estimate from Fig. 7.4.5a indicates a lower longitudinal stress at the cgc of the section by CURDI4 and thus a lower total prestress force at this section. This in turn would produce a different set of primary and secondary moments and also final stresses from those found by Hood experimentally. It is difficult to assess the friction effects in the experimental Hood model, which was built of short plexiglass segments glued together. Each segment had a straight prestressing duct, resulting in a piecewise linear tendon profile approximating the more realistic parabolic tendon. Thus, differences between the assumed friction coefficient in CURDI4 and the actual friction in the experimental model could account for the differences in the longitudinal stresses in Fig. 7.4.5a.

The transverse radial stresses due to prestressing are shown in Fig. 7.4.5b. Agreement between CURDI4 analytical values and Hood experimental values is excellent in the top slab, however, it is not so good in the webs and the bottom slab. The prestressing force exerts a local radial horizontal force component on each web due to the horizontal curvature of the bridge model, which causes high local plate bending moments. CURDI4 incorporates these effects by replacing the actual local radial forces, due to prestressing between the longitudinal joints, by applied work equivalent, consistent nodal forces and moments (see also Section 5.3.1 for a more complete explanation). This procedure, like any finite element procedure, results in discontinuities in internal transverse moments and stresses for actual loads between the joints. These discontinuities can be decreased and the accuracy of the local stresses increased by using a finer

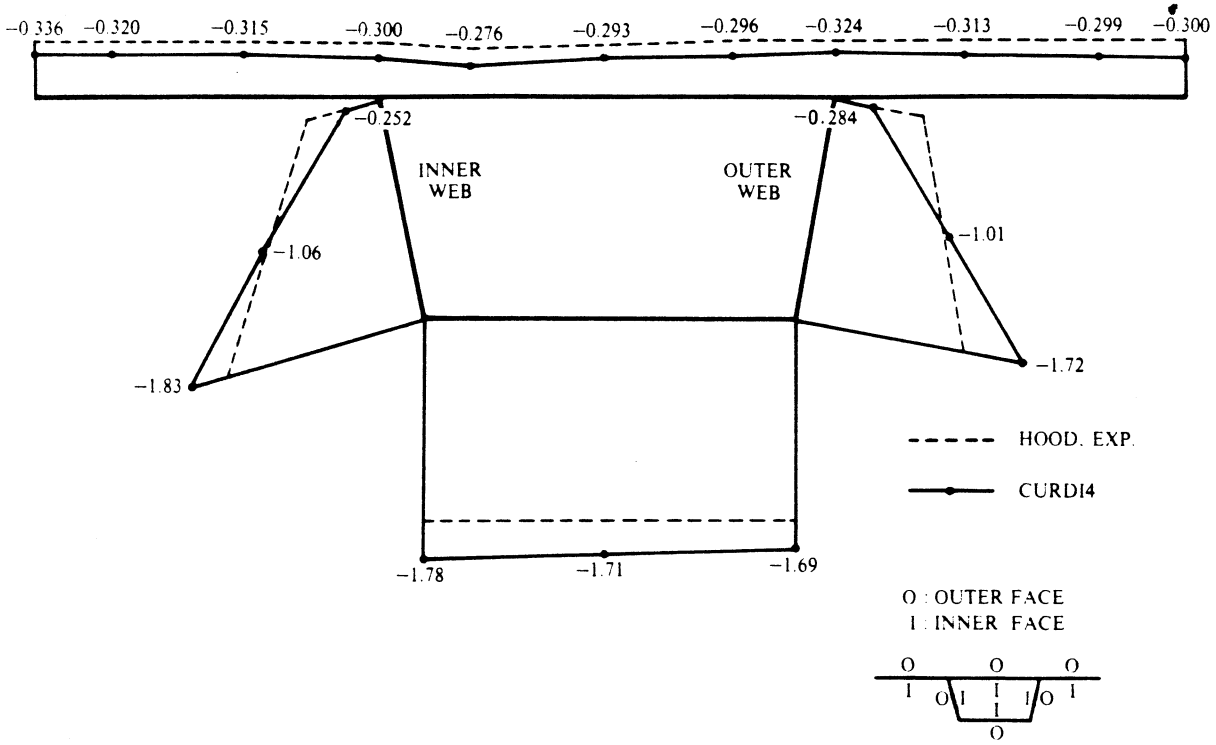

(a) LONGITUDINAL TANGENTIAL STRESSES (MPa)

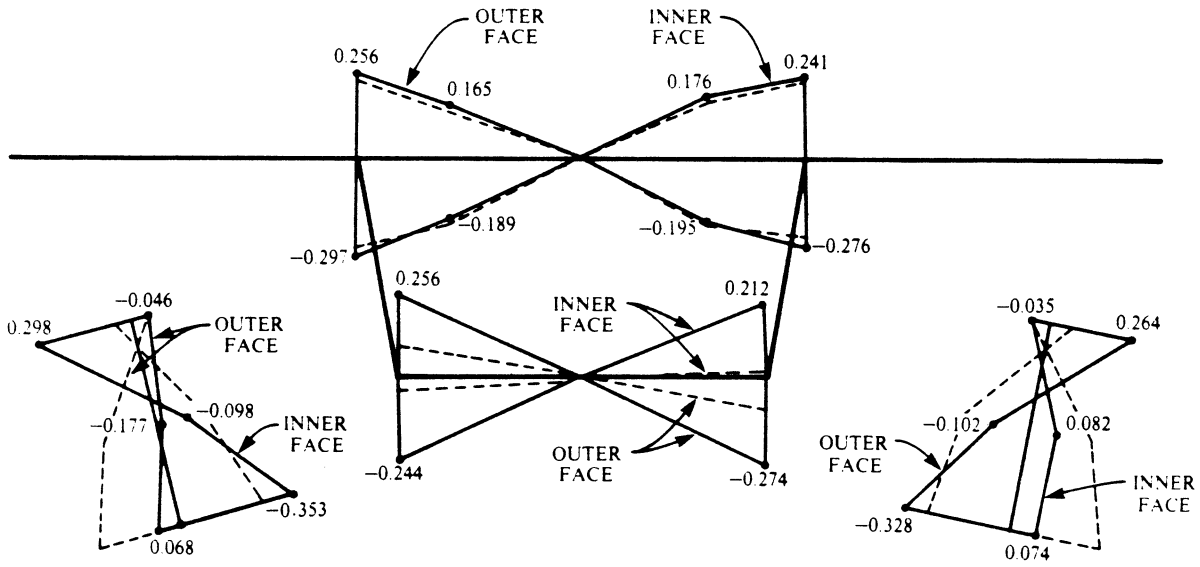

(b) TRANSVERSE RADIAL STRESSES (MPa)

FIG. 7.4.5 STRESSES (MPa) AT MIDSPAN DUE TO PRESTRESSING

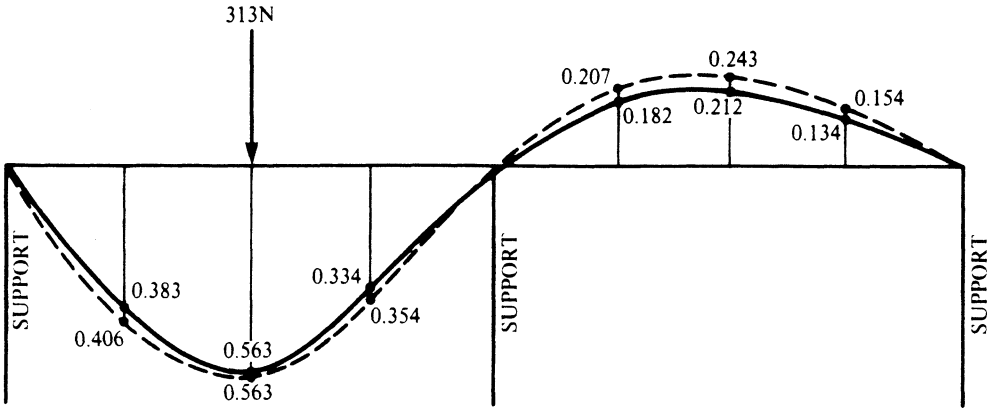

(a) DUE TO A 313N POINT LOAD AT TOP OF INNER WEB

——— AT TOP OF INNER WEB

– – – – AT TOP OF OUTER WEB

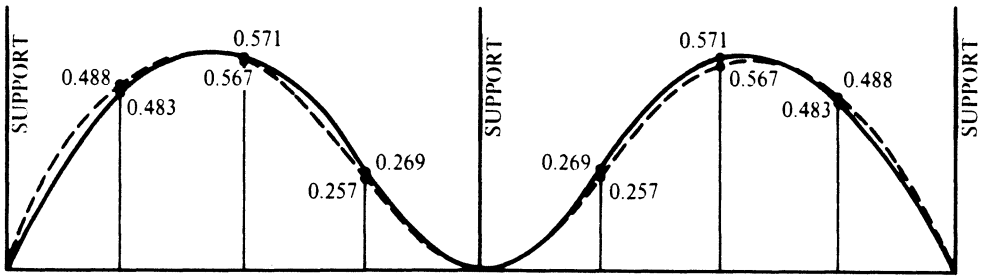

(b) DUE TO PRESTRESS

FIG. 7.4.6 LONGITUDINAL VARIATIONS OF VERTICAL DISPLACEMENT (mm) AT THE TOPS OF THE INNER AND OUTER WEBS

finite strip mesh size. A good measure of the accuracy of the results is to check the equilibrium of internal transverse moments from the strips acting on the joints. This should indicate if a refinement of mesh size is needed to achieve a desired accuracy.

The longitudinal variation of the vertical displacements at the tops of inner and outer webs (Fig. 7.4.6b) indicates essentially no differences due to the prestressing loads.

7.4.4 Conclusions

Analytical results from CURDI4 were in good agreement with experimental model results for a single concentrated load, except in the web directly under the load. For the case of prestressing alone, difficulties in estimating the actual friction losses gave some differences in the analytical and experimental results for longitudinal stresses. Transverse stresses in the top slab, for prestressing alone, were in good agreement, but in the webs and bottom slab significant differences existed due to the local effects of the radial prestress forces.

This example demonstrates the need for a careful study of the results for curved prestressed box girder bridges and also suggests that the effect of upper and lower bound estimates of prestress losses and of finite strip mesh sizes should be considered in certain cases.

7.5 Example 5 - Two Span Circularly Curved Four-Cell Bridge with Vertical Exterior Webs

This example illustrates the versatility of the program CURDI4 by analyzing a two span, circularly curved, four-cell bridge using curved finite strip theory. The results are then compared with Example 3, where a straight four-cell bridge with the same cross-section was studied employing the straight finite strip option in CURDI4.

7.5.1 Structure Geometry, Prestressing and Load Cases

The selected cross-section and the material properties are the same as in Example 3. The two span arrangement is unsymmetrical with 150 ft and 162 ft spans measured along the centerline (Fig. 7.5.1). The bridge is circularly curved in plan with a radius of 400 ft to the centerline. Rigid unmoveable diaphragms support the bridge at the two ends and the middle support. Five parallel vertical webs divide the cross-section into four rectangular cells. The top deck slab with a cantilever portion on either side and a bottom deck complete the cross-section (Fig. 7.3.1).

The same three load cases are considered as in Example 3:

Case 1: Dead load of the bridge.

Case 2: P13 truck in one lane.

Case 3: Longitudinal panel prestressing tendon in all webs.

The dead load includes the weight of the top and bottom deck slabs as well as the five webs and is the same as in Example 3. The P13 truck wheel load arrangement is fully discussed in Example 3 (Fig. 7.3.3). The panel tendons are idealized by one tendon in each web, all having the same vertical parabolic profile (Fig. 7.3.1) measured angularly along the span. The tendon geometry was automatically generated by CURDI4.

The results of the curved four-cell bridge are compared with that of the straight four-cell bridge in Example 3, bearing in mind that they have identical cross-sections, loads and spans measured along the centerline.

7.5.2 Analytical Models

An analytical model of the bridge was obtained by dividing it into

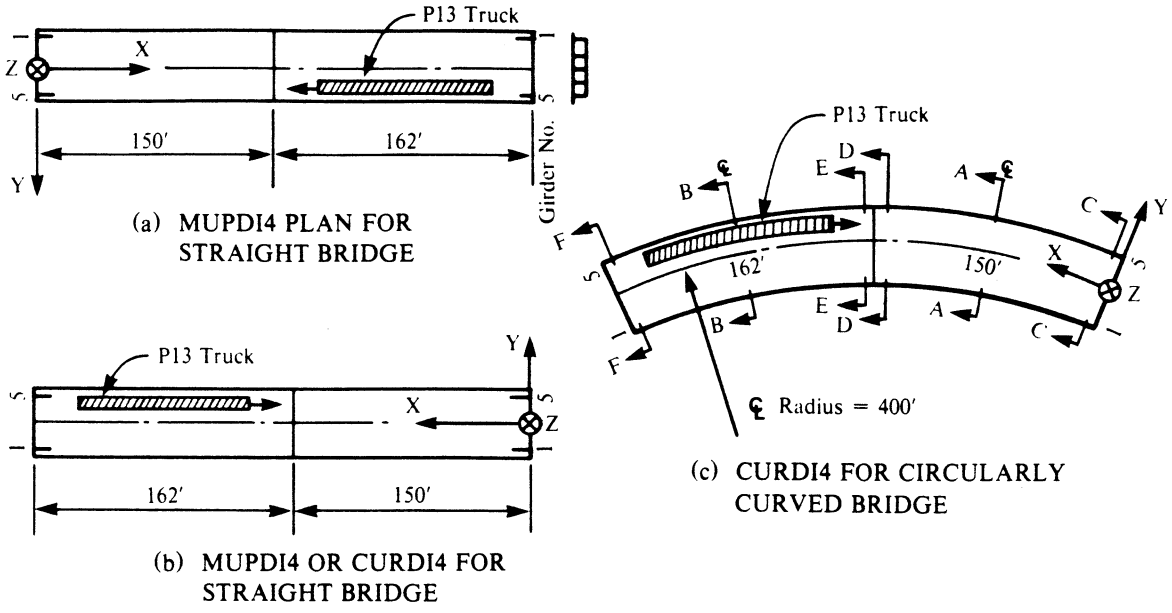

FIG. 7.5.1 PLAN GEOMETRY AND SECTION LOCATIONS FOR CIRCULARLY CURVED FOUR CELL BRIDGE

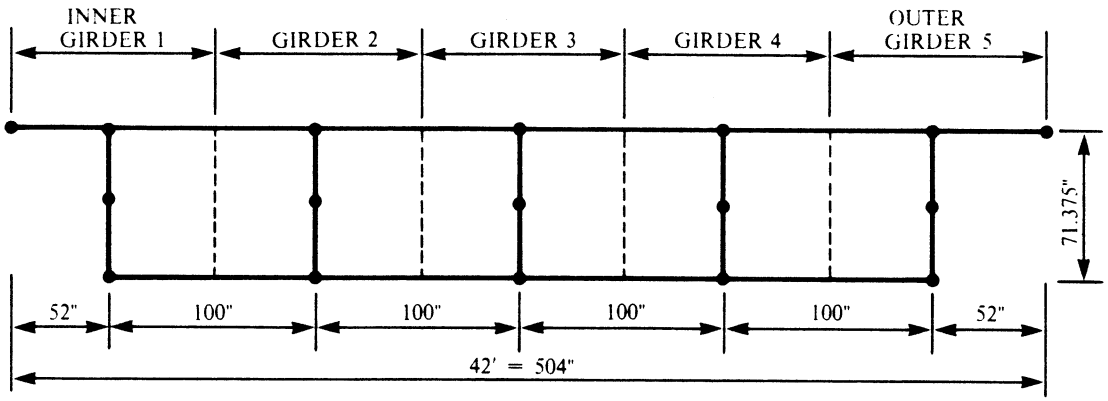

FIG. 7.5.2 ANALYTICAL MODEL 1 (COARSE MESH) OF CROSS-SECTION FOR CURDI4 ANALYSIS

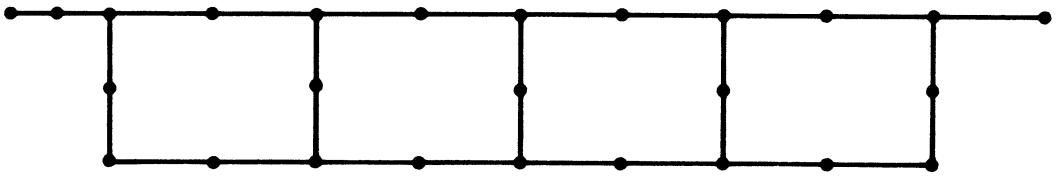

FIG. 7.5.3 ANALYTICAL MODEL 2 (FINE MESH) OF CROSS-SECTION FOR CURDI4 ANALYSIS

curved finite strips, each strip extending longitudinally along the whole span.

The plan geometry, global coordinate system XYZ, and section locations for the curved circularly curved four-cell bridge analyzed by CURDI4 are shown in Fig.7.5.1c. Note that for CURDI4, the radial global axis Y must have a positive direction outward away from the center of horizontal curvature requiring the origin, coordinate system and girder number locations shown in Fig. 7.5.1c. For the similar straight bridge analyzed in Example 3, either the orientation shown in Figs. 7.5.1a or 7.5.1b could be used in the MUPDI4 analysis.

Because the accuracy of the analytical model used in CURDI4 depends on the number of finite strips used, a coarse finite strip mesh 1 (Fig. 7.5.2) and a finer mesh 2 (Fig. 7.5.3) are studied in the analysis of the curved bridge. 100 terms are included in the Fourier series representation of the loading and prestressing.

The cross-section is divided into five girders, each girder comprising one web and a portion of the top and bottom deck slabs. Stresses in each girder are integrated to obtain individual girder and total section moments, shears and axial forces.

The dead load is automatically computed internally by CURDI4 from the input weight of the concrete of 155 pcf. The P13 truck wheel loads are modelled as line loads of zero transverse width and a longitudinal length for each equal to the length of a wheel pad contact surface on the deck. Prestressing tendons are discretized into straight segments. The tendon forces are transferred to the surrounding structure at the ends of the segments. For a more complete explanation of all load cases, refer to Chapter 3.

7.5.3 Discussion of Results

The girder moments and shears reveal the effect of the horizontal curvature of the bridge. Inner girders 1 and 2 (Figs. 7.5.1, 7.5.2 and 7.5.3) are of shorter span measured along the circumferential webs than the

outer girders 4 and 5. Tables 7.5.1 and 7.5.2 summarize the individual girder and total section moments and shears at the various sections indicated in Fig. 7.5.1. The results for coarse mesh 1 are given, but very little difference was found using fine mesh 2.

A careful study of Table 7.5.1 for moments indicates that for dead load and prestressing relatively small differences in the percentage of the total moment taken by inner girders 1 and 2 exist as compared to outer girders 4 and 5. For the transversely unsymmetrical P13 truck loading, somewhat larger percentages of the section moment are taken by girders 4 and5 in the loaded region, but even for this case, the excellent load distributing ability of the four cell box is evident, because girders 1 and 2 still carry a sizeable portion of the total moment.

Comparing moment values for the curved bridge in Table 7.5.1 with those found in Table 7.3.1 for the straight bridge, with the same cross-section and centerline spans, both found using the CURDI4 program, it can be noted that the girder and total section moments are quite similar in magnitude and distribution and not significantly different even for the the unsymmetrical P13 truck load.

A similar comparison of the total section shears for the curved and straight bridges given in Tables 7.5.2 and 7.3.2 indicates similar values at all sections except one. However, for the transversely unsymmetrical P13 truck load, some longitudinal redistribution of the total section shears occurs. With respect to the transverse distribution of the total section shears to the individual girders, significant differences exist between the curved and straight bridges for all three load cases, which should be taken into account in design.

The longitudinal compressive and tensile membrane stresses at midspan Section B-B are approximately constant across the width of the bridge (Fig. 7.5.4) and nearly the same as in the straight bridge of Example 3.

The transverse radial slab moments (Figs. 7.5.5 and 7.5.6) provide a useful check of moment equilibrium at the joints. The finite strip method,

TABLE 7.5.1 SUMMARY OF INDIVIDUAL GIRDER AND TOTAL SECTION MOMENTS (FT-KIPS) (COARSE MESH 1)

SECTION	GIRDER	DEAD LOAD		P13 TRUCK LOAD		PRESTRESS	
		MOMENT	% OF TOTAL	MOMENT	% OF TOTAL	MOMENT	% OF TOTAL
(1)	(2)	(3)	(4)	(5)	(6)	(7)	(8)
SECTION A - A	1	2495	17.5	- 389	17.8	- 2292	14.8
	2	3175	22.3	- 492	22.4	- 3801	24.5
	3	3132	22.0	- 481	21.9	- 3709	23.9
	4	3100	21.7	- 471	21.5	- 3632	23.5
	5	2354	16.5	- 358	16.4	- 2055	13.3
	TOTAL	14260	100	-2191	100	-15490	100
CENTER BENT	1	-5844	17.2	- 584	13.8	5096	20.2
	2	-7242	21.4	- 763	18.0	5287	21.0
	3	-7299	21.5	- 883	20.8	5132	20.4
	4	-7373	21.8	-1054	24.9	4994	19.8
	5	-6147	18.1	- 954	22.5	4704	18.7
	TOTAL	-33900	100	-4239	100	25210	100
SECTION B - B	1	3433	17.5	1012	16.0	- 2294	14.8
	2	4364	22.3	1318	20.8	- 3801	24.6
	3	4305	22.0	1370	21.7	- 3705	24.0
	4	4258	21.7	1460	23.0	- 3624	23.4
	5	3239	16.5	1171	18.5	- 2049	13.2
	TOTAL	19600	100	6331	100	-15470	100

TABLE 7.5.2 SUMMARY OF INDIVIDUAL GIRDER AND TOTAL SECTION SHEARS (KIPS)(COARSE MESH 1)

SECTION	GIRDER	DEAD LOAD		P13 TRUCK LOAD		PRESTRESS	
		SHEAR	% OF TOTAL	SHEAR	% OF TOTAL	SHEAR	% OF TOTAL
(1)	(2)	(3)	(4)	(5)	(6)	(7)	(8)
SECTION C - C	1	-61.7	14.2	1.5	5.0	86.8	22.2
	2	-86.8	20.0	5.4	18.9	85.7	21.9
	3	-88.4	20.4	5.8	20.1	83.0	21.2
	4	-89.0	20.5	6.1	21.3	78.8	20.2
	5	-107.8	24.9	10.0	34.7	56.5	14.5
	TOTAL	-433.7	100	28.8	100	390.8	100
SECTION D - D	1	156.4	16.8	6.4	20.6	-167.8	22.2
	2	194.9	21.0	5.0	16.1	-164.8	21.8
	3	198.4	21.4	7.0	22.5	-158.6	20.9
	4	198.4	21.4	9.6	30.9	-150.9	19.9
	5	180.3	19.4	3.1	10.0	-115.2	15.2
	TOTAL	928.5	100	31.1	100	-757.4	100
SECTION E - E	1	-155.2	16.0	0.9	-0.5	157.9	22.5
	2	-201.9	20.9	-23.5	13.1	153.5	21.9
	3	-206.2	21.3	-30.7	17.1	147.4	21.0
	4	-206.9	21.4	-49.2	27.4	139.8	19.9
	5	-198.5	20.5	-77.1	43.0	103.6	14.8
	TOTAL	-968.6	100	-179.5	100	702.2	100
SECTION F - F	1	64.1	12.8	-7.8	-5.7	-82.7	22.6
	2	99.5	19.8	14.4	10.5	-80.5	22.0
	3	101.9	20.3	19.7	14.3	-77.8	21.3
	4	103.3	20.6	39.1	28.3	-73.4	20.1
	5	132.7	26.5	72.5	52.6	-51.3	14.0
	TOTAL	501.5	100	137.9	100	-365.6	100

by the nature of its formulation as a numerical and therefore not necessarily exact method, satisfies internal moment equilibrium at the joints only approximately. The degree of accuracy depends on the fineness of the mesh and the type of loading. In general, the accuracy increases with mesh refinement. Loads that are not applied at joints are transformed by CURDI4 into energy equivalents which are then applied at the joints as substitutes in an energy sense. This approximation is inherent to the finite strip method and is the most important factor that contributes to inexact satisfaction of moment equilibrium at joints. It is therefore advisable to put joints at points where concentrated loads are applied. In the case of a uniformly distributed load like dead load, this is not possible. Prestressing, which is idealized by many concentrated loads whose points of application vary in position and are of a very large number, is also of concern. If more accurate results are desired in such cases, it is necessary to use a mesh refinement until satisfactory transverse moment equilibrium is obtained.

The coarse mesh (Fig. 7.5.5) satisfies radial moment equilibrium adequately at the joints for the truck load, which is applied only at joints. The dead load and prestressing results have a relatively large moment unbalance at the joints for the coarse mesh 1 (Fig. 7.5.5). The fine mesh (Fig. 7.5.6) satisfies moment equilibrium adequately at the joints for dead load. On the other hand, the prestressing moment equilibrium is still poor although better than for coarse mesh 1. In order to give a satisfactory modelling of transverse, e.g. radial bending due to prestressing in curved bridges it is recommended that more finite strips be used to model the webs which contain the longitudinal panel tendons.

Transverse and longitudinal variations of vertical displacements for each of the load cases are depicted in Figs. 7.5.7 and 7.5.8. As expected outer girder 5 deflects more than inner girder 1, however, the transverse and torsional stiffness of the four cell box is quite effective in resisting distortion and twist in the curved bridge.

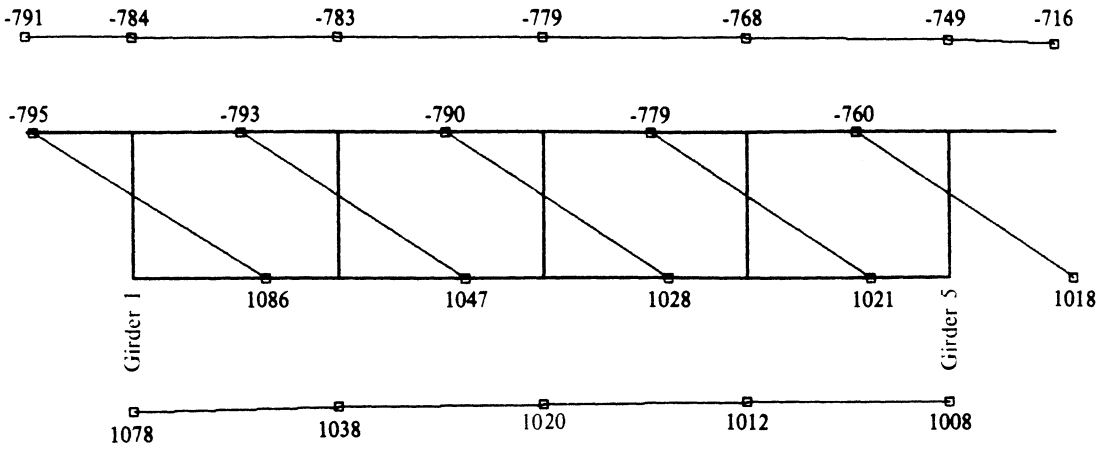

(a) DEAD LOAD

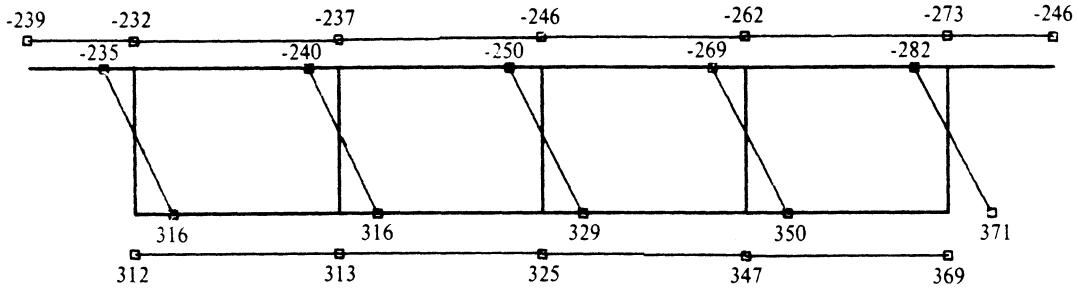

(b) P13 TRUCK LOAD

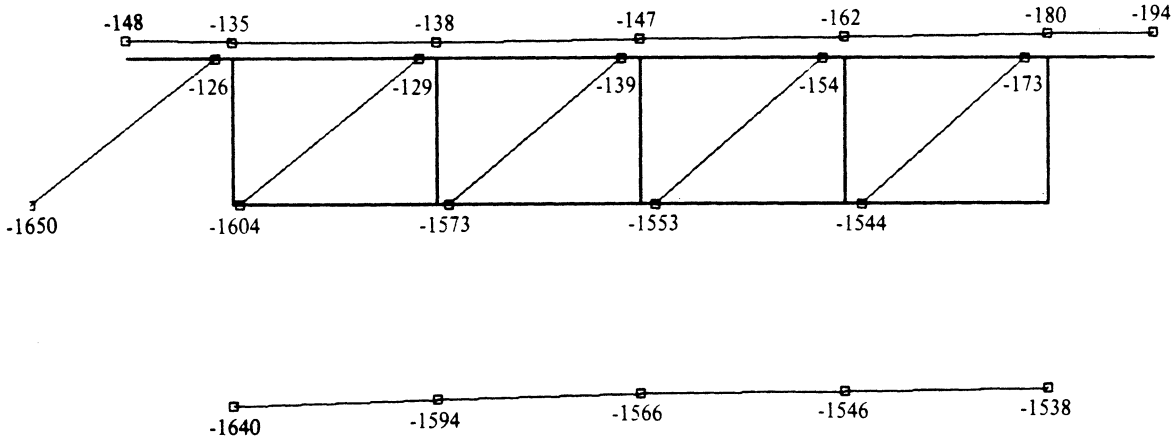

(c) PRESTRESS

FIG. 7.5.4 LONGITUDINAL MEMBRANE STRESSES σ_x (psi) AT MIDSPAN SECTION B-B (COARSE MESH 1)

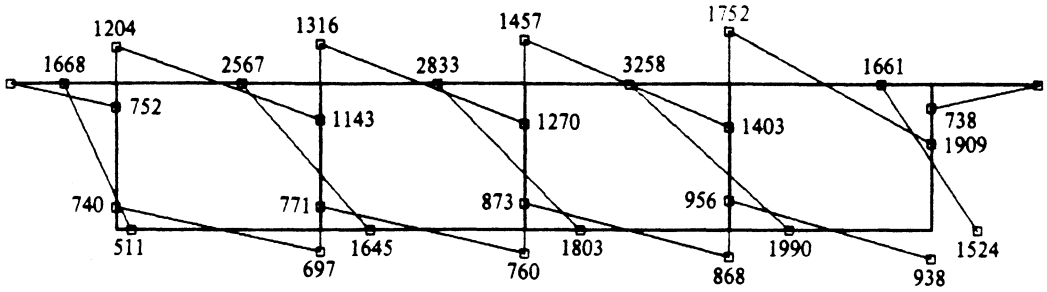

(a) DEAD LOAD

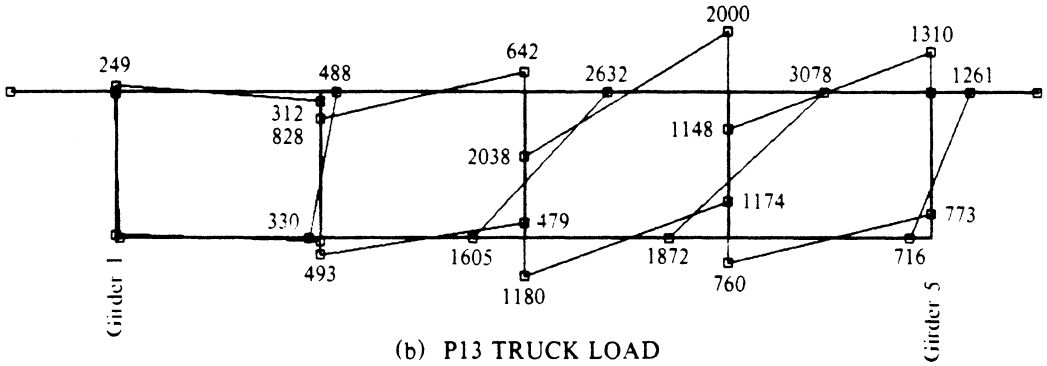

(b) P13 TRUCK LOAD

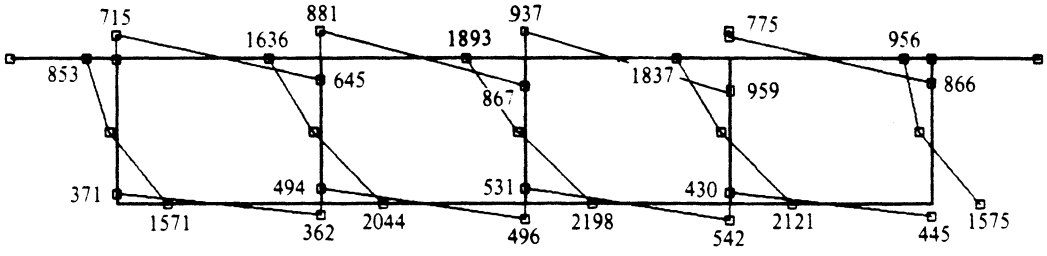

(c) PRESTRESS

FIG. 7.5.5 TRANSVERSE MOMENTS M_y (in.-lb/in.) AT MIDSPAN SECTION B-B (COARSE MESH 1)

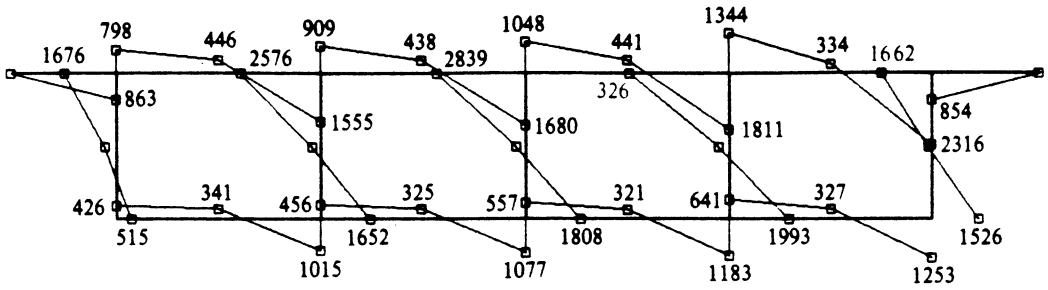

(a) DEAD LOAD

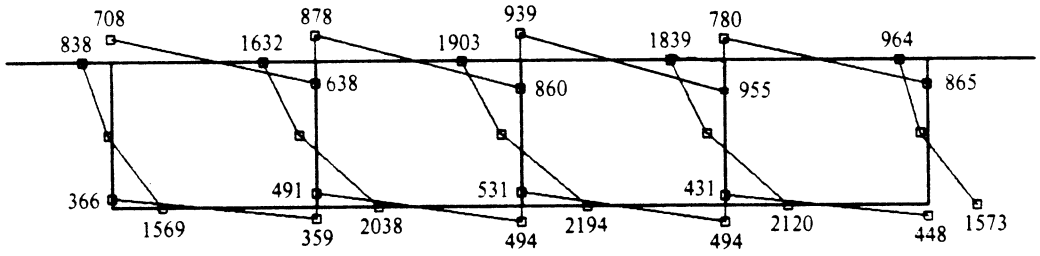

(b) PRESTRESS

FIG. 7.5.6 TRANSVERSE MOMENTS M_y (in.-lb/in.) AT MIDSPAN SECTION B-B (FINE MESH 2)

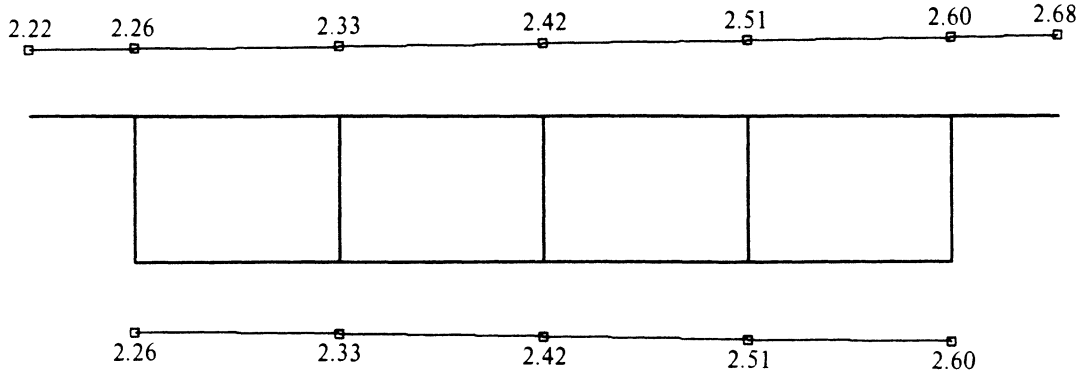

(a) DEAD LOAD

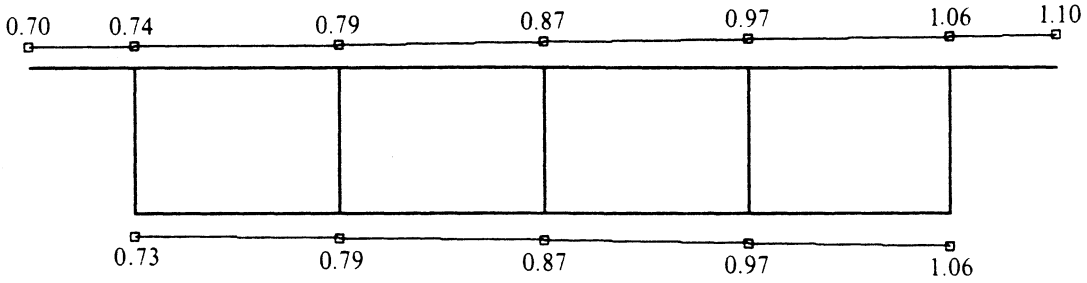

(b) P13 TRUCK LOAD

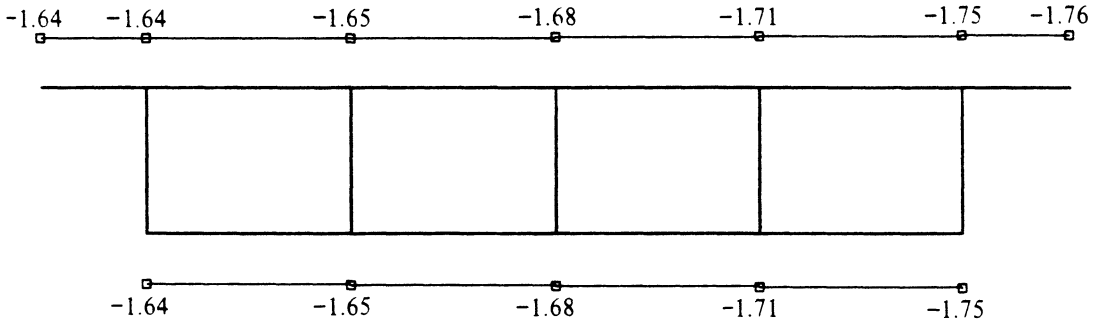

(c) PRESTRESS

FIG. 7.5.7 VERTICAL DISPLACEMENTS (in.) AT MIDSPAN SECTION (COARSE MESH 1)

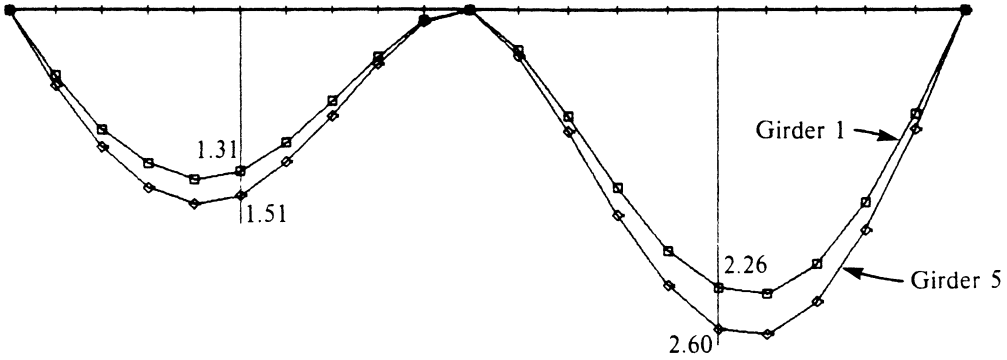

(a) DEAD LOAD

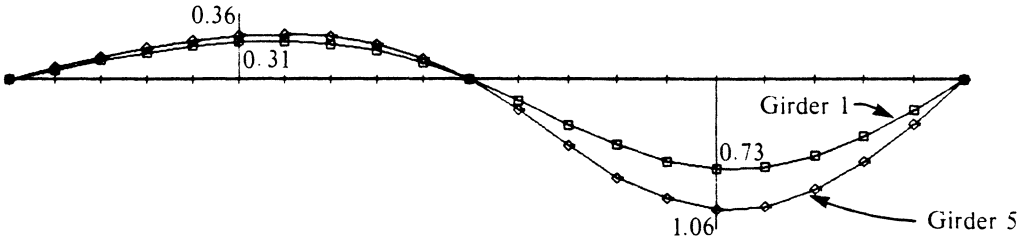

(b) P13 TRUCK LOAD

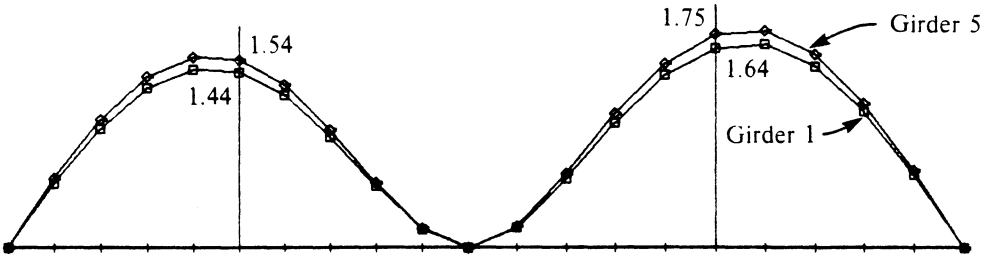

(c) PRESTRESS

FIG. 7.5.8 LONGITUDINAL VARIATIONS OF VERTICAL DISPLACEMENTS (in.) AT TOPS OF INNER GIRDER 1 AND OUTER GIRDER 5 (COARSE MESH 1)

7.5.4 Conclusions

The basic behavior of the curved bridge in this Example 5 was similar to that of the straight bridge of Example 3, with the exception that the effect of longitudinal prestressing must be carefully evaluated due to the radial force components generated in the curved bridge case.

7.6 Example 6 - Three Span Multi-Cell Prestressed Box Girder Bridge of Arbitrary Plan Geometry

This example is used to demonstrate the versatility of the CELL4 computer program in analyzing a complex post-tensioned box girder bridge of arbitrary plan geometry subjected to general loadings, and to illustrate how the computer results should be interpreted.

7.6.1 Structure Geometry, Prestressing and Load Cases

A three span, continuous, post-tensioned bridge designed as part of the highway connection to the airport in San Juan, Puerto Rico was chosen for the analysis. The geometry of the bridge in plan is defined in Fig. 7.6.1. The four supports (left abutment; bent 2A; bent 2B, and right abutment) are oriented in different skew directions (Fig. 7.6.1). The top and bottom slab edges and the webs of the bridge are circular in plan, except for a short length near the right abutment, where they follow a straight path tangent to the circular arc. The two interior support bents 2A and 2B divide the length of the bridge into three spans of approximately 95, 100 and 175 ft. measured along the centerline of the bridge. The cross-section, shown in Fig. 7.6.2c with centerline dimensions and element thicknesses, consists of seven cells with six vertical interior webs and sloping exterior webs. The horizontal radius R = 273.3 ft. shown in Fig. 7.6.1 is to the exterior web at the edge of bridge shown in Fig. 7.6.2c.

Each of the six vertical interior webs is post-tensioned by a longitudinal panel tendon without friction and having a tendon profile along the length of the web as defined parametrically in Fig. 7.6.2b. Vertical distances to the cgs shown are from the bottom slab exterior surface. Note that each web has a different length and tendon point locations at ten equal divisions along each of the three spans were determined automatically in CELL4 using the parametric input option. The total longitudinal prestress force for the entire cross-section was 17,516 kips which was divided among the six girder vertical web panel tendons as follows: 3338 kips to each of the two exterior vertical webs and 2710 kips

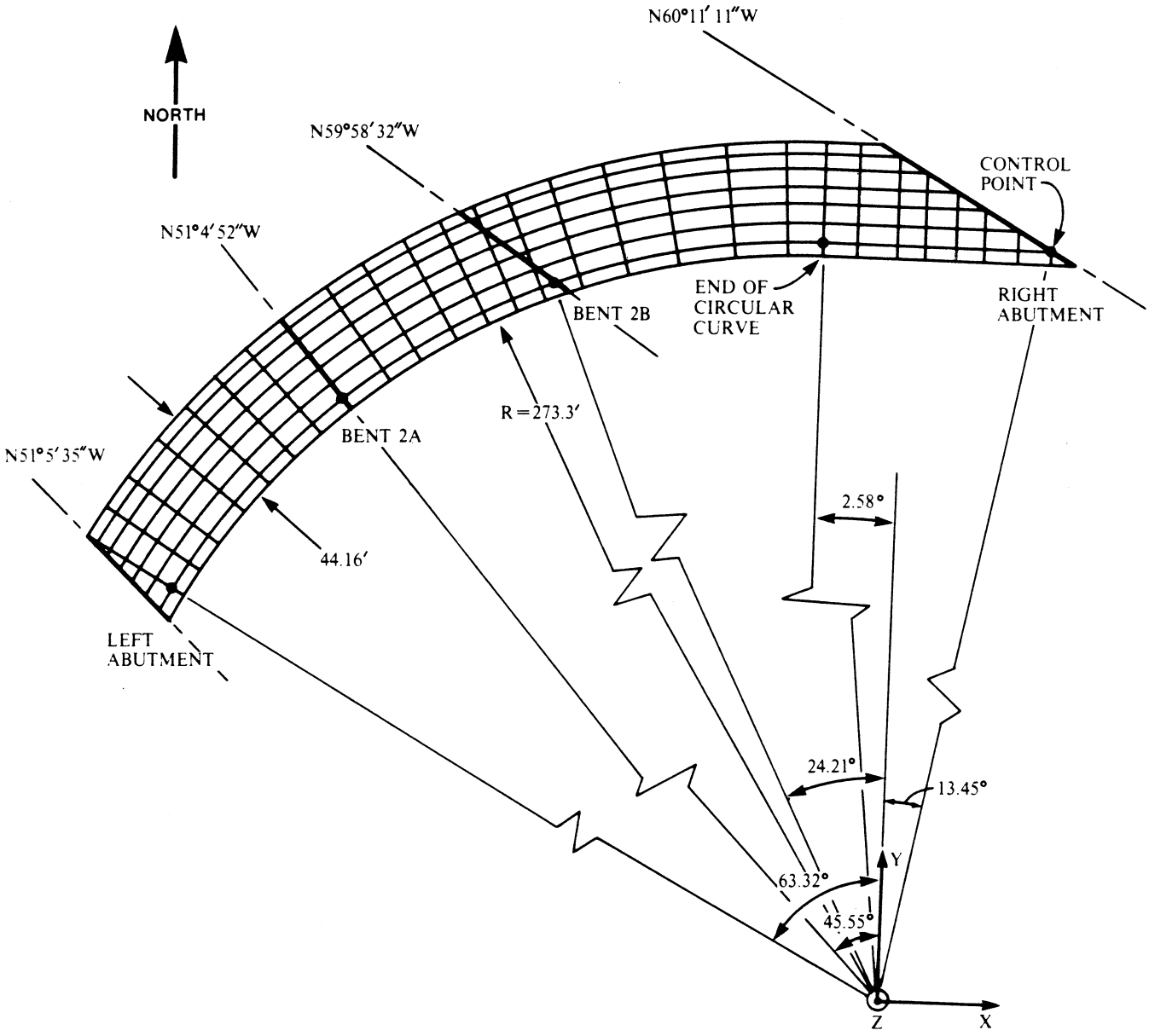

FIG. 7.6.1 GEOMETRY OF THE BRIDGE IN PLAN

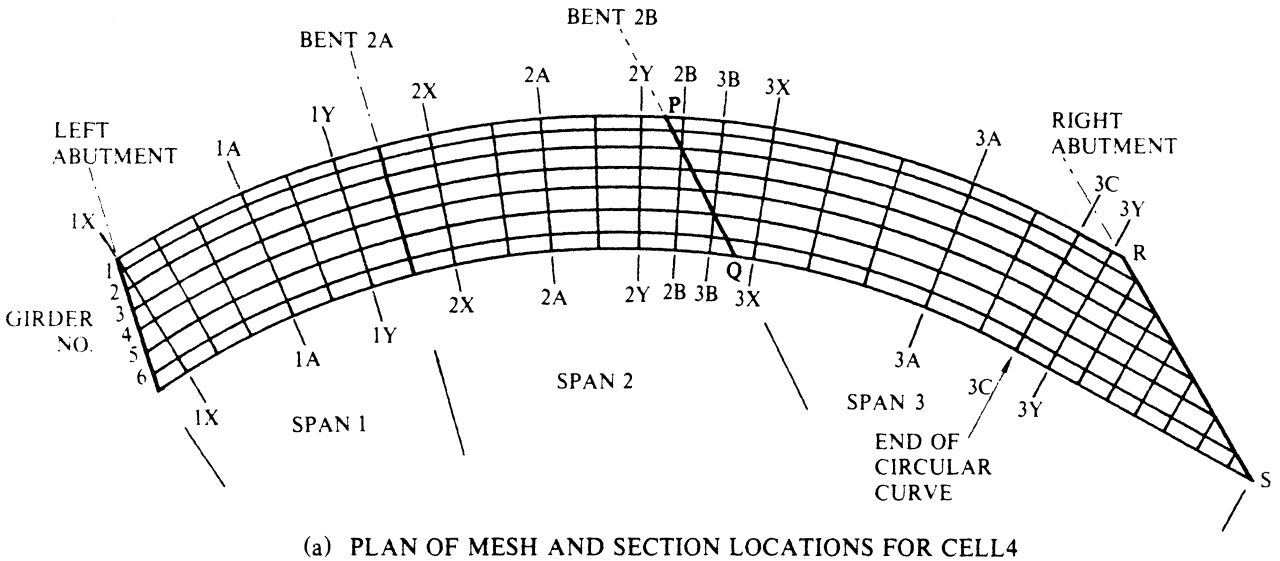

(a) PLAN OF MESH AND SECTION LOCATIONS FOR CELL4

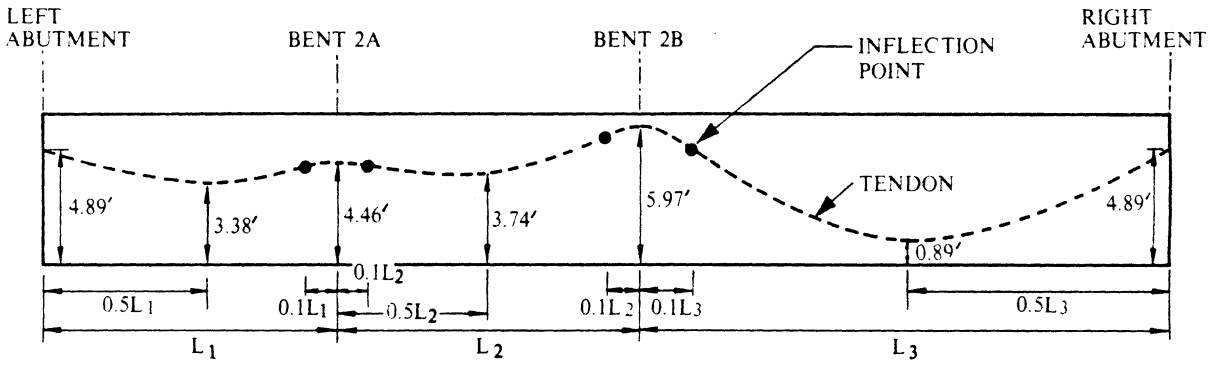

(b) TYPICAL PANEL TENDON PROFILE FOR VERTICAL WEB

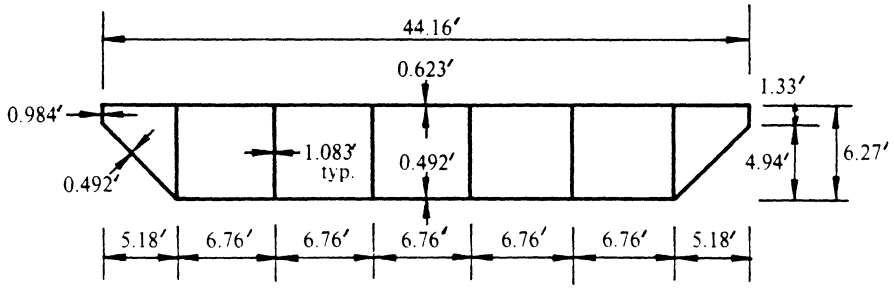

(c) CROSS-SECTIONAL DIMENSIONS

FIG. 7.6.2 PLAN OF MESH, SECTION LOCATIONS, TENDON PROFILE AND CROSS-SECTIONAL DIMENSIONS

to each of the four interior vertical webs. Friction and anchor slip were not considered in the anlaysis.

A total of five different load cases were analyzed by CELL4. They may be summarized as follows:

Case 1 - Uniform vertical load of 1.0 ksf over the entire top deck surface. This loading was used to check overall statics in CELL4 using an easily calculated total applied load.

Case 2 - Dead load of the bridge (Fig. 7.6.3a) calculated automatically in CELL4 from the input unit weight density of 150 pcf.

Case 3 - Longitudinal prestressing without friction and anchorage slip (Fig. 7.6.3b). Parametric input was used in CELL4.

Case 4 - AASHTO HS20 truck live loads in all three lanes, located to produce maximum moment in Span III (Fig. 7.6.3c).

Case 5 - AASHTO lane live loads in all three lanes, located to produce maximum negative moment over interior support bent 2B (Fig. 7.6.3d).

For the live loads no impact or lane reduction factors were included and the location of the AASHTO HS20 truck was selected (Fig. 7.6.3c) such that the middle heavy wheel load is placed at the location where the maximum dead load positive moment occurs.

7.6.2 Analytical Models

Several analytical models of increasing complexity are possible.

1. A planar grid consisting of a single line of one dimensional beam elements, with 6DOF at each end, along the longitudinal axis of the total bridge cross-section, rigidly connected and supported by transverse one dimensional elements at the supports oriented in the direction of the end abutments and the interior support bents. Model 1 will hereafter be termed the SAPIV model.
2. A planar grid consisting of six lines of one dimensional beam elements, with 6DOF at each end, along the six longitudinal axes of

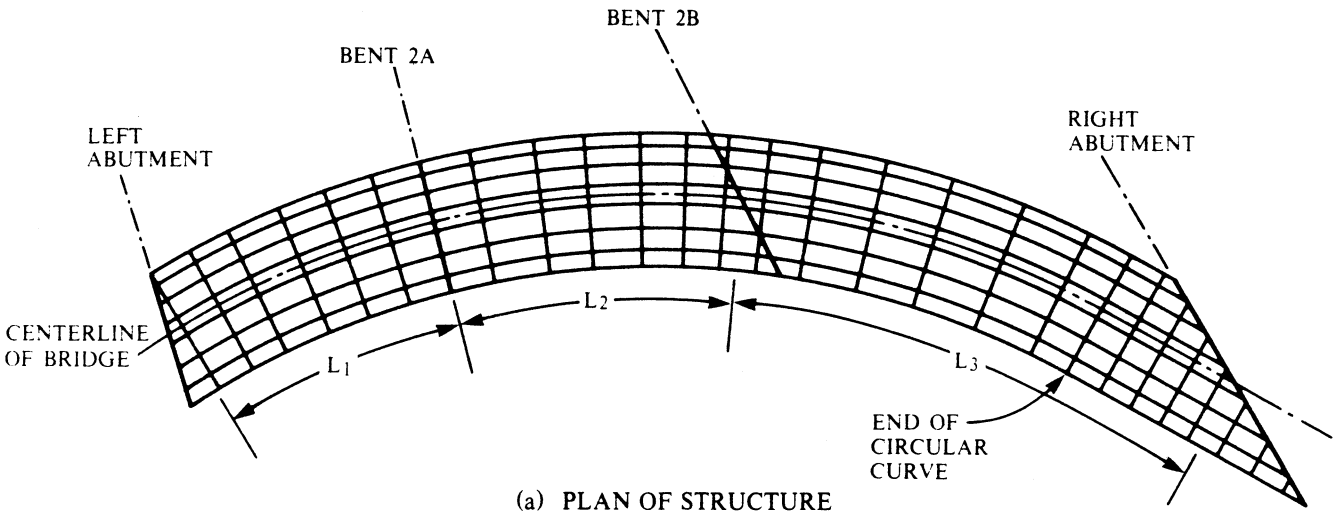

(a) PLAN OF STRUCTURE

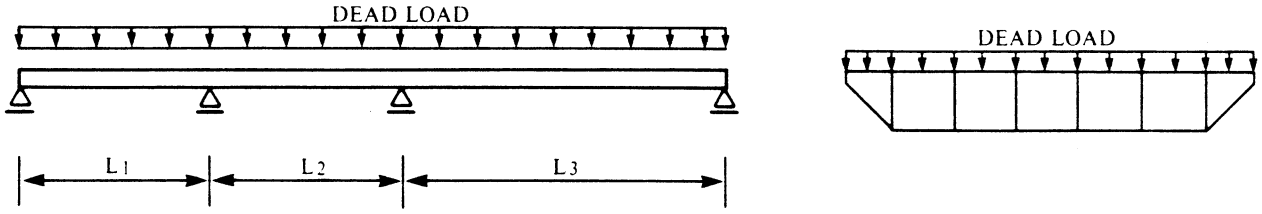

(b) LOAD CASE 2 - DEAD LOAD

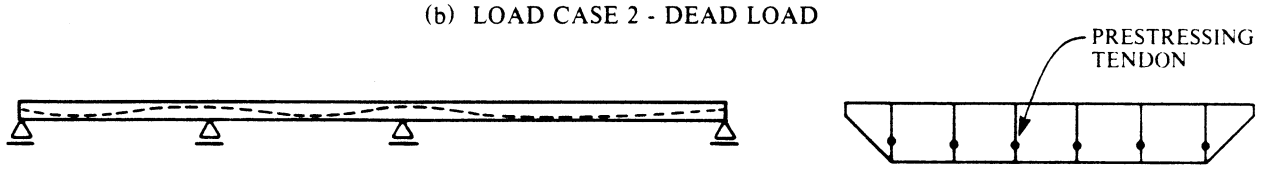

(c) LOAD CASE 3 - PRESTRESS

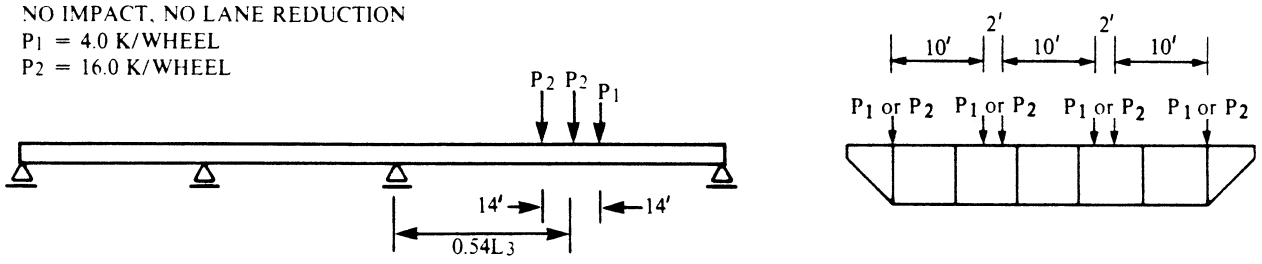

(d) LOAD CASE 4 - HS20 TRUCK ON SPAN 3

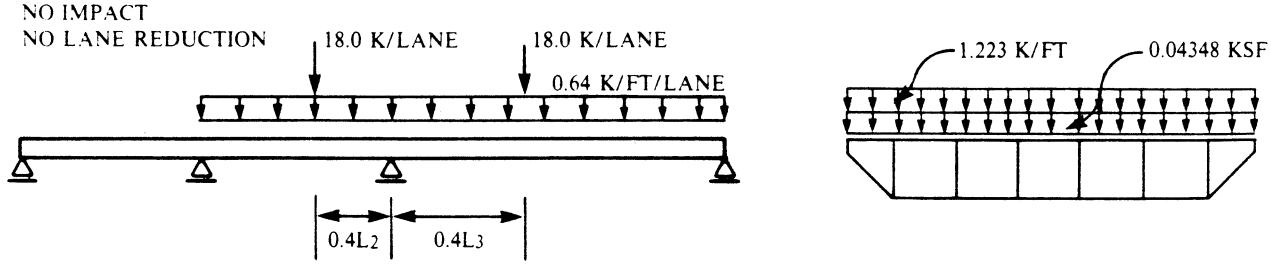

(e) LOAD CASE 5 - AASHTO LANE LOADS ON SPANS 2 AND 3

FIG. 7.6.3 SUMMARY OF VARIOUS LOAD CASES

the girder webs, supported by transverse one dimensional elements at the supports, oriented in the direction of the end abutments and the interior support bents, and in addition connected transversely at specified intervals in each span by one dimensional elements simulating the transverse bending stiffness of the bridge or diaphragms between longitudinal girders.

3. An orthotropic slab having the plan geometry and support conditions of the actual bridge, with appropriate bending and torsional stiffnesses assigned to the slab in the longitudinal and transverse direction to simulate the actual bridge.

4. A finite element model in which the top and bottom slabs, the longitudinal webs, and the transverse diaphragms or supports are modelled with two dimensional finite elements incorporating both in plane membrane stiffnesses and plate bending stiffnesses. Model 4 will hereafter be termed the CELL4 model.

For any of these analytical computer models, extensive preliminary calculations are necessary to determine input values of nodal point coordinates, element properties, external and prestressing loads, etc. Only models 1 and 4 were analyzed and results will be presented for them.

Model 1 was analyzed in a previous investigation using the SAPIV computer program [21]. The entire bridge cross-section was treated as a single longitudinal member along the bridge centerline with the following section properties: distances from the cgc of the section to the fibers at the mid-thickness of the top and bottom slabs of c_t = 2.76 ft and c_b = 3.51 ft; cross-sectional area A = 94.54 ft^2; moment of inertia about horizontal and vertical axes through the cgc, I_3 = 587 ft^4 and I_2 = 15451 ft^4; and torsional stiffness constant J_1 = 1478 ft^4. The concrete material properties were: modulus of elasticity E = 3600 ksi; Poisson's ratio ν = 0.15; and unit weight density w = 150 pcf.

In the SAPIV model, the longitudinal beam member was supported transversely by transverse members at the two end abutments and at the two

interior bents 2A and 2B. These transverse members were rigidly connected to the longitudinal beam member. The two end abutment members were each externally supported vertically at two points, under girder webs 1 and 6, respectively, (Fig. 7.6.2), and the two interior bents 2A and 2B were each externally supported vertically at two points, under girder webs 2 and 5, respectively.

In order to simplify the loads input into the SAPIV program, additional radial rigid members were attached to the longitudinal bridge member at a number of points along the longitudinal span forming a mesh of nodal points (Fig. 7.6.2). Thus nodal points were established on the transverse members at the six girder lines at which input loads due to dead load, live load, and prestressing could be calculated externally and specified and then be automatically transferred internally in SAPIV to the longitudinal bridge member axis used in the analysis. It should be emphasized in the SAPIV model there was only one longitudinal member and the function of the transverse members between supports was only to simplify the load input. Even with this, extensive calculations had to be carried out externally for the input data needed in SAPIV. While the SAPIV model can yield results for the longitudinal variation of centerline displacements and total sectional forces and moments, it cannot give any information on the transverse distribution of these quantities. In addition it can only approximate the detailed structural behavior of the complex bridge structure of this example. SAPIV does have the distinct advantage that the total internal sectional forces and moments obtained will be in equilibrium with the input external loads. This is not necessarily the case in finite element solutions, such as used in CELL4.

The finite element model 4, which was analyzed by CELL4, utilized the mesh layout shown in Fig. 7.6.2a. It consisted of top and bottom deck slab elements, longitudinal interior vertical web spar elements, exterior sloping web special elements and transverse vertical web spar elements at the abutments and interior bents. External vertical supports were

specified only at girder webs 1 and 6 for the two end abutment supports and at girder webs 2 and 5 for the two interior bent supports 2A and 2B. Automatic generation of dead loads and equivalent prestressing loads at the nodes was performed internally in CELL4 from the minimum input data necessary.

For purposes of determining, by automatic stress integration in CELL4, the individual girder and total section forces and moments, the cross-section (Fig. 7.6.2c) was divided into six longitudinal girders. Girders 1 and 6 were the outer and inner exterior girders, respectively, and each included the exterior sloping web and the first interior vertical web, as well as the tributary top and bottom deck slabs. Girders 2, 3, 4, 5 were the interior girders and each included a vertical interior web and its tributary top and bottom deck slabs.

All five load cases were analyzed by CELL4 for which reactions; displacements; element internal stresses and moments; and integrated individual girder and total section forces and moments were output.

7.6.3 Discussion of Results

From the large amount of output obtained from CELL4, selected results are tabulated and plotted for load cases 1 to 5. Comparisons between CELL4 and SAPIV results are made for total reactions, center-line deflections and total section vertical shears and moments. Transverse distributions of displacements and stresses from CELL4 are also shown.

7.6.3.1 Vertical Reactions and Static Checks

Table 7.6.1 gives a summary of the vertical reactions by CELL4 for all load cases. Also compared in the last two lines of Table 7.6.1 is the total sum of all the reactions versus the known applied load. The agreement is excellent.

A study of the individual reactions in Table 7.6.1 indicates support at obtuse corners of the longest span III carry the largest reactions.

A comparison of the total vertical reactions at the four transverse supports as obtained by SAPIV and CELL4 for the dead load Case 2 is given

in Table 7.6.2. The diaphragm weights, which were included in Table 7.6.1, are excluded in this Table 7.6.2 to be consistent with the loadings used in SAPIV. The agreement is quite close, considering the differences in the analytical models used in CELL4 and SAPIV.

It is important in finite element solutions such as used in CELL4 to make static checks between internal and external forces, since only with adequate mesh refinements will the internal stresses found yield satisfactory static checks. For this purpose, the section integration of internal stresses capability of CELL4 is very useful. As an example, Table 7.6.3 summarizes for load case 1 of 1 ksf uniform load, the total vertical shear V, moment M and torque T at Sections 3C and 3Y (Fig. 7.6.2a) as obtained by statics from the external reactions (Table 7.6.1) and the applied load of 1 psf and then by CELL4 from the integration of the internal stresses at these same sections. It can be seen that the agreement is quite good for moments and torques and also is better at Section 3C, which is further away from the support than Section 3Y. The shear forces by statics and CELL4 differ by 10.5 and 13.9% at the same two sections, again indicating that extrapolation procedures and mesh refinement may be needed if accurate values of shears are required.

Table 7.6.4 presents CELL4 results for the total internal dead load shear acting at sections adjacent to the four external supports for which the external reactions are given in Table 7.6.2 and are again shown on line (3) of Table 7.6.4. Values of the sum of the internal shears on lines (1) and (2), which were found by two different extrapolation procedures should equal the value shown on line (3) to satisfy statics. Shears found on line (1) were determined by extrapolation of the CELL4 total section shear force curve shown in Fig. 7.6.4a. Shears found in line (2) were determined by extrapolation of the CELL4 individual girder shear force curves (not shown) and then summing them to get the total section shear force. It can be seen in Table 7.6.4 that the latter method generally gives better results.

TABLE 7.6.1 SUMMARY OF VERTICAL REACTIONS FOR VARIOUS LOAD CASES

SEC.	GIRDER	1.0 KSF UNIF. LOAD		DEAD LOAD		HS 20 TRUCK LOAD		AASHTO LANE LOAD		PRE-STRESS
		(KIPS)	% TOT.	(KIPS)	% TOT.	(KIPS)	% TOT.	(KIPS)	% TOT.	(KIPS)
(1)	(2)	(3)	(4)	(5)	(6)	(7)	(8)	(9)	(10)	(11)
LEFT ABUT.	1	1050	59.9	402	58.4	4.2	68.9	-3.6	67.9	- 16
	6	703	40.1	286	41.6	1.9	31.1	-1.7	32.1	- 21
	TOTAL	1753	100	688	100	6.1	100	-5.3	100	- 37
BENT 2A	2	2357	56.3	834	55.7	3.9	-10.4	52.4	66.0	-207
	5	1826	43.7	662	44.3	-41.3	110.4	27.0	34.0	231
	TOTAL	4183	100	1496	100	-37.4	100	79.4	100	24
BENT 2B	2	838	12.4	328	13.8	-46.7	-33.0	72.3	18.7	887
	5	5942	87.6	2043	86.2	188.3	133.0	315.0	81.3	-836
	TOTAL	6780	100	2371	100	141.6	100	387.3	100	51
RIGHT ABUT.	1	3128	86.3	1144	81.5	120.4	113.9	153.6	88.9	-340
	6	497	13.7	260	18.5	-14.7	-13.9	19.1	11.1	302
	TOTAL	3625	100	1404	100	105.7	100	172.7	100	-38
TOTAL REACTION		16341		5959		216		634		0
TOTAL LOAD		16300		5960		216		635		0

TABLE 7.6.2 COMPARISONS OF TOTAL VERTICAL REACTIONS (KIPS) BY SAPIV AND CELL4 (CASE 2: DEAD LOAD)

PROGRAM	LEFT ABUTMENT	BENT 2A	BENT 2B	RIGHT ABUTMENT	TOTAL REACTION
	(KIPS)	(KIPS)	(KIPS)	(KIPS)	(KIPS)
(1)	(2)	(3)	(4)	(5)	(6)
SAPIV	561	1299	2244	1124	5228
CELL4	571	1381	2234	1184	5370
$\frac{\text{CELL4}}{\text{SAPIV}}$	1.018	1.063	0.996	1.053	1.027

TABLE 7.6.3 COMPARISONS OF EXTERNAL AND INTERNAL SECTION SHEARS, MOMENTS AND TORQUES (CASE 1: 1KSF UNIFORM LOAD)

	EXTERNAL STATICS	INTERNAL CELL4	$\frac{\text{CELL4}}{\text{STATICS}}$
(1)	(2)	(3)	(4)
Shear V_{3c} (kips)	1314	1176	.895
Moment M_{3c} (ft-kips)	46818	45216	.966
Torque T_{3c} (ft-kips)	56207	55196	.982
Shear V_{3y} (kips)	1857	1599	.861
Moment M_{3y} (ft-kips)	27318	26110	.956
Torque T_{3y} (ft-kips)	56207	52037	.926

TABLE 7.6.4 COMPARISON OF EXTRAPOLATED INTERNAL SHEAR FORCES (KIPS) WITH EXTERNAL SUPPORT REACTIONS (KIPS) (CASE 2 - DEAD LOAD)

QUANTITY	LEFT ABUTMENT	BENT 2A	BENT 2B	RIGHT ABUTMENT
(1)	(2)	(3)	(4)	(5)
(1) Total Internal Section Shear	485(85%)	950(69%)	1770(79%)	1050(89%)
(2) Sum of Internal Girder Shears	495(87%)	1165(84%)	1900(85%)	1040(88%)
(3) External Reaction	571(100%)	1381(100%)	2234(100%)	1184(100%)

7.6.3.2 Longitudinal Variations of Internal Shears, Moments and Displacements

A complete tabulation of individual girder and total section shears and moments as obtained by CELL4 is given in Tables 7.6.5 and 7.6.6 for all load cases. Values are given at selected sections (Fig. 7.6.2a) along the span. A study of such results is very useful in determining load distribution for complex bridge geometries.

Plots of the longitudinal variation of the total section shear forces and moments as obtained by CELL4 and SAPIV are given in Fig. 7.6.4 to 7.6.7 for load cases (Fig 7.6.3); 2-dead load; 3-prestress; 4-AASHTO truck live load; and 5-AASHTO lane live load. Note that extrapolated values are used at certain sections in the CELL4 plots. The SAPIV results are in general agreement with the CELL4 results indicating that the simplified beam grid model used in SAPIV can capture the dominant longitudinal behavior. However, note how SAPIV overestimates the moment in the longest span.

The longitudinal variations of the centerline vertical displacement for load cases (Fig. 7.6.3): 2-dead load; and 3-prestress are shown in Fig. 7.6.8. Again it can be seen that CELL4 values are smaller than SAPIV values in Span III because of the capability of CELL4 to capture the true stiffness of the bridge in the highly skewed Span 3 (Fig. 7.6.2a).

7.6.3.3 Transverse Distributions of Displacements and Stresses

The transverse distributions of vertical displacements and longitudinal membrane stresses at midspan section 3A (Fig. 7.6.2a) of Span III and of the membrane shear stresses at Sections 2B and 3B, just to the left and right of Bent 2B (Fig. 7.6.2a), obtained by CELL4, are shown in Figs. 7.6.9 to 7.6.16 for load cases (Fig. 7.6.3): 2-dead load; 3-prestress; 4-AASHTO truck live load; and 5-AASHTO lane live load.

A study of these plots shows that at midspan Section 3A the longitudinal stresses remain relatively uniform accross the section illustrating that under these imposed loadings the cross-section behaves as a beam in which plane sections remain plane. Vertical displacements at

TABLE 7.6.5 SUMMARY OF INTERNAL SHEAR AT VARIOUS SECTIONS FOR DIFFERENT LOAD CASES

SEC	GIRDER	1 KSF UNIF. LOAD		DEAD LOAD		HS20 TRUCK LOAD		AASHTO LANE LOAD		PRESTRESS	
		SHEAR KIPS	% TOTAL	SHEAR KIPS	% TOTAL	SHEAR KIPS	% TOTAL	SHEAR KIPS	% TOTAL	SHEAR KIPS	% TOTAL
1X	1	-459.0	36.3	-160.0	37.9	-2.2	37.8	1.7	32.9	121.3	15.9
	2	-176.0	13.9	-56.3	13.3	-0.9	15.1	0.6	12.2	150.6	19.7
	3	-140.6	11.1	-43.1	10.2	-0.7	11.8	0.7	12.7	139.1	18.2
	4	-132.0	10.4	-40.5	9.6	-0.7	12.0	0.6	11.8	132.5	17.4
	5	-138.2	10.9	-44.1	10.4	-0.7	11.7	0.7	13.2	127.8	16.7
	6	-220.1	17.4	-78.1	18.5	-0.7	11.5	0.9	17.1	91.8	12.0
	TOTAL	-1266.1	100.0	-422.3	100.0	-5.7	100.0	5.1	100.0	763.2	100.0
1Y	1	239.1	17.7	78.5	17.5	-0.6	15.5	-0.8	-28.4	-80.3	21.4
	2	221.8	16.4	74.1	16.5	-0.4	9.0	1.2	43.6	-61.3	16.4
	3	209.3	15.5	69.6	15.5	-0.5	12.5	0.7	24.7	-57.3	15.3
	4	205.0	15.1	68.3	15.2	-1.0	24.0	0.3	12.1	-51.7	13.8
	5	216.1	16.0	72.3	16.1	-1.5	34.7	0.5	16.1	-47.7	12.7
	6	262.4	19.4	86.8	19.3	-0.2	4.3	0.9	31.9	-76.4	20.4
	TOTAL	1353.9	100.0	449.5	100.0	-4.2	100.0	2.9	100.0	-374.7	100.0
2X	1	-202.6	28.2	-67.3	28.0	0.4	1.4	-9.9	31.3	92.8	35.7
	2	-140.4	19.5	-47.1	19.6	2.6	9.6	-5.5	17.3	52.1	20.0
	3	-119.9	16.7	-39.8	16.6	3.3	12.3	-5.0	15.7	45.0	17.3
	4	-110.4	15.3	-36.7	15.3	4.3	15.9	-4.6	14.5	36.0	13.9
	5	-113.9	15.8	-38.5	16.0	5.5	20.4	-4.3	13.6	26.5	10.2
	6	-32.1	4.5	-11.0	4.6	10.8	40.4	-2.4	7.6	7.6	2.9
	TOTAL	-719.5	100.0	-240.5	100.0	26.7	100.0	-31.8	100.0	260.0	100.0
2Y	1	220.9	13.8	72.3	13.7	-1.3	-4.0	21.4	18.0	-162.9	18.2
	2	232.6	14.5	77.6	14.7	2.2	7.0	17.9	15.1	-110.8	12.4
	3	233.1	14.6	76.8	14.5	3.0	9.7	17.9	15.1	-141.5	15.8
	4	259.3	16.2	85.6	16.2	5.9	18.9	18.6	15.6	-155.7	17.4
	5	316.7	19.8	105.6	20.0	8.8	28.4	21.1	17.8	-153.3	17.2
	6	337.9	21.1	111.1	21.0	12.4	40.0	21.9	18.5	-168.9	18.9
	TOTAL	1600.7	100.0	528.8	100.0	31.0	100.0	118.8	100.0	-893.3	100.0
3X	1	-3.6	0.1	2.2	-0.3	-0.7	0.7	-3.9	2.6	40.6	3.2
	2	-226.3	8.4	-74.7	8.4	-7.8	7.7	-14.0	9.2	137.4	10.9
	3	-330.9	12.3	-109.2	12.3	-12.5	12.3	-19.3	12.6	181.9	14.4
	4	-483.0	18.0	-160.1	18.0	-18.2	18.0	-27.2	17.8	217.0	17.2
	5	-558.7	20.8	-186.3	21.0	-20.5	20.3	-31.0	20.4	215.9	17.1
	6	-1080.0	40.3	-360.3	40.6	-41.7	41.1	-57.0	37.4	469.7	37.2
	TOTAL	-2682.6	100.0	-888.5	100.0	-101.3	100.0	-152.3	100.0	1262.6	100.0
3Y	1	1103.9	69.0	373.3	70.6	49.1	51.6	55.3	66.5	-391.2	43.8
	2	416.3	26.0	138.8	26.3	19.5	20.6	20.9	25.1	-204.6	22.9
	3	227.6	14.2	72.2	13.7	14.6	15.3	11.8	14.2	-142.5	15.9
	4	131.7	8.2	39.5	7.5	11.8	12.4	7.3	8.8	-107.8	12.1
	5	68.2	4.3	19.6	3.7	8.6	9.1	4.2	5.1	-76.1	8.5
	6	-348.6	-21.8	-115.0	-21.8	-8.5	-9.0	-16.4	-19.8	28.6	-3.2
	TOTAL	1599.1	100.0	528.4	100.0	95.1	100.0	83.1	100.0	-893.7	100.0

TABLE 7.6.6 SUMMARY OF INTERNAL MOMENT AT VARIOUS SECTIONS FOR DIFFERENT LOAD CASES

SEC	GIRDER	1 KSF UNIF. LOAD		DEAD LOAD		HS20 TRUCK LOAD		AASHTO LANE LOAD		PRESTRESS	
		MOMENT FT-KIP	% TOTAL	MOMENT FT-KIP	% TOTAL	MOMENT FT-KIP	% TOTAL	MOMENT FT-KIP	% TOTAL	MOMENT FT-KIP	% TOTAL
1A	1	5216.1	17.4	1730.8	17.4	48.9	17.3	-40.4	16.3	1015.5	-311.6
	2	4844.2	16.2	1603.9	16.2	44.5	15.7	-38.8	15.7	-652.5	200.2
	3	4808.4	16.0	1588.5	16.0	45.5	16.0	-39.4	15.9	-630.8	193.5
	4	4820.2	16.1	1592.4	16.1	45.9	16.2	-40.5	16.4	-599.2	183.8
	5	4920.5	16.4	1629.3	16.4	47.0	16.6	-40.9	16.5	-587.0	180.1
	6	5353.6	17.9	1776.6	17.9	51.6	18.2	-47.6	19.2	1128.1	-346.1
	TOTAL	29963.1	100.0	9921.7	100.0	283.5	100.0	-247.6	100.0	-325.9	100.0
2A	1	-79.9	5.0	-14.1	3.0	-145.4	16.5	120.9	18.5	1461.5	43.3
	2	-163.7	10.2	-44.0	9.4	-140.5	15.9	107.6	16.5	-169.1	-5.0
	3	-203.1	12.7	-58.6	12.5	-141.5	16.1	106.8	16.3	-76.9	-2.3
	4	-264.6	16.6	-79.3	16.9	-143.1	16.2	105.7	16.2	24.9	0.7
	5	-311.3	19.5	-93.8	20.0	-145.1	16.5	106.4	16.3	121.1	3.6
	6	-575.8	36.0	-179.9	38.3	-165.5	18.8	105.8	16.2	2015.0	59.7
	TOTAL	-1598.4	100.0	-469.6	100.0	-881.2	100.0	653.3	100.0	3376.6	100.0
2B	1	-9854.5	18.0	-3258.5	18.0	-336.9	16.0	-621.4	18.5	6799.6	21.4
	2	-9221.1	16.8	-3052.4	16.9	-293.1	13.9	-592.6	17.6	4704.3	14.8
	3	-8360.1	15.3	-2752.4	15.2	-294.4	14.0	-526.6	15.7	4481.2	14.1
	4	-8076.5	14.8	-2654.6	14.7	-326.7	15.5	-495.2	14.7	4494.2	14.2
	5	-9060.6	16.6	-2993.1	16.6	-390.9	18.6	-533.3	15.9	4609.4	14.5
	6	-10160.4	18.6	-3364.8	18.6	-462.1	22.0	-588.8	17.5	6658.8	21.0
	TOTAL	-54733.3	100.0	-18076.0	100.0	-2104.3	100.0	-3358.0	100.0	31747.7	100.0
3B	1	-6688.1	9.5	-2206.8	9.4	-287.4	10.2	-440.8	10.4	6106.8	15.7
	2	-7471.1	10.6	-2466.4	10.5	-315.1	11.2	-474.0	11.2	4632.7	11.9
	3	-10160.7	14.4	-3365.0	14.3	-414.1	14.7	-613.6	14.5	5496.4	14.1
	4	-13293.6	18.8	-4418.1	18.8	-523.4	18.6	-780.4	18.5	6366.4	16.3
	5	-17709.0	25.1	-5912.4	25.2	-679.9	24.2	-1014.7	24.0	7639.6	19.6
	6	-15360.5	21.7	-5112.4	21.8	-590.3	21.0	-895.8	21.2	8735.3	22.4
	TOTAL	-70683.1	100.0	-23461.2	100.0	-2810.3	100.0	-4219.3	100.0	38977.4	100.0
3A	1	11556.5	17.4	3818.2	17.5	666.8	17.2	630.5	17.4	-3033.2	12.0
	2	10658.5	16.1	3516.7	16.1	622.9	16.0	583.2	16.0	-4474.6	17.8
	3	10596.0	16.0	3491.0	16.0	629.3	16.2	581.0	16.0	-4563.5	18.1
	4	10653.5	16.1	3508.3	16.1	634.4	16.3	585.3	16.1	-4677.7	18.6
	5	10813.0	16.3	3562.8	16.3	636.5	16.4	594.8	16.4	-4818.8	19.1
	6	11980.5	18.1	3952.5	18.1	696.3	17.9	658.7	18.1	-3614.2	14.4
	TOTAL	66258.0	100.0	21849.6	100.0	3886.4	100.0	3633.6	100.0	-25182.0	100.0

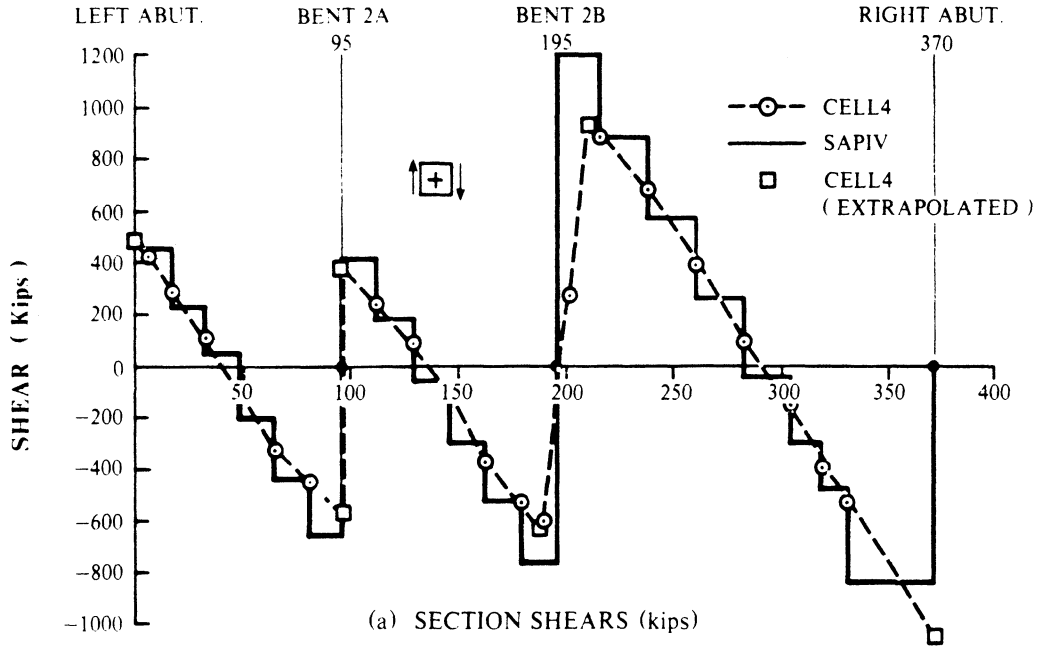

(a) SECTION SHEARS (kips)

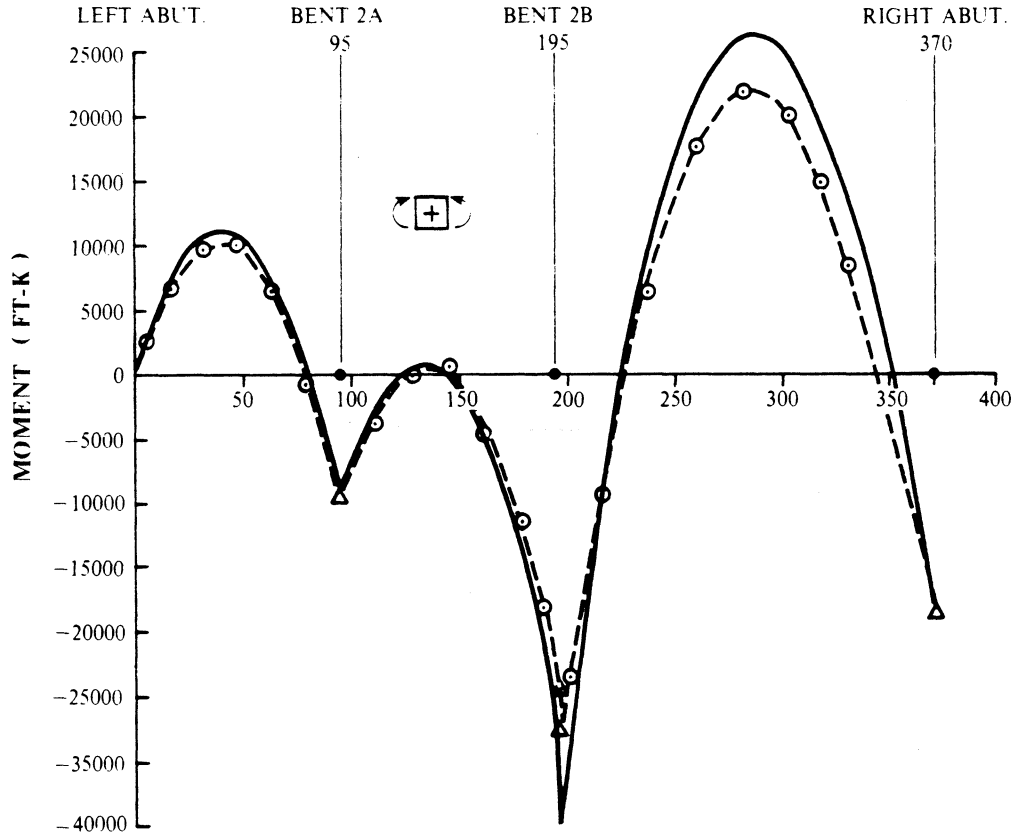

(b) SECTION MOMENTS (ft-kips)

FIG. 7.6.4 LONGITUDINAL VARIATION OF SECTION SHEARS

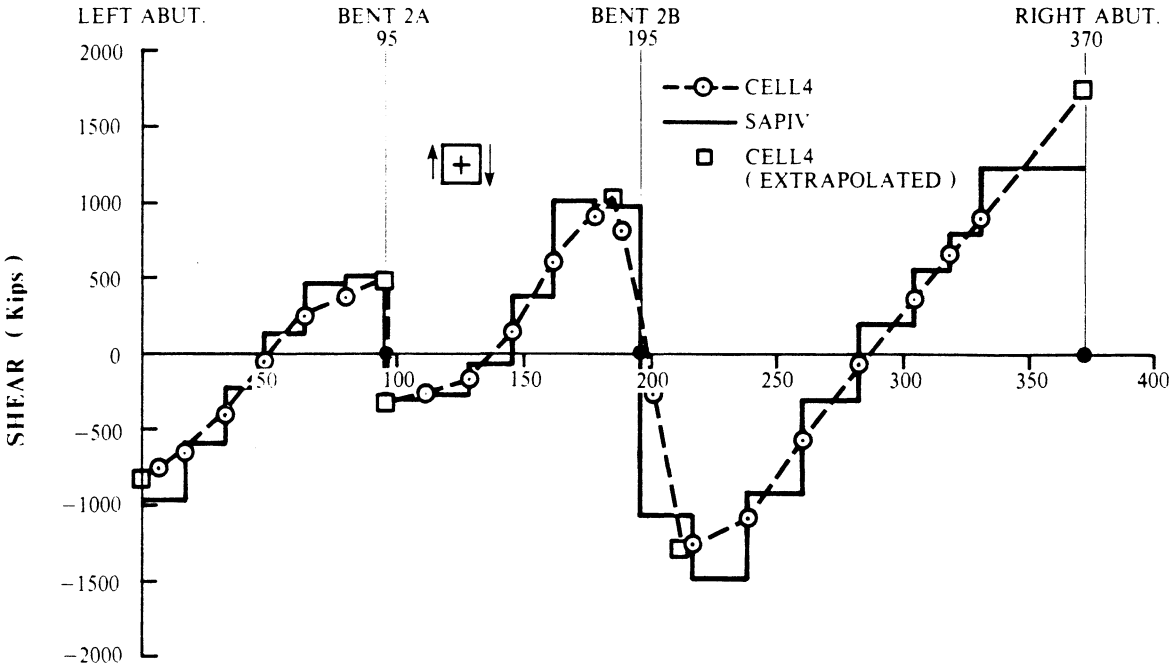

(a) SECTION SHEARS (kips)

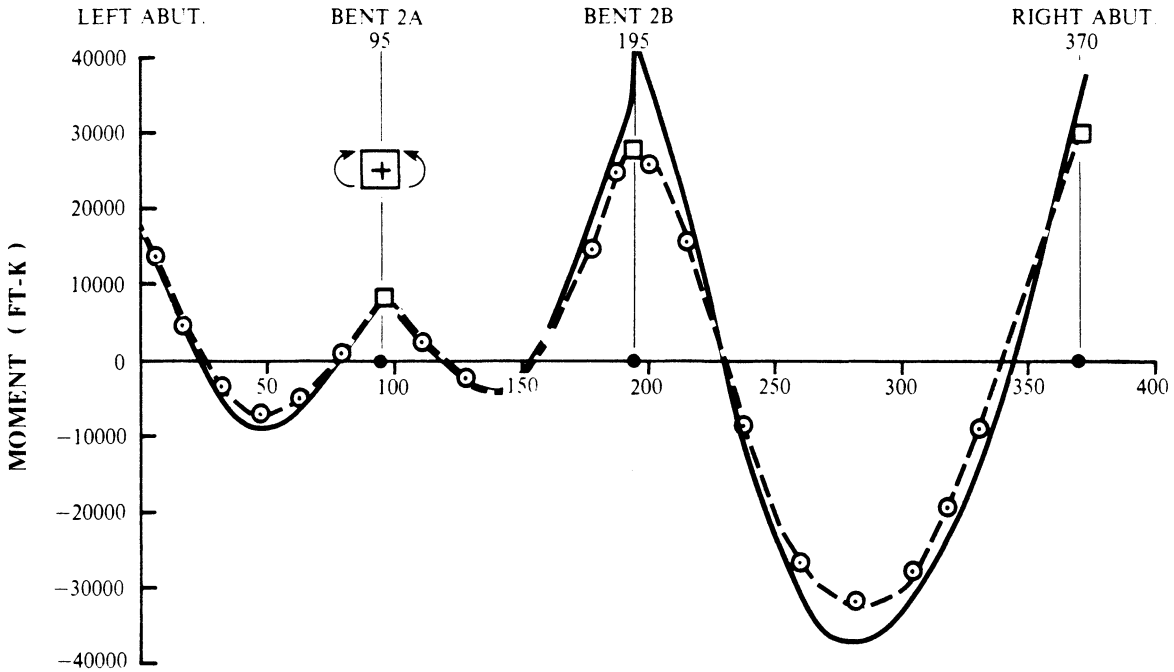

(b) SECTION MOMENTS (ft-kips)

FIG. 7.6.5 LONGITUDINAL VARIATION OF SECTION SHEARS AND MOMENTS FOR PRESTRESS

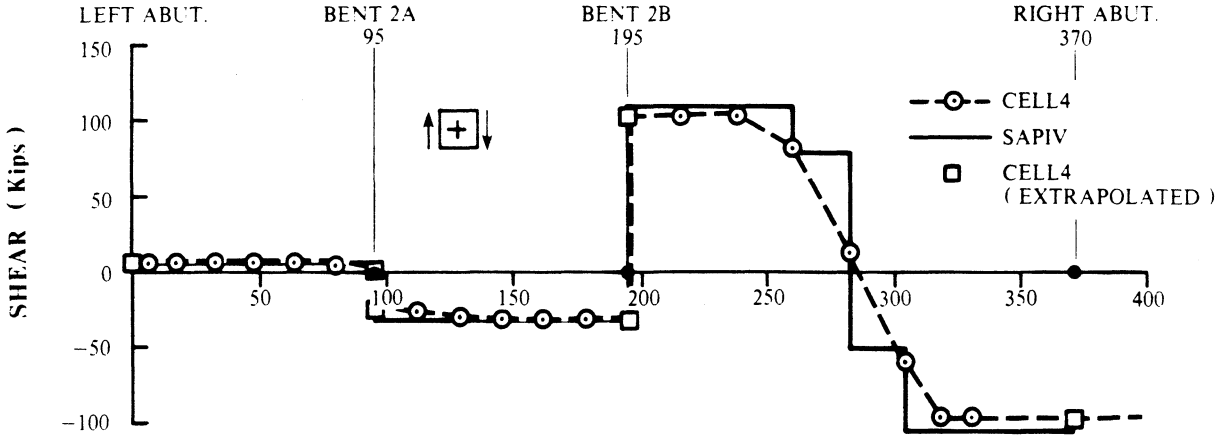

(a) SECTION SHEARS (kips)

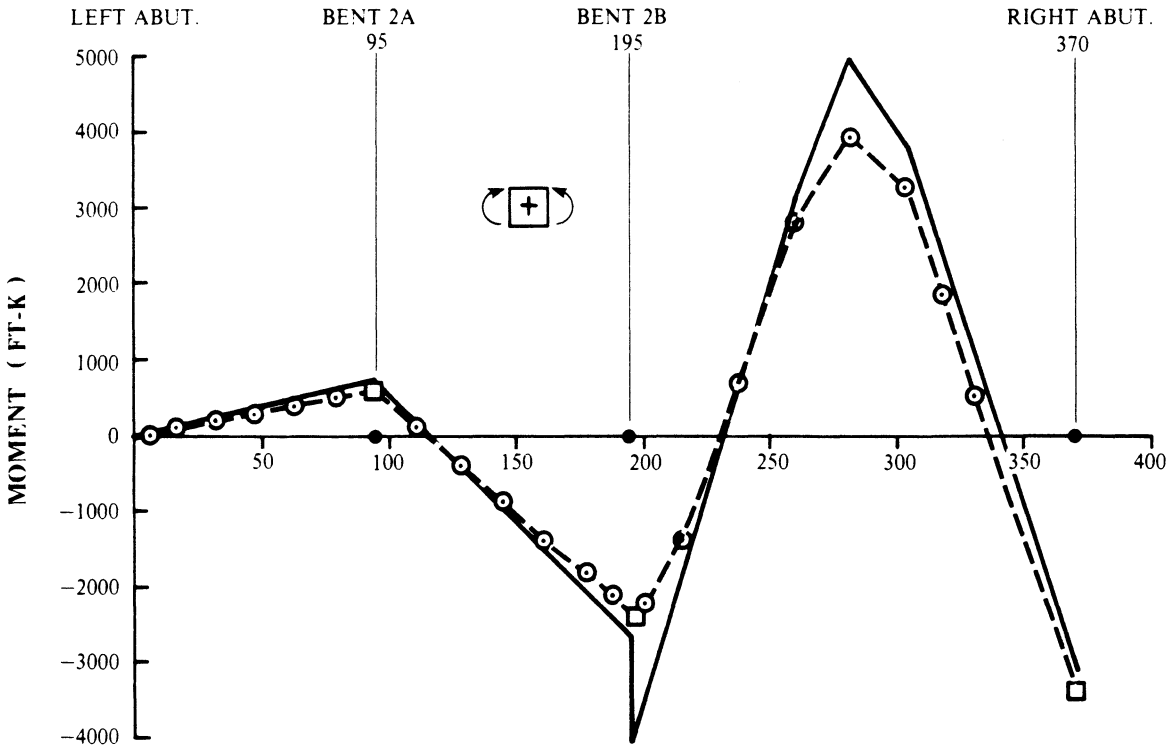

(b) SECTION MOMENTS (ft-kips)

FIG. 7.6.6 LONGITUDINAL VARIATION OF SECTION SHEARS AND MOMENTS FOR AASHTO HS20 LANE LIVE LOAD

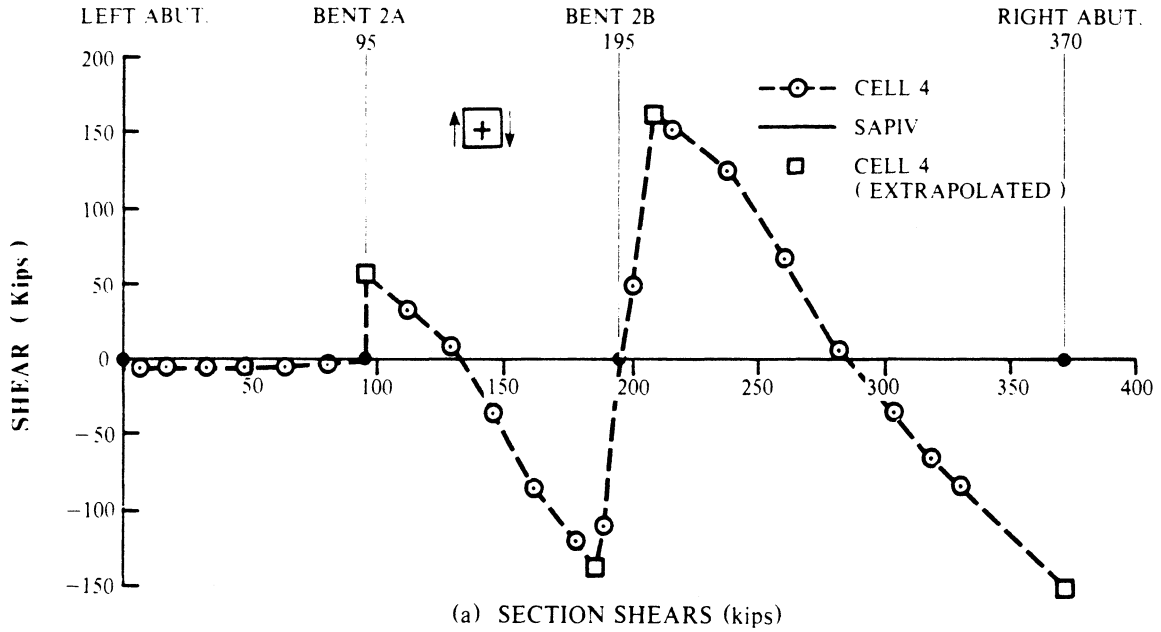

(a) SECTION SHEARS (kips)

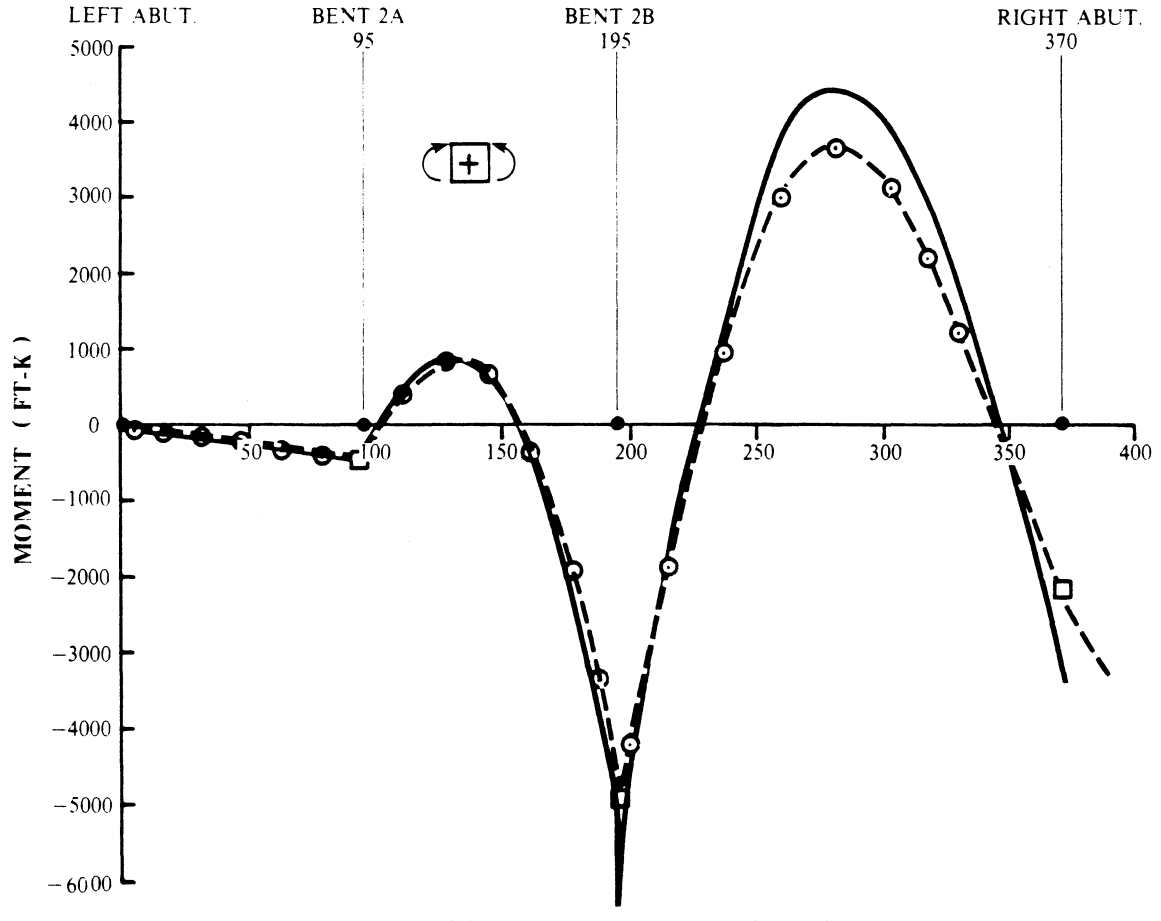

(b) SECTION MOMENTS (ft-kips)

FIG. 7.6.7 LONGITUDINAL VARIATION OF SECTION SHEARS AND MOMENTS FOR AASHTO LANE LIVE LOAD

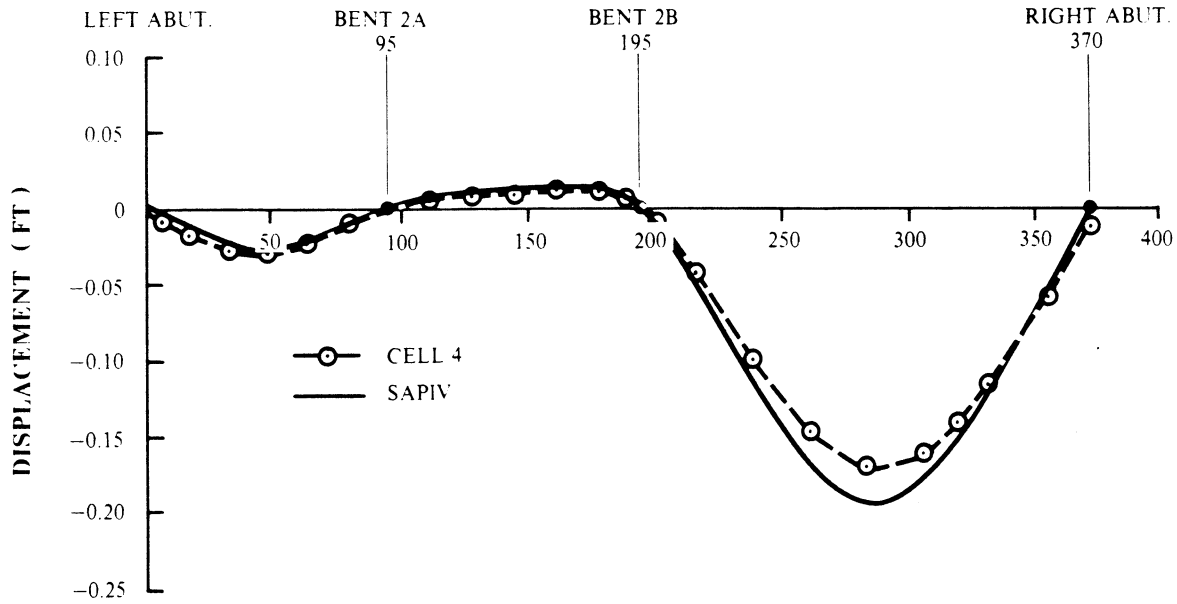

(a) DEAD LOAD DISPLACEMENTS (ft)

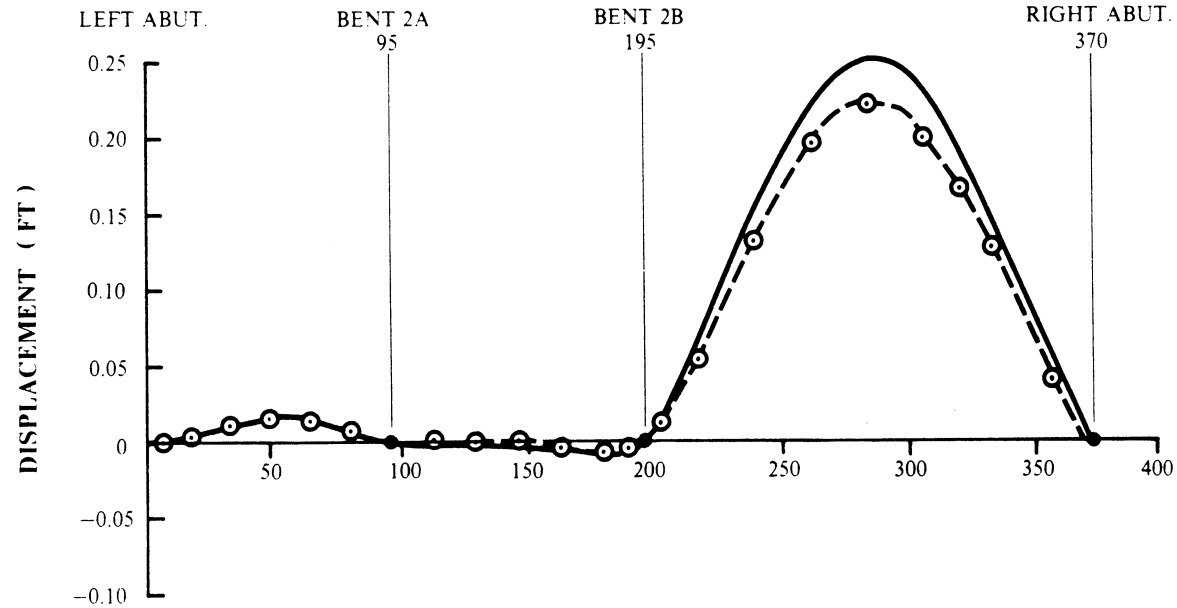

(b) PRESTRESS DISPLACEMENTS (ft)

FIG. 7.6.8 LONGITUDINAL VARIATION OF CENTERLINE VERTICAL DISPLACEMENTS FOR DEAD LOAD AND PRESTRESS

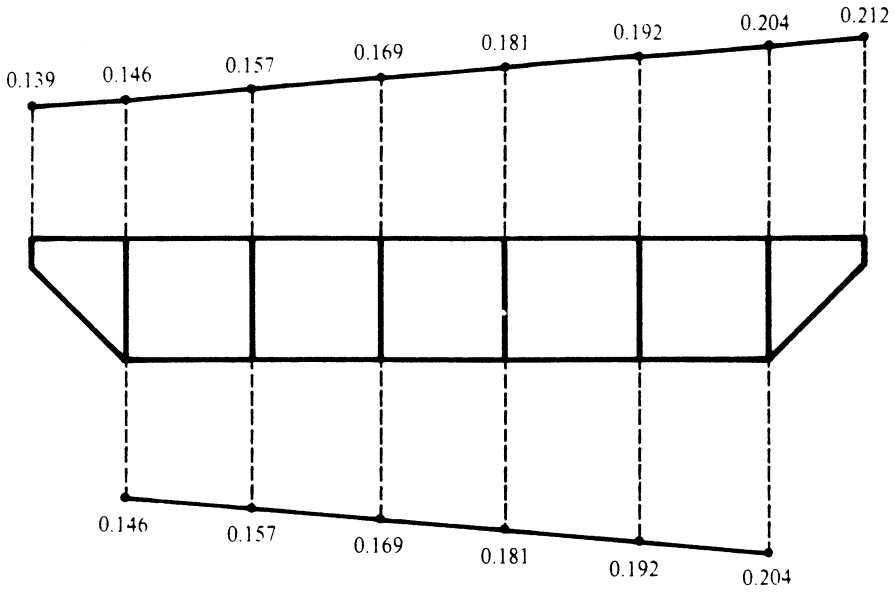

(a) VERTICAL DISPLACEMENTS (ft)

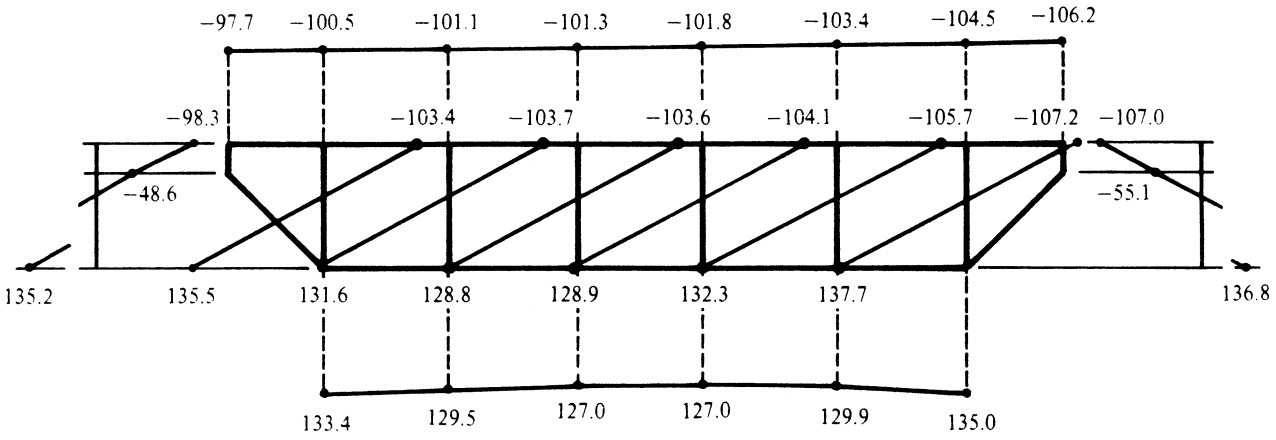

(b) LONGITUDINAL MEMBRANE STRESSES (ksf)

FIG. 7.6.9 TRANSVERSE DISTRIBUTION OF VERTICAL DISPLACEMENTS AND LONGITUDINAL MEMBRANE STRESSES AT MIDSPAN SECTION 3A (SPAN 3) FOR DEAD LOAD

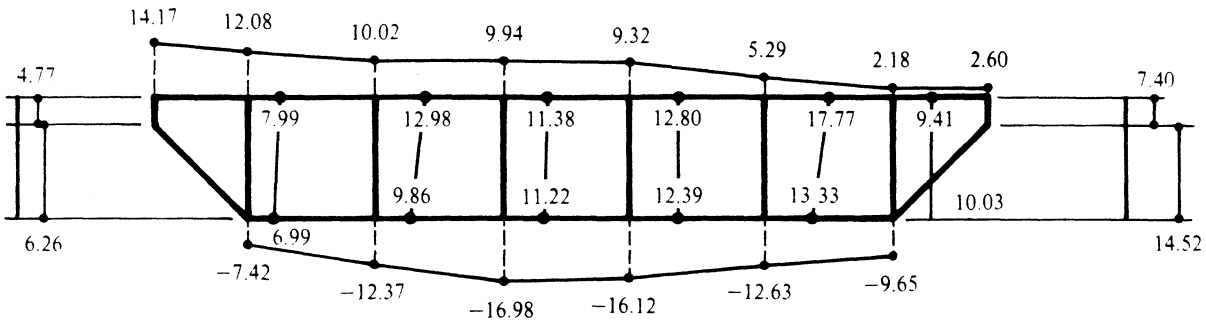

(a) LEFT OF BENT 2B, SECTION 2B

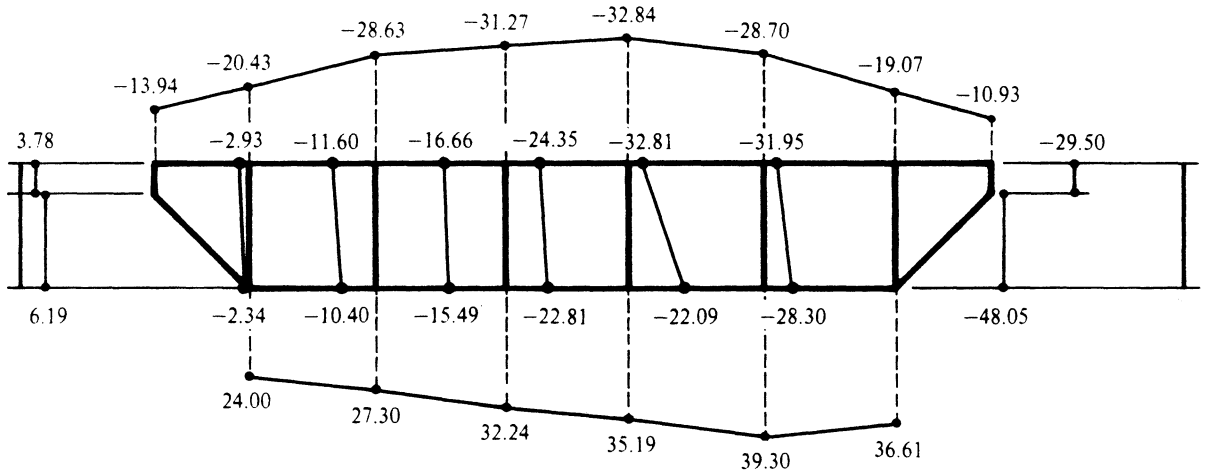

(b) RIGHT OF BENT 2B, SECTION 3B

FIG. 7.6.10 TRANSVERSE DISTRIBUTION OF MEMBRANE SHEAR STRESSES (ksf) AT SECTION 2B AND 3B (LEFT AND RIGHT OF BENT 2B) FOR DEAD LOAD

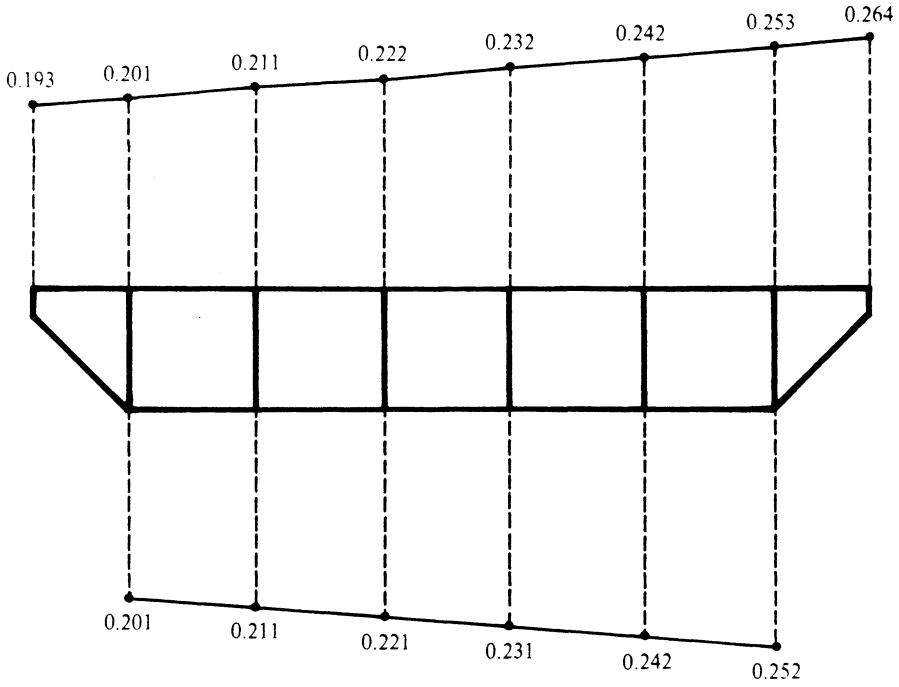

(a) VERTICAL DISPLACEMENTS (ft)

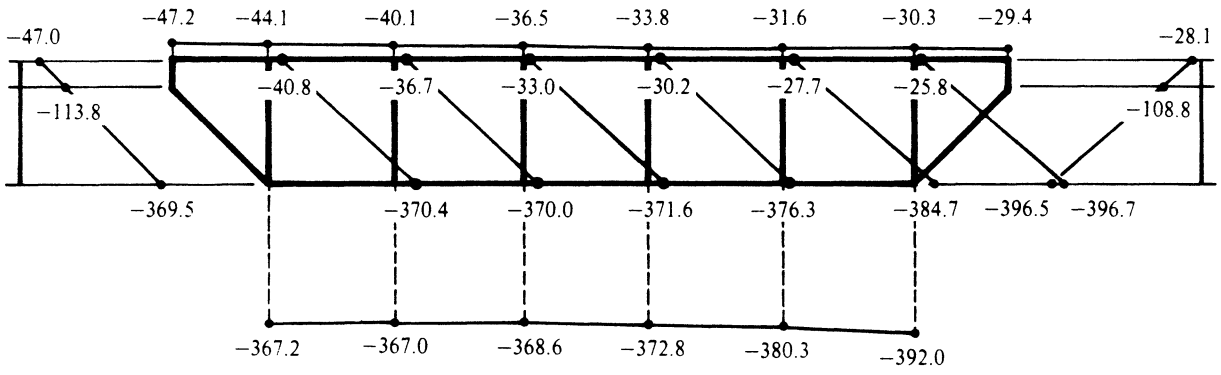

(b) LONGITUDINAL MEMBRANE STRESSES (ksf)

FIG. 7.6.11 TRANSVERSE DISTRIBUTION OF VERTICAL DISPLACEMENTS AND LONGITUDINAL MEMBRANE STRESSES AT MIDSPAN SECTION 3A (SPAN 3) FOR PRESTRESS

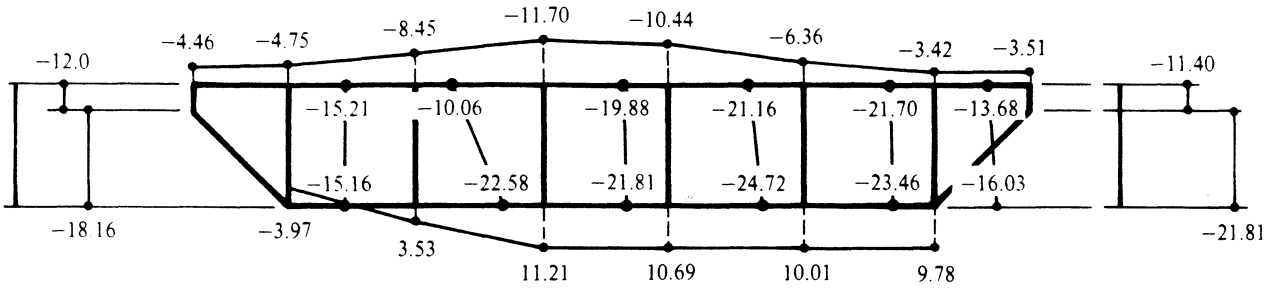

(a) LEFT OF BENT 2B, SECTION 2B

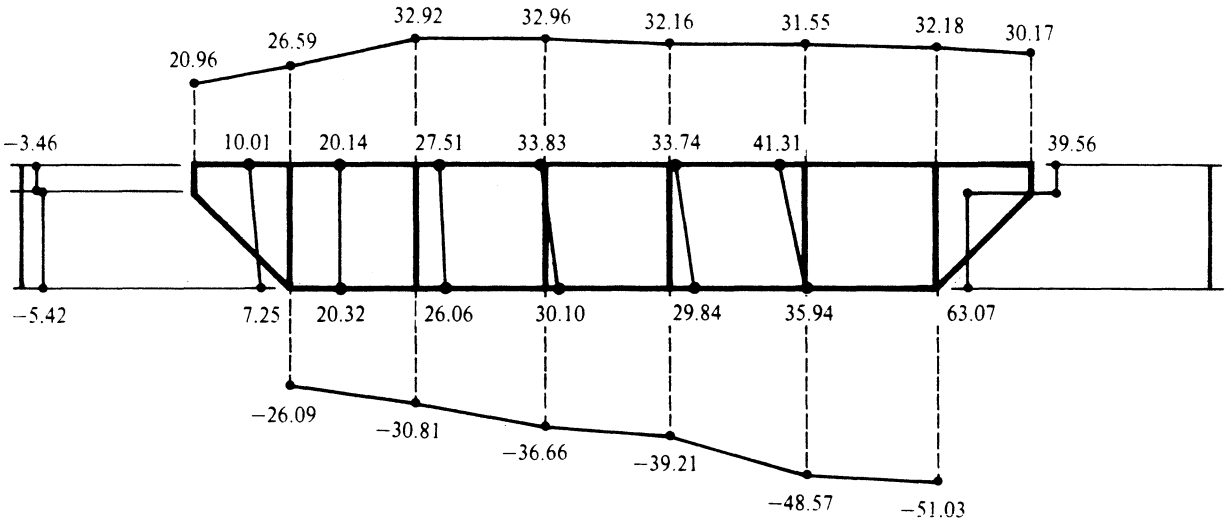

(b) RIGHT OF BENT 2B, SECTION 3B

FIG. 7.6.12 TRANSVERSE DISTRIBUTION OF MEMBRANE SHEAR STRESSES (ksf) AT SECTION 2B AND 3B (LEFT AND RIGHT OF BENT 2B) FOR PRESTRESS

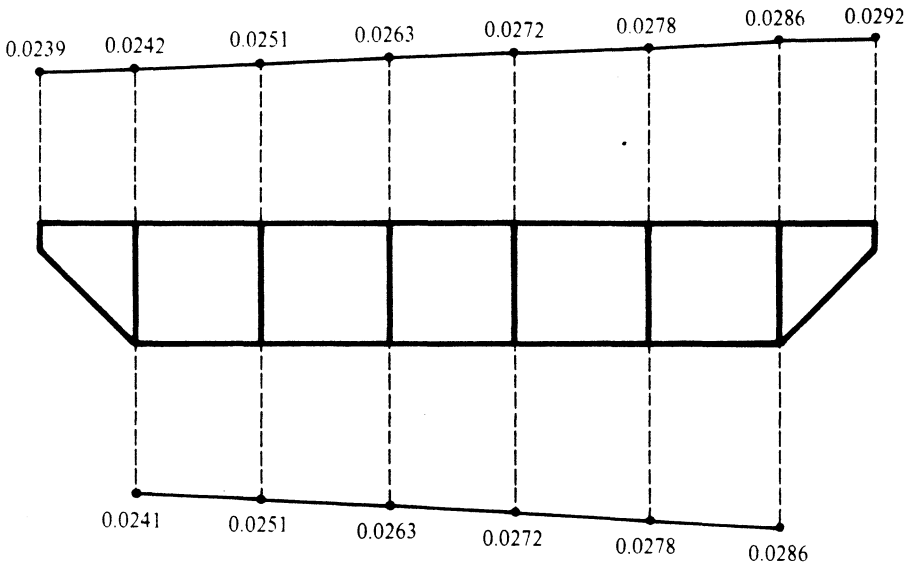

(a) VERTICAL DISPLACEMENTS (ft)

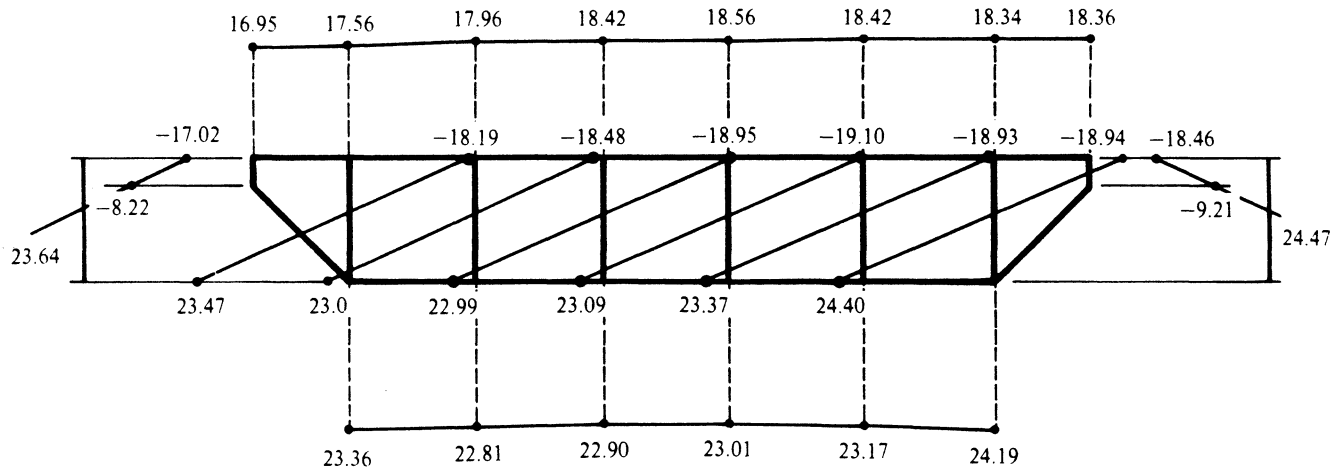

(b) LONGITUDINAL MEMBRANE STRESSES (ksf)

FIG. 7.6.13 TRANSVERSE DISTRIBUTION OF VERTICAL DISPLACEMENTS AND LONGITUDINAL MEMBRANE STRESSES AT MIDSPAN SECTION 3A (SPAN 3) FOR AASHTO HS 20 TUCK LIVE LOADS

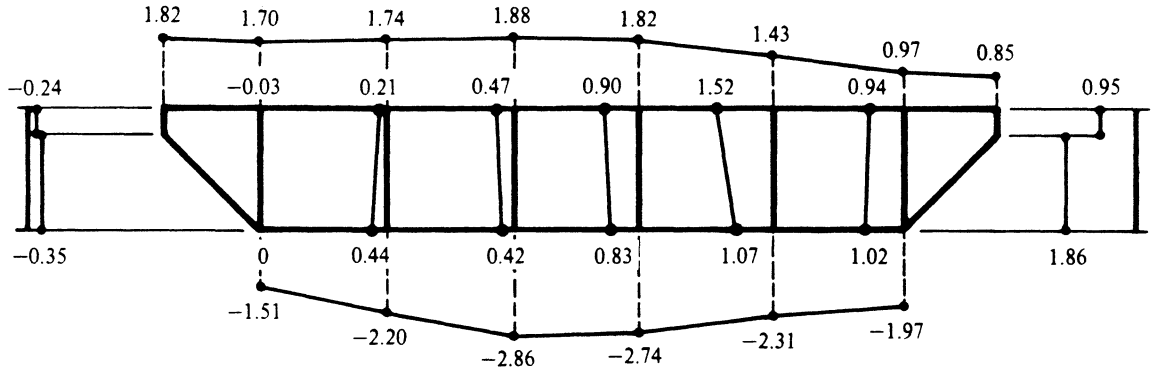

(a) LEFT OF BENT 2B, SECTION 2B

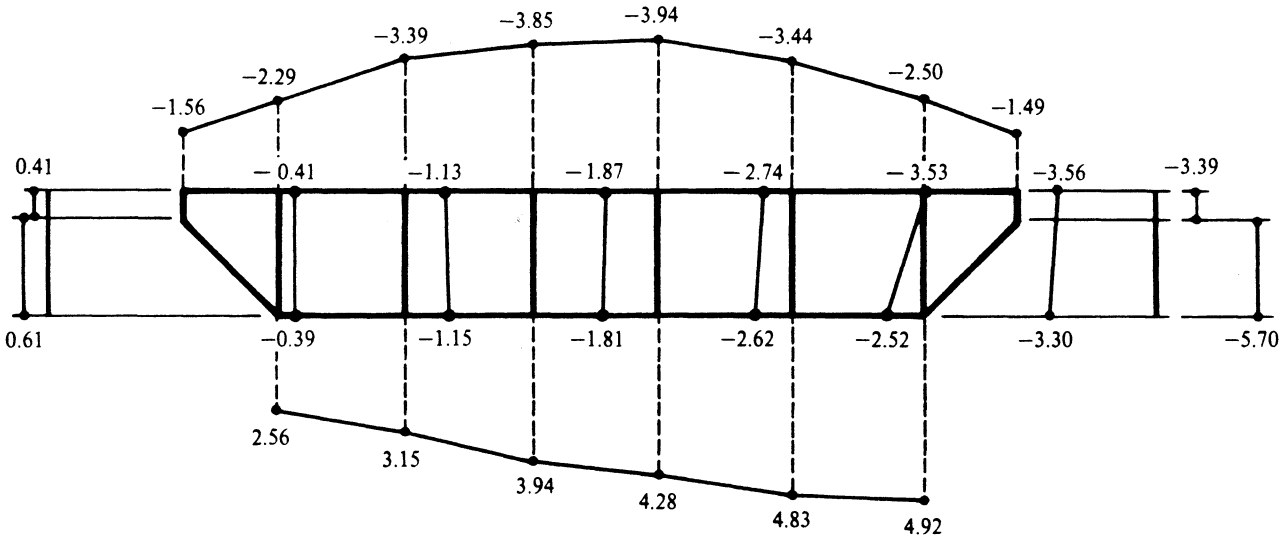

(b) RIGHT OF BENT 2B, SECTION 3B

FIG. 7.6.14 TRANSVERSE DISTRIBUTION OF MEMBRANE SHEAR STRESSES (ksf) AT SECTION 2B AND 3B (LEFT AND RIGHT OF BENT 2B) FOR AASHTO HS 20 TRUCK LIVE LOADS

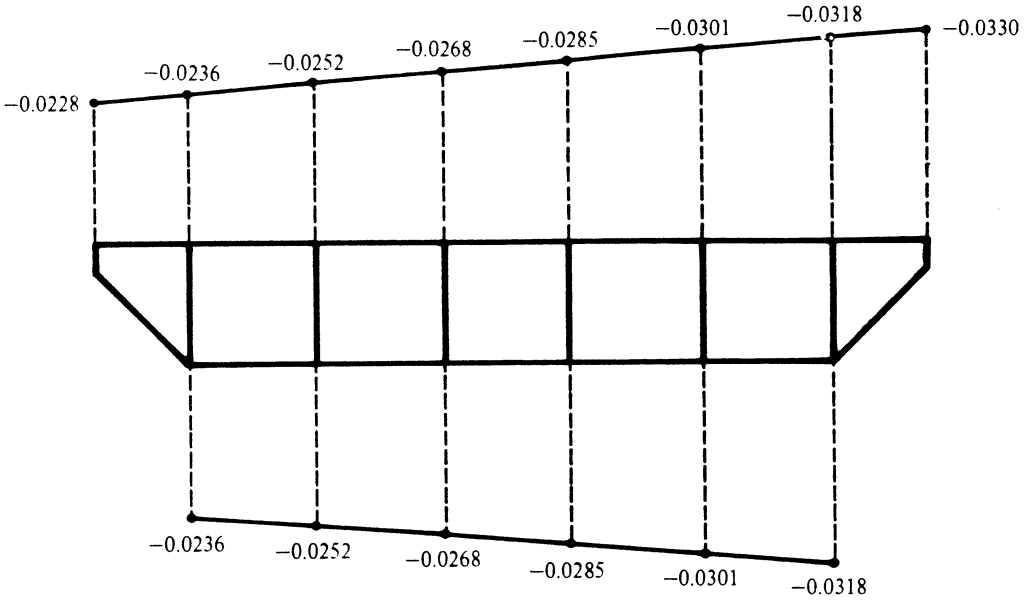

(a) VERTICAL DISPLACEMENTS (ft)

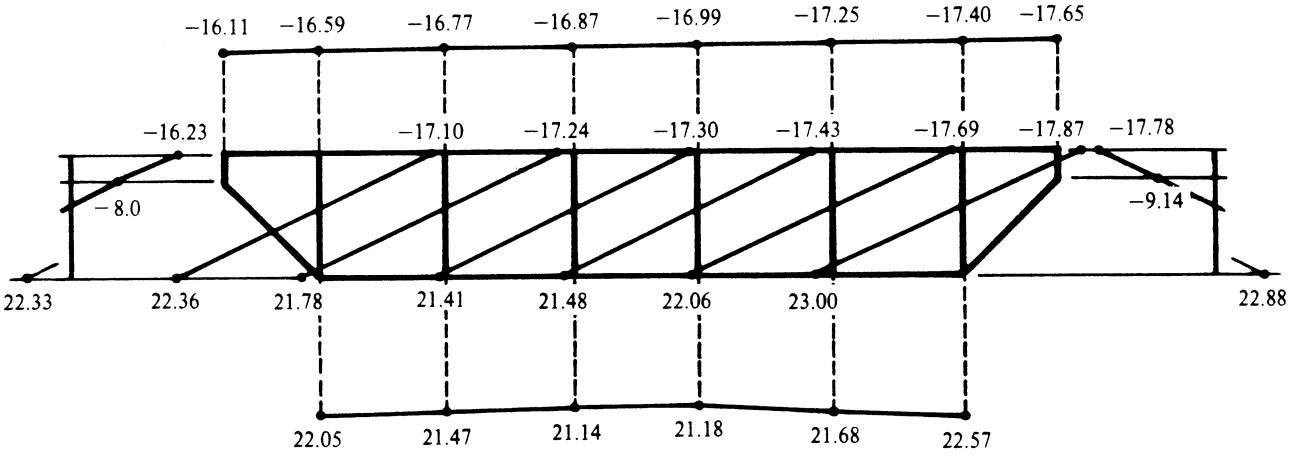

(b) LONGITUDINAL MEMBRANE STRESSES (ksf)

FIG. 7.6.15 TRANSVERSE DISTRIBUTION OF VERTICAL DISPLACEMENTS AND LONGITUDINAL MEMBER STRESSES AT MIDSPAN SECTION 3A (SPAN 3) FOR AASHTO LANE LIVE LOAD

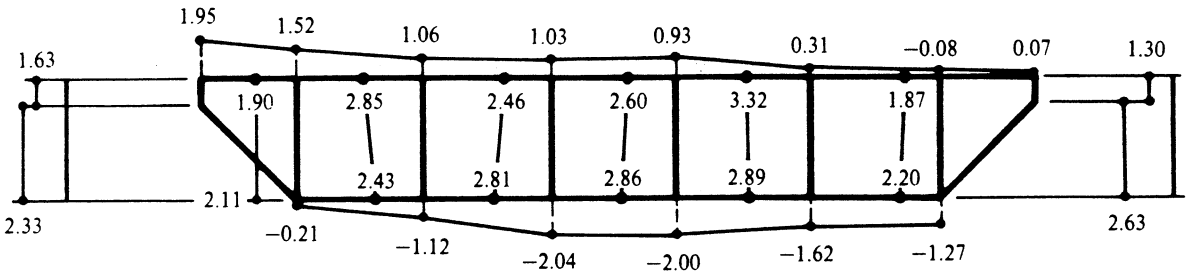

(a) LEFT OF BENT 2B, SECTION 2B

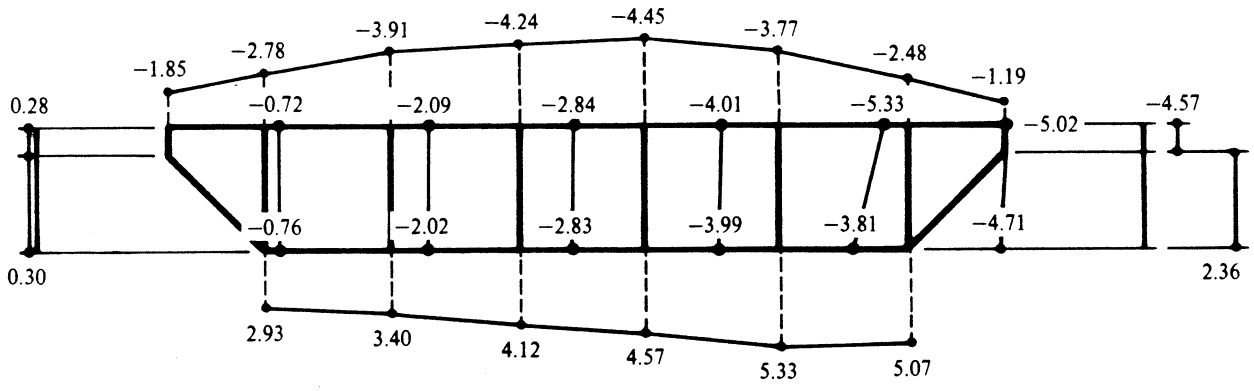

(b) RIGHT OF BENT 2B, SECTION 3B

FIG. 7.6.16 TRANSVERSE DISTRIBUTION OF MEMBRANE SHEAR STRESS (ksf) AT SECTION 2B AND 3B (LEFT AND RIGHT OF BENT 2B) FOR AASHTO LANE LIVE LOAD

Section 3A are largest at girder web 6 (the longest in Span 3) and smallest at girder web 1 (the shortest in Span 3) with almost a linear variation between them indicating a rotation of the section with little transverse distortion.

The membrane shear stress plots reveal a definite non-uniform distribution across the width of the bridge at Sections 2B and 3B, with the largest shear stresses occurring near the obtuse corner of Span 3 at Section 3B. This indicates that particular care should be exercised in evaluating web shear reinforcing requirements in highly skewed bridges. The CELL4 program can be used as an aid in making this evaluation.

7.6.4 Conclusions

By using good engineering judgment and proper interpretation, the CELL4 program can be used to obtain a complete evaluation of both longitudinal and transverse distributions of displacements, reactions, internal forces and moments, and internal stresses. Refinement of mesh and extrapolation of results for shear forces and stresses may be required to obtain satisfactory results. Static checks should always be made using the CELL4 automatic capabilities for integration of internal stresses to obtain section forces and moments.

Using a carefully selected planar grid model, consisting of a single line of one dimensional elements, properly supported, the SAPIV program can be used to get a good estimate of the longitudinal variation of centerline vertical displacements and total section shear forces, moments, and reactions.

8. SUMMARY AND CONCLUSIONS

The primary purpose of this research study, which was to write three new computer programs MUPDI4, CURDI4, and CELL4, was achieved. These programs incorporate automatic prestressing options as well as several other new features, which make it possible to perform detailed linear elastic analyses of prestressed concrete box girder bridges subjected to a variety of external loadings as well as longitudinal and transverse prestressing.

Single or multi-cell box girder bridges which are straight, circularly curved or of arbitrary geometry in plan and which have vertical, sloping or curved exterior webs can be analyzed. Simple and continuous spans, with or without interior rigid or flexible diaphragms and external supporting systems can be treated.

It can be concluded from the numerical examples given that the three computer programs can be used to study a variety of problems, which previously could not be done easily. It should be emphasized that care should be exercised in modelling the structure to be analyzed and interpreting the results obtained. Guidelines for doing this are described in the numerical examples. The automatic integration of element forces option, which gives individual girder and total section moment shears and axial forces, provides a powerful tool for studying load distribution and also for performing static checks.

9. ACKNOWLEDGEMENTS

This research program was sponsored by the Business and Transportation Agency, Department of Transportation, State of California, and the Federal Highway Administration, United States Department of Transportation.

The contents of this report reflect the views of the authors who are responsible for the facts and the accuracy of the data presented herein. The contents do not necessarily reflect the official views or policies of the State of California or the Federal Highway Administration. This report does not constitute a standard, specification or regulation.

The assistance, interest and support of the bridge engineering staff of CALTRANS is gratefully acknowledged, especially that of R. E. Davis of the Research and Development Section, who maintained a close and keen interest in the research program in all its stages.

The visual appearance of the report was aided by the excellent efforts of the graphics staff composed of R. Steele and N. Spersrud, and the word processing staff composed of N. Northern and E. Eisman.

The support of the Computer Center of the University of California, Berkeley, which provided its facilities was also of great assistance to the project.

10. REFERENCES

1. Scordelis, A. C., "Analysis of Simply Supported Box Girder Bridges," Structural Engineering and Structural Mechanics Report No. SESM 66-17, University of California, Berkeley, October 1966 (PB 175 646), 114 pgs.

2. Lin, C. S., and Scordelis, A. C., "Computer Program for Bridges on Flexible Bents," Structural Engineering and Structural Mechanics Report No. UC SESM 71-24, University of California, Berkeley, December 1971 (PB 210 171), 147 pgs.

3. DeFries-Skene, A., and Scordelis, A. C., "Direct Stiffness Solution for Folded Plates," Journal of the Structural Division, Proceedings of the American Society of Civil Engineers, Volume 90, No. ST-3, June 1964, pp. 15-47.

4. Scordelis, A. C., Davis, R. E., and Lo, K. S., "Load Distribution in Concrete Box Girder Bridges," ACI Proceedings of First International Symposium on Concrete Bridge Design, Toronto, Canada, April 1967, ACI Publication SP-23, 1969, pp. 117-136.

5. Scordelis, A. C., and Davis, R. E., "Stresses in Continuous Concrete Box Girder Bridges," ACI Proceedings of Second International Symposium on Concrete Bridge Design, Chicago, April 1969, ACI Publication SP-26, 1971, pp. 284-319.

6. Scordelis, A. C., "Analytical Solutions for Box Girder Bridges," Proceedings, Conference on Modern Developments in Bridge Design and Construction, Cardiff, Great Britain, April 1971, pp. 200-216.

7. Scordelis, A. C., "Analytical and Experimental Studies of Multi-Cell Concrete Box Girder Bridges," Bulletin of the International Association for Shell and Spatial Structures, Madrid, No. 58, August 1975, pp. 9-22.

8. Meyer, C., and Scordelis, A. C., "Analysis of Curved Folded Plate Structures," Structural Engineering and Structural Mechanics Report No. UC SESM 70-8, University of California, Berkeley, June 1970 (PB 193 535), 75 pgs.

9. Meyer, C., "Analysis and Design of Curved Box Girder Bridges," Structural Engineering and Structural Mechanics Report No. UC SESM 70-22, University of California, Berkeley, December 1970 (PB 197 289), 202 pgs.

10. Kabir, A. F., and Scordelis, A. C., "Computer Program for Curved Bridges on Flexible Bents," Structural Engineering and Structural Mechanics Report No. UC SESM 74-10, University of California, Berkeley, September 1974 (PB 242 470/AS), 170 pgs.

11. Sorensen, S. I., and Scordelis, A. C., "Computer Program For Curved Prestressed Box Girder Bridges," Structures and Materials Research Report No. UC SESM 80-10, Department of Civil Engineering, University of California, Berkeley, December 1980, 67 pgs.

12. Meyer, C., and Scordelis, A. C., "Analysis of Curved Folded Plate Structures," Journal of the Structural Division, Proceedings of the American Society of Civil Engineers, Volume 98, No. ST-1, January 1972, pp. 2459-2480.

13. Aslam, M., and Godden., W. G., "Model Studies of Multicell Curved Box-Girder Bridges," Journal of the Engineering Mechanics Division, Proceedings of the American Society of Civil Engineers, Volume 101, No. EM-3, June 1975.

14. Willam, K. J., and Scordelis, A. C., "Computer Program for Cellular Structures of Arbitrary Plan Geometry," Structural Engineering and Structural Mechanics Report No. UC SESM 70-10, University of California, Berkeley, September 1970 (PB 196 143), 157 pgs.

15. Willam, K. J., and Scordelis, A. C., "Cellular Structures of Arbitrary Plan Geometry," Journal of the Structural Division, Proceedings of the American Society of Civil Engineers, Volume 98, No. ST-7, July 1972, pp. 1377-1394.

16. Godden, W. G., and Aslam, M., "Model Studies of Skew Multicell Girder Bridges," Journal of the Engineering Mechanics Division, Proceedings of the American Society of Civil Engineers, Volume 99, No. EM-1, February 1973.

17. Wilson, E. L., and Hoit, M. I., "A Computer Adaptive Language for the Develoment of Structural Analysis Programs," Computers and Structures, Vol 19, No. 3, pp. 321-338, 1984.

18. Prestressed Concrete Institute and Post-Tensioning Institute, Post-Tensioned Box Girder Bridge Manual, PCI and PTI, 1978.

19. Scordelis, A. C., "Berkeley Computer Programs for the Analysis of Concrete Box Girder Bridges," Proceedings, NATO-Advanced Study Institute on Analysis and Design of Bridges, Cesme, Turkey, July 1982, pp. 1-71.

20. Hood, J. A., "An Investigation of a Curved Single Cell Box Girder Bridge," Report No. 138, School of Civil Engineering, University of Aukland, New Zealand, October 1976.

21. Bathe, K.-J., Wilson, E. L., and Peterson, F. E., "SAP IV - A structural Analysis Program for Static and Dynamic Response of Linear Systems," Earthquake Engineering Research Center Report No. EERC 73-11, University of California, Berkeley, June, 1973.

APPENDIX A

PUBLICATIONS ON RESEARCH ON

REINFORCED AND PRESTRESSED CONCRETE BOX GIRDER BRIDGES

The attached publications are on research conducted in the Division of Structural Engineering and Structural Mechanics, University of California, Berkeley, 94720, under the supervision of Professor A. C. Scordelis. Much of this research was sponsored by the State of California, Department of Transportation.

Inquiries regarding these publications may be sent to:

Professor A. C. Scordelis
Department of Civil Engineering
729 Davis Hall
University of California
Berkeley, California 94720

Unfortunately, the supply of some of the research reports has been exhausted. However, most of these publications have been placed on file with the U.S. Department of Commerce and may be obtained on request for cost of reproduction by writing to the following address:

National Technical Information Service
Operations Division
Springfield, Virginia 22151

The accession number (shown in parentheses on reference list A) should be specified when ordering a particular report.

RESEARCH REPORTS AND TECHNICAL PAPERS PUBLISHED ON RESEARCH ON BOX GIRDER BRIDGES PERFORMED IN THE DIVISION OF STRUCTURAL ENGINEERING AND STRUCTURAL MECHANICS, UNIVERSITY OF CALIFORNIA, BERKELEY

A. **Research Reports**

1. Scordelis, A. C., "Analysis of Simply Supported Box Girder Bridges," Structural Engineering and Structural Mechanics Report No. SESM 66-17, University of California, Berkeley, October 1966 (PB 175 646), 114 pgs.

2. Scordelis, A. C., "Analysis of Continuous Box Girder Bridges," Structural Engineering and Structural Mechanics Report No. SESM 67-25, University of California, Berkeley, November 1967 (PB 178 355), 188 pgs.

3. Scordelis, A. C., and Meyer, C., "Wheel Load Distribution in Concrete Box Girder Bridges," Structural Engineering and Structural Mechanics Report No. SESM 69-1, University of California, Berkeley, January 1969 (PB 183 923), 143 pgs.

4. Willam, K. J., and Scordelis, A. C., "Analysis of Orthotropic Folded Plates with Eccentric Stiffeners," Structural Engineering and Structural Mechanics Report No. SESM 70-2, University of California, Berkeley, February 1970 (PB 191 051), 130 pgs.

5. Meyer, C., and Scordelis, A. C., "Computer Program for Prismatic Folded Plates with Plate and Beam Elements," Structural Engineering and Structural Mechanics Report No. SESM 70-3, University of California, Berkeley, February 1970 (PB 191 050), 118 pgs.

6. Meyer, C., and Scordelis, A. C., "Analysis of Curved Folded Plate Structures," Structural Engineering and Structural Mechanics Report No. UC SESM 70-8, University of California, Berkeley, June 1970 (PB 193 535), 75 pgs.

7. Willam, K. J., and Scordelis, A. C., "Computer Program for Cellular Structures of Arbitrary Plan Geometry," Structural Engineering and Structural Mechanics Report No. UC SESM 70-10, University of California, Berkeley, September 1970 (PB 196 143), 157 pgs.

8. Meyer, C., "Analysis and Design of Curved Box Girder Bridges," Structural Engineering and Structural Mechanics Report No. UC SESM 70-22, University of California, Berkeley, December 1970 (PB 197 289), 202 pgs.

9. Bouwkamp, J. G., Scordelis, A. C., and Wasti, S. T., "Structural Behavior of a Two Span Reinforced Concrete Box Girder Bridge Model, Volume I," Structural Engineering and Structural Mechanics Report No. UC SESM 71-15, University of California, Berkeley, April 1971 (PB 199 187), 134 pgs.

10. Bouwkamp, J. G., Scordelis, A. C., and Wasti, S. T., "Structural Behavior of a Two Span Reinforced Concrete Box Girder Bridge Model, Volume II," Structural Engineering and Structural Mechanics Report No. UC SESM 71-16, University of California, Berkeley, April 1971 (PB 210 431), 196 pgs.

11. Bouwkamp, J. G., Scordelis, A. C., and Wasti, S. T., "Structural Behavior of a Two Span Reinforced Concrete Box Girder Bridge Model, Volume III," Structural Engineering and Structural Mechanics Report No. UC SESM 71-17, University of California, Berkeley, April 1971 (PB 199 187), 260 pgs.

12. Meyer, C., and Scordelis, A. C., "Computer Program for Non-Prismatic Folded Plates with Plate and Beam Elements," Structural Engineering and Structural Mechanics Report No. UC SESM 71-23, University of California, Berkeley, December 1971 (PB 220 197), 154 pgs.

13. Lin, C. S., and Scordelis, A. C., "Computer Program for Bridges on Flexible Bents," Structural Engineering and Structural Mechanics Report No. UC SESM 71-24, University of California, Berkeley, December 1971 (PB 210 171), 147 pgs.

14. Godden, W. G., and Aslam, M., "Model Studies of Skew Box Girder Bridges," Structural Engineering and Structural Mechanics Report No. UC SESM 71-26, University of California, Berkeley, December 1971 (PB 223 120), 186 pgs.

15. Comartin, C. D., and Scordelis, A. C., "Analysis and Design of Skew Box Girder Bridges," Structural Engineering and Structural Mechanics Report No. UC SESM 72-14, University of California, Berkeley, December 1972 (PB 226 793), 172 pgs.

16. Godden, W. G., and Aslam, M., "Model Studies of Curved Box Girder Bridges," Structural Engineering and Structural Mechanics Report No. UC SESM 73-5, University of California, Berkeley, March 1973 (PB 226 842/AS), 121 pgs.

17. Scordelis, A. C., Bouwkamp, J. G., and Larsen, P. K., "Structural Behavior of a Curved Two Span Reinforced Concrete Box Girder Bridge Model, Volume I," Structural Engineering and Structural Mechanics Report No. UC SESM 74-5, University of California, Berkeley, September 1974 (PB 242 523/AS), 136 pgs.

18. Scordelis, A. C., Bouwkamp, J. G., and Larsen, P. K., "Structural Behavior of a Curved Two Span Reinforced Concrete Box Girder Bridge Model, Volume II," Structural Engineering and Structural Mechanics Report No. UC SESM 74-6, University of California, Berkeley, September 1974 (PB 242 524/AS), 337 pgs.

19. Scordelis, A. C., Bouwkamp, J. G., and Larsen, P. K., "Structural Behavior of a Curved Two Span Reinforced Concrete Box Girder Bridge Model, Volume III," Structural Engineering and Structural Mechanics Report No. UC SESM 74-7, University of California, Berkeley, September 1974 (PB 242 525/AS), 450 pgs.

20. Kabir, A. F., and Scordelis, A. C., "Computer Program for Curved Bridges on Flexible Bents," Structural Engineering and Structural Mechanics Report No. UC SESM 74-10, University of California, Berkeley, September 1974 (PB 242 470/AS), 170 pgs.

21. Van Zyl, S. F., "Analysis of Curved Segmentally Erected Prestressed Concrete Box Girder Bridges," Structural Engineering and Structural Mechanics Report No. UC SESM 78-2, University of California, Berkeley, January 1978 (PB 284 939/AS), 265 pgs.

22. Scordelis, A. C., Bouwkamp, J. G., Wasti, S. T., and Anicic, D., "Structural Behavior of a Skew Two Span Reinforced Concrete Box Girder Bridge Model, Volume I," Structural Engineering and Structural Mechanics Report No. UC SESM 80-1, University of California, Berkeley, June 1980, 164 pgs.

23. Scordelis, A. C., Bouwkamp, A. C., Wasti, S. T., and Anicic, D., "Structural Behavior of a Skew Two Span Reinforced Concrete Box Girder Bridge Model, Volume II," Structural Engineering and Structural Mechanics Report No. UC SESM 80-2, University of California, Berkeley, June 1980, 407 pgs.

24. Scordelis, A. C., Bouwkamp, A. C., Wasti, S. T., and Anicic, D., "Structural Behavior of a Skew Two Span Reinforced Concrete Box Girder Bridge Model, Volume III," Structural Engineering and Structural Mechanics Report No. UC SESM 80-3, University of California, Berkeley, June 1980, 122 pgs.

25. Scordelis, A. C., Bouwkamp, A. C., Wasti, S. T., and Anicic, D., "Structural Behavior of a Skew Two Span Reinforced Concrete Box Girder Bridge Model, Volume IV," Structural Engineering and Structural Mechanics Report No. UC SESM 80-4, University of California, Berkeley, June 1980, 498 pgs.

26. Sorensen, S. I., and Scordelis, A. C., "Computer Program For Curved Prestressed Box Girder Bridges," Structures and Materials Research Report No. UC SESM 80-10, Department of Civil Engineering, University of California, Berkeley, December 1980, 67 pgs.

27. Sorensen, S. I., and Scordelis, A. C., "Computer Program For Curved Prestressed Slabs," Structures and Materials Research Report No. UC SESM 80-11, Department of Civil Engineering, University of California, Berkeley, December 1980, 66 pgs.

28. Seible, F., "Nonlinear Analysis and Ultimate Strength of Multi-Cell Reinforced Concrete Box Girder Bridges," Structural Engineering and Structural Mechanics Report No. UC SESM 82-2, University of California, Berkeley, February 1982 (PB 84 104462), 228 pgs.

29. Kang, Y. J., "Nonlinear Geometric, Material and Time Dependent Analysis of Reinforced and Prestressed Concrete Frames," Ph.D. Dissertation, Division of Structural Engineering and Structural Mechanics, University of California, Berkeley, Report No. UC-SESM 77-1, January 1977 (PB 272 930/AS), 243 pgs.

B. Technical Papers

1. DeFries-Skene, A., and Scordelis, A. C., "Direct Stiffness Solution for Folded Plates," Journal of the Structural Division, Proceedings of the American Society of Civil Engineers, Volume 90, No. ST-3, June 1964, pp. 15-47.

2. Scordelis, A. C., Davis, R. E., and Lo, K. S., "Load Distribution in Concrete Box Girder Bridges," ACI Proceedings of First International Symposium on Concrete Bridge Design, Toronto, Canada, April 1967, ACI Publication SP-23, 1969, pp. 117-136.

3. Scordelis, A. C., and Davis, R. E., "Stresses in Continuous Concrete Box Girder Bridges," ACI Proceedings of Second International Symposium on Concrete Bridge Design, Chicago, April 1969, ACI Publication SP-26, 1971, pp. 284-319.

4. Lo., K. S., and Scordelis, A. C., "Finite Segment Analysis of Folded Plates," Journal of the Structural Division, Proceedings of the American Society of Civil Engineers, Volume 95, No. ST-5, May 1969, pp. 831-852.

5. Willam, K. J., and Scordelis, A. C., "Analysis of Ecentrically Stiffened Folded Plates," Proceedings of IASS Symposium on Folded Plates and Prismatic Structures, Vienna, September 1970, pp. 1-27.

6. Scordelis, A. C., "Analytical Solutions for Box Girder Bridges," Proceedings, Conference on Modern Developments in Bridge Design and Construction, Cardiff, Great Britain, April 1971, pp. 200-216.

7. Bouwkamp, J. G., Scordelis, A. C., and Wasti, S. T., "Structural Behavior of a Reinforced Concrete Box Girder Bridge," Proceedings, Conference on Modern Developments in Bridge Design and Construction, Cardiff, Great Britain, April 1971, pp. 318-333.

8. Meyer, C., and Scordelis, A. C., "Analysis of Curved Folded Plate Structures," Journal of the Structural Division, Proceedings of the American Society of Civil Engineers, Volume 98, No. ST-1, January 1972, pp. 2459-2480.

9. Willam, K. J., and Scordelis, A. C., "Cellular Structures of Arbitrary Plan Geometry," Journal of the Structural Division, Proceedings of the American Society of Civil Engineers, Volume 98, No. ST-7, July 1972, pp. 1377-1394.

10. Godden, W. G., and Aslam, M., "Model Studies of Skew Multicell Girder Bridges," Journal of the Engineering Mechanics Division, Proceedings of the American Society of Civil Engineers, Volume 99, No. EM-1, February 1973.

11. Scordelis, A. C., Bouwkamp, J. G., and Wasti, S. T., "Study of AASHO Loadings on a Concrete Box Girder Bridge," Highway Research Record No. 428, Highway Research Board, Washington, D. C., 1973, pp. 22-31.

12. Scordelis, A. C., Bouwkamp, J. G., and Wasti, S. T., "Structural Response of a Concrete Box Girder Bridge," Journal of the Structural Division, Proceedings of the American Society of Civil Engineers, Volume 99, No. ST-10, October 1973, pp. 2031-2048.

13. Scordelis, A. C., Bouwkamp, J. G., and Wasti, S. T., "Ultimate Strength of a Concrete Box Girder Bridge," Journal of the Structural Division, Proceedings of the American Society of Civil Engineers, Volume 100, No. ST-1, January 1974, pp. 31-49.

14. Aslam, M., and Godden., W. G., "Model Studies of Multicell Curved Box-Girder Bridges," Journal of the Engineering Mechanics Division, Proceedings of the American Society of Civil Engineers, Volume 101, No. EM-3, June 1975.

15. Scordelis, A. C., "Folded Plates for Bridges," Bulletin of the International Association for Shell and Spatial Structures, Madrid, No. 57, April 1975, pp. 29-38.

16. Scordelis, A. C., "Analytical and Experimental Studies of Multi-Cell Concrete Box Girder Bridges," Bulletin of the International Association for Shell and Spatial Structures, Madrid, No. 58, August 1975, pp. 9-22.

17. Scordelis, A. C., and Larsen, P. K., "Structural Response of Curved RC Box Girder Bridge," Journal of the Structural Division, Proceedings of the American Society of Civil Engineers, Volume 103, No. ST-8, August 1977, pp. 1507-1524.

18. Scordelis, A. C., Larsen, P. K., and Elfgren, L. G., "Ultimate Strength of Curved RC Box Girder Bridge," Journal of the Structural Division, Proceedings of the American Society of Civil Engineers, Volume 103, No. ST-8, August 1977, pp. 1525-1542.

19. Van Zyl, S. F., and Scordelis, A. C., "Analysis of Curved Prestressed Segmental Bridges," Journal of the Structural Division, Proceedings of the American Society of Civil Engineers, Volume 105, No. ST-11, November 1979, pp. 2399-2417.

20. Scordelis, A. C., Elfgren, L. G., and Larsen, P. K., "Time Dependent Behavior of Concrete Box Girder Bridges," Journal of the American Concrete Institute, Title No, 76-9, January 1979, pp. 159-177.

21. Bouwkamp, J. G., Scordelis, A. C., and Wasti, S. T., "Failure Study of A Skew Box Girder Bridge Model," Final Report, 11th Congress, Vienna, International Association for Bridge and Structural Engineering, August 31 - September 5, 1980, pp. 855-860.

22. Hellesland, J., and Scordelis, A. C., "Analysis of RC Bridge Columns Under Imposed Deformations," Final Report, IABSE Colloquium on Advanced Mechanics of Reinforced Concrete, Delft, June 1981, pp. 545-560.

23. Ketchum, M. A., and Scordelis, A. C., "Nonlinear Analysis of a Prestressed Concrete Bridge," Final Report, IABSE Colloquium on Advanced Mechanics of Reinforced Concrete, Delft, June 1981, pp. 561-576.

24. Scordelis, A. C., Wasti, S. T., and Seible, F., "Structural Response of Skew RC Box Girder Bridge," Journal of the Structural Division, Proceedings of the American Society of Civil Engineers, Vol. 108, No. ST-1, January 1982, pp. 89-104.

25. Scordelis, A. C., Bouwkamp, J. G., Wasti, S. T., and Seible, F., "Ultimate Strength of Skew RC Box Girder Bridge," Journal of the Structural Division, Proceedings of the American Society of Civil Engineers, Vol. 108, No. ST-1, January 1982, pp. 105-121.

26. Kang, Y. J., and Scordelis, A. C., "Nonlinear Analysis of Prestressed Concrete Frames," Journal of the Structural Division, Proceedings of the American Society of Civil Engineers, Vol. 106, No. ST-2, February 1980, pp. 445-472.

27. Scordelis, A. C., "Berkeley Computer Programs for the Analysis of Concrete Box Girder Bridges," Proceedings, NATO-Advanced Study Institute on Analysis and Design of Bridges, Cesme, Turkey, July 1982, pp. 1-71.

28. Wasti, S. T., and Scordelis, A. C., "Comparative Structural Behavior of Straight, Curved and Skew Reinforced Concrete Box Girder Bridge Models," Proceedings, NATO-Advanced Study Institute on Analysis and Design of Bridges, Cesme, Turkey, July 1982, pp. 101-121.

29. Seible, F., and Scordelis, A. C., "Nonlinear Behavior and Failure Analysis of Multi-cell RC Box Girder Bridges," Proceedings, International Conference on Short and Medium Span Bridges, Toronto, Canada, Vol. 1, August 1982, pp. 391-405.

30. Scordelis, A. C., and Seible, F., "Time Dependent Behavior of a Skew Reinforced Concrete Box Girder Bridge," American Concrete Institute, Concrete International: Design and Construction, Vol. 5, No. 1, January 1983, pp. 82-92.

31. Seible, F., and Scordelis, A. C., "Nonlinear Analysis of Multi-cell RC Box Girder Bridges," Journal of Engineering Structures, Vol. 5, January 1983, pp. 45-57.

32. Scordelis, A. C., Bouwkamp, J. G., Wasti, S. T., and Seible, F., "Response of a 45^{o} Skew RC Box Girder Bridge Model To AASHTO Trucks and Overload Construction Vehicles," Transportation Research Record No. 871, Transportation Research Board, National Academy of Science, Washington, D.C., 1983, pp. 57-65.

APPENDIX B: MUPDI4 USER'S GUIDE

MUPDI4: A COMPUTER PROGRAM FOR THE ELASTIC ANALYSIS OF STRAIGHT, PRISMATIC, PRESTRESSED CELLULAR FOLDED PLATE STRUCTURES WITH OPTIONAL INTERMEDIATE DIAPHRAGMS AND SUPPORTS

Programmed at the Department of Civil Engineering
University of California, Berkeley

Faculty Investigator: Professor A. C. Scordelis

Author: M. A. Ketchum

Date: February, 1985

Considerable effort has gone into the development and testing of this program, which can analyze a particular class of structure. It is based on the conditions and assumptions described in this report. The program should be used only under these conditions and assumptions and the output must be interpreted appropriately by a qualified person.

Although the program has been extensively tested, no warranty is made regarding the accuracy and reliability of the program, and the authors assume no responsibility in this respect.

MUPDI4 INPUT DATA FORMAT:

1. TITLE (20A4) - 1 line

Col. 1 - 80	TITLE	Title of the problem to be printed with output

2. STRUCTURE CONTROL DATA (F10.0,6I5) - 1 line

Col. 1 - 10	SPAN	Total overall structure length
Col. 11 - 16	NJT	Number of joints in the folded plate system
Col. 16 - 20	NEL	Number of plate elements
Col. 21 - 25	NET	Number of plate element material types
Col. 26 - 30	NDIAPH	Total number of diaphragms and frame bents
Col. 31 - 35	NBT	Number of flexible supporting frame bent types
Col. 36 - 40	NFMD	Number of flexible movable diaphragm types

3. LOAD AND PRESTRESSING CONTROL DATA (5I5) - 1 line

Col. 1 - 5	NLCAS	Number of load cases
Col. 6 - 10	NCONL	Number of joint loads
Col. 11 - 15	NSURL	Number of plate surface loads
Col. 16 - 20	NPT	Number of panel tendons
Col. 21 - 25	NST	Number of slab tendon groups

4. ANALYSIS CONTROL DATA (4I5,F10.0,2I5) - 1 line

Col. 1 - 5	NXP	Number of cross sections at which output of joint displacements, element stresses and displacements, and integrated section shears, moments and axial forces is required
Col. 6 - 10	NCHECK	Check on use of odd and even harmonics +1 to use odd series only (symmetric) 0 to include all series -1 to use even series only (anti-symmetric)
Col. 11 - 15	MHARM	Maximum term number of Fourier series to be used in the harmonic analysis
Col. 16 - 20	NBOX	Number of girders defined in the folded plate system for longitudinal girder shear, moment and axial force integration
Col. 21 - 30	SCLM	Scale factor for girder moment output
Col. 31 - 35	KFRAME	Bent internal force evaluation option 0 to skip bent internal force evaluation 1 to perform bent internal force evaluation
Col. 36 - 40	MODE	Data check mode option 0 for execution mode 1 for data check mode

5. FOLDED PLATE JOINT COORDINATE DATA (I5,2F10.0,I5) - 2 to NJT lines

Joint coordinates may be input or generated in any sequence of joint numbers. However, the coordinates of all joints must be specified or generated.

Col. 1 - 5	N	Joint number
Col. 6 - 15	Y(N)	Y- (horizontal) coordinate of joint N
Col. 16 - 25	Z(N)	Z- (vertical) coordinate of joint N
Col. 26 - 30	KN	Joint increment for automatic coordinate generation. Separate lines must be given for the first and last joints, and the increment is entered with the data for the first joint only. Leave blank for no generation.

6. FOLDED PLATE JOINT BOUNDARY CONDITION DATA (10I5) - 1 to NJT lines

Joint boundary conditions may be input or generated in any sequence of joint numbers. However, the boundary conditions of all joints must be specified or generated.

Col. 1 - 5	NFST	Joint number of the first joint in a series of joints with identical boundary condition specifications
Col. 6 - 10	NLST	Joint number of the last joint in the series
Col. 11 - 15	KN	Joint increment for automatic generation between first and last joint in a series
Col. 16 - 20	LC(1)	Index for horizontal (Y) displacement
Col. 21 - 25	LC(2)	Index for vertical (Z) displacement
Col. 26 - 30	LC(3)	Index for (XX) rotation
Col. 31 - 35	LC(4)	Index for longitudinal (X) displacement

In Cols. 16 - 35 the indices takes the following values:
0 for non zero displacement evaluated by program
1 for prescribed zero displacement

Col. 36 - 40	JF(1)	Index for horizontal (Y) restraint from intermediate diaphragms or bents
Col. 41 - 45	JF(2)	Index for vertical (Z) restraint from intermediate diaphragms or bents
Col. 46 - 50	JF(3)	Index for rotational (XX) restraint from intermediate diaphragms or bents

In Cols. 36 - 50 the indices take the following values:
0 to consider restraint from diaphragms or bents
1 to neglect restraint from diaphragms or bents

7. PLATE ELEMENT MATERIAL TYPE DATA (I5,3F10.0) - NET lines

Provide one line per plate element material type.

Col. 1 - 5	I	Material type number
Col. 6 - 15	EMOD(I)	Modulus of elasticity of plate
Col. 16 - 25	PRAT(I)	Poisson's ratio of plate
Col. 26 - 35	WGT(I)	Unit weight of material, for computing dead load

8. PLATE ELEMENT DATA (4I5,F10.0,3I5,F10.0) - NEL lines

The location and type of each plate element, and girder numbers for stress integration are specified here. Plate stresses and moments are integrated to find girder moments about the Y axis, and forces in the X and Z directions. Each plate element can belong to one or two girders. Stress integration is performed only if called for with a non zero value of NBOX in input section 4. Integration accuracy depends on the number of transverse sections (NSEC) specified. NSEC = 4 is a recommended minimum value. Provide one line per plate element.

Col. 1 - 5	I	Plate element number
Col. 6 - 10	NPI(I)	Joint i of element I
Col. 11 - 15	NPJ(I)	Joint j of element I
Col. 16 - 20	KPL(I)	Plate element material type of element I
Col. 21 - 30	THK(I)	Plate thickness
Col. 31 - 35	NSEC(I)	Number of element transverse subdivisions for output of internal forces and displacements, e.g. use 4 for output at quarter points. If NSEC(I) = 0, no internal forces or displacements will be output for element I.
Col. 36 - 40	NGL(1,I)	First girder number to which this element belongs. If it belongs to two girders, list that which is nearest to joint I first. Girder numbers must be between 1 and NBOX.
Col. 41 - 45	NGL(2,I)	Second girder number to which this element belongs. Use zero if no second girder.
Col. 46 - 55	XDIV(I)	Horizontal (Y) distance from the dividing point to joint I if the element belongs to two girders, input as a positive number. Neglected if NGL(2,I) = 0

9. PLATE ELEMENT OUTPUT CONTROL DATA (14I5) - 1 line

Plate element results may include 14 components at each location in each element. Output of some or all of these components may be suppressed by flagging them here. These control codes apply to all plate elements.

Col. 1 - 5	LSTR(1)	N_x	Output code (Longitudinal membrane force)
Col. 6 - 10	LSTR(2)	N_y	Output code (Transverse membrane force)
Col. 11 - 15	LSTR(3)	N_{xy}	Output code (Membrane shear force)
Col. 16 - 20	LSTR(4)	S_x	Output code (Longitudinal membrane stress)
Col. 21 - 25	LSTR(5)	S_y	Output code (Transverse membrane stress)
Col. 26 - 30	LSTR(6)	S_{xy}	Output code (Membrane shear stress)
Col. 31 - 35	LSTR(7)	M_x	Output code (Moment on X-face)
Col. 36 - 40	LSTR(8)	M_y	Output code (Moment on Y-face)
Col. 41 - 45	LSTR(9)	M_{xy}	Output code (Twisting moment)
Col. 46 - 50	LSTR(10)	Q_x	Output code (Slab shear on X-face)
Col. 51 - 55	LSTR(11)	Q_y	Output code (Slab shear on Y-face)
Col. 56 - 60	LSTR(12)	U	Output code (Longitudinal displacement)
Col. 61 - 65	LSTR(13)	V	Output code (Transverse displacement)
Col. 66 - 70	LSTR(14)	W	Output code (Normal displacement)

Each Output Code may take one of the following values:
0 to skip output of the indicated results component
1 to include output of the indicated results component

10. DIAPHRAGM / BENT INTERACTION DATA (I5,2F10.0,2I5) - NDIAPH lines

Provide one line per intermediate diaphragm or support, omit if NDIAPH = 0

Col. 1 - 5	I	Diaphragm or bent number
Col. 6 - 15	DIAPHX(I)	X-coordinate of diaphragm location
Col. 16 - 25	DIADEL(I)	Diaphragm or bent interaction thickness in the longitudinal direction
Col. 26 - 30	KODIA(I)	Diaphragm classification code 1 for externally supported rigid diaphragm 2 for movable rigid diaphragm 3 for flexible supporting frame bent 4 for flexible movable diaphragm
Col. 31 - 35	KDIP(I)	Type number of flexible diaphragm or bent. Leave blank for rigid diaphragm (KODIA equals 1 or 2 above). See input sections 17 and 18 for type number descriptions.

11. LONGITUDINAL OUTPUT COORDINATE DATA (8F10.0) - 1 or more lines

Col. 1 - 80	XP(I)	X-coordinates of the transverse sections at which results are required. The total number of X-coordinates provided must equal NXP. Use additional lines if necessary.

12. LOAD CASE MULTIPLIERS FOR DEAD LOAD (8F10.0) - 1 or more lines

Col. 1 - 80	FLCM(I)	Factor by which plate element dead load is multiplied for load case I. This load is applied in the global Z-direction. Use additional lines if necessary.

13. FOLDED PLATE JOINT LOAD DATA (2I5,6F10.0) - NCONL lines

Joint loads may be applied over a portion or the entire length of the joint. More than one load may be applied on each joint, but each load requires a separate data line. Provide one line per joint load. No data required if NCONL = 0.

Col. 1 - 5	LJT(I)	Joint number
Col. 6 - 10	LCJ(I)	Load case number
Col. 11 - 20	CONHL(I)	Total horizontal (Y) force
Col. 21 - 30	CONVL(I)	Total vertical (Z) force
Col. 31 - 40	CONM(I)	Total (XX) moment
Col. 41 - 50	CONS(I)	Total longitudinal (X) force P (must be balanced by another CONS somewhere on the structure)
Col. 51 - 60	CONXI(I)	X-coordinate of the center of the load
Col. 61 - 70	CONDEL(I)	Length along the X-axis over which the distributed load is applied. For concentrated load, CONDEL = 0.

14. FOLDED PLATE SURFACE LOAD DATA (2I5,4F10.0) - NSURL lines

Surface loads may be applied over a portion or the entire length of the plate element. All loads are applied over the full width of the plate element. More than one load may be applied on each plate element, but each load requires a separate data line. Provide one line per plate surface load. No data required if NSURL = 0.

Col. 1 - 5	LEL(I)	Plate element number
Col. 6 - 10	LCL(I)	Load case number
Col. 11 - 20	SURHL(I)	Horizontal (Y) load intensity (force per unit vertically projected area or width of plate)
Col. 21 - 30	SURVL(I)	Vertical (Z) load intensity (force per unit horizontally projected area or width of plate)
Col. 31 - 40	SURXI(I)	X-coordinate of center of the distributed load
Col. 41 - 50	SURDEL(I)	Length along the X-axis over which the distributed load is applied.

For SURDEL = 0, loads are input as force per unit projected width of plate

15. SLAB PRESTRESSING TENDONS DATA SET

Slab tendons are input in groups with uniform spacing and identical stressing, profile, and cross section. This data set is required only if slab tendons are called for with parameter NST in input section 3. Provide one set of lines 15-a through 15-d for each slab tendon group. Slab tendon group numbers must be ascending consecutive integers starting with 1.

a. SLAB TENDON CONTROL, JACKING, and FRICTION DATA - 2 lines

First line (2I5,2F10.0,2I5)

Col. 1 - 5	I	Tendon group identification number
Col. 6 - 10	NTEND	Number of tendons in the group
Col. 11 - 20	SDIS	Uniform tendon spacing in the X-direction
Col. 21 - 30	SORD	X-coordinate of center of tendon group
Col. 31 - 35	NSPAN	Number of transverse spans for this tendon group
Col. 36 - 40	KDTP	Code for method of computing tendon forces = 0 for method B (without smoothing) = 1 for method A (with smoothing)

Second line (8F10.0)

Col. 1 - 10	FENDA	Jacking force at end A of each tendon 0 for end B jacking only
Col. 11 - 20	FENDB	Jacking force at end B of each tendon 0 for end A jacking only
Col. 21 - 30	CFC	Curvature friction coefficient
Col. 31 - 40	WFC	Wobble friction coefficient
Col. 41 - 50	AREA	Area of each tendon cross section
Col. 51 - 60	EMOD	Modulus of elasticity of tendon
Col. 61 - 70	SLIP	Anchorage slip distance
Col. 71 - 80	FRAT	Force ratio (final force / initial force)

Initial force is force at transfer, computed by the program based on jacking forces and losses due to friction and anchorage slip. Final force equals initial force minus the user's estimate of all other losses.

b. SLAB TENDON TRANSVERSE SPAN DEFINITION DATA - NSPAN * 2 lines

Slab tendon transverse spans are described by the folded plate system joints lying along their lengths. The first and last joint numbers defining an interior span must match the corresponding joint numbers in the neighboring spans.

First line - (3I5)

Col. 1 - 5	J	Transverse span number
Col. 6 - 10	NIJT(J)	Number of folded plate system joints lying within this span
Col. 11 - 15	KGM(J)	Geometry mode code for span or portion J 0 or blank for parametric geometry input 1 for direct tendon point coordinate input

Second line - (16I5) - use additional lines if necessary

Col. 1 - 80	IJTN(I)	Joint numbers defining the span, ordered from one end to the other

c. SLAB TENDON GEOMETRY DATA - 2 or more lines per slab tendon span

Geometry for span or portion J is input either parametrically or directly as specified with KGM(J). Each span or portion J must be described in increasing numerical order. If KGM(J) = 0 for the particular span or portion, follow the parametric geometry input specification. If KGM(J) = 1 for the particular span or portion, follow the direct tendon point coordinate input specification.

-- PARAMETRIC TENDON DATA - 2 lines per span

Use when geometry mode code KGM(J) = 0

First line - (I5,5X,5F10.0) - all values positive or zero

Col. 1 - 5	J	Span number
Col. 11 - 20	RLLT	Percentage of transverse span length from left end of span to left end of tendon
Col. 21 - 30	RLLI	Percentage of transverse span length from left end of transverse span to left tendon inflection point. If 0, no inflection point occurs left of the point of zero tendon slope (low point for a tendon in a vertical plate element).
Col. 31 - 40	RLLP	Percentage of transverse span length from left end of transverse span to point of zero tendon slope. If 0, there is no point of zero tendon slope.
Col. 41 - 50	RLRI	Percentage of transverse span length from right tendon inflection point to right end of transverse. If 0, no inflection point occurs right of the point of zero tendon slope.
Col. 51 - 60	RLRT	Percentage of transverse span length from right end of tendon to right end of span

Second line - (6F10.0)

Col. 1 - 10	YLT	Y-coordinate of left end of tendon
Col. 11 - 20	ZLT	Z-coordinate of left end of tendon
Col. 21 - 30	YLP	Y-coordinate of point of zero tendon slope
Col. 31 - 40	ZLP	Z-coordinate of point of zero tendon slope
Col. 41 - 50	YRT	Y-coordinate of right end of tendon
Col. 51 - 60	ZRT	Z-coordinate of right end of tendon

-- DIRECT INPUT TENDON DATA - 1 line / defining joint - (I5,2F10.0)

Use when geometry mode code KGM(J) = 1. Specify tendon point coordinates at each joint defining the span.

Col. 1 - 5	J	Tendon point number in this portion
Col. 6 - 15	YZ(1,J)	Y-coordinate of tendon point
Col. 16 - 25	YZ(2,J)	Z-coordinate of tendon point

d. SLAB TENDON LOAD CASE MULTIPLIERS (8F10.0) - 1 or more lines

Col. 1 - 80	FSLC(I)	Factor by which equivalent tendon loads are multiplied for load case I. Use additional lines if necessary.

16. PANEL PRESTRESSING TENDONS DATA SET - 1 set per panel tendon

Required only if panel prestressing tendons are called for with parameter NPT in input section 3. Provide one set of lines 16-a through 16-d for each panel tendon. Panel tendon numbers must be ascending consecutive integers starting with 1.

a. PANEL TENDON CONTROL, JACKING, and FRICTION DATA - 2 lines

First line (5I5)

Col. 1 - 5	I	Tendon identification number
Col. 6 - 10	NSPAN	Number of spans or portions for this tendon
Col. 11 - 15	LENDA	Span or portion number of tendon end A
Col. 16 - 20	LENDB	Span or portion number of tendon end B
Col. 21 - 25	KDTP	Code for method of computing tendon forces = 0 for method B (without smoothing) = 1 for method A (with smoothing)

Second line (8F10.0)

Col. 1 - 10	FENDA	Jacking force at end A (0 for end B jacking only)
Col. 11 - 20	FENDB	Jacking force at end B (0 for end A jacking only)
Col. 21 - 30	CFC	Curvature friction coefficient
Col. 31 - 40	WFC	Wobble friction coefficient
Col. 41 - 50	AREA	Area of tendon cross section
Col. 51 - 60	EMOD	Modulus of elasticity of tendon
Col. 61 - 70	SLIP	Anchorage slip distance at each jacking end
Col. 71 - 80	FRAT	Force ratio (final force / initial force)

Initial force is force at transfer, computed by the program based on jacking forces and losses due to friction and anchorage slip. Final force equals initial force minus the user's estimate of all other losses.

b. PANEL TENDON SPAN or PORTION CONTROL DATA (I5,2(F10.0,I5)) - NSPAN lines

Panel tendon geometry is specified separately for each span or portion of the tendon. Spans or portions need not correspond to the actual spans of the folded plate system. For computation of equivalent concentrated forces on the structure, each span or portion of the curved tendon is discretized as a number of straight segments. The patch ratio defines the length over which each equivalent force will be distributed onto the structure. The geometry of each tendon span or portion may be input either parametrically or by direct specification of the tendon coordinates at the tendon points (ends of the segments).

Col. 1 - 5	J	Span or portion identification number
Col. 6 - 15	PLH(J)	Length of span or portion J
Col. 16 - 20	NSG(J)	Number of segments in span or portion J Default number of segments = 10
Col. 21 - 30	DEL(J)	Patch ratio (patch length / segment length) Default patch ratio = 1.0
Col. 31 - 35	KGM(J)	Geometry mode code for span or portion J 0 or blank for parametric geometry input 1 for direct tendon point coordinate input

c. PANEL TENDON GEOMETRY DATA

Geometry for span or portion J is input either parametrically or directly as specified with KGM(J). Each span or portion J must be described, J = LENDA to LENDB, in increasing numerical order. If KGM(J) = 0 for the particular span or portion, follow the parametric geometry input specification. If KGM(J) = 1 for the particular span or portion, follow the direct tendon point coordinate input specification.

-- PARAMETRIC TENDON DATA - 2 lines per span

Use when geometry mode code KGM(J) = 0

First line - (I5,5X,5F10.0) - all values positive or zero

Col. 1 - 5	J	Span number
Col. 11 - 20	RLLT	Percentage of span length from left end of span to left end of tendon
Col. 21 - 30	RLLI	Percentage of span length from left end of span to left tendon inflection point. If 0, no inflection point occurs left of the point of zero tendon slope (low point for a tendon in a vertical plate element).
Col. 31 - 40	RLLP	Percentage of span length from left end of span to point of zero tendon slope. If 0, there is no point of zero tendon slope.
Col. 41 - 50	RLRI	Percentage of span length from right tendon inflection point to right end of span. If 0, no inflection point occurs right of the point of zero tendon slope.
Col. 51 - 60	RLRT	Percentage of span length from right end of tendon to right end of span

Second line - (6F10.0)

Col. 1 - 10	YLT	Y-coordinate of left end of tendon
Col. 11 - 20	ZLT	Z-coordinate of left end of tendon
Col. 21 - 30	YLP	Y-coordinate of point of zero tendon slope
Col. 31 - 40	ZLP	Z-coordinate of point of zero tendon slope
Col. 41 - 50	YRT	Y-coordinate of right end of tendon
Col. 51 - 60	ZRT	Z-coordinate of right end of tendon

-- DIRECT INPUT TENDON DATA - NSG(J)+1 lines / portion - (I5,2F10.0)

Use when geometry mode code KGM(J) = 1. Specify coordinates of each tendon point in increasing tendon point number order.

Col. 1 - 5	J	Tendon point number in this portion
Col. 6 - 15	XYZ(2,J)	Y-coordinate of tendon point
Col. 16 - 25	XYZ(3,J)	Z-coordinate of tendon point

d. PANEL TENDON LOAD CASE MULTIPLIERS (8F10.0) - 1 or more lines

Col. 1 - 80	FPLC(I)	Factor by which equivalent tendon loads are multiplied for load case I. Use additional lines if necessary.

17. FLEXIBLE SUPPORTING FRAME BENT DATA SET - NBT sets

Required only if flexible supporting frame bents are called for with parameter NBT in input section 2. Provide one set of the following data per type of supporting bent. Type numbers must be ascending consecutive integers starting with 1. Frame coordinates in this section refer to the local X-Y system of the planar frame bent. No gravity or external loads may be applied on any frame bent. Repeat this input section for each flexible supporting frame bent type.

a. BENT TYPE CONTROL DATA (6I5) - 1 line

Col. 1 - 5	I	Bent type number
Col. 6 - 10	NUMNP	Number of nodal points in bent
Col. 11 - 15	NUMEL	Number of frame elements in bent
Col. 16 - 20	NUMMAT	Number of frame material types in bent
Col. 21 - 25	NUMETP	Number of frame element section types in bent
Col. 26 - 30	NUMSPR	Number of elastic support types in bent

b. BENT NODAL POINT COORDINATE DATA (I5,2F10.0,I5) - 2 to NUMNP lines

Node coordinates may be input or generated in any sequence of node numbers. However, the coordinates of all nodes must be specified or generated. Coordinates refer to the local X-Y system of the bent.

Col. 1 - 5	J	Nodal point number
Col. 6 - 15	X(J)	X-coordinate of node
Col. 16 - 25	Y(J)	Y-coordinate of node
Col. 26 - 30	KGN	Node increment for automatic coordinate generation. Separate lines must be given for the first and last nodes, and the increment is entered with the data for the first node only. Use 0 for no generation.

c. ELASTIC SUPPORT DATA (I5,3F10.0) - NUMSPR lines

Col. 1 - 5	N	Identification number
Col. 6 - 15	SP(1,N)	X- component of spring stiffness
Col. 16 - 25	SP(2,N)	Y- component of spring stiffness
Col. 26 - 35	SP(3,N)	ZZ- rotational spring stiffness

d. NODAL BOUNDARY CONDITION DATA (9I5) - 1 to NUMNP lines

Node boundary conditions may be input or generated in any sequence of node numbers. However, the boundary conditions of all nodes must be specified or generated. Coordinates refer to the local X-Y system of the bent.

Col. 1 - 5	NFST	Node number of the first node in a series of nodes with identical boundary condition specifications
Col. 6 - 10	NLST	Node number of the last node in the series
Col. 11 - 15	KN	Node increment for automatic generation between first and last node in a series
Col. 16 - 20	ID(1,N)	Index for horizontal (X) boundary condition
Col. 21 - 25	ID(2,N)	Index for vertical (Y) boundary condition
Col. 26 - 30	ID(3,N)	Index for rotation (ZZ) boundary condition

In Cols. 16 - 30 the indices take the following values:
1 for prescribed zero displacement
0 otherwise

Col. 31 - 35	NPSTP(N)	Elastic support identification number. (Leave blank if no elastic support).
Col. 36 - 40	NFP(N)	Corresponding joint number in the folded plate system. (Leave blank if not connected to folded plate system at this node).
Col. 41 - 45	KNFP	Folded plate joint number generation increment.

e. FRAME ELEMENT MATERIAL PROPERTY DATA (I5,2F10.0) - NUMMAT lines

Col. 1 - 5	I	Material identification number
Col. 6 - 15	EMOD(I)	Young's modulus of material
Col. 16 - 25	PRAT(I)	Poisson's ratio of material

f. FRAME ELEMENT SECTION PROPERTY DATA (I5,3F10.0) - NUMETP lines

Col. 1 - 5	I	Section identification number
Col. 6 - 15	SECP(1,I)	Axial area
Col. 16 - 25	SECP(2,I)	Shear area (leave blank to neglect shear deformation)
Col. 26 - 35	SECP(3,I)	Moment of inertia

g. ELEMENT DATA (5I5,4X,I6) - NUMEL lines

Col. 1 - 5	L	Identification number
Col. 6 - 10	NODE(1,L)	Element node I
Col. 11 - 15	NODE(2,L)	Element node J
Col. 16 - 20	NMAT(L)	Material identification number
Col. 21 - 25	NPRP(L)	Section property identification number
Col. 30 - 35	MERC(L)	Six-digit element end release code

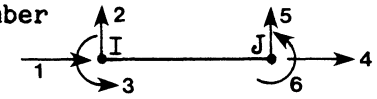

In Cols. 30 - 35, the codes take the following values:
1 for displacement independent of node
0 for displacement dependent on node
Digits 1 to 6 of the code correspond to the element degrees of freedom as shown.

18. FLEXIBLE MOVABLE DIAPHRAGM DATA SET - NFMD sets

Required only if flexible movable diaphragms are called for with parameter NFMD in input section 2. Provide one set of the following data per type of flexible movable diaphragm. Type numbers must be ascending consecutive integers starting with 1. Flexible diaphragms are modelled as straight prismatic beams parallel to the global Y- axis. No gravity or external loads may be applied on any flexible movable diaphragm. Repeat this input section for each flexible movable diaphragm type.

a. DIAPHRAGM TYPE CONTROL DATA (2I5) - 1 line

Col. 1 - 5	Diaphragm type number
Col. 6 - 10	Input option code, for form of next line 1 for option 1 2 for option 2

b. DIAPHRAGM PROPERTY DATA - use either option 1 or 2

Option 1: Rectangular cross section located at mean Z- coordinate of folded plate system (4F10.0) - 1 line

Col. 1 - 10	DITH	Diaphragm thickness in X- direction
Col. 11 - 20	DIDP	Diaphragm depth (centroidal axis assumed at mid-depth)
Col. 21 - 30	DIFE	Modulus of elasticity of diaphragm
Col. 31 - 40	DIFN	Poisson's ratio of diaphragm

Option 2: Arbitrary cross section (6F10.0) - 1 line

Col. 1 - 10	DIFI	Moment of inertia of diaphragm cross section
Col. 11 - 20	DIFA	Area of diaphragm cross section
Col. 21 - 30	DIFS	Shear area of diaphragm cross section (leave blank to neglect shear deformation)
Col. 31 - 40	DIFZ	Z- coordinate of diaphragm centroidal axis
Col. 41 - 50	DIFE	Modulus of elasticity of diaphragm
Col. 51 - 60	DIFN	Poisson's ratio of diaphragm

APPENDIX C: CURDI4 USER'S GUIDE

CURDI4: A COMPUTER PROGRAM FOR THE ELASTIC ANALYSIS OF CIRCULARLY CURVED, PRISMATIC, PRESTRESSED CELLULAR FOLDED PLATE STRUCTURES WITH OPTIONAL INTERMEDIATE DIAPHRAGMS AND SUPPORTS

Programmed at the Department of Civil Engineering
University of California, Berkeley

Faculty Investigator: Professor A. C. Scordelis

Authors: M. A. Ketchum
P. P. van der Walt

Date: March, 1985

Considerable effort has gone into the development and testing of this program, which can analyze a particular class of structure. It is based on the conditions and assumptions described in this report. The program should be used only under these conditions and assumptions and the output must be interpreted appropriately by a qualified person.

Although the program has been extensively tested, no warranty is made regarding the accuracy and reliability of the program, and the authors assume no responsibility in this respect.

CURDI4 INPUT DATA FORMAT

1. **TITLE** (20A4) - 1 line

Col. 1 - 80	TITLE	Title of the problem to be printed with output.

2. **STRUCTURE CONTROL DATA** (6I5) - 1 line

Col. 1 - 5	NJT	Number of joints in the finite strip system.
Col. 6 - 10	NEL	Number of strip elements.
Col. 11 - 15	NET	Number of finite strip material sets.
Col. 16 - 20	NDIAPH	Total number of diaphragms and frame bents.
Col. 21 - 25	NBT	Number of flexible supporting frame bent types.
Col. 26 - 30	NFMD	Number of flexible movable diaphragm types.

3. **ANALYSIS OPTIONS** (4I5) - 1 line

Col. 1 - 5	ICR	Longitudinal coordinate option. 0 for input/output in angular degrees. +1 for input/output in arc lengths.
Col. 6 - 10	ISB	Straight bridge option. 0 for curved bridge using curved finite strip theory, ICR can be input as either 0 or +1. +1 for straight bridge using straight finite strip theory, ICR is automatically set to +1 by CURDI4.
Col. 11 - 15	IMA	Isotropy option. -1 for inputting constitutive relations directly. 0 for isotropic material properties, plate bending and membrane material properties identical. +1 for orthotropic material properties, plate bending and membrane material properties can be different.
Col. 16 - 20	IAX	Axisymmetry option. 0 for non-axisymmetrical cases. +1 for axisymmetrical shell, loads axisymmetrical also.

4. **LOAD AND PRESTRESSING CONTROL DATA** (5I5) - 1 line

Col. 1 - 5	NLCAS	Number of load cases.
Col. 6 - 10	NCONL	Number of joint loads.
Col. 11 - 15	NSURL	Number of finite strip surface loads.
Col. 16 - 20	NPT	Number of panel tendons.
Col. 21 - 25	NST	Number of slab tendon groups.

5. **ANALYSIS CONTROL DATA** (6I5) - 1 line

Col. 1 - 5	NXP	Number of cross-sections at which output of joint displacements and element stresses and displacements, and integrated section shears, moments and axial forces are required.
Col. 6 - 10	NCHECK	Check on use of odd and even harmonics. +1 to use odd series only (symmetric). 0 to include all series. -1 to use even series only (anti-symmetric).
Col. 11 - 15	MHARM	Maximum term number of Fourier series to be used in the harmonic analysis.
Col. 16 - 20	NBOX	Number of girders defined in the finite strip system for longitudinal girder shear, moment and axial force integration.
Col. 21 - 25	KFRAME	Bent internal force evaluation option. 0 to skip bent internal force evaluation. +1 to perform bent internal force evaluation.
Col. 26 - 30	MODE	Data check mode option. 0 for execution mode. +1 for data check mode.

6. **GEOMETRY CONTROL DATA** (2F10.0) - 1 line

Col. 1 - 10	TETAO	If ISB = 0 and ICR = 0:	Total angle subtended for circularly curved bridge in degrees.
		If ISB = 0 and ICR = +1:	Total span of circularly curved bridge measured along reference line.
		If ISB = +1:	Total span for straight bridge.
Col. 11 - 20	R	If ISB = 0 and ICR = 0:	Horizontal radius to reference line for circularly curved bridge.
		If ISB = 0 and ICR = +1:	Horizontal radius to reference line for circularly curved bridge.
		If ISB =+ 1:	Leave blank.

7. **FINITE STRIP JOINT COORDINATE DATA** (I5, 2F10.0, I5) - NJT lines for no joint generation.

Joint coordinates may be input or generated in any sequence of joint

numbers. However, the coordinates of <u>all</u> joints must be specified or generated.

Col. 1 - 5	N	Joint number.
Col. 6 - 15	Y(N)	Y- (horizontal) coordinate of joint N.
Col. 16 - 25	Z(N)	Z- (vertical) coordinate of joint N.
Col. 26 - 30	KN	Joint increment for automatic coordinate generation. Separate lines must be given for the first and last joints, and the increment is entered with the data for the first joint only. Leave blank for no generation.

8. **<u>FINITE STRIP JOINT BOUNDARY CONDITION DATA</u>** (10I5) - NJT lines for no boundary condition generation.

Joint boundary conditions may be input or generated in any sequence of joint numbers. However, the boundary conditions of <u>all</u> joints must be specified or generated.

Col. 1 - 5	NFST	Joint number of the first joint in a series of joints with identical boundary condition specifications.
Col. 6 - 10	NLST	Joint number of the last joint in the series.
Col. 11 - 15	KN	Joint increment for automatic generation between first and last joint in a series.
Col. 16 - 20	II(1)	Index for horizontal (Y) displacement.
Col. 21 - 25	II(2)	Index for vertical (Z) displacement.
Col. 26 - 30	II(3)	Index for (XX) rotation.
Col. 31 - 35	II(4)	Index for longitudinal (X) displacement.
	In Cols. 16 - 35 the indices take the following values:	
		0 for non-zero displacement evaluated by CURDI4.
		+1 for prescribed zero displacement.
Col. 36 - 40	IJ(1)	Index for horizontal (Y) restraint from intermediate diaphragms or bents.
Col. 41 - 45	IJ(2)	Index for vertical (Z) restraint from intermediate diaphragms or bents.
Col. 46 - 50	IJ(3)	Index for rotational (XX) restraint from intermediate diaphragms or bents.
	In Cols. 36 - 50 the indices take the following values:	
		0 to consider restraint from diaphragms or bents.
		+1 for no restraint from diaphragms or bents.

9. **<u>FINITE STRIP MATERIAL SET DATA</u>**

Finite strip material sets may be input in any desired sequence. Material sets must all be of the same type, e.g. isotropic or polar-orthotropic as specified by the IMA control parameter. A total number of NET material sets must be specified. CURDI4 assumes that the finite strip

weight density acts in the positive global Z - direction defined in Section 7.

If IMA = -1: (I5, 4F10.0/5X,5F10.0) - 2 lines per material set, 2 x NET lines total. Input polar-orthotropic constitutive material laws directly.

First Line (I5, 4F10.0)

Col. 1 - 5	I	Material set number.	
Col. 6 - 15	THM(I)	D_{11}	membrane properties
Col. 16 - 25	THB(I)	D_{12}	
Col. 26 - 35	ETM(I)	D_{22}	
Col. 36 - 45	ETB(I)	D_{33}	

Second Line (5X, 5F10.0)

Col. 6 - 15	ESM(I)	D_{44}	bending properties
Col. 16 - 25	ESB(I)	D_{45}	
Col. 26 - 35	GM(I)	D_{55}	
Col. 36 - 45	GB(I)	D_{66}	
Col. 46 - 55	WGT(I)	Unit weight density.	

If IMA = 0: (I5, 3F10.0) - 1 line per material set, NET lines total. Input isotropic material properties, membrane and plate bending constants identical.

Col. 1 - 5	I	Material set number.
Col. 6 - 15	ESB(I)	Modulus of elasticity.
Col. 16 - 25	PRB(I)	Poisson's ratio.
Col. 26 - 35	WGT(I)	Unit weight density.

If IMA = +1: (I5, 5F10.0/5X, 5F10.0) - 2 lines per material set, 2 x NET lines total. Input polar orthotropic material properties, membrane and plate bending constants separately.

First Line: Membrane Characteristics (I5, 5F10.0)

Col. 1 - 5	I	Material set number.
Col. 6 - 15	THM(I)	Effective thickness.
Col. 16 - 25	ETM(I)	Modulus of elasticity in longitudinal direction.
Col. 26 - 35	ESM(I)	Modulus of elasticity in transverse direction.
Col. 36 - 45	GM(I)	Shear modulus.
Col. 46 - 55	PRM(I)	Poisson's ratio.

Second Line: Bending Characteristics (5X, 6F10.0)

Col. 6 - 15	THB(I)	Effective thickness.

Col. 16 - 25	ETB(I)	Modulus of elasticity in longitudinal direction.
Col. 26 - 35	ESB(I)	Modulus of elasticity in transverse direction.
Col. 36 - 45	GB(I)	Shear modulus.
Col. 46 - 55	PRB(I)	Poisson's ratio.
Col. 56 - 65	WGT(I)	Unit weight density.

10. FINITE STRIP ELEMENT DATA

The location and type of each strip element, and girder numbers for stress integration are specified here. Finite strip stresses and moments are integrated to find girder moments about the Y axis, and forces in the X and Z - directions. Each strip element can belong to one or two girders. Girder members must be smaller or equal than NBOX in Section 5. Stress integration is performed only if called for with a non-zero value of NBOX. Integration accuracy depends on the number of transverse sections (NSEC) specified. NSEC = 2 is a recommended minimum value. If the stresses to be integrated are highly nonlinear between element joints, more transverse sections might be necessary. Provide one line per element. Elements can be input in any desired sequence. However, all finite strip elements must be specified.

		If IMA = -1 or IMA = +1: (7I5, F10.0) - NEL lines total.
Col. 1 - 5	I	Finite strip element number.
Col. 6 - 10	NPI(I)	Joint I of element I.
Col. 11 - 15	NPJ(I)	Joint J of element I.
Col. 16 - 20	KPL(I)	Material set number to which element I belongs.
Col. 21 - 25	NSEC(I)	Number of element transverse subdivisions for output of internal forces and displacements, e.g. use 4 for output at quarter points. If NSEC(I) = 0, no internal forces or displacements will be output for element I.
Col. 26 - 30	NGL(1,I)	First girder number to which this element belongs. If it belongs to two girders, list that which is nearest to joint I first.
Col. 31 - 35	NGL(2,I)	Second girder number to which this element belongs. Use zero if no second girder.
Col. 36 - 45	XDIV(I)	Horizontal (Y) distance from the dividing point to joint I if the element belongs to two girders. The sign of the Y - distance corresponds to the gobal Y-direction defined in Section 7. Leave blank if NGL(2,I) = 0.
		If IMA = 0: (3I5, F10.0, 4I5, F10.0) - NEL lines total.
Col. 1 - 5	I	Finite strip element number.
Col. 6 - 10	NPI(I)	Joint I of element I.
Col. 11 - 15	NPJ(I)	Joint J of element I.

Col. 16 - 25	THM(I)	Thickness of element I, membrane and plate thicknesses identical.
Col. 26 - 30	KPL(I)	Material set number to which element I belongs.
Col. 31 - 35	NSEC(I)	Number of element transverse subdivisions for output of internal forces and displacements, e.g. use 4 for output at quarter points. If NSEC(I) = 0, no internal forces or displacements will be output for element I.
Col. 36 - 40	NGL(1,I)	First girder number to which this element belongs. If it belongs to two girders, list that which is nearest to joint I first.
Col. 41 - 45	NGL(2,I)	Second girder number to which this element belongs. Use zero if no second girder.
Col. 46 - 55	XDIV(I)	Horizontal (Y) distance from the dividing point to joint I if the element belongs to two girders. The sign of the Y - distance corresponds to the global Y - direction defined in Section 7. Leave blank if NGL(2,I) = 0.

11. **FINITE STRIP ELEMENT OUTPUT CONTROL DATA** (12I5) - 1 line.

Finite strip element results may include 12 components at each location in each element. Output of some or all of these components may be suppressed by flagging them here. These control codes apply to all elements.

Col. 1 - 5	LSTRES(1)	N_x	Output code (longitudinal membrane force).
Col. 6 - 10	LSTRES(2)	N_y	Output code (transverse membrane force.
Col. 11 - 15	LSTRES(3)	N_{xy}	Output code (membrane shear force).
Col. 16 - 20	LSTRES(4)	S_x	Output code (longitudinal membrane stress).
Col. 21 - 25	LSTRES(5)	S_y	Output code (transverse membrane stress).
Col. 26 - 30	LSTRES(6)	S_{xy}	Output code (membrane shear stress).
Col. 31 - 35	LSTRES(7)	M_x	Output code (moment on X - face).
Col. 36 - 40	LSTRES(8)	M_y	Output code (moment on Y - face).
Col. 41 - 45	LSTRES(9)	M_{xy}	Output code (twisting moment).
Col. 46 - 50	LSTRES(10)	U	Output code (longitudinal displacement).
Col. 51 - 55	LSTRES(11)	V	Output code (transverse displacement).
Col. 56 - 60	LSTRES(12)	W	Output code (normal displacement).

Each output code may take one of the following values:
0 to skip output of the indicated results component.
+1 to include output of the indicated results component.

12. **DIAPHRAGM/BENT INTERACTION DATA** (I5, 2F10.0, 2I5) - NDIAPH lines

Provide one line per intermediate diaphragm or frame bent, omit if NDIAPH = 0

Col. 1 - 5	I	Diaphragm or bent number.
Col. 6 - 15	DIAPHX(I)	If ISB = 0 and ICR = 0: X - coordinate of diaphragm location measured in angular degrees.
		If ISB = 0 and ICR = +1: X - coordinate of diaphragm location measured along reference line.
		If ISB = +1: X - coordinate of diaphragm location for straight bridge.
Col. 16 - 25	DIADEL(I)	If ISB = 0 and ICR = 0: Interaction thickness of diaphragm measured in angular degrees.
		If ISB = 0 and ICR = +1: Interaction thickness of diaphragm measured along reference line.
		If ISB = +1: Interaction thickness of diaphragm for straight bridge.
Col. 26 - 30	KODIA	Diaphragm classification code. 1 for externally supported rigid diaphragm. 2 for movable rigid diaphragm. 3 for flexible supporting frame bent. 4 for flexible movable diaphragm.
Col. 31 - 35	KDIP	Type number of flexible diaphragm or bent. Leave blank for rigid diaphragm (KODIA equals 1 or 2 above). See input sections 20 and 21 for type number descriptions.

13. **LONGITUDINAL OUTPUT COORDINATE DATA** (8F10.0) - 1 or more lines

Col. 1 - 80	XPT(I)	X - coordinates of the transverse sections at which results are required. Use additional lines if necessary. Total number of X - coordinates must be equal to NXP.
		If ISB = 0 and ICR = 0: X - coordinates measured in angular degrees.
		If ISB = 0 and ICR = +1: X - coordinates measured along reference line.

	If ISB = +1:	X - coordinates for straight bridge measured as distance along span.

14. **SCALE FACTOR FOR MOMENT INTEGRATION** (F10.0) - 1 line

Col. 1 - 10	XPT(NXP+1)	Scale factor by which computed girder moments are multiplied for output.

15. **LOAD CASE MULTIPLIERS FOR DEAD LOAD** (8F10.0) - 1 or more lines

Col. 1 - 80	FLCM(I)	Factor by which finite strip dead load is multiplied for load case I. Input in sequential order. Total number of factors must be equal to NLCAS. Use additional lines if necessary.

16. **FINITE STRIP JOINT LOAD DATA** (2I5, 6F10.0) - NCONL lines

Joint loads may be applied over a portion or entire length of the joint. More than one load may be applied on each joint, but each load requires a separate data line. Provide one line per joint load. No data required if NCONL = 0. Positive coordinate directions are defined in input Section 7.

Col. 1 - 5	LJT(I)	Joint number.
Col. 6 - 10	LCJ(I)	Load case number.
Col. 11 - 20	CONHL(I)	Total horizontal (Y) force.
Col. 21 - 30	CONVL(I)	Total vertical (Z) force.
Col. 31 - 40	CONM(I)	Total (XX) moment.
Col. 41 - 50	CONS(I)	Total longitudinal (X) force P (must be balanced by another CONS somewhere on the structure).
Col. 51 - 60	CONXI(I)	If ISB = 0 and ICR = 0: X - coordinate of center of load measured in angular degrees.
		If ISB = 0 and ICR = +1: X - coordinate of center of load measured along reference line.
		If ISB = +1: X - coordinate of center of load for straight bridge.
Col. 61 - 70	CONDEL(I)	Length along the X - axis over which the distributed load is applied. For concentrated load, CONDEL = 0.
		If ISB = 0 and ICR = 0: Input in angular degrees.

If ISB = 0 and ICR = +1:	Take length along reference line.
If ISB = +1:	Take length along X - axis for straight bridge.

17. **FINITE STRIP SURFACE LOAD DATA** (2I5, 6F10.0) - NSURL lines

Surface loads may be applied over a portion or the entire length of the finite strip element. All loads are applied over the full width of the strip element. More than one load may be applied on each strip element, but each load requires a separate data line. Provide one line per strip surface load. No data required if NSURL = 0. Positive coordinate directions are taken as in input Section 7.

Col. 1 - 5	LEL(I)	Element number.
Col. 6 - 10	LCL(I)	Load case number.
Col. 11 - 20	SURHL(I,1)	Horizontal (Y) load intensity (force per unit vertically projected area or width of finite strip) at joint I of element I.
Col. 21 - 30	SURHL(I,2)	Horizontal (Y) load intensity (force per unit vertically projected area or width of finite strip) at joint J of element I.
Col. 31 - 40	SURVL(I,1)	Vertical (Z) load intensity (force per unit horizontally projected area or width of finite strip) at joint I of element I.
Col. 41 - 50	SURVL(I,2)	Vertical (Z) load intensity (force per unit horizontally projected area or width of finite strip) at joint J of element I.
Col. 51 - 60	SURXI(I)	If ISB = 0 and ICR = 0: X - coordinate of the center of the load measured in angular degrees.
		If ISB = 0 and ICR =+1: X - coordinate of the center of the load measured along the reference line.
		If ISB = +1: X - coordinate of the center of the load for straight bridge.
Col. 61 - 70	SURDEL(I)	Length along the X - axis over which the distributed load is applied. For concentrated load, SURDEL(I) = 0.
		If ISB = 0 and ICR = 0: Input in angular degrees.
		If ISB = 0 and ICR =+1: Take length along reference line.
		If ISB = +1: Take length along X - axis for straight bridge.

For SURDEL(I) = 0, loads are input as force per unit projected width of the relevant strip.

18. SLAB PRESTRESSING TENDONS DATA SET

Slab tendons are input in groups with uniform spacing and identical stressing, profile, and cross-sectional area. This data set is required only if slab prestressing tendons are called for with parameter NST in input section 4. Provide one set of lines 18-a through 18-d for each slab tendon group. Slab tendon group numbers must be ascending consecutive integers starting with 1.

a. SLAB TENDON CONTROL, JACKING, and FRICTION DATA - 2 lines

First Line (2I5, 2F10.0, 2I5)

Col. 1 - 5	I	Tendon group identification number.
Col. 6 - 10	NTEND	Number of tendons in the group.
Col. 11 - 20	XDIS	Uniform tendon spacing in the X - direction. If ISB = 0 and ICR = 0: Measured in angular degrees. If ISB = 0 and ICR = +1: Measured along reference line. If ISB = +1: Spacing for straight bridge.
Col. 21 - 30	XORD	X - coordinate of center of tendon group. If ISB = 0 and ICR = 0: Measured in angular degrees. If ISB = 0 and ICR = +1: Measured along reference line. If ISB = +1: X - coordinate for straight bridge.
Col. 31 - 35	NSPAN	Number of transverse spans for this tendon group.
Col. 36 - 40	KDTP	Code for method of computing tendon forces. 0 for method B (without smoothing). +1 for method A (with smoothing).

Second Line (8F10.0)

Col. 1 - 10	FENDA	Jacking force at end A of each tendon. 0 for end B jacking only.
Col. 11 - 20	FENDB	Jacking force at end B of each tendon. 0 for end A jacking only.
Col. 21 - 30	CFC	Curvature friction coefficient.
Col. 31 - 40	WFC	Wobble friction coefficient.
Col. 41 - 50	AREA	Area of each tendon cross section.
Col. 51 - 60	EMOD	Modulus of elasticity of tendon.
Col. 61 - 70	SLIP	Anchorage slip distance.
Col. 71 - 80	FRAT	Force ratio (final force/initial force).

Initial force is force at transfer, computed by the program based on jacking forces and losses due to

friction and anchorage slip. Final force equals initial force minus the user's estimate of all other losses.

b. SLAB TENDON TRANSVERSE SPAN DEFINITION DATA - (NSPAN) x 2 lines

Slab tendon transverse spans are described by the finite strip system joints lying along their lengths. The first and last joint numbers defining an interior span must match the corresponding joint numbers in the neighboring spans.

First Line (3I5)

Col. 1 - 5	J	Transverse span number.
Col. 6 - 10	NIJT(J)	Number of finite strip system joints lying within this span.
Col. 11 - 15	KGM(J)	Geometry mode code for span or portion J. 0 or blank for parametric geometry input. +1 for direct tendon point coordinate input.

Second Line (16I5) Use additional lines if necessary.

Col. 1 - 80	IJTN(I)	Joint numbers defining the span, ordered from one end to the other.

c. SLAB TENDON GEOMETRY DATA - 2 or more lines per slab tendon span

Geometry for span or portion J is input either parametrically or directly as specified with KGM(J). Each span or portion J must be described in increasing numerical order. If KGM(J) = 0 for the particular span or portion, follow the parametric geometry input specification. If KGM(J) = 1 for the particular span or portion, follow the direct tendon point coordinate input specification.

PARAMETRIC TENDON DATA - 2 lines per span

Use when geometry mode code KGM(J) = 0

First Line (I5, 5X, 5F10.0) - all values positive or zero

Col. 1 - 5	J	Span number
Col. 11 - 20	RLLT	Percentage of transverse span length from left end of span to left end of tendon.
Col. 21 - 30	RLLI	Percentage of transverse span length from left end of transverse span to left tendon inflection point. If 0, no inflection point occurs left of the point of zero tendon slope (low point for a tendon in a vertical plate element).
Col. 31 - 40	RLLP	Percentage of transverse span length from left end of transverse span to point of zero

		tendon slope. If 0, there is no point of zero tendon slope.
Col. 41 - 50	RLRI	Percentage of transverse span length from right tendon inflection point to right end of transverse span. If 0, no inflection point occurs right of the point of zero tendon slope.
Col. 51 - 60	RLRT	Percentage of transverse span length from right end of tendon to right end of span.

Second Line (6F10.0)

Col. 1 - 10	YLT	Y - coordinate of left end of tendon.
Col. 11 - 20	ZLT	Z - coordinate of left end of tendon.
Col. 21 - 30	YLP	Y - coordinate of point of zero tendon slope.
Col. 31 - 40	ZLP	Z - coordinate of point of zero tendon slope.
Col. 41 - 50	YRT	Y - coordinate of right end of tendon.
Col. 51 - 60	ZRT	Z - coordinate of right end of tendon.

DIRECT INPUT TENDON DATA - 1 line/defining point - (I5, 2F10.0)

Use when geometry mode code KGM(J) = 1. Specify tendon point coordinates at each joint defining the span.

Col. 1 - 5	J	Tendon point number in this portion.
Col. 6 - 15	YZ(1,J)	Y - coordinate of tendon point.
Col. 16 - 25	YZ(2,J)	Z - coordinate of tendon point.

d. SLAB TENDON LOAD CASE MULTIPLIERS (8F10.0) - 1 or more lines

Col. 1 - 80	FSLC(I)	Factor by which equivalent tendon loads are multiplied for load case I. Use additional lines if necessary.

19. **PANEL PRESTRESSING TENDONS DATA SET** - 1 set per panel tendon

Required only if panel prestressing tendons are called for with parameter NPT in input section 4. Provide one set of lines 19-a through 19-d for each panel tendon. Panel tendon numbers must be ascending consecutive integers starting with 1.

a. PANEL TENDON CONTROL, JACKING, and FRICTION DATA - 2 lines

First Line (5I5)

Col. 1 - 5	I	Tendon identification number.
Col. 6 - 10	NSPAN	Number of spans or portions for this tendon.
Col. 11 - 15	LENDA	Span or portion number of tendon end A.
Col. 16 - 20	LENDB	Span or portion number of tendon end B.
Col. 21 - 25	KDTP	Code for method of computing tendon force. = 0 for method B (without smoothing).

=+1 for method A (with smoothing).

Second Line (8F10.0)

Col. 1 - 10	FENDA	Jacking force at end A (0 for end B jacking only).
Col. 11 - 20	FENDB	Jacking force at end B (0 for end A jacking only).
Col. 21 - 30	CFC	Curvature friction coefficient.
Col. 31 - 40	WFC	Wobble friction coefficient.
Col. 41 - 50	AREA	Area of tendon cross-section.
Col. 51 - 60	EMOD	Modulus of elasticity of tendon.
Col. 61 - 70	SLIP	Anchorage slip distance at each jacking end.
Col. 71 - 80	FRAT	Force ratio (final force / initial force). Initial force is force at transfer, computed by the program based on jacking forces and losses due to friction and anchorage slip. Final force equals initial force minus the user's estimate of all other losses.

b. PANEL TENDON SPAN or PORTION CONTROL DATA (I5, 2(F10.0,I5)) - NSPAN lines

Panel tendon geometry is specified separately for each span or portion of the tendon. Spans or portions need not correspond to the actual spans of the finite strip system. For computation of equivalent concentrated forces on the structure, each span or portion of the curved tendon is discretized as a number of straight segments. The patch ratio defines the length over which each equivalent force will be distributed onto the structure. The geometry of each tendon span or portion may be input either parametrically or by direct specification of the tendon coordinates at the tendon points (ends of the segments).

Col. 1 - 5	J	Span or portion identification number.
Col. 6 - 15	PLH(J)	Length of span or portion J. If ISB = 0 and ICR = 0: Input in angular degrees. If ISB = 0 and ICR = +1: Measured along reference line. If ISB = +1: Length for straight bridge.
Col. 16 - 20	NSG(J)	Number of segments in span or portion J. Default number of segments = 10.
Col. 21 - 30	DEL(J)	Patch ratio (patch length / segment length). Default patch ratio = 1.0.
Col. 30 - 35	KGM(J)	Geometry mode code for span or portion J. 0 or blank for parametric geometry input. +1 for direct tendon point coordinate input.

c. PANEL TENDON GEOMETRY DATA

Geometry for span or portion J is input either parametricaly or directly as specified with KGM(J). Each span or portion J must be described, J = LENDA to LENDB, in increasing numerical order. If KGM(J) = 0 for the particular span or portion, follow the parametric geometry input specification. If KGM(J) = 1 for the particular span or portion, follow the direct tendon point coordinate input specification.

PARAMETRIC TENDON DATA - 2 lines per span

Use when geometry mode code KGM(J) = 0

First Line - (I5, 5X, 5F10.0) - all values positive or zero

Col. 1 - 5	J	Span number.
Col. 11 - 20	RLLT	Percentage of span length from left end of span to left end of tendon.
Col. 21 - 30	RLLI	Percentage of span length from left end of span to left tendon inflection point. If 0, no inflection point occurs left of the point of zero tendon slope (low point for a tendon in a vertical strip element).
Col. 31 - 40	RLLP	Percentage of span length from left end of span to point of zero tendon slope. If 0, there is no point of zero tendon slope.
Col. 41 - 50	RLRI	Percentage of span length from right tendon inflection point to right end of span. If 0, no inflection point occurs right of the point of zero tendon slope.
Col. 51 - 60	RLRT	Percentage of span length from right end of tendon to right end of span.

Second Line - (6F10.0)

Col. 1 - 10	YLT	Y - coordinate of left end of tendon.
Col. 11 - 20	ZLT	Z - coordinate of left end of tendon.
Col. 21 - 30	YLP	Y - coordinate of point of zero tendon slope.
Col. 31 - 40	ZLP	Z - coordinate of point of zero tendon slope.
Col. 41 - 50	YRT	Y - coordinate of right end of tendon.
Col. 51 - 60	ZRT	Z - coordinate of right end of tendon.

DIRECT INPUT TENDON DATA- NSG(J)+1 lines/portion - (I5, 2F10.0)

Use when geometry mode code KGM(J) = +1. Specify coordinates of each tendon point in increasing tendon point number order.

Col. 1 - 5	J	Tendon point number in this portion.
Col. 6 - 15	XYZ(2,J)	Y - coordinate of tendon point.
Col. 16 - 25	XYZ(3,J)	Z - coordinate of tendon point.

d. PANEL TENDON LOAD CASE MULTIPLIERS (8F10.0) - 1 or more lines

Col. 1 - 80	FPLC(I)	Factor by which equivalent tendon loads are multiplied for load case I. Use additional lines if necessary.

20. **FLEXIBLE SUPPORTING FRAME BENT DATA SET** - NBT sets

Required only if flexible supporting frame bents are called for with parameter NBT in input section 2. Provide one set of the following data per type of supporting bent. Type numbers must be ascending consecutive integers starting with +1. Frame coordinates in this section refer to the local X-Y system of the planar frame bent. No gravity or external loads may be applied on any frame bent. Repeat this input section for each flexible supporting frame bent type.

a. BENT TYPE CONTROL DATA (6I5) - 1 line

Col. 1 - 5	I	Bent type number.
Col. 6 - 10	NUMNP	Number of nodal points in bent.
Col. 11 - 15	NUMEL	Number of frame elements in bent.
Col. 16 - 20	NUMMAT	Number of frame material types in bent.
Col. 21 - 25	NUMETP	Number of frame element section types in bent.
Col. 26 - 30	NUMSPR	Number of elastic support types in bent.

b. BENT NODAL POINT COORDINATE DATA (I5, 2F10.0, I5) - 2 to NUMNP lines

Node coordinates may be input or generated in any sequence of node numbers. However, the coordinates of <u>all</u> nodes must be specified or generated. Coordinates refer to the local X-Y system of the bent.

Col. 1 - 5	J	Nodal point number.
Col. 6 - 15	X(J)	X - coordinate of node.
Col. 16 - 25	Y(J)	Y - coordinate of node.
Col. 26 - 30	KGN	Node increment for automatic coordinate generation. Separate lines must be given for the first and last nodes, and the increment is entered with the data for the first node only. Use 0 for no generation.

c. ELASTIC SUPPORT DATA (I5, 3F10.0) - NUMSPR lines

Col. 1 - 5	N	Identification number.
Col. 6 - 15	SP(1,N)	X - component of spring stiffness.
Col. 16 - 25	SP(2,N)	Y - component of spring stiffness.
Col. 26 - 35	SP(3,N)	ZZ - rotational spring stiffness.

d. NODAL BOUNDARY CONDITION DATA (9I5) - 1 to NUMNP lines

Node boundary conditions may be input or generated in any sequence of

node numbers. However, the boundary conditions of <u>all</u> nodes must be specified or generated. Coordinates refer to the local X - Y system of the bent.

Col. 1 - 5	NFST	Node number of the first node in a series of nodes with identical boundary condition specifications.
Col. 6 - 10	NLST	Node number of the last node in the series.
Col. 11 - 15	KN	Node increment for automatic generation between first and last node in a series.
Col. 16 - 20	ID(1,N)	Index for horizontal (X) boundary condition.
Col. 21 - 25	ID(2,N)	Index for vertical (Y) boundary condition.
Col. 26 - 30	ID(3,N)	Index for rotation (ZZ) boundary condition.
		In Cols. 16 - 30 the indices take the following values: +1 for prescribed zero displacement. 0 otherwise.
Col. 31 - 35	NPSTP(N)	Elastic support identification number. (Leave blank if no elastic support).
Col. 36 - 40	NFP(N)	Corresponding joint number in the finite strip system. (Leave blank if not connected to finite strip system at this node.)
Col. 41 - 45	KNFP	Joint number generation increment.

e. FRAME ELEMENT MATERIAL PROPERTY DATA (I5, 2F10.0) - NUMMAT lines

Col. 1 - 5	I	Material identification number.
Col. 6 - 15	EMOD(I)	Young's modulus of material.
Col. 16 - 25	PRAT(I)	Poisson's ratio of material.

f. FRAME ELEMENT SECTION PROPERTY DATA (I5, 3F10.0) - NUMETP lines

Col. 1 - 5	I	Section identification number.
Col. 6 - 15	SECP(1,I)	Axial area.
Col. 16 - 25	SECP(2,I)	Shear area (leave blank to neglect shear deformation).
Col. 26 - 35	SECP(3,I)	Moment of inertia.

g. ELEMENT DATA (5I5, 4X, I6) - NUMEL lines

Col. 1 - 5	L	Identification number.
Col. 6 - 10	NODE(1,L)	Element node I.
Col. 11 - 15	NODE(2,L)	Element node J.
Col. 16 - 20	NMAT(L)	Material identification number.
Col. 21 - 25	NPRP(L)	Section property identification number.
Col. 30 - 35	MERC(L)	Six-digit element end release code.
		In Cols. 30 - 35, the codes take the following values: +1 for displacement independent of node. 0 for displacement dependent on node.
		Digits 1 to 6 of the code correspond to the element degrees of freedom as shown.

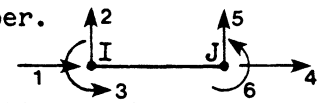

21. **FLEXIBLE MOVABLE DIAPHRAGM DATA SET** - NFMD sets

Required only if flexible movable diaphragms are called for with parameter NFMD in input section 2. Provide one set of the following data per type of flexible movable diaphragm. Type numbers must be ascending consecutive integers starting with 1. Flexible diaphragms are modelled as straight prismatic beams parallel to the global Y-axis. No gravity or external loads may be applied on any flexible movable diaphragm. Repeat this input section for each flexible movable diaphragm type.

a. DIAPHRAGM TYPE CONTROL DATA (2I5) - 1 line

Col. 1 - 5	Diaphragm type number
Col. 6 - 10	Input option code, for form of next line. +1 for option 1. +2 for option 2.

b. DIAPHRAGM PROPERTY DATA - Use either option 1 or 2

Option 1: Rectangular cross section located at mean Z - coordinate of finite strip system (4F10.0) - 1 line

Col. 1 - 10	DITH	Diaphragm thickness in X - direction. If ISB = 0 and ICR = 0: Input in angular degrees. If ISB = 0 and ICR = +1: Thickness measured along finite strip system reference line. If ISB = +1: Thickness of diaphragm for straight bridge.
Col. 11 - 20	DIDP	Diaphragm depth (centroidal axis assumed at mid-depth).
Col. 21 - 30	DIFE	Modulus of elasticity of diaphragm.
Col. 31 - 40	DIFN	Poisson's ratio of diaphragm.

Option 2: Arbitrary cross section (6F10.0) - 1 line

Col. 1 - 10	DIFI	Moment of inertia of diaphragm cross section.
Col. 11 - 20	DIFA	Area of diaphragm cross section.
Col. 21 - 30	DIFS	Shear area of diaphragm cross section (leave blank to neglect shear deformation).
Col. 31 - 40	DIFZ	Z - coordinate of diaphragm centroidal axis.
Col. 41 - 50	DIFE	Modulus of elasticity of diaphragm.
Col. 51 - 60	DIFN	Poisson's ratio of diaphragm.

In Cols. 1 - 30, the moment of inertia, area of cross section and shear area are to be determined at the location of the reference line of the finite strip system.

APPENDIX D: CELL4 USER'S GUIDE

CELL4: A COMPUTER PROGRAM FOR THE ELASTIC FINITE ELEMENT ANALYSIS OF PRESTRESSED CELLULAR STRUCTURES OF ARBITRARY PLAN GEOMETRY AND CONSTANT DEPTH

Programmed at the Department of Civil Engineering
University of California, Berkeley

Faculty Investigator: Professor A. C. Scordelis

Author: E. C. Chan

Date: March, 1985

Considerable effort has gone into the development and testing of this program, which can analyze a particular class of structure. It is based on the conditions and assumptions described in this report. The program should be used only under these conditions and assumptions and the output must be interpreted appropriately by a qualified person.

Although the program has been extensively tested, no warranty is made regarding the accuracy and reliability of the program, and the authors assume no responsibility in this respect.

CELL4 INPUT SPECIFICATIONS

1. **START FLAG** (A4) - 1 line

Col. 1 - 4	CHECK	Each problem has to begin with the word "START" from the first column which initiates the input of each new problem.

2. **TITLE** (20A4) - 1 line

Col. 1 - 80	HED	Title of problem to be printed with output.

3. **INPUT CONTROL DATA** (9I5, F10.0, I5) - 1 line

Col. 1 - 5	NUMELD	Number of top deck plate elements.
Col. 6 - 10	NBEAM	Number of vertical web elements.
Col. 11 - 15	NUMSPW	Number of special web elements.
Col. 16 - 20	NUMNPD	Number of nodal points in the top deck.
Col. 21 - 25	NUMNPW	Number of intermediate nodes between top and bottom deck.
Col. 26 - 30	NMAT	Number of different material types including different thicknesses.
Col. 31 - 35	NUMBC	Total number of nodes with specified kinematic constraints imposed on the top and bottom deck nodes and any intermediate nodes (max. = 200).
Col. 36 - 40	NDSP	Number of boundary spring elements (max. = 200).
Col. 41 - 45	NBLKL	Specified block length of structural stiffness matrix. If it is input as 0, the block length is computed internally using the current bandwidth and a blank common length of 100000.
Col. 46 - 55	AH	Height of the box structure, and this is constant for the entire structure.
Col. 56 - 60	ICHECK	Code for execution mode 1 = input check 0 = problem execution

Note: Both NUMELD, NBEAM and NUMSPW must be input as values greater than zero. In the case where either kind of element type does not exist, a dummy element with zero thickness must be used.

4. **PRESTRESSING CONTROL DATA** (8I5) - 1 line

One blank line is required if prestressing is not considered.

Col. 1 - 5	NTDPT	Number of top deck panel tendons.
Col. 6 - 10	NTDST	Number of top deck slab tendons.
Col. 11 - 15	NBDPT	Number of bottom deck panel tendons.

Col. 16 - 20	NBDST	Number of bottom deck slab tendons.
Col. 21 - 25	NWPT	Number of panel tendons in the vertical webs.
Col. 26 - 30	NSWPT	Number of panel tendons in the special webs.
Col. 31 - 35	MXSEG	Maximum number of tendon segments in any discretized tendon. MXSEG = NUMELD if MXSEG is input as 0.
Col. 36 - 40	MXTP	Maximum number of tendon points in any discretized tendon. MXTP = NUMNPD if MXTP is input as 0.

5. **TOP DECK NODAL COORDINATE DATA** (2I5, 2F10.0, 3I5)
- 1 to NUMNPD lines

Input 1 line for each top deck node unless automatic nodal point generation is used.

Col. 1 - 5	N	Top deck node number.
Col. 6 - 10	IBOT(N)	Code for bottom deck node directly below. 0 = bottom deck node does exist. 1 = bottom deck node does not exist.
Col. 11 - 20	XORD(N)	Global X - coordinate of top deck node N.
Col. 20 - 30	YORD(N)	Global Y - coordinate of top deck node N.
Col. 31 - 35	NDIF	Generation parameter for one way generation. One way generation is activated if previous nodes are omitted and NDIF $\neq$ 0. In this case, the coordinates are generated at equal intervals along line joining the first and last nodes of a string, and the node number is increased by NDIF.

If two way generation is desired, the following data must be added, provided that two strings of nodes have been defined.

Col. 35 - 40	MOD	Difference in node numbers between adjacent string of nodes for two way generation.
Col. 41 - 45	NLIM	Last node number up to which two way generation is activated.

6. **INTERMEDIATE NODAL COORDINATE DATA** (3I5, 3F10.0, 3I5)
- 1 to NUMNPW lines

Skip this input if NUMNPW = 0, or else input 1 line for every node lying between the top and bottom deck unless automatic nodal point generation is used.

Col. 1 - 5	N	Intermediate node number (type 2 in Fig. 6.6).
Col. 6 - 10	NREF(1)	Top deck nodes defining the auxillary yy axis where the yy axis is + ve from NREF(1) to NREF(2), (Fig. 6.1).
Col. 11 - 15	NREF(2)	

Col. 16 - 25	XORD(N)	Global X - coordinate of node N if NREF(1) = NREF(2) = 0, or input 0 if NREF(1) = NREF(2) ≠ 0.
Col. 26 - 35	YORD(N)	Global Y - coordinate of node N if NREF(1) = NREF(2) = 0 or local yy coordinate if NREF(1) = NREF(2) ≠ 0.
Col. 36 - 45	ZORD(N)	Global Z - coordinate of node N.
Col. 46 - 50	NDIF	Node generation parameter, one way generation is activated if previous nodes are omitted. The coordinates are generated at equal intervals between the first and last node of a string and the node numbers are increased by NDIF. If NDIF is left blank, the node numbers are increased by 1.

If two way generation is desired, the following data must be added provided two strings of nodes have been defined.

Col. 47 - 50	MOD	Difference in node numbers between adjacent string of nodes for two way generation.
Col. 51 - 55	NLIM	Last node number up to which two way generation is activated.

7. MATERIAL DATA

The material numbers N described below must be numbered sequentially.

a. CONTROL DATA (3I5) - 1 line

Col. 1 - 5	NISO	Number of different isotropic material including the thickness.
Col. 6 - 10	NORTHO	Number of different orthotropic material including thickness.
Col. 11 - 15	NANISO	Number of different anisotropic material including the thickness.

b. ISOTROPIC MATERIAL (I5 , 3F10.0) - 1 line/isotropic material

Skip this input if NISO = 0

Col. 1 - 5	N	Material number, must be input sequentially.
Col. 6 - 15	E1(N)	Modulus of elasticity.
Col. 16 - 25	PR(N)	Poisson's ratio.
Col. 26 - 35	TH(N)	Thickness of element, assumed to be constant over the element.

c. ORTHOTROPIC MATERIAL (I5 , 6F10.0) - 1 line/orthotropic material

Skip this input if NORTHO = 0

Col. 1 - 5	N	Material number, must be input sequentially following the isotropic material.
Col. 6 - 15	E1(N)	Elastic modulus in principal direction of orthotropy x_1.
Col. 16 - 25	E2(N)	Elastic modulus in principal direction of orthotropy x_2.
Col. 26 - 35	G12(N)	Shear modulus.
Col. 36 - 45	PR(N)	Mean Poisson's ratio, $\nu = \sqrt{\nu_{12}\ \nu_{21}}$.
Col. 46 - 55	ANG(N)	Angle in degrees between local element x - axis and the principal axis of orthotropy x_1. Use right hand rule for + direction.
Col. 56 - 65	TH(N)	Thickness of element, assumed to be constant over the element.

d. ANISOTROPIC MATERIAL - 2 line/anisotropic material

Skip the following input if NANISO = 0

First line - plate bending stiffness coefficients in element local coordinate system (I5, 6F10.0)

Col. 1 - 5	N	Material number, must be input sequentially following orthotropic material.
Col. 5 - 15	DM(I,1,1)	Element 1, 1 of (3 x 3) material law I.
Col. 16 - 25	DM(1,2,2)	Element 2, 2 of (3 x 3) material law I.
Col. 26 - 35	DM(I,3,3)	Element 3, 3 of (3 x 3) material law I.
Col. 36 - 45	DM(I,1,2)	Element 1, 2 of (3 x 3) material law I.
Col. 46 - 55	DM(I,1,3)	Element 1, 3 of (3 x 3) material law I.
Col. 56 - 65	DM(I,2,3)	Element 2, 3 of (3 x 3) material law I.

Second line - membrane stiffness coefficients in element local coordinate system (6F10.0)

Col. 1 - 10	DS(I,1)	Element 1, 1 of (3 x 3) material law I.
Col. 11 - 20	DS(I,2)	Element 2, 2 of (3 x 3) material law I.
Col. 21 - 30	DS(I,3)	Element 3, 3 of (3 x 3) material law I.
Col. 31 - 40	DS(I,4)	Element 1, 2 of (3 x 3) material law I.
Col. 41 - 50	DS(I,5)	Element 1, 3 of (3 x 3) material law I.
Col. 51 - 60	DS(I,6)	Element 2, 3 of (3 x 3) material law I.

8. **DECK ELEMENT DATA** (10I5) 1 to NUMELD lines

Col. 1 - 5	L	Deck element number.
Col. 5 - 25	NP(4)	Element nodal array, listed counter-clockwise when viewed from above.
Col. 26 - 30	MA	Material number of top deck elements.
Col. 31 - 35	MB	Material number of bottom deck element MB = 0 if no bottom deck element exists.

One way generation is activated if previous element numbers are omitted, in which case, the following data

are added.

Col. 36 - 40	NDIF	Difference in corresponding node numbers of adjacent element in a string where one way generation isused. If NDIF is left blank, NDIF is set to 1 in the generation.

If two way generation is desired, the following data must be added, provided that two strings of elements have been defined.

Col. 41 - 45	MOD	Difference in node numbers of adjacent string of elements for two way generation.
Col. 46 - 50	NLIM	Last deck element number up to which two way generation is activated.

9. **VERTICAL WEB ELEMENT DATA** (7I5) 1 To NBEAM lines.

The transverse web elements, if they exist, must be numbered first.

Col. 1 - 5	L	Vertical web element number.
Col. 6 - 15	NBP(2)	Element nodal array, listed nodes in increasing node numbers.
Col. 16 - 20	MC	Material number.

One way generation is activated if previous elements are omitted, in which case, the following data must be added.

Col. 21 - 25	NDIF	Difference in corresponding node numbers of adjacent element in a string where one way generationis used. If NDIF is left blank, NDIF is set to 1 in the generation.

If two way generation is desired, the following data must be added, provided that two strings of elements have been defined.

Col. 26 - 30	MOD	Difference in node numbers of adjacent string of elements for two way generation.
Col. 31 - 35	NLIM	Last vertical web element number up to which two way generation is activated.

10. **SPECIAL WEB ELEMENT DATA** (9I5) - 1 to NUMSPW line

Transverse special web elements, if they exist, must be numbered first.

Col. 1 - 5	L	Special web element number.
Col. 6 - 25	NPW(4)	Special web element nodal array, numbered counter clockwise from NPW(1) to NPW(4), NPW(1) and NPW(4) are nodes closer to the top deck with NPW(4) greater than or equal to NPW(1). NPW(2) and NPW(3) are nodes closer to the bottom deck. If NPW(4) equals NPW(3), it collapses into a triangle.
Col. 26 - 30	MC	Material number.

One way generation is activated if previous elements are omitted, in which case, the following data must be added.

Col. 31 - 35	NDIF	Difference in corresponding node numbers of adjacent elements in a string for one way generation. If NDIF is left blank, NDIF is set to 1 in the generation.

If two way generation is desired, the following data are required, provided that two strings of elements have been defined.

Col. 36 - 40	MOD	Difference in node numbers of adjacent string of elements for two way generation.
Col. 41 - 45	NLIM	Last special web element number up to which two way generation is activated.

11. **DISPLACEMENT BOUNDARY CONDITION DATA** (I5, 6L5, 2F10.0) - 1 to NUMBC lines

Kinematic constraints must be applied separately for each constrained top and bottom node, and each intermediate node between top and bottom decks. A sufficient number of kinematic constraints together with the boundary spring supports described in paragraph 12 must be imposed on the structure to remove any possible rigid body motion.

Col. 1 - 5	M	Nodal point number at which kinematic constraints are applied.
Col. 6 - 10	J1	Code for U - displacement along X - axis.
Col. 11 - 15	J2	Code for V - displacement along Y - axis.
Col. 16 - 20	J3	Code for W - displacement along global Z - axis.
Col. 21 - 25	J4	Code for θ_X - rotation about X - axis.
Col. 26 - 30	J5	Code for θ_Y - rotation about Y - axis. Boundary condition code for above: T = Constrained 0 = Free to move
Col. 31 - 35	JB	Set JB = T for constraint being applied to bottom deck if node M is part of the deck system. Set JB = T for constraint being applied to θ_Z - rotation about global Z - axis when node M is lying between the top and bottom deck.

Omit subsequent data if the above kinematic constraints act in the global coordinate direction. However, if a displacement or a rotation component is constrained in a direction which differs from the global X, Y axes then an angle must be specified separately for each of these constraints. The first angle is denoted by ALF for the displacement constraint V and is taken from the + global X axis to the direction along which the node remains free to displace $\overline{U}$. The second angle is denoted by BET for the rotational constraint θ_Y and is taken from the + global X-axis to the axis about which the node remains free to rotate, $\overline{\theta}_X$. Use right

hand rule for + direction of both angles. The corresponding orthogonal components $\overline{V}$ and $\overline{\theta}_Y$ are set to zero if the constraint for V or θ_Y was set true, T.

Col. 17 - 26	ALF	Angle of skew for constraint $\overline{V}$ in degrees.
Col. 27 - 36	BET	Angle of skew for constraint $\overline{\theta}_Y$ in degrees.

Nonzero displacement boundary conditions can be imposed by applying the corresponding kinematic constraints and by specifying the magnitude of given displacements in the input for nodal loads.

12. **ELASTIC SPRING SUPPORT DATA** (7I5 , 4F10.0, I5) - 1 to NDSP lines.

Boundary springs must be applied separately for top and bottom deck nodes and intermediate nodes if they exist. They can be used to simulate elastic support and support movement and to obtain support reactions.

Col. 1 - 5	N	Boundary spring element number.	
Col. 6 - 10	NI(1)	Node at which the boundary spring element is placed.	
Col. 11 - 15	NI(2)	Node a	Leave columns 16-30 blank if only node a is needed to define spring direction.
Col. 16 - 20	NI(3)	Node b	
Col. 21 - 25	NI(4)	Node c	
Col. 26 - 30	NI(5)	Node d	
Col. 31 - 35	JT	Code for spring in top deck JT = 1, for spring attached to top deck. JT = 0, for spring attached to bottom deck node or intermediate node.	
Col. 36 - 45	SPT	Translational spring stiffness.	
Col. 46 - 55	SPR	Rotational spring stiffness.	
Col. 56 - 65	TD	Translational elastic displacement of spring N.	
Col. 66 - 75	TR	Rotational elastic displacement of spring N.	

Note: For translational rigid support, SPT is typically set a large value (say 10^{10}) and likewise for SPR in rotational rigid support. The values of TD and TR are used to simulate elastic support movement.

Col. 76 - 80	NDIF	Generation parameter The node NI(1) at which the boundary spring element is placed, is incremented by NDIF if consecutive boundary spring elements are missing in a string. The generated boundary elements all have the same orientation, spring stiffness and displacement as the first one in the string.

13. TOP DECK PANEL TENDON DATA

Skip this input if there is no top deck panel tendon, input sequentially otherwise.

a. TENDON CONTROL, JACKING AND FRICTION DATA - 2 lines

First line - Tendon control data (3I5)

Col. 1 - 5	KTIC	Tendon geometry input code KTIC = 0, input tendon point coordinates directly. KTIC = 1, tendon points are generated parabolically.
Col. 6 - 10	KTFC	Tendon force computation code. KTFC = 0, tendon forces are computed by method B in which the tendon forces are consistent with the discretized tendon profile. KTFC = 1, tendon forces are computed by method A in which averaging is done on the tendon forces, computed by method B, at the left and right side of tendon point. (See definition of method A and B in Chapter 3.)
Col. 11 - 15	NPORT	Number of portions making up the tendon.

Second line - Jacking force and friction data (7F10.0)

Col. 1 - 10	FEND(1)	Jacking force from end A, FEND(1) = 0 for jacking from end B only.
Col. 11 - 20	FEND(2)	Jacking force from end B, FEND(2) = 0 for jacking from end A only.
Col. 21 - 30	CRC	Curvature friction coefficient in force / radian.
Col. 31 - 40	WFC	Wobble friction coefficient in force / length of tendon.
Col. 41 - 51	AREA	Cross sectional area of tendon. AREA = 0, anchorage slip losses is ignored.
Col. 51 - 60	EMOD	Modulus of elasticity of prestressing tendon EMOD = 0, anchorage slip losses is ignored.
Col. 61 - 70	SLIP	Anchorage slip distance at each end A and B. SLIP = 0, anchorage slip losses is ignored.

b. TENDON GEOMETRY DATA

DIRECT INPUT OF TENDON POINTS

Skip this input if parabolic generation is used, KTIC = 1

CONTROL DATA (I5) - 1 line

Col. 1 - 5 NTP Number of tendon points along the tendon.

TENDON POINT COORDINATES (2F10.0 , 2I5) - 1 To NTP lines

Input sequentially starting from tendon point 1 at jack end A.

Col. 1 - 10	XI(J)	Global X - coordinate of tendon point J.
Col. 11 - 20	YI(J)	Global Y - coordinate of tendon point J.
Col. 21 - 25	NODI(J)	Node NI of top deck closest to tendon point J.
Col. 26 - 30	NODJ(J)	Node NJ of top deck such that tendon point J lies between NI and NJ, with NJ belonging to the same element as node NI.

Note that NODI(J) and NODJ(J) must form a boundary between adjacent elements. If tendon point J falls on a nodal point NODI(J), then NODI(J) = NODJ(J).

PARABOLIC TENDON POINT GENERATION

Skip the following series of cards if KTIC = 0, otherwise input sequentially starting from portion 1 of jack end A up to NPORT portions.

CHARACTERISTIC X - COORDINATE OF TENDON PORTION (3F10.0) - 1 line

Col. 1 - 30 XX(3) Global X - coordinates of 3 points lying on the X - parabola.

CHARACTERISTIC Y - COORDINATE OF TENDON PORTION (3F10.0) - 1 line

Col. 1 - 30 YY(3) Global Y - coordinates of 3 points with corresponding XX(3) coordinates and lying on the X - parabola.

Note: XX(1) and YY(1) must be the coordinate of the start of a tendon portion, while (XX(2), YY(2)) and (XX(3), YY(3)) are arbitrary points on the tendon portion. If (XX(1), YY(1)), (XX(2), YY(2)) and (XX(3), YY(3)) are colinear, the parabola degenerates into a straight line.

TENDON PORTION PATH DATA (4I5) - 1 line

Col. 1 - 5	NDS	Deck element number which contains the first tendon segment of the current portion.
Col. 1 - 10	NDE	Deck element number which contains the last tendon segment of the current portion.

Col. 11 - 15	NI	Node NI of top deck nearest to the start of the tendon portion.
Col. 16 - 20	NJ	Node NJ of top deck such that tendon point J lies between NI and NJ, with NJ belonging to the same element of NI.

14. BOTTOM DECK PANEL TENDON DATA

Skip this input if there is no bottom deck panel tendon, input sequentially otherwise from bottom deck panel tendon 1.

a. TENDON CONTROL, JACKING AND FRICTION DATA - 2 lines

First line - Tendon control data (3I5)

Col. 1 - 5	KTIC	Tendon geometry input code KTIC = 0, input tendon point coordinate directly. KTIC = 1, tendon points are generated parabolically.
Col. 6 - 10	KTFC	Tendon force computation code. KTFC = 0, tendon forces are computed by method B in which the tendon forces are consistent with the discretized tendon profile. KTFC = 1, tendon forces are computed by method A in which averaging is done on the tendon forces, computed by method B, at the left and right side of tendon point. (See definition of method A and B in Chapter 3.)
Col. 11 - 15	NPORT	Number of portions making up the tendon.

Second line - Jacking force and friction data (7F10.0)

Col. 1 - 10	FEND(1)	Jacking force from end A, FEND(1) = 0 for jacking from end B only.
Col. 11 - 20	FEND(2)	Jacking force from end B, FEND(2) = 0 for jacking from end A only.
Col. 21 - 30	CRC	Curvature friction coefficient in force / radian.
Col. 31 - 40	WFC	Wobble friction coefficient in force / length of tendon.
Col. 41 - 51	AREA	Cross sectional area of tendon. AREA = 0, anchorage slip losses is ignored.
Col. 51 - 60	EMOD	Modulus of elasticity of prestressing tendon EMOD = 0, anchorage slip losses is ignored.
Col. 61 - 70	SLIP	Anchorage slip distance at each end A and B. SLIP = 0, anchorage slip losses is ignored.

b. TENDON GEOMETRY DATA

DIRECT INPUT OF TENDON POINTS

Skip this input if parabolic generation is used, KTIC = 1

CONTROL DATA (I5) - 1 line

Col. 1 - 5	NTP	Number of tendon points along the tendon.

TENDON POINT COORDINATES (2F10.0 , 2I5) - 1 To NTP lines

Input sequentially starting from tendon point 1 at jack end A.

Col. 1 - 10	XI(J)	Global X - coordinate of tendon point J.
Col. 11 - 20	YI(J)	Global Y - coordinate of tendon point J.
Col. 21 - 25	NODI(J)	Node NI of top deck closest to tendon point J.
Col. 26 - 30	NODJ(J)	Node NJ of top deck such that tendon point J lies between NI and NJ, with NJ belonging to the same element as node NI.

Note that NODI(J) and NODJ(J) must form a boundary between adjacent elements. If tendon point J falls on a nodal point NODI(J), then NODI(J) = NODJ(J).

PARABOLIC TENDON POINT GENERATION

Skip the following series of cards if KTIC = 0, otherwise input sequentially starting from portion 1 of jack end A up to NPORT portions.

CHARACTERISTIC X - COORDINATE OF TENDON PORTION (3F10.0) - 1 line

Col. 1 - 30	XX(3)	Global X - coordinates of 3 points lying on the X - parabola.

CHARACTERISTIC Y - COORDINATE OF TENDON PORTION (3F10.0) - 1 line

Col. 1 - 30	YY(3)	Global Y - coordinates of 3 points with corresponding XX(3) coordinates and lying on the X - parabola.

Note: XX(1) and YY(1) must be the coordinate of the start of a tendon portion, while (XX(2), YY(2)) and (XX(3), YY(3)) are arbitrary points on the tendon portion. If (XX(1), YY(1)), (XX(2), YY(2)) and (XX(3), YY(3)) are colinear, the parabola degenerates into a straight line.

TENDON PORTION PATH DATA (4I5) - 1 line

Col. 1 - 5	NDS	Deck element number which contains the first tendon segment of the current portion.
Col. 1 - 10	NDE	Deck element number which contains the last tendon segment of the current portion.
Col. 11 - 15	NI	Node NI of top deck nearest to the start of the tendon portion.
Col. 16 - 20	NJ	Node NJ of top deck such that tendon point J lies between NI and NJ, with NJ belonging to the same element of NI.

15. **TOP DECK SLAB TENDON DATA**

Skip this input if there is no top deck slab tendon, input sequentially otherwise from top deck slab tendon 1.

a. **TENDON CONTROL, JACKING AND FRICTION DATA** - 2 lines

First Line - Tendon control data (3I5)

Col. 1 - 5	KTIC	Tendon geometry input code KTIC = 0, input tendon point coordnate directly. KTIC = 1, tendon points are generated by a given parametric input.
Col. 6 - 10	KTFC	Tendon force computation code. KTFC = 0, tendon forces are computed by method B in which the tendon forces are consistent with the discretized tendon profile. KTFC = 1. Tendon forces are computed by method A in which averaging is done on the tendon forces, computed by method B, at the left and right side of tendon point. (See Chapter 3 for definition of Method A and Method B.)
Col. 11 - 15	NPORT	Number of portions making up the tendon.

Second Line - Jacking force and friction data (7F10.0)

Col. 1 - 10	FEND(1)	Jacking force from end A, FEND(1) = 0 for jacking from end B only.
Col. 11 - 20	FEND(2)	Jacking force from end B, FEND(2) = 0 for jacking from end A only.
Col. 21 - 30	CFC	Curvature friction coefficient in force / radian.
Col. 31 - 40	WFC	Wobble friction coefficient in force / length of tendon.
Col. 41 - 50	AREA	Cross sectional area of tendon.

		AREA = 0, anchorage slip losses is ignored.
Col. 51 - 60	EMOD	Modulus of elasticity of prestressing tendon. EMOD = 0, anchorage slip losses is ignored.
Col. 61 - 70	SLIP	Anchorage slip distance at each end. SLIP = 0, anchorage slip losses is ignored.

b. TENDON GEOMETRY DATA

DIRECT INPUT OF TENDON POINTS

Skip this input if parametric generation is used, KTIC = 1.

CONTROL DATA (I5) 1 line

Col. 1 - 5	NTP	Number of tendon points along the tendon.

TENDON POINT COORDINATES (3F10.0 , 2I5) NTP line

Input sequentially starting from tendon point 1 at jack end A.

Col. 1 - 10	XI(J)	Global X - coordinate of tendon point J.
Col. 11 - 20	YI(J)	Global Y - coordinate of tendon point J.
Col. 21 - 30	ZI(J)	Eccentricity measured from the plate mid-thickness, positive in the Z - direction.
Col. 31 - 35	NODI(J)	Node NI of top deck closest to tendon point J.
Col. 36 - 40	NODJ(J)	Node NJ of top deck with tendon point J belonging to the same element as NI and lying between NI and NJ.

PARABOLIC TENDON POINT GENERATION

Skip the following input if KTIC = 0, otherwise input sequentially starting from portion 1 of jack end A up to NPORT portions.

CHARACTERISTIC X - COORDINATE OF TENDON PORTION (3F10.0) - 1 line

Col. 1 - 30	XX(3)	Global X - coordinates of any 3 pointslying on the Y - parabola.

CHARACTERISTIC Y - COORDINATE OF TENDON PORTION (3F10.0) - 1 line

Col. 1 - 30	YY(3)	Global Y - coordinates of any 3 points with corresponding XX(3) coordinates and lying on the Y - parabola.

TENDON PROFILE IN Z - COORDINATE - 3 lines (See Figs. 3.5, 3.6)

First Line (3F10.0)

Col. 1 - 10	RLLI	Fraction of total developed length, projected on X - Y plane of portion, at which the inflection point nearer to the start of portion occurs, measured from the start of portion.
Col. 11 - 20	RLLP	Fraction of total developed length, projected on X - Y plane of portion, at which the low point with zero slope occurs, measured from the start of portion.
Col. 21 - 30	RLRI	Fraction of total developed length projected on X - Y plane of portion, at which the inflection point nearer to portion end occurs, measured from the end of portion.

Note that the projected lengths are measured along the top deck.

Second Line (3F10.0)

Col. 1 - 10	ZLT	Eccentricity of the start of the portion, measured from mid-surface of plate and + ve in the Z - direction.
Col. 11 - 20	ZLP	Eccentricity of the low point with zero slope of the portion, measured from mid-surface of plate and + ve in the Z - direction.
Col. 21 - 30	ZRT	Eccentricity of the end of tendon portion, measured from mid-surface of plate and + ve in the Z - direction.

Third Line (4I5)

Col. 1 - 5	NDS	Deck element number which contains the first tendon segment of the current portion.
Col. 6 - 10	NDE	Deck element number which contains the last tendon segment of the current portion.
Col. 11 - 15	NI	Node NI of top deck closest to the start of the tendon portion.
Col. 16 - 20	NJ	Node NJ of top deck such that J lies between NI and NJ with NJ belonging to the same element of NI.

16. **BOTTOM DECK SLAB TENDON DATA**

Skip this input if there is no bottom deck slab tendon, input sequentially otherwise from bottom deck slab tendon 1.

a. **TENDON CONTROL, JACKING AND FRICTION DATA** - 2 lines

First Line - Tendon control data (3I5)

Col. 1 - 5	KTIC	Tendon geometry input code KTIC = 0, input tendon point coordnate directly.

		KTIC = 1, tendon points are generated by a given parametric input.
Col. 6 - 10	KTFC	Tendon force computation code. KTFC = 0, tendon forces are computed by method B in which the tendon forces are consistent with the discretized tendon profile. KTFC = 1. Tendon forces are computed by method A in which averaging is done on the tendon forces, computed by method B, at the left and right side of tendon point. (See Chapter 3 for definition of Method A and Method B.)
Col. 11 - 15	NPORT	Number of portions making up the tendon.

Second Line - Jacking force and friction data (7F10.0)

Col. 1 - 10	FEND(1)	Jacking force from end A, FEND(1) = 0 for jacking from end B only.
Col. 11 - 20	FEND(2)	Jacking force from end B, FEND(2) = 0 for jacking from end A only.
Col. 21 - 30	CFC	Curvature friction coefficient in force / radian.
Col. 31 - 40	WFC	Wobble friction coefficient in force / length of tendon.
Col. 41 - 50	AREA	Cross sectional area of tendon. AREA = 0, anchorage slip losses is ignored.
Col. 51 - 60	EMOD	Modulus of elasticity of prestressing tendon. EMOD = 0, anchorage slip losses is ignored.
Col. 61 - 70	SLIP	Anchorage slip distance at each end. SLIP = 0, anchorage slip losses is ignored.

b. TENDON GEOMETRY DATA

DIRECT INPUT OF TENDON POINTS

Skip this input if parametric generation is used, KTIC = 1.

CONTROL DATA (I5) 1 line

Col. 1 - 5	NTP	Number of tendon points along the tendon.

TENDON POINT COORDINATES (3F10.0 , 2I5) NTP line

Input sequentially starting from tendon point 1 at jack end A.

Col. 1 - 10	XI(J)	Global X - coordinate of tendon point J.
Col. 11 - 20	YI(J)	Global Y - coordinate of tendon point J.

Col. 21 - 30	ZI(J)	Eccentricity measured from the plate mid-thickness, positive in the Z - direction.
Col. 31 - 35	NODI(J)	Node NI of top deck closest to tendon point J.
Col. 36 - 40	NODJ(J)	Node NJ of top deck with tendon point J belonging to the same element as NI and lying between NI and NJ.

PARABOLIC TENDON POINT GENERATION

Skip the following input if KTIC = 0, otherwise input sequentially starting from portion 1 of jack end A up to NPORT portions.

CHARACTERISTIC X - COORDINATE OF TENDON PORTION (3f10.0) - 1 line

Col. 1 - 30	XX(3)	Global X - coordinates of any 3 points lying on the Y - parabola.

CHARACTERISTIC Y - COORDINATE OF TENDON PORTION (3F10.0) 1 line

Col. 1 - 30	YY(3)	Global Y - coordinates of any 3 points with corresponding XX(3) coordinates and lying on the Y - parabola.

TENDON PROFILE IN Z - COORDINATE - 3 lines (See Figs. 3.5, 3.6)

First Line (3F10.0)

Col. 1 - 10	RLLI	Fraction of total developed length projected on X - Y plane of portion, at which the inflection point nearer to the start of portion occurs, measured from the start of portion.
Col. 11 - 20	RLLP	Fraction of total developed length projected on X - Y plane of portion, at which the low point with zero slope occurs, measured from the start of portion.
Col. 21 - 30	RLRI	Fraction of total developed length projected on X - Y plane of portion, at which the inflection point nearer to portion end occurs, measured from the end of portion.

Note that the projected lengths are measured along the top deck.

Second Line (3F10.0)

Col. 1 - 10	ZLT	Eccentricity of the start of the portion, measured from mid-surface of plate and + ve in the Z - direction.

Col. 11 - 20	ZLP	Eccentricity of the low point with zero slope of the portion, measured from mid-surface of plate and + ve in the Z - direction.
Col. 21 - 30	ZRT	Eccentricity of the end of tendon portion, measured from mid-surface of plate and +ve in the Z - direction.

Third Line (4I5)

Col. 1 - 5	NDS	Deck element number which contains the first tendon segment of the current portion.
Col. 6 - 10	NDE	Deck element number which contains the last tendon segment of the current portion.
Col. 11 - 15	NI	Node NI of top deck closest to the start of the tendon portion.
Col. 16 - 20	NJ	Node NJ of top deck such that J lies between NI and NJ with NJ belonging to the same element of NI.

17. VERTICAL WEB PANEL TENDON DATA

Skip this input if there is no panel tendon in vertical webs, input sequentially otherwise.

a. TENDON CONTROL, JACKING AND FRICTION DATA- 2 lines

First Line - Tendon control data (3I5)

Col. 1 - 5	KTIC	Tendon geometry input code KTIC = 0, input tendon point coordinate directly. KTIC = 1, tendon profile is generated by a given parametric input.
Col. 6 - 10	KTFC	Tendon force computation code. KTFC = 0, tendon forces are computed by method B in which the tendon forces are consistent with the discretized tendon profile. KTFC = 1, tendon forces are computed by method A in which averaging is done on the tendon forces, computed by method B, at the left and right side of tendon point.
Col. 11 - 15	NPORT	Number of portions making up the tendon.

Second Line - Jacking force and friction data (7F10.0)

Col. 1 - 10	FEND(1)	Jacking force from end A, FEND(1) = 0 for jacking from end B only.
Col. 11 - 20	FEND(2)	Jacking force from end B, FEND(2) = 0 for jacking from end A only.
Col. 21 - 30	CFC	Curvature friction coefficient in force / radian.

Col. 31 - 40	WFC	Wobble friction coefficient in force / length of tendon.
Col. 41 - 50	AREA	Cross sectional area of tendon. AREA = 0, anchorage slip losses is ignored.
Col. 51 - 60	EMOD	Modulus of elasticity of prestressing tendon. EMOD = 0, anchorage slip losses is ignored.
Col. 61 - 70	SLIP	Anchorage slip distance at each end A and B. SLIP = 0, anchorage slip losses is ignored.

b. TENDON GEOMETRY DATA

DIRECT INPUT OF TENDON POINTS

Skip this input if parametric generation is used, KTIC = 1.

CONTROL DATA (I5) - 1 line.

Col. 1 - 5	NTP	Number of tendon points along the tendon.

TENDON POINT COORDINATES (F10.0 , I5) - 1 to NTP lines

Input sequentially starting from tendon point 1 at jack end A.

Col. 1 - 10	ZI(J)	Global Z - coordinate of tendon point J.
Col. 11 - 20	NODI(J)	Node NI of top deck directly above tendon point J.

PARAMETRIC TENDON PROFILE GENERATION

Skip the following input if KTIC = 0, otherwise input sequentially starting from portion 1 of jack end A up to NPORT portions.

TENDON PROFILE DATA - 3 lines (See Figs. 3.5, 3.6)

First Line (3F10.0)

Col. 1 - 10	RLLI	Fraction of total projected length on X - Y plane of portion at which the inflection point nearer to the start of portion occurs, measured from the start of portion.
Col. 11 - 20	RLLP	Fraction of total projected length on X - Y plane of portion at which the low point with zero slope occurs, measured from the start of portion.
Col. 21 - 30	RLRI	Fraction of total projected length on X - Y plane of portion at which the inflection point nearer to the portion end occurs, measured from the end of portion.

Second Line (3F10.0)

Col. 1 - 10	ZLT	Global Z - coordinate of the start of portion.
Col. 11 - 20	ZLP	Global Z - coordinate of the low point with zero slope.
Col. 21 - 30	ZRT	Global Z - coordinate of the end of portion.

Third Line (3I5)

Col. 1 - 5	NBS	Vertical web element number which contains the first segment of the portion.
Col. 6 - 10	NBE	Vertical web element number which contains the last segment of the portion.
Col. 11 - 15	NNS	Node on the top deck directly above the start of tendon portion.

18. **SPECIAL WEB PANEL TENDON DATA**

Skip this input if there is no panel tendon in special web elements, input sequentially otherwise.

a. **TENDON CONTROL, JACKING AND FRICTION DATA** - 2 lines

First Line - Tendon control data (3I5)

Col. 1 - 5	KTIC	Tendon geometry input code. KTIC must be input as 0 or leave blank, because no parametric tendon profile generation can be used for special web panel tendons.
Col. 5 - 10	KTFC	Tendon force computation code. KTFC = 0, tendon forces are computed by method B. KTFC = 1, tendon forces are computed by method A.
Col. 11 - 15	NPORT	Number of portions making up the tendon.

Second Line - Jacking force and friction data (7F10.0)

Col. 1 - 10	FEND(1)	Jacking force from end A, FEND(1) = 0 for jacking from end B only.
Col. 11 - 20	FEND(2)	Jacking force from end B. FEND(2) = 0 for jacking from end A only.
Col. 21 - 30	CFC	Curvature friction coefficient in force / radian.
Col. 31 - 40	WFC	Wobble friction coefficient in force / length of tendon.
Col. 41 - 50	AREA	Cross sectional area of tendon. AREA = 0, anchorage slip losses is ignored.

Col. 51 - 60	EMOD	Modulus of elasticity of prestressing tendon. EMOD = 0, anchorage slip losses is ignored.
Col. 61 - 70	SLIP	Anchorage slip distance at each end A and B. SLIP = 0, anchorage slip losses is ignored.

b. TENDON GEOMETRY DATA

CONTROL DATA

Col. 1 - 5	NTP	Number of tendon points along the tendon.

TENDON POINT COORDINATES (3F10.0 , 2I5) -1 to NTP line

Input sequentially starting from tendon point 1 at jack end A.

Col. 1 - 10	XI(J)	Global X - coordinate of tendon point J.
Col. 11 - 20	YI(J)	Global Y - coordinate of tendon point J.
Col. 21 - 30	ZI(J)	Global Z - coordinate of tendon point J.
Col. 31 - 35	NODI(J)	Node NI closest to the tendon point J.
Col. 36 - 40	NODJ(J)	Node NJ in which J is lying between NI and NJ, with NJ belonging to the same element of NI.

19. **LOAD FLAG** (A4) - 1 Line

Col. 1 - 4	CHECK	Each load case has to begin with the word "LOAD" in the first 4 columns.

20. **LOADING CONTROL DATA** (3I5, 3F10.0)

Col. 1 - 5	NLD	Number of nodes with concentrated forces and moments. These must be applied separately at top and bottom deck nodes.
Col. 5 - 10	NLL	Number of different live load intensities acting on the top deck elements in the Z - direction NLL = 0, no live load is included.
Col. 11 - 15	NDL	Code for dead load NDL = 1, dead load is included. NDL = 0, no dead load is included.
Col. 16 - 25	PLL	Live load intensity (force / area + ve in Z - direction.

If NLL = 1, this PLL is assumed to act on all top deck plate elements. If NLL > 1 the remaining 2nd through NLL live load intensities together with the top deck elements over which they act on, have to be specified in paragraph 22.

Col. 26 - 35	PDL	Unit weight density (force / volume) for dead load computation. PDL = 0 if NDL = 0.
Col. 36 - 45	PPL	Fraction of prestressing load included.

If PPL = 0, prestressing load is not included.

21. **CONCENTRATED NODAL LOAD DATA** (I5, 2L5, 5F10.0) - 1 to NLD line

Skip these input if NLD = 0, or input one line for each loaded top or bottom node.

Col. 1 - 5	M	Loaded node number.
Col. 6 - 10	TBOT	Code for force(or displacement) acting at bottom deck. TBOT = T, force (or displacement) acts at bottom deck. TBOT = 0, force (or displacement) acts at top deck.
Col. 11 - 15	TDIS	Code for non-zero displacement boundary condition. TDIS = T, FORCE(5) are input as displacements and rotations. TDIS = 0, FORCE(5) are input as forces and moments.
Col. 16 - 25	FORCE(1)	Nodal force (or displacement) in global X - direction.
Col. 26 - 35	FORCE(2)	Nodal force (or displacement) in global Y - direction.
Col. 36 - 45	FORCE(3)	Nodal force (or displacement) in global Z - direction.
Col. 46 - 55	FORCE(4)	Nodal moment (or rotation) about global X - direction.
Col. 56 - 65	FORCE(5)	Nodal moment (or rotation) about global Y - direction.

NOTE: No nodal loads can be applied to intermediate nodes between top and bottom decks except the dead load and prestressing load.

22. **LIVE LOAD INTENSITIES DATA** - 1 to (NLL - 1) lines

Skip this input if NLL $\leq$ 1 in paragraph 20. For each additional live load intensity NLL > 1, the following input are needed.

First Line (2I5 , F10.0)

Col. 1 - 5	I	Live load number.
Col. 6 - 10	NEL	Total number of deck elements subjected to this live load.
Col. 11 - 20	PLL	Live load intensity in force / area.

Second Line (16I5) 1 to (NEL - 1)/16 + 1 lines

Col. 1 - 80	NOLL(NEL)	Sequential list of top deck elements

subjected to live load number I having intensity PLL.

23. **OUTPUT CONTROL DATA** (4I5, 2X, 8I1, 2I5, F10.0)

Col. 1 - 5	T1	Code for global nodal displacements. 1 = Output 0 = No output
Col. 6 - 10	T2	Code for global generalized forces obtained by multiplying the stiffness by the displacement. 1 = Output 0 = No output
Col. 11 - 15	T3	Code for integrated sectional forces. 1 = Output 0 = No Output
Col. 16 - 20	NSTO	Total number of nodes, deck nodes and intermediate nodes, at which internal stresses are output for deck nodes, the stresses in the top and bottom deck together with the stresses in the top and bottom of the vertical web are output if they exist. 0 = No output -1 = Output for all nodal points >0 = Output only at NSTO nodes listed in paragraph 24.
Col. 23 - 26	TD(4)	Output code for stresses in the deck elements where TD(1) = code for stresses in global direction. TD(2) = code for principal stresses. TD(3) = code for stresses in the direction described by common angle ALF. TD(4) = code for stresses in the direction described by different angles ANG(I) for every NSTO node. 1 = Output 0 = No output
Col. 27 - 28	TW(2)	Output code for internal forces in the vertical web elements where TW(1) = code for stresses in the element's local coordinate system. TW(2) = code for principal stresses. 1 = Output 0 = No output
Col. 29 - 30	TSW(2)	Output code for internal stresses in the special web elements where TSW(1) = code for stresses in the element's local coordinate system. TSW(2) = code for principal stresses. 1 = Output

0 = No output

Col. 31 - 35 NDIA — Total number of vertical web elements idealizing transverse diaghragms.

Col. 36 - 40 NDIAS — Total number of special web elements idealizing transverse diaghragms.

Col. 41 - 50 ALF — Angle in degrees from global X - axis to the direction X', along which the normal nodal stress σ_{xx} of the deck elements only are computed and output. This angle is common to all deck elements, for different angles, use the option TD(4) = 1. Use right hand rule for + ve direction of ALF, and for ALF = 0.0, the output direction coincides with global X - axis.

24. **NODE NUMBERS FOR OUTPUT OF INTERNAL FORCES** (16I5)

Skip this input if NSTO 0, otherwise use as many lines as needed for NSTO nodes.

Col. 1 - 80 NPS(NSTO) — List of node numbers (including deck and intermediate nodes) in increasing order where internal stresses are to be output.

25. **DIRECTIONS OF STRESS OUTPUT** (BF10.0)

Skip this input if NSTO = 0 or TD(4) = 0, otherwise input for all NSTO nodes defined in paragraph 24 in increasing order, the angle with respect to global X - axis where $_{rr}$ is output.

Col. 1 - 80 ANG(NSTO) — Angle in degrees from global X - axis for each of NSTO node. Use right hand rule for + ve direction.

Although the value of ANG(NSTO) has no effect at intermediate nodes in the special web elements, they must be input in order that NPS(NSTO) and ANG(NSTO) form a pair in specifying the location and the direction of stresses to be output. If NSTO = -1, the angles for all nodal points are needed to input although no NPS(NSTO) is specified in paragraph 24.

If no sectional internal forces are desired, T3 = 0, skip to paragraph 28. If T3 = 1, the following sets of input must be input sequentially.

26. **SECTIONAL INTERNAL FORCES CONTROL DATA** (5I5)

Col. 1 - 5 NUMSEC — Number of cross sections for which sectional internal force resultants are to be calculated and output.

Col. 6 - 10 MDECK — Maximum number of top deck elements framing into a section used in integration.

Col. 11 - 15	MWEB	Maximum number of vertical web elements framing into a section used in integration.
Col. 16 - 20	MSPWEB	Maximum number of special web elements framing into a section used in integration.
Col. 21 - 25	MAXNS	Maximum number of nodal points (including deck and intermediate nodes) lying on a section.

27. **SECTIONAL GEOMETRY DATA**

The following set of input describing the configuration of each cross section are required, (See Fig. 6.6).

a. Control Card (7I5, 3F10.0)

Col. 1 - 5	NSEC	Cross section number.
Col. 6 - 10	NDECK	Number of top deck elements adjacent to section NSEC.
Col. 11 - 15	NWEB	Number of vertical web elements adjacent to section NSEC.
Col. 16 - 20	NSWEB	Number of special web elements adjacent to section NSEC.
Col. 21 - 25	NUMNOD	Number of nodes lying on section NSEC (including deck and intermediate nodal points).
Col. 26 - 30	NGIRD	Number of girders belonging to this section.
Col. 31 - 35	IFC	Code for sectional force averaging IFC = 0, no averaging is used and only those elements lying on one side of section are needed to be input in the following sections c through e. IFC = 1, averaging is used, and all elements adjacent to this section are needed to be input in the following sections c through e.
Col. 35 - 45	XO	Global X - coordinate of reference point in the cross section at which sectional force resultants are to be calculated.
Col. 46 - 55	YO	Global Y - coordinate of reference point in the cross section at which sectional force resultants are to be calculated.
Col. 56 - 65	ZO	Global Z - coordinate of reference point in the cross section at which sectionsl force resultants are to be calculated.

If XO and YO = 0, the default for the reference point is located at mid-width of the top deck. If ZO = 0, the default is set to mid-depth of the cross-section.

Note: (1) The sectional force resultants are computed in the directions normal to the tangent to the section at the reference point. The tangential direction B of the

section is determined by the vector joining the first and last nodes of the NUMNOD nodes listed in input section b in paragraph 27. The local C coincides with the global Z axis with local A perpendicular to both B and C. (See Fig. 6.6.)All six resultants (three forces and three moments) will be output with respect to this set of local axes.

(2) Cross sections can be generated if intermediate sections are missing. In this case, all deck element numbers vertical web element numbers, special web element numbers and the reference point coordinates are generated using the data from the first and last sections in a string. NGIRD and IFC are set to those from the first section.

b. LIST OF NODE NUMBERS (16I5)

Node numbers for nodes lying on the section. Use as many lines as required by NUMNOD nodes.

Col. 1 - 80 NNPS(NUMNOD) Node numbers lying on the section.

Note: The first and last node numbers must lie on the top deck only.

c. LIST OF DECK ELEMENTS (3I5)

Skip if NDECK = 0, otherwise input in increasing order of the top deck elements.

Col. 1 - 5	I	Element number.
Col. 6 - 10	NDGRD(1)	First girder it belongs to.
Col. 11 - 15	NDGRD(2)	Second girder it belongs to.

d. LIST OF VERTICAL WEB ELEMENTS (2I5)

Skip if NWEB = 0, otherwise list in increasing order of vertical web elements.

Col. 1 - 5	I	Element number.
Col. 6 - 10	NWGRD	Girder it belongs to.

e. LIST OF SPECIAL WEB ELEMENTS (2I5)

Skip if NSWEB = 0, otherwise list in increasing order of special web elements.

Col. 1 - 5	I	Element number.
Col. 6 - 10	NSWGRD	Girder it belongs to.

28. **NEXT FLAG** (A4)

Col. 1 - 4	CHECK	Running control flag. = LOAD in first 4 columns, new load case is required and input continues in paragraph 20. = STOP in first 4 columns, the program stops.

APPENDIX E:

LISTINGS OF INPUT DATA FOR

NUMERICAL EXAMPLES IN CHAPTER 7

RUN BY COMPUTER PROGRAMS

MUPDI4, CURDI4 AND CELL4

```
EXAMPLE 1:  MUPDI4: MESH 1: SIMPLE SPAN (162 FT): SINGLE CELL BOX: CURVED WEBS
     162.0   10   10    1    0    0    0
   2    0    4    0    0
  11    1  100    2        1.0    0    0
   1   -15.00        0.00
   2    -8.25        0.00
   3    -6.60        4.00
   4    -2.60        5.65
   5     0.00        0.00
   6     0.00        5.65
   7     2.60        5.65
   8     6.60        4.00
   9     8.25        0.00
  10    15.00        0.00
   1   10    1    0    0    0    0
   1  518400.0        0.15      0.155
   1    1    2    1        0.95    4    1
   2    9   10    1        0.95    4    2
   3    2    5    1        0.95    4    1
   4    5    9    1        0.95    4    2
   5    2    3    1        1.50    4    1
   6    3    4    1        1.50    4    1
   7    9    8    1        1.50    4    2
   8    8    7    1        1.50    4    2
   9    4    6    1        0.75    2    1
  10    6    7    1        0.75    2    2
   1    1    1    1    1    1    1    1    1    1    1    1    1    1
      0.0         8.1        16.2        24.3        32.4        40.5        48.6        56.7
     64.8        72.9        81.0
      1.0         0.0
   4    2         0.0   0.042667        81.0       162.0
   2    2         0.0   0.042667        81.0       162.0
   4    2         0.0        0.40        81.0         3.0
   2    2         0.0        0.40        81.0         3.0
```



```
EXAMPLE 1:  MUPDI4: MESH 2: SIMPLE SPAN (162 FT): SINGLE CELL BOX: CURVED WEBS
     162.0   14   14    1    0    0    0
   2    0    4    0    0
  11    1  100    2        1.0    0    0
   1   -15.00        0.00
   2    -8.25        0.00
   3    -7.82        2.16
   4    -6.60        4.00
   5    -4.76        5.22
   6    -2.60        5.65
   7     0.00        0.00
   8     0.00        5.65
   9     2.60        5.65
  10     4.76        5.22
  11     6.60        4.00
  12     7.82        2.16
  13     8.25        0.00
  14    15.00        0.00
   1   14    1    0    0    0    0
   1  518400.0        0.15      0.155
   1    1    2    1        0.95    4    1
   2   13   14    1        0.95    4    2
   3    2    7    1        0.95    4    1
   4    7   13    1        0.95    4    2
   5    2    3    1        1.50    2    1
   6    3    4    1        1.50    2    1
   7    4    5    1        1.50    2    1
   8    5    6    1        1.50    2    1
   9   13   12    1        1.50    2    2
  10   12   11    1        1.50    2    2
  11   11   10    1        1.50    2    2
  12   10    9    1        1.50    2    2
  13    6    8    1        0.75    2    1
  14    8    9    1        0.75    2    2
   1    1    1    1    1    1    1    1    1    1    1    1    1    1
      0.0         8.1        16.2        24.3        32.4        40.5        48.6        56.7
     64.8        72.9        81.0
      1.0         0.0
   4    2         0.0   0.042667        81.0       162.0
   2    2         0.0   0.042667        81.0       162.0
   4    2         0.0        0.40        81.0         3.0
   2    2         0.0        0.40        81.0         3.0
```

```
EXAMPLE 2:  MUPDI4: SIMPLE SPAN (162 FT): SINGLE CELL BOX: VERTICAL WEBS
     162.0    12    12     1     0     0     0
     5     0    16     4     1
    11     1   100     2        1.0     0     0
     1     15.00        0.00
     2     11.125       0.00
     3      7.25        0.00
     4      7.25        5.65
     5      3.625       0.00
     6      0.00        0.00
     7      0.00        5.65
     8     -3.625       0.00
     9     -7.25        0.00
    10     -7.25        5.65
    11    -11.125       0.00
    12    -15.00        0.00
     1    12     1     0     0     0     0
     1  518400.0        0.15      0.155
     1     1     2     1        0.95     2     1
     2     2     3     1        0.95     2     1
     3     9    11     1        0.95     2     2
     4    11    12     1        0.95     2     2
     5     3     5     1        0.95     2     1
     6     5     6     1        0.95     2     1
     7     6     8     1        0.95     2     2
     8     8     9     1        0.95     2     2
     9     3     4     1        1.50     6     1
    10     9    10     1        1.50     6     2
    11     4     7     1        0.75     4     1
    12     7    10     1        0.75     4     2
     0     0     0     1     1     1     0     1     0     0     1     0     0     0
       0.0         8.1        16.2        24.3        32.4        40.5        48.6        56.7
      64.8        72.9        81.0
       1.0         0.0         0.0         0.0         0.0
     1     2         0.0   0.042667        81.0       162.0
     2     2         0.0   0.042667        81.0       162.0
     3     2         0.0  -0.042667        81.0       162.0
     4     2         0.0  -0.042667        81.0       162.0
     5     2         0.0   0.042667        81.0       162.0
     6     2         0.0   0.042667        81.0       162.0
     7     2         0.0  -0.042667        81.0       162.0
     8     2         0.0  -0.042667        81.0       162.0
     1     2         0.0        0.40        81.0         3.0
     2     2         0.0        0.40        81.0         3.0
     3     2         0.0       -0.40        81.0         3.0
     4     2         0.0       -0.40        81.0         3.0
     5     2         0.0        0.40        81.0         3.0
     6     2         0.0        0.40        81.0         3.0
     7     2         0.0       -0.40        81.0         3.0
     8     2         0.0       -0.40        81.0         3.0
     1   108         1.5        81.0     3     1
      45.0         0.0         0.0         0.0         0.0         0.0         0.0         1.0
     1     3     1
     1     2     3
```



```
     2     5     0
     3     5     6     8     9
     3     3     1
     9    11    12
     1     15.0      -0.04167
     2     11.125    -0.22917
     3      7.25     -0.41667
     2        0.0        20.0        50.0        20.0         0.0
      7.25   -0.41667         0.0       0.125      -7.25    -0.41667
     1     -7.25     -0.41667
     2    -11.125    -0.22917
     3    -15.0      -0.04167
        0.0         0.0         0.0         0.0         1.0
     1     1     1     1     1
  3640.0         0.0         0.00        0.0000      0.157  4032000.0      0.000       1.0
     1      162.0    20
     1              0.0         0.0        50.0         0.0         0.0
       7.25        2.025       7.25        5.108       7.25        2.025
        0.0         0.0         1.0
     2     1     1     1     1
  3640.0         0.0         0.00        0.0000      0.157  4032000.0      0.000       1.0
     1      162.0    20
     1              0.0         0.0        50.0         0.0         0.0
      -7.25        2.025      -7.25        5.108      -7.25        2.025
        0.0         0.0         1.0
     3     1     1     1     1
  4266.0      4266.0         0.25        0.0002      0.157  4032000.0     0.0156       1.0
     1      162.0    20
     1              0.0         0.0        50.0         0.0         0.0
       7.25        2.025       7.25        5.108       7.25        2.025
        0.0         0.0         0.0         1.0
     4     1     1     1     1
  4266.0      4266.0         0.25        0.0002      0.157  4032000.0     0.0156       1.0
     1      162.0    20
     1              0.0         0.0        50.0         0.0         0.0
      -7.25        2.025      -7.25        5.108      -7.25        2.025
        0.0         0.0         0.0         1.0
```

```
EXAMPLE 2:  MUPDI4: SIMPLE SPAN (162 FT): SINGLE CELL BOX: SLOPING WEBS
     162.0   12   12    1    0    0    0
   5    0   16    4    1
  11    1  100    2       1.0    0    0
   1   15.00       0.00
   2   11.875      0.00
   3    8.75       0.00
   4    7.25       5.65
   5    4.375      0.00
   6    0.00       0.00
   7    0.00       5.65
   8   -4.375      0.00
   9   -8.75       0.00
  10   -7.25       5.65
  11  -11.875      0.00
  12  -15.00       0.00
   1   12    1    0    0    0    0
   1  518400.0      0.15     0.155
   1    1    2    1       0.95    2    1
   2    2    3    1       0.95    2    1
   3    9   11    1       0.95    2    2
   4   11   12    1       0.95    2    2
   5    3    5    1       0.95    2    1
   6    5    6    1       0.95    2    1
   7    6    8    1       0.95    2    2
   8    8    9    1       0.95    2    2
   9    3    4    1       1.45    6    1
  10    9   10    1       1.45    6    2
  11    4    7    1       0.75    4    1
  12    7   10    1       0.75    4    2
   0    0    0    1    1    1    0    1    0    0    1    0    0    0
      0.0        8.1       16.2       24.3       32.4       40.5       48.6       56.7
     64.8       72.9       81.0
      1.0        0.0        0.0        0.0        0.0
   1    2        0.0   0.042667       81.0      162.0
   2    2        0.0   0.042667       81.0      162.0
   3    2        0.0  -0.042667       81.0      162.0
   4    2        0.0  -0.042667       81.0      162.0
   5    2        0.0   0.042667       81.0      162.0
   6    2        0.0   0.042667       81.0      162.0
   7    2        0.0  -0.042667       81.0      162.0
   8    2        0.0  -0.042667       81.0      162.0
   1    2        0.0        0.40       81.0        3.0
   2    2        0.0        0.40       81.0        3.0
   3    2        0.0       -0.40       81.0        3.0
   4    2        0.0       -0.40       81.0        3.0
   5    2        0.0        0.40       81.0        3.0
   6    2        0.0        0.40       81.0        3.0
   7    2        0.0       -0.40       81.0        3.0
   8    2        0.0       -0.40       81.0        3.0
   1  108        1.5        81.0    3    1
     45.0        0.0        0.0        0.0        0.0        0.0        0.0        1.0
   1    3    1
   1    2    3
```



```
   2    5    0
   3    5    6    8    9
   3    3    1
   9   11   12
   1   15.0     -0.04167
   2   11.875   -0.22917
   3    8.75    -0.41667
   2       0.0       20.0       50.0       20.0        0.0
     8.75  -0.41667        0.0      0.125     -8.75  -0.41667
   1   -8.75   -0.41667
   2  -11.875  -0.22917
   3  -15.0    -0.04167
      0.0        0.0        0.0        0.0        1.0
   1    1    1    1    1
3640.0          0.0        0.00     0.0000      0.157 4032000.0      0.000        1.0
   1     162.0   20
   1             0.0        0.0       50.0        0.0        0.0
8.2124       2.025      7.3939      5.108      8.2124      2.025
      0.0        0.0        1.0
   2    1    1    1    1
3640.0          0.0        0.00     0.0000      0.157 4032000.0      0.000        1.0
   1     162.0   20
   1             0.0        0.0       50.0        0.0        0.0
-8.2124      2.025     -7.3939      5.108     -8.2124      2.025
      0.0        0.0        1.0
   3    1    1    1    1
4266.0       4266.0          0.25     0.0002      0.157 4032000.0      0.0156       1.0
   1     162.0   20
   1             0.0        0.0       50.0        0.0        0.0
8.2124       2.025      7.3939      5.108      8.2124      2.025
      0.0        0.0        0.0        1.0
   4    1    1    1    1
4266.0       4266.0          0.25     0.0002      0.157 4032000.0      0.0156       1.0
   1     162.0   20
   1             0.0        0.0       50.0        0.0        0.0
-8.2124      2.025     -7.3939      5.108     -8.2124      2.025
      0.0        0.0        0.0        1.0
```

```
EXAMPLE 3:  MUPDI4: STRAIGHT: CONTINUOUS TWO SPAN (150,162 FT): FOUR CELL BOX
    3744.0   12   15    1    1    0    0
     3   14    0    5    0
    23    0   60    5   .083333    0    0
     1     252.0   0
     2     200.0   0
     3     200.0   71.375
     4     100.0   0
     5     100.0   71.375
     6       0.0   0
     7       0.0   71.375
     8    -100.0   0
     9    -100.0   71.375
    10    -200.0   0
    11    -200.0   71.375
    12    -252.0   0
     1   12   11    0    0    0    0    1    1    1
     2   11    1    0    0    0    0    0    0    0
     1    3600.0       0.15  .0000897
     1    1    2    1       7.50    4    1
     2   10   12    1       7.50    4    5
     3    2    4    1       7.50    4    1    2   50
     4    4    6    1       7.50    4    2    3   50
     5    6    8    1       7.50    4    3    4   50
     6    8   10    1       7.50    4    4    5   50
     7    3    5    1       5.75    4    1    2   50
     8    5    7    1       5.75    4    2    3   50
     9    7    9    1       5.75    4    3    4   50
    10    9   11    1       5.75    4    4    5   50
    11    2    3    1       12.0    6    1
    12    4    5    1       12.0    6    2
    13    6    7    1       12.0    6    3
    14    8    9    1       12.0    6    4
    15   10   11    1       12.0    6    5
     0    0    0    1    0    1    0    1    0    0    0    0    0    0
     1    1800.0       36.0    1
        0.0     180.0     360.0     540.0     720.0     900.0    1080.0    1260.0
     1440.0    1620.0    1776.0    1800.0    1824.0    1994.4    2188.8    2383.2
     2577.6    2772.0    2966.4    3160.0    3355.2    3549.6    3744.0
        1.0       0.0       0.0
     8    3       0.0       9.36      0.0       0.0      2124      36.0
     8    3       0.0      17.28      0.0       0.0      2340      36.0
     8    3       0.0      17.28      0.0       0.0      2556      36.0
     8    3       0.0      17.28      0.0       0.0      2772      36.0
     8    3       0.0      17.28      0.0       0.0      2988      36.0
     8    3       0.0      17.28      0.0       0.0      3204      36.0
     8    3       0.0      17.28      0.0       0.0      3420      36.0
    10    3       0.0      16.64      0.0       0.0      2124      36.0
    10    3       0.0      30.72      0.0       0.0      2340      36.0
    10    3       0.0      30.72      0.0       0.0      2556      36.0
    10    3       0.0      30.72      0.0       0.0      2772      36.0
    10    3       0.0      30.72      0.0       0.0      2988      36.0
    10    3       0.0      30.72      0.0       0.0      3204      36.0
    10    3       0.0      30.72      0.0       0.0      3420      36.0
```



```
1    2    1    2    1
1580.0       0.0       0.0       0.0      7.803    29000.0       0.0       1.0
1    1800.0
2    1944.0
1             0.0       0.0      50.0      10.0       0.0
 200.0      30.33     200.0     64.25     200.0      8.25
2             0.0      10.0      50.0       0.0       0.0
 200.0       8.25     200.0     64.25     200.0     30.33
   0.0        1.0       0.0
2    2    1    2    1
1580.0       0.0       0.0       0.0      7.803    29000.0       0.0       1.0
1    1800.0
2    1944.0
1             0.0       0.0      50.0      10.0       0.0
 100.0      30.33     100.0     64.25     100.0      8.25
2             0.0      10.0      50.0       0.0       0.0
 100.0       8.25     100.0     64.25     100.0     30.33
   0.0        1.0       0.0
3    2    1    2    1
1580.0       0.0       0.0       0.0      7.803    29000.0       0.0       1.0
1    1800.0
2    1944.0
1             0.0       0.0      50.0      10.0       0.0
   0.0      30.33       0.0     64.25       0.0      8.25
2             0.0      10.0      50.0       0.0       0.0
   0.0       8.25       0.0     64.25       0.0     30.33
   0.0        1.0       0.0
4    2    1    2    1
1580.0       0.0       0.0       0.0      7.803    29000.0       0.0       1.0
1    1800.0
2    1944.0
1             0.0       0.0      50.0      10.0       0.0
-100.0      30.33    -100.0     64.25    -100.0      8.25
2             0.0      10.0      50.0       0.0       0.0
-100.0       8.25    -100.0     64.25    -100.0     30.33
   0.0        1.0       0.0
5    2    1    2    1
1580.0       0.0       0.0       0.0      7.803    29000.0       0.0       1.0
1    1800.0
2    1944.0
1             0.0       0.0      50.0      10.0       0.0
-200.0      30.33    -200.0     64.25    -200.0      8.25
2             0.0      10.0      50.0       0.0       0.0
-200.0       8.25    -200.0     64.25    -200.0     30.33
   0.0        1.0       0.0
```

```
EXAMPLE 3: CURDI4: STRAIGHT: CONTINUOUS TWO SPAN (150,162FT): FOUR CELL BOX
   27   30    1    1    0    0
    0    1    0    0
    3   14    0    5    0
    9    0  100    5    0    0
   3744.0
    1    -252.0         0
    2    -226.0         0
    3    -200.0         0
    4    -200.0   35.6875
    5    -200.0   71.3750
    6    -150.0         0
    7    -150.0   71.3750
    8    -100.0         0
    9    -100.0   35.6875
   10    -100.0   71.3750
   11     -50.0         0
   12     -50.0   71.3750
   13         0         0
   14         0   35.6875
   15         0   71.3750
   16      50.0         0
   17      50.0   71.3750
   18     100.0         0
   19     100.0   35.6875
   20     100.0   71.3750
   21     150.0         0
   22     150.0   71.3750
   23     200.0         0
   24     200.0   35.6875
   25     200.0   71.3750
   26     226.0         0
   27     252.0         0
    1    2    1    0    0    0    0    1    1    1
   26   27    1    0    0    0    0    1    1    1
    3   25    1    0    0    0    0    0    0    0
    1   3600.0      0.15 0.0000897
    1    1    2      7.50    1    4    1    0
    2    2    3      7.50    1    4    1    0
    3    3    6      7.50    1    4    1    0
    4    6    8      7.50    1    4    2    0
    5    8   11      7.50    1    4    2    0
    6   11   13      7.50    1    4    3    0
    7   13   16      7.50    1    4    3    0
    8   16   18      7.50    1    4    4    0
    9   18   21      7.50    1    4    4    0
   10   21   23      7.50    1    4    5    0
   11   23   26      7.50    1    4    5    0
   12   26   27      7.50    1    4    5    0
   23    5    7      5.75    1    4    1    0
   24    7   10      5.75    1    4    2    0
   25   10   12      5.75    1    4    2    0
   26   12   15      5.75    1    4    3    0
   27   15   17      5.75    1    4    3    0
```



```
   28   17   20      5.75    1    4    4    0
   29   20   22      5.75    1    4    4    0
   30   22   25      5.75    1    4    5    0
   13    3    4     12.00    1    4    1    0
   14    4    5     12.00    1    4    1    0
   15    8    9     12.00    1    4    2    0
   16    9   10     12.00    1    4    2    0
   17   13   14     12.00    1    4    3    0
   18   14   15     12.00    1    4    3    0
   19   18   19     12.00    1    4    4    0
   20   19   20     12.00    1    4    4    0
   21   23   24     12.00    1    4    5    0
   22   24   25     12.00    1    4    5    0
    0    0    0    1    1    1    1    1    0    0    0    0
    1   1800.0     12.0    1    0
        0     180.0     900.0    1620.0    1800.0    1994.0    2772.0
   3549.0    3744.0
0.08333333
      1.0         0         0
   18    3         0      9.36         0         0    2124.0      12.0
   18    3         0     17.28         0         0    2340.0      12.0
   18    3         0     17.28         0         0    2556.0      12.0
   18    3         0     17.28         0         0    2772.0      12.0
   18    3         0     17.28         0         0    2988.0      12.0
   18    3         0     17.28         0         0    3204.0      12.0
   18    3         0     17.28         0         0    3420.0      12.0
   23    3         0     16.64         0         0    2124.0      12.0
   23    3         0     30.72         0         0    2340.0      12.0
   23    3         0     30.72         0         0    2556.0      12.0
   23    3         0     30.72         0         0    2772.0      12.0
   23    3         0     30.72         0         0    2988.0      12.0
   23    3         0     30.72         0         0    3204.0      12.0
   23    3         0     30.72         0         0    3420.0      12.0
    1    2    1    2    1
   1580.0         0         0         0     7.803   29000.0         0       1.0
    1    1800.0    0         0    0
    2    1944.0    0         0    0
    1              0         0      50.0      10.0         0
    200.0     30.33     200.0     64.25     200.0      8.25
    2              0      10.0      50.0         0         0
    200.0      8.25     200.0     64.25     200.0     30.33
         0       1.0         0
    2    2    1    2    1
   1580.0         0         0         0     7.803   29000.0         0       1.0
    1    1800.0    0         0    0
    2    1944.0    0         0    0
    1              0         0      50.0      10.0         0
    100.0     30.33     100.0     64.25       100      8.25
    2              0      10.0      50.0         0         0
    100.0      8.25     100.0     64.25       100     30.33
         0       1.0         0
    3    2    1    2    1
   1580.0         0         0         0     7.803   29000.0         0       1.0
    1    1800.0    0         0    0
```

```
2    1944.0    0         0    0
1              0         0      50.0      10.0         0
     0      30.33         0     64.25         0      8.25
2              0      10.0      50.0         0         0
     0       8.25         0     64.25         0     30.33
     0        1.0         0
4    2    1    2    1
1580.0         0         0         0     7.803   29000.0         0       1.0
1    1800.0    0         0    0
2    1944.0    0         0    0
1              0         0      50.0      10.0         0
-100.0      30.33    -100.0     64.25    -100.0      8.25
2              0      10.0      50.0         0         0
-100.0       8.25    -100.0     64.25    -100.0     30.33
     0        1.0         0
5    2    1    2    1
1580.0         0         0         0     7.803   29000.0         0       1.0
1    1800.0    0         0    0
2    1944.0    0         0    0
1              0         0      50.0      10.0         0
-200.0      30.33    -200.0     64.25    -200.0      8.25
2              0      10.0      50.0         0         0
-200.0       8.25    -200.0     64.25    -200.0     30.33
     0        1.0         0
```



```
EXAMPLE 4: CURDI4: CURVED: TWO SPAN: SINGLE CELL BOX, HOOD MODEL
  16   16    1    1    0    0
   0    0    0    0
   2    1    0    2    0
  13    0  100    2    0    0
79.3333    2000.0
   1    171.00    65.240
  16   -171.00    65.240
   2    146.00    65.240
  15   -146.00    65.240
   3    106.56    64.120
  14   -106.56    64.120
   4     67.12    63.000
  13    -67.12    63.000
   6     38.69    64.505
  10    -38.69    64.505
   8         0    64.505
  12    -60.41    31.500
   5     60.41    31.500
  11    -53.70         0
   7     53.70         0
   9         0         0
   1    3    1    0    0    0    0    1    1    1
  14   16    1    0    0    0    0    1    1    1
   4   13    1    0    0    0    0    0    0    0
   1    6536.0     0.321         0
   1    1    2      9.77    1    4    2    0
   2   15   16      9.77    1    4    1    0
   3    2    3      8.65    1    4    2    0
   4   14   15      8.65    1    4    1    0
   5    3    4     10.89    1    4    2    0
   6   13   14     10.89    1    4    1    0
   7    4    6     10.50    1    4    2    0
   8   10   13     10.50    1    4    1    0
   9    6    8      9.00    1    4    2    0
  10    8   10      9.00    1    4    1    0
  11    9   11      8.00    1    4    1    0
  12    7    9      8.00    1    4    2    0
  13   12   13     14.00    1    4    1    0
  14    4    5     14.00    1    4    2    0
  15   11   12     14.00    1    4    1    0
  16    5    7     14.00    1    4    2    0
   0    0    0    1    1    1    1    1    1    0    0    0
   1  39.66667 1.6666667    1
      0    3.96667   9.91667   19.8333   29.7500  35.70000   39.6667
43.6333   49.5833   59.5000   69.4167   75.3666   79.3333
    1.0
      0         0         0
13    1         0    -313.0         0         0 19.83333 0.237142
 1    5    2    4    1
2224.0    2224.0      0.08         0         0         0         0       1.0
 1 0.833333    1         0    1
 2 38.000000   19        0    1
 3  1.666667    1        0    1
```

```
 4 38.000000   19         0    1
 5  0.833333    1         0    1
 1-62.229111 40.039993
 2-60.876434 33.690002
 3-59.689972 28.119995
 4-58.678146 23.369995
 5-57.838821 19.429993
 6-57.169983 16.289993
 7-56.671509 13.950000
 8-56.349854 12.440000
 9-56.198608 11.730000
10-56.217804 11.820000
11-56.409500 12.720000
12-56.773743 14.430000
13-57.312683 16.960007
14-58.019913 20.279999
15-58.906036 24.440002
16-59.958374 29.380005
17-61.185349 35.139999
18-62.582687 41.699997
19-63.884247 47.809998
20-64.504105 50.720001
 1-64.504105 50.720001
 2-64.504105 50.720001
 1-64.504105 50.720001
 2-63.884247 47.809998
 3-62.582687 41.699997
 4-61.185349 35.139999
 5-59.958374 29.380005
 6-58.906036 24.440002
 7-58.019913 20.279999
 8-57.312683 16.960007
 9-56.773743 14.430000
10-56.409500 12.720000
11-56.217804 11.820000
12-56.198608 11.730000
13-56.349854 12.440000
14-56.671509 13.950000
15-57.169983 16.289993
16-57.838821 19.429993
17-58.678146 23.369995
18-59.689972 28.119995
19-60.876434 33.690002
20-62.229111 40.039993
      0       1.0
 2    5    2    4    1
 2224.0    2224.0      0.08        0         0         0         0       1.0
 1  0.83333    1         0    1
 2 38.00000   19         0    1
 3  1.66667    1         0    1
 4 38.00000   19         0    1
 5  0.83333    1         0    1
 1 62.229111 40.039993
 2 60.876434 33.690002
```



```
 3 59.689972 28.119995
 4 58.678146 23.369995
 5 57.838821 19.429993
 6 57.169983 16.289993
 7 56.671509 13.950000
 8 56.349854 12.440000
 9 56.198608 11.730000
10 56.217804 11.820000
11 56.409500 12.720000
12 56.773743 14.430000
13 57.312683 16.960007
14 58.019913 20.279999
15 58.906036 24.440002
16 59.958374 29.380005
17 61.185349 35.139999
18 62.582687 41.699997
19 63.884247 47.809998
20 64.504105 50.720001
 1 64.504105 50.720001
 2 64.504105 50.720001
 1 64.504105 50.720001
 2 63.884247 47.809998
 3 62.582687 41.699997
 4 61.185349 35.139999
 5 59.958374 29.380005
 6 58.906036 24.440002
 7 58.019913 20.279999
 8 57.312683 16.960007
 9 56.773743 14.430000
10 56.409500 12.720000
11 56.217804 11.820000
12 56.198608 11.730000
13 56.349854 12.440000
14 56.671509 13.950000
15 57.169983 16.289993
16 57.838821 19.429993
17 58.678146 23.369995
18 59.689972 28.119995
19 60.876434 33.690002
20 62.229111 40.039993
      0       1.0
```

```
EXAMPLE 5: CURDI4: CURVED: TWO SPAN (150.162FT): FOUR CELL BOX: COARSE MESH
   17   20    1    1    0
    1    0    0    0
    3   14    0    5    0
    9    0  100    5    0    0
 3744.00   4800.00
    1    -252.0         0
    2    -200.0         0
    3    -200.0   35.6875
    4    -200.0   71.3750
    5    -100.0         0
    6    -100.0   35.6875
    7    -100.0   71.3750
    8         0         0
    9         0   35.6875
   10         0   71.3750
   11     100.0         0
   12     100.0   35.6875
   13     100.0   71.3750
   14     200.0         0
   15     200.0   35.6875
   16     200.0   71.3750
   17     252.0         0
    1   17   16    0    0    0    0    1    1    1
    2   16    1    0    0    0    0    0    0    0
    1    3600.0      0.15 0.0000897
    1    1    2       7.50    1    4    1    0         0
    2   14   17       7.50    1    4    5    0         0
    3    2    5       7.50    1    4    1    2      50.0
    4    5    8       7.50    1    4    2    3      50.0
    5    8   11       7.50    1    4    3    4      50.0
    6   11   14       7.50    1    4    4    5      50.0
    7    4    7       5.75    1    4    1    2      50.0
    8    7   10       5.75    1    4    2    3      50.0
    9   10   13       5.75    1    4    3    4      50.0
   10   13   16       5.75    1    4    4    5      50.0
   11    2    3      12.00    1    4    1    0         0
   12    3    4      12.00    1    4    1    0         0
   13    5    6      12.00    1    4    2    0         0
   14    6    7      12.00    1    4    2    0         0
   15    8    9      12.00    1    4    3    0         0
   16    9   10      12.00    1    4    3    0         0
   17   11   12      12.00    1    4    4    0         0
   18   12   13      12.00    1    4    4    0         0
   19   14   15      12.00    1    4    5    0         0
   20   15   16      12.00    1    4    5    0         0
    0    0    0    1    1    1    1    1    0    0    0    0
    1    1800.0      12.0    1    0
         0     180.0     900.0    1620.0    1800.0    1994.0    2772.0
    3549.0    3744.0
0.08333333
       1.0         0         0
   11    3         0      9.36         0         0    2124.0      12.0
   11    3         0     17.28         0         0    2340.0      12.0
```



```
   11    3         0     17.28         0         0    2556.0      12.0
   11    3         0     17.28         0         0    2772.0      12.0
   11    3         0     17.28         0         0    2988.0      12.0
   11    3         0     17.28         0         0    3204.0      12.0
   11    3         0     17.28         0         0    3420.0      12.0
   14    3         0     16.64         0         0    2124.0      12.0
   14    3         0     30.72         0         0    2340.0      12.0
   14    3         0     30.72         0         0    2556.0      12.0
   14    3         0     30.72         0         0    2772.0      12.0
   14    3         0     30.72         0         0    2988.0      12.0
   14    3         0     30.72         0         0    3204.0      12.0
   14    3         0     30.72         0         0    3420.0      12.0
    1    2    1    2    1
 1580.0         0         0         0     7.803   29000.0         0       1.0
    1    1800.0
    2    1944.0
    1              0         0      50.0      10.0         0
  200.0     30.33     200.0     64.25     200.0      8.25
    2              0      10.0      50.0         0         0
  200.0      8.25     200.0     64.25     200.0     30.33
         0       1.0         0
    2    2    1    2    1
 1580.0         0         0         0     7.803   29000.0         0       1.0
    1    1800.0
    2    1944.0
    1              0         0      50.0      10.0         0
  100.0     30.33     100.0     64.25     100.0      8.25
    2              0      10.0      50.0         0         0
  100.0      8.25     100.0     64.25     100.0     30.33
         0       1.0         0
    3    2    1    2    1
 1580.0         0         0         0     7.803   29000.0         0       1.0
    1    1800.0
    2    1944.0
    1         0         0      50.0      10.0         0
         0     30.33         0     64.25         0      8.25
    2              0      10.0      50.0         0         0
         0      8.25         0     64.25         0     30.33
         0       1.0         0
    4    2    1    2    1
 1580.0         0         0         0     7.803   29000.0         0       1.0
    1    1800.0
    2    1944.0
    1              0         0      50.0      10.0         0
 -100.0     30.33    -100.0     64.25    -100.0      8.25
    2              0     10.00     50.00         0         0
 -100.0      8.25    -100.0     64.25    -100.0     30.33
         0       1.0         0
    5    2    1    2    1
 1580.0         0         0         0     7.803   29000.0         0       1.0
    1    1800.0
    2    1944.0
    1              0         0      50.0      10.0         0
 -200.0     30.33    -200.0     64.25    -200.0      8.25
```

```
2              0      10.0      50.0         0         0
-200.0      8.25    -200.0     64.25    -200.0     30.33
     0       1.0         0
```



```
EXAMPLE 5: CURDI4: CURVED: TWO SPAN (150,162FT): FOUR CELL BOX: FINE MESH
   27   30    1    1    0    0
    1    0    0    0
    3   14    0    5    0
    9    0  100    5    0    0
 3744.0    4800.0
    1    -252.0         0
    2    -226.0         0
    3    -200.0         0
    4    -200.0   35.6875
    5    -200.0   71.3750
    6    -150.0         0
    7    -150.0   71.3750
    8    -100.0         0
    9    -100.0   35.6875
   10    -100.0   71.3750
   11     -50.0         0
   12     -50.0   71.3750
   13         0         0
   14         0   35.6875
   15         0   71.3750
   16      50.0         0
   17      50.0   71.3750
   18     100.0         0
   19     100.0   35.6875
   20     100.0   71.3750
   21     150.0         0
   22     150.0   71.3750
   23     200.0         0
   24     200.0   35.6875
   25     200.0   71.3750
   26     226.0         0
   27     252.0         0
    1    2    1    0    0    0    0    1    1    1
   26   27    1    0    0    0    0    1    1    1
    3   25    1    0    0    0    0    0    0    0
    1  3600.0       0.15 0.0000897
    1    1    2       7.50    1    4    1    0
    2    2    3       7.50    1    4    1    0
    3    3    6       7.50    1    4    1    0
    4    6    8       7.50    1    4    2    0
    5    8   11       7.50    1    4    2    0
    6   11   13       7.50    1    4    3    0
    7   13   16       7.50    1    4    3    0
    8   16   18       7.50    1    4    4    0
    9   18   21       7.50    1    4    4    0
   10   21   23       7.50    1    4    5    0
   11   23   26       7.50    1    4    5    0
   12   26   27       7.50    1    4    5    0
   23    5    7       5.75    1    4    1    0
   24    7   10       5.75    1    4    2    0
   25   10   12       5.75    1    4    2    0
   26   12   15       5.75    1    4    3    0
   27   15   17       5.75    1    4    3    0
```

```
   28   17   20      5.75    1    4    4    0
   29   20   22      5.75    1    4    4    0
   30   22   25      5.75    1    4    5    0
   13    3    4     12.00    1    4    1    0
   14    4    5     12.00    1    4    1    0
   15    8    9     12.00    1    4    2    0
   16    9   10     12.00    1    4    2    0
   17   13   14     12.00    1    4    3    0
   18   14   15     12.00    1    4    3    0
   19   18   19     12.00    1    4    4    0
   20   19   20     12.00    1    4    4    0
   21   23   24     12.00    1    4    5    0
   22   24   25     12.00    1    4    5    0
    0    0    0    1    1    1    1    1    0    0    0    0
    1    1800.0      12.0    1    0
         0     180.0     900.0    1620.0    1800.0    1994.0    2772.0
    3549.0    3744.0
0.08333333
     1.0         0         0
   18    3         0      9.36         0         0    2124.0      12.0
   18    3         0     17.28         0         0    2340.0      12.0
   18    3         0     17.28         0         0    2556.0      12.0
   18    3         0     17.28         0         0    2772.0      12.0
   18    3         0     17.28         0         0    2988.0      12.0
   18    3         0     17.28         0         0    3204.0      12.0
   18    3         0     17.28         0         0    3420.0      12.0
   23    3         0     16.64         0         0    2124.0      12.0
   23    3         0     30.72         0         0    2340.0      12.0
   23    3         0     30.72         0         0    2556.0      12.0
   23    3         0     30.72         0         0    2772.0      12.0
   23    3         0     30.72         0         0    2988.0      12.0
   23    3         0     30.72         0         0    3204.0      12.0
   23    3         0     30.72         0         0    3420.0      12.0
    1    2    1    2    1
   1580.0         0         0         0     7.803   29000.0         0       1.0
    1    1800.0    0         0    0
    2    1944.0    0         0    0
    1              0         0      50.0      10.0         0
     200.0      30.33     200.0     64.25     200.0      8.25
    2              0         0      10.0      50.0         0         0
     200.0      8.25     200.0     64.25     200.0     30.33
         0       1.0         0
    2    2    1    2    1
   1580.0         0         0         0     7.803   29000.0         0       1.0
    1    1800.0    0         0    0
    2    1944.0    0         0    0
    1              0         0      50.0      10.0         0
     100.0      30.33     100.0     64.25       100      8.25
    2              0         0      10.0      50.0         0         0
     100.0      8.25     100.0     64.25       100     30.33
         0       1.0         0
    3    2    1    2    1
   1580.0         0         0         0     7.803   29000.0         0       1.0
    1    1800.0    0         0    0
```



```
    2    1944.0    0         0    0
    1              0         0      50.0      10.0         0
         0     30.33         0     64.25         0      8.25
    2              0      10.0      50.0         0         0
         0      8.25         0     64.25         0     30.33
         0       1.0         0
    4    2    1    2    1
   1580.0         0         0         0     7.803   29000.0         0       1.0
    1    1800.0    0         0    0
    2    1944.0    0         0    0
    1              0         0      50.0      10.0         0
  -100.0      30.33   -100.0     64.25    -100.0      8.25
    2              0      10.0      50.0         0         0
  -100.0       8.25   -100.0     64.25    -100.0     30.33
         0       1.0         0
    5    2    1    2    1
   1580.0         0         0         0     7.803   29000.0         0       1.0
    1    1800.0    0         0    0
    2    1944.0    0         0    0
    1              0         0      50.0      10.0         0
  -200.0      30.33   -200.0     64.25    -200.0      8.25
    2              0      10.0      50.0         0         0
  -200.0       8.25   -200.0     64.25    -200.0     30.33
         0       1.0         0
```

```
START
EXAMPLE 1: CELL4; MESH2; SIMPLE SPAN (162 FT): ANTI-SYMMETRIC BOUNDARY CONDITION
  40    1   45   55   33    5   30    3     67.8          0
   0    0    0    0    0    0    0    0
   1   00.0       180.0
   2   00.0       148.8
   6   10.0        81.0
   7   10.0        40.5
   8   10.0         0.0
   9    97.2       180.0
  10    97.2       148.8
  14   197.2        81.0
  15   197.2        40.5
  16   197.2         0.0
  17    194.4      180.0
  18    194.4      148.8
  22   1194.4       81.0
  23   1194.4       40.5
  24   1194.4        0.0
  25    291.6      180.0
  26    291.6      148.8
  30   1291.6       81.0
  31   1291.6       40.5
  32   1291.6        0.0
  33    388.8      180.0
  34    388.8      148.8
  38   1388.8       81.0
  39   1388.8       40.5
  40   1388.8        0.0
  41    486.0      180.0
  42    486.0      148.8
  46   1486.0       81.0
  47   1486.0       40.5
  48   1486.0        0.0
  49    583.2      180.0
  50    583.2      148.8
  54   1583.2       81.0
  55   1583.2       40.5
  56   1583.2        0.0
  57    680.4      180.0
  58    680.4      148.8
  62   1680.4       81.0
  63   1680.4       40.5
  64   1680.4        0.0
  65    777.6      180.0
  66    777.6      148.8
  70   1777.6       81.0
  71   1777.6       40.5
  72   1777.6        0.0
  73    874.8      180.0
  74    874.8      148.8
  78   1874.8       81.0
  79   1874.8       40.5
  80   1874.8        0.0
  81    972.0      180.0
  82    972.0      148.8
  86   1972.0       81.0
  87   1972.0       40.5
  88   1972.0        0.0
   3          0.0        122.85    -62.64
  83        972.0        122.85    -62.64        8
   4          0.0        100.86    -47.94
```



```
  84        972.0       100.86    -47.94        8
   5          0.0        86.16     -25.95
  85        972.0        86.16     -25.95        8
  13600.     3600.      1560.      0.15                  11.4
  23600.     3600.      1560.      0.15                  9.0
  33600.     3600.      1560.      0.15                  18.0
  41.0       1.0        0.5        0.0                   0.0
  53600.     3600.      1560.      0.15                  36.0
   1    1    2   10    9    1    2
  10   73   74   82   81    1    2    8
  11    2    6   14   10    1
  20   74   78   86   82    1         8
  21    6    7   15   14    1
  30   78   79   87   86    1         8
  31    7    8   16   15    1
  40   79   80   88   87    1         8
   1    1    2    4
   1    2    5    6    2    5
   2    2    4    5    2    5
   3    2    3    4    2    5
   4    2    2    3    2    5
   5    1    1    2    2    5
   6   11   10    2    3    3
  15   83   82   74   75    3    8
  16   12   11    3    4    3
  25   84   83   75   76    3    8
  26   13   12    4    5    3
  35   85   84   76   77    3    8
  36   14   13    5    6    3
  45   86   85   77   78    3    8
   1    T                   T
   1    T                   T    T
   9    T         T         T
   9    T         T         T    T
  17    T         T         T
  17    T         T         T    T
  25    T         T         T
  25    T         T         T    T
  33    T         T         T
  33    T         T         T    T
  41    T         T         T
  41    T         T         T    T
  49    T         T         T
  49    T         T         T    T
  57    T         T         T
  57    T         T         T    T
  65    T         T         T
  65    T         T         T    T
  73    T         T         T
  73    T         T         T    T
  81    T         T         T
  81    T         T         T    T
  82    T                   T
  82    T                   T    T
  83    T                   T    T
  84    T                   T    T
  85    T                   T    T
  86    T                   T
  87    T                   T
  88    T                   T
   1    1    1    9    1    2              1.E10
   2    2    1    9    1    2              1.E10
```

```
   3    1    2                                1.E10
LOAD
UNSYMMETRICAL LIVE LOAD - ONE LANE WITH 0.5*ASSHTO LANE LOAD (ANTI-SYMM. B.C.)
   5    1     -0.000148
  81                                -0.390
  82                                -1.23750
  86                                -1.353750
  87                                -1.01250
  88                                -0.506250
   1         1   -1  10000010          5
  11    8     0    8    8
   1    4     0    4    8    1    00.0        180.       -33.9
   1    2     3    4    5    6    7    8
   1    1
  11    1
  21    1
  31    1
   6    1
  16    1
  26    1
  36    1
   2    8     0    8    8    1    197.2       180.       -33.9
   9   10    11   12   13   14   15   16
   1    1
   2    1
  11    1
  12    1
  21    1
  22    1
  31    1
  32    1
   6    1
   7    1
  16    1
  17    1
  26    1
  27    1
  36    1
  37    1
  10    8     0    8    8    1    1874.8      180.       -33.9
  73   74    75   76   77   78   79   80
   9    1
  10    1
  19    1
  20    1
  29    1
  30    1
  39    1
  40    1
  14    1
  15    1
  24    1
  25    1
  34    1
  35    1
  44    1
  45    1
  11    4     0    4    8    1    0972.0      180.       -33.9
  81   82    83   84   85   86   87   88
  10    1
  20    1
  30    1
```



```
  40    1
  15    1
  25    1
  35    1
  45    1
STOP
```

```
START
EXAMPLE 1: CELL4: MESH2: SIMPLE SPAN (162 FT): SYMMETRIC BOUNDARY CONDITION
   40    1   45   55   33    5   30    2     67.8           0
    0    0    0    0    0    0    0    0
    1    00.0       180.0
    2    00.0       148.8
    6    10.0       81.0
    7    10.0       40.5
    8    10.0       0.0
    9     97.2      180.0
   10     97.2      148.8
   14    197.2      81.0
   15    197.2      40.5
   16    197.2      0.0
   17     194.4     180.0
   18     194.4     148.8
   22    1194.4     81.0
   23    1194.4     40.5
   24    1194.4     0.0
   25     291.6     180.0
   26     291.6     148.8
   30    1291.6     81.0
   31    1291.6     40.5
   32    1291.6     0.0
   33     388.8     180.0
   34     388.8     148.8
   38    1388.8     81.0
   39    1388.8     40.5
   40    1388.8     0.0
   41     486.0     180.0
   42     486.0     148.8
   46    1486.0     81.0
   47    1486.0     40.5
   48    1486.0     0.0
   49     583.2     180.0
   50     583.2     148.8
   54    1583.2     81.0
   55    1583.2     40.5
   56    1583.2     0.0
   57     680.4     180.0
   58     680.4     148.8
   62    1680.4     81.0
   63    1680.4     40.5
   64    1680.4     0.0
   65     777.6     180.0
   66     777.6     148.8
   70    1777.6     81.0
   71    1777.6     40.5
   72    1777.6     0.0
   73     874.8     180.0
   74     874.8     148.8
   78    1874.8     81.0
   79    1874.8     40.5
   80    1874.8     0.0
   81     972.0     180.0
   82     972.0     148.8
   86    1972.0     81.0
   87    1972.0     40.5
   88    1972.0     0.0
    3          0.0        122.85    -62.64
   83        972.0        122.85    -62.64        8
    4          0.0        100.86    -47.94
```



```
   84        972.0        100.86    -47.94        8
    5          0.0        86.16     -25.95
   85        972.0        86.16     -25.95        8
    13600.    3600.     1560.     0.15                  11.4
    23600.    3600.     1560.     0.15                  9.0
    33600.    3600.     1560.     0.15                  18.0
    41.0      1.0       0.5       0.0                   0.0
    53600.    3600.     1560.     0.15                  36.0
     1    1    2   10    9    1    2
   10   73   74   82   81    1    2    8
   11    2    6   14   10    1
   20   74   78   86   82    1         8
   21    6    7   15   14    1
   30   78   79   87   86    1         8
   31    7    8   16   15    1
   40   79   80   88   87    1         8
    1    1    2    4
    1    2    5    6    2    5
    2    2    4    5    2    5
    3    2    3    4    2    5
    4    2    2    3    2    5
    5    1    1    2    2    5
    6   11   10    2    3    3
   15   83   82   74   75    3    8
   16   12   11    3    4    3
   25   84   83   75   76    3    8
   26   13   12    4    5    3
   35   85   84   76   77    3    8
   36   14   13    5    6    3
   45   86   85   77   78    3    8
    1             T         T
    1             T         T         T
    9             T         T
    9             T         T         T
   17             T         T
   17             T         T         T
   25             T         T
   25             T         T         T
   33             T         T
   33             T         T         T
   41             T         T
   41             T         T         T
   49             T         T
   49             T         T         T
   57             T         T
   57             T         T         T
   65             T         T
   65             T         T         T
   73             T         T
   73             T         T         T
   81    T        T         T    T
   81    T        T         T    T    T
   82    T                       T
   82    T                       T    T
   83    T                       T    T
   84    T                       T    T
   85    T                       T    T
   86    T                       T
   87    T                       T
   88    T                       T
    1    1    1    9    1    2              1.E10
    2    2    1    9    1    2              1.E10
```

```
LOAD
DEAD LOAD OF BRIDGE
                1          0.0000897
    1           1   -1  10000010          5
   11    8      0    8    8
    1    4      0    4    8    1    00.0        180.       -33.9
    1    2      3    4    5    6    7    8
    1    1
   11    1
   21    1
   31    1
    6    1
   16    1
   26    1
   36    1
    2    8      0    8    8    1    197.2       180.       -33.9
    9   10     11   12   13   14   15   16
    1    1
    2    1
   11    1
   12    1
   21    1
   22    1
   31    1
   32    1
    6    1
    7    1
   16    1
   17    1
   26    1
   27    1
   36    1
   37    1
   10    8      0    8    8    1    1874.8      180.       -33.9
   73   74     75   76   77   78   79   80
    9    1
   10    1
   19    1
   20    1
   29    1
   30    1
   39    1
   40    1
   14    1
   15    1
   24    1
   25    1
   34    1
   35    1
   44    1
   45    1
   11    4      0    4    8    1    0972.0      180.       -33.9
   81   82     83   84   85   86   87   88
   10    1
   20    1
   30    1
   40    1
   15    1
   25    1
   35    1
   45    1
LOAD
```



```
UNSYMMETRICAL LIVE LOAD - ONE LANE WITH 0.5 * ASSHTO LANE LOAD (SYMM. B.C.)
    5    1      -0.000148
   81                          -0.390
   82                          -1.23750
   86                          -1.353750
   87                          -1.01250
   88                          -0.506250
    1           1   -1  10000010          5
   11    8      0    8    8
    1    4      0    4    8    1    00.0        180.       -33.9
    1    2      3    4    5    6    7    8
    1    1
   11    1
   21    1
   31    1
    6    1
   16    1
   26    1
   36    1
    2    8      0    8    8    1    197.2       180.       -33.9
    9   10     11   12   13   14   15   16
    1    1
    2    1
   11    1
   12    1
   21    1
   22    1
   31    1
   32    1
    6    1
    7    1
   16    1
   17    1
   26    1
   27    1
   36    1
   37    1
   10    8      0    8    8    1    1874.8      180.       -33.9
   73   74     75   76   77   78   79   80
    9    1
   10    1
   19    1
   20    1
   29    1
   30    1
   39    1
   40    1
   14    1
   15    1
   24    1
   25    1
   34    1
   35    1
   44    1
   45    1
   11    4      0    4    8    1    0972.0      180.       -33.9
   81   82     83   84   85   86   87   88
   10    1
   20    1
   30    1
   40    1
   15    1
```

```
   25    1
   35    1
   45    1
STOP
```



```
START
EXAMPLE 1: CELL4: MESH1: SIMPLE SPAN (162 FT): SYMMETRIC BOUNDARY CONDITION
   40    1   20   55   11    4   28    6     67.8          0
    0    0    0    0    0    0    0    0    0
    1    00.0       180.0
    2    00.0       148.8
    4    10.0       81.0
    5    10.0       40.5
    6    10.0       0.0
    7     97.2      180.0
    8     97.2      148.8
   10    197.2      81.0
   11    197.2      40.5
   12    197.2      0.0
   13     194.4     180.0
   14     194.4     148.8
   16    1194.4     81.0
   17    1194.4     40.5
   18    1194.4     0.0
   19     291.6     180.0
   20     291.6     148.8
   22    1291.6     81.0
   23    1291.6     40.5
   24    1291.6     0.0
   25     388.8     180.0
   26     388.8     148.8
   28    1388.8     81.0
   29    1388.8     40.5
   30    1388.8     0.0
   31     486.0     180.0
   32     486.0     148.8
   34    1486.0     81.0
   35    1486.0     40.5
   36    1486.0     0.0
   37     583.2     180.0
   38     583.2     148.8
   40    1583.2     81.0
   41    1583.2     40.5
   42    1583.2     0.0
   43     680.4     180.0
   44     680.4     148.8
   46    1680.4     81.0
   47    1680.4     40.5
   48    1680.4     0.0
   49     777.6     180.0
   50     777.6     148.8
   52    1777.6     81.0
   53    1777.6     40.5
   54    1777.6     0.0
   55     874.8     180.0
   56     874.8     148.8
   58    1874.8     81.0
   59    1874.8     40.5
   60    1874.8     0.0
   61     972.0     180.0
   62     972.0     148.8
   64    1972.0     81.0
   65    1972.0     40.5
   66    1972.0     0.0
    3          0.0        100.86    -47.94
    9          97.2       100.86    -47.94
   15          194.4      100.86    -47.94
```

```
   21          291.6      100.86     -47.94
   27          388.8      100.86     -47.94
   33          486.0      100.86     -47.94
   39          583.2      100.86     -47.94
   45          680.4      100.86     -47.94
   51          777.6      100.86     -47.94
   57          874.8      100.86     -47.94
   63          972.0      100.86     -47.94
    13600.     3600.      1560.      0.15                  11.4
    23600.     3600.      1560.      0.15                  9.0
    33600.     3600.      1560.      0.15                  18.0
    41.0       1.0        0.5        0.0                   0.0
    1    1     2    8     7     1    2
   10   55    56   62    61     1    2     6
   11    2     4   10     8     1
   20   56    58   64    62     1          6
   21    4     5   11    10     1
   30   58    59   65    64     1          6
   31    5     6   12    11     1
   40   59    60   66    65     1          6
    1    1     2    4
    1    9     8    2     3     3
   10   63    62   56    57     3     6
   11   10     9    3     4     3
   20   64    63   57    58     3     6
    1              T           T
    1              T           T          T
    7              T           T
    7              T           T          T
   13              T           T
   13              T           T          T
   19              T           T
   19              T           T          T
   25              T           T
   25              T           T          T
   31              T           T
   31              T           T          T
   37              T           T
   37              T           T          T
   43              T           T
   43              T           T          T
   49              T           T
   49              T           T          T
   55              T           T
   55              T           T          T
   61    T         T           T     T
   61    T         T           T     T    T
   62    T                           T
   62    T                           T    T
   63    T                           T    T
   64    T                           T
   65    T                           T
   66    T                           T
    1    1     1    7     1     2    T      1.E10
    2    1     1    7     1     2           1.E10
    3    2     1    7     1     2    T      1.E10
    4    2     1    7     1     2           1.E10
    5    3     1    7     1     2           1.E10
    6    4     1    7     1     2    T      1.E10
LOAD
               1          0.0000897
    1          1   24  10000010
```



```
    1    2     3    4     5     6     7     8     9    10    11    12    31    32    33    34
   35   36    61   62    63    64    65    66
    3    4     0    2     6
    1    4     0    2     6     1972.0      180.0      -33.9
   66   65    64   63    62    61
   10    1
   20    1
   30    1
   40    1
   10    1
   20    1
    2    4     0    2     6     1486.0      180.0      -33.9
   36   35    34   33    32    31
    5    1
   15    1
   25    1
   35    1
    5    1
   15    1
    3    4     0    2     6     10.0        180.0      -33.9
    1    2     3    4     5     6
    1    1
   11    1
   21    1
   31    1
    1    1
   11    1
STOP
```

```
START
EXAMPLE 2: CELL4: SIMPLE SPAN (162 FT): VERTICAL WEBS: SYMMETRIC BOUNDARY COND.
   40   12    1   55    0    5   28    3     67.8          0
    0    0    0    0    1    0   10   11
    1    00.0       180.0
    2    00.0       136.5
    3    00.0       93.0
    4    10.0       46.5
    5    10.0       0.0
    6     97.2      180.0
    7     97.2      136.5
    8     97.2      93.0
    9    197.2      46.5
   10    197.2      0.0
   11     194.4     180.0
   12     194.4     136.5
   13     194.4     93.0
   14    1194.4     46.5
   15    1194.4     0.0
   16     291.6     180.0
   17     291.6     136.5
   18     291.6     93.0
   19    1291.6     46.5
   20    1291.6     0.0
   21     388.8     180.0
   22     388.8     136.5
   23     388.8     93.0
   24    1388.8     46.5
   25    1388.8     0.0
   26     486.0     180.0
   27     486.0     136.5
   28     486.0     93.0
   29    1486.0     46.5
   30    1486.0     0.0
   31     583.2     180.0
   32     583.2     136.5
   33     583.2     93.0
   34    1583.2     46.5
   35    1583.2     0.0
   36     680.4     180.0
   37     680.4     136.5
   38     680.4     93.0
   39    1680.4     46.5
   40    1680.4     0.0
   41     777.6     180.0
   42     777.6     136.5
   43     777.6     93.0
   44    1777.6     46.5
   45    1777.6     0.0
   46     874.8     180.0
   47     874.8     136.5
   48     874.8     93.0
   49    1874.8     46.5
   50    1874.8     0.0
   51     972.0     180.0
   52     972.0     136.5
   53     972.0     93.0
   54    1972.0     46.5
   55    1972.0     0.0
  13600.      3600.      1560.      0.15              11.4
  23600.      3600.      1560.      0.15              9.0
  33600.      3600.      1560.      0.15              18.0
```



```
   41.0        1.0         0.5         0.0                    0.0
   53600.      3600.       1560.       0.15                   36.0
    1    1    2    7    6    1    2
   10   46   47   52   51    1    2    5
   11    2    3    8    7    1    2
   20   47   48   53   52    1    2    5
   21    3    4    9    8    1
   30   48   49   54   53    1         5
   31    4    5   10    9    1
   40   49   50   55   54    1         5
    1    1    2    5
    2    2    3    5
    3    3    8    3
   12   48   53    3    5
    1    1    1    2    2    4
    1         T         T
    1         T         T         T
    6         T         T
    6         T         T         T
   11         T         T
   11         T         T         T
   16         T         T
   16         T         T         T
   21         T         T
   21         T         T         T
   26         T         T
   26         T         T         T
   31         T         T
   31         T         T         T
   36         T         T
   36         T         T         T
   41         T         T
   41         T         T         T
   46         T         T
   46         T         T         T
   51    T    T         T    T
   51    T    T         T    T    T
   52    T                   T
   52    T                   T    T
   53    T                   T
   53    T                   T    T
   54    T                   T
   55    T                   T
    1    1    1    6    1    2              1.E10
    2    2    1    6    1    2              1.E10
    3    3    1    6    1    2              1.E10
    1    1    1
3640.
0.0         1.0         0.0
-24.3      -61.2996    -61.2996
    3   12    3
LOAD
PRESTRESSING IN VERTICAL WEB WITHOUT FRICTION LOSSES
                                          1.0
    1         1   -1  10001000    2
   11    8    2    0    5
    1    4    1    0    5    1    00.0        180.       -23.292
    1    2    3    4    5
    1    1
   11    1
   21    1
   31    1
```

```
     3    1
     2    8    2    0    5    1    197.2       180.       -23.292
     6    7    8    9   10
     1    1
     2    1
    11    1
    12    1
    21    1
    22    1
    31    1
    32    1
     3    1
     4    1
    10    8    2    0    5    1    1874.8      180.       -23.292
    46   47   48   49   50
     9    1
    10    1
    19    1
    20    1
    29    1
    30    1
    39    1
    40    1
    11    1
    12    1
    11    4    1    0    5    1    0972.0      180.       -23.292
    51   52   53   54   55
    10    1
    20    1
    30    1
    40    1
    12    1
LOAD
DEAD LOAD OF BRIDGE
                1          0.0000897
     1          1   -1  10001000    2
    11    8    2    0    5
     1    4    1    0    5    1    00.0        180.       -23.292
     1    2    3    4    5
     1    1
    11    1
    21    1
    31    1
     3    1
     2    8    2    0    5    1    197.2       180.       -23.292
     6    7    8    9   10
     1    1
     2    1
    11    1
    12    1
    21    1
    22    1
    31    1
    32    1
     3    1
     4    1
    10    8    2    0    5    1    1874.8      180.       -23.292
    46   47   48   49   50
     9    1
    10    1
    19    1
    20    1
```



```
    29    1
    30    1
    39    1
    40    1
    11    1
    12    1
    11    4    1    0    5    1    0972.0      180.       -23.292
    51   52   53   54   55
    10    1
    20    1
    30    1
    40    1
    12    1
STOP
```

```
START
EXAMPLE 2: CELL4: SIMPLE SPAN (162 FT): VERTICAL WEBS: SYMM. AASHTO LANE LOAD
   40   12    1   55    0    5   28    3     67.8          0
    0    0    0    0    1    0   10   11
    1    00.0       180.0
    2    00.0       136.5
    3    00.0       93.0
    4    10.0       46.5
    5    10.0       0.0
    6     97.2      180.0
    7     97.2      136.5
    8     97.2      93.0
    9    197.2      46.5
   10    197.2      0.0
   11     194.4     180.0
   12     194.4     136.5
   13     194.4     93.0
   14    1194.4     46.5
   15    1194.4     0.0
   16     291.6     180.0
   17     291.6     136.5
   18     291.6     93.0
   19    1291.6     46.5
   20    1291.6     0.0
   21     388.8     180.0
   22     388.8     136.5
   23     388.8     93.0
   24    1388.8     46.5
   25    1388.8     0.0
   26     486.0     180.0
   27     486.0     136.5
   28     486.0     93.0
   29    1486.0     46.5
   30    1486.0     0.0
   31     583.2     180.0
   32     583.2     136.5
   33     583.2     93.0
   34    1583.2     46.5
   35    1583.2     0.0
   36     680.4     180.0
   37     680.4     136.5
   38     680.4     93.0
   39    1680.4     46.5
   40    1680.4     0.0
   41     777.6     180.0
   42     777.6     136.5
   43     777.6     93.0
   44    1777.6     46.5
   45    1777.6     0.0
   46     874.8     180.0
   47     874.8     136.5
   48     874.8     93.0
   49    1874.8     46.5
   50    1874.8     0.0
   51     972.0     180.0
   52     972.0     136.5
   53     972.0     93.0
   54    1972.0     46.5
   55    1972.0     0.0
  13600.      3600.      1560.      0.15              11.4
  23600.      3600.      1560.      0.15              9.0
  33600.      3600.      1560.      0.15              18.0
```



```
    41.0        1.0        0.5        0.0                  0.0
   53600.      3600.      1560.       0.15                36.0
    1    1    2    7    6    1    2
   10   46   47   52   51    1    2    5
   11    2    3    8    7    1    2
   20   47   48   53   52    1    2    5
   21    3    4    9    8    1
   30   48   49   54   53    1         5
   31    4    5   10    9    1
   40   49   50   55   54    1         5
    1    1    2    5
    2    2    3    5
    3    3    8    3
   12   48   53    3    5
    1    1    1    2    2    4
    1         T         T
    1         T         T         T
    6         T         T
    6         T         T         T
   11         T         T
   11         T         T         T
   16         T         T
   16         T         T         T
   21         T         T
   21         T         T         T
   26         T         T
   26         T         T         T
   31         T         T
   31         T         T         T
   36         T         T
   36         T         T         T
   41         T         T
   41         T         T         T
   46         T         T
   46         T         T         T
   51    T    T         T    T
   51    T    T         T    T    T
   52    T                   T
   52    T                   T    T
   53    T                   T
   53    T                   T    T
   54    T                   T
   55    T                   T
    1    1    1    6    1    2              1.E10
    2    2    1    6    1    2              1.E10
    3    3    1    6    1    2              1.E10
    1    1    1
3640.
0.0         1.0        0.0
-24.3      -61.2996   -61.2996
    3   12    3
LOAD
SYMMETRIC ASSHTO LANE LOAD (NO IMPACT FACTOR)
    5    1      -0.0002962
   51                              -1.0875
   52                              -2.175
   53                              -2.25
   54                              -2.325
   55                              -1.1625
    1         1   -1  10001000    2
   11    8    2    0    5
    1    4    1    0    5    1    00.0        180.       -23.292
```

```
    1    2    3    4    5
    1    1
   11    1
   21    1
   31    1
    3    1
    2    8    2    0    5    1    197.2      180.       -23.292
    6    7    8    9   10
    1    1
    2    1
   11    1
   12    1
   21    1
   22    1
   31    1
   32    1
    3    1
    4    1
   10    8    2    0    5    1    1874.8     180.       -23.292
   46   47   48   49   50
    9    1
   10    1
   19    1
   20    1
   29    1
   30    1
   39    1
   40    1
   11    1
   12    1
   11    4    1    0    5    1    0972.0     180.       -23.292
   51   52   53   54   55
   10    1
   20    1
   30    1
   40    1
   12    1
STOP
```



```
START
EXAMPLE 2: CELL4: SIMPLE SPAN (162 FT): VERTICAL WEBS: ANTI-SYMM. AASHTO LANE LD
   40   12    1   55    0    5   28    3     67.8          0
    0    0    0    0    1    0   10   11
    1    00.0       180.0
    2    00.0       136.5
    3    00.0       93.0
    4    10.0       46.5
    5    10.0       0.0
    6     97.2      180.0
    7     97.2      136.5
    8     97.2      93.0
    9    197.2      46.5
   10    197.2      0.0
   11     194.4     180.0
   12     194.4     136.5
   13     194.4     93.0
   14    1194.4     46.5
   15    1194.4     0.0
   16     291.6     180.0
   17     291.6     136.5
   18     291.6     93.0
   19    1291.6     46.5
   20    1291.6     0.0
   21     388.8     180.0
   22     388.8     136.5
   23     388.8     93.0
   24    1388.8     46.5
   25    1388.8     0.0
   26     486.0     180.0
   27     486.0     136.5
   28     486.0     93.0
   29    1486.0     46.5
   30    1486.0     0.0
   31     583.2     180.0
   32     583.2     136.5
   33     583.2     93.0
   34    1583.2     46.5
   35    1583.2     0.0
   36     680.4     180.0
   37     680.4     136.5
   38     680.4     93.0
   39    1680.4     46.5
   40    1680.4     0.0
   41     777.6     180.0
   42     777.6     136.5
   43     777.6     93.0
   44    1777.6     46.5
   45    1777.6     0.0
   46     874.8     180.0
   47     874.8     136.5
   48     874.8     93.0
   49    1874.8     46.5
   50    1874.8     0.0
   51     972.0     180.0
   52     972.0     136.5
   53     972.0     93.0
   54    1972.0     46.5
   55    1972.0     0.0
  13600.     3600.     1560.     0.15              11.4
  23600.     3600.     1560.     0.15              9.0
  33600.     3600.     1560.     0.15              18.0
```

```
  41.0        1.0        0.5        0.0                    0.0
  53600.      3600.      1560.      0.15                   36.0
   1    1    2    7    6    1    2
  10   46   47   52   51    1    2    5
  11    2    3    8    7    1    2
  20   47   48   53   52    1    2    5
  21    3    4    9    8    1
  30   48   49   54   53    1         5
  31    4    5   10    9    1
  40   49   50   55   54    1         5
   1    1    2    5
   2    2    3    5
   3    3    8    3
  12   48   53    3    5
   1    1    1    2    2    4
   1    T         T         T
   1    T         T         T    T
   6    T         T         T
   6    T         T         T    T
  11    T         T         T
  11    T         T         T    T
  16    T         T         T
  16    T         T         T    T
  21    T         T         T
  21    T         T         T    T
  26    T         T         T
  26    T         T         T    T
  31    T         T         T
  31    T         T         T    T
  36    T         T         T
  36    T         T         T    T
  41    T         T         T
  41    T         T         T    T
  46    T         T         T
  46    T         T         T    T
  51    T         T         T
  51    T         T         T    T
  52    T                   T
  52    T                   T    T
  53    T                   T
  53    T                   T    T
  54    T                   T
  55    T                   T
   1    2    1    6    1    2              1.E10
   2    3    1    6    1    2              1.E10
   3    3    2                             1.E10
   1    1    1
3640.
0.0        1.0        0.0
-24.3      -61.2996   -61.2996
   3   12    3
LOAD
ANTI-SYMMETRIC ASSHTO LANE LOAD (NO IMPACT FACTOR)
   5    1      -0.0002962
  51                                -1.0875
  52                                -2.175
  53                                -2.25
  54                                -2.325
  55                                -1.1625
   1         1   -1  10001000    2
  11    8    2    0    5
   1    4    1    0    5    1    00.0        180.       -23.292
```



```
   1    2    3    4    5
   1    1
  11    1
  21    1
  31    1
   3    1
   2    8    2    0    5    1    197.2       180.       -23.292
   6    7    8    9   10
   1    1
   2    1
  11    1
  12    1
  21    1
  22    1
  31    1
  32    1
   3    1
   4    1
  10    8    2    0    5    1    1874.8      180.       -23.292
  46   47   48   49   50
   9    1
  10    1
  19    1
  20    1
  29    1
  30    1
  39    1
  40    1
  11    1
  12    1
  11    4    1    0    5    1    0972.0      180.       -23.292
  51   52   53   54   55
  10    1
  20    1
  30    1
  40    1
  12    1
STOP
```

```
START
EXAMPLE 2: CELL4: SIMPLE SPAN (162 FT): VERTICAL WEBS: PANEL PRESTRESS/FRICTION
   40   12    1   55    0    5   28    3     67.8          0
    0    0    0    0    1    0   10   11
    1    00.0       180.0
    2    00.0       136.5
    3    00.0       93.0
    4    10.0       46.5
    5    10.0       0.0
    6     97.2      180.0
    7     97.2      136.5
    8     97.2      93.0
    9    197.2      46.5
   10    197.2      0.0
   11     194.4     180.0
   12     194.4     136.5
   13     194.4     93.0
   14    1194.4     46.5
   15    1194.4     0.0
   16     291.6     180.0
   17     291.6     136.5
   18     291.6     93.0
   19    1291.6     46.5
   20    1291.6     0.0
   21     388.8     180.0
   22     388.8     136.5
   23     388.8     93.0
   24    1388.8     46.5
   25    1388.8     0.0
   26     486.0     180.0
   27     486.0     136.5
   28     486.0     93.0
   29    1486.0     46.5
   30    1486.0     0.0
   31     583.2     180.0
   32     583.2     136.5
   33     583.2     93.0
   34    1583.2     46.5
   35    1583.2     0.0
   36     680.4     180.0
   37     680.4     136.5
   38     680.4     93.0
   39    1680.4     46.5
   40    1680.4     0.0
   41     777.6     180.0
   42     777.6     136.5
   43     777.6     93.0
   44    1777.6     46.5
   45    1777.6     0.0
   46     874.8     180.0
   47     874.8     136.5
   48     874.8     93.0
   49    1874.8     46.5
   50    1874.8     0.0
   51     972.0     180.0
   52     972.0     136.5
   53     972.0     93.0
   54    1972.0     46.5
   55    1972.0     0.0
    13600.     3600.     1560.     0.15              11.4
    23600.     3600.     1560.     0.15              9.0
    33600.     3600.     1560.     0.15              18.0
```



```
    41.0       1.0       0.5       0.0                 0.0
    53600.     3600.     1560.     0.15                36.0
     1    1    2    7    6    1    2
    10   46   47   52   51    1    2    5
    11    2    3    8    7    1    2
    20   47   48   53   52    1    2    5
    21    3    4    9    8    1
    30   48   49   54   53    1         5
    31    4    5   10    9    1
    40   49   50   55   54    1         5
     1    1    2    5
     2    2    3    5
     3    3    8    3
    12   48   53    3    5
     1    1    1    2    2    4
     1         T         T
     1         T         T         T
     6         T         T
     6         T         T         T
    11         T         T
    11         T         T         T
    16         T         T
    16         T         T         T
    21         T         T
    21         T         T         T
    26         T         T
    26         T         T         T
    31         T         T
    31         T         T         T
    36         T         T
    36         T         T         T
    41         T         T
    41         T         T         T
    46         T         T
    46         T         T         T
    51    T    T         T    T
    51    T    T         T    T    T
    52    T                   T
    52    T                   T    T
    53    T                   T
    53    T                   T    T
    54    T                   T
    55    T                   T
     1    1    1    6    1    2              1.E10
     2    2    1    6    1    2              1.E10
     3    3    1    6    1    2              1.E10
     1    1    1
4266.0              0.25      0.0000167 22.6      28000.    0.1875
0.0        1.0      0.0
-24.3     -61.2996  -61.2996
    3   12    3
LOAD
PRESTRESSING IN VERTICAL WEB WITH ANCHORAGE SLIP AND FRICTION LOSSES
                                        1.0
     1         1   -1  10001000    2
    11    8    2    0    5
     1    4    1    0    5    1    00.0       180.       -23.292
     1    2    3    4    5
     1    1
    11    1
    21    1
    31    1
```

```
    3    1
    2    8    2    0    5    1    197.2      180.       -23.292
    6    7    8    9   10
    1    1
    2    1
   11    1
   12    1
   21    1
   22    1
   31    1
   32    1
    3    1
    4    1
   10    8    2    0    5    1    1874.8     180.       -23.292
   46   47   48   49   50
    9    1
   10    1
   19    1
   20    1
   29    1
   30    1
   39    1
   40    1
   11    1
   12    1
   11    4    1    0    5    1    0972.0     180.       -23.292
   51   52   53   54   55
   10    1
   20    1
   30    1
   40    1
   12    1
STOP
```



```
START
EXAMPLE 2: CELL4: SIMPLE SPAN (162 FT): VERTICAL WEBS: SLAB PRESTRESS-NO FRICT.
   40   10    1   55    0    4   28    6     67.8          0
    0   10    0    0    0    0   10   11
    1    00.0       180.0
    2    00.0       136.5
    3    00.0       93.0
    4    10.0       46.5
    5    10.0       0.0
    6     97.2      180.0
    7     97.2      136.5
    8     97.2      93.0
    9    197.2      46.5
   10    197.2      0.0
   11     194.4     180.0
   12     194.4     136.5
   13     194.4     93.0
   14    1194.4     46.5
   15    1194.4     0.0
   16     291.6     180.0
   17     291.6     136.5
   18     291.6     93.0
   19    1291.6     46.5
   20    1291.6     0.0
   21     388.8     180.0
   22     388.8     136.5
   23     388.8     93.0
   24    1388.8     46.5
   25    1388.8     0.0
   26     486.0     180.0
   27     486.0     136.5
   28     486.0     93.0
   29    1486.0     46.5
   30    1486.0     0.0
   31     583.2     180.0
   32     583.2     136.5
   33     583.2     93.0
   34    1583.2     46.5
   35    1583.2     0.0
   36     680.4     180.0
   37     680.4     136.5
   38     680.4     93.0
   39    1680.4     46.5
   40    1680.4     0.0
   41     777.6     180.0
   42     777.6     136.5
   43     777.6     93.0
   44    1777.6     46.5
   45    1777.6     0.0
   46     874.8     180.0
   47     874.8     136.5
   48     874.8     93.0
   49    1874.8     46.5
   50    1874.8     0.0
   51     972.0     180.0
   52     972.0     136.5
   53     972.0     93.0
   54    1972.0     46.5
   55    1972.0     0.0
  13600.      3600.      1560.      0.15              11.4
  23600.      3600.      1560.      0.15              9.0
  33600.      3600.      1560.      0.15              18.0
```

```
  41.0        1.0         0.5         0.0                    0.0
    1    1    2    7    6    1    2
   10   46   47   52   51    1    2    5
   11    2    3    8    7    1    2
   20   47   48   53   52    1    2    5
   21    3    4    9    8    1
   30   48   49   54   53    1         5
   31    4    5   10    9    1
   40   49   50   55   54    1         5
    1    3    8    3
   10   48   53    3    5
    1    1    1    2    2    4
    1              T         T
    1              T         T         T
    6              T         T
    6              T         T         T
   11              T         T
   11              T         T         T
   16              T         T
   16              T         T         T
   21              T         T
   21              T         T         T
   26              T         T
   26              T         T         T
   31              T         T
   31              T         T         T
   36              T         T
   36              T         T         T
   41              T         T
   41              T         T         T
   46              T         T
   46              T         T         T
   51    T         T         T    T
   51    T         T         T    T    T
   52    T                        T
   52    T                        T    T
   53    T                        T
   53    T                        T    T
   54    T                        T
   55    T                        T
    1    1    1    6    1    2    T    1.E10
    2    1    1    6    1    2         1.E10
    3    2    1    6    1    2    T    1.E10
    4    2    1    6    1    2         1.E10
    5    3    1    6    1    2    T    1.E10
    6    3    1    6    1    2         1.E10
    1    1    2
243.
48.6        48.6        48.6
180.        90.         0.0
0.0         0.0         0.2
-1.5        -1.5        5.0
    1   11    1    6
48.6        48.6        48.6
93.         40.         0.0
0.5         1.0         0.0
5.0         0.5         0.5
   21   31    3    8
    1    1    2
243.
145.8       145.8       145.8
180.        90.         0.0
```



```
0.0         0.0         0.2
-1.5        -1.5        5.0
    2   12    6   11
145.8       145.8       145.8
93.         40.         0.0
0.5         1.0         0.0
5.0         0.5         0.5
   22   32    8   13
    1    1    2
243.
243.        243.        243.
180.        90.         0.0
0.0         0.0         0.2
-1.5        -1.5        5.0
    3   13   11   16
243.        243.        243.
93.         40.         0.0
0.5         1.0         0.0
5.0         0.5         0.5
   23   33   13   18
    1    1    2
243.
340.2       340.2       340.2
180.        90.         0.0
0.0         0.0         0.2
-1.5        -1.5        5.0
    4   14   16   21
340.2       340.2       340.2
93.         40.         0.0
0.5         1.0         0.0
5.0         0.5         0.5
   24   34   18   23
    1    1    2
243.
437.4       437.4       437.4
180.        90.         0.0
0.0         0.0         0.2
-1.5        -1.5        5.0
    5   15   21   26
437.4       437.4       437.4
93.         40.         0.0
0.5         1.0         0.0
5.0         0.5         0.5
   25   35   23   28
    1    1    2
243.
534.6       534.6       534.6
180.        90.         0.0
0.0         0.0         0.2
-1.5        -1.5        5.0
    6   16   26   31
534.6       534.6       534.6
93.         40.         0.0
0.5         1.0         0.0
5.0         0.5         0.5
   26   36   28   33
    1    1    2
243.
631.8       631.8       631.8
180.        90.         0.0
0.0         0.0         0.2
-1.5        -1.5        5.0
```

```
    7   17   31   36
631.8      631.8      631.8
93.         40.         0.0
0.5         1.0         0.0
5.0         0.5         0.5
   27   37   33   38
    1    1    2
243.
729.       729.       729.
180.        90.         0.0
0.0         0.0         0.2
-1.5       -1.5         5.0
    8   18   36   41
729.       729.       729.
93.         40.         0.0
0.5         1.0         0.0
5.0         0.5         0.5
   28   38   38   43
    1    1    2
243.
826.2      826.2      826.2
180.        90.         0.0
0.0         0.0         0.2
-1.5       -1.5         5.0
    9   19   41   46
826.2      826.2      826.2
93.         40.         0.0
0.5         1.0         0.0
5.0         0.5         0.5
   29   39   43   48
    1    1    2
243.
923.4      923.4      923.4
180.        90.         0.0
0.0         0.0         0.2
-1.5       -1.5         5.0
   10   20   46   51
923.4      923.4      923.4
93.         40.         0.0
0.5         1.0         0.0
5.0         0.5         0.5
   30   40   48   53
LOAD
SINGLE CELL WITH VERTICAL WEB - SLAB PRESTRESSING (FRICTION EFFECTS IGNORED)
                                      1.0
    1         1   -1  10001000
   11    8    2    0    5
    1    4    1    0    5    1    00.0       180.       -33.9
    1    2    3    4    5
    1    1
   11    1
   21    1
   31    1
    1    1
    2    8    2    0    5    1    197.2      180.       -33.9
    6    7    8    9   10
    1    1
    2    1
   11    1
   12    1
   21    1
   22    1
```



```
   31    1
   32    1
    1    1
    2    1
   10    8    2    0    5    1    1874.8     180.       -33.9
   46   47   48   49   50
    9    1
   10    1
   19    1
   20    1
   29    1
   30    1
   39    1
   40    1
    9    1
   10    1
   11    4    1    0    5    1    0972.0     180.       -33.9
   51   52   53   54   55
   10    1
   20    1
   30    1
   40    1
   10    1
STOP
```

```
START
EXAMPLE 2: CELL4: SIMPLE SPAN (162 FT): SLOPING WEBS: SYMMETRIC BOUNDARY COND.
   50    2   11   66    0    5   29    3     67.8          0
    0    0    0    0    0    1   10   11
    1    00.0       180.0
    2    00.0       136.5
    3    00.0       93.0
    4    10.0       75.0
    5    10.0       37.5
    6    10.0       0.0
    7     97.2      180.0
    8     97.2      136.5
    9     97.2      93.0
   10    197.2      75.0
   11    197.2      37.5
   12    197.2      0.0
   13     194.4     180.0
   14     194.4     136.5
   15     194.4     93.0
   16    1194.4     75.0
   17    1194.4     37.5
   18    1194.4     0.0
   19     291.6     180.0
   20     291.6     136.5
   21     291.6     93.0
   22    1291.6     75.0
   23    1291.6     37.5
   24    1291.6     0.0
   25     388.8     180.0
   26     388.8     136.5
   27     388.8     93.0
   28    1388.8     75.0
   29    1388.8     37.5
   30    1388.8     0.0
   31     486.0     180.0
   32     486.0     136.5
   33     486.0     93.0
   34    1486.0     75.0
   35    1486.0     37.5
   36    1486.0     0.0
   37     583.2     180.0
   38     583.2     136.5
   39     583.2     93.0
   40    1583.2     75.0
   41    1583.2     37.5
   42    1583.2     0.0
   43     680.4     180.0
   44     680.4     136.5
   45     680.4     93.0
   46    1680.4     75.0
   47    1680.4     37.5
   48    1680.4     0.0
   49     777.6     180.0
   50     777.6     136.5
   51     777.6     93.0
   52    1777.6     75.0
   53    1777.6     37.5
   54    1777.6     0.0
   55     874.8     180.0
   56     874.8     136.5
   57     874.8     93.0
   58    1874.8     75.0
```



```
   59    1874.8     37.5
   60    1874.8     0.0
   61     972.0     180.0
   62     972.0     136.5
   63     972.0     93.0
   64    1972.0     75.0
   65    1972.0     37.5
   66    1972.0     0.0
    13600.      3600.      1560.      0.15                11.4
    23600.      3600.      1560.      0.15                9.0
    33600.      3600.      1560.      0.15                17.4
    41.0        1.0        0.5        0.0                 0.0
    53600.      3600.      1560.      0.15                36.
    1    1    2    8    7    1    2
   10   55   56   62   61    1    2    6
   11    2    3    9    8    1    2
   20   56   57   63   62    1    2    6
   21    3    4   10    9    1
   30   57   58   64   63    1         6
   31    4    5   11   10    1
   40   58   59   65   64    1         6
   41    5    6   12   11    1
   50   59   60   66   65    1         6
    1    1    2    5
    2    2    3    5
    1    3    3    4    3    5
    2   10    9    3    4    3
   11   64   63   57   58    3    6
    1              T         T
    1              T         T         T
    7              T         T
    7              T         T         T
   13              T         T
   13              T         T         T
   19              T         T
   19              T         T         T
   25              T         T
   25              T         T         T
   31              T         T
   31              T         T         T
   37              T         T
   37              T         T         T
   43              T         T
   43              T         T         T
   49              T         T
   49              T         T         T
   55              T         T
   55              T         T         T
   61    T         T         T    T
   61    T    T              T    T    T
   62    T                        T
   62    T                        T    T
   63    T                        T
   63    T                        T    T
   64    T                        T
   65    T                        T
   66    T                        T
    1    1    1    7    1    2              1.E10
    2    2    1    7    1    2              1.E10
    3    3    1    7    1    2              1.E10
    0    1    1
3640.0
```

```
   11
0.0        81.45       -24.30        4    3
97.2       83.32       -31.33       10    9
194.4      84.99       -37.62       16   15
291.6      86.46       -43.17       22   21
388.8      87.74       -47.98       28   27
486.0      88.82       -52.05       34   33
583.2      89.70       -55.38       40   39
680.4      90.39       -57.97       46   45
777.6      90.88       -59.82       52   51
874.8      91.18       -60.93       58   57
972.0      91.27       -61.30       64   63
LOAD
PRESTRESSING IN SLOPING EXTERIOR WEB (FRICTION IGNORED)
                                      1.0
    1          1   -1  10001010     2    1
   11   10     0    2    6
    1    5     0    1    6    1     00.0        180.        -23.292
    1    2     3    4    5    6
    1    1
   11    1
   21    1
   31    1
   41    1
    2    1
    2   10     0    2    6    1     197.2       180.        -23.292
    7    8     9   10   11   12
    1    1
    2    1
   11    1
   12    1
   21    1
   22    1
   31    1
   32    1
   41    1
   42    1
    2    1
    3    1
   10   10     0    2    6    1     1874.8      180.        -23.292
   55   56    57   58   59   60
    9    1
   10    1
   19    1
   20    1
   29    1
   30    1
   39    1
   40    1
   49    1
   50    1
   10    1
   11    1
   11    5     0    1    6    1     0972.0      180.        -23.292
   61   62    63   64   65   66
   10    1
   20    1
   30    1
   40    1
   50    1
   11    1
LOAD
```



```
DEAD LOAD OF BRIDGE
                1          0.0000897
    1           1   -1  10001010     2    1
   11   10     0    2    6
    1    5     0    1    6    1     00.0        180.        -23.292
    1    2     3    4    5    6
    1    1
   11    1
   21    1
   31    1
   41    1
    2    1
    2   10     0    2    6    1     197.2       180.        -23.292
    7    8     9   10   11   12
    1    1
    2    1
   11    1
   12    1
   21    1
   22    1
   31    1
   32    1
   41    1
   42    1
    2    1
    3    1
   10   10     0    2    6    1     1874.8      180.        -23.292
   55   56    57   58   59   60
    9    1
   10    1
   19    1
   20    1
   29    1
   30    1
   39    1
   40    1
   49    1
   50    1
   10    1
   11    1
   11    5     0    1    6    1     0972.0      180.        -23.292
   61   62    63   64   65   66
   10    1
   20    1
   30    1
   40    1
   50    1
   11    1
STOP
```

```
START
EXAMPLE 2: CELL4: SIMPLE SPAN (162 FT); SLOPING WEBS; SYMM. AASHTO LANE LOAD
   50    2   11   66    0    5   29    3     67.8          0
    0    0    0    0    0    1   10   11
    1    00.0       180.0
    2    00.0       136.5
    3    00.0       93.0
    4    10.0       75.0
    5    10.0       37.5
    6    10.0       0.0
    7     97.2      180.0
    8     97.2      136.5
    9     97.2      93.0
   10    197.2      75.0
   11    197.2      37.5
   12    197.2      0.0
   13     194.4     180.0
   14     194.4     136.5
   15     194.4     93.0
   16    1194.4     75.0
   17    1194.4     37.5
   18    1194.4     0.0
   19     291.6     180.0
   20     291.6     136.5
   21     291.6     93.0
   22    1291.6     75.0
   23    1291.6     37.5
   24    1291.6     0.0
   25     388.8     180.0
   26     388.8     136.5
   27     388.8     93.0
   28    1388.8     75.0
   29    1388.8     37.5
   30    1388.8     0.0
   31     486.0     180.0
   32     486.0     136.5
   33     486.0     93.0
   34    1486.0     75.0
   35    1486.0     37.5
   36    1486.0     0.0
   37     583.2     180.0
   38     583.2     136.5
   39     583.2     93.0
   40    1583.2     75.0
   41    1583.2     37.5
   42    1583.2     0.0
   43     680.4     180.0
   44     680.4     136.5
   45     680.4     93.0
   46    1680.4     75.0
   47    1680.4     37.5
   48    1680.4     0.0
   49     777.6     180.0
   50     777.6     136.5
   51     777.6     93.0
   52    1777.6     75.0
   53    1777.6     37.5
   54    1777.6     0.0
   55     874.8     180.0
   56     874.8     136.5
   57     874.8     93.0
   58    1874.8     75.0
```



```
   59    1874.8     37.5
   60    1874.8     0.0
   61     972.0     180.0
   62     972.0     136.5
   63     972.0     93.0
   64    1972.0     75.0
   65    1972.0     37.5
   66    1972.0     0.0
    13600.      3600.      1560.      0.15                  11.4
    23600.      3600.      1560.      0.15                  9.0
    33600.      3600.      1560.      0.15                  17.4
    41.0        1.0        0.5        0.0                   0.0
    53600.      3600.      1560.      0.15                  36.
    1   1   2   8   7   1   2
   10  55  56  62  61   1   2   6
   11   2   3   9   8   1   2
   20  56  57  63  62   1   2   6
   21   3   4  10   9   1
   30  57  58  64  63   1       6
   31   4   5  11  10   1
   40  58  59  65  64   1       6
   41   5   6  12  11   1
   50  59  60  66  65   1       6
    1   1   2   5
    2   2   3   5
    1   3   3   4   3   5
    2  10   9   3   4   3
   11  64  63  57  58   3   6
    1       T       T
    1       T       T       T
    7       T       T
    7       T       T       T
   13       T       T
   13       T       T       T
   19       T       T
   19       T       T       T
   25       T       T
   25       T       T       T
   31       T       T
   31       T       T       T
   37       T       T
   37       T       T       T
   43       T       T
   43       T       T       T
   49       T       T
   49       T       T       T
   55       T       T
   55       T       T       T
   61   T   T       T   T
   61   T   T       T   T   T
   62   T                   T
   62   T                   T   T
   63   T                   T
   63   T                   T   T
   64   T                   T
   65   T                   T
   66   T                   T
    1   1   1   7   1   2           1.E10
    2   2   1   7   1   2           1.E10
    3   3   1   7   1   2           1.E10
    0   1   1
3640.0
```

```
   11
0.0        81.45       -24.30         4    3
97.2       83.32       -31.33        10    9
194.4      84.99       -37.62        16   15
291.6      86.46       -43.17        22   21
388.8      87.74       -47.98        28   27
486.0      88.82       -52.05        34   33
583.2      89.70       -55.38        40   39
680.4      90.39       -57.97        46   45
777.6      90.88       -59.82        52   51
874.8      91.18       -60.93        58   57
972.0      91.27       -61.30        64   63
LOAD
ASSHTO SYMMETRIC LANE LOAD (NO IMPACT FACTOR)
    6    1     -0.0002962
   61                                -1.0875
   62                                -2.175
   63                                -1.5375
   64                                -1.3875
   65                                -1.875
   66                                -0.9375
    1         1   -1  10001010     2    1
   11   10    0    2    6
    1    5    0    1    6    1     00.0        180.       -23.292
    1    2    3    4    5    6
    1    1
   11    1
   21    1
   31    1
   41    1
    2    1
    2   10    0    2    6    1     197.2       180.       -23.292
    7    8    9   10   11   12
    1    1
    2    1
   11    1
   12    1
   21    1
   22    1
   31    1
   32    1
   41    1
   42    1
    2    1
    3    1
   10   10    0    2    6    1     1874.8      180.       -23.292
   55   56   57   58   59   60
    9    1
   10    1
   19    1
   20    1
   29    1
   30    1
   39    1
   40    1
   49    1
   50    1
   10    1
   11    1
   11    5    0    1    6    1     0972.0      180.       -23.292
   61   62   63   64   65   66
   10    1
```



```
   20    1
   30    1
   40    1
   50    1
   11    1
STOP
```

```
START
EXAMPLE 2: CELL4: SIMPLE SPAN (162 FT): SLOPING WEBS: ANTI-SYMM. AASHTO LANE LD
   50    2   11   66    0    5   29    3     67.8          0
    0    0    0    0    0    1   10   11
    1    00.0       180.0
    2    00.0       136.5
    3    00.0       93.0
    4    10.0       75.0
    5    10.0       37.5
    6    10.0       0.0
    7     97.2      180.0
    8     97.2      136.5
    9     97.2      93.0
   10    197.2      75.0
   11    197.2      37.5
   12    197.2      0.0
   13     194.4     180.0
   14     194.4     136.5
   15     194.4     93.0
   16    1194.4     75.0
   17    1194.4     37.5
   18    1194.4     0.0
   19     291.6     180.0
   20     291.6     136.5
   21     291.6     93.0
   22    1291.6     75.0
   23    1291.6     37.5
   24    1291.6     0.0
   25     388.8     180.0
   26     388.8     136.5
   27     388.8     93.0
   28    1388.8     75.0
   29    1388.8     37.5
   30    1388.8     0.0
   31     486.0     180.0
   32     486.0     136.5
   33     486.0     93.0
   34    1486.0     75.0
   35    1486.0     37.5
   36    1486.0     0.0
   37     583.2     180.0
   38     583.2     136.5
   39     583.2     93.0
   40    1583.2     75.0
   41    1583.2     37.5
   42    1583.2     0.0
   43     680.4     180.0
   44     680.4     136.5
   45     680.4     93.0
   46    1680.4     75.0
   47    1680.4     37.5
   48    1680.4     0.0
   49     777.6     180.0
   50     777.6     136.5
   51     777.6     93.0
   52    1777.6     75.0
   53    1777.6     37.5
   54    1777.6     0.0
   55     874.8     180.0
   56     874.8     136.5
   57     874.8     93.0
   58    1874.8     75.0
```



```
   59    1874.8     37.5
   60    1874.8     0.0
   61     972.0     180.0
   62     972.0     136.5
   63     972.0     93.0
   64    1972.0     75.0
   65    1972.0     37.5
   66    1972.0     0.0
    13600.      3600.      1560.      0.15                  11.4
    23600.      3600.      1560.      0.15                  9.0
    33600.      3600.      1560.      0.15                  17.4
    41.0        1.0        0.5        0.0                   0.0
    53600.      3600.      1560.      0.15                  36.
     1    1    2    8    7    1    2
    10   55   56   62   61    1    2    6
    11    2    3    9    8    1    2
    20   56   57   63   62    1    2    6
    21    3    4   10    9    1
    30   57   58   64   63    1         6
    31    4    5   11   10    1
    40   58   59   65   64    1         6
    41    5    6   12   11    1
    50   59   60   66   65    1         6
     1    1    2    5
     2    2    3    5
     1    3    3    4    3    5
     2   10    9    3    4    3
    11   64   63   57   58    3    6
     1    T         T         T
     1    T         T         T    T
     7    T         T         T
     7    T         T         T    T
    13    T         T         T
    13    T         T         T    T
    19    T         T         T
    19    T         T         T    T
    25    T         T         T
    25    T         T         T    T
    31    T         T         T
    31    T         T         T    T
    37    T         T         T
    37    T         T         T    T
    43    T         T         T
    43    T         T         T    T
    49    T         T         T
    49    T         T         T    T
    55    T         T         T
    55    T         T         T    T
    61    T         T         T
    61    T         T         T    T
    62    T                   T
    62    T                   T    T
    63    T                   T
    63    T                   T    T
    64    T                   T
    65    T                   T
    66    T                   T
     1    2    1    7    1    2              1.E10
     2    3    1    7    1    2              1.E10
     3    3    2                             1.E10
     0    1    1
3640.0
```

```
   11
0.0        81.45       -24.30         4    3
97.2       83.32       -31.33        10    9
194.4      84.99       -37.62        16   15
291.6      86.46       -43.17        22   21
388.8      87.74       -47.98        28   27
486.0      88.82       -52.05        34   33
583.2      89.70       -55.38        40   39
680.4      90.39       -57.97        46   45
777.6      90.88       -59.82        52   51
874.8      91.18       -60.93        58   57
972.0      91.27       -61.30        64   63
LOAD
ASSHTO ANTI-SYMMETRIC LANE LOAD (NO IMPACT FACTOR)
    6    1      -0.0002962
   61                                -1.0875
   62                                -2.175
   63                                -1.5375
   64                                -1.3875
   65                                -1.875
   66                                -0.9375
    1          1   -1  10001010     2    1
   11   10     0    2     6
    1    5     0    1     6    1    00.0        180.       -23.292
    1    2     3    4     5    6
    1    1
   11    1
   21    1
   31    1
   41    1
    2    1
    2   10     0    2     6    1    197.2       180.       -23.292
    7    8     9   10    11   12
    1    1
    2    1
   11    1
   12    1
   21    1
   22    1
   31    1
   32    1
   41    1
   42    1
    2    1
    3    1
   10   10     0    2     6    1    1874.8      180.       -23.292
   55   56    57   58    59   60
    9    1
   10    1
   19    1
   20    1
   29    1
   30    1
   39    1
   40    1
   49    1
   50    1
   10    1
   11    1
   11    5     0    1     6    1    0972.0      180.       -23.292
   61   62    63   64    65   66
   10    1
```



```
   20    1
   30    1
   40    1
   50    1
   11    1
STOP
```

```
START
EXAMPLE 2: CELL4: SIMPLE SPAN (162 FT): SLOPING WEBS: PANEL PRESTRESS/FRICTION
   50    2   11   66    0    5   29    3     67.8          0
    0    0    0    0    0    1   10   11
    1    00.0       180.0
    2    00.0       136.5
    3    00.0       93.0
    4    10.0       75.0
    5    10.0       37.5
    6    10.0       0.0
    7     97.2      180.0
    8     97.2      136.5
    9     97.2      93.0
   10    197.2      75.0
   11    197.2      37.5
   12    197.2      0.0
   13     194.4     180.0
   14     194.4     136.5
   15     194.4     93.0
   16    1194.4     75.0
   17    1194.4     37.5
   18    1194.4     0.0
   19     291.6     180.0
   20     291.6     136.5
   21     291.6     93.0
   22    1291.6     75.0
   23    1291.6     37.5
   24    1291.6     0.0
   25     388.8     180.0
   26     388.8     136.5
   27     388.8     93.0
   28    1388.8     75.0
   29    1388.8     37.5
   30    1388.8     0.0
   31     486.0     180.0
   32     486.0     136.5
   33     486.0     93.0
   34    1486.0     75.0
   35    1486.0     37.5
   36    1486.0     0.0
   37     583.2     180.0
   38     583.2     136.5
   39     583.2     93.0
   40    1583.2     75.0
   41    1583.2     37.5
   42    1583.2     0.0
   43     680.4     180.0
   44     680.4     136.5
   45     680.4     93.0
   46    1680.4     75.0
   47    1680.4     37.5
   48    1680.4     0.0
   49     777.6     180.0
   50     777.6     136.5
   51     777.6     93.0
   52    1777.6     75.0
   53    1777.6     37.5
   54    1777.6     0.0
   55     874.8     180.0
   56     874.8     136.5
   57     874.8     93.0
   58    1874.8     75.0
```



```
   59    1874.8     37.5
   60    1874.8     0.0
   61     972.0     180.0
   62     972.0     136.5
   63     972.0     93.0
   64    1972.0     75.0
   65    1972.0     37.5
   66    1972.0     0.0
    13600.      3600.      1560.      0.15                  11.4
    23600.      3600.      1560.      0.15                  9.0
    33600.      3600.      1560.      0.15                  17.4
    41.0        1.0        0.5        0.0                   0.0
    53600.      3600.      1560.      0.15                  36.
     1    1    2    8    7    1    2
  10   55   56   62   61    1    2    6
  11    2    3    9    8    1    2
  20   56   57   63   62    1    2    6
  21    3    4   10    9    1
  30   57   58   64   63    1         6
  31    4    5   11   10    1
  40   58   59   65   64    1         6
  41    5    6   12   11    1
  50   59   60   66   65    1         6
   1    1    2    5
   2    2    3    5
   1    3    3    4    3    5
   2   10    9    3    4    3
  11   64   63   57   58    3    6
   1         T         T
   1         T         T         T
   7         T         T
   7         T         T         T
  13         T         T
  13         T         T         T
  19         T         T
  19         T         T         T
  25         T         T
  25         T         T         T
  31         T         T
  31         T         T         T
  37         T         T
  37         T         T         T
  43         T         T
  43         T         T         T
  49         T         T
  49         T         T         T
  55         T         T
  55         T         T         T
  61    T    T         T    T
  61    T    T         T    T    T
  62    T                   T
  62    T                   T    T
  63    T                   T
  63    T                   T    T
  64    T                   T
  65    T                   T
  66    T                   T
   1    1    1    7    1    2         1.E10
   2    2    1    7    1    2         1.E10
   3    3    1    7    1    2         1.E10
   0    1    1
4266.0              0.25      0.0000167 22.6      28000.     0.1875
```

```
   11
0.0        81.45       -24.30         4    3
97.2       83.32       -31.33        10    9
194.4      84.99       -37.62        16   15
291.6      86.46       -43.17        22   21
388.8      87.74       -47.98        28   27
486.0      88.82       -52.05        34   33
583.2      89.70       -55.38        40   39
680.4      90.39       -57.97        46   45
777.6      90.88       -59.82        52   51
874.8      91.18       -60.93        58   57
972.0      91.27       -61.30        64   63
LOAD
PRESTRESSING IN SLOPING EXT. WEB WITH ANCHORAGE SLIP AND FRICTION LOSSES
                                      1.0
    1          1   -1  10001010     2    1
   11   10     0    2    6
    1    5     0    1    6    1     00.0        180.       -23.292
    1    2     3    4    5    6
    1    1
   11    1
   21    1
   31    1
   41    1
    2    1
    2   10     0    2    6    1     197.2       180.       -23.292
    7    8     9   10   11   12
    1    1
    2    1
   11    1
   12    1
   21    1
   22    1
   31    1
   32    1
   41    1
   42    1
    2    1
    3    1
   10   10     0    2    6    1     1874.8      180.       -23.292
   55   56    57   58   59   60
    9    1
   10    1
   19    1
   20    1
   29    1
   30    1
   39    1
   40    1
   49    1
   50    1
   10    1
   11    1
   11    5     0    1    6    1     0972.0      180.       -23.292
   61   62    63   64   65   66
   10    1
   20    1
   30    1
   40    1
   50    1
   11    1
STOP
```



```
START
EXAMPLE 3: CELL4: STRAIGHT: CONTINUOUS TWO SPAN (150,162 FT): FOUR CELL BOX
  200  124     1  231     0     7     2    15     071.375
    0    0     0    0     5     0    20    21
    1   10.0          504.0
  111   11800.0       504.0          11
    2    0.0          452.0
  112    1800.0       452.0          11
    3    0.0          402.0
  113    1800.        402.0          11     1   120
   11   10.0          0.0
  121   11800.0       0.0            11
  122   11994.4       504.0
  221   13744.0       504.0          11
  123    1994.4       452.0
  222    3744.0       452.0          11
  124    1994.4       402.0
  223    3744.0       402.0          11     1   230
  132   11994.4       0.0
  231   13744.0       0.0            11
    13600.0     3600.0     1565.2     0.15                  7.5
    23600.0     3600.0     1565.2     0.15                  5.75
    33600.0     3600.0     1565.2     0.15                  9.5
    43600.0     3600.0     1565.2     0.15                  12.0
    53600.0     3600.0     1565.2     0.15                  6.0
    63600.0     3600.0     1565.2     0.15                  24.0
    73600.0     3600.0     1565.2     0.15                  0.0
    1   12     1    2   13     3     0
   20  221   210  211  222     3     0    11
   21   13     2    3   14     1     2
   40  222   211  212  223     1     2    11
   41   14     3    4   15     1     2
   60  223   212  213  224     1     2    11    20   180
  181   21    10   11   22     3     0
  200  230   219  220  231     3     0    11
    1    2     3    6
    9  112   113    6
   17  222   223    6
   24  229   230    6
   25    2    13    4
   45    4    15    4    11
   64  213   224    4    11    20   124
    1    2     2    3     3    7
  112    T     T                 T
  120    T                       T
    1    2    12    1     2    1          1.E10
    5   10    12    1     2    1          1.E10                  2
    6  112    12    1     2    1          1.E10
   10  120    12    1     2    1          1.E10                  2
   11  222    12    1     2    1          1.E10
   15  230    12    1     2    1          1.E10                  2
    1    1     2
1580.      1580.
0.0        0.5        0.1
-30.33     -64.25     -8.25
   25   34     2
0.1        0.5        0.0
-8.25      -64.25     -30.33
   35   44   112
    1    1     2
1580.      1580.
0.0        0.5        0.1
```

```
-30.33    -64.25    -8.25
   45   54    4
0.1       0.5       0.0
-8.25     -64.25    -30.33
   55   64  114
    1    1    2
1580.     1580.
0.0       0.5       0.1
-30.33    -64.25    -8.25
   65   74    6
0.1       0.5       0.0
-8.25     -64.25    -30.33
   75   84  116
    1    1    2
1580.     1580.
0.0       0.5       0.1
-30.33    -64.25    -8.25
   85   94    8
0.1       0.5       0.0
-8.25     -64.25    -30.33
   95  104  118
    1    1    2
1580.     1580.
0.0       0.5       0.1
-30.33    -64.25    -8.25
  105  114   10
0.1       0.5       0.0
-8.25     -64.25    -30.33
  115  124  120
LOAD
4 CELL BOX GIRDER BRIDGE - DEAD LOAD ANALYSIS
             1          0.0000897
    1        1   -1  10001000   24
   40   10    5    0   11
    1   10    5    0   11    5
   12   13   14   15   16   17   18   19   20   21   22
    1    1
   21    1
   41    2
   61    2
   81    3
  101    3
  121    4
  141    4
  161    5
  181    5
   25    1
   45    2
   65    3
   85    4
  105    5
   20   10    5    0   11    5
  221  222  223  224  225  226  227  228  229  230  231
   20    1
   40    1
   60    2
   80    2
  100    3
  120    3
  140    4
  160    4
  180    5
```



```
  200    5
   44    1
   64    2
   84    3
  104    4
  124    5
   21   10    5    0   11    5
    1    2    3    4    5    6    7    8    9   10   11
    1    1
   21    1
   41    2
   61    2
   81    3
  101    3
  121    4
  141    4
  161    5
  181    5
   25    1
   45    2
   65    3
   85    4
  105    5
   40   10    5    0   11    5
  210  211  212  213  214  215  216  217  218  219  220
   20    1
   40    1
   60    2
   80    2
  100    3
  120    3
  140    4
  160    4
  180    5
  200    5
   44    1
   64    2
   84    3
  104    4
  124    5
LOAD
4 CELL BOX GIRDER BRIDGE - LIVE LOAD DUE TO P13 TRUCK
   27
  129                              -1.91
  140                              -6.16
  151                              -9.39
  162                              -9.39
  173                              -10.56
  184                              -9.39
  195                              -9.39
  206                              -9.39
  217                              -3.52
  130                              -2.42
  141                              -7.84
  152                              -11.95
  163                              -11.94
  174                              -13.44
  185                              -11.94
  196                              -11.95
  207                              -11.94
  218                              -4.48
  131                              -4.33
```

```
142                                    -14.0
153                                    -21.34
164                                    -21.33
175                                    -24.0
186                                    -21.33
197                                    -21.34
208                                    -21.33
219                                    -8.0
  1         1   -1  10001000   24
 40   10    5    0   11
  1   10    5    0   11    5
  1    2    3    4    5    6    7    8    9   10   11
  1    1
 21    1
 41    2
 61    2
 81    3
101    3
121    4
141    4
161    5
181    5
 25    1
 45    2
 65    3
 85    4
105    5
 20   10    5    0   11    5
210  211  212  213  214  215  216  217  218  219  220
 20    1
 40    1
 60    2
 80    2
100    3
120    3
140    4
160    4
180    5
200    5
 44    1
 64    2
 84    3
104    4
124    5
 21   10    5    0   11    5
 12   13   14   15   16   17   18   19   20   21   22
  1    1
 21    1
 41    2
 61    2
 81    3
101    3
121    4
141    4
161    5
181    5
 25    1
 45    2
 65    3
 85    4
105    5
 40   10    5    0   11    5
```



```
221  222  223  224  225  226  227  228  229  230  231
 20    1
 40    1
 60    2
 80    2
100    3
120    3
140    4
160    4
180    5
200    5
 44    1
 64    2
 84    3
104    4
124    5
LOAD
4 CELL BOX GIRDER BRIDGE - PRSTRESS ANALYSING - FRICTION EFFECTS IGNORED
                                       1.0
  1         1   -1  10001000   24
 40   10    5    0   11
  1   10    5    0   11    5
  1    2    3    4    5    6    7    8    9   10   11
  1    1
 21    1
 41    2
 61    2
 81    3
101    3
121    4
141    4
161    5
181    5
 25    1
 45    2
 65    3
 85    4
105    5
 20   10    5    0   11    5
210  211  212  213  214  215  216  217  218  219  220
 20    1
 40    1
 60    2
 80    2
100    3
120    3
140    4
160    4
180    5
200    5
 44    1
 64    2
 84    3
104    4
124    5
 21   10    5    0   11    5
 12   13   14   15   16   17   18   19   20   21   22
  1    1
 21    1
 41    2
 61    2
 81    3
```

```
  101    3
  121    4
  141    4
  161    5
  181    5
   25    1
   45    2
   65    3
   85    4
  105    5
   40   10    5    0   11    5
  221  222  223  224  225  226  227  228  229  230  231
   20    1
   40    1
   60    2
   80    2
  100    3
  120    3
  140    4
  160    4
  180    5
  200    5
   44    1
   64    2
   84    3
  104    4
  124    5
STOP
```



```
START
EXAMPLE 6: CELL4: THREE SPAN (96,100,175 FT): MULTI-CELL BOX: ARBITRARY PLAN
  182  171  111  210   53    6    2    8     6.27          1
    0    0    0    0    6    0   28   29
    1    1   -283.68    142.55
    3        -279.54    139.24
    4        -274.15    134.89
    5        -268.77    130.54
    6        -263.36    126.18
    7        -257.95    121.81
    8        -252.54    117.44
    9    1   -248.40    114.10
   11    0   -279.05    140.22
   12    0   -273.01    137.19
   13    0   -266.98    134.16
   14    0   -260.94    131.12
   15    0   -254.90    128.09
   16    0   -248.86    125.05
   17    1   -244.23    122.73
   19    1   -278.18    153.00
   21    0   -273.64    150.50
   22    0   -267.72    147.24
   23    0   -261.81    143.99
   24    0   -255.88    140.73
   25    0   -249.96    137.47
   26    0   -244.04    134.22
   27    1   -239.50    131.72
   29    1   -269.59    167.67
   31    0   -265.19    164.94
   32    0   -259.45    161.37
   33    0   -253.72    157.80
   34    0   -247.98    154.23
   35    0   -242.24    150.66
   36    0   -236.50    147.09
   37    1   -232.10    144.36
   39    1   -260.25    181.83
   41    0   -256.01    178.86
   42    0   -250.47    174.99
   43    0   -244.93    171.12
   44    0   -239.39    167.25
   45    0   -233.85    163.38
   46    0   -228.31    159.51
   47    1   -224.06    156.54
   49    1   -250.18    195.46
   51    0   -246.10    192.27
   52    0   -240.77    188.11
   53    0   -235.45    183.95
   54    0   -230.12    179.79
   55    0   -224.80    175.63
   56    0   -219.47    171.47
   57    1   -215.39    168.28
   59    1   -239.35    208.58
   61    0   -235.45    205.18
   62    0   -230.35    200.73
   63    0   -225.26    196.30
   64    0   -220.16    191.86
   65    0   -215.07    187.42
   66    0   -209.97    182.98
   67    1   -206.07    179.57
   69    1   -229.28    219.61
   71        -225.23    216.34
   72        -219.95    212.08
```

73		-214.68	207.82
74		-209.40	203.56
75		-204.11	199.29
76		-198.83	195.02
77	1	-194.78	191.75
79	1	-215.10	233.51
81	0	-211.59	229.70
82	0	-207.01	224.73
83	0	-202.44	219.76
84	0	-197.86	214.79
85	0	-193.28	209.82
86	0	-188.70	204.85
87	1	-185.19	201.04
89	1	-201.64	245.22
91	0	-198.35	241.22
92	0	-194.06	236.00
93	0	-189.77	230.79
94	0	-185.48	225.56
95	0	-181.18	220.34
96	0	-176.89	215.12
97	1	-173.60	211.12
99	1	-187.55	256.16
101	0	-184.49	251.98
102	0	-180.50	246.53
103	0	-176.51	241.08
104	0	-172.52	235.63
105	0	-168.52	230.17
106	0	-164.53	224.72
107	1	-161.47	220.54
109	1	-172.82	266.32
111	0	-170.00	261.98
112	0	-166.32	256.31
113	0	-162.65	250.64
114	0	-158.97	244.97
115	0	-155.29	239.30
116	0	-151.61	233.63
117	1	-148.79	229.29
119	1	-157.59	275.61
121	0	-155.02	271.11
122	0	-151.66	265.24
123	0	-148.31	259.38
124	0	-144.95	253.51
125	0	-141.60	247.65
126	0	-138.24	241.78
127	1	-135.67	237.28
129	1	-154.58	277.35
131		-149.30	274.30
132	1	-147.97	280.89
134	0	-145.56	276.31
135	0	-142.41	270.32
136	0	-139.26	264.35
137		-135.48	266.31
138	0	-136.11	258.37
139		-128.46	262.26
140	0	-132.96	252.39
141	0	-129.81	246.41
142	1	-127.39	241.83
144	1	-135.08	287.31
146	0	-132.87	282.62
147	0	-130.00	276.51
148	0	-127.12	270.40
149	0	-124.25	264.28

150	0	-121.37	258.16
151	0	-118.50	252.04
152		-114.20	254.02
153	1	-116.29	247.36
155	1	-108.71	250.85
157	1	-120.42	293.76
159	0	-118.45	288.96
160	0	-115.89	282.71
161	0	-113.33	276.46
162	0	-110.77	270.21
163	0	-108.20	263.95
164	0	-105.64	257.70
165	1	-103.67	252.91
167	1	-98.32	301.87
169	0	-96.71	296.95
170	0	-94.62	290.52
171	0	-92.53	284.10
172	0	-90.44	277.67
173	0	-88.34	271.25
174	0	-86.25	264.82
175	1	-84.65	259.89
177	1	-75.68	308.33
179	0	-74.44	303.30
180	0	-72.83	296.73
181	0	-71.22	290.18
182	0	-69.61	283.61
183	0	-68.00	277.05
184	0	-66.39	270.48
185	1	-65.15	265.45
187	1	-52.62	313.09
189	0	-51.76	307.98
190	0	-50.64	301.31
191	0	-49.52	294.66
192	0	-48.40	287.99
193	0	-47.28	281.32
194	0	-46.16	274.66
195	1	-45.30	269.55
197	1	-29.22	316.13
199	0	-28.74	310.97
200	0	-28.12	304.24
201	0	-27.50	297.52
202	0	-26.87	290.79
203	0	-26.25	284.06
204	0	-25.63	277.33
205	1	-25.15	272.17
207	1	-14.29	317.16
209	0	-14.06	311.98
210	0	-13.75	305.23
211	0	-13.45	298.49
212	0	-13.15	291.73
213	0	-12.84	284.98
214	0	-12.54	278.23
215	1	-12.30	273.05
217	1	-1.98	317.71
219		-1.75	312.54
220		-1.45	305.79
221		-1.15	299.04
222		-0.84	292.28
223		-0.54	285.53
224		-0.24	278.78
225	1	0.0	273.60
227	1	1.84	317.88

229		10.55	313.09
230		10.85	306.34
231		11.16	299.58
232		11.46	292.83
233		11.77	286.08
234		12.07	279.32
235	1	12.31	274.14
237		21.92	306.84
238		22.22	300.09
239		22.53	293.33
240		22.83	286.58
241		23.14	279.82
242	1	23.38	274.65
244		33.29	300.59
245		33.59	293.84
246		33.90	287.08
247		34.20	280.32
248	1	34.44	275.15
250		44.66	294.33
251		44.96	287.58
252		45.27	280.83
253	1	45.51	275.64
255		56.03	288.08
256		56.33	281.33
257	1	56.57	276.15
259		67.40	281.83
260	1	67.64	276.65
263	1	76.11	277.04

2	-283.68	142.55	-1.33
10	-248.40	114.10	-1.33
18	-244.23	122.73	-1.33
20	-278.18	153.00	-1.33
28	-239.50	131.72	-1.33
30	-269.59	167.67	-1.33
38	-232.10	144.36	-1.33
40	-260.25	181.83	-1.33
48	-224.06	156.54	-1.33
50	-250.18	195.46	-1.33
58	-215.39	168.28	-1.33
60	-239.35	208.58	-1.33
68	-206.07	179.57	-1.33
70	-229.28	219.61	-1.33
78	-194.78	191.75	-1.33
80	-215.10	233.51	-1.33
88	-185.19	201.04	-1.33
90	-201.64	245.22	-1.33
98	-173.60	211.12	-1.33
100	-187.55	256.16	-1.33
108	-161.47	220.54	-1.33
110	-172.82	266.32	-1.33
118	-148.79	229.29	-1.33
120	-157.59	275.61	-1.33
128	-135.67	237.28	-1.33
130	-154.58	277.35	-1.33
133	-147.97	280.89	-1.33
143	-127.39	241.83	-1.33
145	-135.08	287.31	-1.33
154	-116.29	247.36	-1.33
156	-108.71	250.85	-1.33
158	-120.42	293.76	-1.33
166	-103.67	252.91	-1.33
168	-98.32	301.87	-1.33

176	-84.65	259.89	-1.33
178	-75.68	308.33	-1.33
186	-65.15	265.45	-1.33
188	-52.62	313.09	-1.33
196	-45.30	269.55	-1.33
198	-29.22	316.13	-1.33
206	-25.15	272.17	-1.33
208	-14.29	317.16	-1.33
216	-12.30	273.05	-1.33
218	-1.98	317.71	-1.33
226	0.0	273.60	-1.33
228	1.84	317.88	-1.33
236	12.31	274.14	-1.33
243	23.38	274.65	-1.33
249	34.44	275.15	-1.33
254	45.51	275.64	-1.33
258	56.57	276.15	-1.33
261	67.64	276.65	-1.33
262	76.11	277.04	-1.33

1	5.19E5	5.19E5	2.26E5	0.15		0.623
2	5.19E5	5.19E5	2.26E5	0.15		0.492
3	5.19E5	5.19E5	2.26E5	0.15		1.083
4	5.19E5	5.19E5	2.26E5	0.15		0.984
5	5.19E5	5.19E5	2.26E5	0.15		0.492
6	5.19E5	5.19E5	2.26E5	0.15		2.67

1	1	3	11	1	1	0	
2	1	11	21	19	1	0	
3	19	21	31	29	1	0	
13	119	121	131	129	1	0	10
14	129	131	134	132	1	0	
15	132	134	146	144	1	0	
16	144	146	159	157	1	0	
17	157	159	169	167	1	0	
23	217	219	229	227	1	0	10
24	3	4	12	11	1	?	
25	11	12	22	21	1	2	
35	111	112	122	121	1	2	10
36	121	122	135	131	1	2	
37	131	135	134	131	1	2	
38	134	135	147	146	1	2	
39	146	147	160	159	1	2	
40	159	160	170	169	1	2	
46	219	220	230	229	1	2	10
47	229	230	237	229	1	2	
48	4	5	13	12	1	2	
49	12	13	23	22	1	2	
59	112	113	123	122	1	2	10
60	122	123	136	135	1	2	
61	135	136	137	135	1	2	
62	135	137	148	147	1	2	
63	147	148	161	160	1	2	
64	160	161	171	170	1	2	
70	220	221	231	230	1	2	10
71	230	231	238	237	1	2	
72	237	238	244	237	1	2	
73	5	6	14	13	1	2	
74	13	14	24	23	1	2	
84	113	114	124	123	1	2	10
85	123	124	138	136	1	2	
86	136	138	139	137	1	2	
87	137	139	149	148	1	2	
88	148	149	162	161	1	2	

```
 89  161  162  172  171    1    2
 95  221  222  232  231    1    2   10
 96  231  232  239  238    1    2
 97  238  239  245  244    1    2
 98  244  245  250  244    1    2
 99    6    7   15   14    1    2
100   14   15   25   24    1    2
110  114  115  125  124    1    2   10
111  124  125  140  138    1    2
112  138  140  150  139    1    2
113  139  150  149  139    1    2
114  149  150  163  162    1    2
115  162  163  173  172    1    2
121  222  223  233  232    1    2   10
122  232  233  240  239    1    2
123  239  240  246  245    1    2
124  245  246  251  250    1    2
125  250  251  255  250    1    2
126    7    8   16   15    1    2
127   15   16   26   25    1    2
137  115  116  126  125    1    2   10
138  125  126  141  140    1    2
139  140  141  151  150    1    2
140  150  151  152  150    1    2
141  150  152  164  163    1    2
142  163  164  174  173    1    2
148  223  224  234  233    1    2   10
149  233  234  241  240    1    2
150  240  241  247  246    1    2
151  246  247  252  251    1    2
152  251  252  256  255    1    2
153  255  256  259  255    1    2
154    8    9   17   16    1    0
155   16   17   27   26    1    0
165  116  117  127  126    1    0   10
166  126  127  142  141    1    0
167  141  142  153  151    1    0
168  151  153  155  152    1    0
169  152  155  165  164    1    0
170  164  165  175  174    1    0
176  224  225  235  234    1    0   10
177  234  235  242  241    1    0
178  241  242  248  247    1    0
179  247  248  253  252    1    0
180  252  253  257  256    1    0
181  256  257  260  259    1    0
182  259  260  263  259    1    0
  1    3    4    6
  6   71   72    6
 11  131  135    6
 12  135  137    6
 13  137  139    6
 14  139  150    6
 15  150  152    6
 16  229  237    6
 17  237  244    6
 18  244  250    6
 19  250  255    6
 20  255  259    6
 21    3   11    3
 22   11   21    3
 34  131  134    3   10
```



```
 35  134  146    3
 36  146  159    3
 37  159  169    3
 43  219  229    3   10
 44    4   12    3
 45   12   22    3
 55  112  122    3   10
 56  122  135    3
 57  135  147    3
 58  147  160    3
 59  160  170    3
 65  220  230    3   10
 66  230  237    3
 67    5   13    3
 68   13   23    3
 78  113  123    3   10
 79  123  136    3
 80  136  137    3
 81  137  148    3
 82  148  161    3
 83  161  171    3
 89  221  231    3   10
 90  231  238    3
 91  238  244    3
 92    6   14    3
 93   14   24    3
103  114  124    3   10
104  124  138    3
105  138  139    3
106  139  149    3
107  149  162    3
108  162  172    3
114  222  232    3   10
115  232  239    3
116  239  245    3
117  245  250    3
118    7   15    3
119   15   25    3
129  115  125    3   10
130  125  140    3
131  140  150    3
132  150  163    3
133  163  173    3
139  223  233    3   10
140  233  240    3
141  240  246    3
142  246  251    3
143  251  255    3
144    8   16    3
145   16   26    3
155  116  126    3   10
156  126  141    3
157  141  151    3
158  151  152    3
159  152  164    3
160  164  174    3
166  224  234    3   10
167  234  241    3
168  241  247    3
169  247  252    3
170  252  256    3
171  256  259    3
```

```
  1    1    2    3    3    6
  2    8    8   10    9    6
  3   69   70   71   71    6
  4   76   76   78   77    6
  5  129  130  131  131    6
  6  152  152  156  155    6
  7  227  228  229  229    6
  8  259  259  262  263    6
  9    1    2   20   19    4
 10   19   20   30   29    4
 20  119  120  130  129    4   10
 21  129  130  133  132    4
 22  132  133  145  144    4
 23  144  145  158  157    4
 24  157  158  168  167    4
 30  217  218  228  227    4   10
 31    2    3   11    2    5
 32    2   11   21   20    5
 33   20   21   31   30    5
 43  120  121  131  130    5   10
 44  130  131  134  133    5
 45  133  134  146  145    5
 46  145  146  159  158    5
 47  158  159  169  168    5
 53  218  219  229  228    5   10
 54   10    8   16   18    5
 55   18   16   26   28    5
 65  118  116  126  128    5   10
 66  128  126  141  143    5
 67  143  141  151  154    5
 68  154  151  152  156    5
 69  156  152  164  166    5
 70  166  164  174  176    5
 76  226  224  234  236    5   10
 77  236  234  241  243    5
 78  243  241  247  249    5
 79  249  247  252  254    5
 80  254  252  256  258    5
 81  258  256  259  261    5
 82  261  259  262  261    5
 83    9   10   18   17    4
 84   17   18   28   27    4
 94  117  118  128  127    4   10
 95  127  128  143  142    4
 96  142  143  154  153    4
 97  153  154  156  155    4
 98  155  156  166  165    4
 99  165  166  176  175    4
105  225  226  236  235    4   10
106  235  236  243  242    4
107  242  243  249  248    4
108  248  249  254  253    4
109  253  254  258  257    4
110  257  258  261  260    4
111  260  261  262  263    4
135    T    T                   T
150    T                        T
  1    3    1    3   11    3        1.E10
  2    8    1    3   11    3        1.E10
  3   72    1    3   11    3        1.E10
  4   75    1    3   11    3        1.E10
  5  135    1    3   11    3        1.E10
```



```
  6  150    1    3   11    3        1.E10
  7  229    1    3   11    3        1.E10
  8  259    1    3   11    3        1.E10
  1    1    3
3338.0    3338.0
0.0       0.5       0.1
-1.626    -3.136    -2.056
 21   27    3
0.1       0.5       0.1
-2.056    -2.776    -0.546
 28   33   71
0.1       0.5       0.0
-0.546    -5.626    -1.626
 34   43  131
  1    1    3
2710.0    2710.0
0.0       0.5       0.1
-1.626    -3.136    -2.056
 44   50    4
0.1       0.5       0.1
-2.056    -2.776    -0.546
 51   56   72
0.1       0.5       0.0
-0.546    -5.626    -1.626
 57   66  135
  1    1    3
2710.0    2710.0
0.0       0.5       0.1
-1.626    -3.136    -2.056
 67   73    5
0.1       0.5       0.1
-2.056    -2.776    -0.546
 74   80   73
0.1       0.5       0.0
-0.546    -5.626    -1.626
 81   91  137
  1    1    3
2710.0    2710.0
0.0       0.5       0.1
-1.626    -3.136    -2.056
 92   98    6
0.1       0.5       0.1
-2.056    -2.776    -0.546
 99  105   74
0.1       0.5       0.0
-0.546    -5.626    -1.626
106  117  139
  1    1    3
2710.0    2710.0
0.0       0.5       0.1
-1.626    -3.136    -2.056
118  124    7
0.1       0.5       0.1
-2.056    -2.776    -0.546
125  131   75
0.1       0.5       0.0
-0.546    -5.626    -1.626
132  143  150
  1    1    3
3338.0    3338.0
0.0       0.5       0.1
-1.626    -3.136    -2.056
```

```
  144  150    8
0.1       0.5       0.1
-2.056    -2.776    -0.546
  151  158   76
0.1       0.5       0.0
-0.546    -5.626    -1.626
  159  171  152
LOAD
UNIFORM PRESSURE OF 1 KSF ON THE TOP BRIDGE DECK
         1     -1.0
    1    0    1   -1  00011010   20    8
     63.32     63.32     63.52     63.80     64.10     64.40     64.72     65.06
     65.34     65.34     63.32     63.32     63.32     63.32     63.32     63.32
     63.32     63.32     61.19     61.19     61.19     61.19     61.19     61.19
     61.19     61.19     61.19     61.19     58.12     58.12     58.12     58.12
     58.12     58.12     58.12     58.12     58.12     58.12     55.06     55.06
     55.06     55.06     55.06     55.06     55.06     55.06     55.06     55.06
     52.00     52.00     52.00     52.00     52.00     52.00     52.00     52.00
     52.00     52.00     48.93     48.93     48.93     48.93     48.93     48.93
     48.93     48.93     48.93     48.93     46.24     46.24     46.15     46.04
     45.93     45.81     45.68     45.55     45.45     45.45     42.65     42.65
     42.65     42.65     42.65     42.65     42.65     42.65     42.65     42.65
     39.43     39.43     39.43     39.43     39.43     39.43     39.43     39.43
     39.43     39.43     36.21     36.21     36.21     36.21     36.21     36.21
     36.21     36.21     36.21     36.21     32.98     32.98     32.98     32.98
     32.98     32.98     32.98     32.98     32.98     32.98     29.76     29.76
     29.76     29.76     29.76     29.76     29.76     29.76     29.76     29.76
     29.16     29.16     28.56     27.78     27.78     27.78     27.78     27.78
     26.96     27.78     26.10     27.78     27.78     27.78     27.78     25.18
     25.18     25.18     25.18     25.18     25.18     25.18     25.18     24.21
     25.18     25.18     23.46     23.46     22.29     22.29     22.29     22.29
     22.29     22.29     22.29     22.29     22.29     22.29     18.04     18.04
     18.04     18.04     18.04     18.04     18.04     18.04     18.04     18.04
     13.79     13.79     13.79     13.79     13.79     13.79     13.79     13.79
     13.79     13.79      9.54      9.54      9.54      9.54      9.54      9.54
      9.54      9.54      9.54      9.54      5.28      5.28      5.28      5.28
      5.28      5.28      5.28      5.28      5.28      5.28      2.58      2.58
      2.58      2.58      2.58      2.58      2.58      2.58      2.58      2.58
      2.58      2.58      2.58      2.58      2.58      2.58      2.58      2.58
      2.58      2.58      2.58      2.58      2.58      2.58      2.58      2.58
      2.58      2.58      2.58      2.58      2.58      2.58      2.58      2.58
      2.58      2.58      2.58      2.58      2.58      2.58      2.58      2.58
      2.58      2.58      2.58      2.58      2.58      2.58      2.58
   24   14   12    8   10
    1    7    6    4   10    6
    1    2    3    4    5    6    7    8   10    9
    1    1
   24    1    2
   48    2    3
   73    3    4
   99    4    5
  126    5    6
  154    6
   21    1
   44    2
   67    3
   92    4
  118    5
  144    6
    9    1
   31    1
```



```
   54    6
   83    6
    2    7    6    4   10    6
    1    2   11   12   13   14   15   16   18   17
    1    1
   24    1    2
   48    2    3
   73    3    4
   99    4    5
  126    5    6
  154    6
   21    1
   44    2
   67    3
   92    4
  118    5
  144    6
    9    1
   31    1
   54    6
   83    6
    3   14   12    8   10    6    1
   19   20   21   22   23   24   25   26   28   27
    2    1
    3    1
   25    1    2
   26    1    2
   49    2    3
   50    2    3
   74    3    4
   75    3    4
  100    4    5
  101    4    5
  127    5    6
  128    5    6
  155    6
  156    6
   22    1
   23    1
   45    2
   46    2
   68    3
   69    3
   93    4
   94    4
  119    5
  120    5
  145    6
  146    6
    9    1
   10    1
   32    1
   33    1
   55    6
   56    6
   84    6
   85    6
    7   14   12    8   10    6    1
   59   60   61   62   63   64   65   66   68   67
    6    1
    7    1
   29    1    2
```

```
 30   1   2
 53   2   3
 54   2   3
 78   3   4
 79   3   4
104   4   5
105   4   5
131   5   6
132   5   6
159   6
160   6
 26   1
 27   1
 49   2
 50   2
 72   3
 73   3
 97   4
 98   4
123   5
124   5
149   6
150   6
 13   1
 14   1
 36   1
 37   1
 59   6
 60   6
 88   6
 89   6
  8   7   6   4  10   6
 69  70  71  72  73  74  75  76  78  77
  7   1
 30   1   2
 54   2   3
 79   3   4
105   4   5
132   5   6
160   6
 27   1
 50   2
 73   3
 98   4
124   5
150   6
 14   1
 37   1
 60   6
 89   6
  9   7   6   4  10   6
 69  70  71  72  73  74  75  76  78  77
  8   1
 31   1   2
 55   2   3
 80   3   4
106   4   5
133   5   6
161   6
 28   1
 51   2
 74   3
```



```
 99   4
125   5
151   6
 15   1
 38   1
 61   6
 90   6
 10  14  12   8  10   6   1
 79  80  81  82  83  84  85  86  88  87
  8   1
  9   1
 31   1   2
 32   1   2
 55   2   3
 56   2   3
 80   3   4
 81   3   4
106   4   5
107   4   5
133   5   6
134   5   6
161   6
162   6
 28   1
 29   1
 51   2
 52   2
 74   3
 75   3
 99   4
100   4
125   5
126   5
151   6
152   6
 15   1
 16   1
 38   1
 39   1
 61   6
 62   6
 90   6
 91   6
 14  14  12   8  10   6   1
119 120 121 122 123 124 125 126 128 127
 12   1
 13   1
 35   1   2
 36   1   2
 59   2   3
 60   2   3
 84   3   4
 85   3   4
110   4   5
111   4   5
137   5   6
138   5   6
165   6
166   6
 32   1
 33   1
 55   2
```

```
 56   2
 78   3
 79   3
103   4
104   4
129   5
130   5
155   6
156   6
 19   1
 20   1
 42   1
 43   1
 65   6
 66   6
 94   6
 95   6
 15   7   6   4  10   6
129 130 131 135 137 139 150 152 156 155
 13   1
 36   1   2
 61   2   3
 86   3   4
112   4   5
140   5   6
168   6
 33   1
 56   2
 80   3
105   4
131   5
158   6
 20   1
 43   1
 68   6
 97   6
 16   7   6   4  10   6
129 130 131 135 137 139 150 152 156 155
 14   1
 37   1   2
 62   2   3
 87   3   4
113   4   5
141   5   6
169   6
 34   1
 57   2
 81   3
106   4
132   5
159   6
 21   1
 44   1
 69   6
 98   6
 17  14  12   8  10   6   1
157 158 159 160 161 162 163 164 166 165
 16   1
 17   1
 39   1   2
 40   1   2
 63   2   3
```



```
 64   2   3
 88   3   4
 89   3   4
114   4   5
115   4   5
141   5   6
142   5   6
169   6
170   6
 36   1
 37   1
 58   2
 59   2
 82   3
 83   3
107   4
108   4
132   5
133   5
159   6
160   6
 23   1
 24   1
 46   1
 47   1
 69   6
 70   6
 98   6
 99   6
 23  14  12   8  10   6   1
217 218 219 220 221 222 223 224 226 225
 22   1
 23   1
 45   1   2
 46   1   2
 69   2   3
 70   2   3
 94   3   4
 95   3   4
120   4   5
121   4   5
147   5   6
148   5   6
175   6
176   6
 42   1
 43   1
 64   2
 65   2
 88   3
 89   3
113   4
114   4
138   5
139   5
165   6
166   6
 29   1
 30   1
 52   1
 53   1
 75   6
```

```
  76    6
 104    6
 105    6
  24    7    6    4   10    6
 227  228  229  237  244  250  255  259  262  263
  23    1
  47    1    2
  72    2    3
  98    3    4
 125    4    5
 153    5    6
 182    6
  43    1
  66    2
  91    3
 117    4
 143    5
 171    6
  30    1
  53    1
  82    6
 111    6
LOAD
PRESTRESSING LOAD ON BRIDGE EXCLUDING FRICTION AND ANCHORAGE SLIP LOSSES
                                    1.0
   1    0    1   -1  00011010   20    8
    63.32     63.32     63.52     63.80     64.10     64.40     64.72     65.06
    65.34     65.34     63.32     63.32     63.32     63.32     63.32     63.32
    63.32     63.32     61.19     61.19     61.19     61.19     61.19     61.19
    61.19     61.19     61.19     61.19     58.12     58.12     58.12     58.12
    58.12     58.12     58.12     58.12     58.12     58.12     55.06     55.06
    55.06     55.06     55.06     55.06     55.06     55.06     55.06     55.06
    52.00     52.00     52.00     52.00     52.00     52.00     52.00     52.00
    52.00     52.00     48.93     48.93     48.93     48.93     48.93     48.93
    48.93     48.93     48.93     48.93     46.24     46.24     46.15     46.04
    45.93     45.81     45.68     45.55     45.45     45.45     42.65     42.65
    42.65     42.65     42.65     42.65     42.65     42.65     42.65     42.65
    39.43     39.43     39.43     39.43     39.43     39.43     39.43     39.43
    39.43     39.43     36.21     36.21     36.21     36.21     36.21     36.21
    36.21     36.21     36.21     36.21     32.98     32.98     32.98     32.98
    32.98     32.98     32.98     32.98     32.98     32.98     29.76     29.76
    29.76     29.76     29.76     29.76     29.76     29.76     29.76     29.76
    29.16     29.16     28.56     27.78     27.78     27.78     27.78     27.78
    26.96     27.78     26.10     27.78     27.78     27.78     27.78     25.18
    25.18     25.18     25.18     25.18     25.18     25.18     25.18     24.21
    25.18     25.18     23.46     23.46     22.29     22.29     22.29     22.29
    22.29     22.29     22.29     22.29     22.29     22.29     18.04     18.04
    18.04     18.04     18.04     18.04     18.04     18.04     18.04     18.04
    13.79     13.79     13.79     13.79     13.79     13.79     13.79     13.79
    13.79     13.79      9.54      9.54      9.54      9.54      9.54      9.54
     9.54      9.54      9.54      9.54      5.28      5.28      5.28      5.28
     5.28      5.28      5.28      5.28      5.28      5.28      2.58      2.58
     2.58      2.58      2.58      2.58      2.58      2.58      2.58      2.58
     2.58      2.58      2.58      2.58      2.58      2.58      2.58      2.58
     2.58      2.58      2.58      2.58      2.58      2.58      2.58      2.58
     2.58      2.58      2.58      2.58      2.58      2.58      2.58      2.58
     2.58      2.58      2.58      2.58      2.58      2.58      2.58      2.58
     2.58      2.58      2.58      2.58      2.58      2.58      2.58
  24   14   12    8   10
   1    7    6    4   10    6
   1    2    3    4    5    6    7    8   10    9
```



```
   1    1
  24    1    2
  48    2    3
  73    3    4
  99    4    5
 126    5    6
 154    6
  21    1
  44    2
  67    3
  92    4
 118    5
 144    6
   9    1
  31    1
  54    6
  83    6
   2    7    6    4   10    6
   1    2   11   12   13   14   15   16   18   17
   1    1
  24    1    2
  48    2    3
  73    3    4
  99    4    5
 126    5    6
 154    6
  21    1
  44    2
  67    3
  92    4
 118    5
 144    6
   9    1
  31    1
  54    6
  83    6
   3   14   12    8   10    6    1
  19   20   21   22   23   24   25   26   28   27
   2    1
   3    1
  25    1    2
  26    1    2
  49    2    3
  50    2    3
  74    3    4
  75    3    4
 100    4    5
 101    4    5
 127    5    6
 128    5    6
 155    6
 156    6
  22    1
  23    1
  45    2
  46    2
  68    3
  69    3
  93    4
  94    4
 119    5
 120    5
```

```
145   6
146   6
  9   1
 10   1
 32   1
 33   1
 55   6
 56   6
 84   6
 85   6
  7  14  12   8  10   6   1
 59  60  61  62  63  64  65  66  68  67
  6   1
  7   1
 29   1   2
 30   1   2
 53   2   3
 54   2   3
 78   3   4
 79   3   4
104   4   5
105   4   5
131   5   6
132   5   6
159   6
160   6
 26   1
 27   1
 49   2
 50   2
 72   3
 73   3
 97   4
 98   4
123   5
124   5
149   6
150   6
 13   1
 14   1
 36   1
 37   1
 59   6
 60   6
 88   6
 89   6
  8   7   6   4  10   6
 69  70  71  72  73  74  75  76  78  77
  7   1
 30   1   2
 54   2   3
 79   3   4
105   4   5
132   5   6
160   6
 27   1
 50   2
 73   3
 98   4
124   5
150   6
 14   1
```



```
 37   1
 60   6
 89   6
  9   7   6   4  10   6
 69  70  71  72  73  74  75  76  78  77
  8   1
 31   1   2
 55   2   3
 80   3   4
106   4   5
133   5   6
161   6
 28   1
 51   2
 74   3
 99   4
125   5
151   6
 15   1
 38   1
 61   6
 90   6
 10  14  12   8  10   6   1
 79  80  81  82  83  84  85  86  88  87
  8   1
  9   1
 31   1   2
 32   1   2
 55   2   3
 56   2   3
 80   3   4
 81   3   4
106   4   5
107   4   5
133   5   6
134   5   6
161   6
162   6
 28   1
 29   1
 51   2
 52   2
 74   3
 75   3
 99   4
100   4
125   5
126   5
151   6
152   6
 15   1
 16   1
 38   1
 39   1
 61   6
 62   6
 90   6
 91   6
 14  14  12   8  10   6   1
119 120 121 122 123 124 125 126 128 127
 12   1
 13   1
```

```
 35   1    2
 36   1    2
 59   2    3
 60   2    3
 84   3    4
 85   3    4
110   4    5
111   4    5
137   5    6
138   5    6
165   6
166   6
 32   1
 33   1
 55   2
 56   2
 78   3
 79   3
103   4
104   4
129   5
130   5
155   6
156   6
 19   1
 20   1
 42   1
 43   1
 65   6
 66   6
 94   6
 95   6
 15   7    6    4   10    6
129 130  131  135  137  139  150  152  156  155
 13   1
 36   1    2
 61   2    3
 86   3    4
112   4    5
140   5    6
168   6
 33   1
 56   2
 80   3
105   4
131   5
158   6
 20   1
 43   1
 68   6
 97   6
 16   7    6    4   10    6
129 130  131  135  137  139  150  152  156  155
 14   1
 37   1    2
 62   2    3
 87   3    4
113   4    5
141   5    6
169   6
 34   1
 57   2
```



```
 81   3
106   4
132   5
159   6
 21   1
 44   1
 69   6
 98   6
 17  14   12    8   10    6    1
157 158  159  160  161  162  163  164  166  165
 16   1
 17   1
 39   1    2
 40   1    2
 63   2    3
 64   2    3
 88   3    4
 89   3    4
114   4    5
115   4    5
141   5    6
142   5    6
169   6
170   6
 36   1
 37   1
 58   2
 59   2
 82   3
 83   3
107   4
108   4
132   5
133   5
159   6
160   6
 23   1
 24   1
 46   1
 47   1
 69   6
 70   6
 98   6
 99   6
 23  14   12    8   10    6    1
217 218  219  220  221  222  223  224  226  225
 22   1
 23   1
 45   1    2
 46   1    2
 69   2    3
 70   2    3
 94   3    4
 95   3    4
120   4    5
121   4    5
147   5    6
148   5    6
175   6
176   6
 42   1
 43   1
```

```
  64    2
  65    2
  88    3
  89    3
 113    4
 114    4
 138    5
 139    5
 165    6
 166    6
  29    1
  30    1
  52    1
  53    1
  75    6
  76    6
 104    6
 105    6
  24    7    6    4   10    6
 227  228  229  237  244  250  255  259  262  263
  23    1
  47    1    2
  72    2    3
  98    3    4
 125    4    5
 153    5    6
 182    6
  43    1
  66    2
  91    3
 117    4
 143    5
 171    6
  30    1
  53    1
  82    6
 111    6
LOAD
GRAVITY LOAD OF THE BRIDGE
                1          0.15
    1    0    1   -1  00011010   20    8
     63.32     63.32     63.52     63.80     64.10     64.40     64.72     65.06
     65.34     65.34     63.32     63.32     63.32     63.32     63.32     63.32
     63.32     63.32     61.19     61.19     61.19     61.19     61.19     61.19
     61.19     61.19     61.19     61.19     58.12     58.12     58.12     58.12
     58.12     58.12     58.12     58.12     58.12     58.12     55.06     55.06
     55.06     55.06     55.06     55.06     55.06     55.06     55.06     55.06
     52.00     52.00     52.00     52.00     52.00     52.00     52.00     52.00
     52.00     52.00     48.93     48.93     48.93     48.93     48.93     48.93
     48.93     48.93     48.93     48.93     46.24     46.24     46.15     46.04
     45.93     45.81     45.68     45.55     45.45     45.45     42.65     42.65
     42.65     42.65     42.65     42.65     42.65     42.65     42.65     42.65
     39.43     39.43     39.43     39.43     39.43     39.43     39.43     39.43
     39.43     39.43     36.21     36.21     36.21     36.21     36.21     36.21
     36.21     36.21     36.21     36.21     32.98     32.98     32.98     32.98
     32.98     32.98     32.98     32.98     32.98     32.98     29.76     29.76
     29.76     29.76     29.76     29.76     29.76     29.76     29.76     29.76
     29.16     29.16     28.56     27.78     27.78     27.78     27.78     27.78
     26.96     27.78     26.10     27.78     27.78     27.78     27.78     25.18
     25.18     25.18     25.18     25.18     25.18     25.18     25.18     24.21
     25.18     25.18     23.46     23.46     22.29     22.29     22.29     22.29
     22.29     22.29     22.29     22.29     22.29     22.29     18.04     18.04
```



```
     18.04     18.04     18.04     18.04     18.04     18.04     18.04     18.04
     13.79     13.79     13.79     13.79     13.79     13.79     13.79     13.79
     13.79     13.79      9.54      9.54      9.54      9.54      9.54      9.54
      9.54      9.54      9.54      9.54      5.28      5.28      5.28      5.28
      5.28      5.28      5.28      5.28      5.28      5.28      2.58      2.58
      2.58      2.58      2.58      2.58      2.58      2.58      2.58      2.58
      2.58      2.58      2.58      2.58      2.58      2.58      2.58      2.58
      2.58      2.58      2.58      2.58      2.58      2.58      2.58      2.58
      2.58      2.58      2.58      2.58      2.58      2.58      2.58      2.58
      2.58      2.58      2.58      2.58      2.58      2.58      2.58      2.58
      2.58      2.58      2.58      2.58      2.58      2.58      2.58
 24   14   12    8   10
  1    7    6    4   10    6
  1    2    3    4    5    6    7    8   10    9
  1    1
 24    1    2
 48    2    3
 73    3    4
 99    4    5
126    5    6
154    6
 21    1
 44    2
 67    3
 92    4
118    5
144    6
  9    1
 31    1
 54    6
 83    6
  2    7    6    4   10    6
  1    2   11   12   13   14   15   16   18   17
  1    1
 24    1    2
 48    2    3
 73    3    4
 99    4    5
126    5    6
154    6
 21    1
 44    2
 67    3
 92    4
118    5
144    6
  9    1
 31    1
 54    6
 83    6
  3   14   12    8   10    6    1
 19   20   21   22   23   24   25   26   28   27
  2    1
  3    1
 25    1    2
 26    1    2
 49    2    3
 50    2    3
 74    3    4
 75    3    4
100    4    5
```

```
101   4   5
127   5   6
128   5   6
155   6
156   6
 22   1
 23   1
 45   2
 46   2
 68   3
 69   3
 93   4
 94   4
119   5
120   5
145   6
146   6
  9   1
 10   1
 32   1
 33   1
 55   6
 56   6
 84   6
 85   6
  7  14  12   8  10   6   1
 59  60  61  62  63  64  65  66  68  67
  6   1
  7   1
 29   1   2
 30   1   2
 53   2   3
 54   2   3
 78   3   4
 79   3   4
104   4   5
105   4   5
131   5   6
132   5   6
159   6
160   6
 26   1
 27   1
 49   2
 50   2
 72   3
 73   3
 97   4
 98   4
123   5
124   5
149   6
150   6
 13   1
 14   1
 36   1
 37   1
 59   6
 60   6
 88   6
 89   6
  8   7   6   4  10   6
```



```
 69  70  71  72  73  74  75  76  78  77
  7   1
 30   1   2
 54   2   3
 79   3   4
105   4   5
132   5   6
160   6
 27   1
 50   2
 73   3
 98   4
124   5
150   6
 14   1
 37   1
 60   6
 89   6
  9   7   6   4  10   6
 69  70  71  72  73  74  75  76  78  77
  8   1
 31   1   2
 55   2   3
 80   3   4
106   4   5
133   5   6
161   6
 28   1
 51   2
 74   3
 99   4
125   5
151   6
 15   1
 38   1
 61   6
 90   6
 10  14  12   8  10   6   1
 79  80  81  82  83  84  85  86  88  87
  8   1
  9   1
 31   1   2
 32   1   2
 55   2   3
 56   2   3
 80   3   4
 81   3   4
106   4   5
107   4   5
133   5   6
134   5   6
161   6
162   6
 28   1
 29   1
 51   2
 52   2
 74   3
 75   3
 99   4
100   4
125   5
```

```
126    5
151    6
152    6
 15    1
 16    1
 38    1
 39    1
 61    6
 62    6
 90    6
 91    6
 14   14   12    8   10    6    1
119  120  121  122  123  124  125  126  128  127
 12    1
 13    1
 35    1    2
 36    1    2
 59    2    3
 60    2    3
 84    3    4
 85    3    4
110    4    5
111    4    5
137    5    6
138    5    6
165    6
166    6
 32    1
 33    1
 55    2
 56    2
 78    3
 79    3
103    4
104    4
129    5
130    5
155    6
156    6
 19    1
 20    1
 42    1
 43    1
 65    6
 66    6
 94    6
 95    6
 15    7    6    4   10    6
129  130  131  135  137  139  150  152  156  155
 13    1
 36    1    2
 61    2    3
 86    3    4
112    4    5
140    5    6
168    6
 33    1
 56    2
 80    3
105    4
131    5
158    6
```



```
 20    1
 43    1
 68    6
 97    6
 16    7    6    4   10    6
129  130  131  135  137  139  150  152  156  155
 14    1
 37    1    2
 62    2    3
 87    3    4
113    4    5
141    5    6
169    6
 34    1
 57    2
 81    3
106    4
132    5
159    6
 21    1
 44    1
 69    6
 98    6
 17   14   12    8   10    6    1
157  158  159  160  161  162  163  164  166  165
 16    1
 17    1
 39    1    2
 40    1    2
 63    2    3
 64    2    3
 88    3    4
 89    3    4
114    4    5
115    4    5
141    5    6
142    5    6
169    6
170    6
 36    1
 37    1
 58    2
 59    2
 82    3
 83    3
107    4
108    4
132    5
133    5
159    6
160    6
 23    1
 24    1
 46    1
 47    1
 69    6
 70    6
 98    6
 99    6
 23   14   12    8   10    6    1
217  218  219  220  221  222  223  224  226  225
 22    1
```

```
  23    1
  45    1    2
  46    1    2
  69    2    3
  70    2    3
  94    3    4
  95    3    4
 120    4    5
 121    4    5
 147    5    6
 148    5    6
 175    6
 176    6
  42    1
  43    1
  64    2
  65    2
  88    3
  89    3
 113    4
 114    4
 138    5
 139    5
 165    6
 166    6
  29    1
  30    1
  52    1
  53    1
  75    6
  76    6
 104    6
 105    6
  24    7    6    4   10    6
 227  228  229  237  244  250  255  259  262  263
  23    1
  47    1    2
  72    2    3
  98    3    4
 125    4    5
 153    5    6
 182    6
  43    1
  66    2
  91    3
 117    4
 143    5
 171    6
  30    1
  53    1
  82    6
 111    6
LOAD
LIVE LOAD (TRUCK LOAD) FOR MAXIMUM POSITIVE MOMENT ON SPAN 3
  18
 179                              -4.923
 180                              -3.816
 181                              -6.030
 182                              -6.030
 183                              -3.816
 184                              -4.923
 189                             -21.744
```



```
190                              -16.851
191                              -26.636
192                              -26.636
193                              -16.851
194                              -21.744
199                              -9.333
200                              -7.234
201                              -11.433
202                              -11.433
203                              -7.234
204                              -9.333
  1    0    1   -1  00011010   20    8
  63.32     63.32     63.52     63.80     64.10     64.40     64.72     65.06
  65.34     65.34     63.32     63.32     63.32     63.32     63.32     63.32
  63.32     63.32     61.19     61.19     61.19     61.19     61.19     61.19
  61.19     61.19     61.19     61.19     58.12     58.12     58.12     58.12
  58.12     58.12     58.12     58.12     58.12     58.12     55.06     55.06
  55.06     55.06     55.06     55.06     55.06     55.06     55.06     55.06
  52.00     52.00     52.00     52.00     52.00     52.00     52.00     52.00
  52.00     52.00     48.93     48.93     48.93     48.93     48.93     48.93
  48.93     48.93     48.93     48.93     46.24     46.24     46.15     46.04
  45.93     45.81     45.68     45.55     45.45     45.45     42.65     42.65
  42.65     42.65     42.65     42.65     42.65     42.65     42.65     42.65
  39.43     39.43     39.43     39.43     39.43     39.43     39.43     39.43
  39.43     39.43     36.21     36.21     36.21     36.21     36.21     36.21
  36.21     36.21     36.21     36.21     32.98     32.98     32.98     32.98
  32.98     32.98     32.98     32.98     32.98     32.98     29.76     29.76
  29.76     29.76     29.76     29.76     29.76     29.76     29.76     29.76
  29.16     29.16     28.56     27.78     27.78     27.78     27.78     27.78
  26.96     27.78     26.10     27.78     27.78     27.78     27.78     25.18
  25.18     25.18     25.18     25.18     25.18     25.18     25.18     24.21
  25.18     25.18     23.46     23.46     22.29     22.29     22.29     22.29
  22.29     22.29     22.29     22.29     22.29     22.29     18.04     18.04
  18.04     18.04     18.04     18.04     18.04     18.04     18.04     18.04
  13.79     13.79     13.79     13.79     13.79     13.79     13.79     13.79
  13.79     13.79      9.54      9.54      9.54      9.54      9.54      9.54
   9.54      9.54      9.54      9.54      5.28      5.28      5.28      5.28
   5.28      5.28      5.28      5.28      5.28      5.28      2.58      2.58
   2.58      2.58      2.58      2.58      2.58      2.58      2.58      2.58
   2.58      2.58      2.58      2.58      2.58      2.58      2.58      2.58
   2.58      2.58      2.58      2.58      2.58      2.58      2.58      2.58
   2.58      2.58      2.58      2.58      2.58      2.58      2.58      2.58
   2.58      2.58      2.58      2.58      2.58      2.58      2.58      2.58
   2.58      2.58      2.58      2.58      2.58      2.58      2.58
 24   14   12    8   10
  1    7    6    4   10    6
  1    2    3    4    5    6    7    8   10    9
  1    1
 24    1    2
 48    2    3
 73    3    4
 99    4    5
126    5    6
154    6
 21    1
 44    2
 67    3
 92    4
118    5
144    6
  9    1
```

```
 31   1
 54   6
 83   6
  2   7   6   4  10   6
  1   2  11  12  13  14  15  16  18  17
  1   1
 24   1   2
 48   2   3
 73   3   4
 99   4   5
126   5   6
154   6
 21   1
 44   2
 67   3
 92   4
118   5
144   6
  9   1
 31   1
 54   6
 83   6
  3  14  12   8  10   6   1
 19  20  21  22  23  24  25  26  28  27
  2   1
  3   1
 25   1   2
 26   1   2
 49   2   3
 50   2   3
 74   3   4
 75   3   4
100   4   5
101   4   5
127   5   6
128   5   6
155   6
156   6
 22   1
 23   1
 45   2
 46   2
 68   3
 69   3
 93   4
 94   4
119   5
120   5
145   6
146   6
  9   1
 10   1
 32   1
 33   1
 55   6
 56   6
 84   6
 85   6
  7  14  12   8  10   6   1
 59  60  61  62  63  64  65  66  68  67
  6   1
  7   1
```



```
 29   1   2
 30   1   2
 53   2   3
 54   2   3
 78   3   4
 79   3   4
104   4   5
105   4   5
131   5   6
132   5   6
159   6
160   6
 26   1
 27   1
 49   2
 50   2
 72   3
 73   3
 97   4
 98   4
123   5
124   5
149   6
150   6
 13   1
 14   1
 36   1
 37   1
 59   6
 60   6
 88   6
 89   6
  8   7   6   4  10   6
 69  70  71  72  73  74  75  76  78  77
  7   1
 30   1   2
 54   2   3
 79   3   4
105   4   5
132   5   6
160   6
 27   1
 50   2
 73   3
 98   4
124   5
150   6
 14   1
 37   1
 60   6
 89   6
  9   7   6   4  10   6
 69  70  71  72  73  74  75  76  78  77
  8   1
 31   1   2
 55   2   3
 80   3   4
106   4   5
133   5   6
161   6
 28   1
 51   2
```

```
 74   3
 99   4
125   5
151   6
 15   1
 38   1
 61   6
 90   6
 10  14   12    8   10    6    1
 79  80   81   82   83   84   85   86   88   87
  8   1
  9   1
 31   1    2
 32   1    2
 55   2    3
 56   2    3
 80   3    4
 81   3    4
106   4    5
107   4    5
133   5    6
134   5    6
161   6
162   6
 28   1
 29   1
 51   2
 52   2
 74   3
 75   3
 99   4
100   4
125   5
126   5
151   6
152   6
 15   1
 16   1
 38   1
 39   1
 61   6
 62   6
 90   6
 91   6
 14  14   12    8   10    6    1
119 120  121  122  123  124  125  126  128  127
 12   1
 13   1
 35   1    2
 36   1    2
 59   2    3
 60   2    3
 84   3    4
 85   3    4
110   4    5
111   4    5
137   5    6
138   5    6
165   6
166   6
 32   1
 33   1
```



```
 55   2
 56   2
 78   3
 79   3
103   4
104   4
129   5
130   5
155   6
156   6
 19   1
 20   1
 42   1
 43   1
 65   6
 66   6
 94   6
 95   6
 15   7    6    4   10    6
129 130  131  135  137  139  150  152  156  155
 13   1
 36   1    2
 61   2    3
 86   3    4
112   4    5
140   5    6
168   6
 33   1
 56   2
 80   3
105   4
131   5
158   6
 20   1
 43   1
 68   6
 97   6
 16   7    6    4   10    6
129 130  131  135  137  139  150  152  156  155
 14   1
 37   1    2
 62   2    3
 87   3    4
113   4    5
141   5    6
169   6
 34   1
 57   2
 81   3
106   4
132   5
159   6
 21   1
 44   1
 69   6
 98   6
 17  14   12    8   10    6    1
157 158  159  160  161  162  163  164  166  165
 16   1
 17   1
 39   1    2
 40   1    2
```

```
 63    2    3
 64    2    3
 88    3    4
 89    3    4
114    4    5
115    4    5
141    5    6
142    5    6
169    6
170    6
 36    1
 37    1
 58    2
 59    2
 82    3
 83    3
107    4
108    4
132    5
133    5
159    6
160    6
 23    1
 24    1
 46    1
 47    1
 69    6
 70    6
 98    6
 99    6
 23   14   12    8   10    6    1
217  218  219  220  221  222  223  224  226  225
 22    1
 23    1
 45    1    2
 46    1    2
 69    2    3
 70    2    3
 94    3    4
 95    3    4
120    4    5
121    4    5
147    5    6
148    5    6
175    6
176    6
 42    1
 43    1
 64    2
 65    2
 88    3
 89    3
113    4
114    4
138    5
139    5
165    6
166    6
 29    1
 30    1
 52    1
 53    1
```



```
 75    6
 76    6
104    6
105    6
 24    7    6    4   10    6
227  228  229  237  244  250  255  259  262  263
 23    1
 47    1    2
 72    2    3
 98    3    4
125    4    5
153    5    6
182    6
 43    1
 66    2
 91    3
117    4
143    5
171    6
 30    1
 53    1
 82    6
111    6
LOAD
LIVE LOAD (LANE LOAD) FOR MAXIMUM NEGATIVE MOMENT AT BENT 2B
 32    2
 99                              -1.189
101                              -2.740
102                              -3.103
103                              -3.103
104                              -3.103
105                              -3.103
106                              -2.740
107                              -1.189
109                              -1.979
111                              -4.561
112                              -5.165
113                              -5.165
114                              -5.165
115                              -5.165
116                              -4.561
117                              -1.979
177                              -2.639
179                              -6.083
180                              -6.888
181                              -6.888
182                              -6.888
183                              -6.888
184                              -6.083
185                              -2.639
187                              -0.528
189                              -1.218
190                              -1.379
191                              -1.379
192                              -1.379
193                              -1.379
194                              -1.218
195                              -0.528
  2  133-0.04348
  8    9   10   11   12   13   14   15   16   17   18   19   20   21   22   23
 31   32   33   34   35   56   37   38   39   40   41   42   43   44   45   46
 47   55   56   57   58   59   60   61   62   63   64   65   66   67   68   69
```

```
 70   71   72   80   81   82   83   84   85   86   87   88   89   90   91   92
 93   94   95   96   97   98  106  107  108  109  110  111  112  113  114  115
116  117  118  119  120  121  122  123  124  125  133  134  135  136  137  138
139  140  141  142  143  144  145  146  147  148  149  150  151  152  153  161
162  163  164  165  166  167  168  169  170  171  172  173  174  175  176  177
178  179  180  181  182
  1    0    1   -1  00011010   20    8
    63.32        63.32        63.52        63.80        64.10        64.40        64.72        65.06
    65.34        65.34        63.32        63.32        63.32        63.32        63.32        63.32
    63.32        63.32        61.19        61.19        61.19        61.19        61.19        61.19
    61.19        61.19        61.19        61.19        58.12        58.12        58.12        58.12
    58.12        58.12        58.12        58.12        58.12        58.12        55.06        55.06
    55.06        55.06        55.06        55.06        55.06        55.06        55.06        55.06
    52.00        52.00        52.00        52.00        52.00        52.00        52.00        52.00
    52.00        52.00        48.93        48.93        48.93        48.93        48.93        48.93
    48.93        48.93        48.93        48.93        46.24        46.24        46.15        46.04
    45.93        45.81        45.68        45.55        45.45        45.45        42.65        42.65
    42.65        42.65        42.65        42.65        42.65        42.65        42.65        42.65
    39.43        39.43        39.43        39.43        39.43        39.43        39.43        39.43
    39.43        39.43        36.21        36.21        36.21        36.21        36.21        36.21
    36.21        36.21        36.21        36.21        32.98        32.98        32.98        32.98
    32.98        32.98        32.98        32.98        32.98        32.98        29.76        29.76
    29.76        29.76        29.76        29.76        29.76        29.76        29.76        29.76
    29.16        29.16        28.56        27.78        27.78        27.78        27.78        27.78
    26.96        27.78        26.10        27.78        27.78        27.78        27.78        25.18
    25.18        25.18        25.18        25.18        25.18        25.18        25.18        24.21
    25.18        25.18        23.46        23.46        22.29        22.29        22.29        22.29
    22.29        22.29        22.29        22.29        22.29        22.29        18.04        18.04
    18.04        18.04        18.04        18.04        18.04        18.04        18.04        18.04
    13.79        13.79        13.79        13.79        13.79        13.79        13.79        13.79
    13.79        13.79         9.54         9.54         9.54         9.54         9.54         9.54
     9.54         9.54         9.54         9.54         5.28         5.28         5.28         5.28
     5.28         5.28         5.28         5.28         5.28         5.28         2.58         2.58
     2.58         2.58         2.58         2.58         2.58         2.58         2.58         2.58
     2.58         2.58         2.58         2.58         2.58         2.58         2.58         2.58
     2.58         2.58         2.58         2.58         2.58         2.58         2.58         2.58
     2.58         2.58         2.58         2.58         2.58         2.58         2.58         2.58
     2.58         2.58         2.58         2.58         2.58         2.58         2.58         2.58
     2.58         2.58         2.58         2.58         2.58         2.58         2.58
 24   14   12    8   10
  1    7    6    4   10    6
  1    2    3    4    5    6    7    8   10    9
  1    1
 24    1    2
 48    2    3
 73    3    4
 99    4    5
126    5    6
154    6
 21    1
 44    2
 67    3
 92    4
118    5
144    6
  9    1
 31    1
 54    6
 83    6
  2    7    6    4   10    6
  1    2   11   12   13   14   15   16   18   17
```



```
  1    1
 24    1    2
 48    2    3
 73    3    4
 99    4    5
126    5    6
154    6
 21    1
 44    2
 67    3
 92    4
118    5
144    6
  9    1
 31    1
 54    6
 83    6
  3   14   12    8   10    6    1
 19   20   21   22   23   24   25   26   28   27
  2    1
  3    1
 25    1    2
 26    1    2
 49    2    3
 50    2    3
 74    3    4
 75    3    4
100    4    5
101    4    5
127    5    6
128    5    6
155    6
156    6
 22    1
 23    1
 45    2
 46    2
 68    3
 69    3
 93    4
 94    4
119    5
120    5
145    6
146    6
  9    1
 10    1
 32    1
 33    1
 55    6
 56    6
 84    6
 85    6
  7   14   12    8   10    6    1
 59   60   61   62   63   64   65   66   68   67
  6    1
  7    1
 29    1    2
 30    1    2
 53    2    3
 54    2    3
 78    3    4
```

```
 79   3   4
104   4   5
105   4   5
131   5   6
132   5   6
159   6
160   6
 26   1
 27   1
 49   2
 50   2
 72   3
 73   3
 97   4
 98   4
123   5
124   5
149   6
150   6
 13   1
 14   1
 36   1
 37   1
 59   6
 60   6
 88   6
 89   6
  8   7   6   4  10   6
 69  70  71  72  73  74  75  76  78  77
  7   1
 30   1   2
 54   2   3
 79   3   4
105   4   5
132   5   6
160   6
 27   1
 50   2
 73   3
 98   4
124   5
150   6
 14   1
 37   1
 60   6
 89   6
  9   7   6   4  10   6
 69  70  71  72  73  74  75  76  78  77
  8   1
 31   1   2
 55   2   3
 80   3   4
106   4   5
133   5   6
161   6
 28   1
 51   2
 74   3
 99   4
125   5
151   6
 15   1
```



```
 38   1
 61   6
 90   6
 10  14  12   8  10   6   1
 79  80  81  82  83  84  85  86  88  87
  8   1
  9   1
 31   1   2
 32   1   2
 55   2   3
 56   2   3
 80   3   4
 81   3   4
106   4   5
107   4   5
133   5   6
134   5   6
161   6
162   6
 28   1
 29   1
 51   2
 52   2
 74   3
 75   3
 99   4
100   4
125   5
126   5
151   6
152   6
 15   1
 16   1
 38   1
 39   1
 61   6
 62   6
 90   6
 91   6
 14  14  12   8  10   6   1
119 120 121 122 123 124 125 126 128 127
 12   1
 13   1
 35   1   2
 36   1   2
 59   2   3
 60   2   3
 84   3   4
 85   3   4
110   4   5
111   4   5
137   5   6
138   5   6
165   6
166   6
 32   1
 33   1
 55   2
 56   2
 78   3
 79   3
103   4
```

```
104    4
129    5
130    5
155    6
156    6
 19    1
 20    1
 42    1
 43    1
 65    6
 66    6
 94    6
 95    6
 15    7    6    4   10    6
129  130  131  135  137  139  150  152  156  155
 13    1
 36    1    2
 61    2    3
 86    3    4
112    4    5
140    5    6
168    6
 33    1
 56    2
 80    3
105    4
131    5
158    6
 20    1
 43    1
 68    6
 97    6
 16    7    6    4   10    6
129  130  131  135  137  139  150  152  156  155
 14    1
 37    1    2
 62    2    3
 87    3    4
113    4    5
141    5    6
169    6
 34    1
 57    2
 81    3
106    4
132    5
159    6
 21    1
 44    1
 69    6
 98    6
 17   14   12    8   10    6    1
157  158  159  160  161  162  163  164  166  165
 16    1
 17    1
 39    1    2
 40    1    2
 63    2    3
 64    2    3
 88    3    4
 89    3    4
114    4    5
```



```
115    4    5
141    5    6
142    5    6
169    6
170    6
 36    1
 37    1
 58    2
 59    2
 82    3
 83    3
107    4
108    4
132    5
133    5
159    6
160    6
 23    1
 24    1
 46    1
 47    1
 69    6
 70    6
 98    6
 99    6
 23   14   12    8   10    6    1
217  218  219  220  221  222  223  224  226  225
 22    1
 23    1
 45    1    2
 46    1    2
 69    2    3
 70    2    3
 94    3    4
 95    3    4
120    4    5
121    4    5
147    5    6
148    5    6
175    6
176    6
 42    1
 43    1
 64    2
 65    2
 88    3
 89    3
113    4
114    4
138    5
139    5
165    6
166    6
 29    1
 30    1
 52    1
 53    1
 75    6
 76    6
104    6
105    6
 24    7    6    4   10    6
```

```
  227  228  229  237  244  250  255  259  262  263
   23    1
   47    1    2
   72    2    3
   98    3    4
  125    4    5
  153    5    6
  182    6
   43    1
   66    2
   91    3
  117    4
  143    5
  171    6
   30    1
   53    1
   82    6
  111    6
STOP
```